A window into magmatic systems: mineralogical constraints on the nature and timing of magma interactions and ascent

Rosa Didonna

BSc, MSc

Department of Earth and Environmental Sciences

Presented to Macquarie University in fulfilment of the requirements for the degree of Doctor of Philosophy

January 2020

Per te Manuel

Abstract

Investigations into the time evolution of sub-volcanic magmatic systems are invaluable in order to improve our understanding of volcanic behaviours and associated hazards. The magmatic pathway from source to surface is usually complex and may involve many different processes, such as fractional crystallisation, magma mingling/mixing, and assimilation of wall rock in contact with the magma. These processes are recorded in the erupted deposits and can be found both at macroscopic (e.g., inclusions in the host rock, banded pumice, and xenoliths) and microscopic scales (e.g., rock-forming mineral textures and compositional zoning patterns).

This thesis focused on mineral-scale studies of volcanic rocks in order to decipher the magmatic histories of volcanoes located in different tectonic settings: Soufriere Hills Volcano at Montserrat Island (Lesser Antilles; subduction zone), Gede Volcano in West Java (Indonesia; subduction zone), and Waitomokia Volcano (New Zealand; intraplate zone).

Soufrière Hills Volcano has been studied through mineralogical textures and chemical compositions of plagioclase in its volcanic rocks. Diffusion modelling of magnesium in these plagioclase reveals timescales for magmatic interactions (basaltic andesite intrusion into the andesitic host) ranging from a few hours up to two months prior the eruption, inferred to be related to syn-eruptive processes.

Gede Volcano produced rocks with plagioclase phenocrysts originally crystallised from the host andesite. These plagioclase show resorption areas from 20 to 400 microns in thickness, which imply timescales ranging from 1 to 10 days between the intrusion of new magma in the host and the eruption.

Waitomokia Volcano has been characterised through olivine core compositions and zoning patterns within juvenile material produced during progressive eruption stages (from initial phreatomagmatic to final magmatic phase). It has been found that magma ascent from the mantle source to the surface is rapid, and yet that magma mixing has an important role in this small-volume plumbing system.

In this work, the recognition of magmatic interactions via mixing and mingling processes within all the volcanic systems investigated shows complexity either in small- and large-scale volcanic systems. The findings from this work about the timescales of storage, transport and evolution of magma have important implications in the understanding of eruption triggers. The results for these three volcanoes are particularly relevant due to their location nearby populous cities, and therefore this work provides powerful results to support the interpretation of the monitoring signals, fundamental in case of future unrest situation.

Statement of Originality

This work has not previously been submitted for a degree or diploma in any university. To the best of my knowledge and belief, the thesis contains no material previously published or written by another person except where due reference is made in the thesis itself.

(Signed) Date: 29/01/2020

Rosa Didonna

Acknowledgements

Special thanks to my principal supervisor *Heather Handley* (MQ, Macquarie University) for giving me this amazing opportunity and fuel my passion and determination for this project. Thank you for your support and encouragement to stay in Australia despite difficult times. If I didn't give up, it was becasue of your inspiration as a scientist and mother at the same time.

I am extremely grateful to my supervisor, *Fidel Costa* (EOS, Earth Observatory of Singapore). This thesis would not have been possible without your guidance, dedication, enthusiasm, patience and passion for this project. Also, thank you for giving me the opportunity to come to Singapore and collaborate with such an incredible research group at EOS.

Thank you to my co-supervisor, Professor Simon Turner, for the encouragement and constructive discussion during our meetings.

Thank you to my examiners Michel Pichavant, Marie Edmonds and Marco Fiorentini for their comments and suggestions that improved this work.

Thank you to the analytical team during laboratory work: Timothy Murphy (MQ), Dr Lilu Cheng and Dr Jason Herrin (EOS), and Steve Craven (MQ) - for your assistance, guidance and support during lab work. Thank you for sharing your knowledge!

Turker Topal (MQ), your invaluable help with the matlab code, the long discussions and most of all for your friendship.

To the wonderful people who have been a mentor thought my phd: Elena Belousova, Orsola De Marco and Jennifer Rowland – models of stength as scientists, women and mothers at the same time.

To people who contributed with their discussions, suggestions or just for sharing their knowledge: Benat Oliveira Bravo, Nathan Daczko, Jon Adams, Rachel Bezard, Steven Hansen (MQ), Helena Albert, Cristina Widiwijayanti and Gareth Gabbro (EOS).

Lucy McGee (MQ), I especially thank you for these three years of discussions and encouragement.

Those who have been a source of strength: my cousins Claudia and Angela Iacobellis, Ramón Abud Alcalá, Montgarri Castillo Oliver, Coti Manassero, Marina Veter, Marco DiVincenzo, Hindol Ghatak, Simone Vez, Vito, Francesco Cataldo- thank you for all the laughs, tears and encouragement in completing this thesis during these adventurous years!

To everybody who has been a part of this adventure at Macquarie University: Anthony Lanati, Thusitha Bandara Nimalsiri, Laura Otter, Michael Förster, Catarina Vila Pouca, Louise Goode, Kim, Robyn, Sinan, Milena, Lauren, Ananuer, Yoanne, Lou, Gullielme, Toosin, Peter Wieland, Marthe and anybody else that I have forgotten!!!—The Italian team, *Alessandro Maini*, Valentina Bracetti, Roberto Iaconi, Edoardo Lanari and Emilio Lomonaco.

To the amazing people that I've met at EOS in Singapore: Helena, Alex, Fabio, Sara, Chris, Asif, George, Marcus, Olivier and Tommaso - thank you for all the trips, adventures, amazing dinners, dancing and incredible laughs after a long day at work!

People who were helping me with my son when I was travelling for a conference, to Singapore or when I was working and writing this thesis: Ottavio, Alyson, Kylie, Cristine, Rachele, Cinzia, Santino, Salam and her family (the best landlord and neighbours ever!)

Thank you to my parents, my sister Dalia and my big Italian family (zii, cugini e nonna) for your unconditional love, encouragement and financial support that helped to make this thesis a dream come true.

Finally, the most important person to thank is to Manuel, my son, for his patience, support and enthusiasm to live our hectic life travelling around the world with or without me. He has an incredible passion for life and capacity to make me feel loved and proud of him every single day.

This work was funded by Macquarie University Research Excellence Scholarship (MQRES) (2015081) associated with an Australian Research Council Discovery Project (DP150100328).

Table of contents

Chapter 1. Introduction 1

1.1. General introduction and motivation 3

1.2. Volcanic plumbing system: magma pathway from the source to the surface 5

1.3. Magmatic processes responsible for triggering volcanic eruptions 7

1.4. Understanding magmatic processes: linking mineral texture with chemical zoning in crystals 8

1.5. Diffusion and Magmatic Timescales 9

1.6. Aims of this thesis and selection of case studies 10

1.7. Outline of the thesis 11

1.8. Author contributions 12

Chapter 2. Dynamics and timescales of mafic-silicic magma interactions at Soufrière Hills Volcano, Montserrat 21

Abstract 23

2.1. Introduction 25

2.2. Geology and petrology of Soufrière Hills Volcano (1995-2010 eruption) 26

2.2.1. Previous models of mafic-silicic magma interactions at SVH 28

2.3. Sample details and analytical techniques 30

2.4. Modelling approach and parameters used for calculating melt compositions and timescales 31

2.4.1. Partition coefficient and melt equivalent of magnesium (Mg)..... 32
2.4.2. Temperature..... 33
2.4.3. Diffusion coefficient of Mg in plagioclase..... 35
2.4.4. Numerical modelling 35

2.5. Mineral assemblages, textures, and compositions 36

2.5.1. Plagioclase textures and zoning patterns..... 38

2.6. Melt compositions and temperatures in equilibrium with plagioclase 40

2.6.1. Bulk-rock and glass compositions and their relationship to magmatic temperature..... 43
2.6.2. Andesite magma 43
2.6.3. Basaltic-andesite magmas 44
2.6.4. Calculated melt compositions in equilibrium with the host and enclave..... 44

2.7. Estimated timescales from diffusion modelling.....47

2.7.1. Calculated timescales of magmatic interaction to eruption 48
2.7.2. Uncertainties..... 50

2.8. Magma end-members and processes inferred from petrology, plagioclase zoning, and calculated melt compositions 50

2.8.1 Andesite and basaltic andesite magmas prior to interaction 50
2.8.2. Interaction between the host andesite and intruding basalt..... 52

2.9. Timescales between the last interaction and eruption.....53

2.10. A variety of time scales for the SHV magmatic system.....55

2.11. Conclusion.....57

Appendix A 65

A.1. 1-Stage model 67
A.2. 2-Stage model 71
A.3. Electron backscattered (BSE) images of MT35 rock. 75
A.4. Electron backscattered (BSE) images of MT35 rock. 77
A.5. Overview of all the temperature proposed in literature.....76
A.6. Summary of phase equilibrium experiments from Couch et al. (2003).....76
A.7. FeO and MgO vs An content for interior part to the rim of plagioclase 79
A.8. Description of one-stage and two stage models.....80

Chapter 3. Insights into the dynamics of magma mixing through texture and compositional zoning recorded in crystals: Gede Volcano as a case study 81

Abstract 83

3.1. Introduction.....85

3.2. Geological background 87

3.3. Samples and Methods 89

3.3.1. Scanning electron microscope (SEM) and electron microprobe (EMPA) 90
3.3.2. In-situ trace element analysis by laser-ICP MS 91

3.4. Melt composition calculations 91

3.5. Mineral texture and compositional zoning 92

3.5.1. Plagioclase 93
3.5.2. Pyroxene: clinopyroxene and orthopyroxene 96
3.5.4. Melt compositions 99

3.6. Discussion 100

3.6.1. Macroscopic and geochemical evidence for magmatic interactions 101
3.6.2. Insights into magma mingling/mixing using mineral texture and composition . 103
3.6.3. Implications for magmatic processes at Gede Volcanic Complex (GVC) 105

3.7. Conclusions.....106

Chapter 4. Rapid magma ascent from olivine morphology and zoning patterns: Waitomokia Volcano, Auckland Volcanic Field, New Zealand 111

Abstract 113

4.1. Introduction 115

4.2. Geological background 117

4.2.1. Waitomokia Volcano 118

4.3. Sample selection and analytical methods 119

4.3.1. Scanning electron microscope (SEM) and electron microprobe (EMPA) analyses 120

4.4. Results: Mineralogy and petrography 122

4.4.1. Olivine 122
4.4.2. Clinopyroxene 127
4.4.3. Estimation of the temperature and pressure of crystallisation 128

4.5. Discussion 129

4.5.1. Magmatic environments inferred from olivine core compositions 129
4.5.2. Magma evolution, interaction and transport to the surface 130
4.5.3. Implications for the temporal evolution of Waitomokia volcano 133

4.6. Conclusion 137

Appendix C 145

C.1. Samples analyses in this study and collected during two different field trips 147
C.2. Whole rock data from selected samples 147

Chapter 5. Insights into volatile transport and eruption triggering at explosive volcanoes 149

Abstract 151

5.1. Introduction 153

5.2. Timescales of eruption triggers: application of Uranium series chemistry 153

5.3. The 1995-2010AD eruption of Soufrière Hills Volcano and the significance of enclave formation 154

5.4. Methods 158

5.5. Petrography of MT35 and MT75 158

5.6. U-Th-Ra-Pb results 160

5.7. Millennial-scale magma additions and decadal-scale volatile fluxes 160

Appendix D 167

D.1. U-Th, Th-Ra and Ra-Pb plots of the studied serial sections compared to enclave and andesite data. 169
D.2. MT35 X-ray map from Tornado 170
D.3 MT75 X-ray map from Tornado 171

Chapter 6. Conclusions **173**

6.1. Conclusions and future work 175

6.2. Timescales of mafic-silicic magma interactions at Soufrière Hills volcano 175

6.3. Unravel the nature and dynamics of magmatic system at Gede volcano 175

6.4. Constrain magma ascent dynamics throughout the formation of Waitomokia volcano through textural and compositional investigation of minerals 176

6.5. Shed light on the level of complexity in sub-volcanic magmatic plumbing systems at different scales using detailed mineralogical studies 176

6.6. Summary and broader implications of this work 177

6.7. Future directions 177

List of Figures

Chapter 1. Introduction 1

Figure 1. Pictures of the Soufriere Hills Volcano, Gede and Waitomokia Volcano 4
Figure 2. Magmatic system in which magma accumulates and evolves 5
Figure 3. Transcrustal magmatic system 6
Figure 4. Conditions that control eruptions for an idealised magma reservoir 7

Chapter 2. Dynamics and timescales of mafic-silicic magma interactions at Soufrière Hills Volcano, Montserrat 21

Figure 1. Rock sample (MT35) from deposits of the dome collapse 26
Figure 2. Satellite image of the Soufrière Hills Volcano (Montserrat Island, Lesser Antilles) 27
Figure 3 . Summary of previous models of plumbing system at SHV. 29
Figure 4. Comparison of MgO vs SiO2 in andesite (host rock) and basaltic andesite (enclave) between the five phases of extrusive activity 34
Figure 5. Backscattered electron image of a whole thin section 'MT2E' 37
Figure 6. Representative plagioclase phenocrysts, in enclave and host, characterized on the base of anorthite content (An) against MgO composition 39
Figure 7. BSE images of plagioclase from enclave (basaltic andesite) 41
Figure 8. BSE images of plagioclase from andesite host 42
Figure 9. Calculated MgO in the melt at three different temperatures 46
Figure 10. H6 plagioclase as case study for Type I (host andesite) 48
Figure 11. Diffusion models for plagioclase in host and enclaves 49
Figure 12. Schematic representation of the sequence of four events resulting from the interaction of andesite and intruding basalt 53
Figure 13. Timescales gained using different methods 56

Chapter 3. Insights into the dynamics of magma mixing through texture and compositional zoning recorded in crystals: Gede Volcano as a case study 81

Figure 1. Tectonic setting of Java within the Sunda arc, Indonesia 86
Figure 2. Location map of samples from the Old Quaternary to the Young Gede erupted deposits 87
Figure 3. Juvenile scoria from pyroclastic flows 89
Figure 4. Whole rock compositions of the samples investigated in this study 90
Figure 5. G13 from Old Gede microscopic picture 92
Figure 6. G51 from Young Gede microscopic picture 93
Figure 7. Histograms on the variation in anorthite (An) composition for the plagioclase phenocrysts 94
Figure 8. Variation in An for core-middle-rim compositions against FeO, K_2O, Al_2O_3 and Na_2O 96
Figure 9. Classification of clinopyroxene in the basis of Mg, Fe and Ca 97
Figure 10. Variation of An content in Sr concentration in calculated melt from Blundy and Wood (1991) for samples showing dark and light melt (b) Variation of Ba in calculated melt against An content. 99
Figure 11. Variation of An content in Sr (a) and (Ba) concentration in calculated melt 100
Figure 12. Variation of Ba and Sr concentration in plagioclase 101
Figure 13. Sr/Ba ratios variations correlated with An composition plagioclase 102
Figure 14. Calculated melt of Ba against the Sr melt from Blundy and Wood (1991) 104

Chapter 4. Rapid magma ascent from olivine morphology and zoning patterns: Waitomokia Volcano, Auckland Volcanic Field, New Zealand 111

Figure 1. Location map of the Auckland Volcanic Field (AVF) and its eruptive centres 116
Figure 2. Changes in the geomorphology of the Waitomokia area since 1950 to present day 119
Figure 3. Location of the twelve samples selected for detailed textural and compositional analysis 121
Figure 4. Textural and zoning features of the different olivine 123
Figure 5. Schematic representation of a common olivine crystal 124
Figure 6. Histograms showing the distribution of Fo (mol.%) in olivine core and rim 124
Figure 7. BSE images and Fo, CaO and Ni content profiles 125
Figure 8. CaO, NiO and MnO contents as a function of Fo content in olivine 126
Figure 9. BSE showing sector and oscillatory zoning in clinopyroxene microphenocrysts 127
Figure 10. Compositions of clinopyroxene cores and rims of microphenocrysts and clinopyroxene

rims on olivine.....128
Figure 11. Estimated T and P of clinopyroxene crystallization within Waitomokia rocks 132
Figure 12. CaO content (wt.%) against Fo content (mol.%) for olivine cores and rims.....134
Figure 13. Olivine Fo (mol.%) zoning profiles subdivided by Group 1, 2 and 3 during the eruptive stages. 135
Figure 14. Schematic model showing the development of the magmatic plumbing system at Waitomokia volcano 136

Chapter 5. Insights into volatile transport and eruption triggering at explosive volcanoes 149

Figure 1: U-series data for sample MT35 from Phase V of the SHV eruption.....154
Figure 2: U-series data for sample MT75 from Phase V of the SHV eruption.....155
Figure 3: The $(^{210}Pb/^{226}Ra)_0$ signatures of the studied samples related to the enclave formation mechanism.....161

Supplementary Data.....179

A1. Major element composition of plagioclase from Soufrière Hills Volcano, Montserrat.....180
A1.2. Major element composition of pyroxene from Soufrière Hills Volcano, Montserrat.....234

B1.1. Major element composition of plagioclase from Gede volcano.....272
B1.2. Major element composition of orthopyroxene Gede volcano.....272
B1.3. Major element composition of clinopyroxene from Gede volcano.....283
B1.4. Major element composition of olivine from Gede volcano.....284

B2. Trace element composition of plagioclase from Gede volcano.....285
B3. Calculation of Sr-Ba melt composition from Gede volcano.....298

C1.1. Major element composition of clinopyroxene from the Waitomokia volcano.....299
C1.2. Major element composition of olivine from the Waitomokia volcano.....300
C1.3. Major element composition of clinopyroxene, olivine and glass from the Waitomokia volcano....348

D1.1. Major element composition of plagioclase from Soufrière Hills Volcano, Montserrat.....349
D1.2. Major element composition of orthopyroxene from Soufrière Hills Volcano, Montserrat.....350

Chapter 1

Introduction

1.1. General introduction and motivation

Volcanic eruptions are one of the most fascinating phenomena on Earth. Billions of people are living in cities built on volcanic areas, so understanding the magmatic processes that trigger eruptions is fundamental for interpreting the eruption behaviours and for mitigating volcanic hazards (Sparks et al., 1977). Despite advances in the ability to forecast volcanic eruptions (e.g., monitoring of ground movements, gas emissions seismic activity), it is still unclear what triggers the destabilisation of the system, and the ascent of magma leading to an eruption. Therefore, it is crucial to investigate the sub-volcanic magmatic plumbing system, and the magmatic processes, such as magma mingling and mixing, assimilation and transport towards the surface (Blundy and Cashman, 2008; Costa et al., 2013; Davidson et al., 2001a, b; Edmonds and Wood, 2018; Eichelberger, 1980, Kahl et al., 2011). Erupted rocks could preserve in their texture the different evolutions experienced by the magma and can show both macroscopic evidence (banded pumice and host rocks with inclusions; Bacon, 1986; Clynne, 1999; Harford and Sparks, 2001; Mortazavi and Sparks, 2004; Murphy et al., 2000; Plail et al., 2018) and microscopic information (mineral textures and chemical zoning in minerals; Andersen et al., 2018; Berlo et al., 2007; Fabbro et al., 2017; Morgavi et al., 2013; Zellmer et al., 2003).

In this study are examined detailed mineralogical and compositional analyses of the crystal populations on some rock samples, with a special focus on investigating the chemical textural zoning patterns. This study aims to constrain the pre-eruptive conditions in the magma plumbing system and the time changes at three different volcanic areas. These areas are characterised by different magmatic processes and timescales between unrest and eruption. The three volcanoes investigated are Soufriere Hills Volcano at Montserrat Island (Lesser Antilles), Gede Volcano in West Java (Indonesia), and Waitomokia Volcano (New Zealand). Understanding the reasons behind the timescale diversity on the magmatic processes (from long -over decades-, to short-month/years-, to syneruptive -hours/days) is crucial in order to improve our knowledge volcanic hazards and associated risks (Albert et al., 2016, 2019; Berlo et al., 2007; Fabbro et al., 2017; Kahl et al., 2011, 2013, 2015; Plail et al., 2018; Ruth et al., 2018; Turner et al., 2004; Zellmer et al., 2003).

Figure 1: (a) Soufriere Hills Volcano, Montserrat Island (13 January 2017). Photo provided by Victoria Miller (Montserrat Volcano Observatory). (b) Overview of Auckland Volcanic Field in 1955 (Waitomokia Volcano indicated by arrow). Photo by Whites Aviation Ltd. (c) Gede Volcano, West Java, Indonesia. Photo by Heather Handley.

1.2. Volcanic plumbing system: magma pathway from the source to the surface

Our understanding of how magma reaches the surface has changed over the past century. The formation, storage and chemical differentiation of magma are the dominant processes extending over the volcanic plumbing system. In the past, the model of the magma plumbing system was quite simplified, with a magma chamber of spherical geometry and a melt injection from below (Daly, 1911). Subsequent geochemical and geophysical techniques, however, have revealed a more complex magmatic system, which the upper part in the shallow crust is the area of magma accumulation that is more likely modified by replenishment of new magma from greater depth (Berlo et al., 2007; Browne and Gardner, 2006; Zellmer et al., 2003). Such a complex system is characterised by magma interactions, that generates mingling and mixing processes (Laumonier et al., 2014), and are sometimes associated with crustal assimilation leading to the eruption (DePaolo, 1981a). These processes could also reach the lower crust (see, e.g., Annen et al., 2005), where initial fractionation and melt segregation start from a deep hot zone and propagates to the shallow crust (Fig. 2). Residual and crustal melts from different areas of a hot zone can also interact with others before the ascent.

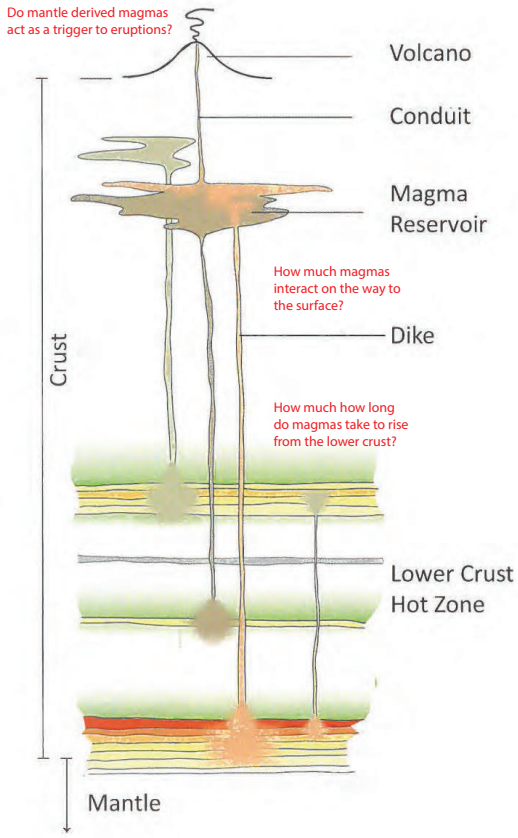

Figure 2: Magmatic system in which magma accumulates and evolves. Transport pathways may extend directly from the mantle to the surface, or magma may be stored in one or more reservoirs in the crust (modified from Annen et al., 2006).

Based on thermal, mechanical and dynamic principles a multiphase model was proposed for magma interactions, comprising crystal-melt-volatile components identified as 'mush'. This crystal-rich mush is dominated by the transfer of crystal and melt (Bachmann and Bergantz, 2008; Marsh, 1996), where new batches of magma replenish the system and interstitial melts are mobilised producing a magma reservoir (Bachmann and Bergantz, 2003; 2004).

The development of extensive and complex magma storage models was supported by Cashman et al. (2017), which suggest that melts can be produced in the deep crustal level, and transferred through the mid and upper levels (Fig. 3). The vertical extension of this magmatic complex is linked with the destabilisation of melt lenses that could amalgamate and form magma chamber, as proposed for the Soufrière Hills Volcano (Christopher et al., 2015). Melt that percolates upwards and reacts with crystals ('reactive melt flow') has a critical role in controlling storage, accumulation and differentiation in the mid-lower crustal reservoir (Solano et al., 2014).

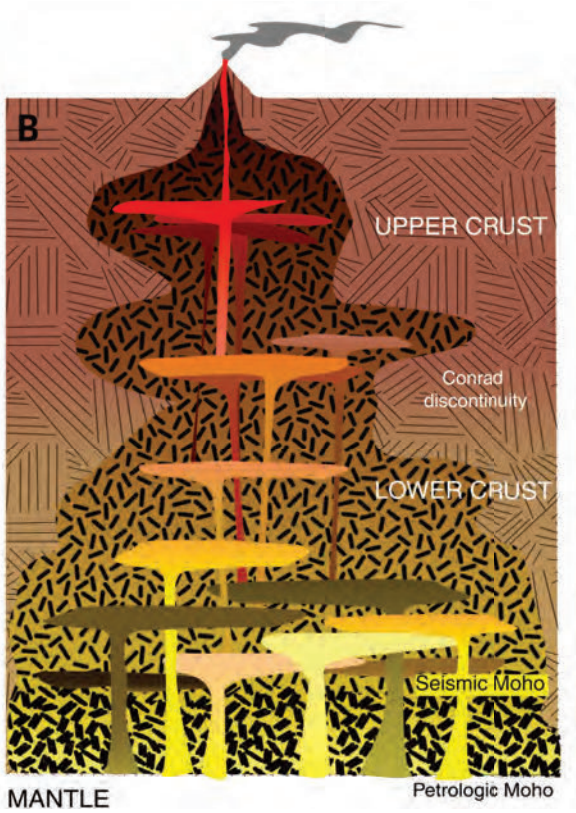

Figure 3: Transcrustal magmatic system proposed by Christopher et al. (2015) and Cashman et al. (2017), where the deep crust experiences processes producing melt lenses that are transferred to mid- and upper crustal levels. The vertical connectivity between lenses could destabilise the melt lenses.

The formation, storage and interaction of melts are influenced by the mechanical proprieties and behaviour of the crust, including the ability to deform, flow or fracture. The magma interaction with country rocks could incorporate S as sulfate or sulfite, generating immiscible sulfide liquid and producing the accumulation of Ni, Cu, Co, Au and platinum group elements PGEs (Barnes

and Robertson, 2019). All these proprieties evolve over the life cycle of the volcano. The several competing drivers that force magma to rise and to oppose movement are involved in what makes magma movements and eruptions so difficult to forecast (Melnik and Sparks, 2005), and strongly affect the style, intensity, magnitude and duration of volcanic eruptions (Acocella, 2014). The investigation of the mechanisms that magma experienced since its formation through its ascent to the surface can shed light on the trigger of volcanic eruptions.

1.3. Magmatic processes responsible for triggering volcanic eruptions

Many studies have been conducted on the triggering mechanisms of volcanic eruptions, based on physical and thermodynamic models and laboratory experiments. Regions where magma accumulates and stalls can control the eruption dynamics by developing accumulation of gas, overpressure and segregation of melt from crystals (Blundy and Cashman, 2008; Cashman et al., 2017; Edmonds and Woods, 2018; Pioli et al., 2009; Plail et al., 2018; Ruth et al., 2018; Sparks et al., 1977; Stock et al., 2016). These processes could be generated by an injection of new magma, triggered by the contrast in chemical and physical properties (e.g. temperature, pressure and composition) with mingling and mixing processes leading to the eruption (Anderson, 1976; Bachmann and Bergantz, 2006; Bacon and Barnes, 1978; Clynne, 1999; Degruyter et al., 2016; Eichelberger, 1980; Huber et al., 2010; Oldenburg et al., 1989; Reid and Vazquez, 2017; Scaillet et al., 2000; Sparks et al., 1977; Trial and Spera, 1990).

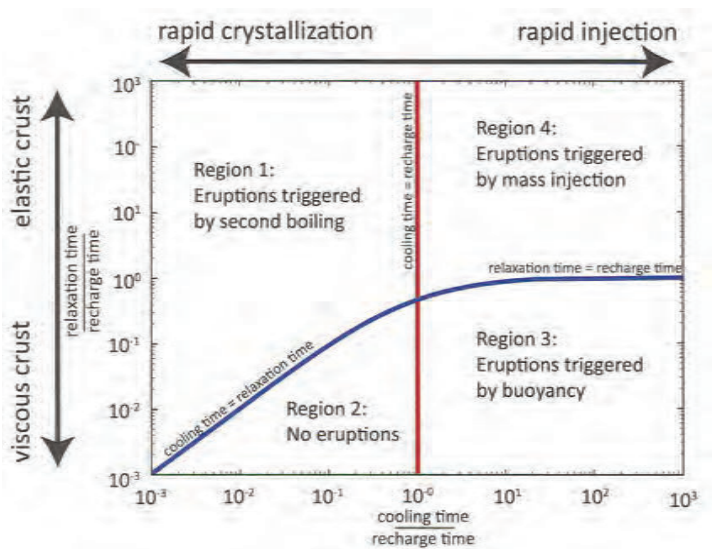

Figure 4: Conditions that control eruptions for an idealised magma reservoir. The horizontal axis is the ratio of heat supplied by new magma injection to the heat lost by conduction to the surrounding crust. The vertical axis is the ratio of the timescale for viscous relaxation of chamber overpressure compared to the timescales for recharge. Whether or how an eruption is triggered depends on the interplay of the rate of mass injection into the reservoir, the gas content of magma and the size of the reservoir (modified from Degruyter and Huber, 2014).

Recharge, magma mingling, and mixing events can be associated with crustal contamination (Andrews et al., 2008; Davidson et al., 2001b; TEPLEY III et al., 2000). However, the discrimination of the individual processes involved in the evolution of the magmatic system is still difficult, due to the complexity of the system and the simultaneity of several processes.

Degruyter et al. (2016) predicted in their idealized model, different triggering mechanisms, depending on the magma flux into the reservoir and on the behaviour of the surrounding crust. For instance, in Fig. 4 are represented the conditions that control eruptions for an idealised magma reservoir, as a function of the ratio between the heat supplied by a recharge input of new magma and the heat lost by conduction to the surrounding crust. This ratio is correlated with the ratio between the timescale for viscous relaxation of chamber overpressure and the timescale of recharge. The conditions that trigger an eruption depend on the interplay among the mass injection rate into the reservoir, the buoyancy, and the content of gas (which in turn is linked with the formation of bubbles driven by crystallization -second boiling), and the size of the reservoir (Edmonds and Woods, 2018). The interactions of volatile in the recently active volcanic system have also been investigated using short-lived Ra-Pb isotopes (Berlo and Turner, 2010; Turner et al., 2004). Unravelling nature and timescales of the processes that drive the eruptions will have a powerful impact on the forecast of future eruptions.

1.4. Understanding magmatic processes: linking mineral texture with chemical zoning in crystals

Erupted rocks exhibit various types of texture and assemblage of crystals, which record the unique experiences in the plumbing system before being erupted. Magmatic processes such as fractional crystallisation, magma mingling/mixing, assimilation and the transport from the source towards the surface are imprinted on the final texture of crystal population (Cashman, 1990; Costa and Chakraborty, 2004; Davidson et al., 2007a; Davidson et al., 2007b; Jerram and Martin, 2008; Martin et al., 2010; Turner et al., 2003; Wallace and Bergantz, 2002).

Crystals can crystallize directly from the melt (phenocrysts) or can be recycled from various environments (antecrysts), and often show compositional zoning patterns linked to changes in physical and chemical conditions of the melts (Berlo et al., 2007; Browne et al., 2006; Costa et al., 2013; Davidson et al., 2001a; Gill et al., 2006). Xenocrysts are foreign to the magma and have been incorporated during ascent; they frequently show new overgrowths or reaction rims as a consequence of the interaction with the magma (Jerram and Martin, 2008).

Although whole-rock analyses are commonly used in the study of magmatic processes,

the identification of crystal populations in terms of mineral texture (e.g. crystal, shape, pattern) provides a powerful tool to investigate magmatic processes. Micro XRF Tornado analyses and Backscattered Electron (BSE) images (using grey scales) show textures of individual crystals that can be combined with geochemical analyses, so revealing a rich history recorded prior to the eruption. For example, this approach has been used in plagioclase-oriented studies in Santorini (Fabbro et al., 2017; Flaherty et al., 2018) and Unzen (Browne and Gardner, 2006), and in olivine-oriented studies in Calbuco Volcano (Morgado et al., 2019) and the San Pedro Complex (Costa and Dungan, 2005).

The study here presented is focused both on small (Waitomokia Volcano) and large-scale volcanic systems (Soufrière Hills and Gede Volcanoes). In these three different systems, selected for their relevance on the society in case of eruptions, minerals such as olivine and plagioclase recorded a unique history of their pathway to the surface.

The re-equilibration of trace elements and their surrounding liquid is a powerful feature to understand magmatic processes that the whole-rock composition is not able to reveal. For the Waitomokia Volcano, olivine was used to track the crystal growth through the chemical re-equilibration of Mg-Fe between melt and crystal phases. For the Soufrière Hills Volcano, Mg re-equilibration in plagioclase was instead modelled, and the investigation provided to be relatively complex due to the dependence on anorthite composition and temperature of partitioning and diffusivity (Costa et al., 2003). Finally, for the Gede Volcano plagioclase was examined, in this case exploring the partition between Sr and Ba concentrations in the melt, and studying how the ratio Sr/Ba is correlated with the anorthite content in plagioclase from different populations.

1.5. Diffusion and Magmatic Timescales

One of the current topics for modern volcanology is the investigation of the timescales of the processes that lead to an eruption. Deciphering magmatic processes is complex, due to various timescales and dynamics involved in the formation of the final erupted rocks (Costa and Morgan, 2011). In the last decade, a routine approach based on the determination of the magmatic processes duration as recorded in the crystal cargo (Costa et al., 2008 and references therein). The goal of this approach is to model the diffusion of concentration gradients within a mineral to obtain both the duration of magma mixing (Andersen et al., 2018; Costa et al., 2013; Costa and Chakraborty, 2004) and magma residence time (Allan et al., 2013; Fabbro et al., 2017; Flaherty et al., 2018; Rubin et al., 2017), when possible combining seismic data (Albert et al., 2019; Albert et al., 2016; Kahl et al., 2011; Rae et al., 2016). This technique is a powerful tool, when to active volcanoes, can

assist with the interpretation of monitoring signals and improved forecasting of volcano behaviour (Kahl et al., 2011; Kahl et al., 2013; Kahl et al., 2015; Morgan et al., 2006).

An additional timescale approach is based on the relative of U-Th isotope in samples. This technique can be used to identify the relative age relationship between compositionally different magmas and to provide information on timescales less than 350 kyrs (Bourdon et al., 2003; Condomines et al., 2003).

1.6. Aims of this thesis and selection of case studies

The main aim of this thesis is to use chemical and textural zoning patterns recorded in volcanic rock minerals to determine the detailed dynamics of magmatic processes and the triggering events of volcanic eruptions. To this purpose three volcanoes have been selected as study target: Soufrière Hills Volcano in Montserrat Island, Gede in West Java (Indonesia) and Waitomokia in Auckland Volcanic Field (New Zealand).

Soufrière Hills Volcano is an explosive subduction zone volcano in the Caribbean, last erupted in 2010 after 15 years of volcanic activity, when the collapse of the eruptive column generated pyroclastic flows that destroyed the capital city of Plymouth. The volcano has been extensively monitored in recent decades, becoming a convenient natural laboratory for multidisciplinary analyses.

Gede volcano is a subduction zone volcano in West Java (Indonesia) located close to the densely populated capital city of Jakarta. Currently, records report only gas emissions and a few volcanic tremors, but this large volcanic complex is characterised by a history of pyroclastic flows and blocks and ash flows. This volcano lacks a detailed plagioclase investigation, which makes it particularly suitable for a study aiming at strengthening this fundamental for forecasting eruptions.

Waitomokia volcano is a small-volume basaltic volcano in the intraplate Auckland Volcanic Field of the North Island of New Zealand. In the contest of this thesis, it could represent the simplest scenario among the three case studies.

These three volcanoes have been selected not only based on their geological setting, but also their proximity to populated cities. The results of this study can improve the monitoring signal interpretation to better understand the relative times between unrest and future eruptions.

In particular, the objectives of this thesis are to:

1. Elucidate the timescales of mafic-silicic magma interactions at Soufrière Hills volcano, through modelling the diffusive re-equilibration of Mg in plagioclase;

2. Unravel the nature and dynamics of the magmatic system at Gede volcano;

3. Constrain the magma ascent dynamics involved in the formation of Waitomokia volcano through textural and compositional investigation of minerals;

4. Shed light on the level of complexity in sub-volcanic magmatic plumbing systems at different spatial and temporal scales, making use of detailed mineralogical studies

1.7. Outline of the thesis

This thesis is composed of six chapters, each written manuscript presentation requirements and therefore including a general introduction, a methodology section, a discussion, and its bibliography. The introductory chapter (this one) and the conclusive chapter (Chapter 6) connect the work done in this thesis and provide the general framework for the studies performed.

Chapter 2 show the textural and compositional study focused on plagioclase crystals produced at Soufrière Hills volcano (Montserrat). The aim is to investigate the magmatic interactions with an implemented model in Matlab code to estimate the residence time of the magma in the shallow reservoir prior to eruption. In this code, the diffusion of Mg in plagioclase is modelled taking into account the compositional dependence on anorthite content and temperature, and the diffusion equation is solved numerically by the finite difference method proposed by Costa et al. (2003).

Chapter 3 is dedicated to the investigation of the volcanic rocks produced at Gede Volcano. In order to clarify the relative importance of processes such as fractional crystallisation, crustal contamination, and/or magma mingling/mixing in triggering the eruptions, geochemical analyses and calculation of the partition coefficient of Sr and Ba between plagioclase and surrounding melt were performed.

Chapter 4 provide the detailed mineralogical characterisation of erupted materials at Waitomokia volcano, one of the many basaltic volcanic centres in Auckland Volcanic Field. This material combines textural and compositional features developed during the evolution of the monogenetic eruption.

Chapter 5 details a study of U-Th-Ra-Pb isotopes across the interface of two compositionally

different magmas at Soufrière Hills volcano, which elucidates the triggering mechanisms of eruptions. To this aim, two samples were investigated in detail, one of which is the rock studied in Chapter 2. This complement the above investigation at Soufrière Hills volcano.

Finally, Chapter 6 summarises this study and highlight the important new insights from the selected case studies.

1.8. Author contributions

This project is part of Australian Research Council Discovery Project (DP150100328) on the timescales of mixing and volatile transfer leading to volcanic eruptions at Soufrière Hills volcano (Montserrat) awarded to Assoc. Prof. Heather Handley, Prof. Simon Turner (both from Macquarie University) Prof. Mark Reagan (University of Iowa) and Prof. Jenni Barclay (University of East Anglia) in collaboration with Assoc. Prof. Fidel Costa (Earth Observatory of Singapore).

Chapter 2: The project, initially conceived by Heather Handley was developed by the author and Fidel Costa. The author was responsible for 100% of data collection and 90% of data processing, interpretation of results, implementation of the Matlab code and writing. Samples for the study were provided by Jenni Barclay. Proofreading of this chapter was conducted external to the supervisory panel.

Chapter 3: The project concept was initially conceived by Heather Handley and further developed by the author. The author is responsible for 70% of data collection and 95% of data analysis and writing. Heather Handley provided the samples studied.

Chapter 4: The project was conceived by Heather Handley. The author participated in one of the two field trips to the volcano and is responsible for 100% of data collection and 85% for data analysis and writing. Samples were collected by Rebecca Griffis, Heather Handley and the author.

Chapter 5: This project was conceived by Heather Handley and Simon Turner as part of the Australian Research Council Discovery Project on Soufrière Hills volcano (Montserrat). The author is responsible for 100% of the petrographic description of the samples, collection of mineralogical data (by micro-XRF Tornado) and electron microprobe analyses (EMPA). Samples were provided by Melissa Plail and the main author is Dr Lucy McGee (University of South Australia).

References

Acocella, V., 2014. Great challenges in volcanology: how does the volcano factory work? Frontiers in Earth Science, 2: 4.

Albert, H., Costa, F., Di Muro, A., Herrin, J., Métrich, N. and Deloule, E., 2019. Magma interactions, crystal mush formation, timescales, and unrest during caldera collapse and lateral eruption at ocean island basaltic volcanoes (Piton de la Fournaise, La Réunion). Earth and Planetary Science Letters, 515: 187-199.

Albert, H., Costa, F. and Martí, J., 2016. Years to weeks of seismic unrest and magmatic intrusions precede monogenetic eruptions. Geology, 44(3): 211-214.

Allan, A.S., Morgan, D.J., Wilson, C.J. and Millet, M.-A., 2013. From mush to eruption in centuries: assembly of the super-sized Oruanui magma body. Contributions to Mineralogy and Petrology, 166(1): 143-164.

Andersen, N.L., Singer, B.S., Costa, F., Fournelle, J., Herrin, J.S. and Fabbro, G.N., 2018. Petrochronologic perspective on rhyolite volcano unrest at Laguna del Maule, Chile. Earth and Planetary Science Letters, 493: 57-70.

Anderson, A.T., 1976. Magma Mixing - Petrological Process and Volcanological Tool. Journal of Volcanology and Geothermal Research, 1(1): 3-33.

Andrews, B.J., Gardner, J.E. and Housh, T.B., 2008. Repeated recharge, assimilation, and hybridization in magmas erupted from El Chichón as recorded by plagioclase and amphibole phenocrysts. Journal of Volcanology and Geothermal Research, 175(4): 415-426.

Bachmann, O. and Bergantz, G., 2008. The magma reservoirs that feed supereruptions. Elements, 4(1): 17-21.

Bachmann, O. and Bergantz, G.W., 2003. Rejuvenation of the Fish Canyon magma body: A window into the evolution of large-volume silicic magma systems. Geology, 31(9): 789-792.

Bachmann, O. and Bergantz, G.W., 2004. On the origin of crystal-poor rhyolites: extracted from batholithic crystal mushes. Journal of Petrology, 45(8): 1565-1582.

Bachmann, O. and Bergantz, G.W., 2006. Gas percolation in upper-crustal silicic crystal mushes as a mechanism for upward heat advection and rejuvenation of near-solidus magma bodies. Journal

of Volcanology and Geothermal Research, 149(1-2): 85-102.

Bacon, K.J. and Barnes, G.T., 1978. 2-Component Monolayers .4. Excess Enthalpies and Entropies of Mixing in Octadecanol-Docosyl Sulfate System. Journal of Colloid and Interface Science, 67(1): 70-77.

Barnes SJ, and Robertson JC (2019). Time scales and length scales in magma flow pathways and the origin of magmatic Ni-Cu-PGE ore deposits. Geosci Front 10:77-87 doi:10.1016/j.gsf.2018.02.006

Berlo, K., Blundy, J., Turner, S. and Hawkesworth, C., 2007. Textural and chemical variation in plagioclase phenocrysts from the 1980 eruptions of Mount St. Helens, USA. Contributions to Mineralogy and Petrology, 154(3): 291-308.

Berlo, K. and Turner, S., 2010. Pb-210-Ra-226 disequilibria in volcanic rocks. Earth and Planetary Science Letters, 296(3-4): 155-164.

Blundy, J. and Cashman, K., 2008. Petrologic reconstruction of magmatic system variables and processes. Reviews in Mineralogy and Geochemistry, 69(1): 179-239.

Bourdon, B., Turner, S., Henderson, G.M. and Lundstrom, C.C., 2003. Introduction to U-series geochemistry. Reviews in mineralogy and geochemistry, 52(1): 1-21.

Browne, B.L., Eichelberger, J.C., Patino, L.C., Vogel, T.A., Uto, K. and Hoshizumi, H., 2006. Magma mingling as indicated by texture and Sr/Ba ratios of plagioclase phenocrysts from Unzen volcano, SW Japan. Journal of Volcanology and Geothermal Research, 154(1-2): 103-116.

Browne, B.L. and Gardner, J.E., 2006. The influence of magma ascent path on the texture, mineralogy, and formation of hornblende reaction rims. Earth and Planetary Science Letters, 246(3-4): 161-176.

Cashman, K.V., 1990. Textural Constraints on the Kinetics of Crystallization of Igneous Rocks. Modern Methods of Igneous Petrology : Understanding Magmatic Processes, 24: 259-314.

Cashman, K.V., Sparks, R.S.J. and Blundy, J.D., 2017. Vertically extensive and unstable magmatic systems: a unified view of igneous processes. Science, 355(6331): eaag3055.

Christopher, T., Blundy, J., Cashman, K., Cole, P., Edmonds, M., Smith, P., Sparks, R. and Stinton, A., 2015. Crustal-scale degassing due to magma system destabilization and magma-gas decoupling

at Soufrière ills Volcano, Montserrat. Geochemistry, Geophysics, Geosystems, 16(9): 2797-2811.

Clynne, M.A., 1999. A complex magma mixing origin for rocks erupted in 1915, Lassen Peak, California. Journal of Petrology, 40(1): 105-132.

Condomines, M., Gauthier, P.-J. and Sigmarsson, O., 2003. Timescales of magma chamber processes and dating of young volcanic rocks. Reviews in Mineralogy and Geochemistry, 52(1): 125-174.

Costa, F., Andreastuti, S., de Maisonneuve, C.B. and Pallister, J.S., 2013. Petrological insights into the storage conditions, and magmatic processes that yielded the centennial 2010 Merapi explosive eruption. Journal of Volcanology and Geothermal Research, 261: 209-235.

Costa, F. and Chakraborty, S., 2004. Time scales of igneous differentiation obtained from diffusion modeling of compositional zoning in olivine. Geochimica Et Cosmochimica Acta, 68(11): A642-A642.

Costa, F., Chakraborty, S. and Dohmen, R., 2003. Diffusion coupling between trace and major elements and a model for calculation of magma residence times using plagioclase. Geochimica Et Cosmochimica Acta, 67(12): 2189-2200.

Costa, F., Dohmen, R. and Chakraborty, S., 2008. Time Scales of Magmatic Processes from Modeling the Zoning Patterns of Crystals. Minerals, Inclusions and Volcanic Processes, 69: 545-594.

Costa, F. and Dungan, M., 2005. Short time scales of magmatic assimilation from diffusion modeling of multiple elements in olivine. Geology, 33(10): 837-840.

Daly, R.A., 1911. The nature of volcanic action, Proceedings of the American Academy of Arts and Sciences. JSTOR, pp. 47-122.

Davidson, J., Tepley, F., Palacz, Z. and Meffan-Main, S., 2001a. Magma recharge, contamination and residence times revealed by in situ laser ablation isotopic analysis of feldspar in volcanic rocks. Earth and Planetary Science Letters, 184(2): 427-442.

Davidson, J., Tepley III, F., Palacz, Z. and Meffan-Main, S., 2001b. Magma recharge, contamination and residence times revealed by in situ laser ablation isotopic analysis of feldspar in volcanic rocks. Earth and Planetary Science Letters, 184(2): 427-442.

Davidson, J.P., Morgan, D.J. and Charlier, B.L.A., 2007a. Isotopic microsampling of magmatic rocks. Elements, 3(4): 253-259.

Davidson, J.P., Morgan, D.J., Charlier, B.L.A., Harlou, R. and Hora, J.M., 2007b. Microsampling and isotopic analysis of igneous rocks: Implications for the study of magmatic systems. Annual Review of Earth and Planetary Sciences, 35: 273-311.

Degruyter, W., Huber, C., Bachmann, O., Cooper, K.M. and Kent, A.J., 2016. Magma reservoir response to transient recharge events: The case of Santorini volcano (Greece). Geology, 44(1): 23-26.

DePaolo, D.J., 1981a. Trace element and isotopic effects of combined wallrock assimilation and fractional crystallization. Earth and planetary science letters, 53(2): 189-202.

DePaolo, D.J., 1981b. Trace-Element and Isotopic Effects of Combined Wallrock Assimilation and Fractional Crystallization. Earth and Planetary Science Letters, 53(2): 189-202.

Edmonds, M. and Woods, A.W., 2018. Exsolved volatiles in magma reservoirs. Journal of Volcanology and Geothermal Research.

Eichelberger, J.C., 1980. Vesiculation of Mafic Magma during Replenishment of Silicic Magma Reservoirs. Nature, 288(5790): 446-450.

Fabbro, G.N., Druitt, T.H. and Costa, F., 2017. Storage and Eruption of Silicic Magma across the Transition from Dominantly Effusive to Caldera-forming States at an Arc Volcano (Santorini, Greece). Journal of Petrology, 58(12): 2429-2464.

Flaherty, T., Druitt, T., Tuffen, H., Higgins, M.D., Costa, F. and Cadoux, A., 2018. Multiple timescale constraints for high-flux magma chamber assembly prior to the Late Bronze Age eruption of Santorini (Greece). Contributions to Mineralogy and Petrology, 173(9): 75.

Gill, J., Reagan, M., Tepley, F. and Malavassi, E., 2006. Arenal Volcano, Costa Rica: Magma genesis and volcanological processes - Introduction. Journal of Volcanology and Geothermal Research, 157(1-3): 1-8.

Harford, C.L. and Sparks, R.S.J., 2001. Recent remobilisation of shallow-level intrusions on Montserrat revealed by hydrogen isotope composition of amphiboles. Earth and Planetary Science Letters, 185(3-4): 285-297.

Huber, C., Bachmann, O. and Manga, M., 2010. Two competing effects of volatiles on heat transfer in crystal-rich magmas: thermal insulation vs defrosting. Journal of Petrology, 51(4): 847-867.

Jerram, D.A. and Martin, V.M., 2008. Understanding crystal populations and their significance through the magma plumbing system. Geological Society, London, Special Publications, 304(1): 133-148.

Kahl, M., Chakraborty, S., Costa, F. and Pompilio, M., 2011. Dynamic plumbing system beneath volcanoes revealed by kinetic modeling, and the connection to monitoring data: An example from Mt. Etna. Earth and Planetary Science Letters, 308(1-2): 11-22.

Kahl, M., Chakraborty, S., Costa, F., Pompilio, M., Liuzzo, M. and Viccaro, M., 2013. Compositionally zoned crystals and real-time degassing data reveal changes in magma transfer dynamics during the 2006 summit eruptive episodes of Mt. Etna. Bulletin of Volcanology, 75(2): 692.

Kahl, M., Chakraborty, S., Pompilio, M. and Costa, F., 2015. Constraints on the nature and evolution of the magma plumbing system of Mt. Etna Volcano (1991–2008) from a combined thermodynamic and kinetic modelling of the compositional record of minerals. Journal of Petrology, 56(10): 2025-2068.

Laumonier, M., Scaillet, B., Pichavant, M., Champallier, R., Andujar, J. and Arbaret, L., 2014. On the conditions of magma mixing and its bearing on andesite production in the crust. Nature communications, 5: 5607.

Marsh, B.D., 1996. Solidification fronts and magmatic evolution. Mineralogical Magazine, 60(398): 5-40.

Martin, V.M., Davidson, J., Morgan, D. and Jerram, D.A., 2010. Using the Sr isotope compositions of feldspars and glass to distinguish magma system components and dynamics. Geology, 38(6): 539-542.

Melnik, O. and Sparks, R., 2005. Controls on conduit magma flow dynamics during lava dome building eruptions. Journal of Geophysical Research: Solid Earth, 110(B2).

Morgado, E., Morgan, D., Harvey, J., Parada, M., Castruccio, A., Brahm, R., Gutierrez, F., Georgiev, B. and Hammond, S., 2019. Localised heating and magmatic intensive conditions prior to the 22-23 April 2015 Calbuco volcano eruption (Southern Chile). Bulletin of Volcanology.

Morgan, D., Blake, S., Rogers, N., De Vivo, B., Rolandi, G. and Davidson, J., 2006. Magma chamber recharge at Vesuvius in the century prior to the eruption of AD 79. Geology, 34(10): 845-848.

Morgavi, D., Perugini, D., De Campos, C.P., Ertl-Ingrisch, W., Lavallée, Y., Morgan, L. and Dingwell, D.B., 2013. Interactions between rhyolitic and basaltic melts unraveled by chaotic mixing experiments. Chemical Geology, 346: 199-212.

Mortazavi, M. and Sparks, R., 2004. Origin of rhyolite and rhyodacite lavas and associated mafic inclusions of Cape Akrotiri, Santorini: the role of wet basalt in generating calcalkaline silicic magmas. Contributions to Mineralogy and Petrology, 146(4): 397-413.

Oldenburg, C.M., Spera, F.J., Yuen, D.A. and Sewell, G., 1989. Dynamic Mixing in Magma Bodies - Theory, Simulations, and Implications. Journal of Geophysical Research-Solid Earth and Planets, 94(B7): 9215-9236.

Pioli, L., Azzopardi, B. and Cashman, K., 2009. Controls on the explosivity of scoria cone eruptions: Magma segregation at conduit junctions. Journal of Volcanology and Geothermal Research, 186(3-4): 407-415.

Plail, M., Edmonds, M., Woods, A.W., Barclay, J., Humphreys, M.C., Herd, R.A. and Christopher, T., 2018. Mafic enclaves record syn-eruptive basalt intrusion and mixing. Earth and Planetary Science Letters, 484: 30-40.

Rae, A.S., Edmonds, M., Maclennan, J., Morgan, D., Houghton, B., Hartley, M.E. and Sides, I., 2016. Time scales of magma transport and mixing at Kīlauea Volcano, Hawai'i. Geology, 44(6): 463-466.

Reid, M.R. and Vazquez, J.A., 2017. Fitful and protracted magma assembly leading to a giant eruption, Youngest Toba Tuff, Indonesia. Geochemistry, Geophysics, Geosystems, 18(1): 156-177.

Rubin, A.E., Cooper, K.M., Till, C.B., Kent, A.J., Costa, F., Bose, M., Gravley, D., Deering, C. and Cole, J., 2017. Rapid cooling and cold storage in a silicic magma reservoir recorded in individual crystals. Science, 356(6343): 1154-1156.

Ruth, D.C., Costa, F., de Maisonneuve, C.B., Franco, L., Cortés, J.A. and Calder, E.S., 2018. Crystal and melt inclusion timescales reveal the evolution of magma migration before eruption. Nature communications, 9(1): 2657.

Scaillet, B., Whittington, A., Martel, C., Pichavant, H. and Holtz, F., 2000. Phase equilibrium constraints on the viscosity of silicic magmas II: implications for mafic-silicic mixing processes. Transactions of the Royal Society of Edinburgh-Earth Sciences, 91: 61-72.

Solano, J., Jackson, M., Sparks, R. and Blundy, J., 2014. Evolution of major and trace element composition during melt migration through crystalline mush: implications for chemical differentiation in the crust. American Journal of Science, 314(5): 895-939.

Sparks, S.R.J., Sigurdsson, H. and Wilson, L., 1977. Magma Mixing - Mechanism for Triggering Acid Explosive Eruptions. Nature, 267(5609): 315-318.

Stock, M.J., Humphreys, M.C., Smith, V.C., Isaia, R. and Pyle, D.M., 2016. Late-stage volatile saturation as a potential trigger for explosive volcanic eruptions. Nature Geoscience, 9(3): 249.

TEPLEY III, F., Davidson, J., Tilling, R. and Arth, J.G., 2000. Magma mixing, recharge and eruption histories recorded in plagioclase phenocrysts from El Chichon Volcano, Mexico. Journal of Petrology, 41(9): 1397-1411.

Trial, A.F. and Spera, F.J., 1990. Mechanisms for the Generation of Compositional Heterogeneities in Magma Chambers. Geological Society of America Bulletin, 102(3): 353-367.

Turner, S., Black, S. and Berlo, K., 2004. Pb-210-Ra-226 and Ra-228-Th-232 systematics in young arc lavas: implications for magma degassing and ascent rates. Earth and Planetary Science Letters, 227(1-2): 1-16.

Turner, S., George, R., Jerram, D.A., Carpenter, N. and Hawkesworth, C., 2003. Case studies of plagioclase growth and residence times in island arc lavas from Tonga and the Lesser Antilles, and a model to reconcile discordant age information. Earth and Planetary Science Letters, 214(1-2): 279-294.

Wallace, G.S. and Bergantz, G.W., 2002. Wavelet-based correlation (WBC) of zoned crystal populations and magma mixing. Earth and Planetary Science Letters, 202(1): 133-145.

Zellmer, G.F., Sparks, R.S.J., Hawkesworth, C.J. and Wiedenbeck, M., 2003. Magma emplacement and remobilization timescales beneath Montserrat: Insights from Sr and Ba zonation in plagioclase phenocrysts. Journal of Petrology, 44(8): 1413-1431.

Chapter 2

Dynamics and timescales of mafic-silicic magma interactions at Soufrière Hills Volcano, Montserrat

Rosa Didonna[1], Fidel Costa [2,3], Heather Handley[1], Simon Turner[1], Jenni Barclay[4]

[1]*Department of Earth and Environmental Sciences, Macquarie University, Sydney, NSW, Australia*
[2]*Earth Observatory of Singapore, Nanyang Technological University, Singapore*
[3]*Asian School of the Environment, Nanyang Technological University, Singapore*
[4]*School of Environmental Science, University of East Anglia, Norwich, UK*

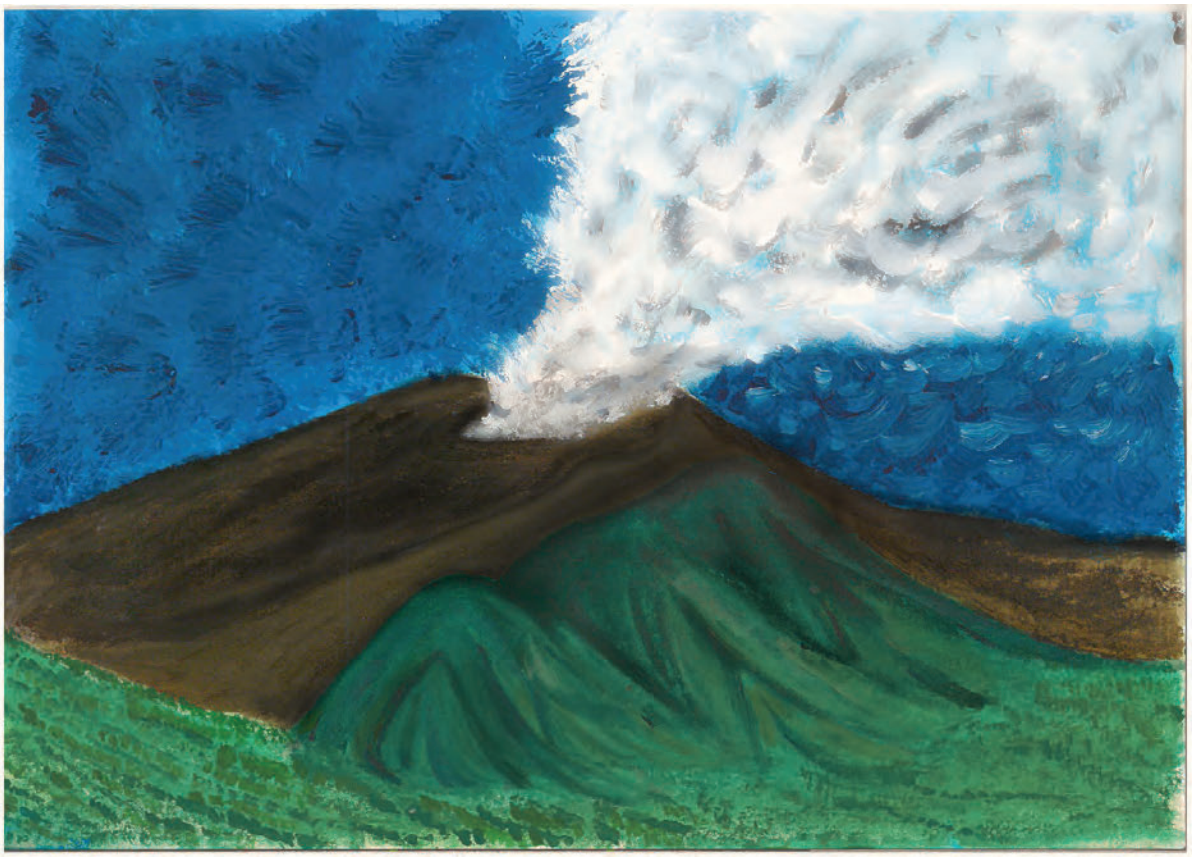

Soufriere Hills Volcano, Montserrat Island- Watercolours- Rosa,2017

Abstract

Mafic magma intrusions into silica-rich reservoirs are commonly proposed to drive andesitic eruptions of arc volcanoes. However, the mafic-silicic magma interactions are very complex, involving large gradients of physical and chemical properties that evolve over time, and, thus, the dynamics and timescales of such processes and how they may relate to eruption are still unclear. Here, we investigated the dynamics of magma mingling/mixing using chemical and textural zoning patterns recorded in plagioclase crystals from the last eruption (11th February 2010) at Soufrière Hills Volcano, Montserrat Island. This eruption is by now a classic example of interactions between two different magmas: an andesite that is the bulk of the erupted magma and basaltic andesite magma that occurs as enclaves of varying proportions during the course of the eruption. The textural characteristics of plagioclase were examined through backscattered electron images and detailed electron microprobe traverses. We find that many crystals are made of two well-defined zones that record the processes and timescales of mafic-silicic interaction: (1) an interior, often characterised by patchy, dusty and oscillatory zoning, and (2) an overgrowth zone (rim), of a different composition in anorthite content and Mg concentration than the core. We used anorthite and Mg concentrations to track the details of the magma mixing, and we modelled the timescales of such interactions via Mg re-equilibration in plagioclase. Results of few hours up to 2 months are reflecting syn-eruptive mixing that could be facilitating by the eruption itself. This study provides a useful support to interpret the monitoring signals and the relative timeframe between unrest and eruption that is characteristic of Soufrière Hills Volcano.

2.1. Introduction

Volcanic rocks erupted upon the Earth's surface reflect the variety of processes occurring in the plumbing system prior to eruption. Magma mingling and mixing processes between magmas characterised by different chemical and physical properties and by diverse volatile contents are recognised as commonly processes and have been proposed as key drivers for triggering eruptions (Bacon and Barnes, 1978; Clynne, 1999; Edmonds and Woods, 2018; Eichelberger, 1980; Oldenburg et al., 1989; Scaillet et al., 2000; Sparks et al., 1977; Trial and Spera, 1990). Such magma interactions are recorded in rocks both at the macroscopic level (such as quenched mafic inclusions; see, e.g., Barclay et al., 2010; Browne et al., 2006a; Clynne, 1999; Feeley and Dungan, 1996; Murphy et al., 1998; Pichavant et al., 2002; Plail et al., 2014), and at the microscopic level (in crystal textural and chemical zoning; see, e.g., Browne et al., 2006b; Costa et al., 2013; Costa and Chakraborty, 2004; Costa et al., 2008; Costa and Dungan, 2005; Kent et al., 2010; Longpre et al., 2014; Tomiya and Takahashi, 2005). However, there are still many unclear aspects about the complex and varied dynamics and timescales of such interactions, about their link with the eruption styles, and about their relationship with the evaluation of the volcano hazard.

Mineral textures and chemical zoning can be used to investigate magma recharge, interaction and assimilation in magma reservoirs (Davidson et al., 2007; Blundy and Cashman, 2008; Costa et al., 2008; Kahl et al., 2013; Singer et al., 2016; Streck, 2008). Crystal zoning patterns record changes of their environment, and therefore they may reveal the magma composition and its changes over time (Costa et al., 2008; Turner and Costa, 2007). Such timescales reveal important information about the magmatic processes that occur before (e.g., intrusion of new magma, mixing) or during the eruption (e.g., syn-eruptive processes) and can be correlated with various time series of geophysical and geochemical monitoring data (Costa et al., 2013; Kahl et al., 2011; Rae et al., 2016; Sparks et al., 1977).

In this study we focus on the deposits produced during the last eruption (11th February 2010) of Soufrière Hills Volcano (SHV), at Montserrat Island in the Lesser Antilles. This eruption contains widespread geological and petrological evidence of magma mingling/mixing between the host andesite (Fig. 1a; Barclay et al., 1998; Christopher et al., 2014; Couch et al., 2001; Devine et al., 1998; Humphreys et al., 2009; Murphy et al., 2000), and basaltic andesite enclaves (Fig. 1b; Barclay et al., 2010; Christopher et al., 2014; Mann, 2013; Murphy et al., 1998, 2000; Plail et al., 2013). Previous studies have used a range of approaches to estimate the duration of magma interactions at SHV. A short timescale of a few days to a few weeks was inferred for andesite erupted from 1995 to 2002 (Devine et al., 2003), based on the chemical zoning patterns of TiO_2 in

Figure1. Rock sample (MT35) from deposits of the dome collapse (11th February 2010). Host andesite (lighter grey region) and basaltic andesite enclave (darker grey region in the centre).

titanomagnetite crystals. These results were interpreted in the framework of a quick remobilization of a silicic magma that was heated prior to eruption (Devine et al., 1998; Devine and Rutherford, 2014). It is still not clear if the compositional zoning in titanomagnetite phenocrysts are linked only to the changes in temperature or also due to changes in fO_2. However, small changes in fO_2 occurred due to the magma being heated rather than to reduction processes by the invading basalt (Devine et al., 2003) interpreting the high TiO_2 contents of titanomagnetite rims due to the rise in the temperature of the host magma and not in fO_2 changes.

In contrast, Zellmer et al. (2003b) obtained the much longer timescales of 15-320 years for the same samples, based on the re-equilibration of Sr and Ba concentrations in plagioclase phenocrysts. Although these results appear to be contradictory, they may also simply reflect the complexity of a system that involves multiple magma injections over a range of timescales, ranging from reactivation of a crystal-rich system (long timescale) to the last event that leads to eruption (short timescale) (e.g., Turner and Costa, 2007). In this study, we look at plagioclase but we focus also on the features recorded by the changes of Ca/Na and Mg, which are a robust record of mafic and silicic melt interactions. Our timescale results support the interpretation of the monitoring data at SHV, which remain active despite it ceased to erupt new magma at the surface since 2010.

2.2. Geology and petrology of Soufrière Hills Volcano (1995-2010 eruption)

Soufrière Hills Volcano is an island arc volcano located in the southern part of Montserrat Island (Lesser Antilles; see Fig.2), formed by the westward subduction of the Atlantic crust beneath the Caribbean plate, happening at the rate of ~2 cm yr-1 (Minster and Jordan, 1978). Montserrat island

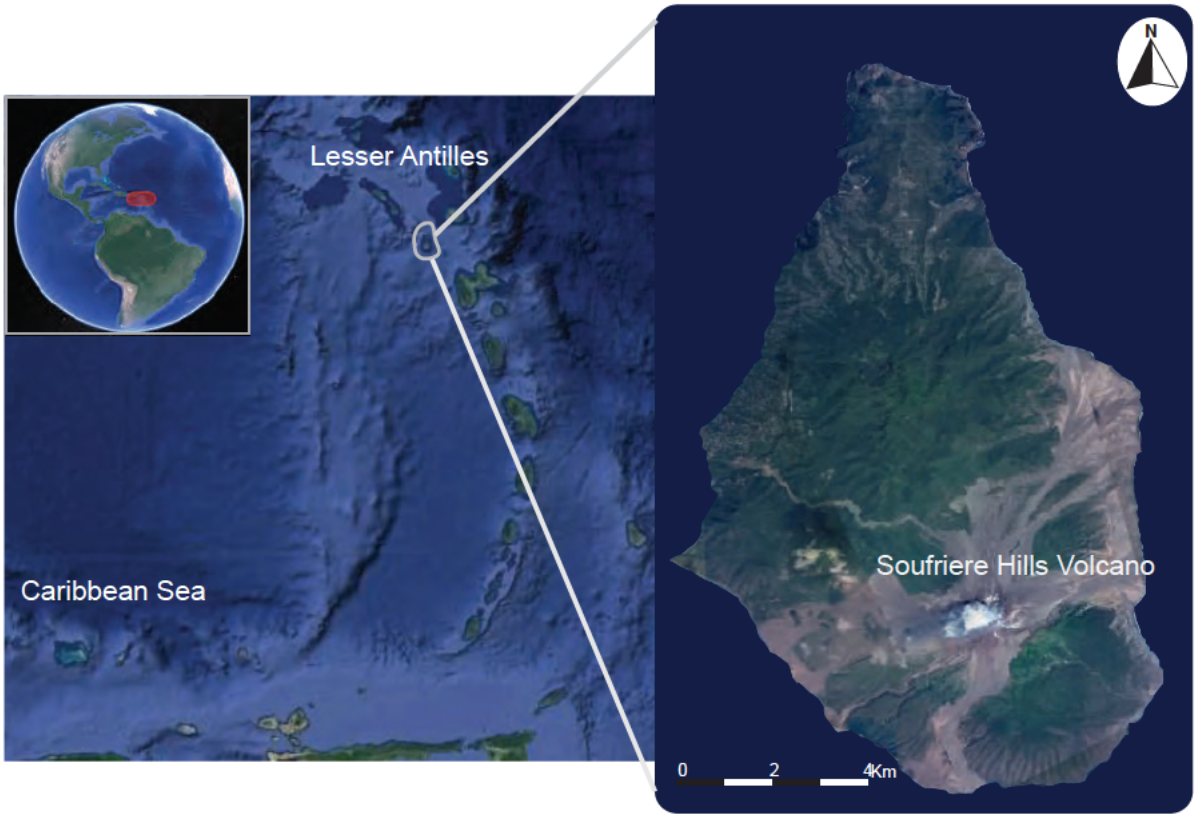

Figure 2. Soufrière Hills Volcano located in the Southern part of Montserrat Island, Lesser Antilles.

comprises four volcanic centres: Silver Hills (active in the period 2600-1200 ka ago), Centre Hills (950-550 ka ago), the SHV (282 ka to present) and the South Soufrière Hills volcano (131-128 ka ago) (Coussens et al., 2017; Harford et al., 2002). Andesitic lavas, with abundant mafic enclaves, are predominant in all of these volcanic centres, except South Soufrière Hills, which is the only basaltic volcano on the island (Cassidy et al., 2015).

In July 1995, after three years of intense seismicity focused at less than 7 km depth, SHV started to erupt (Aspinall et al., 1998; Young et al., 1998). The activity of the volcano in the period 1995-2010 is one of the best monitored in the world, and the island has become a natural laboratory for investigating magmatic processes and volcanic hazard mitigation. The 1995-2010 period of eruptive activity of SHV was characterised by episodic lava dome growth and collapse, often accompanied by vulcanian explosive events (Druitt and Kokelaar, 2002; Ryan et al., 2010; Sparks et al., 2000; Wadge et al., 2014). The eruption comprised five phases of extrusion (I-V), each separated by a hiatus of activity. Each phase is distinct in terms of the mass of andesitic lava erupted and of the volume of mafic enclaves. Between Phase III and Phases IV-V, the length of the eruptive phase decreased from years to months, and the average extrusion rate increased (Christopher et al., 2014; Wadge et al., 2014). Most erupted rocks are andesitic and contain ubiquitous sub-rounded mafic enclaves of several centimetres in diameter (Murphy et al., 2000; Murphy et al., 1998; Plail

et al., 2014). The SHV andesite is crystal-rich (30-40 vol.% phenocrysts), with limited changes in composition over time. It consists of plagioclase, hornblende, orthopyroxene, Fe-Ti oxides, minor quartz and rare zircon, in a groundmass of plagioclase, orthopyroxene, clinopyroxene, Fe-Ti oxides and rhyolitic interstitial glass (Barclay et al., 1998; Christopher et al., 2014; Couch et al., 2001; Devine et al., 1998; Humphreys et al., 2009; Murphy et al., 2000).

The proportion of mafic enclaves increased throughout the eruption, from ~1% volume of the erupted material in Phase I (1997), to approximately 5-7% volume in Phase IV (Barclay et al., 2010), and 3-8% vol. in Phase V (Barclay et al., 2010; Komorowski et al., 2010; Murphy et al., 2000; Plail et al., 2014). The mafic enclaves contain phenocrysts of plagioclase, amphibole, orthopyroxene, in a diktytaxitic groundmass of elongate plagioclase ± clinopyroxene ± high-Al-amphibole ± orthopyroxene ± Fe-Ti oxides. Some enclaves contain embayed quartz with rims of clinopyroxene and rare zircon (Humphreys et al., 2009; Murphy et al., 2000; Plail et al., 2014). Plail et al. (2014) classified the enclaves in three types (A, B, and C) defining different textural degrees of interaction between the andesite and the invading more mafic magma. Type A enclaves are the more basaltic ones, with a narrow range in composition and characterised by chilled margins, high-Al amphibole, and high vesicularity. Type B enclaves have a broader range in composition (basaltic andesite), lacks chilled margins, has low vesicularity, and high-Al amphibole is rare. Finally, type C enclaves are composite, with a mafic interior (Type A) and hybrid exterior (Type B) (Christopher et al., 2014; Plail et al., 2014).

2.2.1. Previous models of mafic-silicic magma interactions at SVH

A number of past studies led to a variety of conceptual models for the magma storage and interactions at SHV (Fig.3a). Zellmer et al. (2003a; b) proposed a model with repeated intrusion in the upper crust characterised by small volumes of andesitic magma, which then crystallised during degassing and cooling (Fig. 3a1). Influx of hotter and more mafic magma into the andesitic bodies led to their remobilisation and mixing via convective processes. Magma heating and remobilization were inferred by Sr and Ba zoning in plagioclase, and constrained the duration of crystal growth and residence time from 10 years to a few hundred years (Zellmer et al., 2003a; Zellmer et al., 2003b). Christopher et al. (2015) proposed a magmatic system lying below SHV made of vertical crustal-scale crystal-melt mush (Fig. 3a2). In this scenario, during unrest (without eruption), melt and fluid layers become unstable and start to amalgamate and mix. Eruption occurs when there is a major destabilisation of the mush system, with mixing between a wide range of magmas characterised by different depths, composition, and ages.

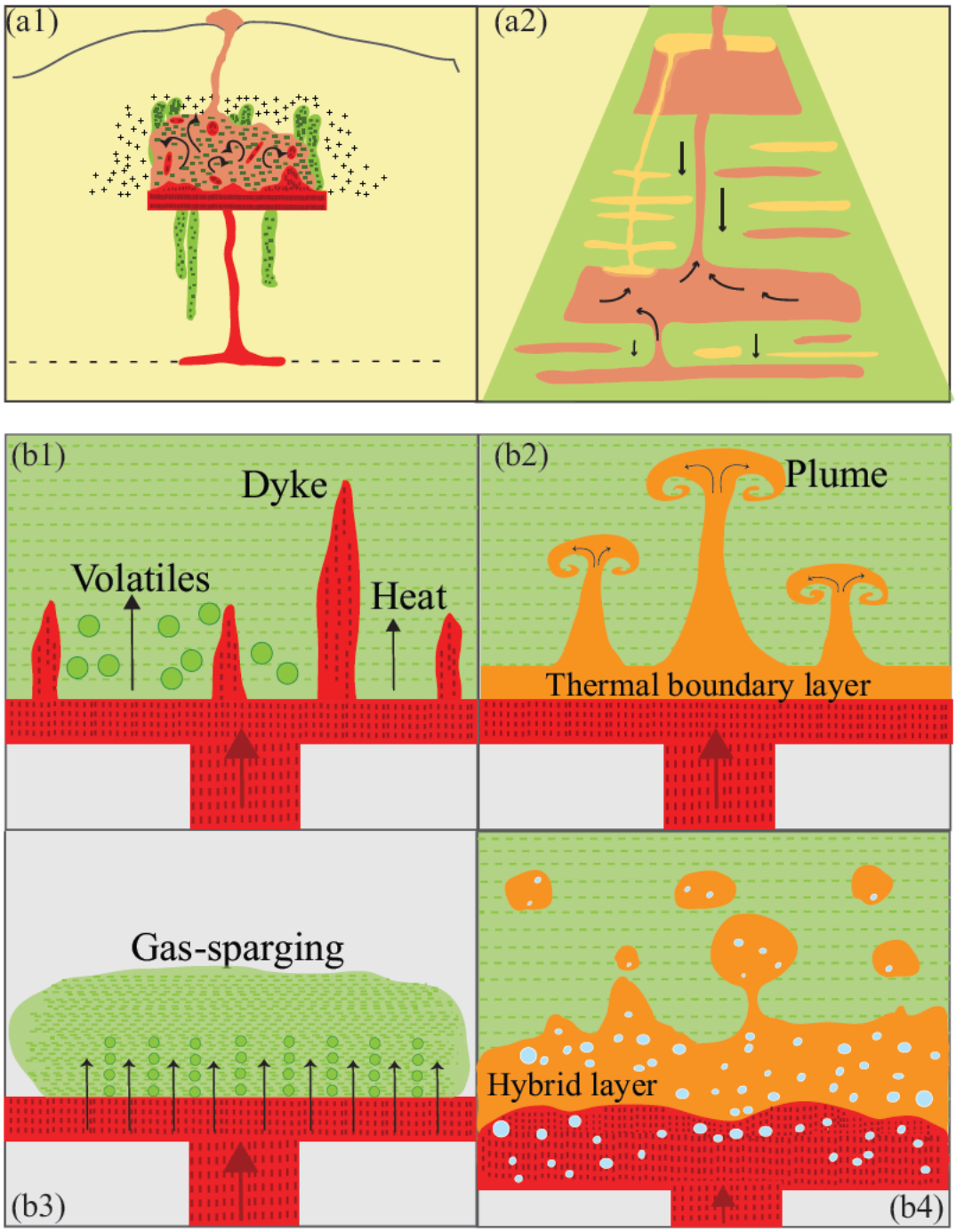

Figure3. (a) Schematic representation of the storage system at SVH, for the 1995-2010 eruption. (a1) Influx of hotter and more mafic magma into the andesitic bodies produced remobilisation and mixing between different compositional magmas producing convective processes (Zellmer et al. 2003a; Zellmer et al. 2003b). (a2) Vertical crustal magmatic mush, where melt and fluid layers become unstable during the periods of unrest (without eruption). The major destabilisation of the mush system triggered the eruption, with gases release and magma mixing characterising by different sources, composition and ages (Christopher et al. 2015). (b) Summary of previous models at the interface between engulfing magma and host. (b1) Model proposed by Murphy et al. (2000), where an intrusion of mafic magma (red) underplated the andesitic host magma (green). Thermal convection produce mixing that generated dikes of mafic magma into host andesite. (b2) In Couch et al. (2001), convective self-mixing produced convective plumes in a thermal boundary layer (orange) between mafic magma (red) and andesite (green). (b3) Bachmann and Bergantz (2006) proposed that the remobilization of andesitic magma resulted by 'gas-sparging' due to the migration upward of a hot fluid volatile phase from the mafic magma (red) to the volatile-saturated silicic magma (green). (b4) Detailed explanation of enclave formation illustrated by Plail et al. (2010, 2018), where the enclaves are the result of a hybrid layer (orange) between the mafic magma (red) and andesitic host magma (green).

Other studies focused on the more detailed mechanism of interactions at the interface between an intruding mafic magma and the andesitic host (Fig. 3b). Murphy et al. (2000) proposed that intrusion of hotter and mafic magma below andesitic magma led to thermal convection, to mixing of crystals from different parts of the resident magma, and to fragmentation of the intruding mafic dikes, which resulted in the mafic enclaves (Fig. 3b1). The remobilisation of the andesite magma occurred due to convective self-mixing, driven by thermal conduction from the lower to the upper part of the reservoir, developing convective plumes (Fig. 3b2; Couch et al., 2001). In other models, andesite remobilization requires mafic magma intrusion but also 'gas sparging' (Fig. 3b3), which includes the upward migration of a hot fluid (volatile) phase from the mafic magma to the volatile-saturated silicic mush, crossing the interface by infiltration or through small clusters of bubbles (Bachmann and Bergantz, 2006). Finally, the increases in volume and size (up to 80 cm) of ther mafic enclaves during the last phase of eruption (Phase V, Barclay et al., 2010; Plail et al., 2014) has been interpreted as the result of a more extensively developed boundary layer between the andesite and the basalt that developed since the beginning of the eruption (Fig. 3b4; Plail et al., 2018).

2.3. Sample details and analytical techniques

In this study, we focused on a Type A enclave hosted in andesite (sample MT35) collected from deposits of the dome collapse that took place on 11th February 2010 (Phase V), as reported in Plail (2013). The bulk-rock andesite has 60.5 wt.% SiO_2 and 2.6 wt.% MgO. The mafic enclave is a basaltic andesite with 52 wt.% SiO_2 and 4.8 wt.% MgO (Fig. 4; Plail, 2013), therefore lying in the middle of the compositional range for the enclaves typical of SHV (49-56 wt.% SiO_2 and 3.5-5.5 wt.% MgO).

Ten polished and thin sections of sample MT35 [MT1 (a, b, c, d), MT2 (e, f, g), and MT3 (h, l, m)] were investigated using a variety of methods. Optical microscope analyses were conducted as a preliminary investigation into the mineral assemblages in the host andesite and enclave. Approximately 80 backscattered electron (BSE) images of orthopyroxene (56) and plagioclase (24) were obtained using a Zeiss EVO MA15 scanning electron microscope with accelerating voltage of 15 kV at Macquarie University (Sydney, Australia). Brightness and contrast were varied to accentuate the textures. A large resolution (5256 × 12236 pixels) backscattered electron image of section MT2e was acquired using a Field Emission Scanning Electron Microscope (JSM-7800F) at Nanyang Technological University (NTU), Singapore. A super hybrid lens (SHL) provided extreme resolution of 0.8 nm at 15 kV.

Quantitative analyses of minerals and glass were done using an electron microprobe (JEOL 8230/8530) at Nanyang Technological University (NTU), Singapore. The operating conditions for plagioclase were an accelerating voltage of 15 kV and a beam current of 10 nA for Si, Al, Ca, Na, K, Fe (ka), and 80 nA for P, Mg, Ti, Mn (ka). For pyroxene, the same elements were measured, but the beam current was set to 20 nA. The standards used were Plagioclase (Astimex block) for Al ka and Ca ka, Apatite for P ka, Albite for Na ka and Si ka, Rutile for Ti ka, Specularite for Fe ka and Orthoclase. The counting times were set to 10 seconds for Na, 20 seconds for Al and Si, 30 seconds for Ca, 40 seconds for K, Fe and Mn, and 80 seconds for Mg, Ti and P (ka). High-resolution profiles of approximately 1 micrometer (μm) spacing were obtained across compositional gradients in plagioclase and pyroxene as identified in greyscale changes in the BSE images.

Detailed analyses of plagioclase were obtained of section MT2e, which was selected as representative of the different plagioclase textures. In total, 21 plagioclase crystals were measured: 12 from the andesite (approximately 1000 data points) and 9 from the enclave (approximately 800 data points). Electron microprobe traverses were obtained perpendicular to one of crystal margins or composition gradients, and distant from other margins (corners of the crystals) to avoid artefacts of diffusion along multiple dimensions or skewed length of the gradient (e.g., Costa et al., 2003; Costa et al., 2008).

Mineral symbols and members are used in the following manner: Anorthite content [%An =100 × molar Ca/(Na+Ca+K)], Magnesium (Mg)-number [Mg# =100 × molar Mg/(Mg+Fe*); where Fe* = is total iron], while end-members of pyroxene were calculated according to Deer et al. (1992).

2.4. Modelling approach and parameters used for calculating melt compositions and timescales

A main objective of this study was to determine the magmatic processes and timescales recorded in the crystals prior to, during and after the quenching in the host andesite. This is not a straightforward problem due to the significant temporal changes in temperature and composition at the boundary of the crystals, and it requires the use of crystal-melt partition relationships and of the modelling of the diffusive equilibration of elements. Initially, orthopyroxene crystals were studied for modelling the Mg/Fe gradients. However, given the rarity of the orthopyroxene crystals in the studied samples (e.g., only a few strongly zoned), we re-focused our attention on plagioclase phenocrysts. Diffusion timescales were determinated using an original matlab code based on equation (7) from Costa et al. (2003). The re-equilibration of Mg in plagioclase is relatively complex due to the

dependence of the partitioning and diffusivity by anorthite composition and temperature (Costa et al., 2003). The following paragraphs describe step by step the modelling approach, including the computation of the Magnesium partition coefficient, the used range of temperatures, the diffusion coefficients used in the numerical modelling and their relative uncertainties. In the modelling, the multidimensional effect of diffusive flux in different directions of the plagioclase crystals were not considered.

2.4.1. Partition coefficient and melt equivalent of magnesium (Mg)

Experimental partition coefficients between plagioclase and melt have been obtained using a variety of temperatures, pressures and/or melt compositions (Bindeman et al., 1998; Blundy and Wood, 1991; Dohmen and Blundy, 2014; Putirka, 2005). The partition coefficient (K) of a trace element i can be defined by the equilibrium partitioning of trace elements between crystal (plag; C_i^{plag}) and melt (liq; C_i^{liq}):

$$K_i^{\mathrm{plag/liq}} = \frac{C_i^{\mathrm{plag}}}{C_i^{\mathrm{liq}}} \tag{1}$$

Here, we calculated the Mg compositions in equilibrium with plagioclase using equation (2) given by Bindeman et al. (1998), which is dependent on An content and temperature. However, the equation proposed by Bindeman et al. (1998) has been obtained for a range in An content ($An_{40\text{-}80}$) comparable to those in our samples:, which justify the use of equation (2):

$$K = \exp\left(\frac{AX_{\mathrm{An}} + B}{RT}\right) \tag{2}$$

where A and B are empirical coefficients, X_{An} is the An molar fraction, R is the molar gas constant and T is the temperature (in Kelvin). The concentrations of Mg in plagioclase (C_i^{plag}) were obtained from EMPA detailed analyses, and then we calculated the equivalent melt (C_i^{liq}), which strongly depends on the temperature assumed. The 'equivalent melt' refers to the composition of the melt that the crystal grew or equilibrated with, and follows the proposition by Fabbro et al. (2017).

2.4.2. Temperature

Previous estimates of SHV magma temperature (see Table 1; Barclay et al., 1998, Christopher et al., 2014; Devine and Rutherford, 2014; Humphreys et al., 2009; Murphy et al., 2000; Plail, 2013) indicate 850 °C for the andesite host, but we investigated the effects of temperature variation on the enclave from 850 to 1100 °C for both melt composition calculations and diffusion models. The calculated melt Mg in equilibrium with plagioclase was compared with published bulk-rock data, melt inclusions and glass composition (Table 2) for the same eruption (Phase IV-V) and for the same rock (MT35) analysed in this work (Fig. 4).

Table 1. Summary of temperature estimated for host (andesite) and enclave (basaltic andesite) since the eruption started in 1995 until the last eruption in 2010. References from literature and methods adopted for gained the temperature are also reported.

Temperature	
Host	Enclave
$820-840$ (1)	$1020-1050(2)^{\star}$
$851 \pm 20(2)^{\star}$	$1074-1196(6)^{\wedge}$
$1100^{\star\star}$	1000 (6)*
$834-850$ (3)***	1070 (6)**
$820-840$ (4)***	$809-947$ (6)$^{\wedge\wedge\wedge}$
840 ± 7 (5)***	$907-1016$ (7)$^{\wedge\wedge}$
$903-1142$ (6)$^{\wedge}$	$1074-1196$ (8)$^{\wedge}$
$800-900$ (6)*	$903-1305$ (8)**
1000 (6)**	$1097-1154$ (8)$^{\sim}$
$791-809$ (6)***	
844 (6)$^{\wedge\wedge\wedge}$	
$824-965$ (8)*	
1018 (8)**	
920 (8)$^{\wedge\wedge}$	
833 (8)$^{\wedge\wedge\wedge}$	

(1) Barclay et al., 1998 (Method: Experiments)
(2) Murphy et al, 1998, 2000 (Method: *Opx phenocrysts core; **Opx reversed zoned rim)
(3) Devine et al., 1998a (Method: ***Oxides thermometry)
(4) Devine et al., 2003
(5) Devine and Rutherford, 2014
(6) Humphreys et al., 2009 (Method: ^ Two-pyroxene from Anderson et al., 1993)
(7) Plail, 2013 (PhD thesis, Method: ^^ Plag-melt equilibria from Putirka 2008)
(8) Christopher et al., 2014 (^^^ Horneblende-plagioclase equilibria from Holland&Blundy1994; ~ Cpxmelt)

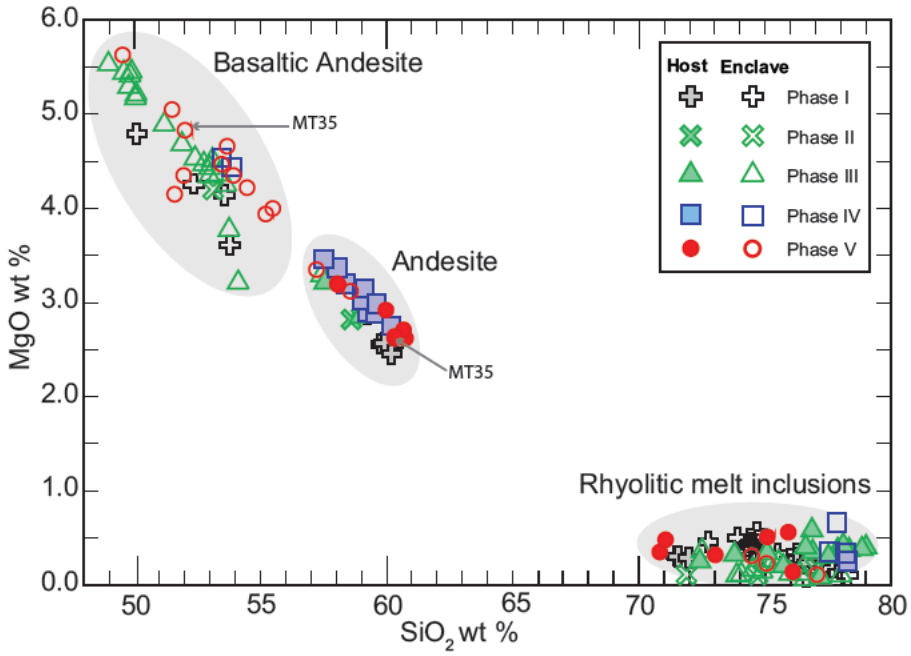

Figure 4. Comparison of MgO vs SiO_2 in andesite (host rock) and basaltic andesite (enclave) between the five phases of extrusive activity (from 1995 to 2010). Closed symbols represent andesite and open symbols are basaltic andesite. Phase I (Barclay et al., 1998; Christopher et al., 2014; Devine and Rutherford, 2014; Zellmer et al., 2003; Mann, 2010); Phase II (Christopher et al., 2014; Humphreys et al., 2010; Mann, 2010); Phase III and IV (Christopher et al., 2014; Humphreys et al., 2010; Plail, 2013), and Phase V (Christopher et al., 2014; Devine and Rutherford, 2014; Plail, 2013). MT35 are the host and enclave compositions that we have studied.

These comparisons provided additional support for estimating the various temperatures. We acknowledge the complexity of the mafic-silicic magma interactions: the host can be reheated, and the enclave cooled down between incorporation and quenching with the host (Barclay et al., 1998; Christopher et al, 2014; Couch et al., 2001; Devine et al., 1998; Humphreys et al., 2009; Plail, 2013; Plail et al., 2014, 2018).

Table 2. MgO composition content in rocks erupted during the last eruption in February 2010. Values were calculated from previous authors though bulk rock analyses and melt inclusions.

MgO wt% compositions			
Host		Enclave	
Bulk rock(1)	Melt inclusions(2)(3)	Bulk rock(1)	Melt inclusions(1)
2.62	0.14	4.15	0.23
2.92	0.32	4.83 (MT35 rock)	0.11
3.19	0.35	5.05	0.31
2.71	0.48	4.35	
2.64	0.51	5.63	

(1) Plail, 2013 (PhD thesis)
(2) Christopher et al., 2014
(3) Devine and Rutherford, 2014

2.4.3. Diffusion coefficient of Mg in plagioclase

Diffusion timescales were investigated using plagioclase in the host andesite and enclave. Given the slow diffusivity of An (Grove et al., 1984), in order to provide well-defined initial conditions, we focused on phenocryst with large and abrupt changes in An content. We selected Mg as element representative for the mafic component of the system and for which the An-dependent diffusion coefficients have been experimentally determined by Van Orman et al. (2014). The experiments cover the largest range of plagioclase composition (between An_{23} and An_{93}), and the range of temperature includes those for SHV andesite and basaltic andesite (800 and 1150 °C):

$$D_{\mathrm{Mg}}^{\mathrm{plag}} = \exp\left[(-6.06 \pm 1.10) - (7.96 \pm 0.42)\, X_{\mathrm{An}} - \frac{287000 \pm 10000}{RT}\right] \tag{3}$$

where D^{plag}_{Mg} is espressed in $m^2\ s^{-1}$ while T, R, and X_{An} have the same units as equation (2).

2.4.4. Numerical modelling

Mg-diffusion modelling was carried out in one dimension using equation (7) from Costa et al. (2003), and solved numerically by a finite difference method. A similar approach has been applied to other volcanic systems (Druitt et al., 2012; Fabbro et al., 2017; Flaherty et al., 2018). Changes in Mg composition in plagioclase (C_{Mg}) were calculated using equation (6) in Costa et al. (2003):

$$\frac{\partial C_{\mathrm{Mg}}}{\partial t} = \frac{\partial}{\partial x}\left(D_{\mathrm{Mg}}\frac{\partial C_{\mathrm{Mg}}}{\partial x} - D_{\mathrm{Mg}} C_{\mathrm{Mg}} \frac{A}{RT}\frac{\partial X_{\mathrm{An}}}{\partial x}\right) \tag{4}$$

where D_{Mg} is the diffusion coefficient of Mg in plagioclase and A is the parameter that represents the variation of the partition coefficient of Mg with An as in equation (2) above.

Equation (4) is expanded as:

$$\frac{\partial C_{\mathrm{Mg}}}{\partial t} = D_{\mathrm{Mg}}\frac{\partial^2 C_{\mathrm{Mg}}}{\partial x^2} + \frac{\partial C_{\mathrm{Mg}}}{\partial x}\frac{\partial D_{\mathrm{Mg}}}{\partial x} - \frac{A}{RT}\left(D_{\mathrm{Mg}}\frac{\partial C_{\mathrm{Mg}}}{\partial x}\frac{\partial X_{\mathrm{An}}}{\partial x} + C_{\mathrm{Mg}}\frac{\partial D_{\mathrm{Mg}}}{\partial x}\frac{\partial X_{\mathrm{An}}}{\partial x} + D_{\mathrm{Mg}} C_{\mathrm{Mg}}\frac{\partial^2 X_{\mathrm{An}}}{\partial x^2}\right) \tag{5}$$

and solved with a finite difference method as:

$$\frac{C_{i,j+1}-C_{i,j}}{\Delta t} = D_{i,j}\frac{C_{i+1,j}-2C_{i,j}+C_{i-1,j}}{\Delta x^2} + \frac{(C_{i+1,j}-C_{i,j})(D_{i+1,j}-D_{i,j})}{\Delta x^2} - \frac{A}{RT}\left(D_{i,j}\frac{(C_{i+1,j}-C_{i,j})(X_{\mathrm{An}i+1,j}-X_{\mathrm{An}i,j})}{\Delta x^2} + C_{i,j}\frac{(D_{i+1,j}-D_{i,j})(X_{\mathrm{An}i+1,j}-X_{\mathrm{An}i,j})}{\Delta x^2} + D_{i,j}C_{i,j}\frac{(X_{\mathrm{An}i+1,j}-2X_{\mathrm{An}i,j}+X_{\mathrm{An}i-1,j})}{\Delta x^2}\right) \quad (6)$$

where i and j describe the discrete spatial and temporal steps, respectively. Δx is the distance step and Δt the time step for each iteration,

A step function was used for the initial conditions, and at the edge of the crystal it has been considered an open boundary. The step function represents a large and sharp An jumps in the modelled crystals, while the open boundary at the rim implies that the crystal can re-equilibrate with a liquid phase that may change composition over time during the mafic-silicic interaction, and allows the occurrence of crystallisation processes of the matrix during quenching of the enclaves. We assumed that the crystal margin is in equilibrium with the surrounding melt.

The best match of the model with the measured data was determined visually. Depending on the shapes of the profiles, we used one- or two-stage models (e.g., Druitt et al., 2012). One-stage models were first used for all plagioclase profiles, where the growth of the crystal was assumed instantaneous without diffusion, followed by the re-equilibration with the melt. Two-stage models were performed to obtain a better fit of some profiles and provided two times, the first one related to the interior part of the crystal and the second one to the crystal as a whole. Such two-step models aim at accounting for the possibility that diffusion and re-equilibration between the crystal interior and the surrounding melt occurred before the crystal grew its rim, as it has been found in other systems (e.g., Santorini; see Druitt et al., 2012; Fabbro et al., 2017).

2.5. Mineral assemblages, textures, and compositions

The MT35 andesite sample is crystal-rich (35-40 vol.% phenocrysts) with a mineral assemblage of plagioclase, amphibole (Amph), orthopyroxene (Opx), Fe-Ti oxides and minor quartz (Qtz). The groundmass is dominated by plagioclase with a wide range of sizes that give a seriate texture to the sample. The groundmass contains microlites of Opx, clinopyroxene (Cpx), Fe-Ti oxides and glass,

with almost no vesicles. Plagioclase is the most abundant mineral and displays a variety of textures and zoning patterns, described in detail below. Single Opx phenocrysts (crystals > 300 μm) are unzoned or have a thin rim (< 10 μm) of Cpx. Amph is unreacted or may contain inclusions of plagioclase and oxides. Qtz has reaction rims of Cpx and magnetite; apatite and rare zircon are also present (Fig 5a).

In the sample MT35, a basaltic andesite enclave (Fig. 5b), many minerals contain a variety of reaction textures that results more developed than in the host (see below), and plagioclase appears to be the most abundant mineral. Phenocrysts of Opx occur as single isolated grains or as glomerocrysts (up to 8 mm), with reaction rims of Cpx, and can be unzoned or reversely zoned (i.e., higher Mg/Fe in rims than in cores). Reacted large Amph, Qtz and Fe-Ti oxides are in lower abundance. Amph (up to 5 mm in size) show reaction rims of Cpx, plagioclase, oxides and/or glass. Phenocrysts of Qtz, with or without reaction rims of Cpx (up to 2 mm in size), are also present. Magnetite is much more abundant than ilmenite, and can be found with a rim of it. Accessory minerals are apatite and rare zircon. The groundmass of the enclave contains euhedral thin laths of plagioclase, amphibole, and pyroxenes as well as vesicles that are bounded by crystal margins, indicative of fast quenching (Fig. 5b).

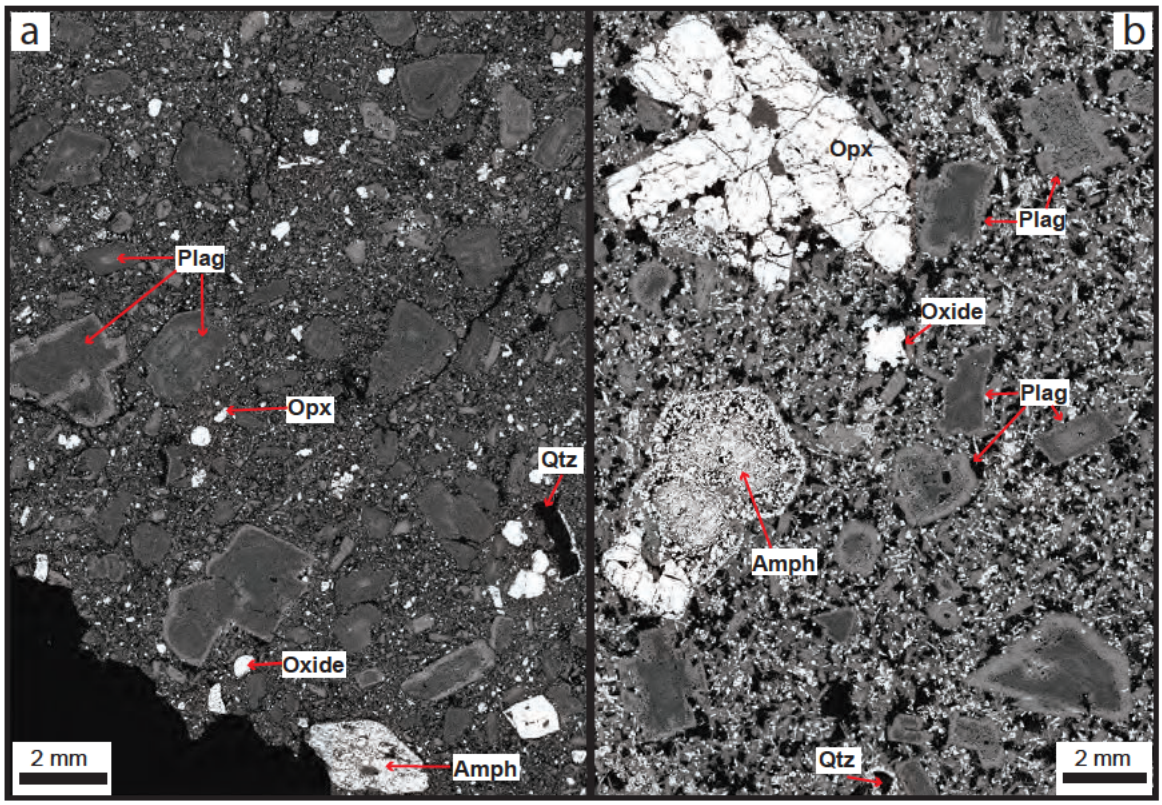

Figure 5. Backscattered electron (BSE) image of a whole thin section 'MT2E' (Phase V, Soufrière Hills Volcano). Clear evidence of interaction between two different magmas: a) andesite and b) basaltic andesite inclusion in the host magmatic andesite.

These assemblage and texture of this minerals are virtually identical to those reported for other SHV enclaves (e.g., Christopher et al., 2015; Plail et al., 2014). Further petrographic and mineralogical details on the SHV andesite can be found in Christopher et al. (2014), Couch et al. (2001), Devine et al. (1998), Humphreys et al. (2009, 2010) and Murphy et al. (1998, 2000), while for the enclaves see Plail et al. (2014) and Mann (2010).

2.5.1. Plagioclase textures and zoning patterns

Plagioclase occurs as phenocrysts (up to ~ 4 mm in size), microphenocrysts (100-300 μm), and microlites (< 100 μm), and exhibits a wide range of textures and compositions in the andesitic host and basaltic andesite enclave (Fig. 5). BSE images (Appendix A3) show that many of the phenocrysts in the enclave and in the host have two well-defined zones: an interior one, often characterised by patchy, dusty and oscillatory zoning; and an overgrowth zone (rim) of a different composition. Some crystals contain an intermediate sieve-textured zone with abundant melt inclusions between the interior and overgrowth zones. The sieve-textured crystals are less abundant in the andesite than in the enclave.

Electron microprobe traverses, from the rim towards the interior of the plagioclase, revealed a wide variation in An contents from approximately 45 to 90 mol%. The EMPA traverses were aimed at characterising the compositional boundary between rim and interior zones, as they highlighted from greyscale changes in the BSE images. A large part of the crystal cores was excluded from analysis due to their patchy, sieve-textured, mineral- and melt-included nature. Traverses across areas with pronounced sieve texture were avoided as these areas are typically a mixture of plagioclase plus other minerals and melt inclusions, which makes it difficult to analyse. For this reason, most of the observations on the different type of textures are based on the BSE images. Combining the BSE images and microprobe traverses allowed us to categorize the plagioclase into two main types.

Type I crystalswere mainly found in the andesite host (~75 vol.%; 10 vol.% in the enclave), tend to be euhedral and show variations in An content from 45 up to 70 mol% (Fig. 6). However, most are characterised by concentration between 45-55 mol% An, are reversely zoned (higher An in the rims than the core), and their interior part with patchy zoning.

Type II crystals have anhedral and sub-rounded interiors (An_{50} to An_{70}) that resemble the Type I crystals. Their interiors are surrounded by largely euhedral Ca-rich overgrowths (An_{75} to An_{90}), and overall, theses crystals display therefore a strong reverse zoning. The transition between the interior and the overgrowth zone is abrupt, typically occurring in < 5 μm. We have further

distinguished between Type IIa crystals, typically lacking a well-defined sieve-textured zone between interior and overgrowth and characterised by a narrow Ca-rich rims (< 20 μm), and Type IIb crystals, defined by a well-developed sieved-textured zone with abundant melt and mineral inclusions between the interior and the overgrowth zone. Some crystals have an outermost rim (<10 μm thick) with lower An (50-65 mol%), but other crystals lack these (Fig. 6). Type IIa crystals are more abundant in the host than in the enclaves, whereas Type IIb dominate the plagioclase in the enclaves (> 90%).

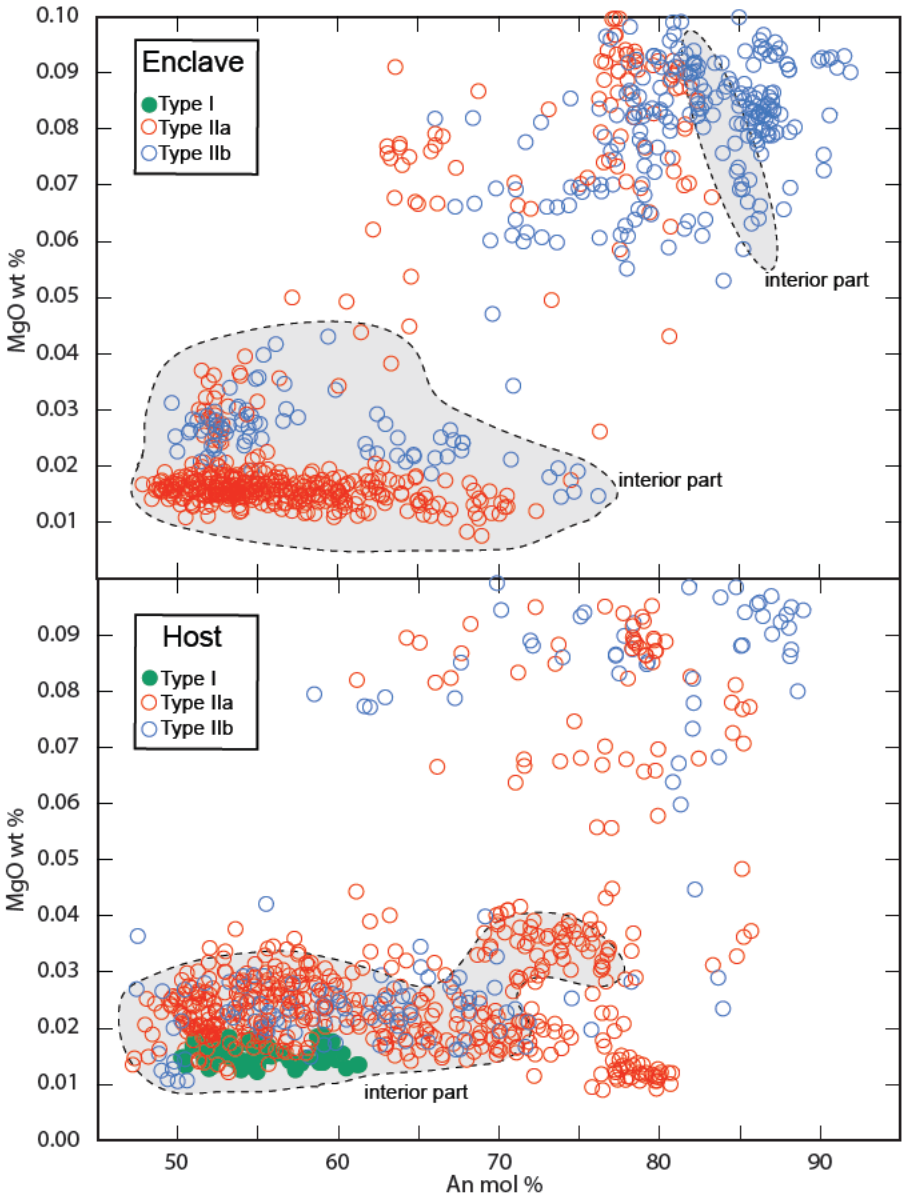

Figure 6. Representative plagioclase phenocrysts, in enclave and host, characterize on the base of anorthite content (An) against MgO composition. Type I have core range of about 50-60 in An and low MgO concentration between 0.01 and 0.02 wt %, also they are most abundant in the host and rare in the enclave. Type II show a wide range in An and MgO wt% composition.

Fe and Mg concentrations typically co-vary with An changes in enclave and host (Fig. 7 and 8). Rim to interior traverses show that many Type I crystals have positively correlated An and MgO concentrations (H10 in the host, Fig. 8) but less well correlated FeO* concentrations. The transition zone between the interior and overgrowth rim is extremely abrupt and narrow (<5 μm). Type II crystals from the enclaves essentially show the same relationships to those of the host, although the width of the transition zone of Mg is greater than for Fe and An (e.g., E2, Fig. 7). Other crystals in the host (e.g., H2, Fig. 8) have changes in An and Fe that are positively correlated between interiors and overgrowths, but the MgO concentrations do not significantly change. The same types of crystals occur in the enclave (E9, Fig. 7), but again the MgO concentration changes are less abrupt than those in An at the transition zone. The interior zones of Type II crystals tend to have higher Mg than those of Type I for the same An content.

2.6. Melt compositions and temperatures in equilibrium with plagioclase

The textural and compositional features of SHV plagioclase suggest that different crystal zones grew from melts having very different compositions and/or thermodynamic variables (e.g., temperature and pressure). The overgrowth/interior compositional gradients have enrichment factors that vary from about 1.5 for An, 1.8 for Fe, to about 4 for Mg, although it can also be much lower and close to 1 for some crystals (e.g., H2; see Fig. 8). The low An, low Mg and low Fe concentrations of the crystal interiors suggest they grew from much more evolved magmas than the high An, Mg and Fe overgrowths. Thus, Type I plagioclase are representative of the more evolve crystal-rich andesitic mingling/mixing end-members.

The sharp transition between the interiors and the overgrowths suggests that the change of the magmatic environment experienced by the crystal was also very abrupt, and the presence of sieve textures and dissolution features indicates that reaction and growth happened concurrently. The same types of plagioclase crystals are found both in the host and in the enclave, which suggest sthat the magmas exchanged mass and heat, and therefore, none of our samples is representative of the end-members magmas (e.g., pre-mingling/mixing) involved in the interaction. Such observations are common to other studies of plagioclase textures and compositions, from mixed dacite to basaltic andesite magmas, and attest the dynamic nature of the mafic-silicic magma interactions (e.g., Feeley and Dungan, 1996; Pichavant et al., 2002; Tomiya and Takahashi, 2005).

Recent numerical simulations of magma mixing and mingling in basaltic systems illustrate the wide range of environments that a crystal may experience over the course of a single intrusion (e.g., Schleicher and Bergantz, 2017). Therefore, it is not straightforward to associate a specific

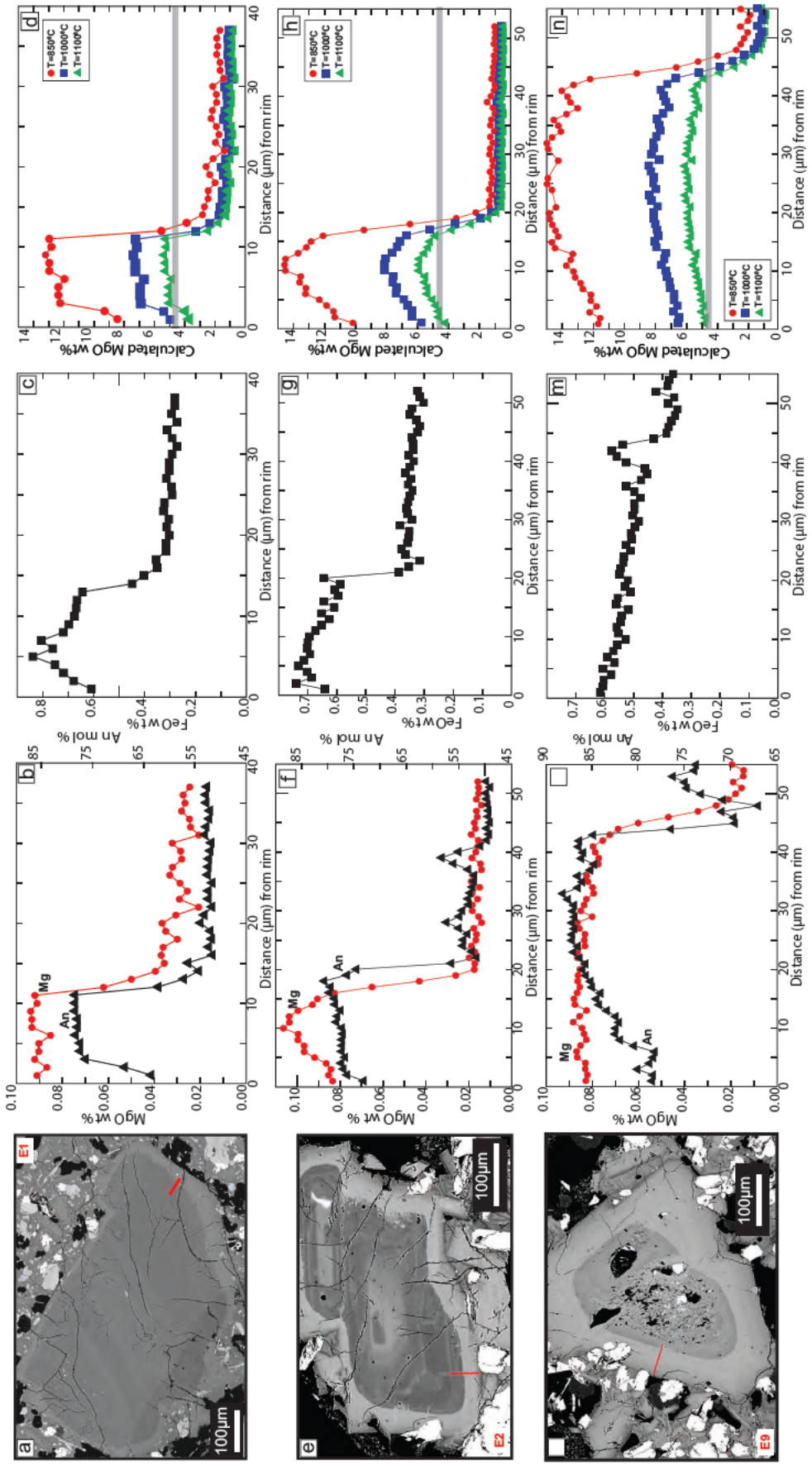

Figure 7. BSE images of plagioclase E1 (a), E2 (e) and E9 (i) from enclave (basaltic andesite). E1 and E2 (Type II plagioclase) show patchy core, with a sharp increase in composition of anorthite (black triangle), MgO (red circle) and FeO content (c) at the boundary between rim and interior part. E9 (Type I plagioclase) has inclusion-rich core and reversed zone rim with higher MgO (l) and FeO (m). Calculation of melts equivalent for MgO content (d, h and n) by Binderman et al. (1998) at 850 °C, 1000 °C and 1100 °C (red circle, blue square and green triangle respectively). Grey line represents the bulk rock composition of Mg (4.83wt%) obtained by Plail (2013) for our sample (MT35).

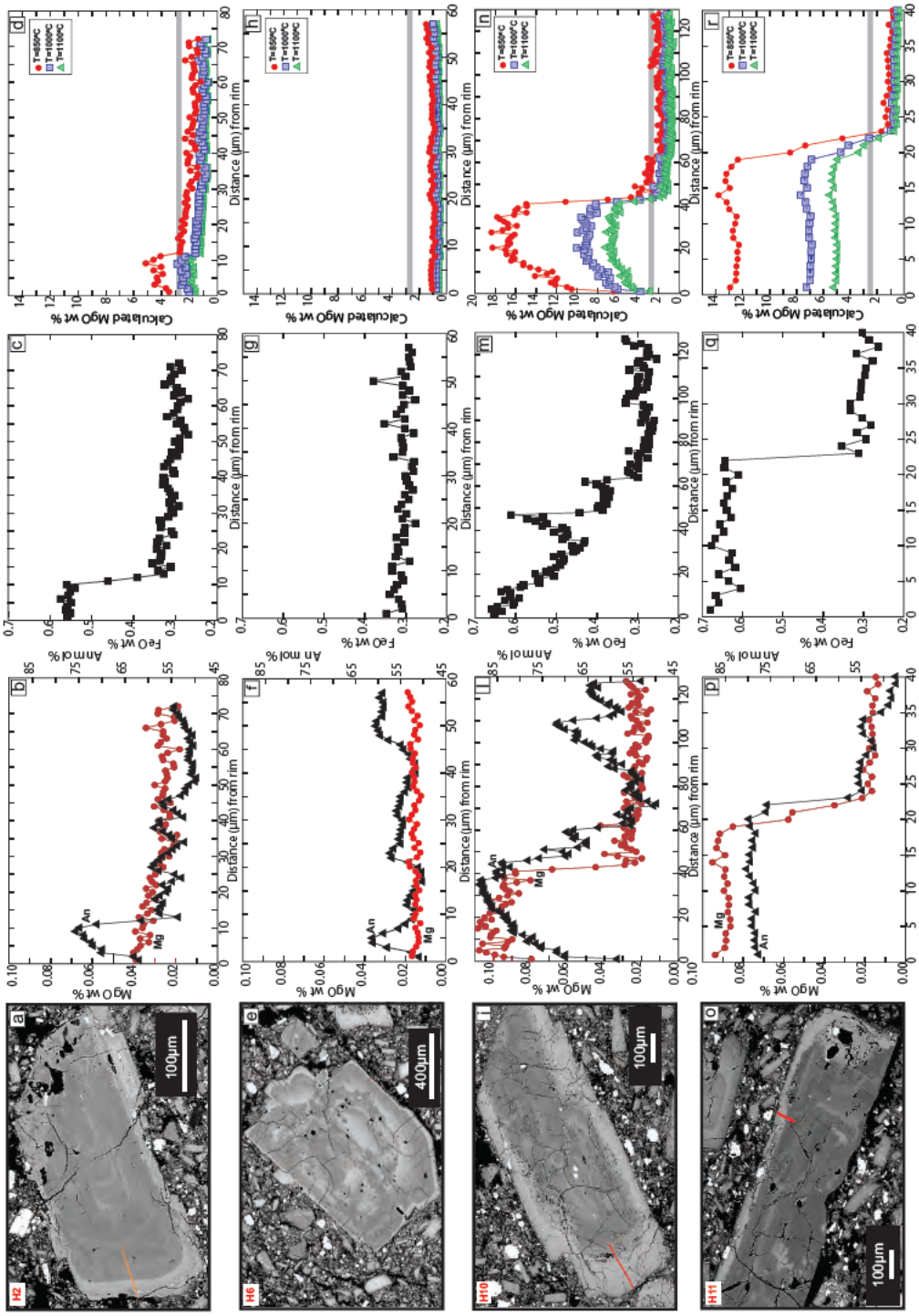

Figure 8. BSE images of plagioclase H2 (a), H6 (e), H10 (i) and H11 (o) from andesite host. Phenocrysts show patchy and sodic core, with a sharp increase in composition of anorthite (black triangle). H2 (Type I plagioclase) reveal no significant change in MgO content (b), indeed An content (b) and FeO (c) are characterized by an abrupt variation at the transition between rim and the interior part. H6 (Type III) has a small rim with a change in An content and no relevant change in MgO (f) and FeO (g). H10 (Type I) has a resorbed and rich-inclusion zone at the boundary with the rim that is marked by a sharp increase of anorthite and MgO content (f), and smooth increase in FeO (g). H11 (Type II) displays a profile with an uphill of An, MgO (b) and FeO (c) content. Calculation of melts equivalent for MgO content (d, h and n) by Binderman et al. (1998) at 850 °C, 1000 °C and 1100 °C (red circle, blue square and green triangle respectively). Grey line represents the bulk rock composition of Mg (2.62 wt%) proposed by Plail (2013) of andesite rock (our sample) during the last eruption in 2010.

plagioclase composition with a given melt composition and/or temperature. In the following, we attempt to associate the Mg and An concentrations of the plagioclase growing in a melt with specific temperature and over time. To this aim, we turn first to the range of temperatures and melt compositions that have been reported for the andesite and mafic enclaves at SHV (Tables 1 and 2).

2.6.1. Bulk-rock and glass compositions and their relationship to magmatic temperature

There are numerous analyses of the host andesite, enclaves, and melt inclusions (MI) from the different phases of SHV eruption (see, e.g., Barclay et al., 1998; Christopher et al., 2014; Devine and Rutherford, 2014; Humphreys et al., 2010; Plail et al., 2014; Zellmer et al., 2003a). The bulk-rock analyses of the mafic enclaves found a concentration of MgO varying between 3.5 and 5.5 wt.% (between 49 and 55 wt.% for SiO_2), while those of the andesite host a MgO concentration between 2.4 and 3.5 wt.% (between 57 and 61 wt.% for SiO_2). Melt inclusions trapped in plagioclase phenocrysts from the enclaves and host are significantly more evolved, with MgO contents between 0.1 and 0.5 wt.%, SiO_2 between 71 and 79 wt.%, and their compositions are independent of whether the MI are in crystals in the host or enclave.

Given the high phenocryst content and the mingled and mixed nature of the rocks (Humphreys et al., 2010; Plail et al., 2014), the bulk-rock compositions are likely not representative of the liquids, but provide reference values for the concentrations from which the plagioclase crystals could have grown. The changes in melt composition are typically associated with temperature changes, and this is another variable that needs to be considered. Extracting meaningful equilibrium temperatures from geothermometers or phase equilibria experiments is difficult because of the mingling and mixing processes that have juxtaposed minerals and melts with different origins. We review the results from the literature below.

2.6.2. Andesite magma

A review of previous work shows that the Opx rims and cores, hornblende-plagioclase, magnetite-ilmenite pairs and phase equilibria, all fall within 850 °C ± 20 °C for the andesite (Table 1). At this temperature and with and about 4-5 wt.% of water in the liquid (100-130 MPa) phase equilibria indicate that the magma would contain > 50% crystals (Barclay et al. 1998; Couch et al., 2003; Rutherford & Devine; 2003) and the liquid would be rhyolitic, probably characterised by compositions akin to the melt inclusions (e.g., 70-78wt% SiO_2, 0.1-0.5wt% MgO). Such a liquid would be in equilibrium with plagioclase An contents, between about 47 and 55 mol% (Appendix

A6). The highest An content close to the liquidus at about 950 °C was found to be about An_{70}. Melt inclusions in plagioclase phenocrysts and hydrogen concentrations in Opx indicate melt water contents of 4-5 wt.% and saturation pressures of 100-130 MPa (Edmonds et al., 2016). In the andesite, some Opx with reverse zoning (higher Mg/Fe in rim than core) experienced significantly higher temperatures, between 1000 and 1100 °C. From this we conclude that the crystal-rich andesite magma was likely stored at about 850 °C, at 100-130MPa, with an interstitial rhyolitic melt with 4-5 wt.% H_2O, and that was in equilibrium with quartz, amphibole and Type I low-An plagioclase (e.g., 45-55). This likely represents one of the mixing/hybridization end members.

2.6.3. Basaltic-andesite magmas

The SHV basaltic andesite enclave geothermometry studies were mainly based on Opx and Cpx compositions, and produced temperatures ranging from about 1000 to 1100°C (Plail, 2013). Plagioclase-melt calculations give a much broader range of temperatures, from about 900 to 1050 °C, whereas those of hornblende and plagioclase thermometry are as low as 850 °C. Hydrogen concentration of Opx in the enclave indicate water contents (about 7 wt.% H_2O) higher than for the andesite, and also somewhat higher pressures of 200-300 MPa (Edmonds et al., 2016). Aside from the Opx and Cpx, it is unclear whether the mafic magma was saturated in plagioclase when it came in contact with the andesite or not, and its crystal content was likely to be quite low given the high water and temperature. Phase-equilibria experiments on a basaltic andesite from neighbouring Mt. Pelée volcano on Martinique Island (Pichavant et al., 2002, 2018), characterised by a bulk-rock composition similar to the SHV enclaves, suggest that the magma would be at near liquidus at 1050°C and about 8 wt.% H_2O, and that with decreasing temperature or content of water the first mineral to crystallise would be Cpx followed by high-An plagioclase. Based on these considerations, we conclude that the basaltic andesite magma initially had a temperature of 1000-1100°C and high pressure (200-300 MPa), and that it was carrying mainly Opx and most of plagioclase inherited from the andesite by mechanical disaggregation during the time.

2.6.4. Calculated melt compositions in equilibrium with the host and enclave

The majority of crystals with An between 45 and 55 mol% and at 850°C could have grown from or equilibrated with melts characterised by 1- 2 wt.% MgO, which is > 50% higher than the MgO of the melt inclusions (Fig. 9). It is unclear if this difference is significant or related to the limitations of the Bindeman et al. (1998) partition relations for An-poor plagioclase (e.g., Longpre et al. 2014). If the temperature increases by 50°C, the MgO decreases by about 2.5 wt.%, thus, it could

be inferred that the crystals re-equilibrated their Mg concentration with hybrid liquids at somewhat higher temperatures than those of the melt inclusions. For the highest An contents (75-85) and a temperature of 1100°C, we calculate liquids characterised by a wide range of MgO concentrations: from about 1 to up to 6 wt.%, which are partly overlapping with the bulk MgO of the enclave. Thus, some of the high An plagioclase could have grown or re-equilibrated with liquids similar to the most mafic erupted magmas, although their lower values would indicate partial equilibration with lower Mg melts that were hybrids. Finally, intermediate An contents between 55 and 75 recover a wide range of MgO in the liquid, that varies between 1 and 4 wt.%, depending on the temperature. These crystals likely recorded a combination of growth and re-equilibration dynamics identified by a range of MgO and temperatures included between the two end-members.

Further insights into the range of liquids and into the sequence of events recorded by the plagioclase crystals can be gathered from deconvolving the information of the traverses from the crystal rims towards their interiors. Melts as calculated in equilibrium with the plagioclase across the range of temperatures described above, show that low An cores from enclave and host re-equilibrated with melts with MgO of 1-2 wt.%. These were likely hybrids of the rhyolite and of the basaltic andesite. The abrupt An shift between cores and rims records a major change in melt MgO, and many of the rims grew or re-equilibrated with liquids with 4-6 wt.% MgO. The high An rims of many crystals found in the andesite record temperature and MgO concentration that are consistent with those of the basaltic andesite enclaves, and that experienced virtually no re-equilibration (e.g., H11 crystal, Fig. 8r) or only very limited re-equilibration (e.g., H10 crystal, Fig. 8n) with the host andesite. If we use the temperature of the host as con strain, these rims appear to have re-equilibrated with liquids characterised by unrealistically high MgO concentrations. However, the interpretation of MgO contents in plagioclase is made complex by the interplay between the temperature variation and its effect on the partitioning relations and liquid compositions. Increasing the temperature from 850 to 1100 °C, decreases the K_D by a factor of 2.5 (for a given An), where the same temperature change could increase the MgO of the melt by a factor of 5 or more (e.g., melt inclusions have < 1 wt.% MgO whereas enclaves have about 6 wt.%). Thus, temperature and MgO in the liquid partly compensate each other, and they are difficult to separate when interpreting MgO concentrations in plagioclase. The diffusivity of Mg in plagioclase (see below) suggests that the incorporation of these crystals in the andesite occurred at a time very close to eruption or during the magma transport to the surface.

Other high An crystal rims in the host record MgO in hybrid liquids with compositions in between the evolved and mafic magmas and are difficult to interpret. The crystals in the enclaves

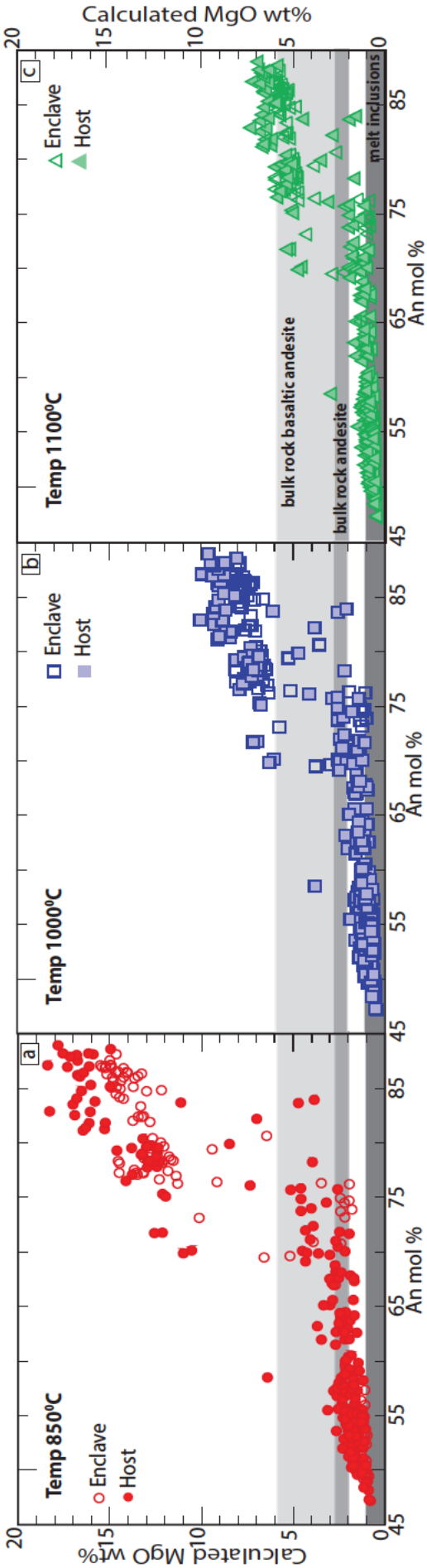

Figure 9. MgO in the melt calculated using Binderman et al. (1998) equation selecting three different temperatures: 850 °C (a), 1000 °C (b) and 1100 °C (c). Lighter grey bar (from 3.5 to 6 wt % of MgO) represent the bulk rock composition of the basaltic andesite enclave yield from previous studies (Phase I-V). Grey bar from 2 to 3.5 wt % of MgO characterize the bulk composition of the andesite produced during all the phases of the eruption. Darker grey bar (from 0 to 1 wt % of MgO) show the concentration of MgO gained from the melt inclusions trapped in plagioclase from literature.

show similar relations to that of the host. The cores grew or equilibrated with liquid MgO that was low in MgO (< 2 wt.%) disregarding the range of temperature we used, whereas the rims record a high MgO and temperature that is coherent with that of the basaltic andesite magma. There is no evidence of quenching and of a temperature drop for the enclaves with the host in terms of re-equilibration of plagioclase MgO, since this would imply extremely high MgO in the liquids (> 10 wt.%).

In conclusion the diffusive re-equilibration between MgO and melt was modelled under specific crystallisation conditions of different plagioclase types (see below). Type I (low-An plagioclase (45-55) represents the phenocrysts that started to crystallise before the intrusion of the mafic magma. We modelled Type I plagioclase at 850-1000-1100°C (Fig. 10) taking into account different MgO concentrations in the melt (0.48-1 wt%). Type II plagioclase (e.g., E1 in Fig. 7) were modelled by two stages of diffusive re-equilibration (Appendix A8): the interior part re-equilibrated as Type I plagioclase and the overgrowth rim with high-An content (70-85) were modelled at high temperature of 1100 °C. The overgrowth rims with an abrupt change in An composition is associated to the interaction between the andesitic host and intrution of basaltic andesite magma.

2.7. Estimated timescales from diffusion modelling

In addition to crystal growth and dissolution processes, there were diffusion within the crystals and between the crystal margins and the surrounding melt (e.g., Costa et al., 2008). In particular, the observation that Mg concentrations are almost constant even with large changes in An, and that in others crystals Mg is significantly smoother than An, both suggest that diffusion between interiors, overgrowths and external liquid has modified them to varying degrees (e.g., Costa et al., 2003). Fe concentrations may also be affected by diffusion in the crystals, however the difficulty of analysing Fe^{2+} and Fe^{3+} at sufficiently high spatial resolution and uncertainty on the different diffusivities partition coefficients (Ruprecht and Worner, 2007; Sato et al., 2005), make the interpretation of Fe profiles more complex. The abrupt changes in An and Mg between outer rims and interior parts in SHV plagioclase are useful for modelling the diffusion of Mg, with relatively little uncertainty on the initial geometry and composition. Re-equilibration between the crystal rims and the matrix melt should provide information on the timescales involved (e.g., Costa et al., 2003, 2008). Possible complications include the wide range in temperatures and in compositional variations that the crystals may have experienced during the magma interaction.

2.7.1. Calculated timescales of magmatic interaction to eruption

We modelled the equilibration degree of plagioclase, which did not show well defined zoning trends (e.g., H6, Fig. 10). Such models can account for the compositional difference for the interior parts characterising Type I and II plagioclase and are an attempt to account for complexities involved in the mafic-silicic interaction, with crystals may have experienced a range of composition and temperature changes over time (Clynne, 1999; Feeley and Dungan, 1996; Schleicher and Bergantz, 2017).

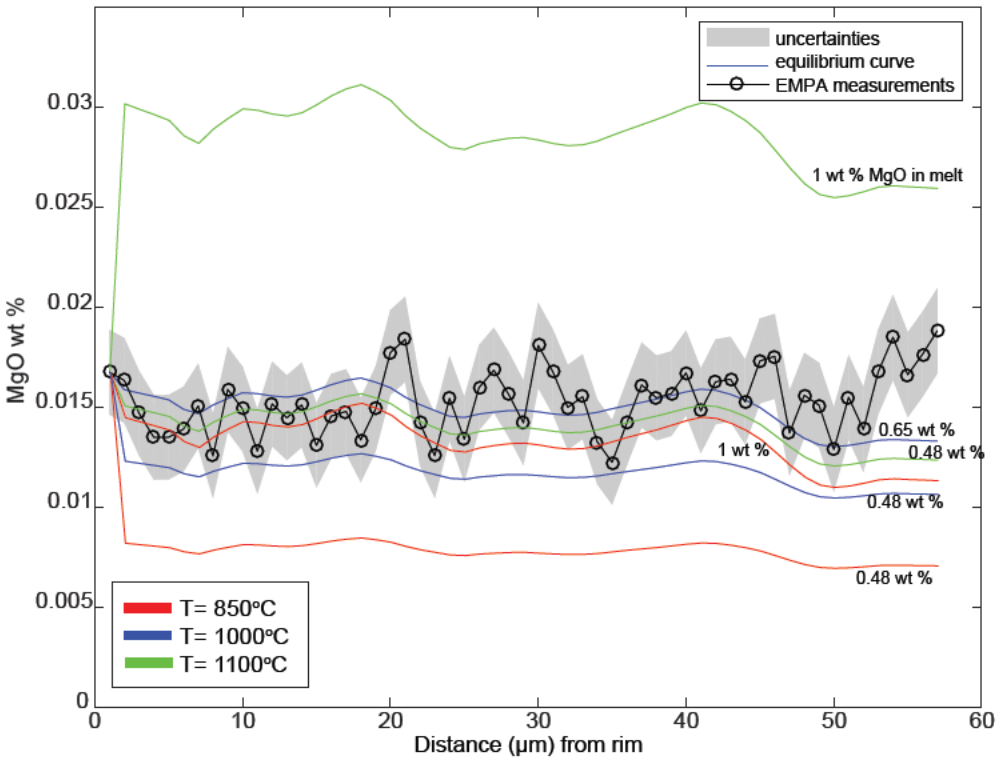

Figure 10. H6 plagioclase as case study for Type I (host andesite). Equilibrium curve calculated with MgO concentration in melt inclusions at different temperature (850 °C, 1000 °C and 1100 °C). Uncertainties of the EMPA analysis are in grey. The equilibrium is gained for MgO of 0.48 wt. % in the melt at 1100 °C.

For Type II plagioclase, we were able to obtain different times, which we believe reflect the various processes that the crystals experienced (Fig. 11). One-and two-stage models (see red curves and blue squares respectively on Fig. 11) were used to fit computed and measured profiles (Fig. 11; Tables 3 and 4). Fig. 11 reports the comparison between the two models, and shows that the best fits were obtained with the two-stage models. The time for the interior part to re-equilibrate at 1100 °C varies from 7 to 22 days in the enclave (Fig. 11a, c, e), and is up to 50 days in the host (Fig. 11b, d, f). The outer parts reveal timescales in the range of hours in both host and enclave, and up to a couple of days for one crystal in the host (H1, Fig. 11b). A summary of the time scales obtained for each crystal and for the different modelling approaches are reported in Tables 3 and 4.

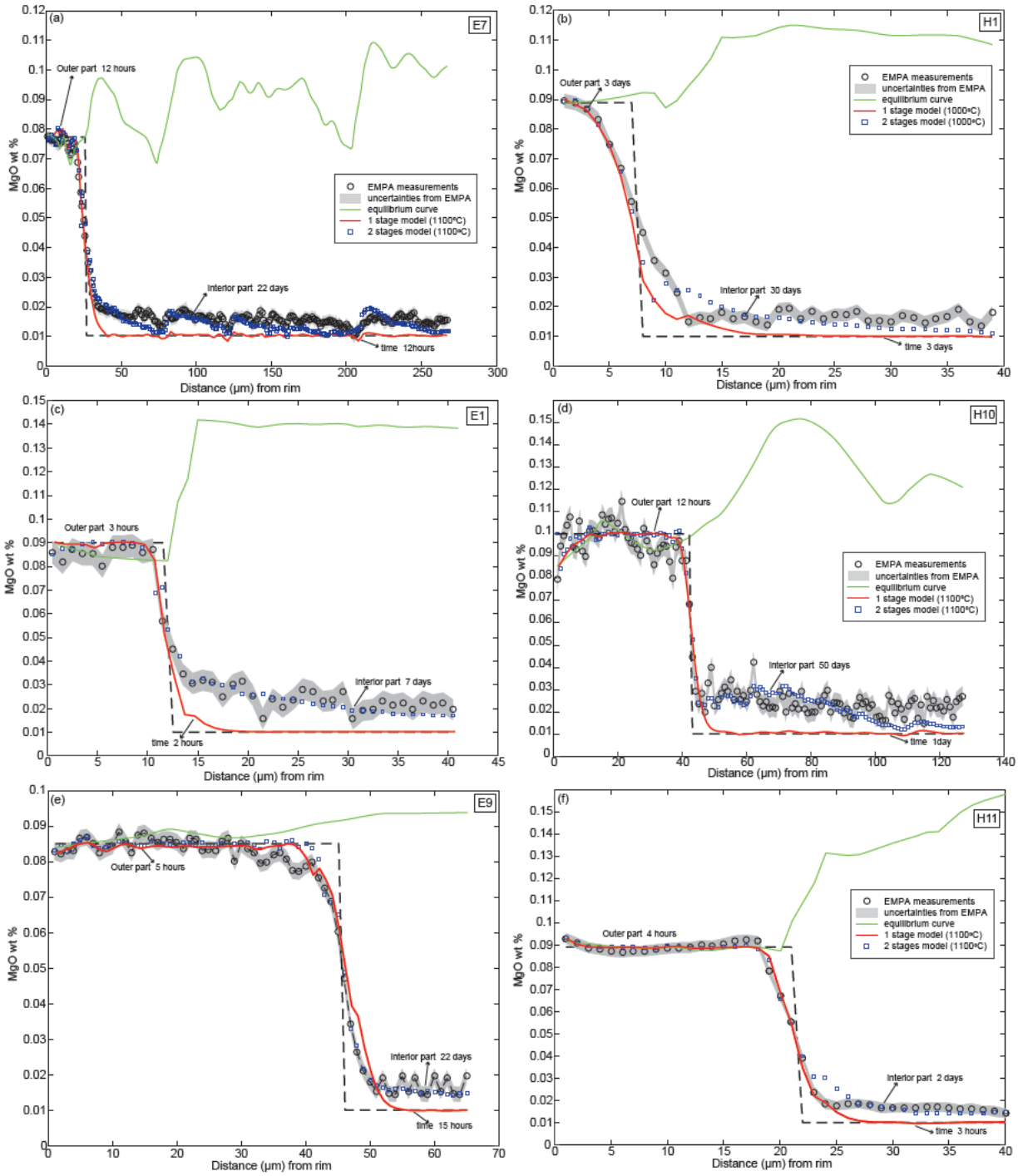

Figure 11. Diffusion models for plagioclase in host and enclaves. Dashed line is the initial condition, calculated on the base of the anorthite content along the EMPA measurements from rim through the interior part. Green continuous line is the equilibrium curve and Mg profiles (black circle) with uncertainty (grey area) from EMPA analysis. Modeled results are in red line for one stage model and in blue square for 2 stages model.

2.7.2. Uncertainties

The main source of uncertainty in the modelling of liquid compositions and timescales is the uncertainty in temperatures. Temperatures were calculated with various methods (see section 4.2 above), which range in from ± 20°C (Barclay et al. 1998) to ± 50°C (Murphy et al. 1998) for the host andesite, while for the basaltic andesite range from 900 to 1000°C (Plail 2013). In Table 3 and 4 we report the results for the timescale with their associated uncertainty. Initial conditions and profile shapes are additional sources of uncertainty, while the crystals selected have large and abrupt An changes assuming a step-wise initial profile reasonable.

A further source of uncertainty is associated with the values of the coefficients for the plagioclase-melt Mg partition that we took from Binderman et al. (1998). Previous works have observed that this effect is probably due to the low An content and to the intermediate-silicic liquid composition (Berlo et al., 2007; Druitt et al., 2012; Longpre et al., 2014). Other calculations would also give very different results, because the relations of partitioning have a very small slope linking An and Mg and they would imply high An and low Mg melts, which appears to be unrealistic (Coote & Shane, 2016).

2.8. Magma end-members and processes inferred from petrology, plagioclase zoning, and calculated melt compositions

Previous studies of the SHV andesite and enclaves proposed that magma mingling resulted in the exchange and incorporation of phenocrysts and microlites from the andesite into the basaltic andesite enclaves and vice versa. These imply also the mechanical disaggregation of mafic enclaves into the andesite magma (Barclay et al., 2010; Humphreys et al., 2013; Plail et al., 2014). An important aspect for understanding these mafic-silicic magma interactions is the ability to distinguish between the likely end-members that were involved and their states before they interacted.

2.8.1. Andesite and basaltic andesite magmas prior to interaction

Although bulk-rock compositions of the host are andesitic, the melt inclusions in plagioclase and pyroxene are rhyolitic, and, thus, significantly more evolved (Fig. 4). Quartz, amphibole, and the dominant plagioclase An_{45-60} (Type I phenocrysts) are in equilibrium with a rhyolitic liquid at about 850 °C, 100 MPa and 4 wt.% H_2O in the melt according to phase equilibria (Couch et al., 2000). At these conditions the magma should contain 40-50% crystals and it likely represent the environmental and rheological state of the andesite magma before the intrusion and partial melting

by the mafic magmas. Plagioclase in the host, andesite groundmass and many of the phenocryst overgrowths are calcic in composition (Fig. 1 in Murphy et al. 1998). The great majority of plagioclase phenocrysts in the enclave (about 90%) are reversely zoned Type II, and their low An interior parts were inherited from the andesite. Given the sparse presence of plagioclase (only about 10%), they did not have a major effect on the bulk-magma composition. The andesite has a lower phenocryst content (30-40 wt.%), therefore it was likely erupted at a slightly higher temperature than 850 °C (Murphy et al., 1998). We find that 75 vol.% of the plagioclase of the andesite are of Type I (Appendix A.4), which represent the phenocrysts before the intrusion of mafic magma. We do not have detailed traverses of these Type I phenocrysts, but BSE images show that their interiors preserve excursions to high An and some cores also have high An contents. These crystals would record any evolution of the andesite magma prior to significant arrival of mafic magma, and they have been investigated by Zellmer. et al. (2003a, b). The enclaves should represent the basaltic end-member. The lack in olivine, indicating that they are already differentiated from basaltic magmas and they may be similar to those found in the older parts of SHV (Cassidy et al., 2015). However, the lack in olivine doesn't necessarily hint a highly fractionated basalt, as it has been show by Pichvant et al.,(2018) on samples from La Soufriere Volcano (Guadaloupe, Lesser Antilles), which found that low-MgO mafic magmas can crystallise olivine under specific conditions of temperature, pressure and fugacity.

We did not find plagioclase phenocrysts (unzoned) with high An (> 80) in our enclave or in the andesite. This suggests that the mafic-end member magma was under-saturated in plagioclase, which is consistent with its high water content (> 7 wt.%; Edmonds et al., 2016) that would have suppressed plagioclase stability. However, if we consider the water content (>7wt.%) not exceptional in evolved basalts from the islands in the Lesser Antilles (Pichavant and Macdonald, 2007), the An-rich plagioclase (>90) have been re-equilibrated to lower An plagioclase (<80) due to the interactions and mixing of magmas. The end-member intruding basaltic andesite end-member was probably close to its liquidus at about 1050 °C since it had only minor amounts of pyroxene phenocrysts (e.g., Murphy et al., 1998), which is in accordance with phase equilibria experiments performed on basaltic andesite from Mount Pelée, which is characterised by a similar composition to the SHV enclaves (Pichavant et al., 2002, 2018).

2.8.2. Interaction between the host andesite and intruding basalt

We propose that the following sequence of events occurred during interaction the between andesite and intruding basalt (Fig. 12).

(1) Andesite stored at relatively low temperature (850 °C) and high crystallinity (40-50%) was in equilibrium with Type I plagioclase, rhyolitic liquid, amphibole and quartz. We know little about the history of this magma before the last intrusion of basalt related to the current eruption. Some insights into this early history may be found in the study proposed by Zellmer et al. (2003b) on the timescales gained from the modelling of the Sr concentration in plagioclase zoning.
The calculated MgO in equilibrium with Type I crystals (about 1 wt.%) is higher than that of the rhyolitic liquid. This has been ascribed to poor calibration of the Bindeman et al. (1998) partition coefficient for low An (discussed in paragraph 2.4.1), or to extensive crystallization of the MI, or/ and to re-equilibrations of the crystals with a liquid that was already partly hybridised with the more mafic magma.

(2) The crystal-rich andesite was reheated, and plagioclase and quartz began to melt. A front of mafic magma reached the interface with the andesite and developed a hybrid zone, where Type I crystals were entrained into the higher temperature/high-Mg magma that was water-rich and at near liquidus conditions. Such magma could be generated by fractionation of a more mafic liquid such as that found in South Soufrière Hills Volcano (Edmonds et al., 2016). Plagioclase of Type I dissolved and generated a sieve texture, but in some instances the plagioclase Mg content increased and re-equilibrated to the higher Mg of the mafic magma. Amphibole and quartz that were retained in this mafic magma were also dissolved and reacted.

(3) At some point the mafic magma cooled quickly, probably because in contact with a larger amount of unheated andesite. This triggered the crystallisation of the high-An rich rims and produced the Type II crystals, which equilibrated with a liquid characterised by about 5 wt.% MgO (e.g., similar to the bulk-rock of enclaves). Following this scenario, Type IIa labels crystals that were less affected by dissolution or reaction induced by the mafic liquid than Type IIb. Such an event of rim growth was followed by, or happened at the same time with, the generation of the diktytaxitic texture, the high An and amphibole of the groundmass.

(4) Some of the Type II crystals from the enclaves were reincorporated in the andesite magma, either during the time of the cooling of the enclaves or later during high strain interactions that led to enclave disaggregation (Humphreys et al., 2009). Most of these Type II in the host still record the equilibration with the same high Mg-liquids, which the enclaves equilibrated with, although we did find one example where partial re-equilibration with the andesite has occurred.

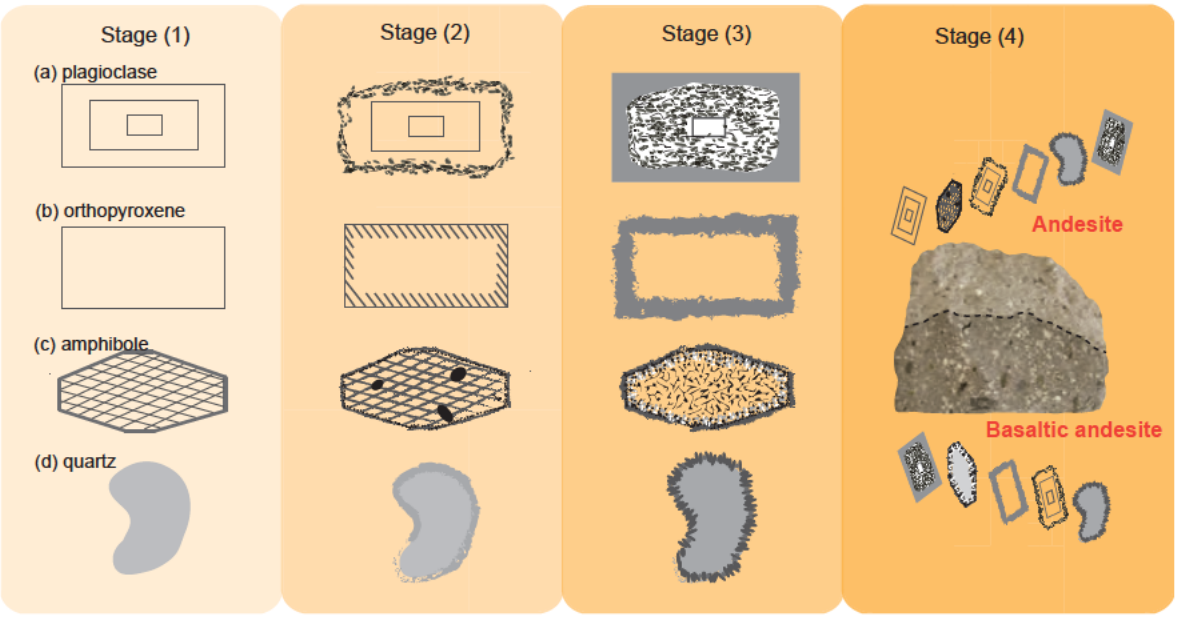

Figure 12. Schematic representation of the sequence of four events that occurred during interaction between the andesite and intruding basalt. (Stage 1) Andesite stored at relatively low temperature (850 °C) and crystallinity of 40-50% (plagioclase, orthopyroxene, amphibole and quartz). (Stage 2) New fresh, and more, mafic magma intruding the andesite that was reheated and crystals began to melt. (Stage 3) After time, the interaction between the two magmas increased and the mafic magma cooled down. (Stage 4) Some of the crystals from the enclaves were reincorporated in the andesite magma. For more details see the text.

2.9. Timescales between the last interaction and eruption

The modelling of the compositional zoning of Mg in plagioclase provides a window into the timescales and processes that occurred during mafic-silicic magma interactions. The interior of some Type IIa and IIb plagioclase have Mg concentrations that are higher than those of Type I with the same An content (Figs. 7 and 8). This suggests that they re-equilibrated with the high Mg of the basaltic melt before they grew with to have high An content rims. We estimated the time it would take to re-equilibrate the interiors of these crystals using the Mg concentration of the lowest of the Type I crystals. We found that the re-equilibration times for the plagioclase in the host ranges from hours to 50 days at 1100 °C, and from 20 to 250 days at 1000 °C (Table 3). For the plagioclase in the enclave, the times vary from 7 to 40 days at 1100 °C, and from 46 days to 300 days at 1000 °C (Table 4). These times could underestimate the real time, because if the crystals were dissolving while diffusion of Mg in the crystal was occurring, any zoning would have disappeared. In addition, our profiles encompass only a limited part of the interiors and, thus, our timescales can not reflect earlier or longer processes that may have occurred before the interactions. Realistic modelling of the Mg concentrations of the entirety of the cores would need to consider 2D or 3D

Table 3. Diffusion timescale using one-stage and two-stage models. Here, results of modelling of plagioclase in the andesitic host are shown that were performed at 1100 °C and 1000 °C, with relative uncertainties.

				1 stage		2 stage			
Plagioclase	Type	Thickness rim (μm)	Temperature (°C)		Uncertainty	Interior part	Uncertainty	Rim	Uncertainty
HOST									
H1	IIa	10	1100	11h	± 3h	35 days	± 10 days	~	~
			1000	3 days	± 1 day	30 days	± 5 days	3 days	± 1 day
H2	IIa	20	1100	90 days	± 2 days	40 days	± 5 days	~	~
			1000	5 days	± 12h	250 days	± 50 days	~	~
H3	IIa	20		~	~	~	~	~	~
H4	I	10		~	~	~	~	~	~
H5	IIa	35		~	~	~	~	~	~
H6	I	5		~	~	~	~	~	~
H7	IIa	35		~	~	~	~	~	~
H8	IIa	40		~	~	~	~	~	~
H9	IIb	45	1100	8h	± 1h	2h	± 1h	~	~
			1000	2 days	± 12h	24h	± 12h	~	~
H10	IIb	40	1100	1 day	± 5h	50 days	± 10 days	12h	± 2h
			1000	5 days	± 1 day	210 days	± 20 days	20 days	± 5 day
H11	IIa	20	1100	3h	± 1h	2 days	± 1 day	4h	± 1h
			1000	9h	± 1h	20 days	± 4 days	24h	± 4h
H12	IIa	15		~	~	~	~	~	~

re-equilibration, which is beyond the scope of this work.

The times that we obtained from the one-stage models come from the modelling of the changes of the Mg concentration between the interior parts and the rims. For these we used very sharp (< 1 μm) initial profiles, even if the length of the transition zone of An and Mg contents is about the same, implying that little diffusion has occurred between interiors and rim. Our models typically reproduce well the data and provide times (at 1100 °C) that range from hours to days (Tables 3 and 4). These are significantly shorter (90 days) than the time obtained from the interior

Table 4. Diffusion timescale using one-stage and two-stage models. Here, results of modelling of plagioclase in the basaltic andesite enclave are shown that were performed at 1100 °C and 1000 °C, with relative uncertainties.

				1 stage		2 stage			
Plagioclase	Type	Thickness rim (μm)	Temperature (°C)		Uncertainty	Interior part	Uncertainty	Rim	Uncertainty
ENCLAVE									
E1	IIa	13	1100	2h	± 1h	7 days	± 1 day	3 h	± 1h
			1000	16h	± 5h	46 days	± 5 days	4 h	± 1h
E2	IIa	20	1100	24h	± 5h	10 days	± 5 days	~	~
			1000	10 days	± 2 days	70 days	± 10 days	~	~
E3	IIa	35	1100	24h	± 10h	40 days	± 10 days	~	~
			1000	8 days	± 2 days	300 days	± 50 days	~	~
E4	IIb	10		~	~	~	~	~	~
E5	IIb	5		~	~	~	~	~	~
E6	IIb	100		~	~	~	~	~	~
E7	IIa	20	1100	12h	± 2h	22 days	± 5 days	12h	± 2h
			1000	3 days	±12h	100 days	± 10 days	2 days	± 12h
E8	IIb	100		~	~	~	~	~	~
E9	IIb	45	1100	16h	± 1h	22 days	± 2 days	5h	± 3h
			1000	5 days	± 1 day	130 days	± 2 days	24h	± 2h

part equilibrations (up to 300 days for the interior parts). With the two-stage models, we obtained short times, ranging from hours to 10 days (in host and enclave), when modelling with 1100 °C, and ranging from hours to 50 days with 1000 °C (Tables 3 and 4).

2.10. A variety of time scales for the SHV magmatic system

In Fig. 13, we compare our timescales with those obtained by other authors using different approaches. Long residence times were proposed as representative of the period between magma heating and remobilization, and have been obtained studying the degree of disequilibrium between the An content in plagioclase and the partitioning of Ba and Sr in the crystals (Zellmer et al., 2003a; Zellmer et al., 2003b). In particular a temperature of 850 °C was used in the diffusion models, and the variation in Sr within the crystal revealed a residence time ranging from 200 to 1,220 years, much longer than our results ranging from hours to days. In our models, temperatures of 1000-1100 °C were considered the most representative of the melt's temperature, when the diffusion processes were developed at the transition zones between the interior parts and the rims. Notice that while decreasing the temperature makes longer timescales, in our models the times obtained at 850 °C never exceed 1 year (Appendix A). It is interesting to notice that for Zellmer et al. (2003b) the timescales of the crystal growth is reasonably shorter than the resident time at magmatic temperature (which ranges from from 15 to 320 years), and that in this framework the complexity of the zoning pattern of plagioclase can reveal a multiple injection of fresh new magma in the magmatic system, followed by mixing of hot magma with the resident magma. However, the oscillatory zoning can be a response due to rapid decompression (without diffusion). We also stress that Zellmer et al. (2003b) looked at the interior of Type I crystals, which we did not investigate.

Higgins and Roberge (2003) calculated the crystal size distribution of plagioclase and amphibole crystals from andesite, and proposed a model based on from those from Devine et al. (1998) and Couch et al. (2001), where the cycle of nucleation and growth are interrupted by the injection of mafic magma. Such an injection induced the dissolution of the small plagioclase, while the larger crystals continued to grow. In this work, we calculated the time using the data from Higgins and Roberge (2003), which show a range from about 300 up to 1000 years (Fig. 13).

The difference between the short timescales of this work and the long timescales obtained by Zellmer et al. (2003b) and the time gained from crystal size distribution proposed by Higgins and Roberge (2003), can be correlated to the sample analysed. A few hundreds years of resident time of plagioclase in the andesitic magma correspond to products erupted between 151±4ka and 1999 (Zellmer et al., 2003b), and between 1995 and 2000 (Higgins and Roberge, 2003). Since that

time, the magmatic system was evolved during the 15 years of eruption, so plagioclase modelled here (from the last eruption in 2010) represented the last interaction with the andesitic host and the more intruded mafic magma suggesting syn-eruptive processes. During the eruption, the magmatic system experienced multiple injections of more mafic magma, and the reheating processes probably erased the previous compositional zoning pattern recorded during previous interactions.

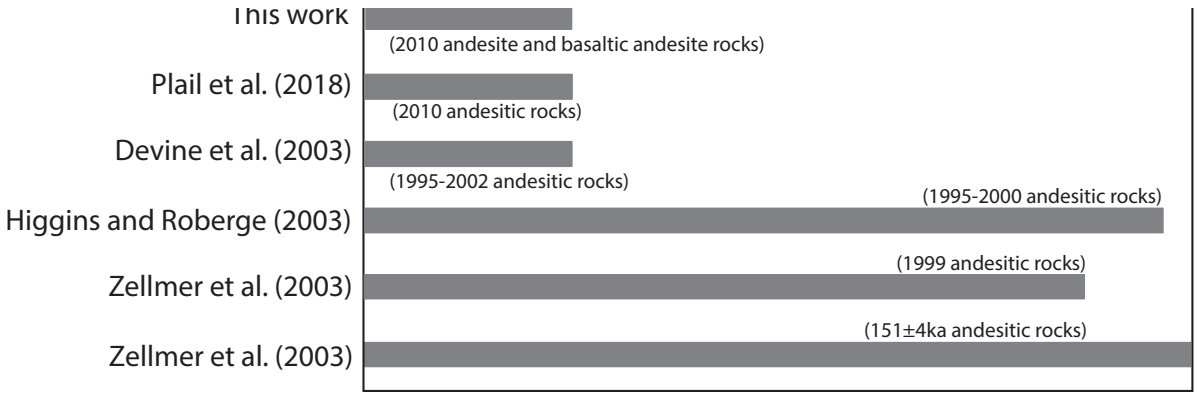

Figure 13. Timescales gained using different methods. Short timescales from few hours to weeks are obtained from the current study, Plail et al. (2008) and Devine et al. (2003). Longer timescales ranging from a few years to more than 1,000 years were yielded by Zellmer et al. (2003) and also calculating the time (this work) from the CSDs data proposed by Higgins and Roberge (2003).

Other studies, using Fe-Ti oxide geothermometry and chemical zoning of titanomagnetite phenocrysts, determined short timescales ranging from days to months (Devine and Rutherford, 2014; Devine et al., 2003). This confirms the magma interaction processes here described, and the relative remobilisation of the hybrid andesitic host magma just before the eruption (Devine and Rutherford, 2014; Devine et al., 2003). Rocks from 1995 to 2010 were analysed, and titanomagnetite crystals showed diffusion gradients in TiO_2 from core to rim, which reflected the intrusion of a new mafic magma into the andesitic host (Devine et al., 1998; Devine and Rutherford, 2014; Devine et al., 2003). Syn-eruptive processes of magma mingling/mixing and eruption were also proposed in a recent work by Plail et al. (2018), where it is invoked a syn-eruptive mechanism for the formation of enclaves through a thermal diffusion model of the interaction between basalt layer and the overlying andesite layer.

The potential injections of new mafic magma could have relevant implications for future eruptions at SHV. The volcano ended the last erupting phase in 2010, and if the injection of magma has completely ceased as suggested by Plail et al. (2018), the volcano can be considered dormant. However, if the supply of mafic magma should increase, the reheating-mingling-mixing processes

will extended in time, with a future re-activation of the system. An alternative hypothesis is that the mafic magma all intruded early in the system, but has been erupted progressively. In other words, what looks like progressive intrusion over time actually be progressive emptying of an early intrusion that happened at one time.

2.11. Conclusion

Rocks erupted at SHV reveal the complexity of the magma storage, which experienced multiple injections of more mafic magma over time. The absence of olivines, the presence of reacted quartz, the disaggregation of mafic enclaves into the andesitic host, the inherited phenocrysts and mineral phases in equilibrium with evolved liquid (dacite-rhyolite), all are proofd of the intricate multistage processes of crystallisation, recharge, mixing and eruption.

The presence of mafic enclaves is unequivocal evidence of magma mixing processes. However, these processes resulted also from the combination of multiple factors, such as the amount of the magma that intruded the host, the contrast in viscosity, and the chemical and physical characteristics of each magma. The trigger of each phase of the eruption at SHV is not correlated with the formation of enclaves as demonstrated by McGee et al. (2019) using U-series disequilibria in host and enclave. However, understanding the time intervals between periods of re-activation of the storage system, unrest, and eruption is crucial for SHV.

Since the last eruption happened on 11th February 2010, the volcano is showing low-levels of unrest, characterised by degassing, inflation and sporadic seismicity (reported and continuously monitored by Montserrat Observatory Volcano, MVO). The timescales inferred in this work through the modelling of diffusive re-equilibration of Mg in plagioclase (up to 2 months) are a beneficial support for interpreting the monitoring signals at SHV. Plagioclase analysed do not preserve a long time recorded from 1995 interaction as show in plagioclase from Zellmer et al. (2003a, b). However, our timescales are consistent with previous results obtained by Devine and Rutherford (2014), and with syn-eruptive processes between compositionally different magmas at the boundary layer interface, as proposed by Plail et al. (2018).

Acknowledgements

This work was funded by Macquarie University Research Excellence Scholarship (MQRES) (2015081) associated with an Australian Research Council Discovery Project (DP150100328). F. Costa acknowledges a National Research Foundation Investigatorship Award (Grant number NRF-NRFI2017-06). We would like to thank Melissa Plail for sharing her sample collection, Steve

Craven for the rock preparations, Lilu Cheng and Jason Herrin for their assistance, respectively, during SEM and EMPA analyses. We are grateful to Turker Topal for his help with Matlab code, Benat Oliveira Bravo for helpful discussion about diffusion modelling processes and Lucy McGee for constructive discussion related to the SHV magmatic system. In addition, Professional editor, John McAndrew, provided copyediting and proofreading services for this chapter according to the guidelines laid out in the university-endorsed national "Guidelines for Editing Research Theses".

References

Aspinall, W.P., Miller, A.D., Lynch, L.L., Latchman, J.L., Stewart, R.C., White, R.A., Power, J.A., 1998. Soufriere Hills eruption, Montserrat, 1995-1997: Volcanic earthquake locations and fault plane solutions. Geophys Res Lett 25, 3397-3400.

Bachmann, O., Bergantz, G.W., 2006. Gas percolation in upper-crustal silicic crystal mushes as a mechanism for upward heat advection and rejuvenation of near-solidus magma bodies. J Volcanol Geoth Res 149, 85-102.

Bacon, K.J., Barnes, G.T., 1978. 2-Component Monolayers .4. Excess Enthalpies and Entropies of Mixing in Octadecanol-Docosyl Sulfate System. J Colloid Interf Sci 67, 70-77.

Barclay, J., Herd, R.A., Edwards, B.R., Christopher, T., Kiddle, E.J., Plail, M., Donovan, A., 2010. Caught in the act: Implications for the increasing abundance of mafic enclaves during the recent eruptive episodes of the Soufriere Hills Volcano, Montserrat. Geophys Res Lett 37.

Barclay, J., Rutherford, M.J., Carroll, M.R., Murphy, M.D., Devine, J.D., Gardner, J., Sparks, R.S.J., 1998. Experimental phase equilibria constraints on pre-eruptive storage conditions of the Soufriere Hills magma. Geophys Res Lett 25, 3437-3440.

Berlo, K., Blundy, J., Turner, S., Hawkesworth, C., 2007. Textural and chemical variation in plagioclase phenocrysts from the 1980 eruptions of Mount St. Helens, USA. Contrib Mineral Petr 154, 291-308.

Bindeman, I.N., Davis, A.M., Drake, M.J., 1998. Ion microprobe study of plagioclase-basalt partition experiments at natural concentration levels of trace elements. Geochim Cosmochim Ac 62, 1175-1193.

Blundy, J.D., Wood, B.J., 1991. Crystal-Chemical Controls on the Partitioning of Sr and Ba

between Plagioclase Feldspar, Silicate Melts, and Hydrothermal Solutions. Geochim Cosmochim Ac 55, 193-209.

Browne, B.L., Eichelberger, J.C., Patino, L.C., Vogel, T.A., Dehn, J., Uto, K., Hoshizumi, H., 2006a. Generation of porphyritic and equigranular mafic enclaves during magma recharge events at Unzen volcano, Japan. J Petrol 47, 301-328.

Browne, B.L., Eichelberger, J.C., Patino, L.C., Vogel, T.A., Uto, K., Hoshizumi, H., 2006b. Magma mingling as indicated by texture and Sr/Ba ratios of plagioclase phenocrysts from Unzen volcano, SW Japan. J Volcanol Geoth Res 154, 103-116.

Cassidy, M., Edmonds, M., Watt, S.F.L., Palmer, M.R., Gernon, T.M., 2015. Origin of Basalts by Hybridization in Andesite-dominated Arcs. J Petrol 56, 325-346.

Christopher, T.E., Humphreys, M.C.S., Barclay, J., Genareau, K., De Angelis, S.M.H., Plail, M., Donovan, A., 2014. Petrological and geochemical variation during the Soufriere Hills eruption, 1995 to 2010, Geol Soc Mem, pp. 317-342.

Clynne, M.A., 1999. A complex magma mixing origin for rocks erupted in 1915, Lassen Peak, California. J Petrol 40, 105-132.

Costa, F., Andreastuti, S., de Maisonneuve, C.B., Pallister, J.S., 2013. Petrological insights into the storage conditions, and magmatic processes that yielded the centennial 2010 Merapi explosive eruption. J Volcanol Geoth Res 261, 209-235.

Costa, F., Dohmen, R., Chakraborty, S., 2008. Time Scales of Magmatic Processes from Modeling the Zoning Patterns of Crystals. Rev Mineral Geochem 69, 545-594.

Costa, F., Dungan, M., 2005. Short time scales of magmatic assimilation from diffusion modeling of multiple elements in olivine. Geology 33, 837-840.

Couch, S., Sparks, R.S.J., Carroll, M.R., 2001. Mineral disequilibrium in lavas explained by convective self-mixing in open magma chambers. Nature 411, 1037-1039.

Coussens, M., Cassidy, M., Watt, S.F.L., Jutzeler, M., Tailing, P.J., Barfod, D., Gernon, T.M., Taylor, R., Hatter, S.J., Palmer, M.R., 2017. Long-term changes in explosive and effusive behaviour at andesitic arc volcanoes: Chronostratigraphy of the Centre Hills Volcano, Montserrat. J Volcanol Geoth Res 333, 15-35.

Deer, W.A., Howie, R.A., Zussman, J., 1992. An introduction to the rock-forming minerals. Longman Scientific & Technical.

Devine, J.D., Murphy, M.D., Rutherford, M.J., Barclay, J., Sparks, R.S.J., Carroll, M.R., Young, S.R., Gardner, J.E., 1998. Petrologic evidence for pre-eruptive pressure-temperature conditions, and recent reheating, of andesitic magma erupting at the Soufriere Hills Volcano, Montserrat, WI. Geophys Res Lett 25, 3669-3672.

Devine, J.D., Rutherford, M.J., 2014. Magma storage region processes of the Soufriere Hills Volcano, Montserrat. Geol Soc Mem 39, 361-381.

Devine, J.D., Rutherford, M.J., Norton, G.E., Young, S.R., 2003. Magma storage region processes inferred from geochemistry of Fe-Ti oxides in andesitic magma, Soufriere Hills Volcano, Montserrat, WI. J Petrol 44, 1375-1400.

Dohmen, R., Blundy, J., 2014. A Predictive Thermodynamic Model for Element Partitioning between Plagioclase and Melt as a Function of Pressure, Temperature and Composition. Am J Sci 314, 1319-1372.

Druitt, T.H., Costa, F., Deloule, E., Dungan, M., Scaillet, B., 2012. Decadal to monthly timescales of magma transfer and reservoir growth at a caldera volcano. Nature 482, 77-U97.

Edmonds, M., Kohn, S.C., Hauri, E.H., Humphreys, M.C.S., Cassidy, M., 2016. Extensive, water-rich magma reservoir beneath southern Montserrat. Lithos 252, 216-233.

Edmonds M, Woods AW (2018) Exsolved volatiles in magma reservoirs J Volcanol Geoth Res

Eichelberger, J.C., 1980. Vesiculation of Mafic Magma during Replenishment of Silicic Magma Reservoirs. Nature 288, 446-450.

Fabbro, G.N., Druitt, T.H., Costa, F., 2017. Storage and Eruption of Silicic Magma across the Transition from Dominantly Effusive to Caldera-forming States at an Arc Volcano (Santorini, Greece). J Petrol 58, 2429-2464.

Feeley, T.C., Dungan, M.A., 1996. Compositional and dynamic controls on mafic-silicic magma interactions at continental arc volcanoes: Evidence from Cordon El Guadal, Tatara San Pedro Complex, Chile. J Petrol 37, 1547-1577.

Flaherty, T., Druitt, T.H., Tuffen, H., Higgins, M.D., Costa, F., Cadoux, A., 2018. Multiple timescale

constraints for high-flux magma chamber assembly prior to the Late Bronze Age eruption of Santorini (Greece). Contrib Mineral Petr 173.

Harford, C.L., Pringle, M.S., Sparks, R.S.J., Young, S.R., 2002. The volcanic evolution of Montserrat using ⁴⁰Ar/³⁹Ar geochronology. Geological Society, London, Memoirs 21, 93-113.

Higgins, M.D., Roberge, J., 2003. Crystal size distribution of plagioclase and amphibole from Soufriere Hills volcano, Montserrat: Evidence for dynamic crystallization-textural coarsening cycles. J Petrol 44, 1401-1411.

Humphreys, M.C.S., Christopher, T., Hards, V., 2009. Microlite transfer by disaggregation of mafic inclusions following magma mixing at SoufriSre Hills volcano, Montserrat. Contrib Mineral Petr 157, 609-624.

Humphreys, M.C.S., Edmonds, M., Christopher, T., Hards, V., 2010. Magma hybridisation and diffusive exchange recorded in heterogeneous glasses from Soufriere Hills Volcano, Montserrat. Geophys Res Lett 37.

Humphreys, M.C.S., Edmonds, M., Plail, M., Barclay, J., Parkes, D., Christopher, T., 2013. A new method to quantify the real supply of mafic components to a hybrid andesite. Contrib Mineral Petr 165, 191-215.

Kahl, M., Chakraborty, S., Costa, F., Pompilio, M., 2011. Dynamic plumbing system beneath volcanoes revealed by kinetic modeling, and the connection to monitoring data: An example from Mt. Etna. Earth Planet Sc Lett 308, 11-22.

Kahl, M., Chakraborty, S., Costa, F., Pompilio, M., Liuzzo, M., Viccaro, M., 2013. Compositionally zoned crystals and real-time degassing data reveal changes in magma transfer dynamics during the 2006 summit eruptive episodes of Mt. Etna. B Volcanol 75.

Kent, A.J.R., Darr, C., Koleszar, A.M., Salisbury, M.J., Cooper, K.M., 2010. Preferential eruption of andesitic magmas through recharge filtering. Nat Geosci 3, 631-636.

Komorowski, J.C., Legendre, Y., Christopher, T., Bernstein, M., Stewart, R., Joseph, E., Fournier, N., Chardot, L., Finizola, A., Wadge, G., Syers, R., Williams, C., Bass, V., 2010. Insights into processes and deposits of hazardous vulcanian explosions at Soufriere Hills Volcano during 2008 and 2009 (Montserrat, West Indies). Geophys Res Lett 37.

Longpre, M.A., Stix, J., Costa, F., Espinoza, E., Munoz, A., 2014. Magmatic Processes and Associated Timescales Leading to the January 1835 Eruption of Cosiguina Volcano, Nicaragua. J Petrol 55, 1173-1201.

Mann CP, Wallace PJ, Stix J (2013) Phenocryst-hosted melt inclusions record stalling of magma during ascent in the conduit and upper magma reservoir prior to vulcanian explosions, Soufriere Hills volcano, Montserrat, West Indies Bulletin of Volcanology 75 doi:ARTN 687 10.1007/s00445-013-0687-4

Mann (2010). Magma chamber dynamics at Soufriere Hills volcano, Montserrat. PhD Thesis submitted to McGill University, Montreal, Quebec.

McGee L et al. (2019) Volatile behaviour in the 1995-2010 eruption of the Soufriere Hills Volcano, Montserrat recorded by U-series disequilibria in mafic enclaves and andesite host Earth and Planetary Science Letters 524 doi:UNSP 115730 10.1016/j.epsl.2019.115730

Minster, J.B., Jordan, T.H., 1978. Present-Day Plate Motions. J Geophys Res 83, 5331-5354.

Murphy, M.D., Sparks, R.S.J., Barclay, J., Carroll, M.R., Brewer, T.S., 2000. Remobilization of andesite magma by intrusion of mafic magma at the Soufriere Hills Volcano, Montserrat, West Indies. J Petrol 41, 21-42.

Murphy, M.D., Sparks, R.S.J., Barclay, J., Carroll, M.R., Lejeune, A.M., Brewer, T.S., Macdonald, R., Black, S., Young, S., 1998. The role of magma mixing in triggering the current eruption at the Soufriere Hills volcano, Montserrat, West Indies. Geophys Res Lett 25, 3433-3436.

Oldenburg, C.M., Spera, F.J., Yuen, D.A., Sewell, G., 1989. Dynamic Mixing in Magma Bodies - Theory, Simulations, and Implications. J Geophys Res-Solid 94, 9215-9236.

Pichavant, M., Martel, C., Bourdier, J.L., Scaillet, B., 2002. Physical conditions, structure, and dynamics of a zoned magma chamber: Mount Pelee (Martinique, Lesser Antilles Arc). J Geophys Res-Sol Ea 107.

Pichavant M, Poussineau S, Lesne P, Solaro C, Bourdier JL (2018) Experimental Parametrization of Magma Mixing: Application to the AD 1530 Eruption of La Soufriere, Guadeloupe (Lesser Antilles) Journal of Petrology 59:257-281 doi:10.1093/petrology/egy030.

Plail, M., Barclay, J., Humphreys, M.C.S., Edmonds, M., Herd, R.A., Christopher, T.E., 2014. Characterization of mafic enclaves in the erupted products of Soufriere Hills Volcano, Montserrat,

2009 to 2010. Geol Soc Mem 39, 343-360.

Plail, M., Edmonds, M., Woods, A.W., Barclay, J., Humphreys, M.C.S., Herd, R.A., Christopher, T., 2018. Mafic enclaves record syn-eruptive basalt intrusion and mixing. Earth Planet Sc Lett 484, 30-40.

Putirka, K.A., 2005. Igneous thermometers and barometers based on plagioclase plus liquid equilibria: Tests of some existing models and new calibrations. Am Mineral 90, 336-346.

Rae, A.S.P., Edmonds, M., Maclennan, J., Morgan, D., Houghton, B., Hartley, M.E., Sides, I., 2016. Time scales of magma transport and mixing at Kilauea Volcano, Hawai'i. Geology 44, 463-466.

Ruprecht, P., Worner, G., 2007. Variable regimes in magma systems documented in palgioclase zoning patterns: El Misti stratovolcano and Andahua monogenetic cones. J Volcanol Geoth Res 165, 142-162.

Ryan, G.A., Loughlin, S.C., James, M.R., Jones, L.D., Calder, E.S., Christopher, T., Strutt, M.H., Wadge, G., 2010. Growth of the lava dome and extrusion rates at Soufriere Hills Volcano, Montserrat, West Indies: 2005-2008. Geophys Res Lett 37.

Sato, H., Holtz, F., Behrens, H., Botcharnikov, R., Nakada, S., 2005. Experimental petrology of the 1991-1995 Unzen dacite, Japan. Part II: Cl/OH partitioning between hornblende and melt and its implications for the origin of oscillatory zoning of hornblende phenocrysts. J Petrol 46, 339-354.

Scaillet, B., Whittington, A., Martel, C., Pichavant, H., Holtz, F., 2000. Phase equilibrium constraints on the viscosity of silicic magmas II: implications for mafic-silicic mixing processes. T Roy Soc Edin-Earth 91, 61-72.

Schleicher, J.M., Bergantz, G.W., 2017. The Mechanics and Temporal Evolution of an Open-system Magmatic Intrusion into a Crystal-rich Magma. J Petrol 58, 1059-1072.

Singer, B.S., Costa, F., Herrin, J.S., Hildreth, W., Fierstein, J., 2016. The timing of compositionally-zoned magma reservoirs and mafic 'priming' weeks before the 1912 Novarupta-Katmai rhyolite eruption. Earth Planet Sc Lett 451, 125-137.

Sparks, R.S.J., Murphy, M.D., Lejeune, A.M., Watts, R.B., Barclay, J., Young, S.R., 2000. Control on the emplacement of the andesite lava dome of the Soufriere Hills volcano, Montserrat by

degassing-induced crystallization. Terra Nova 12, 14-20.

Sparks, S.R.J., Sigurdsson, H., Wilson, L., 1977. Magma Mixing - Mechanism for Triggering Acid Explosive Eruptions. Nature 267, 315-318.

Tomiya, A., Takahashi, E., 2005. Evolution of the magma chamber beneath Usu volcano since 1663: A natural laboratory for observing changing phenocryst compositions and textures. J Petrol 46, 2395-2426.

Trial, A.F., Spera, F.J., 1990. Mechanisms for the Generation of Compositional Heterogeneities in Magma Chambers. Geol Soc Am Bull 102, 353-367.

Turner, S., Costa, F., 2007. Measuring timescales of magmatic evolution. Elements 3, 267-272.

Wadge, G., Voight, B., Sparks, R.S.J., Cole, P.D., Loughlin, S.C., Robertson, R.E.A., 2014. An overview of the eruption of Soufriere Hills Volcano, Montserrat from 2000 to 2010. Geol Soc Mem 39, 1-39.

Young, S.R., Sparks, R.S.J., Aspinall, W.P., Lynch, L.L., Miller, A.D., Robertson, R.E.A., Shepherd, J.B., 1998. Overview of the eruption of Soufriere Hills volcano, Montserrat, 18 July 1995 to December 1997. Geophys Res Lett 25, 3389-3392.

Zellmer, G.F., Hawkesworth, C.J., Sparks, R.S.J., Thomas, L.E., Harford, C.L., Brewer, T.S., Loughlin, S.C., 2003a. Geochemical evolution of the Soufriere Hills volcano, Montserrat, Lesser Antilles volcanic arc. J Petrol 44, 1349-1374.

Zellmer, G.F., Sparks, R.S.J., Hawkesworth, C.J., Wiedenbeck, M., 2003b. Magma emplacement and remobilization timescales beneath Montserrat: Insights from Sr and Ba zonation in plagioclase phenocrysts. J Petrol 44, 1413-1431.

Appendix A

A.1. One-Stage model

Xan = Position of anorthite profile points
C_mes = Measured Mg
dx = distance between each point
T = temperature in Kelvin
A = Parameter from partition coefficient equation
B = Parameter from partition coefficient equation
dt = Time step in seconds
tf = Time frame
Err_Mg = Error of Mg from microprobe analyses

WINDOW 1: main

```
function [Cmg]= main(C_init,Dmg,dDmg_dx,dXan_dx, Art,d2Xan_dx2,dt,dx,Out_Bc)
C_init(1)=Out_Bc;
C_init = [Out_Bc C_init C_init(end)];

dCmg_dx   = diff(C_init)/dx;          % first derivative
d2Cmg_dx2 = diff(C_init,2)/dx^2;      % second derivative


%arranging vector size (ignore first and last elemenets)

C_init    = C_init(2:end-1);
dCmg_dx   = dCmg_dx(2:end);


dCmg_dt= (Dmg .* d2Cmg_dx2) + (dCmg_dx .* dDmg_dx) ...
      - Art*( (Dmg .* dCmg_dx .* dXan_dx) ...
      + (C_init .* dDmg_dx .*dXan_dx )+ (Dmg.*C_init.*d2Xan_dx2));

Cmg = dt*dCmg_dt+C_init;
```

WINDOW 2: diffusion

```
function Cmg=diffusion(Xan,C_init,dt,tf,T,dx,Out_Bc)
% This function made for one stage diffusion

% set constants and time parameters
R    = 8.3144621;
A    = -26100;
T    = T+273;

% find the number of measurements
[~,m]    = size(Xan);

% create empty matrix and vectors
Cmg      = zeros(tf,m);

% make Xan symetric for second derivative calculation
Xan  = [Xan(1) Xan Xan(end)];

% calculate Dmg using Van Orman et al., (2014)  and Check if r is within range
Dmg      = (exp(-6.06 - 7.96 * Xan - (287000 /(R*T))))*10^12;
```

```
if (dt/dx^2)*max(Dmg)>0.5
   errordlg('r is too big');
   return;
end

Cmg(1,:) = C_init;

%calculate derivatives
dDmg_dx          = diff(Dmg)/dx;
dXan_dx          = diff(Xan)/dx;
d2Xan_dx2        = diff(Xan, 2)/dx^2;

%arrange vector sizes
dDmg_dx          = dDmg_dx(2:end);
dXan_dx          = dXan_dx(2:end);
Dmg              = Dmg(2:end-1);

%to increase the speed calculate Art once
Art = (A /(R*T));

%Function takes Cmg values at time is equal to t and returns Cmg at time
%is equal to t+dt
for i=2:tf
   Cmg(i,:)= main(Cmg(i-1,:),Dmg,dDmg_dx,dXan_dx, Art,d2Xan_dx2,dt,dx,Out_Bc);
end
```

WINDOW3: one stage model

```
function Ceq=onestage(Xan,boundary1,Melt1,Melt2,Tk1,Tk2)

% constants and time parameters
R   = 8.3144621;
A   = -26100;
B   = -25700;

% find the number of measurements
[~,m]   = size(Xan);
Tk      = zeros(1,m);

% create empty matrix and vectors
Ceq     = zeros(1,m);

% set equilibrium temperature in Kelvin and find K
Tk(1:boundary1)     = Tk2 + 273;   % stage 2
Tk(boundary1+1:end) = Tk1 + 273;   % stage 1

K = exp((A*Xan+B)./(R*Tk));

% calculate equilibrium curve
Ceq(1:boundary1)     = Melt2 * K(1:boundary1);      %stage 2
Ceq(boundary1+1:end) = Melt1 * K(boundary1+1:end);  %stage 1
```

WINDOW 4:crystal selected

```
filename='E1 Data';

% read from excel sheet
data      = xlsread(filename);
Xan       = data(:,3)';
Cmes      = data(:,5)';
Err_Mg    = data(:,22)';


% find the number of measurements
[~,m]     = size(Xan);
C_init    = zeros(1,m);


% ========== constants for equilibrium ================== %
boundary1 = 12;
Tk1       = 1050;   % temperature for stage 1
Melt1                = 5;    % equilibrium coefficient C liqu- stage1

% ========= constants for diffusion ====================== %
dt        = 60;
tf        = 60*24*20;
dx        = 1;
Td1       =  850;
Td2       =  1050;

% =========== Smooth Data ================================ %
Xan       = (smooth(Xan,0.1,'rlowess'))';
Cmes      = (smooth(Cmes,0.1,'rlowess'))';


% ================== Equilibrium ========================= %
Ceq       = onestage(Xan,boundary1,Melt1,Tk1);
Ceq       = (smooth(Ceq,5.9,'rlowess'))';
Out_Bc    = 0.09;

% ================ initial condition ==================== %
max_val              = 0.09;
min_val              = 0.029;
C_init(1:boundary1)          = max_val;
C_init(boundary1+1:end)  = min_val;


m         = size(Cmes,2);
x         =1:m;
Cmes_up              =Cmes+Err_Mg.*Cmes/100;
Cmes_low             =Cmes-Err_Mg.*Cmes/100;
figure

fill([x fliplr(x)],[Cmes_up fliplr(Cmes_low)], [.8 .8 .8], 'linestyle', 'none')

hold on
plot(C_init,'k--','LineWidth',1.5)
% grid on
% grid minor
set(gca,'YTick',0:0.01:0.15);
```

```
hold on
plot(Ceq, 'k')
hold on
plot(Cmes, 'k-o')
hold on

% ============== Diffusion ========================== %

Cmg1    = mydiffusion(Xan,C_init,dt,tf,Td1,dx,Out_Bc);
Cmg2    = mydiffusion(Xan,C_init,dt,tf,Td2,dx,Out_Bc);

[stratc,endc] = size(Cmg2);
Cmg3    =zeros(1,endc);
Cmg3(1:boundary1)          =Cmg2(60*24*365*3,1:boundary1);
Cmg3(boundary1+1:endc)              =Cmg1(60*24*365*18,boundary1+1:endc);
Cmg3    = (smooth(Cmg3,9,'rlowess'))';

plot(Cmg1(60*24*20,:),'r','LineWidth',1.5) %
hold on

 title([filename ' E1'])
legend('EMPA data uncertanity','initial condition','equi curve','EMPA data','T=850C','T=1050C','Location',
'northeast', 'Orientation', 'vertical')
```

A.2. Two-Stage model

Xan = Position of anorthite profile points
C_mes = Measured Mg
dx = distance between each point
T = temperature in Kelvin
A = Parameter from partition coefficient equation
B = Parameter from partition coefficient equation
dt = Time step in seconds
tf = Time frame
Err_Mg = Error of Mg from microprobe analyses

WINDOW 1: main

```
function [Cmg]= main(C_init,Dmg,dDmg_dx,dXan_dx, Art,d2Xan_dx2,dt,dx,Out_Bc)
C_init(1)=Out_Bc;
C_init = [Out_Bc C_init C_init(end)];

dCmg_dx   = diff(C_init)/dx;          % first derivative
d2Cmg_dx2 = diff(C_init,2)/dx^2;      % second derivative


%arranging vector size (ignore first and last elemenets)

C_init    = C_init(2:end-1);
dCmg_dx   = dCmg_dx(2:end);


dCmg_dt= (Dmg .* d2Cmg_dx2) + (dCmg_dx .* dDmg_dx) ...
      - Art*( (Dmg .* dCmg_dx .* dXan_dx) ...
      + (C_init .* dDmg_dx .*dXan_dx )+ (Dmg.*C_init.*d2Xan_dx2));

Cmg = dt*dCmg_dt+C_init;
```

WINDOW 2: diffusion

```
function Cmg=diffusion(Xan,C_init,dt,tf,T,dx,Out_Bc)
% This function made for two stages diffusion

% set constants and time parameters
R    = 8.3144621;
A    = -26100;
T    = T+273;

% find the number of measurements
[~,m]    = size(Xan);

% create empty matrix and vectors
Cmg      = zeros(tf,m);

% make Xan symetric for second derivative calculation
Xan  = [Xan(1) Xan Xan(end)];

% calculate Dmg using Van Orman et al., (2014)  and Check if r is within range
Dmg      = (exp(-6.06 - 7.96 * Xan - (287000 /(R*T))))*10^12;
```

```
if (dt/dx^2)*max(Dmg)>0.5
   errordlg('r is too big');
   return;
end

Cmg(1,:) = C_init;

%calculate derivatives
dDmg_dx          = diff(Dmg)/dx;
dXan_dx          = diff(Xan)/dx;
d2Xan_dx2        = diff(Xan, 2)/dx^2;

%arrange vector sizes
dDmg_dx          = dDmg_dx(2:end);
dXan_dx          = dXan_dx(2:end);
Dmg              = Dmg(2:end-1);

%to increase the speed calculate Art once
Art = (A /(R*T));

%Function takes Cmg values at time is equal to t and returns Cmg at time
%is equal to t+dt
for i=2:tf
   Cmg(i,:)= main(Cmg(i-1,:),Dmg,dDmg_dx,dXan_dx, Art,d2Xan_dx2,dt,dx,Out_Bc);
end
```

WINDOW3: two stages model

```
function Ceq=twostages(Xan,boundary1,Melt1,Melt2,Tk1,Tk2)

% constants and time parameters
R   = 8.3144621;
A   = -26100;
B   = -25700;

% find the number of measurements
[~,m]     = size(Xan);
Tk        = zeros(1,m);

% create empty matrix and vectors
Ceq     = zeros(1,m);

% set equilibrium temperature in Kelvin and find K
Tk(1:boundary1)          = Tk2 + 273;   % stage 2
Tk(boundary1+1:end)      = Tk1 + 273;   % stage 1

K = exp((A*Xan+B)./(R*Tk));

% calculate equilibrium curve
Ceq(1:boundary1)         = Melt2 * K(1:boundary1);     %stage 2
Ceq(boundary1+1:end)     = Melt1 * K(boundary1+1:end);  %stage 1
```

WINDOW 4:crystal selected

```
filename='H2 Data';

% read from excel sheet
data      = xlsread(filename);
Xan       = data(:,3)';
Cmes      = data(:,5)';
Err_Mg    = data(:,22)';


% find the number of measurements
[~,m]     = size(Xan);
C_init    = zeros(1,m);


% ============constants for equilibrium ================== %
boundary1          = 13;
boundary2          = 6;       % must be smaller then boundary 1
Tk1                = 1020;    % temperature for stage 1
Tk2                = 1020;    % temperature for stage 2
Tk3                = 950;     % temperature for stage 3
Melt1              = 2.3;     % equilibrium coefficient C liqu- stage1
Melt2              = 2.3;     % equilibrium coefficient - stage2
Melt3              = 2.6;     % equilibrium coefficient - stage3


% ============constants for diffusion ==================== %
dt        = 60;                  % time step
tf        = 60*24*365*20;        % time frame -
dx        = 1;                   % distance between  locations
Td1       =  1000;               % before boundary
Td2       =  1050;               % after boundary


% =============Smooth Data ============================== %
Xan       = (smooth(Xan,0.05,'rlowess'))';
Cmes      = (smooth(Cmes,0.05,'rlowess'))';

% ============ Equilibrium ============================== %
Ceq       = twostage(Xan,boundary1,Melt1,Melt2,Tk1,Tk2);
Ceq       = (smooth(Ceq,10,'rlowess'))';
Out_Bc    = 0.04;

% ============= Initial Condition ======================== %
max_val            = 0.06;
min_val            = 0.017;
C_init(1:boundary1)          = max_val;
C_init(boundary1+1:end)  = min_val;


m = size(Cmes,2);
x=1:m;
Cmes_up=Cmes+Err_Mg.*Cmes/100;
Cmes_low=Cmes-Err_Mg.*Cmes/100;
figure

fill([x fliplr(x)],[Cmes_up fliplr(Cmes_low)], [.8 .8 .8], 'linestyle', 'none')
```

```
hold on
plot(C_init,'k--','LineWidth',1.5) %initial condition
grid on
grid minor
set(gca,'YTick',0:0.01:0.15);
hold on
plot(Ceq, 'b') % equilibrium curve
hold on
plot(Cmes, 'k-o') % microprobe data
hold on

% ================= Diffusion ====================== %

Cmg1 = mydiffusion2(Xan,C_init,dt,tf,Td1,dx,Out_Bc);
Cmg2 = mydiffusion2(Xan,C_init,dt,tf,Td2,dx,Out_Bc);

 [stratc,endc]                 = size(Cmg2);
 Cmg3                          =zeros(1,endc);
 Cmg3(1:boundary1)             =Cmg2(60*24*365*3,1:boundary1);
 Cmg3(boundary1+1:endc)=Cmg1(60*24*365*18,boundary1+1:endc);
 Cmg3                          = (smooth(Cmg3,9,'rlowess'))';

plot(Cmg1(60*24*365*18,:),'g--','LineWidth',1.5)
hold on
plot(Cmg2(60*24*365*3,:),'c--','LineWidth',1.5)
hold on
plot(Cmg3, 'r-*', 'LineWidth',1.5)
hold on


title([filename ' Diffusion2'])
legend('EMPA data uncertanity','initial condition','EMPA data','Location', 'northeast', 'Orientation', 'vertical')
```

A3: Electron backscattered (BSE) images of MT35 rock. In red circles are highlighted the plagioclase phenocrysts in host andesite and in green the plagioclase from basaltic andesite enclave.

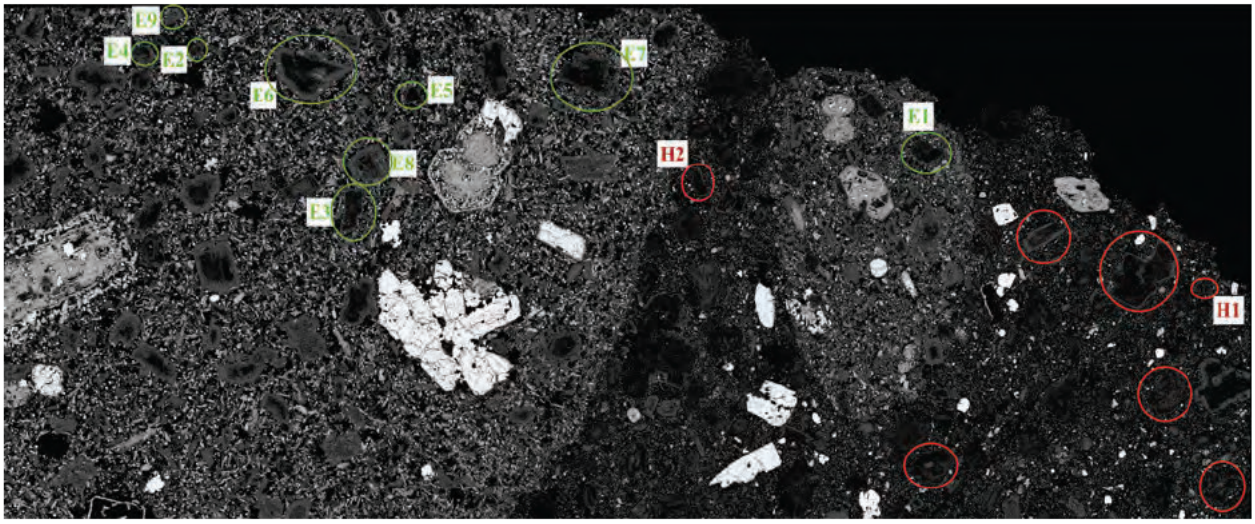

A4: A large backscattered electron image of section MT35 with Type I (blue) mostly found in the andesite host and Type II (red) predominant in the basaltic andesite.

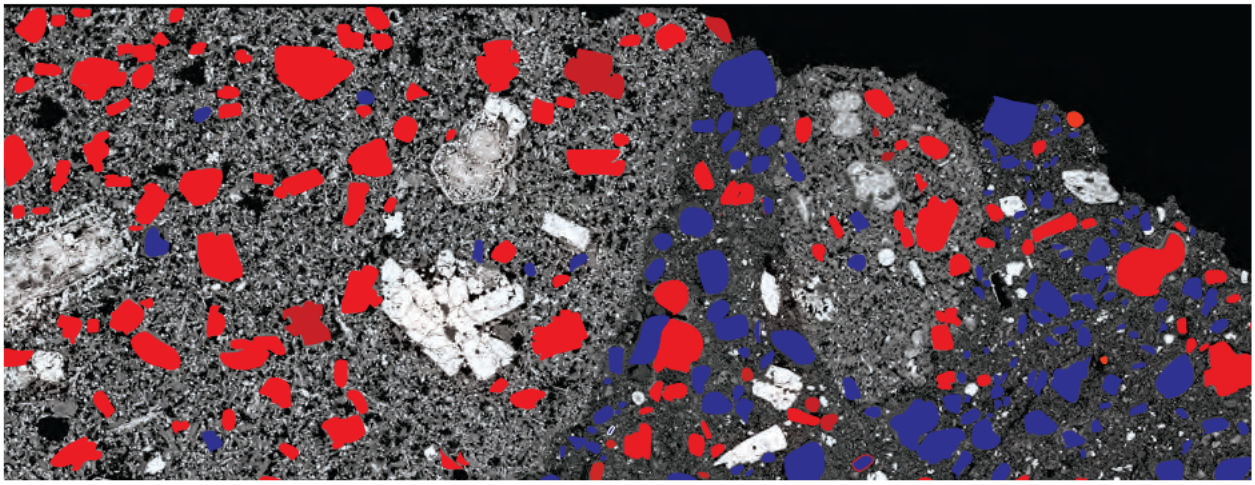

A5: Overview of all the temperature proposed in literature using different approachs

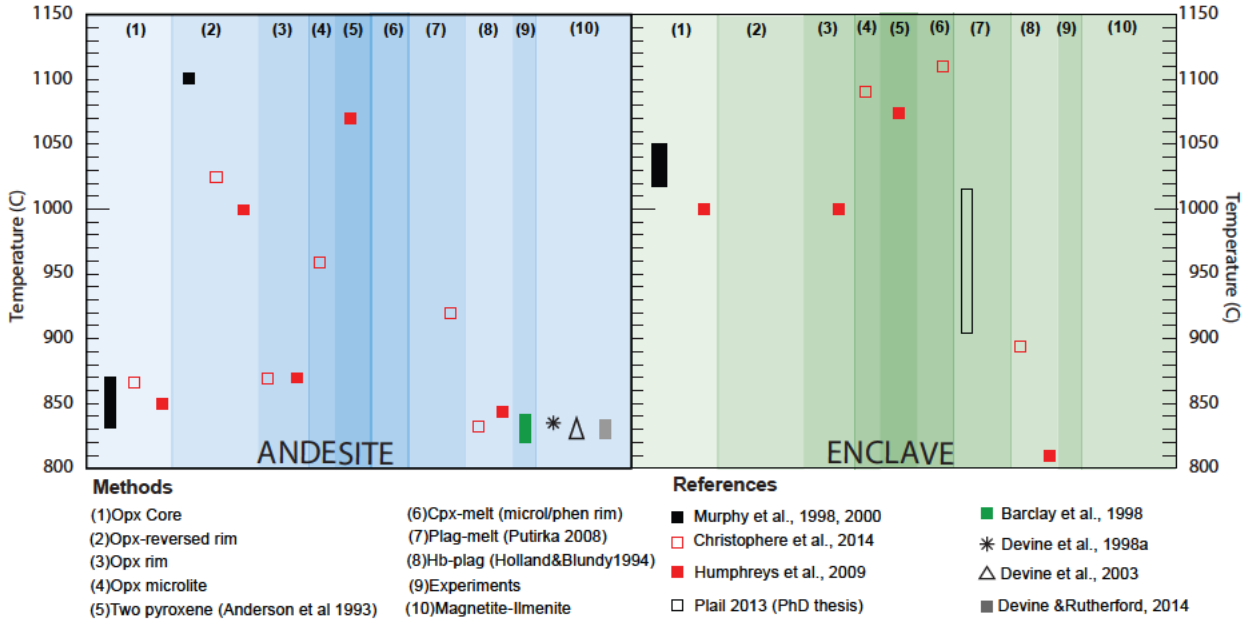

A6: A summary of phase equilibrium experiments from Couch et al. (2003) and Rutherford and Devine (2003) indicating the temperature of the liquid in equilibrium with specific plagioclase anorthite content.

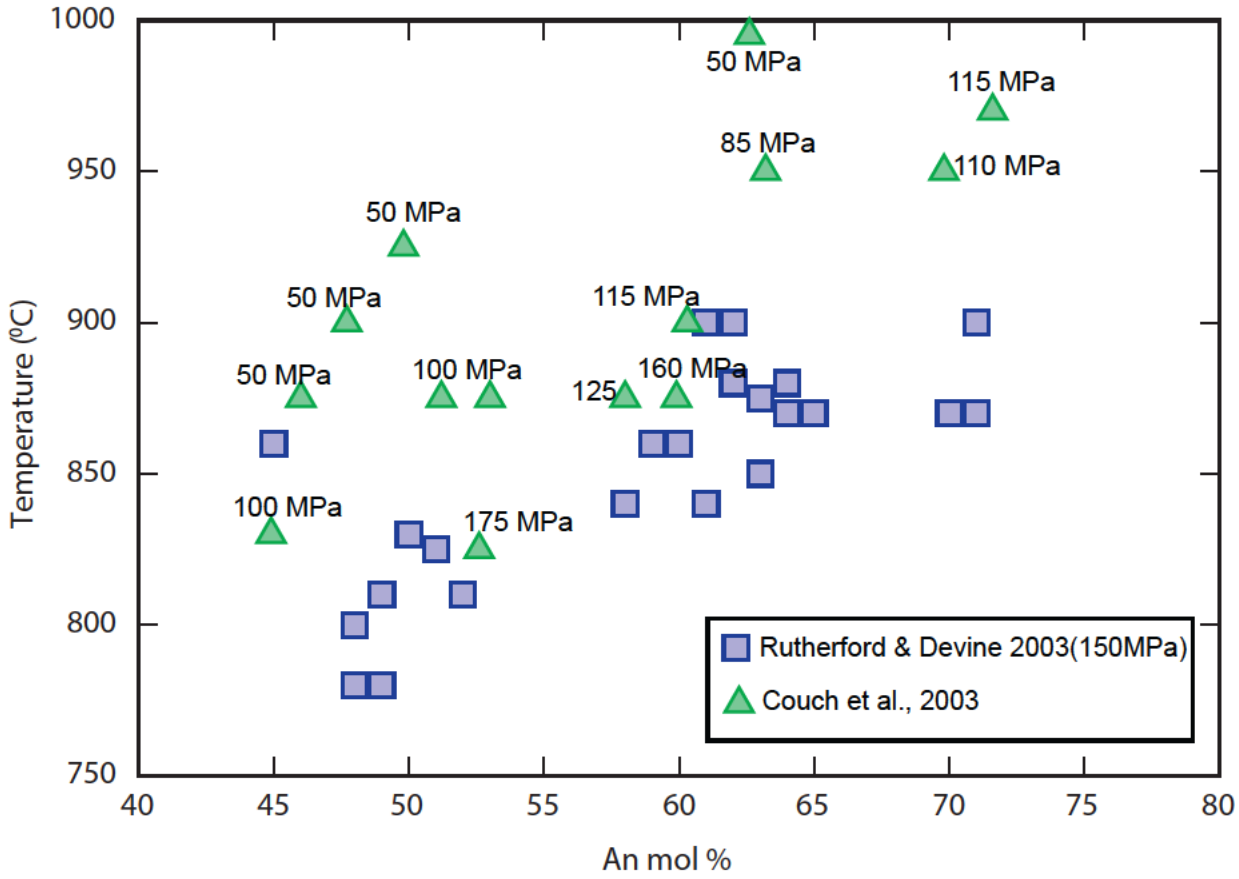

A7: FeO and MgO concentration against An content for interior part to the rim of plagioclase from host.

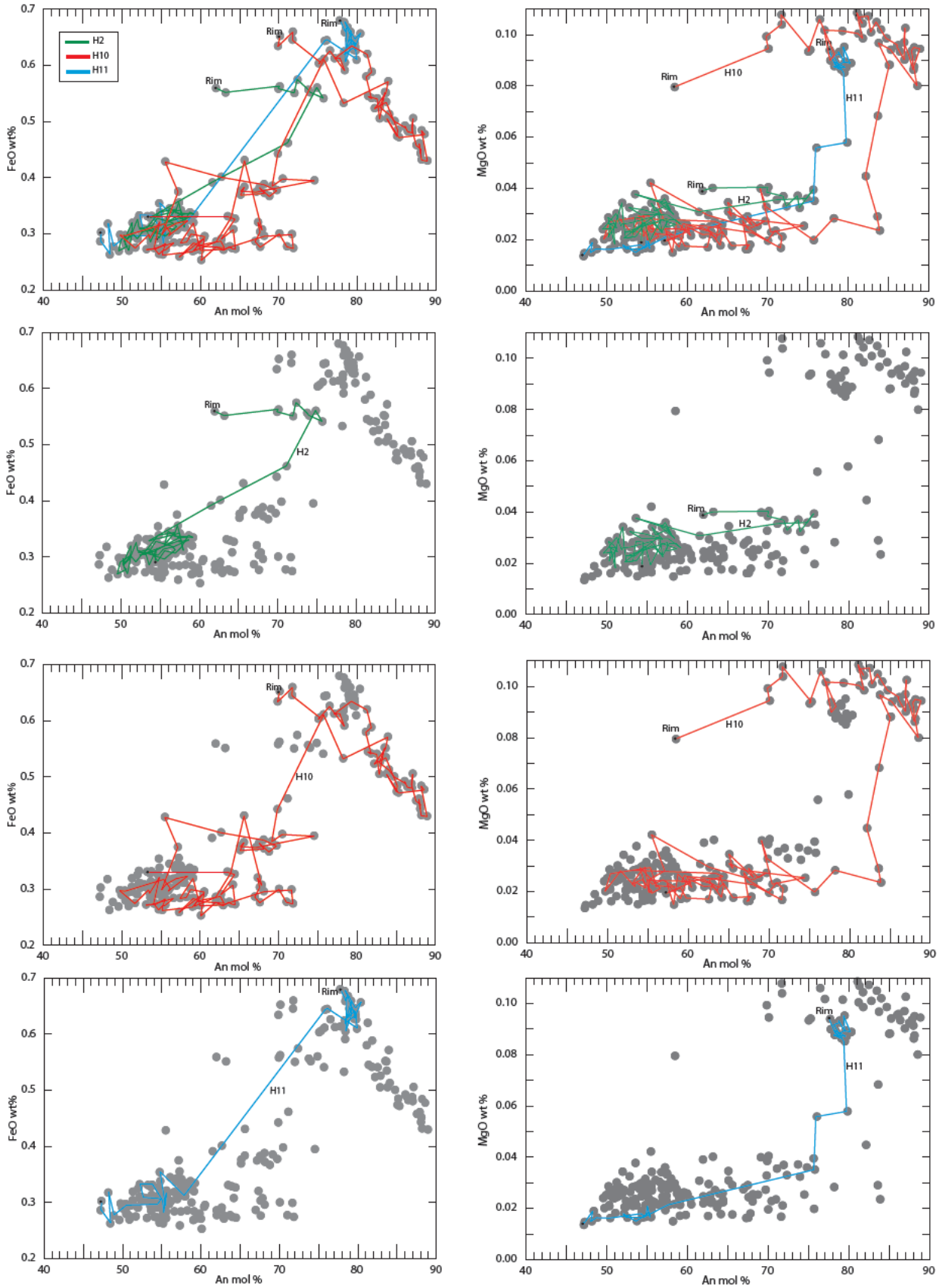

A8: Description of the two modelling approaches adopted in this study (e.g. crystal in enclave E1). (a) 1-step diffusion model of Mg at temperature of 1100°C for defined initial profile (dashed lines). The circles are the measured profile (using a distance space of 1µm each data point) with associated uncertainties from EMPA (grey area). A 1-step model at 1100°C gives a poor fit of maximum 2 hours for the whole crystal. (b) A 2-step model (blue squares) shows a better fit, where first happen the exchange between the interior part and the melt at 1100°C (7 days) followed by exchange the interior part, the rim and the melt at 1100°C (3 hours).

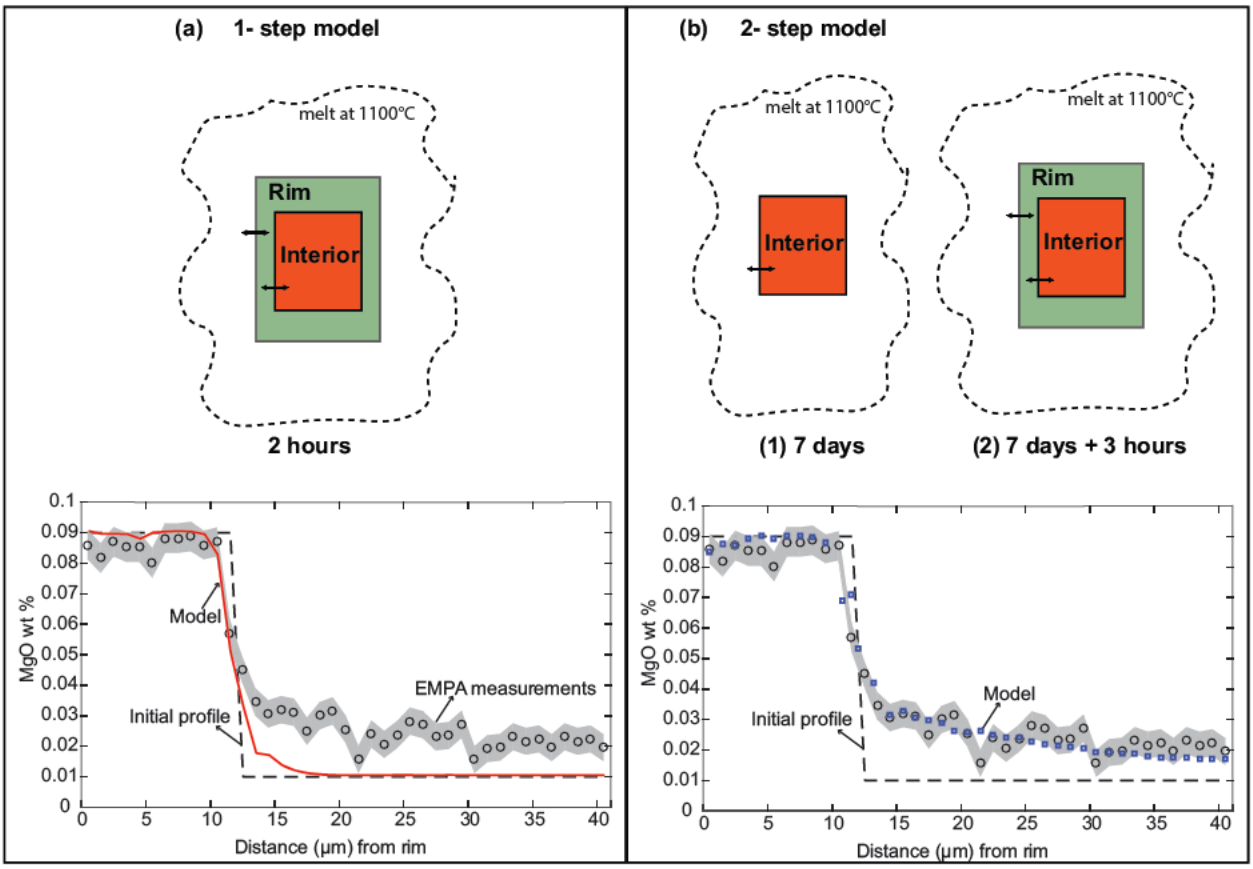

Chapter 3

Insights into the dynamics of magma mixing through texture and compositional zoning recorded in crystals: Gede Volcano as a case study

Rosa Didonna[1], Heather Handley[1], Rachel Bezard[2], Fidel Costa[3,4]

[1]*Department of Earth and Environmental Sciences, Macquarie University, Sydney, NSW, Australia*
[2]*Department of Geosciences, University of Tuebingen, Germany*
[3]*Earth Observatory of Singapore, Nanyang Technological University, Singapore*
[4]*Asian School of the Environment, Nanyang Technological University, Singapore*

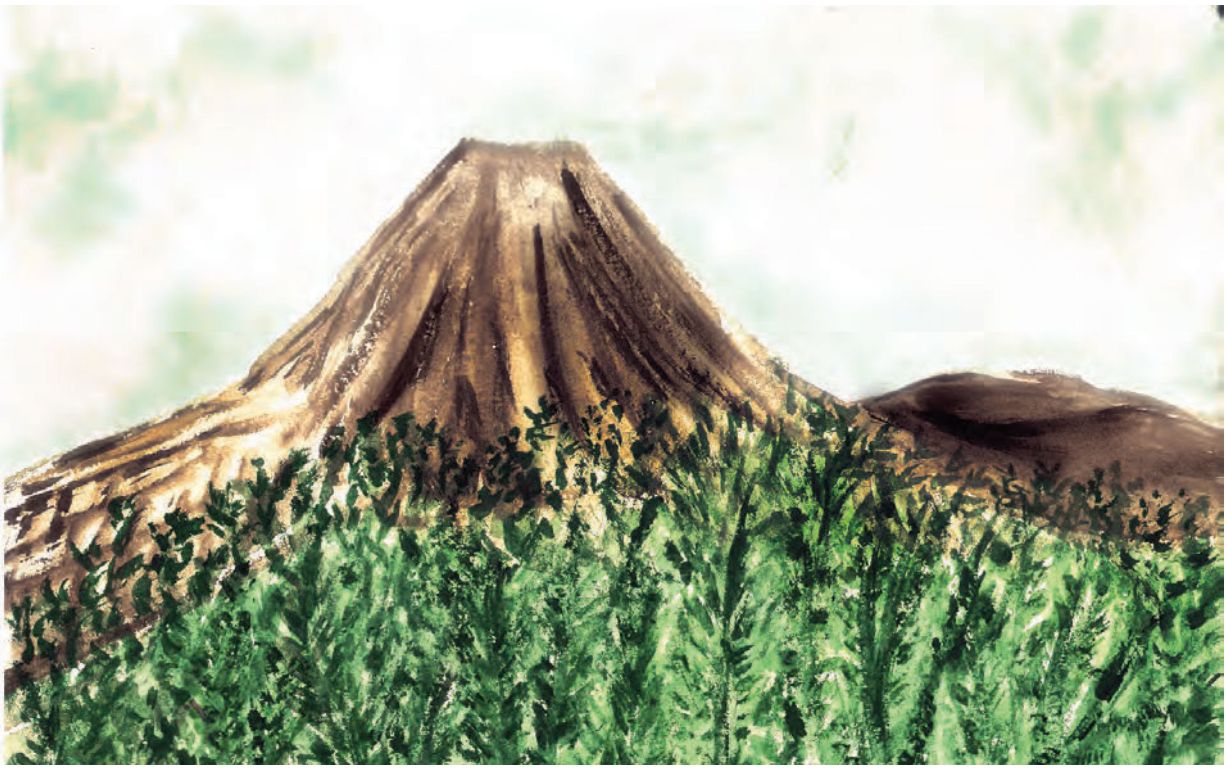

Gede Volcano, West Java, Indonesia- Watercolours- Rosa, 2016

Abstract

Understanding the relative importance of composition-modifying processes such as fractional crystallisation, crustal contamination and magma mixing in arc lavas is needed before the nature of the magmatic source can be established. The negative correlations observed between whole-rock Pb-Sr isotopic ratios and indices of differentiation (SiO_2) in Gede Volcanic Complex volcanic rocks (West Java, Indonesia) suggest a role for the assimilation of crustal material during magmatic differentiation. The negative trends may be attributed to: (1) increasing incorporation of less radiogenic material, such as more isotopically primitive arc rocks or ophiolitic oceanic crust (in the arc crust), during magmatic evolution or, (2) the lowest silica rocks have assimilated the most (by volume) radiogenic crustal material. The latter may represent assimilation of carbonate material, which has been implicated at other Javanese volcanoes (e.g., Merapi) and has important implications for the addition of crustal CO_2 to the magma volatile budget. To further investigate magmatic processes and the potential control of carbonate assimilation on whole-rock geochemical composition at Gede, we have conducted detailed textural and compositional (major and trace element) analysis of minerals within selected rocks along the assimilation trend. The major and trace element compositions and grain profiles in crystals present clear evidence for the interaction of distinct magmas. Reverse zoning in plagioclase and clinopyroxene along with clinopyroxene overgrowths on orthopyroxene suggest that influx of mafic magma is an important process at Gede and may trigger volcanic eruptions. Calculated melt compositions of plagioclase with different textures provide important constraints on the magmatic plumbing system at Gede Volcano and potential eruption triggers.

3.1. Introduction

The geochemical complexity of arc magma compositions and their history are expressed by a combination of multiple processes such as fractional crystallisation, crustal assimilation, magma injection, hybridization, mingling/mixing, and geochemical variation in their source (Davidson et al., 1987; Handley et al., 2014; Hawkesworth et al., 1991; Mcculloch and Gamble, 1991). Volcanic rocks in subduction zone reflect a wide range of magma compositions and only whole-rock analyses can provide "averaged" and representative results, which however are difficult to interpret. The identification of an individual process (e.g. magma mixing) is not straightforward, especially if the magma is completely hybridized. In order to achieve a more comprehensive understanding of these processes, petrological studies combine whole-rock data, mineral compositional data, and textural features of individual phenocrysts.

Compositional zoning in plagioclase, pyroxenes and other minerals are often investigated because their zoning is considered an indicator of the variability of the mineral-growth environment. This allows to trace the history of mineral crystallisation, which is strongly dependent on melt composition, pressure and temperature (Bachmann and Dungan, 2002; Browne et al., 2006b; Cortes et al., 2005; Costa et al., 2013; Fabbro et al., 2017; Feeley and Dungan, 1996; Gardner et al., 1995; Ginibre et al., 2002; Holland and Blundy, 1994; Holtz et al., 2005; Tsuchiyama and Takahashi, 1983).

Plagioclase crystals are frequently selected because they crystallise over a wide range of temperature, and because their persist as a stable crystallising phase throughout cooling and eruption. The compositional and textural zoning patterns are developed and preserved during primary growth due to the relatively slow CaAl-NaSi diffusion inter-change within the crystal structure (Grove et al., 1984).

In the present study, we analysed andesitic lavas from the Gede Volcano (Fig. 1; West Java, Indonesia) and compared Young Gede, Old Gede, Pangrango, Gegerbentang, and Older Quaternary volcanic deposits (Fig. 2). Investigation on zonation patterns and geochemical data on trace elements from phenocrysts of plagioclase, pyroxene and amphibole were conducted using electron microprobe analysis (EMPA) and laser ablation inductively coupled plasma mass spectrometry (LA ICP-MS).

Kinetic processes can be distinguished from the variation of compositional melts by considering the relative behaviour of compatible versus incompatible elements in plagioclase. The coupling between Ba and Sr variations within the crystals and the relative anorthite content can be useful tools to discriminate different magmatic processes such as fractional crystallisation and

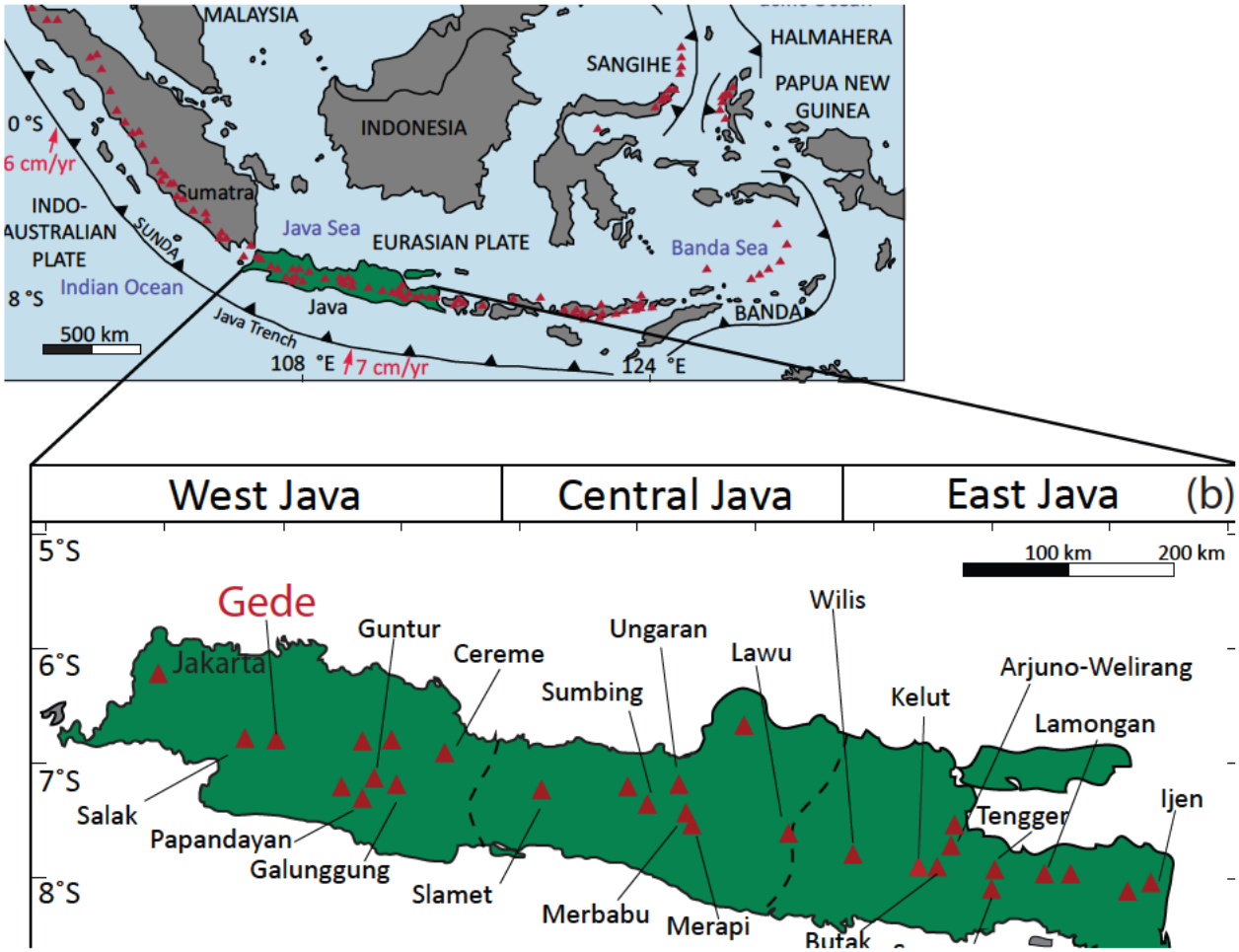

Figure 1: (a) Tectonic setting of Java within the Sunda arc, Indonesia (modified from Goode, 2018). Java trench (black line) is ascribed to the collision and subduction of ocean basement of the Indo-Australian Plate. (b) Map of Java with the location of major volcanoes and Gede Volcano (red font). Volcano names are consistent with those given by the Smithsonian Institution, Global Volcanism Program (http://www.volcano.si.edu/).

recharge events. In this work, we discuss the calculated variation of Ba and Sr melt concentrations variations associated with the crystal texture. The presence of macroscopic evidence of mixing members in the erupted rocks (e.g., banded texture with dark and light zones) makes this volcanic area a wonderful place to examine magmatic interactions and their correlated hybridisation results.

This volcanic area has a relevant importance in terms of volcanic hazard and risk mitigation, because it is located about 60 km south of Jakarta, the capital city of Indonesia with an estimated population of over 10 million of people. Studying how the magmatic system was working during the past eruptions could be an important improvement for providing more realistic future eruption scenarios.

3.2. Geological background

Gede Volcano is a part of Gede Volcanic Complex (GVC) in West Java (Handley et al., 2010) and is inside the Quaternary volcanic front of Sunda Arc (Fig. 1). The northward subduction of the Indo-Australian Plate beneath the Eurasian Plate created the Indonesian subduction system, and the Sunda arc is situated in its western part (Hamilton 1979). The first classification of the GVC was proposed by Neumann van Padang in 1951, which highlighted how the volcanic complex is principally composed by the twin stratovolcanoes of Pangrango (3,019 a.s.l.) to the north-northwest and Gede (2,958 m a.s.l.), which is the only active volcano of the complex.

More recently, a new classification scheme was proposed for the Southeast Asian volcanoes on the basis of volcano morphology, eruption history, and degassing style. Following this new classification, Gede Volcano is considered a "semi-plugged stratocone", based on the summit crater longer axis diameter (≤2500 m from remote sensing data), which is correlated on frequency and VEI's of eruptions and width of pyroclastic apron (Whelley et al., 2015).

Previous studies divided the stratigraphic and morphological deposits of Gede volcano

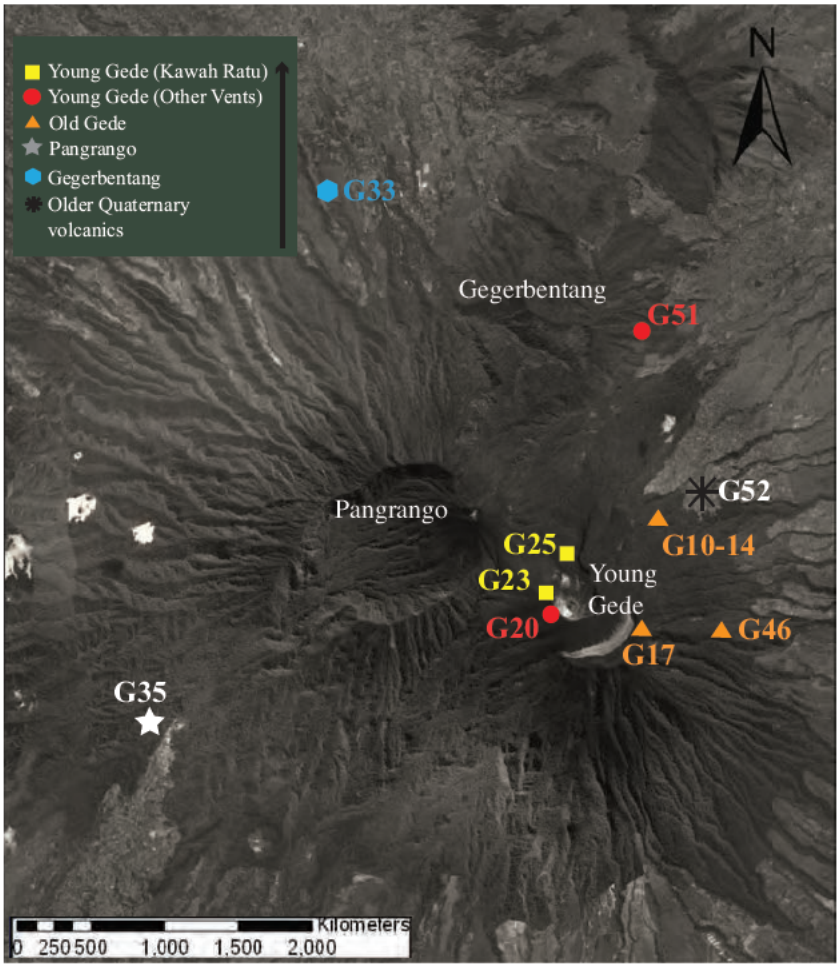

Figure 2: Location map of samples from the Old Quaternary to the Young Gede erupted deposits.

in Young and Old Gede (Situmorang and Hadisantono 1992). Gunung Gumuruh is the crater rim of Old Gede (50-200 m high), that is truncated by Young Gede to the north-west and also the largest (~1600 m in diameter) and oldest crater at Gede. The volcanic deposits of Old Gede are exposed on the south-eastern slope of Gede and form a deeply dissected morphology. Young Gede is marked by several smaller craters (Sela, Ratu, Lanang, Wadon and Baru) and most of the deposits are confined in relatively narrow belts, extending north-east and south-west of the summit due to the topographic highs of Pangrango-Marsigit and Old Gede in the northwest and southeast, respectively. According to recent studies (Belousov et al., 2015) these craters are not older than approximately 10 kyr, while the deposits of Old Gede are >45 kyr, dating back to the late Pleistocene (Situmorang and Hadisantono 1992). The Gegerbentang Complex consists of a series of eroded volcanoes lying to the north of Gede and relatively older than both Gede and Pangrango (Handley et al., 2010). The oldest deposits of Quaternary volcanic material (Older Quaternary Volcanic group) are exposed to the east and south west of Gede (Besar and Koncana, respectively). The basement rocks of the complex and surrounding area are dominated by Tertiary aged volcanogenic and marine sediments (Effendi et al. 1998; Handley et al., 2014).

The present morphology of the volcanic area shows clear evidence of different caldera collapse episodes. The summit of Gumuruh, for instance, has a horseshoe shape open in NNE direction. Volcanoclastic deposits studied by Belousov et al. (2015) do not show any characteristics of debris avalanche deposit of sufficient volume in the corresponding sector of the volcano that could explain the formation of the caldera by lateral gravitational collapse. For that reason, they suggested that this caldera was generated by vertical subsidence with consequent flank emission of lava.

Magmatic history of GVC is discussed in detail by Handley et al., (2010), Krimer (PhD thesis) and Belousov et al. (2015). In these studies, the eruptive history shows multiple episodes of fractional crystallisation and mingling/mixing processes, between basaltic and rhyodacite end-members or fractionation of a hybrid mafic magma. Moreover, basaltic andesite represents another end-member that produces andesite magma with clearly evidence of mingling events in the eruptive products. Textural and mineralogical studies suggested that the magmatic system is an open system with mixing/mingling between magmas, or between magmas and crystal rich-zones due to intrusion of more mafic magma in a crystal-rich silicic reservoir. Therefore, the intrusion of mafic magma could be the result of the periodic seismic crisis recorded at Gede in the last 20 years.

The most recent activities are recorded in deposits produced during the violent eruptions in 1840 and the 1955-57, characterised by phreatomagmatic episodes. Some of the youngest craters

(Kawah Lanang and Kawah Wadon) show hydrothermal activity. Most recently, seismic swarms were recorded in 2006, end of 2010, end of 2011, January-February 2012, and March-April 2012 (Hidayat et al., 2012).

3.3. Samples and Methods

For this study, petrographic analyses were performed on nine volcanic rock samples chosen to characterise different geochronologic units and compositions (Fig. 3), based on previous work by Handley et al. (2010). The youngest volcanic rocks (G23-G25) have been collected from Young Gede (Kawah Ratu) and are basaltic andesite-andesite in composition (Fig. 4). Sample G20 composition is basaltic andesite and represents the oldest deposits from Young Gede (Other Vents). Old Gede deposits (G11-G17, and G46) are basaltic andesites, with G14 the most evolved end-member sample that is andesite in composition.

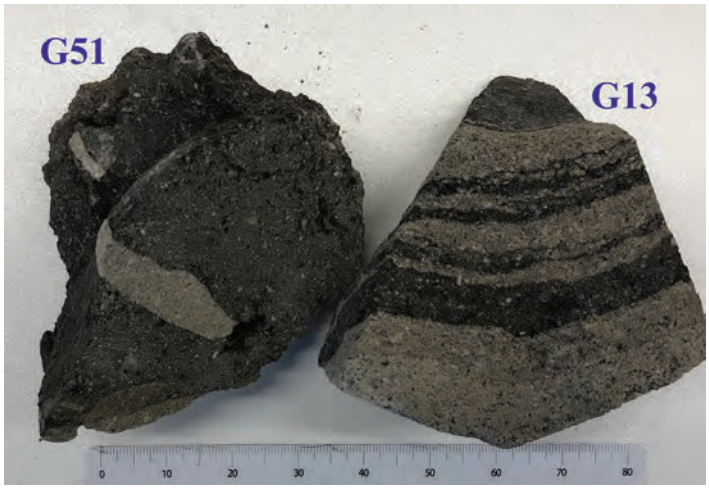

Figure 3: Juvenile scoria from pyroclystic flows that characterised Young Gede (G51) and Old Gede

The lowest silica end-member is represented by G35, a basalt from the twin volcanic centre, Pangrango. Sample G33 is from Gegerbentang, while G51 represents the oldest volcanic rocks in the complex, collected from the older Quaternary Volcanics group. Both these last are basaltic andesite in composition (Fig. 4).

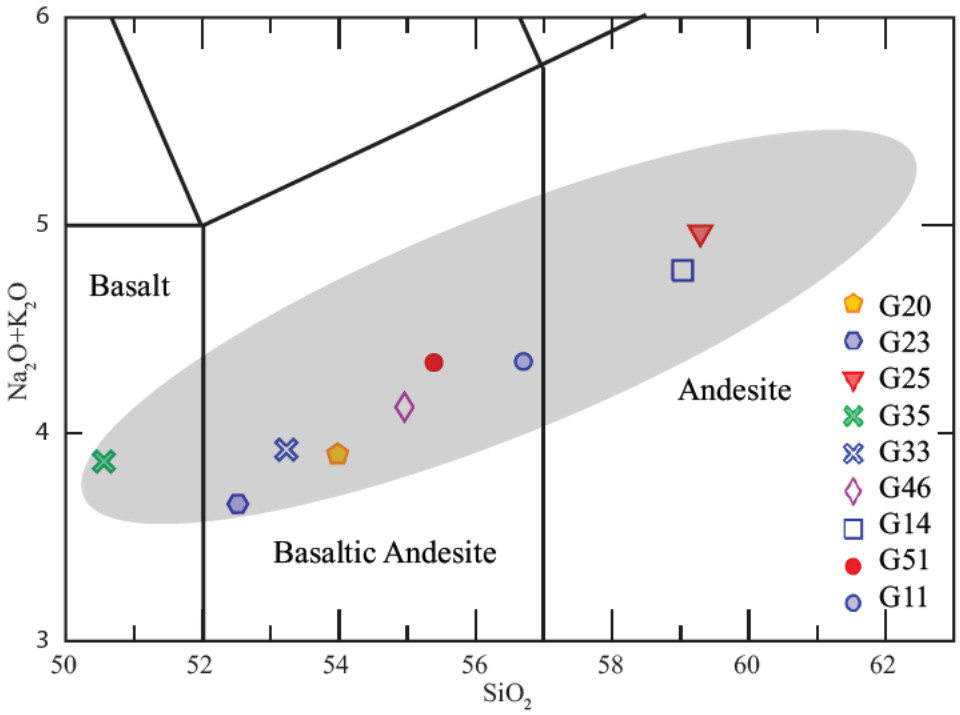

Figure 4: Whole rock compositions of the samples investigated in this study (from Handley et al. (2010). Composition range from basalt to more evolved andesite.

3.3.1. Scanning electron microscope (SEM) and electron microprobe (EMPA) analyses

Over 500 back-scattered electron (BSE) images were collected on thick sections using a Zeiss EVO MA15 Scanning Electron Microscope (SEM) at Macquarie University, with accelerating voltage of 15 kV. Plagioclase (~300 BSE images), clinopyroxene and othopyroxene (~100 BSE images), and olivine (5 BSE images) were investigated and the brightness and contrast in images of individual crystals were varied to accentuate the mineralogical textures. Major element compositions of the lava groundmass were determined using an energy dispersive spectrometer (X-max Oxford Instruments) attached to the Zeiss EVO scanning electron microscope at operating conditions of 20 kV and 8-10 nA. The spectrum was calibrated using a thin pure copper grid attached to each section analysed.

Compositional major element analyses were completed using a CAMECA SX100 electron microprobe (EMPA) at Macquarie University with an accelerating voltage of 15 kV, a 20 nA beam current and a beam diameter of 1-2 µm. The calibration was based on the following standards: orthoclase (K), wollastonite (Ca, Si), albite (Na), hematite (Fe), kyanite (Al), chromium (Cr), rutile (Ti), olivine (Mg). The data points (core-middle-rim) and compositional profile (from

core to rim) were selected with particular care due to the high amount of inclusions, cracks and resorbed areas within the crystals. In total, around 50 individual plagioclase crystals were analysed producing approximately 200 compositional data points. Around 50 data point measurements were carried out on 15 pyroxene crystals (clinopyroxene and orthopyroxene). Due to the low abundance of olivine in the rocks, only limited olivine compositional data was collected. Mineral symbols and members are used according to Deer et al. (1992): Anorthite content [%An =100 × molar Ca/(Na+Ca+K)] for plagioclase, Mg-number [Mg# =100 × molar Mg/(Mg+Fe*); where Fe* = is total iron] for olivine and pyroxene, moreover we calculated the end-members of pyroxene Enstatite (En), Ferrosilite (Fs) and Wollastonite (Wo). The whole dataset is included in electronic supplementary file B1.

3.3.2. In-situ trace element analysis by laser-ICP MS

Based on the combined petrographic SEM and EMPA data, a subset of samples containing the representative plagioclase and pyroxene textural types were selected for trace element analysis.The concentrations of in-situ trace element were determined using a New WaveUP-213 laser ablation system linked to an Agilent 7700 Series ICP-MS system at Macquarie University. Ablation of the samples was performed in a helium chamber using a frequency of 5 Hz and an ablation size of 55 μm for single spots, or a line 120 μm long and 30 μm wide, when rastering was needed. Concentrations and detection limits were obtained using GLITTER software (http://www.glitter-gemoc.com/). The instrument was calibrated using the NIST610 glass standard and the CaO concentration (wt.%) obtained from the electron microprobe was used as an internal standard for each analysis. The BCR-2 standard was analysed at least at the beginning and the end of each analytical session. The trace element dataset can be found in electronic supplementary file B2.

3.4. Melt composition calculations

We used the partition coefficients by Blundy and Wood (1991) to calculate the Sr and Ba contents of melts in equilibrium with measured plagioclase, which depends on An content and temperature, but disgregarding the PH_2O effect. Bedard (2006) conducted a total regression of all partition coefficient data showing a change of 1-2 wt.% of H_2O in the melt could produce an ~100 ppm variation in apparent melt Sr. However, Blundy and Wood (1991) found little difference between the partition coefficient of Sr from experiments both under hydrothermal conditions and silicate melts, suggesting that the effect of the PH_2O is included in the An term of the partition function. Blundy and Wood (1991) proposed the following expressions relative to the partition of Sr and Ba

between plagioclase and melt:

$$RT \ln D_{Sr} = 26800 - 26700 X_{An} \quad (1)$$

$$RT \ln D_{Ba} = 10200 - 38200 X_{An} \quad (2)$$

Where R is the ideal gas constant (8.3145 Jmol-1 K-1) and temperature (T) is expressed in Kelvin. Handley et al. (2010) estimated an average temperature of T=1,273.2 K for the samples selected in this study. The results from these calculations have been compared with the equations on the Sr and Ba partitioning coefficient proposed by Binderman et al. (1998). However, the results do not show significant differences (Electronic Supplementary data B3).

3.5. Mineral texture and compositional zoning

The petrographic details of Gede lavas are given by Handley et al. (2010), and it is found that the majority of GVC contains similar mineral assemblages of plagioclase, clinopyroxene and Fe-Ti oxide ± orthopyroxene ± olivine. Here, we define phenocrysts as crystals >0.5 mm in size, microphenocrysts ~0.1-0.5 mm, and microlites as <0.1 mm. Samples G13 (Fig. 5) and G51 (Fig. 6) clearly show banded textures with dark and lighter areas, which are indicative of interaction of two different melts.

Figure 5: G13 from Old Gede deposits show a clear evidence of two different compositional magmas, where the more mafic magma (dark areas) intruded the more evolved host magma (light areas).

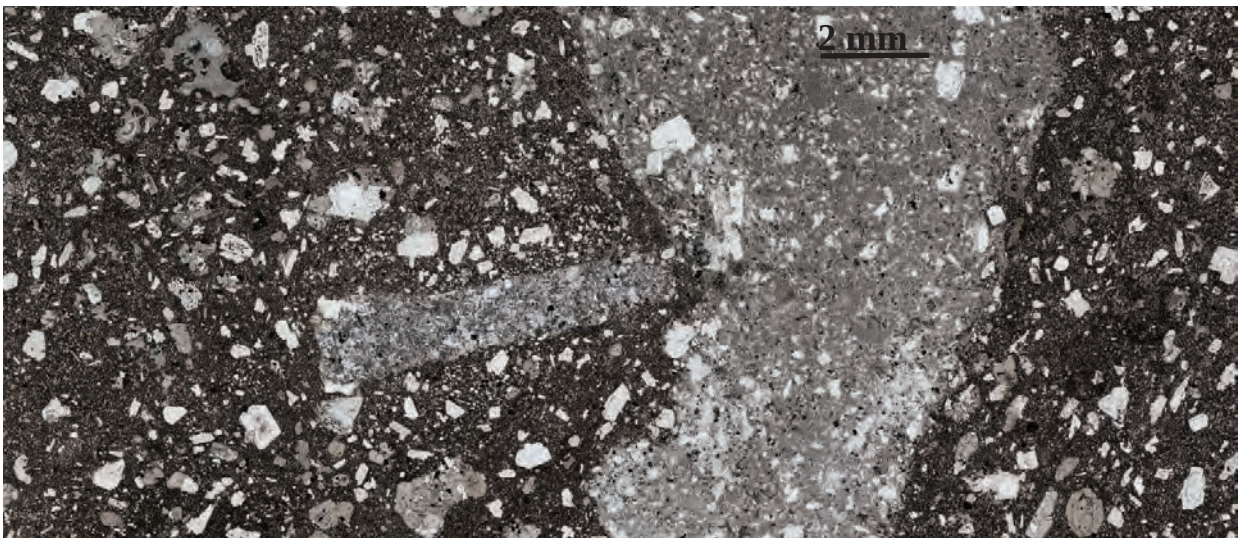

Figure 6: G51 from Young Gede deposits show inclusions of more mafic magma that interact with andesite host.

3.5.1. Plagioclase

Plagioclase up to ~3 mm in size, are euhedral and subehedral in shape and show complex zoning patterns, with the anorthite content (An) ranging from 40 to 90 mol.% (Fig. 7). Plagioclase core, mantle and rim zones were delineated on the basis of An content and of the presence of inclusions and/or resorbed areas (identified through high-resolution BSE images, core-to-rim chemical profiles and in-situ trace element concentrations). Chemical characterisation of plagioclase was challenging due to the abundant dissolution surfaces and resorption zones that could not be analysed.

We identify six plagioclase types, overall divided in two main core populations with high An core content (70-95 wt.%; Types I, II, III, IV) and low An core content (50-65 wt.%; Types V and VI), with mantle and rim zones that exhibit various pattern of alternation of high-low An content as summarised in Table 1. Sr/Ba ratio is also used to classify the plagioclase, as previous studies found that the variability in this ratio is linked to changes in An content (Blundy and Wood 1991; Browne et al. 2006; Nakai et al., 2002).

Type I is characterised by An content ranging between 75-95 wt.% and shows patchy zoning (low An_{70} patchy areas). The whole plagioclase (core-mantle-rim) is generally inclusion-rich, with some plagioclase showing a clear rim and relatively few inclusions. Sr/Ba ratio ranges from 13 to 18 for plagioclase with An_{75-85} and up to 26 for plagioclase with An_{85-95}.

Type II plagioclase display a core/mantle with high An (75-90) and oscillatory zoned rim (up to 100 μm thick), with alternation between high An_{85-90} and low An_{40-65} zones. The core/mantle show areas of patchy texture with low An content and inclusions. In the low An zones the Sr/Ba is ~9 and in the high An zones the Sr/Ba ratio is ~15.

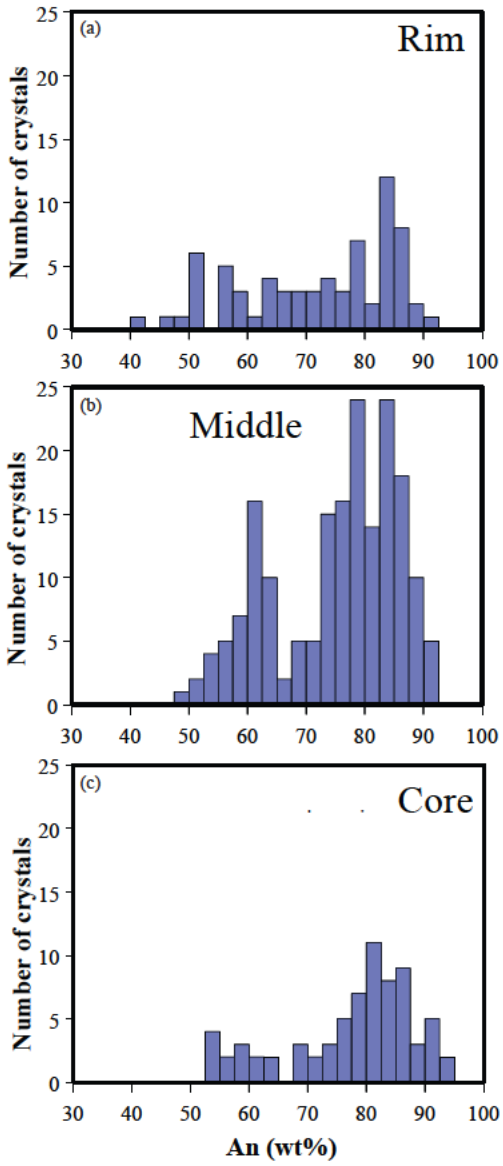

Figure 7: Histograms on the variation in anorthite (An) composition for rim (a), middle (b) and core (c) for the plagioclase phenocrysts.

Type III exhibits a core (up to 100 µm in size) with high An_{75-80}, and a mantle/rim up to 200µm in length characterised by oscillatory zoning with alternation of low An_{50-60} and high An_{75-80}, while the outer rim is low An_{50-55}. The transition between high and low An zone is marked by dissolution surfaces.

Type IV is characterised by a complex texture. It has a core of high An_{80-90} and poor inclusions, followed by a mantle with oscillatory zoning (between low An_{65} and high An_{90}) with resorbed, inclusion-rich regions and dissolution surfaces. The rim is up to 100 µm in thickness and is distinguished by an abrupt decrease in An content (20 mol.% An) and dissolution surfaces at the mantle-core transition. Sr/Ba is ~8 for the low An zone and ranges between 11 to 20 for the high An area.

Table 1: Classification of plagioclase phenocrysts on the basis of An content (core-middle-rim) and Sr/Ba ratio.

Type I	Type II	Type III	Type IV	Type V	Type VI
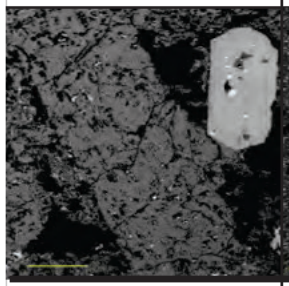	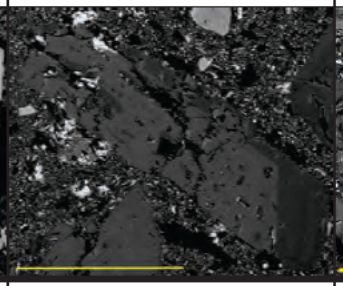	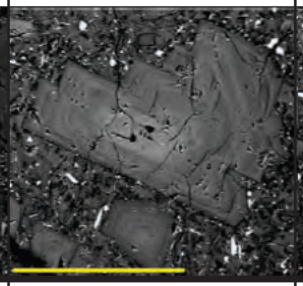	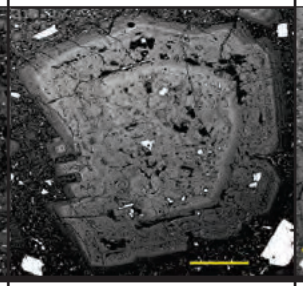	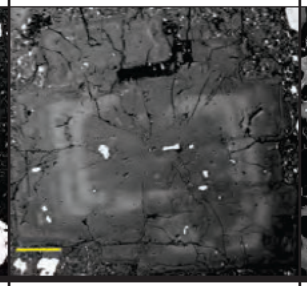	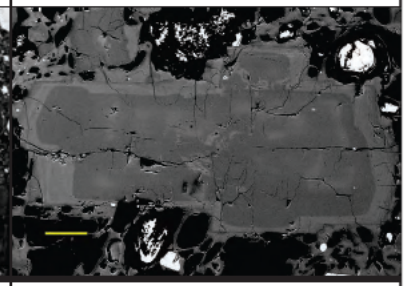
Inclusion-rich with homogeneous An (~80-90), somewhere patchy zones (low An~70)	Core with high An, somewhere patchy zones. Rim with oscillatory zones with low An (~40) and high An (~80-85)	Core with high An (~80-90). Mantle/rim with concentric zones, alternation of high An (75-80) and low An (50-55)	Resorbed core (An~70), inclusion-rich.Transition core/mantle with oscillatory zones. Mantle resorded (70-80), Transition mantle/rim with oscillatory zones. Rim with low An (55-60) and poor-inclusions	Core with low An (~55) and mantle alternated with high An (80-85). Rim poor-inclusions and low An (40-50)	Low An core (~55) and patchy zoned with An zoned of An~65. Oscillatory zoned rim with high An (~75) and poor-inclusions
Sr/Ba ~ 13-17 (low An zones) Sr/Ba ~15-20 (high An zones)	Sr/Ba ~9 (low An zones) Sr/Ba ~15 (high An zones)	Sr/Ba ~13 (rim high An zones) Sr/Ba ~23-24 (core high An zones)	Sr/Ba ~8 (low An zones) Sr/Ba ~11-20 (high An zones)	Sr/Ba ~4 (low An zones) Sr/Ba ~6 (high An zones)	Sr/Ba ~5 (low An zones) Sr/Ba ~8 (high An zones)

Type V plagioclase display a low An core (40-50 mol.%), without inclusions or resorbed surfaces. The mantle is oscillatory zoned with a large contrast in An content (An_{60} and An_{85}). The rim is inclusion- poor, with a dissolution surface at the transition mantle-rim and low An content (50-60 mol.%). Sr/Ba ratios of ~ 4 and ~6 characterise the low and high An zones, respectively.

Finally, Type VI is defined by reversely zoned plagioclase with an increase in An content from core (An~ 50-60) to rim (up to 75 mol.%). Sr/Ba ratio ranges between 3-5.5 for the low An core and up to 8 for the high An rim (Table 1).

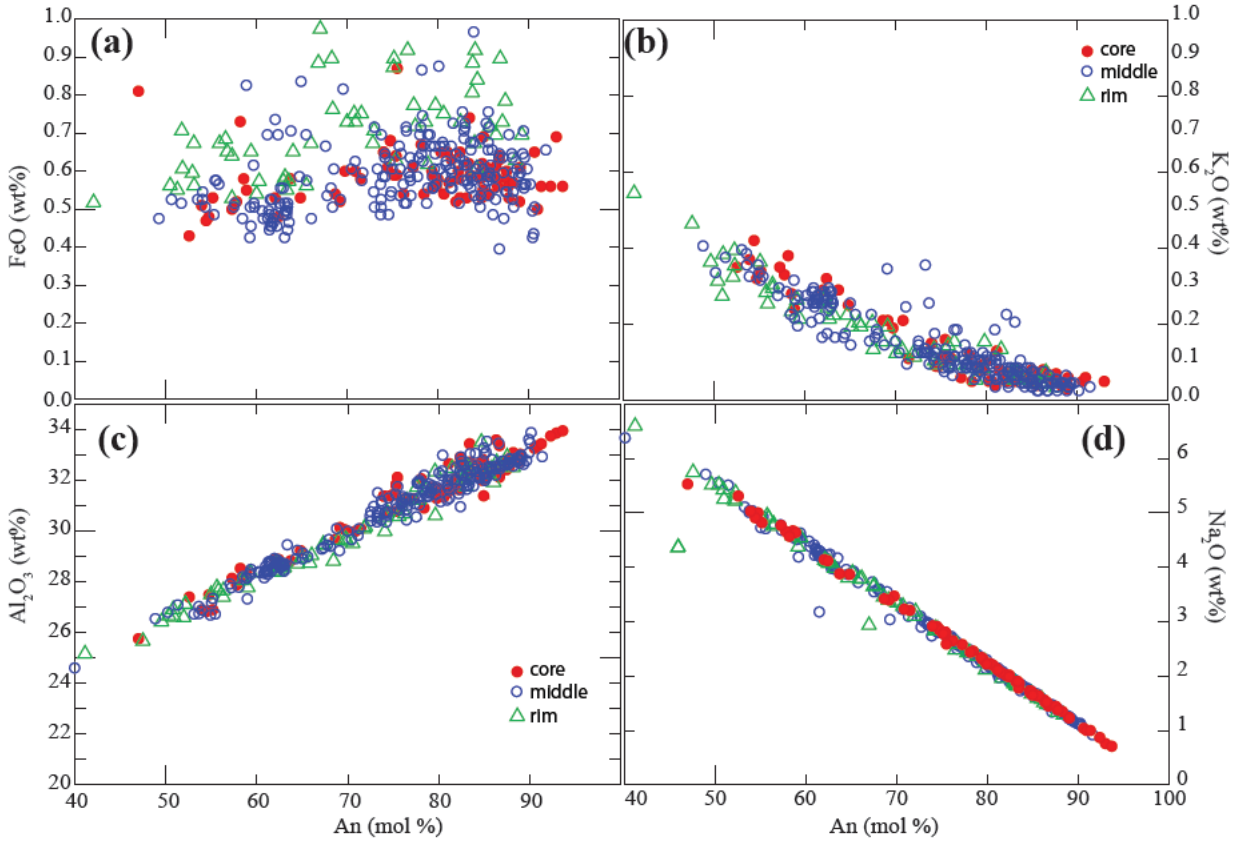

Figure 8: Variation in An for core-middle-rim compositions against FeO (a), K_2O (b) Al_2O_3 (c) and Na_2O (d).

In Fig. 8, FeO, K_2O, Na_2O and Al_2O_3 are plotted versus An content for plagioclase core, middle and rim. These areas all show a negative correlation of An with K_2O and Na_2O, while a positive correlation with Al_2O_3. FeO display scatter variation related with An content and lower FeO for core and middle area of plagioclase.

3.5.2. Pyroxene: clinopyroxene and orthopyroxene

Clinopyroxene crystals are typically subhedral to euhedral with composition of augite (Fig. 9). Pyroxene phenocrysts were classified into four types based on their core, mantle and rim compositions (Table 2).

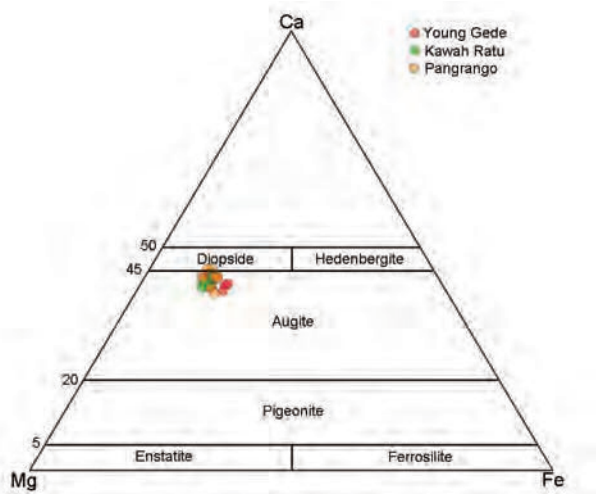

Figure 9: Classification of clinopyroxene in the basis of Mg, Fe and Ca .

Type 1 is the most common type and is characterised by reversely zoned clinopyroxene (an increase in Mg/Fe towards the rim) with a rim of Mg#76, En~44, Fs~14 and Wo~42 and core with Mg#68, En~40, Fs~19 and Wo~41.

Type 2 shows oscillatory core-to-rim zoning with limited fluctuations in Mg# from 73-77. The transition between higher and lower Mg# is often associated with dissolution surfaces and inclusions.

Type 3 exhibits orthopyroxene crystals mantled by clinopyroxene. The orthopyroxene is unzoned, with composition of Mg#76, En~73, Fs~24 and Wo~4. The clinopyroxene corona is reversely zoned with an interior part of Mg#72, En~43, Fs~17 and Wo~41 and the rim of higher Mg#78, En~44, Fs~12 and Wo~44.

Type 4 is defined by individual microphenocrysts of orthopyroxene, which are reversely zoned with a core characterised by Mg#77, En~74, Fs~23 and Wo~3. It was not possible to obtain compositional data points for the rim due to the large amount of inclusions and the small size of the crystals.

Table 2: Classification of pyroxene basis on the Mg # and En, Fs and Wo in core, middle and rim of phenocrysts.

	Type 1	*core*	*mantle/rim*	
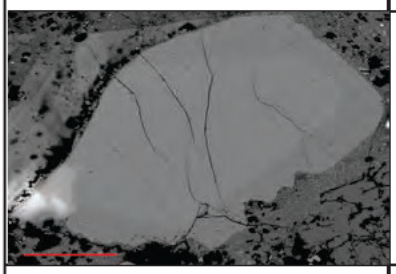	Clinopyroxene reverse zoned with poor inclusions. Increase of Mg# from core to rim	*En~41* *Fs~19* *Wo~40* *Mg#68*	*En~44* *Fs~14* *Wo~42* *Mg#76*	
	Type 2	*core*	*mantle/rim*	
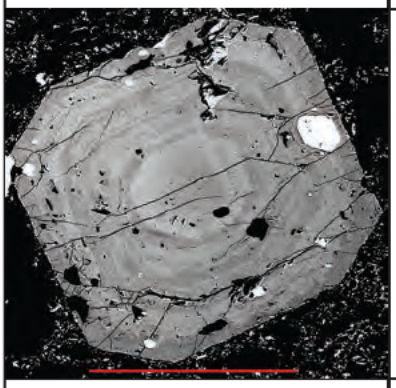	Clinopyroxene with core poor-inclusions. Mantle/ rim oscillatory zones	En~43 Fs~16 Wo~41 Mg#73	Low zone En~45 Fs~16 Wo~39 Mg#74	High zone En~43 Fs~13 Wo~44 Mg#77
	Type 3	*core*	*mantle/rim*	
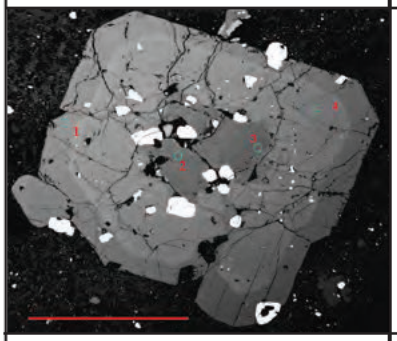	Orthopyroxene mantled by Clinopyroxene.	(point 2) En~70 Fs~27 Wo~3 Mg#72 (point 3) En~70 Fs~28 Wo~3 Mg#72	(point1) En~43 Fs~14 Wo~43 Mg#75	(point4) En~43 Fs~16 Wo~41 Mg#73
	Type 4	*core*	*mantle/rim*	
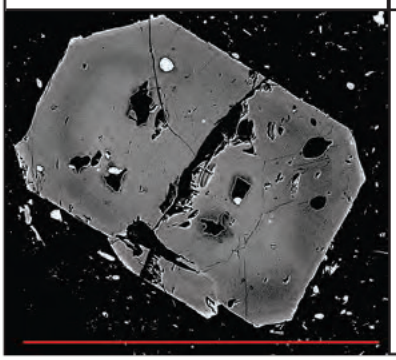	Orthopyroxene reverse zoned, with increase Mg/Fe towards the rim	En~74 Fs~23 Wo~3 Mg#77		

3.5.4. Melt compositions

Partitioning behaviour of Sr and Ba between melt and plagioclase is controlled by various factors such as temperature, composition and pressure (Blundy and Wood, 1991; Giletti and Casserly; 1994; Bindeman et al., 1998; Dohmen and Blundy, 2014; Putirka, 2005). For this work, we used the equations proposed by Blundy and Wood (1991) that were derived from experimental and natural samples to estimate the Sr and Ba partition coefficients in plagioclase based on their dependence on temperature and An content.

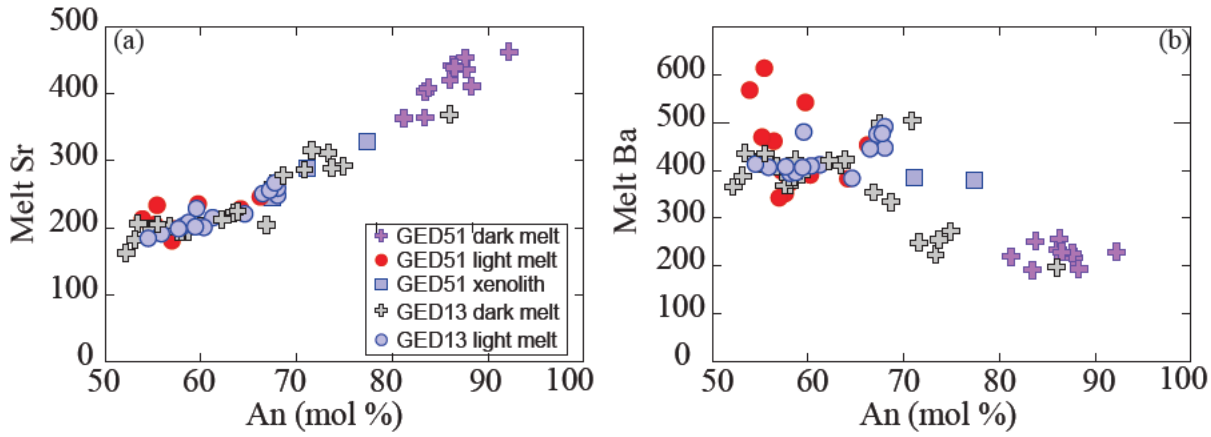

Figure 10: (a) Variation of An content in Sr concentration in calculated melt from Blundy and Wood (1991) for samples showing dark and light melt (b) Variation of Ba in calculated melt against An content.

We assumed a temperature of T=1,273.2 K from geothermobarometry estimations obtained for Gede by Handley et al. (2010). In Fig. 10 are plotted the calculated Ba and Sr melt concentrations versus An content, for samples G13 (banded pumice) and G51 (felsic inclusion in more mafic host rock), which show the light and dark parts of the samples separately. In Fig. 11 the same plot is produced for samples G20, G23, G25 and G35.

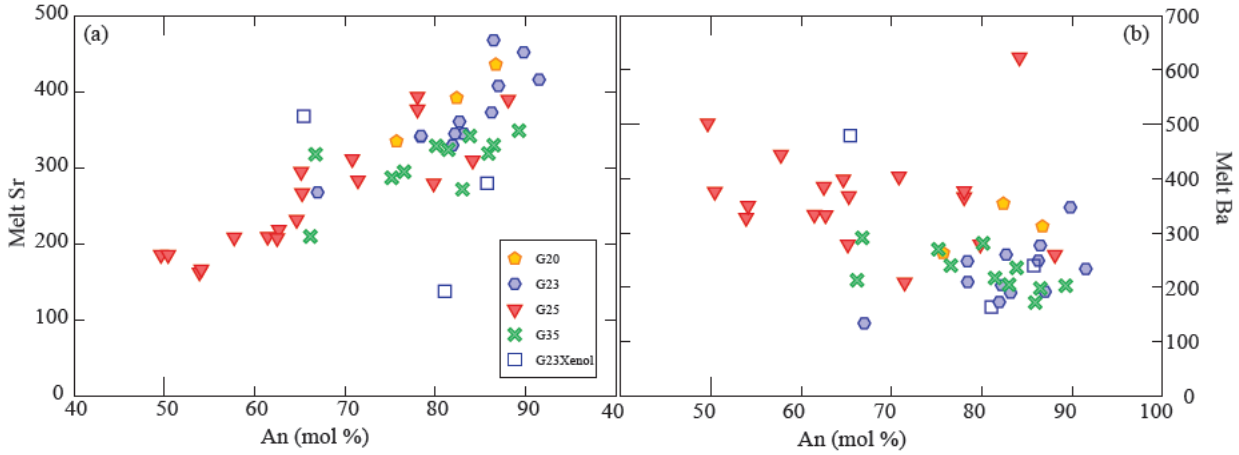

Figure 11:Variation of An content in Sr (a) and (Ba) concentration in calculated melt from Blundy and Wood (1991), for basalt (G35) and basaltic andesite and andesite sample (G25) samples.

3.6. Discussion

Geochemical complexity of arc magmas and their history are investigated combining textural and compositional zoning pattern in plagioclase from eruptive products of Gede Volcano. Results suggest repeated intrusions of basaltic magma into andesite host magma chamber over the lifetime of the volcano. Plagioclase phenocrysts that originally crystallised from the host andesite magma are identified by oscillatory zoning patterns, low An content cores (An_{50-55}) and low Sr/Ba ratio (e.g., Type V and VI). Host-derived plagioclase are disaggregated or engulfed due to the intrusion of more mafic magma producing resorption zones with high An content zones (An_{75-90}) and high Sr/Ba ratio (e.g., Type IV).

Type IV is the most common texture (oscillatory zones and coarsely sieved plagioclase), which are texturally and compositionally identical to those found in plagioclase phenocrysts contained in the inclusions. This reveals that plagioclase were engulfed by intruding magma and recycled back into the host magma over the time (Fig. 12a). Plagioclase with calcic cores (An_{80-90}) are the dominant phase, which link their origin to basaltic magma. However, the interior of some phenocrysts in the inclusions (dark melt) are patchy and oscillatory-zoned, with the same Sr/Ba ratio of the plagioclase in the host (light melt). This suggests that they formed into the andesite host and then recycled back (Fig. 12b).

Pyroxene show different zoning patterns (e.g., well-developed reverse zoning patterns), and the complexity and compositional differenses between evolved cores and more mafic rims are consistent with open-system processes (Table 2) characterised by multiples events of injection, recharge and mingling of different melts over the time.

3.6.1. Macroscopic and geochemical evidence for magmatic interactions

Rocks from Gede Volcano reveal a great diversity in composition of material erupted. Banded pumice and scoria from Old Gede (such as in sample G13) show the macroscopic interaction of two magmas (dark and light in colour) with a different composition as shown by sample G11 (dark part of banded pumice) that is characterised by 56.70 wt.% SiO_2 and by sample G14 (correlated with the light banded part) with 59.03 wt. % SiO_2 (Fig. 4; Handley et al., 2010).

Although Young Gede deposits contain light inclusions, the dark part of sample G51 is less rich in SiO_2 (55.39 wt.%) than the dark part of G11, which can be linked to more evolved melt. Some authors suggested that the origin of the banded pumice could be linked to the flow of magma in the conduits (Koyaguchi, 1985; Blake & Tait, 1986). In particular, when two liquids of different viscosity are simultaneously drawn in the conduit, the resultant flow is unstable, and the two liquids mix. The textural relationship between the black and light bands suggests that differential flow caused the less viscous magma (e.g., dark andesite) to form thin bands that entrain some of

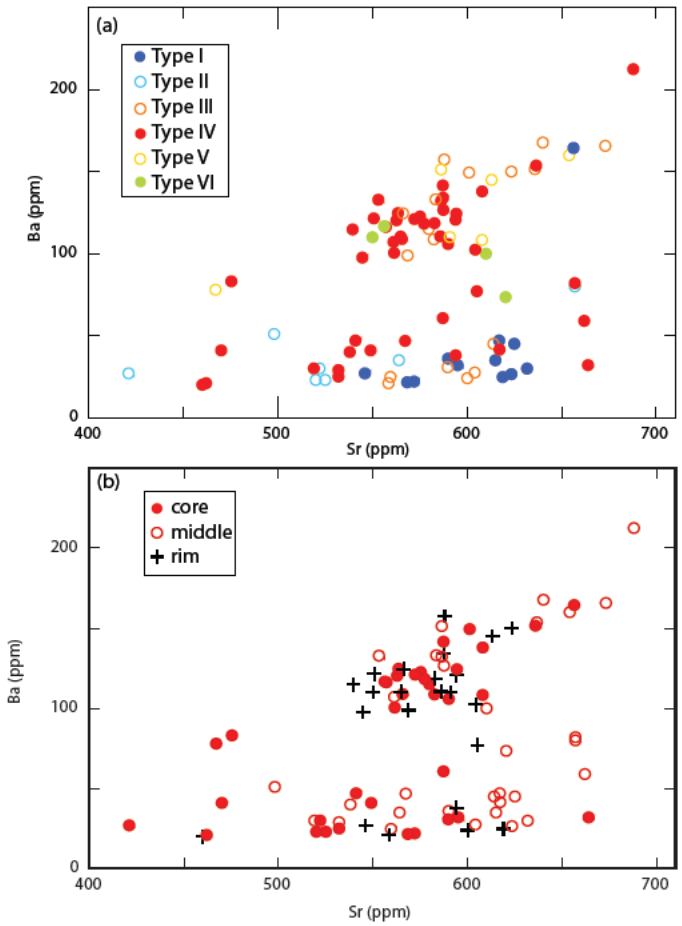

Figure 12: Variation of Ba and Sr concentration in plagioclase based on different texture types (a) and core-middle-rim (b).

the more viscous magma (e.g., light dacite), and that the more viscous magma formed thicker bands that entrained little of less viscous magma (Kouchi & Sunagawa, 1985).

Macroscopic observations on the interaction between different melt compositions (dark part and light part in G13 and G51) were combined with detailed variation in composition of trace element (Sr and Ba) within plagioclase that recorded kinetic processes during the growth of the crystals or during the changes in the melt compositions. The composition of the melt could be modified by different magmatic processes, such as injection of new magma, assimilation of wall rock, and/or contamination of the melt (Berlo et al., 2007; Browne et al., 2006a; Costa et al., 2013; Davidson et al., 2001; Gill et al., 2006) .

Plagioclase phenocrysts display different trends for Sr and Ba concentrations from G13 (Old Gede) and G51 (Young Gede) (Fig.12). Low Ba (<40 ppm) and low Sr (550-650 ppm) are characteristic of the dark melt from G51, which represents the more mafic end-member. The light

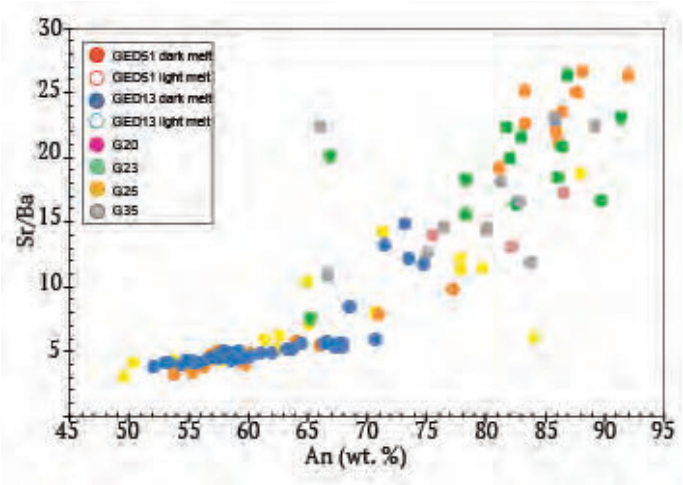

Figure 13: Sr/Ba ratios variations correlated with An composition plagioclase.

melts of G51 and G13 show higher Ba concentration (between 100 and 200 ppm) and higher Sr content (between 540-720 ppm) that are indicative of more evolved melts. The dark G13 melt is the more hybridised in compositions among the other dark/light melts. Other samples from other locations, like G20 and G23 from Young Gede, and G35 from Pangrango exhibit low Ba and Sr concentrations, similar to the G51 dark melt. On the contrary, G25 from Young Gede (Kawah Ratu vent) follows the trend with high Ba and Sr already shown by G13 light melt (Fig. 12).

The behaviour of compatible versus incompatible elements in plagioclase such as Ba and Sr is linked with the variation in An content, with Ba less compatible than Sr with the increase of An content. This implies that the plagioclase types reveal fluctuations in the Sr/Ba ratio.

Plagioclase from the same eruptive vent (Young Gede, Kawah Ratu) show different results in texture type and Sr/Ba ratio (Table 1). The Sr/Ba ratio of plagioclase phenocrysts correlates strongly with the variation in An content, in particular it increases with An content (Browne et al., 2006b) (Fig. 13). This is consistent with the results of Blundy and Wood (1991), which found that the partitioning of Sr and Ba between plagioclase and melt is primarily dependent on the structure of plagioclase crystals, with Ba less compatible than Sr with An content increases (Figs. 10, 11). The change in Sr/Ba ratios with plagioclase composition from our samples is also broadly consistent with predicted changes in Sr and Ba crystal-melt partitioning as a function of changes in plagioclase composition (Blundy and Wood, 1991) (Fig. 13).

3.6.2. Insights into magma mingling/mixing using mineral texture and composition

The history of recharging, mingling, mixing and/or contamination, and crystallisation of minerals, is unveiled by mineral texture and chemical composition of the varieties of mineral types that are found in Gede volcano. The core of each mineral recorded the initial environment where it started to growth, and most of the types (Type I, II, III, IV) are characterised by high An content and high Sr/Ba ratio that represents the melt composition of the more “mafic end-member”. However, inclusions, patchy zoning (Type I, II, III), dissolution surfaces, and alternation of resorption areas (Type IV) are distinctive of these cores. Overgrown mantle and rim exhibit also oscillatory zoning, resorption and dissolution surfaces, which reveal perturbation of the system in terms of temperature, pressure and/or composition, such interaction of melt with different properties. Resorption zones surrounding oscillatory-zoned plagioclase are strongly similar to samples obtained experimentally from plagioclase underwent heating events (Nakamura and Shimakita, 1998; Tsuchiyama, 1985; Tsuchiyama and Takahashi, 1983)

Type I, with the highest An content of about 90 mol.% and Sr/ Ba (16-26), is found in G20 and G23 samples from Young Gede and in the dark melt of sample G51, but also in the Old Gede G13 (dark melt) and in the G35 Pangrango sample. Type II is found in samples G51 (light melt) and G20 (Young Gede) and is the most common type in G35.

Instead, Type V and VI display a low An content (40-60) and low Sr/Ba ratio (4-8), which suggest that they started to grown in more evolved magma. However, Type V is characterised by alternation of high An zones, as show in plagioclase found in sample G25 and in the light melt of G51 and G13. This alternation reveals melt with similar trend for these samples with low melt-Sr and high Melt-Ba (see Fig. 10-11). These Type V with low An core are different from the low core

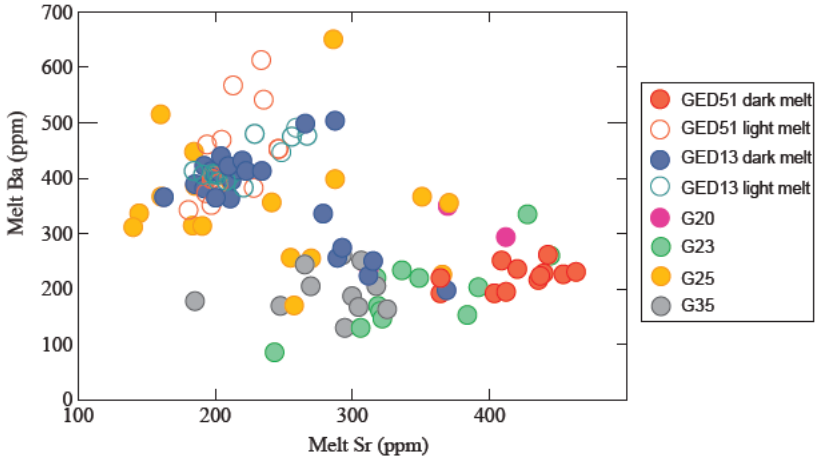

Figure 14: Calculated melt of Ba against the Sr melt from Blundy and Wood (1991).

plagioclase of Type VI, which are delineated by reversed zoned with low An core (50-60 mol. %) and high An rim (75-85 mol.%) commonly found in G13 dark melt.

Type IV are the most common types, found in almost all samples and particularly abundant in samples G13 (dark and light melts), G51 (light melt), G23, G25, and G35. This type is characterised by a complex alternation of resorption and dissolution surfaces, alternated by oscillatory zones with high and low An content, and inclusion that are rich during the transition core/mantle and/or mantle/rim. The elaborated textures reflect multiples events of injection, recharge and mingling of different melts experienced by the magmatic chamber over the time. Moreover, the identification of strong reversely zoned clinopyroxene (Type 1) in all samples, especially in G13 and G51, the oscillatory-zoned clinopyroxene (Type 2), and the orthopyroxene mantle by clinopyroxene (Type 3, commonly found in G25 and G13), supports the complexity and variety of magmatic processes happened before the eruption.

On the basis of the textures and melt compositions, sample G13 (Old Gede) reveals the most complex history in terms of experienced magmatic processes, with more than one recharge event. Sample G25 (Young Gede) covers all texture types identified in this work, and shows a geochemical trend similar to G13 in the dark and light melts. The interior (mantle/core) of Type IV shows multiple resorption areas alternated with oscillatory zoned plagioclase, and Sr/Ba composition simiular to the interiors of the plagioclase found in the light melt of G13. In Type V, the low An (50-60) and low Sr/Ba suggest that they formed from the more evolved magma (G13, light melt), which was intruded by basaltic andesite (G13, dark melt). Type 3 pyroxene are found in the sample G25, in which orthopyroxene mantled by pyroxene is indicative of fractional

crystallisation in the magma chamber (andesite, G13 light melt), as a consequence of an injection of more mafic magma (basaltic andesite; dark melt G13) that produced reversed zoned clinopyroxene rim as Type 1 (Table 2).

More information can be obtained from the thickness of the resorption zone, with the aim of calculating the time necessary for the intruded basaltic andesite to engulf the plagioclase into the host magma (Browne et al 2006). The thickness of resorption areas in Type IV plagioclase ranges from 20 to 400 microns. For a range in temperatures from 950ºC to 1030ºC (Handley et al., 2010), the time necessary to produce such a thickness ranges from 1 to 10 days (Tsuchiyama and Takahashi, 1983; Tsuchiyama 1985; Nakamamura and Shimakita, 1998).

This calculation does not take into account the difference in temperature of the two interacting melts, neither the correlated variation of the An content (as we did in the Chapter 2). However, this result is consistent with the timescales obtained from reversely zoned orthopyroxene at Gede Volcano by Krimer (2015), which found that the time between the last magmatic intrusion and the eruption is less than a month.

3.6.3. Implications for magmatic processes at Gede Volcanic Complex (GVC)

On the basis of this study, it is possible to state that GVC experienced multiple magmatic events at the microscale level between host-andesitic magmas and intrusion of more mafic basaltic andesite , which produced banded features and inclusions in the host magma. Similarities among the different types of plagioclase and pyroxene in the studied samples show evidence of disaggregation of the host magma into the intruded basaltic magma and vice versa. This is suggested by textural and geochemical results that are identical to the ones described in other volcanic systems (e.g., Soufrière Hills Volcano, Humphreys et al., 2010; Lassen Peak, Clynne, 1999; Unzen volcano, Browne and Gardner, 2006; El Chichón volcano, Andrews et al., 2008), such as sieve texture and alternation of resorption zoned were combined with oscillatory zoned.

It is important to evaluate the role of the crustal contamination in arc volcanoes associated with magma mingling/mixing processes (e.g., El Chichón Volcano, Mexico). Previous studies at GVC (Handley et al., 2014; Handley et al., 2010; Handley et al., 2008) shown the negative correlations between whole-rock Pb-Sr isotopic ratios and indices of differentiation (SiO_2), suggesting an assimilation of crustal material during magmatic differentiation. The negative trends may be attributed to: (1) increasing incorporation of less radiogenic material, such as more isotopically primitive arc rocks or ophiolitic oceanic crust (in the arc crust), during magmatic evolution; or, (2) assimilation by the lowest silica rocks of the most (by volume) radiogenic crustal

material. The latter may represent assimilation of carbonate material, which has been implicated at other Javanese volcanoes (e.g., Merapi) and has important implications for the addition of crustal CO_2 to the magma volatile budget.

Future isotopic ($^{87}Sr/^{86}Sr$) analyses of plagioclase are planned to pin down the location and role of contamination during the magma mingling/mixing events. The increase in Sr/Ba ratio, which is correlated with An content in the plagioclase phenocrysts and their relative textures, suggests multiple episodes of injection of more mafic magma into the more evolved silicic magma host .

An important aspect to consider is related to the fact that these processes (magma mingling/mixing and/or contamination) play a crucial role in triggering the eruption. Therefore, the understanding of how they played in the past is a powerful tool for eruption forecasting and for mitigation for the people living close by, as the Jakarta citizens.

3.7. Conclusions

Investigation on individual phenocrysts at GVC via trace element analyses, combined with microprobe analyses and textural information, shed light on the population of plagioclase and pyroxene phenocrysts in magmas with different compositions interacting each other over the time. Plagioclase textures, such as oscillatory zoning or resorption zones, reveal events of phenocrysts exchange between the intruded magma and the host magma.

The findings of this work show:

- magma mixing is the main mechanism that led to the wide range of textures and compositions observed at GVC;
- there are no evidences of crustal assimilation from the trend of Sr and Ba melt composition calculated using the equation proposed by Blundy and Wood (1991);
- the injections of basaltic magma into dacitic/andesitic magma chamber have experienced over time multiple events of replenishments;
- plagioclase reacted to the changes in temperature, pressure and melt compositions producing resorption zones and crystallised rim with composition similar in high An content and Sr/Ba ratio to plagioclase inherited from the intruding basaltic magma.
- Type IV plagioclase is the most common type found in all samples studied, which is characterised by resorption areas from 20 to 400 microns in thickness. Our results yielded timescales from 1 to 10 days to reproduce such a thickness ranges at temperatures 950ºC -1030ºC.

Deeper future isotopic analyses of plagioclase ($^{87}Sr/^{86}Sr$) could clarify the role of crustal contamination at GVC and how the contribution of this process affected the population of plagioclase. Understanding the eruption style at Gede Volcano is important due to the large population living close by. Results from this work can improve the interpretation of monitored data signals, fundamental in case of unrest situation.

Acknowledgements

This work is funded by a Macquarie University Research Excellence Scholarship (MQRES) (2015081) associated with an Australian Research Council Discovery Project (DP150100328). We thank Dave Adams and Will Powell for their assistance, respectively, with the scanning electron microscope and electron microprobe, and laser ablation.

References

Andrews, B.J., Gardner, J.E. and Housh, T.B., 2008. Repeated recharge, assimilation, and hybridization in magmas erupted from El Chichón as recorded by plagioclase and amphibole phenocrysts. Journal of Volcanology and Geothermal Research, 175(4): 415-426.

Bachmann, O. and Dungan, M.A., 2002. Temperature-induced Al-zoning in hornblendes of the Fish Canyon magma, Colorado. American Mineralogist, 87(8-9): 1062-1076.

Belousov A, Belousova M, Krimer D, Costa F, Prambada O, Zaennudin A (2015) Volcaniclastic stratigraphy of Gede Volcano, West Java, Indonesia: How it erupted and when. J Volcanol Geoth Res 301:238-252.

Berlo, K., Blundy, J., Turner, S. and Hawkesworth, C., 2007. Textural and chemical variation in plagioclase phenocrysts from the 1980 eruptions of Mount St. Helens, USA. Contributions to Mineralogy and Petrology, 154(3): 291-308.

Blake, S., Wilson, C., Smith, I. and Walker, G., 1992. Petrology and dynamics of the Waimihia mixed magma eruption, Taupo Volcano, New Zealand. Journal of the Geological Society, 149(2): 193-207.

Browne, B.L., Eichelberger, J.C., Patino, L.C., Vogel, T.A., Dehn, J., Uto, K. and Hoshizumi, H., 2006a. Generation of porphyritic and equigranular mafic enclaves during magma recharge events

at Unzen volcano, Japan. Journal of Petrology, 47(2): 301-328.

Browne, B.L., Eichelberger, J.C., Patino, L.C., Vogel, T.A., Uto, K. and Hoshizumi, H., 2006b. Magma mingling as indicated by texture and Sr/Ba ratios of plagioclase phenocrysts from Unzen volcano, SW Japan. Journal of Volcanology and Geothermal Research, 154(1-2): 103-116.

Browne, B.L. and Gardner, J.E., 2006. The influence of magma ascent path on the texture, mineralogy, and formation of hornblende reaction rims. Earth and Planetary Science Letters, 246(3-4): 161-176.

Clynne, M.A., 1999. A complex magma mixing origin for rocks erupted in 1915, Lassen Peak, California. Journal of Petrology, 40(1): 105-132.

Cortes, J.A., Wilson, M., Condliffe, E., Francalanci, L. and Chertkoff, D.G., 2005. The evolution of the magmatic system of Stromboli volcano during the Vancori period (26-13.8 ky). Journal of Volcanology and Geothermal Research, 147(1-2): 1-38.

Costa, F., Andreastuti, S., de Maisonneuve, C.B. and Pallister, J.S., 2013. Petrological insights into the storage conditions, and magmatic processes that yielded the centennial 2010 Merapi explosive eruption. Journal of Volcanology and Geothermal Research, 261: 209-235.

Davidson, J., Tepley, F., Palacz, Z. and Meffan-Main, S., 2001. Magma recharge, contamination and residence times revealed by in situ laser ablation isotopic analysis of feldspar in volcanic rocks. Earth and Planetary Science Letters, 184(2): 427-442.

Davidson, J.P., Dungan, M.A., Ferguson, K.M. and Colucci, M.T., 1987. Crust-Magma Interactions and the Evolution of Arc Magmas - the San-Pedro-Pellado Volcanic Complex, Southern Chilean Andes. Geology, 15(5): 443-446.

Fabbro, G.N., Druitt, T.H. and Costa, F., 2017. Storage and Eruption of Silicic Magma across the Transition from Dominantly Effusive to Caldera-forming States at an Arc Volcano (Santorini, Greece). Journal of Petrology, 58(12): 2429-2464.

Feeley, T.C. and Dungan, M.A., 1996. Compositional and dynamic controls on mafic-silicic magma interactions at continental arc volcanoes: Evidence from Cordon El Guadal, Tatara San Pedro Complex, Chile. Journal of Petrology, 37(6): 1547-1577.

Gardner, J.E., Rutherford, M., Carey, S. and Sigurdsson, H., 1995. Experimental Constraints on Pre-Eruptive Water Contents and Changing Magma Storage Prior to Explosive Eruptions of Mount

St-Helens Volcano. Bulletin of Volcanology, 57(1): 1-17.

Gill, J., Reagan, M., Tepley, F. and Malavassi, E., 2006. Arenal Volcano, Costa Rica: Magma genesis and volcanological processes - Introduction. Journal of Volcanology and Geothermal Research, 157(1-3): 1-8.

Ginibre, C., Kronz, A. and Worner, G., 2002. High-resolution quantitative imaging of plagioclase composition using accumulated backscattered electron images: new constraints on oscillatory zoning. Contributions to Mineralogy and Petrology, 142(4): 436-448.

Handley, H.K., Blichert-Toft, J., Gertisser, R., Macpherson, C.G., Turner, S.P., Zaennudin, A. and Abdurrachman, M., 2014. Insights from Pb and O isotopes into along-arc variations in subduction inputs and crustal assimilation for volcanic rocks in Java, Sunda arc, Indonesia. Geochimica Et Cosmochimica Acta, 139: 205-226.

Handley, H.K., Macpherson, C.G. and Davidson, J.P., 2010. Geochemical and Sr-O isotopic constraints on magmatic differentiation at Gede Volcanic Complex, West Java, Indonesia. Contributions to Mineralogy and Petrology, 159(6): 885-908.

Handley, H.K., Turner, S.P., Smith, I.E.M. and Stewart, R.B., 2008. Timescales of crustal assimilation at intra-oceanic arcs: U-series and geochemical constraints from Lopevi Volcano, Vanuatu, SW Pacific. Geochimica Et Cosmochimica Acta, 72(12): A348-A348.

Hawkesworth, C.J., Hergt, J.M., Ellam, R.M. and Mcdermott, F., 1991. Element Fluxes Associated with Subduction Related Magmatism. Philosophical Transactions of the Royal Society of London Series a-Mathematical Physical and Engineering Sciences, 335(1638): 393-405.

Holland, T. and Blundy, J., 1994. Non-ideal interactions in calcic amphiboles and their bearing on amphibole-plagioclase thermometry. Contributions to mineralogy and petrology, 116(4): 433-447.

Holtz, F., Sato, H., Lewis, J., Behrens, H. and Nakada, S., 2005. Experimental petrology of the 1991-1995 Unzen dacite, Japan. Part I: Phase relations, phase composition and pre-eruptive conditions. Journal of Petrology, 46(2): 319-337.

Humphreys, M.C.S., Edmonds, M., Christopher, T. and Hards, V., 2010. Magma hybridisation and diffusive exchange recorded in heterogeneous glasses from Soufriere Hills Volcano, Montserrat. Geophysical Research Letters, 37.

Krimer, D., 2015. Unreveling the evolution, dynamics, and timescales of magmatic processes

below Gede Volcano, West Java, Indonesia. PhD Thesis. Asian School of the Environment, Nanyang Technological University, Singapore.

Koyaguchi, T., 1986. Evidence for two-stage mixing in magmatic inclusions and rhyolitic lava domes on Niijima Island, Japan. Journal of volcanology and geothermal research, 29(1-4): 71-98.

Mcculloch, M.T. and Gamble, J.A., 1991. Geochemical and Geodynamical Constraints on Subduction Zone Magmatism. Earth and Planetary Science Letters, 102(3-4): 358-374.

Nakamura, M. and Shimakita, S., 1998. Dissolution origin and syn-entrapment compositional change of melt inclusion in plagioclase. Earth and Planetary Science Letters, 161(1-4): 119-133.

Tsuchiyama, A., 1985. Dissolution kinetics of plagioclase in the melt of the system diopside-albite-anorthite, and origin of dusty plagioclase in andesites. Contributions to Mineralogy and Petrology, 89(1): 1-16.

Tsuchiyama, A. and Takahashi, E., 1983. Melting Kinetics of a Plagioclase Feldspar. Contributions to Mineralogy and Petrology, 84(4): 345-354.

Whelley, P.L., Newhall, C.G. and Bradley, K.E., 2015. The frequency of explosive volcanic eruptions in Southeast Asia. Bulletin of Volcanology, 77(1).

Chapter 4

Rapid magma ascent from olivine morphology and zoning patterns: Waitomokia Volcano, Auckland Volcanic Field, New Zealand

Rosa Didonna[1], Heather Handley[1], Fidel Costa[2,3]

[1]*Department of Earth and Environmental Sciences, Macquarie University, Sydney, NSW, Australia*
[2]*Earth Observatory of Singapore, Nanyang Technological University, Singapore*
[3]*Asian School of the Environment, Nanyang Technological University, Singapore*

Auckland Volcanic Field, New Zealand-Watercolours-Rosa, 2019

Abstract

Olivine and clinopyroxene mineral textures and compositions were determined for stratigraphically-constrained eruptive products of Waitomokia Volcano, a tuff ring and scoria cone complex within the Auckland Volcanic Field, New Zealand. Olivine core compositions reveal two main magmatic environments (ME1 and ME2) in the sub-volcanic magmatic system within the upper mantle. Clinopyroxene-melt thermobarometry suggests that the late crystallisation of clinopyroxene (post-crystallisation of phenocrystic olivine) occurred at the crust-mantle boundary (Moho). CaO, Fo and Ni compositional profiles of olivine indicate differentiation and mixing between magma/s from the two magmatic environments occurred at or below the Moho, which eventually triggered rapid ascent through the crust and the eruption. The eruption of mixed magma resulted in greater olivine compositional diversity in the initial phreatomagmatic stage of the eruption producing the tuff-ring. Over the duration of the eruption and evolution to a more magmatic, scoria cone-building phase, compositional diversity decreased with a dominance of magma erupted that was sourced from the deeper magmatic environment (ME1; evidenced by the presence of only high Fo olivine cores). The reduction in compositional diversity throughout the eruption may indicate exhaustion of the eruptible magma from ME2 and/or a more open ascent pathway for ME1 magma. Skeletal textures of olivine found in rocks throughout the eruption deposits combined with preservation of Mg-Fe zoning suggests moderate degrees of undercooling and relatively fast magmatic ascent from source to surface. The present work indicates the importance of mineral-scale studies in understanding the nature of magma transport, evolution and ascent in magmatic systems traditionally considered to be ‘simple’ and provides important constrains for the assessment of future volcanic hazard and risk within the Auckland Volcanic Field.

4.1. Introduction

The transport, storage, and evolution of magmas play a critical role in controlling the eruptive behaviour of volcanoes. Yet these processes are still poorly constrained for volcanic centres in continental intraplate settings, despite being the source of significant volcanic hazard for populations and infrastructure, and show little predictability in space and time (Albert et al., 2015; Allen and Smith, 1994; Brenna et al., 2010; Cas et al., 2016; Gutmann, 2002; Jankovics et al., 2019; McGee et al., 2012; Schmincke et al., 1983). Elucidating the structure of the pre-eruptive magmatic plumbing systems and the magma ascent pathways and timescales in active continental intraplate volcanic areas, is of paramount importance for accurate assessment of volcanic hazards and their mitigation.

Magma ascent in intraplate continental settings is traditionally thought to be relatively rapid due to the presence and the preservation of mantle xenoliths in erupted volcanic rocks (Spera, 1984; O'Reilly and Griffin, 2011), to the lack of significant crystallisation of shallow crustal minerals (e.g., plagioclase), and to the dominance of basaltic over evolved rock compositions (McBirney et al., 1987). The short time frame between detectable seismicity and eruption for some historical monogenetic eruptions (e.g., Madinah, Saudi Arabia, 1256, Camp et al., 1987; Heimaey, Iceland 1973, Thorarinsson et al., 1973; Ardoukoba, Djibouti, 1978, Smithsonian Institution/SEAN, 1989) also points towards minimal storage time in the crust prior to eruption. However, recent high-resolution, mineral-scale studies investigating crystal textures and zoning patterns have revealed more complex pre-eruptive magmatic histories in small-volume basaltic volcanic systems (e.g., Albert et al., 2016; Brenna et al., 2018; Jankovics et al., 2012). Therefore, it is possible that the textures and compositional profiles of igneous crystals formed during magma transport, storage and evolution en route to the Earth's surface can provide an invaluable window into magmatic plumbing systems, and can help to set constraints on the timescales of magma ascent (Albert et al., 2015; Blundy and Cashman, 2008; Costa et al., 2013; Davidson and Tepley, 1997; Fabbro et al., 2017; Ginibre et al., 2002; Hartley et al., 2016; Kahl et al., 2015; Larsen et al., 1938; Shea et al., 2015).

Olivine, due to its dominance as a major mineral in basaltic volcanic rocks and frequent compositional zoning, has been widely utilised to investigate pre-eruptive magmatic processes and ascent dynamics (e.g., Costa and Chakraborty, 2004; Mattioli et al., 2006; Hartley et al., 2016; Jollands et al., 2016; Gordeychik et al., 2018). Experimental and petrological studies indicate that olivine morphology is linked to both the degree of undercooling (i.e., the difference between the liquidus temperature at which a mineral would crystallise from the melt at equilibrium and the

actual temperature) and the cooling rate (Drever and Johnston, 1957; Donaldson, 1976; Faure et al., 2003; Welsch et al., 2013). During experiment, first the tablet shapes wea yielded and then skeletal followed by dendritic morphologies form with progressively greater degrees of undercooling.

In this work, we conduct a detailed petrological study on juvenile material produced during progressive eruption stages (opening phreatomagmatic to final magmatic phase) by Waitomokia volcano, a tuff ring and scoria cone complex in the Auckland Volcanic Field (AVF; Fig. 1).

Olivine textural characteristics and high-resolution compositional zoning profiles were

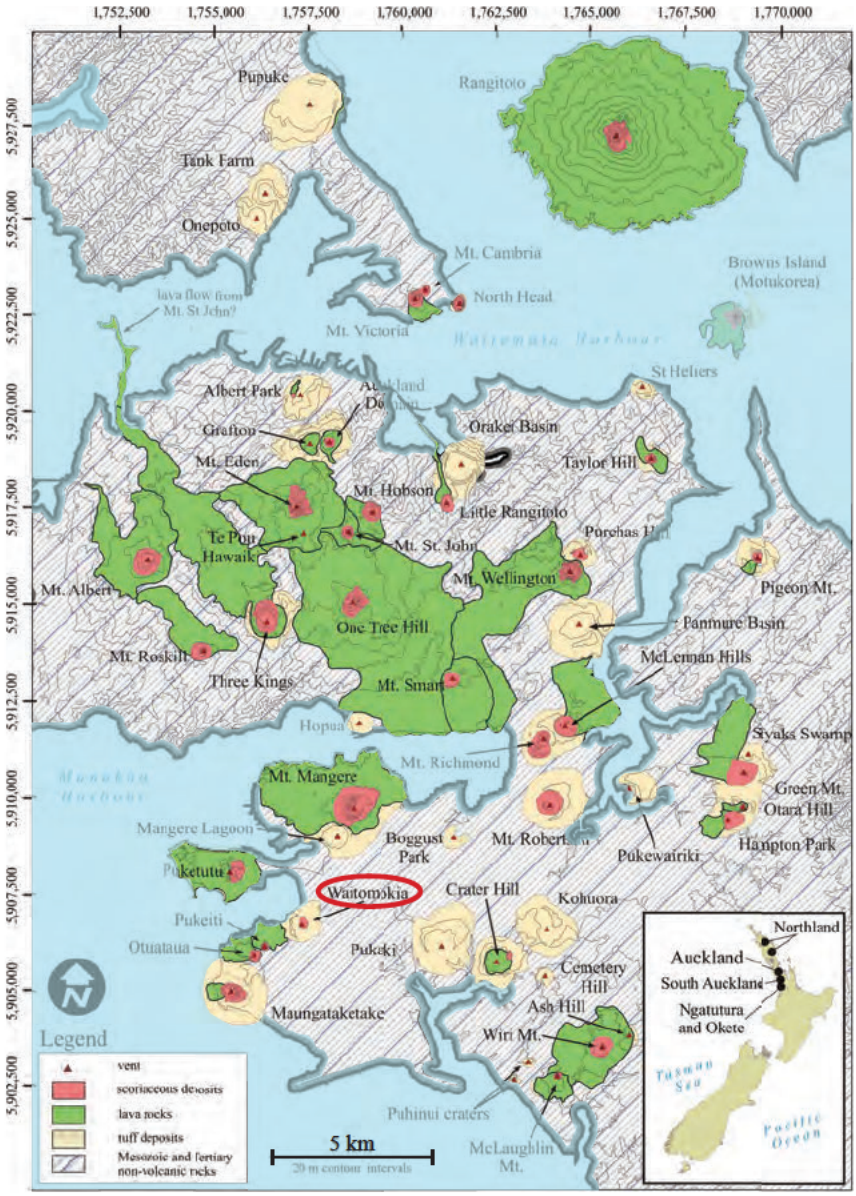

Figure 1: (a) Location map of the Auckland Volcanic Field (AVF) and its eruptive centres (modified from Kereszturi et al., 2013). Deposits from scoria cones, tuff rings and lava deposits are highlighted. The location of Waitomokia volcano is shown by a red circle. Inset (b) shows the general location of the AVF within the North Island, New Zealand. Other volcanic fields are highlighted: South Auckland Volcanic Field (SAVF), Northland, Ngatutura and Okete.

determined in order to constrain the pre-eruptive magmatic history, from source to surface. Waitomokia has excellent continuous exposure of the deposits forming the outer tuff ring rim, providing a strong stratigraphical framework in which to assess changes in magma ascent and transport dynamics throughout monogenetic eruptions. The volcanic complex is located in the southwest of the Auckland Volcanic Field, close to key transport infrastructure such as Auckland International Airport and major arterial roads, and so understanding ascent dynamics in this area is of additional interest.

4.2. Geological background

The AVF in the North Island of New Zealand is an active continental intraplate basaltic volcanic field, containing over 53 volcanic centres spread over an area of ~600km^2 (Hopkins et al., 2017). The basement under the AVF is inferred to comprise Triassic to Late Jurassic-aged sedimentary rocks. However, the oldest rocks observed in outcrop are Miocence-aged poorly consolidated mudstone and sandstone of the Waitemata Group (Kermode, 1992). Since the Late Pliocene (<3 Ma), basaltic volcanism over the wider Auckland area produced three distinctive volcanic areas with the formation of the Auckland, South Auckland, and Nigatutura/Okete volcanic fields (Briggs et al., 1994; Cook et al., 2005; Kereszturi et al., 2013) (Fig 1). Studies on the velocity contrast of the surface beneath AVF (Horspool et al., 2006) suggest that the basalt was generated in the upper mantle by partial melting, with the Moho interpreted to be at 29 ± 1 km depth in the south, and about 26 ± 1 km in the north of the field.

The AVF is located around 250 km away from the active Taupo Volcanic Zone and about 350-400 km away from the active subduction of the Pacific Plate beneath the North Island (Sprung et al., 2007). The field has been active over the last ~250 kyrs and has erupted a total estimated volume of approximately 3.4 km^3 of dense rock equivalent (DRE) (Allen and Smith, 1994), with little evidence of any spatio-temporal pattern in eruptions (Cassidy et al., 2007; Hopkins et al. 2017). The volcanic field is in the city of Auckland, home to approximately one third of New Zealand's population, about 1.66 million people (Allen et al., 1996; Kereszturi et al., 2013; Sporli and Eastwood, 1997) (Fig. 1). The last eruption, which was also the most voluminous (~2 km^3 DRE), took place at Rangitoto volcano around 500 years ago (Linnell et al., 2016; Fig. 1). Many of the AVF volcanoes show a progression from an initial phreatomagmatic phase with tuff rings and maar craters to a magmatic phase producing scoria cones and lava flows e.g., Auckland Domain, Crater Hill, Maungataketake, Waitomokia and Wiri volcanoes (Agustin-Flores et al., 2014; Hayward et al., 2011; Allen and Smith, 1994; Molloy et al., 2009; Kereszturi et al., 2013; Fig. 1).

The erupted products in the AVF vary in composition from alkali basalts to nephelinites, with rare subalkali basalts (Allen et al., 1996; McGee et al., 2012; Mcgee and Smith, 2016; Needham et al., 2011). Whole-rock geochemical studies infer relatively rapid ascent with minimal stalling or storage of magma in the crust (McGee et al., 2011, 2012, 2013; McGee and Smith, 2016) although some volcanic centres show evidence of crustal assimilation through the presence of Os isotope (Hopkins et al., 2016). Few mantle-derived xenoliths have been found in the AVF erupted products, with occurrences generally limited to Pupuke (Spargo, 2007) and Onepoto volcanic centres (Searle, 1961) in the north of the AVF (Fig. 1). Using the whole-rock geochemical compositions for a suite of stratigraphically constrained volcanic rocks from Crater Hill (south AVF), Smith et al. (2008) ascribed the temporal changes in the chemistry of erupted products to the changing degrees of crystal fractionation from the source to the surface.

To date, few detailed mineralogical studies to investigate the crystallisation during magma ascent have been conducted on AVF volcanic rocks utilising mineral textures and chemical zoning patterns. Petrographic description of a number of volcanic rocks from several centres in the AVF was carried out in the 1960s (e.g., Searle, 1961; Searle 1962). A recent study by Brenna et al. (2018) measured major, minor and trace element and OH profiles in the rims of xenocrystic olivine from Pupuke. They showed that magma ascent, at least in the north of the field, may be characterised by the accumulation and storage of magmas in deep mantle source zones for up to a few years prior to rapid magma ascent to the surface (from weeks to less than a month).

4.2.1. Waitomokia Volcano

Waitomokia volcano is a tuff ring and scoria cone complex located in the southwest of the AVF (Figs. 1 and 2a). In Maori language Waitomokia means “water seeping into the ground” (Hayward et al., 2011). Unfortunately, due to extensive quarrying and urban development since the 1950s, the three original scoria cones (~30 m high) within northeast side of the tuff ring crater are no longer present (Fig. 2b). Despite the removal of the cones, circular gravity and magnetic anomalies were measured by Cassidy et al. (2007) in the location of the former cones, indicating that a significant subsurface volume of dense and magnetic rocks is present within the underlying Plio-Pleistocene sediments. The initial tuff ring was created by a number of explosions from different vents, as evidenced by the oval shape of the original tuff ring (Fig. 2a) and by the individual explosion craters on the margin of the tuff ring rim (most evident on the northeast side). Present land use within the tuff ring crater includes a winery with vineyard, a quarry and storage yard. The tuff ring rim deposits formed from ‘wet’ phreatomagmatic activity have been divided into two stages based

Figure 2: Changes in the geomorphology of the Waitomokia area since 1950 (a) to present day (Google Earth image) (b). The aerial photographs in (a) and (c) show the presence of three scoria cones inside the tuff-ring crater (yellow circle) now removed by quarrying. Present land use within the crater consists of a vineyard (d) and quarry and storage yard (historic photographs taken by Whites Aviation Ltd.).

on location of the deposits below (initial phreatomagmatic) or above (late phreatomagmatic) an unconformity within in a road cutting that exposes a 9 m-high continuous section of the western tuff ring rim. Present day deposits representing the youngest 'dry' magmatic phase of the eruption are scarce due to the prior quarrying of the cones. These include minor outcrops of scoria fall, fluidal spatter-bomb-rich units in the northwest of the tuff ring crater, and a massive outcrop of coherent lava in the location of the former western-most scoria cone (sampled as WQW1 in this study; Fig. 3).

4.3. Sample selection and analytical methods

Twenty juvenile lapilli, bomb and lava samples from within the Waitomokia tuff ring were selected for initial petrographic analysis. From this group, 12 samples were selected for detailed microscopic analysis and BSE imaging using Scanning Electron Microscope (SEM) (Fig. 3, Appendix C.1), as they represent the range in eruptive style and volcanic deposits, from the initial (VMA1, VMA7, VMB1A, VMDW2, VMC2, WQE3) to the later (VMC3, VMC4, VMC6) phreatomagmatic

stages, to the further later magmatic phase (WQA1, WQAb, WQW1). The relative stratigraphic relationships of the selected samples are presented in Fig. 3f. Five samples were chosen based on their mineral compositional analysis to represent the three main eruption stages: 1) initial phreatomagmatic stage (VMA1, juvenile lapilli; WQE3, juvenile bomb), 2) late phreatomagmatic stage (VMC3, juvenile lapilli) and 3) final magmatic stage (WQAb, juvenile bomb; WQW1, lava; Fig. 3). Waitomokia whole-rock compositions were taken from Griffis (2013), which range from basanite to alkali basalt (Appendix C.2).

4.3.1. Scanning electron microscope (SEM) and electron microprobe (EMPA) analyses

Back-scattered electron (BSE) images of crystals of olivine (250) and clinopyroxene (50) were produced using a Zeiss EVO MA15 scanning electron microscope (SEM) at Macquarie University, using an accelerating voltage of 15 kV. Brightness and contrast were varied to accentuate the textures and visibility of the zoning.

Elemental analyses of minerals were carried out using a CAMECA SX100 electron microprobe (EMPA) at Macquarie University using an accelerating voltage of 15 kV, a 20 nA beam current, and a beam diameter of 1 micrometre (μm). The counting time was 10 seconds for Fe, Si, and Al, 20 seconds for Cr and Ca, 30 seconds for Na and P, and 40 seconds for K and Ti (ka). High-resolution profiles were realised with 2-4 μm spacing rim-to-core, or rim-to-rim across the compositional gradients, on profiles previously selected from the BSE images. The convolution effect across the sharp boundaries of the chemical changes of the mineral was not considered, however should be <4 μm. Overall, approximately 2000 quantitative analysis points for olivine and 200 points for clinopyroxene were obtained. Detailed profiles of Si, Fe, Mg, Mn, Ca, Ti, Ni, Al, Cr and P were obtained for 30 olivine crystals, while profiles of Si, Al, Fe, Mg, Mn, Ca, Ti, Na, Cr, K and P were determined for 15 clinopyroxene phenocrysts and 10 clinopyroxene microphenocrysts.

We calculated the Mg-number following Deer et al. (1992), where for olivine the total iron FeO (Fe*) was used instead FeO_{tot}: Mg#* = 100 × molar Mg/(Mg+Fe*). However, for clinopyroxene we considered Fe^{2+} (instead FeO) and calculated Mg-number as Mg# = 100 × molar Mg/(Mg+Fe^{2+}) following Droop et al. (1987).

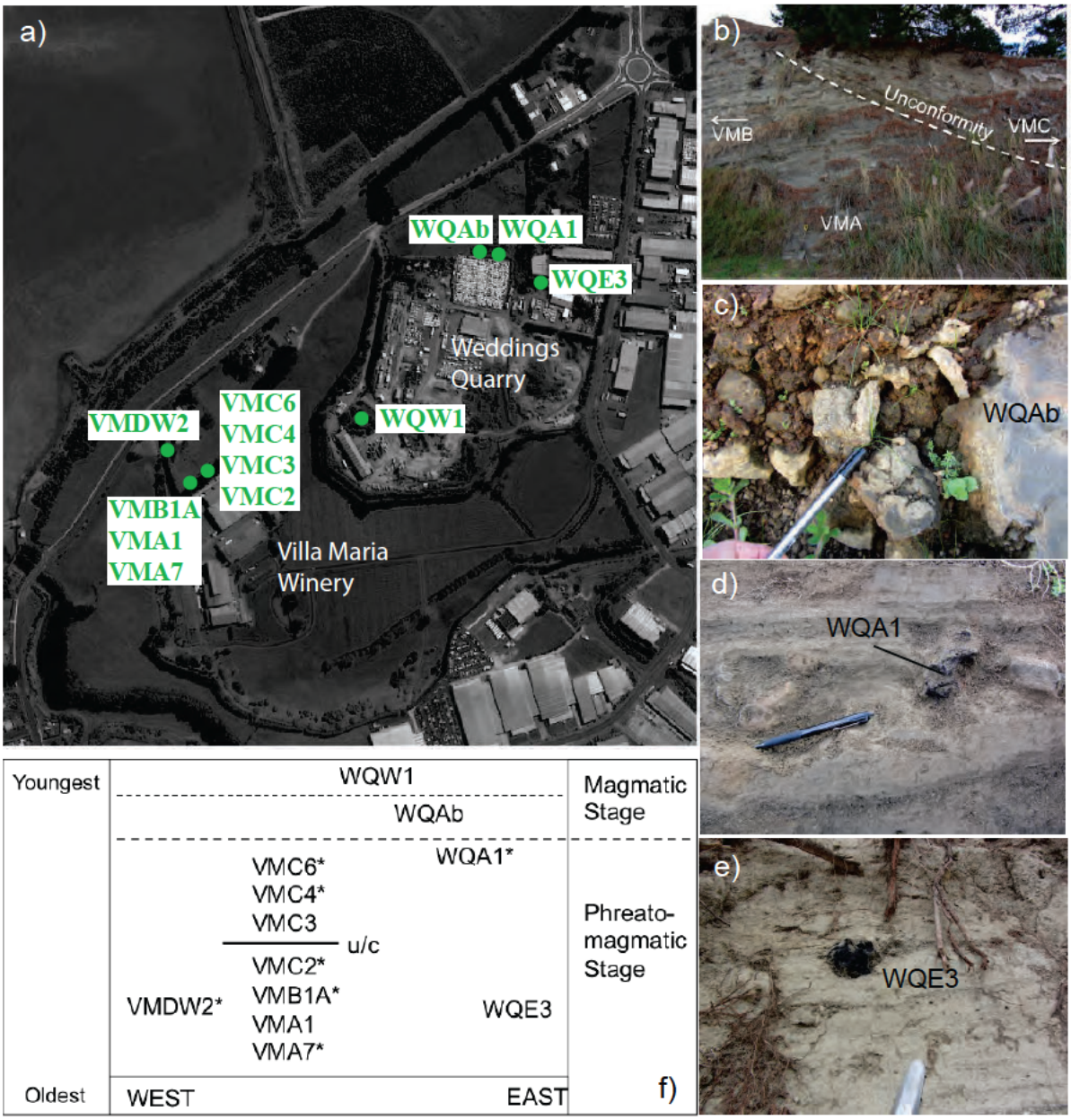

Figure 3: Location of the twelve samples selected for detailed textural and compositional analysis in this work (a). The asterisk denotes samples that underwent analysis by SEM but not EMPA. Image taken from Google Earth. A subset of five deposits of juvenile lapilli VMA1 and VMC3 (b), juvenile bomb WQAb (c), WQW1 (d) and WQE3 (e) were selected to cover the range in eruption style from the beginning of the eruption (phreatomagmatic stage) to the final eruptive magmatic stage (f).

4.4. Results: Mineralogy and petrography

In this work, we use 'phenocryst' to denote a mineral that crystalized directly from the host magma and 'antecrysts' for a mineral that originate in the magma system but has been inherited from liquids that existed at different times and places (Davidson et al., 2007). We define 'xenocrysts' as crystals derived from elsewhere, such as older cumulate material or country rocks (Welsch et al., 2013; Heltz, 1987). Phenocrysts (>300 μm in size), microphenocrysts (100-300 μm) and microlites (<100 μm) are described following the definition of Heltz (1987) as euhedral or skeletal crystals, with or without inclusions.

The juvenille lapilli (VMA1, VMC3) are porphyritic in texture, with olivine as the dominant mineral phase characterised by crystals up to 5 mm in size, followed in order of abundance by microphenocrysts of clinopyroxene in a fine-grained groundmass of plagioclase, clinopyroxene, olivine and oxides. Rounded vesicles are about 100 μm in size and sometimes elliptical/elongated. Juvenile bombs (WQE3, WQAb) are characterised by a similar mineralogical assemblage to the juvenile lapilli, with phenocrysts of olivine up to 5 mm in length, again followed by microphenocrysts of clinopyroxene and oxide. The WQAb groundmass is vesiculated and made of plagioclase, clinopyroxene, olivine and oxides. However, WQE3 groundmass is more vesiculated with rounded vesicles up to 100 μm in size. The lava sample (WQW1) is an olivine-rich alkali basalt, with phenocrysts of olivine as the most abundant mineral and up to 3 mm in size, followed by microphenocrysts of clinopyroxene and oxides in a porphyritic groundmass of plagioclase, clinopyroxene, olivine, oxides and glass. Lithic clasts such as sandstone, silt and clay are present (up to 2-3 mm in size) within the sections of the juvenile lapilli and bombs analysed.

The textures and compositional zoning of each mineral are described below, starting with the samples recovered from the tuff ring and maar craters (VMA1, WQE3), produced during the initial phreatomagmatic phase, followed by the sample produced by the later phreatomagmatic phase (VMC3), to conclude with the samples recovered from the scoria cones and lava (WQAb, WQW1), produced during the final magmatic activity.

4.4.1. Olivine

Olivine phenocrysts show a wide range of habits/shapes based on Welsch et al. (2013), including euhedral and elongate habits along the a-axis, skeletal or dendritic, and groups of polyhedral phenocrysts parallel to each other (Fig. 4). We define as crystal 'core' the compositionally (relatively) homogeneous interior part of the crystal that is clear, and without inclusions. The

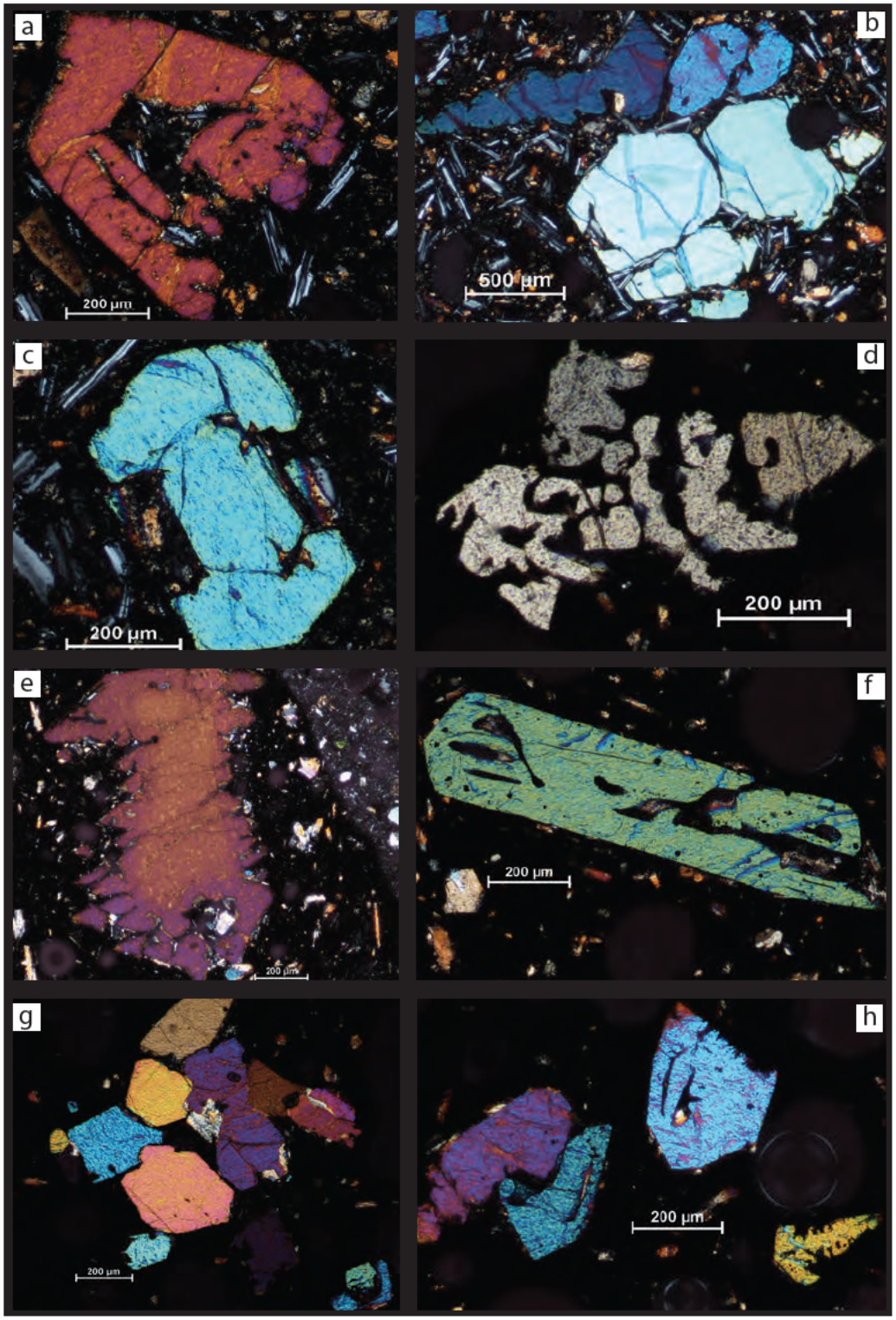

Figure 4: Textural and zoning features of the different olivine found in VMA1, VMC3, WQE3, WQAb, WQW1. Based on the classification by Welsch et al. (2013). Skeletal/dendritic crystals with cavities and inclusions (a, c, d, e, f) and groups of polyhedral units of crystals (b, g, h).

core is surrounded by compositionally distinct 'rims' (20-100 µm wide), that are variably zoned (normal or reverse) and are further subdivided within some crystals into 'inner' and 'outer' rim. In all samples, the outermost olivine rims are coated by a few micrometres-thick rim of clinopyroxene

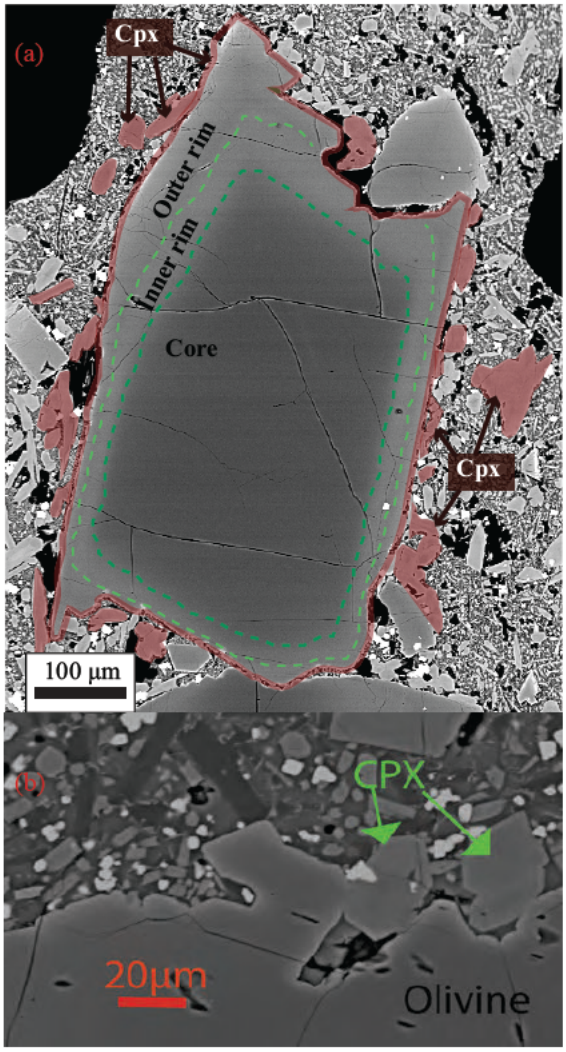

Figure 5: (a) Schematic representation of a common olivine crystal with an interior homogeneous in composition (core) surrounded by an inner and outer rim (green). Characteristic of all olivine is a rim (few micrometers) of clinopyroxene in composition (red). Individual microphenocrysts of clinopyroxene are also in contact with the olivine and present in the groundmass. (b) High-resolution detailed contact between clinopyroxene and olivine.

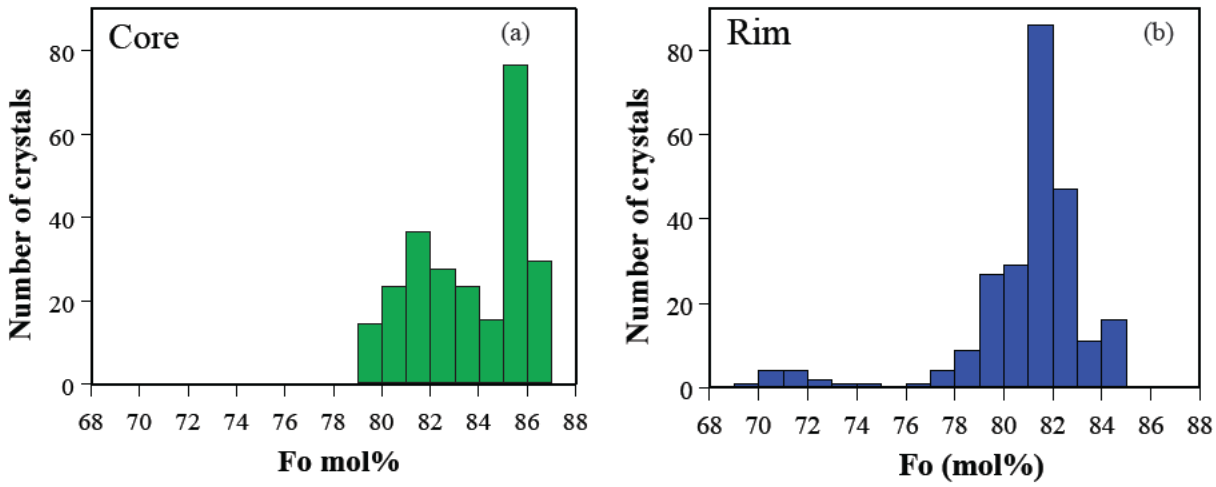

Figure 6: Histograms showing the distribution of Fo (mol.%) in olivine core (a) and rim (b) for samples VMA1, VMC3, WQE3, WQAb and WQW1.

(Fig. 5). Olivine habit appears to be independent of chemical zoning profile.

We identify three main olivine core populations with compositional plateaus at high Fo >85, intermediate Fo_{84-82} and lower Fo<82 contents (Figs. 6a and 7). The majority of olivine rims have an intermediate Fo content of around Fo82 (ranging Fo_{76-85}) with an additional small rim

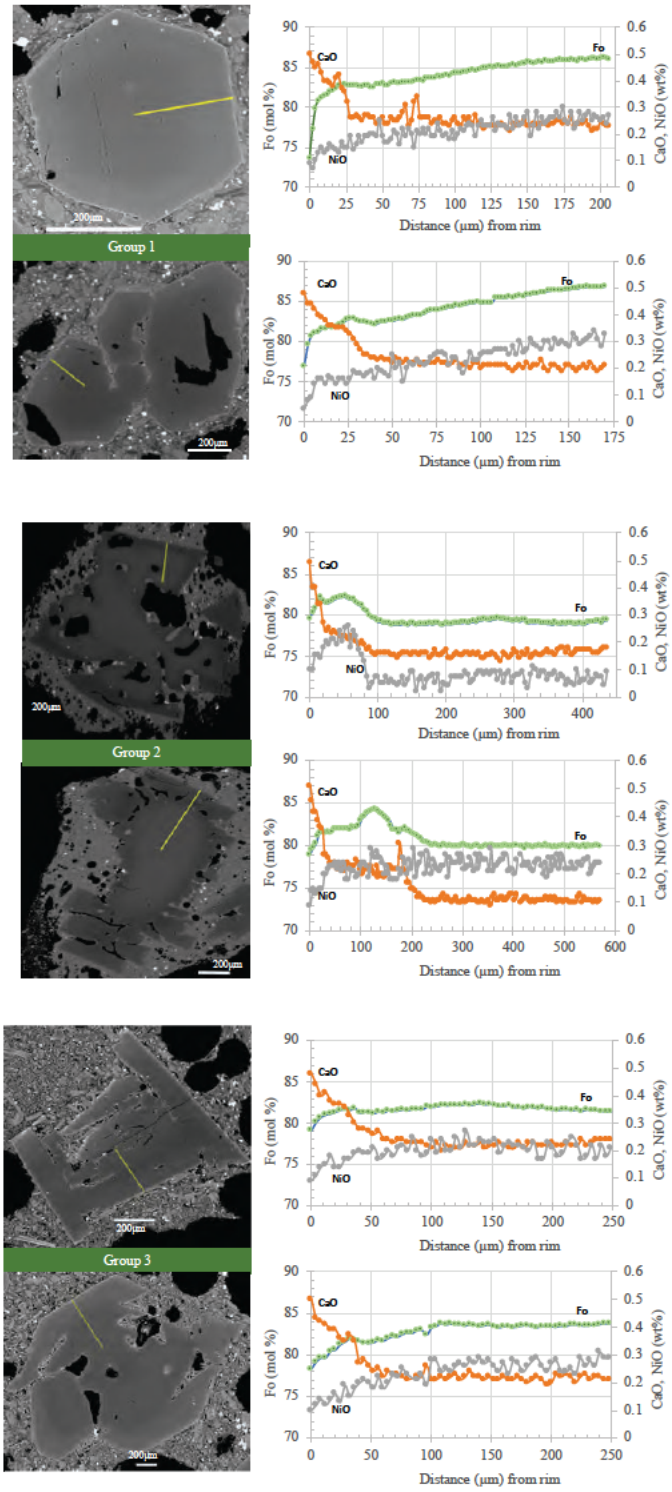

Figure 7: BSE images and Fo, CaO and Ni content profiles, where yellow line shows where the compositional profile was taken. Olivine was classified into three different groups based on zoning patterns and Fo composition of the core and rim. Group 1: normal zoned with high Fo (>85) core composition and rim, with a large decrease towards the rim (to Fo~70) (a, b). Group 2 is reversely zoned and characterised by a core with Fo~78-80 and then an increase in Fo content in the rim (up to Fo~83-85) (c, d). Group 3 is normal zoned, with an intermediate core of Fo<82-84 and rim up to Fo_{79}.

population at lower Fo content (Fo_{69-75}) (Fig. 6b). Based on forsterite zoning patterns and Fo, CaO and NiO contents (Fig. 7) the Waitomokia olivines have been divided into three main groups: Group 1 crystals are normally zoned with Fo content decreasing relatively smoothly from core (>85 mol.%) to rim (76-78 mol.%), CaO content ranging between 0.2-0.5 wt.% and NiO content up to 0.3 wt.% (Figs. 7a and b). Crystals within this group are found in samples representing all stages of the Waitomokia eruption (phreatomagmatic to magmatic). Group 2 is characterised by olivine core plateaux with Fo content relatively lower than Group 1 (Fo_{78-80}) and reverse zoning in the inner rim (Figs. 7c and d). The inner rim shows higher Fo content than the core (up to ~Fo_{82-85}), followed by a decrease in Fo content towards the outer rim (Fo_{79-82}). Group 2 crystals are only found in sample VMA1, from the initial phreatomagmatic stage of the eruption (Fig. 3). The crystal cores have notably lower CaO concentrations (0.1-0.14 wt.%) than the olivine in Groups 1 and 3 (>0.2 wt.%) (Fig. 7). Group 3 olivine crystals are defined by core Fo content plateaus of ~Fo_{82}, which is intermediate between Group 1 and 2 (Fig. 7). Similar to Group 1, Group 3 olivines are normally zoned, with a relatively smooth transition between core and rim concentrations, but with slightly higher rim Fo content relative to Group 1 (Figs. 7e and f).

The olivine rims show a wide range in Fo content (Fig. 8), which correlates negatively

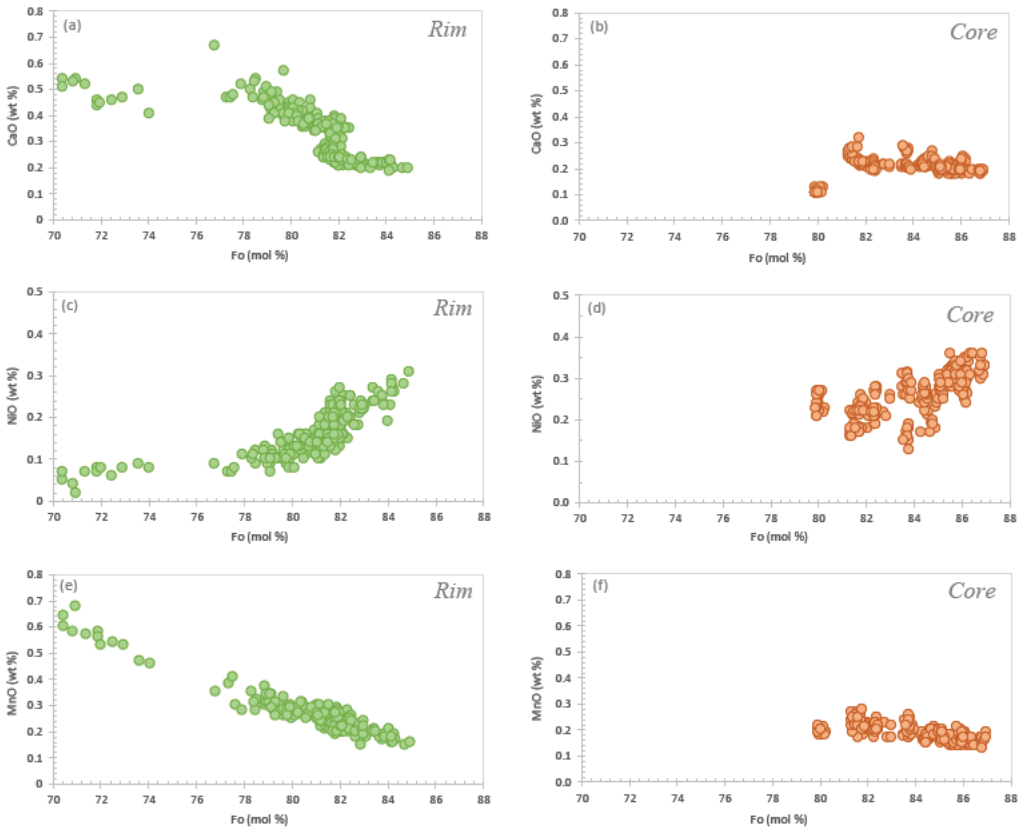

Figure 8: CaO, NiO and MnO contents as a function of Fo content in olivine.

with CaO and MnO (Figs. 8a and e) and positively with NiO contents (Fig. 8c). Based on CaO-Fo relationships, the rims display three different compositional arrays: high Fo-low CaO, intermediate Fo-high CaO and low Fo-high CaO. The transition between the high Fo-low CaO and intermediate Fo-high CaO arrays occurs at Fo_{81-82} with an overlap between the two arrays in Fo content. The low Fo-high CaO rim array is restricted to the Group 1 olivines and the magmatic phase of the eruption (found dominantly in the WQW1 lava sample). All olivine crystals show a minor increase or plateau in Fo content at ~25 μm from the rim (Fig. 7). The olivine rims show a wider range in CaO content overall (0.2-0.6 wt.%) compared to the olivine cores (0.1-0.35 wt.%).

4.4.2. Clinopyroxene

Clinopyroxene occurs as a microphenocrysts (up to 300 μm) and microlites (< 100 μm) in the groundmass and displays complex zoning patterns such as oscillatory and sector zoning (Figs.

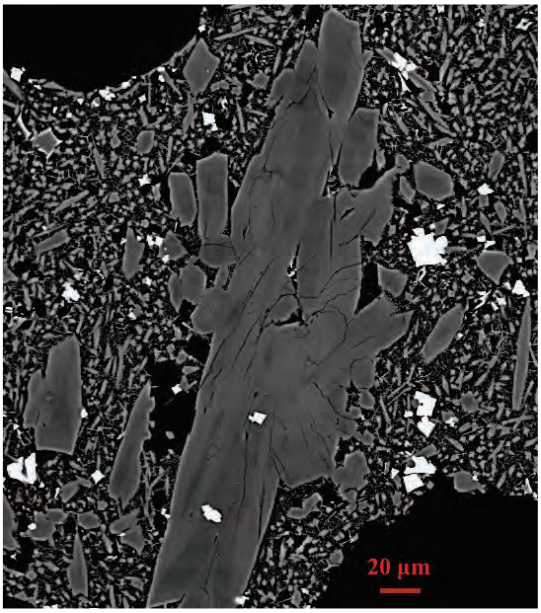

Figure 9: Backscattered electron image showing sector and oscillatory zoning in clinopyroxene microphenocrysts.

5 and 9). Clinopyroxene crystals, approximately 5-10 μm in length, are also found surrounding olivine phenocrysts (Fig. 5). Thin clinopyroxene rims of a few microns in thickness are observed on all olivine crystals (Fig. 5).

Core and rim compositions were obtained for clinopyroxene microphenocrysts and clinopyroxene rims around olivine crystals. Clinopyroxene compositions of $Wo_{42-52}En_{30-41}Fs_{10-17}$ show that all clinopyroxene (microphenocrysts, microlites and rims on olivine crystals) are diopside (Fig. 10), with Mg#* ranging from 62 about to 88 (where * denotes total iron). Structural formula calculations (Droop, 1987) show that most crystals have high calculated Fe^{3+} contents and

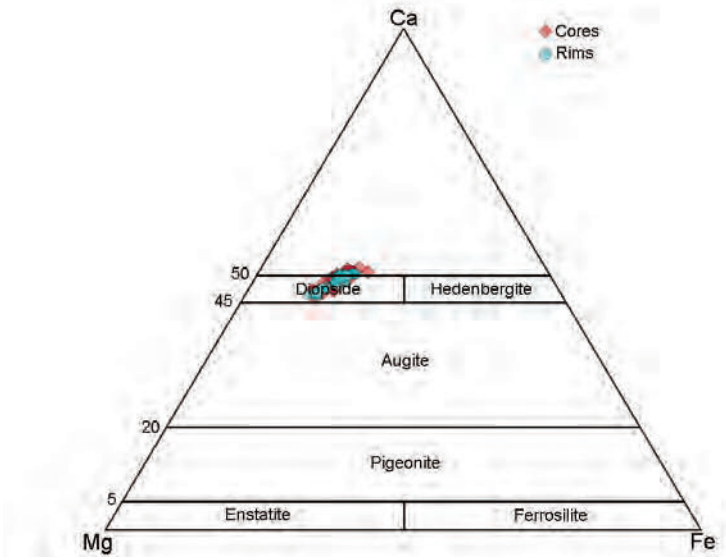

Figure 10: Compositions of clinopyroxene cores and rims of microphenocrysts and clinopyroxene rims on olivine showing a similar range in composition between core and rim.

thus have Mg# values of 76-88 (Electronic Supplementary Data C).

4.4.3. Estimation of the temperature and pressure of crystallisation

Initially, a thermometer of olivine in contact with clinopyroxene (Loucks, 1996) was used to estimate the temperature crystallisation in the magmatic system. However, the results did not show equilibrium between olivine and clinopyroxene, probably because clinopyroxene are too Fe-rich to be in equilibrium with the most Fo-rich olivine (Fo_{87}). Instead, the clinopyroxene-liquid barometer as proposed by Neave and Putirka (2017) was used to compare the results with the ones obtained from Louck (1996) calculation. Following this model, the two equations for temperature (T) and pressure (P) can be used simultaneously to obtain T and P of the clinopyroxene in equilibrium with glass or whole rock compositions. First, we considered T and P independently and results within 1 standard deviation were considered a valid estimation. Then, we tested for equilibrium by comparing clinopyroxene and Mg# in the liquid, assuming a Fe-Mg exchange coefficient of 0.23 ± 0.03.

To represent the composition of the melt from which the clinopyroxene grew we used the composition of the interstitial matrix glass obtained from microprobe analysis (for sample WQW1; Supplementary data C1) and the whole-rock compositions from Griffis (2013) (Appendix C2). Thermobarometric calculations, using clinopyroxene microphenocrysts compositions in equilibrium with the interstitial glass, provided temperatures between 1162 °C and 1183 °C and

pressure ranging from 7.7 kbar to 9.5 kbar (with standard error of ±1.4 kbar), which corresponds to a depth of 25.6 km to 31 km.

4.5. Discussion

The investigation of the textural and compositional features of olivine crystals reveals important constraints on the magma pathway from the source to the surface. By looking at these characteristics within the context of a well-constrained stratigraphy, we are able to document potential changes in magma transport, storage and ascent throughout the course of the eruption, from the initial phreatomagmatic stage to the final magmatic activity. Zoning patterns in crystals provide an opportunity to unravel magmatic processes such as magma recharge or mingling/mixing that reflect changes in magma composition or other environmental factors. Due to the fast chemical re-equilibration of Fo in olivine that could erase the initial stage of crystallisation (Chakraborty, 1997; Costa and Chakraborty, 2004; Costa and Dungan 2005; Dohmen et al, 2007), the preservation of Fo in crystals from Waitomokia implies relatively short magma residence timescales within the plumbing system that will be quantified in future work.

4.5.1. Magmatic environments inferred from olivine core compositions

The relatively small size of the olivine crystals, the dominance of euhedral, skeletal and polyhedral olivine habits, and the absence of resorption features, combined with a core compositions of $Fo_{<87}$ and a lack of observed mantle xenoliths in the volcanic deposits at Waitomokia, all suggest that the olivines in this study do not represent mantle-derived ultramafic xenocrysts, transported to the surface by ascending melt. This contrasts with the large (2-20 mm), anhedral, forsterite-rich ($Fo_{\geq 90}$) olivine xenocrysts observed in volcanic rocks from Pupuke maar in the north of the AVF (Searle, 1962; Spargo, 2007; Brenna et al., 2018). In the AVF, volcanic deposits containing mantle xenoliths and xenocrysts are largely restricted to the North Shore volcanoes such as Onepoto and Pupuke (Searle, 1961; Rodgers et al., 1975; Spargo, 2007), with Cr-spinel compositions suggesting subduction-related origins (Spargo, 2007). The general lack of mantle xenocryst and xenoliths within volcanic rocks from the AVF, compared to other basaltic intraplate volcanic fields (e.g., such as the Newer Volcanics Province in Australia;Wass and Irving, 1976), implies that either magma ascent rate is slow relative to the settling and dissolution rates of the mantle xenoliths (e.g. Spera, 1984; Brearley and Scarfe, 1986), or that the melt transfer mechanism physically filters or blocks their ascent.

The two main populations of olivine core compositions displayed in Fig. 6a suggest that

there were at least two magmatic environments (ME; e.g. Kahl et al., 2011) in which olivine grew prior to eruption at Waitomokia: ME1 with $Fo_{>85}$ and ME2 with ~Fo_{81-82}. The Group 2 reversely zoned olivines belonging to ME2 are characterised by lower CaO content (0.1 wt.%) and by the lowest core Fo contents (~80 mol.%). They may have formed from a relatively more evolved melt compared to that of the other ME2 cores, which underwent a prior crystallisation of a Ca-rich phase such as clinopyroxene ,or they may have formed from a melt composition characterised by lower CaO content. As such, these cores are likely to be xenocrysts or possibly antecrysts and were only found within sample VMA1 from the initial phreatomagmatic phase.

4.5.2. Magma evolution, interaction and transport to the surface

The wide range in olivine rim Fo content (Fo_{69-85}) within Waitomokia volcanic rocks (Fig. 6b), should provide insight into magma pathways and reactions en route to the surface. Calcium content and zoning patterns in olivine have been shown to be strongly controlled by melt composition (silica activity) and pressure (Stormer, 1973). Olivines from more silica-poor alkaline melts, akin to the Waitomokia basanites, are characterised by strong enrichments in calcium content towards olivine rims compared to olivine in more siliceous tholeiitic melts, which show less pronounced enrichment and zoning. At constant pressure, calcium content in olivine is expected to decrease with cooling. However, at constant temperature the calcium content in olivine can increase with decreasing pressure. Therefore, the calcium zoning patterns observed in Waitomokia olivines (Fig. 7) can be used to investigate pressure and temperature changes in the magma. By assessing whether the changes in calcium occur in tandem with changes in Fo and Ni content we will be able to identify changes related to changes in melt composition, versus those related to varying environmental conditions (e.g., temperature and pressure).

The high Fo-low CaO rim population in Fig. 8a overlaps in composition with the main group of core compositions (Fig. 8b) suggesting crystallisation from a similar melt composition or ME/s to which the olivine cores crystallised. However, the increase in CaO at a given Fo content at ~Fo_{81-82} and an intermediate Fo-high CaO rim array (Fig. 8a) implies a change in the conditions of crystallisation, due to either interaction with a melt with contrasting Ca content or change in environmental conditions (e.g., temperature or pressure), or both. The individual Fo, CaO and NiO zoning patterns in olivines of all groups shown in Fig. 7 reveal the following: 1) the constant or slightly decreasing Fo and NiO contents and constant CaO content in the olivine cores from all groups suggests crystallisation of cores from stable respective melt compositions (ME1 and ME2) at constant pressure and stable or decreasing temperature; 2) the reverse zoning in Fo content

observed from the core to the inner rim boundary in Group 2 is accompanied by a slight increase in CaO and increase/plateau in NiO, suggesting, as noted above, that these low Fo cores were incorporated into a more mafic/hotter melt, and are thus xenocrysts or antecrysts; 3) the observed moderate to steep increase in CaO content accompanied by minor increase in Fo content (~1 mol.%) and little change in NiO at around 25 microns from the rim (displayed by olivines in all groups and with variable textures) indicates the interaction and mixing of compositionally-distinct melts prior to the eruption; 4) The steep increase in CaO content within the outermost 25 microns of the rim, accompanied by steep decreases in Fo and NiO content suggest that the crystallisation occurred due to decreasing pressure (higher CaO) and decreasing temperature (lower Fo and NiO), likely during the ascent to the surface. The thin (few μm-wide) Ca-rich clinopyroxene (diopside) coronas displayed by all the olivines within all Waitomokia samples suggests that prior to the eruption the CaO content of the melt became saturated with Ca-rich clinopyroxene. Past petrographic studies of volcanic rocks from the AVF (Searle, 1961), also reported the presence of thin clinopyroxene rims on olivine crystals, which indicates that calcium enrichment of the melt in the late stage of crystallisation is a common process beneath many AVF eruptive centres. We note that in this study we did not taken into consideration the potential impact upon our results of the phase boundary fluorescence effect (PBF) encountered through electron microprobe analysis of calcium content in olivine close to grain boundaries with Ca-rich phases such as diopside (Dalton and Lane, 1996). However, the experiments by Dalton and Lane (1996) suggest that the increase in olivine calcium concentration due to the PBF when olivine is in contact with diopside is around 0.07 wt.% over a distance of a few tens of microns. Therefore, the effect of PBF is not important when compared with the magnitude of the CaO increase observed in the outer rim of olivines (outer 25 microns) in this study, which ranges consistently within most crystals from ~0.2 to 0.5 CaO wt.%.

The estimated pressures and temperatures obtained from clinopyroxene-melt thermobarometry using both the clinopyroxene microphenocryst rim and clinopyroxene corona compositions with groundmass composition (Fig. 11) indicate that the clinopyroxene grew within a relatively restricted range of temperature (~1160-1190 °C) and pressure (~7-10 kbar) equal to approximately 26-31 km depth. This depth corresponds to the inferred depth of the crust-mantle boundary (Moho) beneath the AVF at 26-29 km (Horspool et al., 2006) and indicates potential stalling and crystallisation of melt at the mantle-to-crust transition. The diopside coronas on olivine and small crystal size of the clinopyroxene relative to olivine suggest that clinopyroxene was a late fractionating phase, post-crystallisation of the variably textured olivine phenocrysts. Therefore, we can conclude that olivine crystallisation took place at or below the Moho. A low velocity zone

beneath the AVF was identified at 70-90 km depth which was attributed to a melt-producing region in the upper mantle and source for AVF basalts. Therefore, crystallisation of olivine phenocrysts is proposed to take place between 70-90 km and the Moho.

The chemical zoning pattern in the outer rim of olivine appears to be similar for all three crystal Groups, despite their variation in Fo core content (two main ME), and is also independent of the olivine morphology (euhedral/skeletal/polyhedral). This indicates that at or below the Moho, olivines from ME1 and ME2 were mixed together before, or due to, mixing with an additional

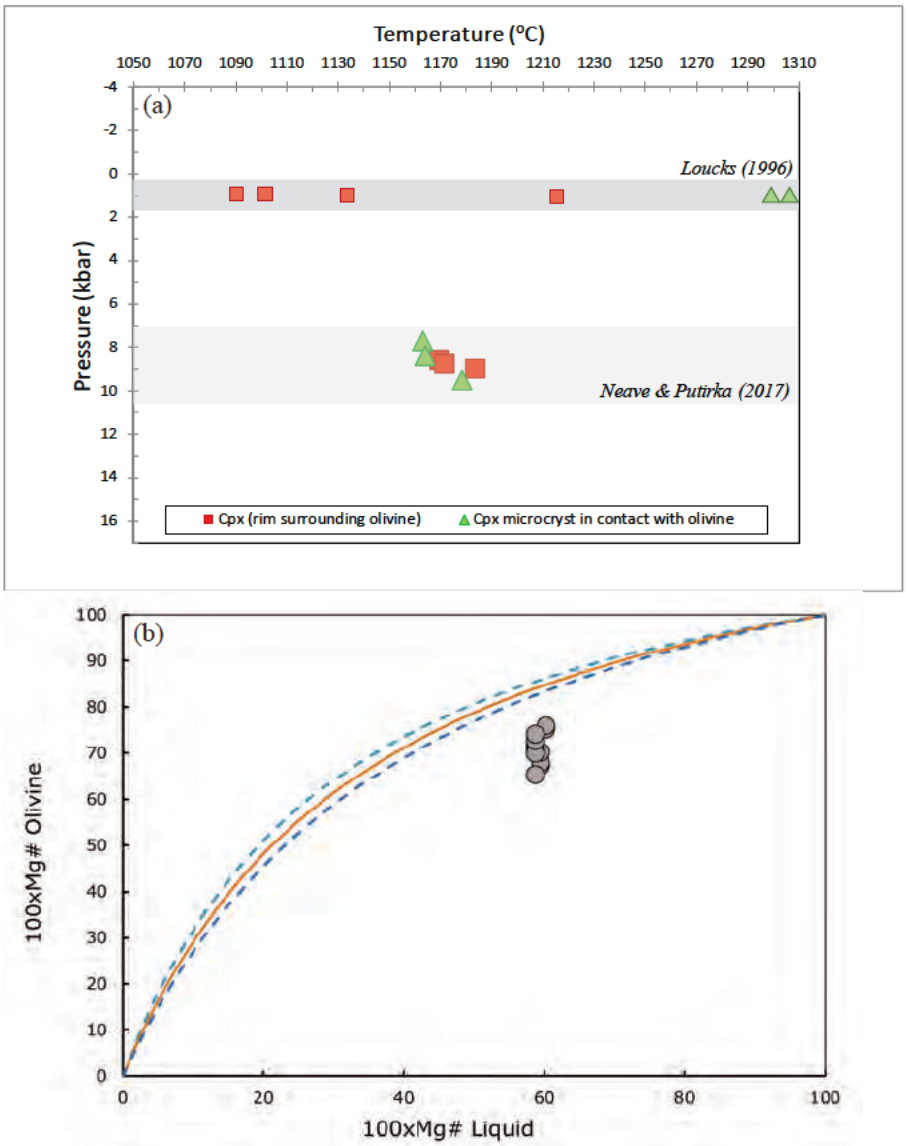

Figure 11: (a) Estimated temperatures and pressures of clinopyroxene crystallization within Waitomokia rocks using the clinopyroxene-melt thermobarometer of Neave and Putirka (2017). This calibration has a standard error of ±1.4 kbar. In comparison, Louks (1996) thermobarometry was used yielding temperatures with a standard error of ± 6°C and constant pressure of 1kbar.(b) Rhodes diagram to test di equilibrium between the core of olivine (grey circles) and the calculated liquid using Putirka (2008).

melt of higher Fo and CaO content (as even the Group 1 high-Fo core plateau olivines show an increase in Fo and CaO at 25 microns in from the rim). This additional and subsequent mixing of magma may have been sufficient to trigger ascent to the surface and eruption at Waitomokia. The importance of accumulation and storage of magmas in deep source zones for the AVF was also recently implicated by Brenna et al. (2018), who also found that magma mixing may be an eruption trigger in basaltic 'monogenetic' volcanic fields.

Experimental researches show that olivine morphology is controlled predominantly by cooling rate and degree of undercooling (degree of supersaturation; see, e.g., Donaldson, 1976; Faure et al., 2003). With increased degrees of undercooling, olivine shape evolves from tablet to skeletal (hopper) to dendritic (swallowtail) (Faure et al., 2003). The abundant skeletal olivine morphologies in the Waitomokia volcanic rocks (Fig. 4) imply moderate degrees of undercooling and moderate to high cooling rates. Whereas, the polyhedral (and euhedral) olivines (e.g., Fig. 4g) suggest a relatively low cooling rate and a decreased growth rate, under near-equilibrium conditions. The polyhedral olivine may have formed by cavity infilling of earlier-formed skeletal olivine (Faure et al., 2003; Welsch et al., 2013) but this is yet to be determined. The chemical re-equilibration of Fo in olivine is relatively fast at magmatic temperatures (Chakraborty, 1997; Costa and Chakraborty, 2004; Costa and Dungan, 2005; Dohmen et al., 2007). Therefore, the preservation of zoning in Fo content in Waitomokia olivines along with skeletal morphologies, likely reflects the relatively fast ascent of magma from source to surface where, at times, melt experienced moderately rapid and large decreases in temperature, after potential events of stalling at the Moho and magma mixing.

Despite their small size, the clinopyroxene microphenocrysts show complex oscillatory and sector zoning patterns (Fig. 9). The oscillatory zoning may have resulted from changes in melt composition due to the inferred magma mixing processes and/or be related to local changes in environmental conditions during growth. Recent studies on clinopyroxene by Welsch et al. (2016) and Ubide et al. (2019) indicate that sector zoning in clinopyroxene appears under near-equilibrium conditions at low degrees of undercooling. Therefore, the euhedral sector-zoned microphenocrysts in this study, showing crystallisation depths corresponding to the Moho, likely formed in an environment with little change in temperature contrasting with the skeletal olivines.

4.5.3. Implications for the temporal evolution of Waitomokia volcano

In order to examine changes in the magmatic plumbing system throughout the eruption, olivine core and rim CaO content versus Fo content is plotted for each individual sample in Fig. 12,

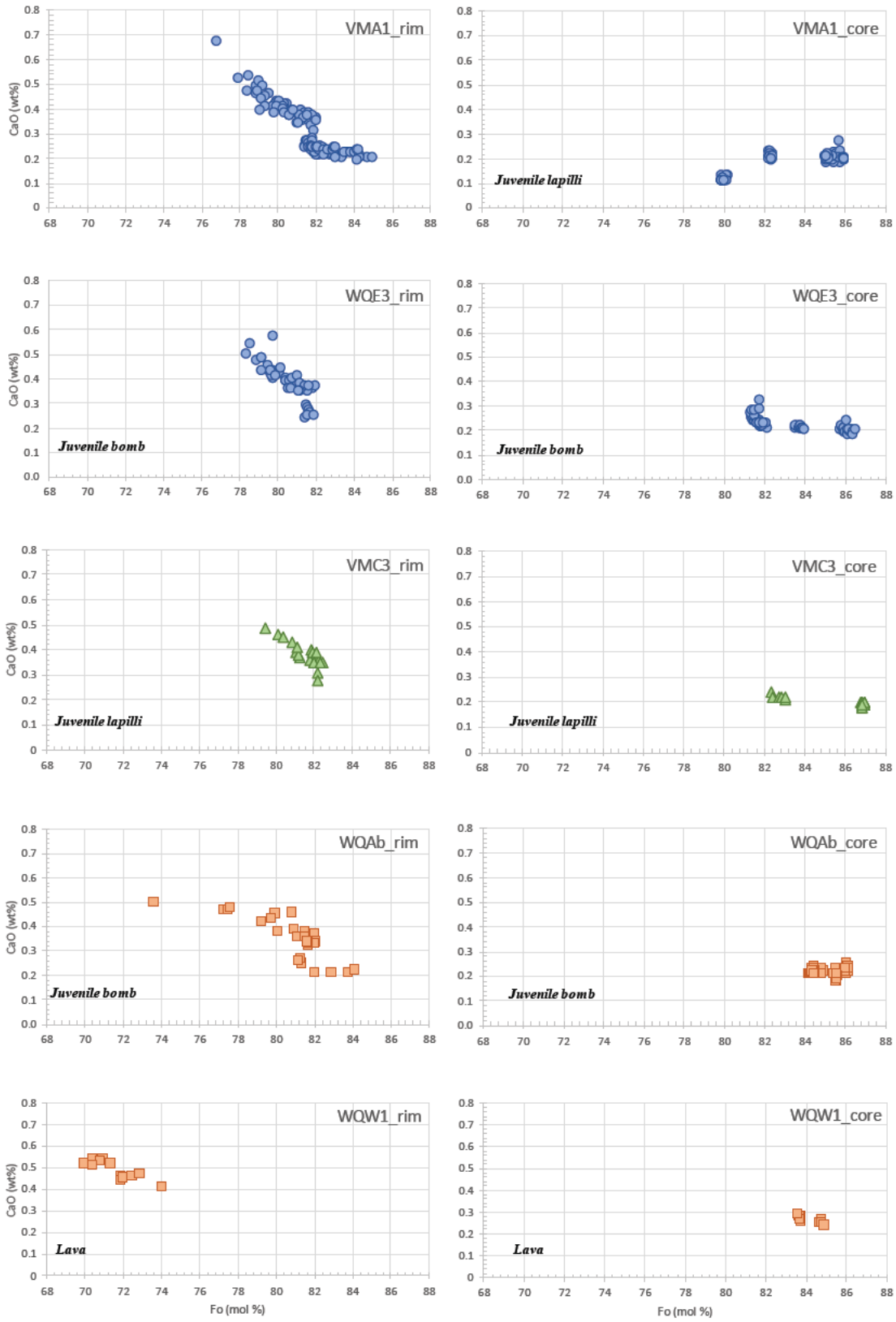

Figure 12: CaO content (wt.%) against Fo content (mol.%) for olivine cores and rims in individual samples: juvenile lapilli VMA1 (a, b) and VMC3 (e, f), juvenile bomb WQE3 (c, d) and WQAb (g, h), and lava deposit WQW1 (i, l).

with a code of colours relative to eruption stage (blue = early phreatomagmatic phase; green = late phreatomagmatic phase; orange = magmatic phase). Fo content profiles from rim to core are also presented for the three eruption stages in Fig. 13. The early phase of the phreatomagmatic eruption (represented by VMA1 and WQE3 from the tuff ring rim) shows a wider range in olivine core composition compared to later stages of the eruption (Fig. 12, blue samples; and Fig. 13a). This is interpreted as due to the complexity involved in the establishment and in the opening of the magmatic system at depth, with crystallisation events happened at different temperatures and depths from a similar parental magma to produce the range in Fo content at a similar CaO content in the cores. During the later phreatomagmatic activity (VMC3), we do not find the reversed zoned olivine of Group 2, but still we have a relatively wide range in Fo core content within the crystals (Figs. 12 and 13b). Towards the more magmatic stages of the eruption the olivine core compositions are high in Fo content and more restricted in range, suggesting dominance of the

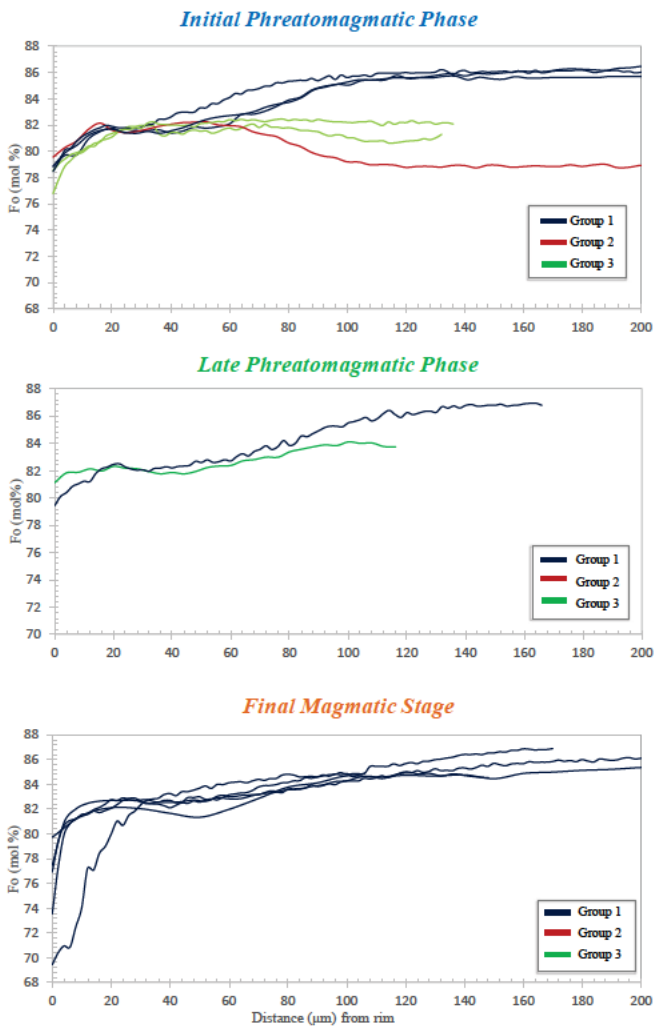

Figure 13: Olivine Fo (mol.%) zoning profiles subdivided by Group 1, 2 and 3 during the eruptive stages: initial phreatomagmatic stage (a), late phreatomagmatic stage (b) and final magmatic stage (c).

involvement of a more mafic/hotter melt in the final phase of the eruption. Interestingly, the lava sample (WQW1) collected from the location of the formed scoria cones that represents ponded lava and the youngest deposit of the eruption sequence, both exhibits relatively high Fo core contents (>83 mol.%; ME1) and the lowest outer rim Fo contents (~70-74 mol.%; Fig. 12). The lack of Fo content between 74 to 83 mol.% in WQW1 olivines, which is in contrast to all the other samples in this study, suggests that this magma may have had little interaction with other magma/s en route to the surface, and/or not stalled for any significant amount of time. The low Fo rims with a steep decrease in Fo (Fig. 13) in WQW1 may be related to crystal growth during cooling as magma ponded in the conduit.

A schematic petrogenetic model for Waitomokia is presented in Fig. 14. We propose that primitive magma ME1 (from the same mantle source or from two different sources, considering the observed variation in CaO content) ascended and intruded at around the transition of the crust-mantle boundary (Moho) as constrained by our thermobarometry results, where magma fractionated in ME2 (Fig. 14a). Further addition/s of magma (from ME1) reached the Moho, mixed and likely triggered fast ascent through the crust (Fig. 14b). The opening phreatomagmatic

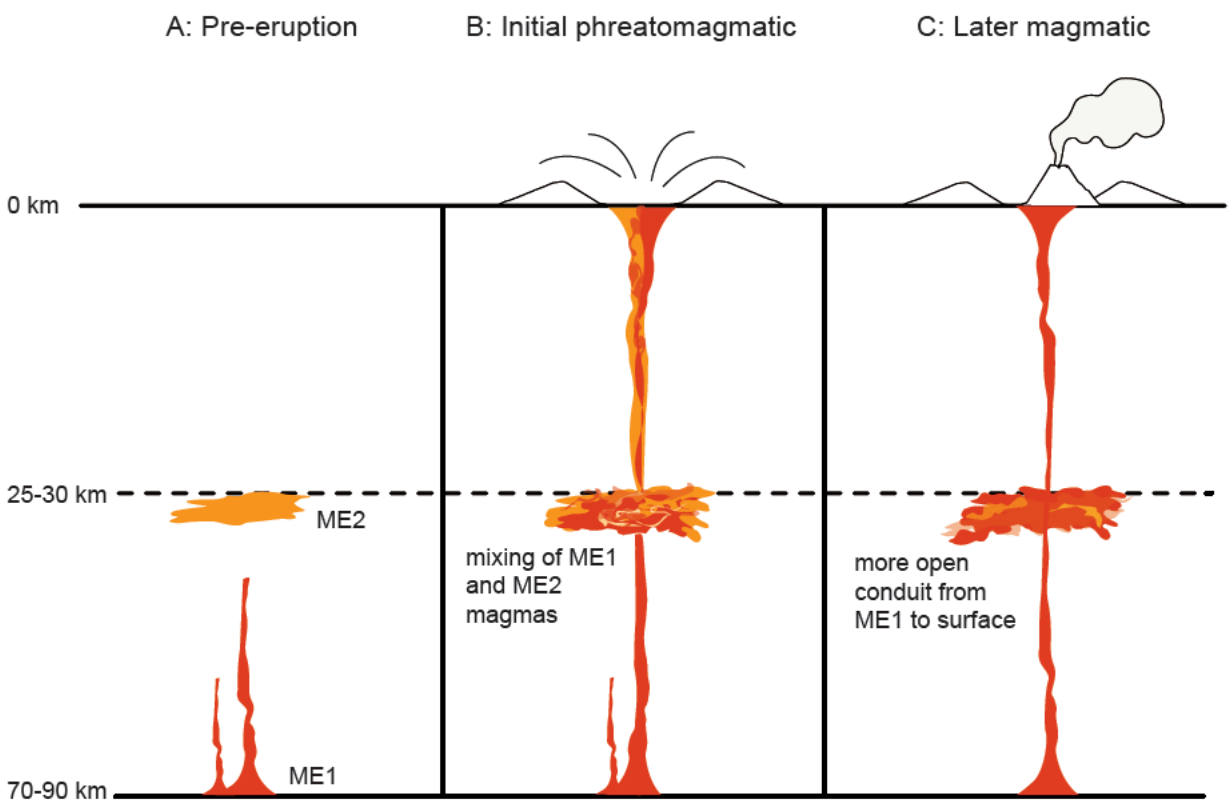

Figure 14: Schematic model showing the development of the magmatic plumbing system at Waitomokia volcano. A) Magma from ME1 is generated by partial melting of the upper mantle around 70-90 km depth (Horspool et al., 2006). ME2 may also be derived from the upper mantle and present at the crust-mantle transition (Moho). Group 1 olivine start to grow in ME1 (Fo >85). Instead Groups 2 and 3 are representative of ME2. B) Interaction between melts from ME1 and ME2 likely triggered the opening pheatomagmatic eruption. All three olivine groups were found within this stage. C) Final magmatic activity, where magma feeding the eruption if dominantly sourced from ME1.

phase of the eruption therefore contained a wide range in Fo core composition due to sourcing magma from ME1 and ME2. However, once the conduit was open, magma from ME1 (high Fo core) was not inhibited by stalling at the Moho in ME2 on ascent. Whether or not the volume of eruptable magma in ME2 had been exhausted in the earlier phreatomagmatic phases of the eruption is unknown. Regardless, there appears to be a reduction in overall compositional complexity through the eruption. A reduction in system complexity as the eruption progressed from initial phreatomagmatic to later magmatic phase was also proposed by Jankovics et al. (2019) in a recent study investigating the compositional and textural diversity in olivine and spinel from a monogenetic basaltic volcano in the Bakony-Balaton Highland Volcanic Field, Eastern Central Europe. More research is required to establish whether this reduction in complexity through time characterises sub-volcanic magmatic plumbing systems within continental intraplate only, or basaltic volcanic fields more broadly. Future work will utilise the compositional zoning patterns in olivine to determine ascent rate through Mg-Fe in olivine diffusion studies to test the ascent hypotheses presented here.

4.6. Conclusion

Mineral textural and compositional analyses of olivine at Waitomokia show a decrese in complexity during the evolution of the sub-volcanic magmatic system feeding the eruption. We reconstructed the history that the olivine crystals recorded by combining shape, texture and compositional zoning patterns, to identify if single or different types of magmas were involved during the evolution of the eruption from phreatomagmatic to magmatic activity. Through the composition of olivine cores were identified at least two different magmatic environments (ME1 and ME2) that played an important role in the evolution of the magmatic system. ME1 likely corresponds to an environment close to the low velocity region in the upper mantle observed from geophysical data at 70-90 km depth (Group 1 olivine). ME2 may have also been produced in the same region ,but represents storage/stalling at the Moho (Group 1 and 3 olivine). The interaction of magma/s from ME1 and ME2 possibly triggered final fast ascent through the crust and produced a wide range of compositions in olivine (Group 1, 2 and 3). During the evolution of the sub-volcanic magmatic system, its complexity decreased due to dominance of the ME1 magma, possible draining eruptible magma from ME2 and opening ascent pathway (Fig. 14c). The skeletal textures observed in olivine suggest moderate undercooling of melt and likely fast magma ascent during transport. Our results provide an important insight into the way continental intraplate basaltic volcanoes behave, and can improve hazard scenarios. This work highlights how even an apparently simple volcanic system,

such as the volcanic field in Auckland, sub-volcanic magmatic systems can be characterised by magmatic interactions between different magma batches.

In future works, we could refine the model proposed here and place additional constraints based on trace element compositions of representative grains, both from the main olivine core and the rim populations, and use the compositional zoning to calculate ascent timescales from source to surface via Mg-Fe diffusion chronometry. Moreover, modelling CaO variability with rhyolite-MELTS program will be a grateful tool to explore the fractional crystallisation of olivine and clinopyroxene over time.

Acknowledgments

This work was funded by a Macquarie University Research Excellence Scholarship (MQRES) (2015081) associated with an Australian Research Council Discovery Project (DP150100328). We thank Rebecca Griffis for sharing samples and whole-rock data. Lucy McGee is thanked for the helpful discussion during fieldwork in 2016. Ian Weddings and Villa Maria Vineyard are thanked for access to the few remaining volcanic deposits at Waitomokia. Warm thanks to Timothy Murphy (Macquarie University) for his assistance with the scanning electron microscope and electron microprobe and for sharing his precious knowledge about the instruments. Thank you also to Helena Albert, Marina Veter and Micheal Forster for helpful discussions about olivine and basaltic volcanic fields.

References

Agustín-Flores, J., Németh, K., Cronin, S.J., Lindsay, J.M., Kereszturi, G., Brand, B.D. and Smith, I.E., 2014. Phreatomagmatic eruptions through unconsolidated coastal plain sequences, Maungataketake, Auckland volcanic field (New Zealand). Journal of Volcanology and Geothermal Research, 276: 46-63.

Albert, H., Costa, F. and Marti, J., 2015. Timing of Magmatic Processes and Unrest Associated with Mafic Historical Monogenetic Eruptions in Tenerife Island. Journal of Petrology, 56(10): 1945-1965.

Albert, H., Costa, F., Martí, J., 2016. Years to weeks of seismic unrest and magmatic intrusions precede monogenetic eruptions. Geology 44, 211–214.

Allen, S.R., Bryner, V.F., Smith, I.E.M. and Ballance, P.F., 1996. Facies analysis of pyroclastic deposits within basaltic tuff-rings of the Auckland volcanic field, New Zealand. New Zealand

Journal of Geology and Geophysics, 39(2): 309-327.

Allen, S.R. and Smith, I.E., 1994. Eruption styles and volcanic hazard in the Auckland. 20: 5-14.

Blundy, J. and Cashman, K., 2008. Petrologic Reconstruction of Magmatic System Variables and Processes. Minerals, Inclusions and Volcanic Processes, 69: 179-239.

BREARLEY M, SCARFE CM (1986) Dissolution Rates of Upper Mantle Minerals in an Alkali Basalt Melt at High Pressure: An Experimental Study and Implications for Ultramafic Xenolith Survival J Petrol 27:1157-1182 doi:10.1093/petrology/27.5.1157

Brenna, M., Cronin, S.J., Smith, I.E.M., Sohn, Y.K., Németh, K., 2010. Mechanisms driving polymagmatic activity at a monogenetic volcano, Udo, Jeju Island, South Korea. Contrib. Mineral. Petrol. 160 (6), 931–950.

Brenna M et al. (2018) Olivine xenocryst diffusion reveals rapid monogenetic basaltic magma ascent following complex storage at Pupuke Maar, Auckland Volcanic Field, New Zealand Earth Planet Sc Lett 499:13-22 doi:10.1016/j.epsl.2018.07.015.

Briggs RM, Okada T, Itaya T, Shibuya H, Smith IEM (1994) K-Ar ages, paleomagnetism, and geochemistry of South Auckland volcanic field, North Island, New Zealand. NZ J Geol Geophys 37:143–153.

Camp, V.E., Hooper, P.R., Roobol, M.J., White, D.L. 1987. The Madinah eruption, Saudi Arabia: magma mixing and simultaneous extrusion of three basaltic chemical types. Bulletin of Volcanology 49: 489-508.

Cas RAF, van Otterloo J, Blaikie TN, van den Hove J (2017) The dynamics of a very large intra-plate continental basaltic volcanic province, the Newer Volcanics Province, SE Australia, and implications for other provinces Geol Soc Spec Publ 446:123-172 doi:10.1144/Sp446.8

Cassidy J, France SJ, Locke CA (2007) Gravity and magnetic investigation of maar volcanoes, Auckland volcanic field, New Zealand J Volcanol Geoth Res 159:153-163 doi:10.1016/j.jvolgeores.2006.06.007

Chakraborty, S., 1997. Rates and mechanisms of Fe-Mg interdiffusion in olivine at 980°–1300° C. Journal of Geophysical Research: Solid Earth, 102(B6): 12317-12331.

Cook C, Briggs RM, Smith IEM, Maas R (2005) Petrology and geochemistry of intraplate basalts in the South Auckland volcanic field, New Zealand: evidence for two coeval magma suites from distinct sources. J Petrol 46:473–503.

Costa, F., Andreastuti, S., de Maisonneuve, C.B. and Pallister, J.S., 2013. Petrological insights into the storage conditions, and magmatic processes that yielded the centennial 2010 Merapi explosive

eruption. Journal of Volcanology and Geothermal Research, 261: 209-235.

Costa, F. and Chakraborty, S., 2004. Decadal time gaps between mafic intrusion and silicic eruption obtained from chemical zoning patterns in olivine. Earth and Planetary Science Letters, 227(3-4): 517-530.

Costa F, Dungan M (2005) Short time scales of magmatic assimilation from diffusion modeling of multiple elements in olivine Geology 33:837-840 doi:10.1130/G21675.1.

Dalton JA, Lane SJ (1996) Electron microprobe analysis of Ca in olivine close to grain boundaries; the problem of secondary X-ray fluorescence Am Mineral 81:194-201 doi:10.2138/am-1996-1-224.

Davidson, J., Morgan, D., Charlier, B., Harlou, R. and Hora, J., 2007. Microsampling and isotopic analysis of igneous rocks: implications for the study of magmatic systems. Annu. Rev. Earth Planet. Sci., 35: 273-311.

Davidson, J.P. and Tepley, F.J., 1997. Recharge in volcanic systems: Evidence from isotope profiles of phenocrysts. Science, 275(5301): 826-829.

Deer WA, Howie RA, Zussman J (1992) An introduction to the rock-forming minerals. Longman Scientific & Technical.

Dohmen, R. and Chakraborty, S., 2007. Fe–Mg diffusion in olivine II: point defect chemistry, change of diffusion mechanisms and a model for calculation of diffusion coefficients in natural olivine. Physics and Chemistry of Minerals, 34(6): 409-430.

Donaldson CH (1976) An experimental investigation of olivine morphology. Contrib Mineral Petrol 57:187–213.

Drever HI, Johnston R (1957) Crystal growth of forsteritic olivine in magmas and melts. Trans R Soc Edinb 63:289–315.

Droop, G., 1987. A general equation for estimating Fe 3+ concentrations in ferromagnesian silicates and oxides from microprobe analyses, using stoichiometric criteria. Mineralogical magazine, 51(361): 431-435.

Fabbro, G.N., Druitt, T.H. and Costa, F., 2017. Storage and Eruption of Silicic Magma across the Transition from Dominantly Effusive to Caldera-forming States at an Arc Volcano (Santorini, Greece). Journal of Petrology, 58(12): 2429-2464.

Faure F, Trolliard G, Nicollet C, Montel J-M (2003) A developmental model of olivine morphology as a function of the cooling rate and the degree of undercooling. Contrib Miner Pet 145(2):251–263.

Ginibre, C., Worner, G. and Kronz, A., 2002. Minor- and trace-element zoning in plagioclase: implications for magma chamber processes at Parinacota volcano, northern Chile. Contributions to Mineralogy and Petrology, 143(3): 300-315.

Gordeychik B, Churikova T, Kronz A, Sundermeyer C, Simakin A, Worner G (2018) Growth of, and diffusion in, olivine in ultra-fast ascending basalt magmas from Shiveluch volcano Sci Rep-Uk 8 doi:ARTN 11775 10.1038/s41598-018-30133-1

Griffis, B. 2013. The volcanological and geochemical evolution of Waitomokia Volcano, Auckland Volcanic Field, New Zealand. Honours Thesis, Macquarie University, Sydney, Australia.

Gutmann, J.T., 2002. Strombolian and effusive activity as precursors to phreatomagmatism: eruptive sequence at maars of the Pinacate volcanic field, Sonora, Mexico. Journal of Volcanology and Geothermal Research, 113(1-2): 345-356.

Jankovics, M.É., Harangi, S., Kiss, B., Ntaflos, T., 2012. Open-system evolution of the Füzes-tó alkaline basaltic magma, western Pannonian Basin: Constraints from mineral tex- tures and compositions. Lithos 140-141, 25–37.

Jankovics ME et al. (2019) Olivine major and trace element compositions coupled with spinel chemistry to unravel the magmatic systems feeding monogenetic basaltic volcanoes J Volcanol Geoth Res 369:203-223 doi:10.1016/j.jvolgeores.2018.11.027

Jollands, M.C., Hermann, J., O'Neill, H.S.C., Spandler, C., Padrón-Navarta, J.A., 2016. Diffusion of Ti and some divalent cations in olivine as a function of tempera- ture, oxygen fugacity, chemical potentials and crystal orientation. J. Petrol. 57, 1983–2010.

Hartley, M.E., Morgan, D.J., Maclennan, J., Edmonds, M. and Thordarson, T., 2016. Tracking timescales of short-term precursors to large basaltic fissure eruptions through Fe–Mg diffusion in olivine. Earth and Planetary Science Letters, 439: 58-70.

Hayward BW, Murdoch G, Maitland G (2011) Volcanoes of Auckland, the essential guide. Auckland University Press, Auckland, New Zealand.

Helz, R.T., 1987. Differentiation behavior of Kilauea Iki lava lake, Kilauea Volcano, Hawaii: an overview of past and current work. Magmatic processes: physicochemical principles, 1: 241-258.

Hopkins JL, Timm C, Millet M-A, Poirier A, Wilson CJN, Leonard GS (2016) Os isotopic constraints on crustal contamination in Auckland Volcanic Field basalts, New Zealand. Chem Geol 439:83–97.

Hopkins, J.L., Wilson, C.J., Millet, M.-A., Leonard, G.S., Timm, C., McGee, L.E., Smith, I.E. and Smith, E.G., 2017. Multi-criteria correlation of tephra deposits to source centres applied in the Auckland Volcanic Field, New Zealand. Bulletin of Volcanology, 79(7): 55.

Horspool, N.A., Savage, M.K., Bannister, S. 2006. Implications for intraplate volcanism and back-arc deformation in northwestern New Zealand, from joint inversion of receiver functions and surface waves. Geophysical Journal International 166: 1466-1483.

Kahl, M., Chakraborty, S., Costa, F., Pompilio, M., 2011. Dynamic plumbing system beneath volcanoes revealed by kinetic modeling, and the connection to monitoring data: an example from Mt. Etna. Earth Planet. Sci. Lett. 308 (1–2), 11–22.

Kahl, M., Chakraborty, S., Pompilio, M. and Costa, F., 2015. Constraints on the nature and evolution of the magma plumbing system of Mt. Etna Volcano (1991–2008) from a combined thermodynamic and kinetic modelling of the compositional record of minerals. Journal of Petrology, 56(10): 2025-2068.

Kereszturi, G., Nemeth, K., Cronin, S.J., Agustin-Flores, J., Smith, I.E.M. and Lindsay, J., 2013. A model for calculating eruptive volumes for monogenetic volcanoes - Implication for the Quaternary Auckland Volcanic Field, New Zealand. Journal of Volcanology and Geothermal Research, 266: 16-33.

Kermode L.O. (1992) Geology of the Auckland urban area. Scale 1:50, 000. Institute of Geological and Nuclear Sciences geological map 2. Institute of Geological and Nuclear Sciences Ltd, Lower Hutt, New Zealand.

Larsen, E.S., Irving, J., Gonyer, F. and Larsen 3rd, E.S., 1938. Petrologic results of a study of the minerals from the Tertiary volcanic rocks of the San Juan region, Colorado. American Mineralogist: Journal of Earth and Planetary Materials, 23(4): 227-257.

Linnell, T., Shane, P., Smith, I., Augustinus, P., Cronin, S., Lindsay, J. and Maas, R., 2016. Long-lived shield volcanism within a monogenetic basaltic field: The conundrum of Rangitoto volcano, New Zealand. Bulletin, 128(7-8): 1160-1172.

Loucks, R.R., 1996. A precise olivine-augite Mg-Fe-exchange geothermometer. Contributions to Mineralogy and Petrology, 125(2-3): 140-150.

Mattioli, M., Renzulli, A., Menna, M. and Holm, P.M., 2006. Rapid ascent and contamination of magmas through the thick crust of the CVZ (Andes, Ollagüe region): Evidence from a nearly aphyric high-K andesite with skeletal olivines. Journal of Volcanology and Geothermal Research, 158(1-2): 87-105.

McBirney, A.R., Taylor, H.P., Armstrong, R.L. 1987 Paricutin re-examined: a classic example of crustal assimilation in calc-alkaline magma. Contributions to Mineralogy and Petrology 95: 4-20.

McGee LE, Beier C, Smith IEM, Turner S (2011) Dynamics of melting beneath a small-scale basaltic system: a U-Th-Ra study from Rangitoto volcano, Auckland Volcanic Field, New Zealand.

Contrib Mineral Petr 162:547–563

McGee, L.E., Millet, M.-A., Smith, I.E., Németh, K. and Lindsay, J.M., 2012. The inception and progression of melting in a monogenetic eruption: Motukorea Volcano, the Auckland Volcanic Field, New Zealand. Lithos, 155: 360-374.

McGee LE, Smith IEM, Millet M-A, Handley H, Lindsay JM (2013) Asthenospheric control of melting processes in a monogenetic ba- saltic system: a case study of the Auckland Volcanic Field, New Zealand. J Petrol 54:2125–2153

McGee, L.E. and Smith, I.E.M., 2016. Interpreting chemical compositions of small scale basaltic systems: A review. Journal of Volcanology and Geothermal Research, 325: 45-60.

Molloy C, Shane P, Augustinus P (2009) Eruption recurrence rates in a basaltic volcanic field based on tephra layers in maar sediments: implications for hazards in the Auckland volcanic field. Geol Soc am Bull 121:1666–1677

Neave, D.A. and Putirka, K.D., 2017. A new clinopyroxene-liquid barometer, and implications for magma storage pressures under Icelandic rift zones. American Mineralogist, 102(4): 777-794.

Needham, A.J., Lindsay, J.M., Smith, I.E.M., Augustinus, P. and Shane, P.A., 2011. Sequential eruption of alkaline and sub-alkaline magmas from a small monogenetic volcano in the Auckland Volcanic Field, New Zealand. Journal of Volcanology and Geothermal Research, 201(1-4): 126-142.

O'Reilly, S.Y., Griffin, W.L. 2011. Rates of magma ascent: constraints from mantle-derived xenoliths. In Timescales of magmatic processes: From core to atmosphere Eds. Dosetto et al. Blackwell Publishing Ltd.

Putirka, K. D.; Thermometers and Barometers for Volcanic Systems (2008). Reviews in Mineralogy and Geochemistry ; 69 (1): 61–120. doi: https://doi.org/10.2138/rmg.2008.69.3

Rodgers, K. A.; Brothers, R. N.; Searle, E. J. 1975: Ultramafic nodules and their host rocks from Auckland, New Zealand. Geological magazine 112: 163-174.

Schmincke, H.-U., Lorenz, V. and Seck, H., 1983. The quaternary Eifel volcanic fields, Plateau uplift. Springer, pp. 139-151.

Searle, E., 1961. The petrology of the Auckland basalts. New Zealand Journal of Geology and Geophysics, 4: 165-204.

Searle, E., 1962. The volcanoes of Auckland city. New Zealand Journal of Geology and Geophysics, 5(2): 193-227.

Shea, T., Lynn, K.J. and Garcia, M.O., 2015. Cracking the olivine zoning code: Distinguishing

between crystal growth and diffusion. Geology, 43(10): 935-938.

Smith IEM, Blake S, Wilson CJN, Houghton BF (2008) Deep-seated fractionation during the rise of a small-volume basalt magma batch: Crater Hill, Auckland, New Zealand. Contrib Mineral Petrol 155: 511–527.

Smithsonian Institution/SEAN 1989. Global Volcanism 1975-1985. Englewood Cliffs, New Jersey, Prentice Hall, and Washington DC, American Geophysical Union, 657 p.

Spargo SRW (2007) The Pupuke volcanic centre: polygenetic magmas in a monogenetic field. MSc thesis. University of Auckland, New Zealand.

Spera, F.J. 1984. Carbon dioxide in petrogenesis III: role of volatiles in the ascent of alkaline magma with special reference to xenolith-bearing mafic lavas. Contributions to Mineralogy and Petrology 88: 217-232.

Sporli, K.B. and Eastwood, V.R., 1997. Elliptical boundary of an intraplate volcanic field, Auckland, New Zealand. Journal of Volcanology and Geothermal Research, 79(3-4): 169-179.

Sprung, P., Schuth, S., Münker, C. and Hoke, L., 2007. Intraplate volcanism in New Zealand: the role of fossil plume material and variable lithospheric properties. Contributions to Mineralogy and Petrology, 153(6): 669-687.

Stormer 1973. Calcium zoning in olivine and its relationship to silica activity and pressure. Geochimica, Comsochimica, Acta 37, 1815-1821.

Thorarinsson, S., Steinthorsson, S., Einarsson, T., Kristmannsdottir, H., Oskarsson, N. 1973. The eruption on Heimaey, Iceland. Nature 241: 372-375.

Ubide, T., Mollo, S., Zhao, J-x., Nazzari, M., Scarlato, P. 2019. Sector-zoned clinopyroxene as a recorder of magma history, eruption triggers and ascent. Geochimica et Cosmochimica Acta 251, 265-283.

Wass, S.Y. & Irving, A.J. 1976. XENMEG - A catalogue of Occurrences of Xenoliths and Megacrysts in Volcanic Rocks of Eastern Australia. The Australian Museum, Sydney.

Welsch B, Faure F, Famin V, Baronnet A, Bachèlery P (2013) Dendritic crystallization: a single process for all the textures of olivine in basalts? J Petrol 54(3):539–574

Welsch B., Hammer J., Baronnet A., Jacob S., Hellebrand E. and Sinton J. (2016) Clinopyroxene in post-shield Haleakala ankaramite: 2. Texture, compositional zoning and supersaturation in the magma. Contrib. Mineral. Petrol. 171, 6. https:// doi.org/10.1007/s00410-015-1213-9.

Appendix C

C.1: Samples analyses in this study from rock collected during two different field trips.

Sample	Field Date	Description	SEM	EMPA
WQAb	2016	Bomb magmatic stage	X	X
VMA1	2013	Lapilli- Tuff ring rim	X	X
VMC3	2013	Lapilli- Later phreat stage	X	X
WQE3	2013	Bomb in a tuff ring	X	X
WQW1	2013	Lava (inner cone)	X	X
VMA7	2013	Lapilli- Tuff ring rim	X	
VMB1A	2013	Lapilli scoria cone	X	
VMC2	2013	Lapilli- Later phreatomagmatic stage	X	
VMC4	2013	Lapilli- Later phreatomagmatic stage	X	
VMC6	2013	Lapilli- Later phreatomagmatic stage	X	
VMDW2	2013	Early stage of phreatomagmatic	X	
WQA1	2013	Bomb magmatic stage	X	

C.2: Whole rock data from selected samples.

Sample	VMC6	VMC2	WQA1	WQC3	WQD1	WQW1
Na_2O	2.89	3.08	3.31	3.43	3.34	3.21
MgO	11.6	11.05	11.4	11.43	11.72	11.34
Al_2O_3	12.69	12.7	12.57	12.54	12.62	13
SiO_2	44.41	45.06	45.11	42.76	43.44	43.94
P_2O_5	0.67	0.66	0.66	0.63	0.65	0.47
K_2O	1.09	1.45	1.44	1.32	1.38	1.21
CaO	9.69	9.47	9.53	9.95	9.98	10.64
TiO_2	2.67	2.66	2.64	2.69	2.73	2.76
Mn_3O_4	0.21	0.20	0.21	0.20	0.21	0.20
Fe_2O_3	14.05	13.82	13.93	13.78	14.09	13.31
LOI	0.01	0.00	0.00	0.00	0.00	0.00
Total	99.97	100.15	100.80	98.7	100.16	100.08

Chapter 5

Insights into volatile transport and eruption triggering at explosive volcanoes

Lucy McGee[1], Simon Turner[1], Mark Reagan[2], Heather Handley[1], Rosa Didonna[1], Kim Berlo[3], Sarah Hansen[2], Steve Sparks[4], Jenni Barclay[5]

[1]*Department of Earth and Environmental Sciences, Macquarie University, Sydney, NSW, Australia*
[2]*Department of Earth and Environmental Sciences, The University of Iowa, Iowa, USA*
[3]*Department of Earth and Planetary Sciences, McGill University, Montreal, Canada*
[4]*School of Earth Sciences, University of Bristol, Bristol, UK*
[5]*School of Environmental Science, University of East Anglia, Norwich, UK*

Abstract

Injection of volatile-rich mafic magma prior to an eruption is thought to be a major trigger controlling episodes of explosive volcanism. However, petrologic knowledge of the timescales from mafic injection to eruption have been limited to crystal-scale studies which record this input as the chemical zoning patterns of minerals. The study of mafic enclaves dispersed within eruption products can provide insights into the interaction between deep and shallow reservoirs. We present the first study of U-Th-Ra-Pb isotopes across the interface of two contrasting mafic enclaves in contact with their host andesite from the last major eruption at Soufrière Hills, Montserrat. The application of these time- and volatile-sensitive isotopes to whole rock samples highlights complexities in the interaction of these components, the enclaves' formation mechanisms and their potential as eruption triggers. Analyses of the enclaves exhibit $(^{210}Pb/^{226}Ra)_0$ ratios consistent with volatile input to the subsurface plumbing system a few decades prior to eruption. Samples of the andesitic host however, which make up the bulk of the eruptive products, are in $(^{210}Pb/^{226}Ra)_0$ equilibrium showing no net volatile loss or gain. This finding supports a role for fresh magma during periods of unrest but challenges the hypothesis that volatile transfer from fresh magma via enclaves is a direct trigger of explosive eruptions.

5.1. Introduction

Explosive volcanic eruptions occur frequently, sometimes within a predictable timeframe and other times without warning. It is still unclear, however, what the main driver of tipping the system from 'dormant' to 'imminent eruption' is. Models of subsurface magmatic plumbing systems are becoming increasingly complex with the addition of multiple new geophysical and geochemical studies from the regional scale of the whole volcano down to the individual crystal scale, and detailed studies of how the many components such as volatiles, crystals, and magmatic reservoirs interact can give valuable insights into the triggering mechanism.

5.2. Timescales of eruption triggers: application of Uranium series chemistry

Sparks et al. (1977) hypothesised that some silicic explosive eruptions are triggered by injection of basic magma causing mixing, convection, the transfer of volatiles and then vesiculation, leading to overpressure and explosive eruption. This mechanism is still widely considered viable but recent work has mainly based this conclusion on micro-scale observations such as crystal 'stratigraphy' and in-depth crystal thermobarometry (e.g. Santorini, (Martin et al., 2008) Quizapu, (Ruprecht and Bachmann, 2010), Earthquake Flat, New Zealand, (Molloy et al., 2008), Calbuco 2015 (Morgado et al., 2019), and glass composition studies (e.g. Eyjafjallajkull 2010, (Sigmarsson et al., 2011) and Pinatubo 1991 (Pallister et al., 1992)). Although these approaches can pinpoint the timing of mafic injection causing reheating and rapid magma composition changes, they cannot constrain the role of volatiles in driving explosive eruption.

Evidence for remobilisation due to injection is the occurrence of mafic enclaves and banded pumice in volcanic rocks. The most recent eruption at Soufrière Hills Volcano (SHV) 1995 to 2010 on the island of Montserrat deposited andesitic dome collapse material containing mafic enclaves (e.g. Barclay et al., 2010; Murphy et al., 2000; Plail et al., 2014). Uranium series radionuclides can be applied to such material to investigate the timescales on which volcanic processes occur, as in addition to their varying half-lives each nuclide has different compatibility within melts, fluids and mineral phases (see Bourdon et al., 2003).

The ^{226}Ra-^{210}Pb pair is key to this study because an intermediary daughter, ^{222}Rn (t½ = 3.8 days), will partition into the volatile phase, thereby making the activity ratio $(^{210}Pb/^{226}Ra)_0$ of recently erupted volcanic rocks a strong indicator of volatile loss or gain prior to eruption (Berlo and Turner 2010; Reagan et al., 2017).

5.3. The 1995-2010AD eruption of Soufrière Hills Volcano and the significance of enclave formation

From 1995 to February 2010 SHV underwent five eruptive phases (Phases I-V) separated by hiatuses in activity during which domes continued to grow. All eruptions contain enclaves that are interpreted to be hybrids resulting from interaction between resident andesite and a basaltic

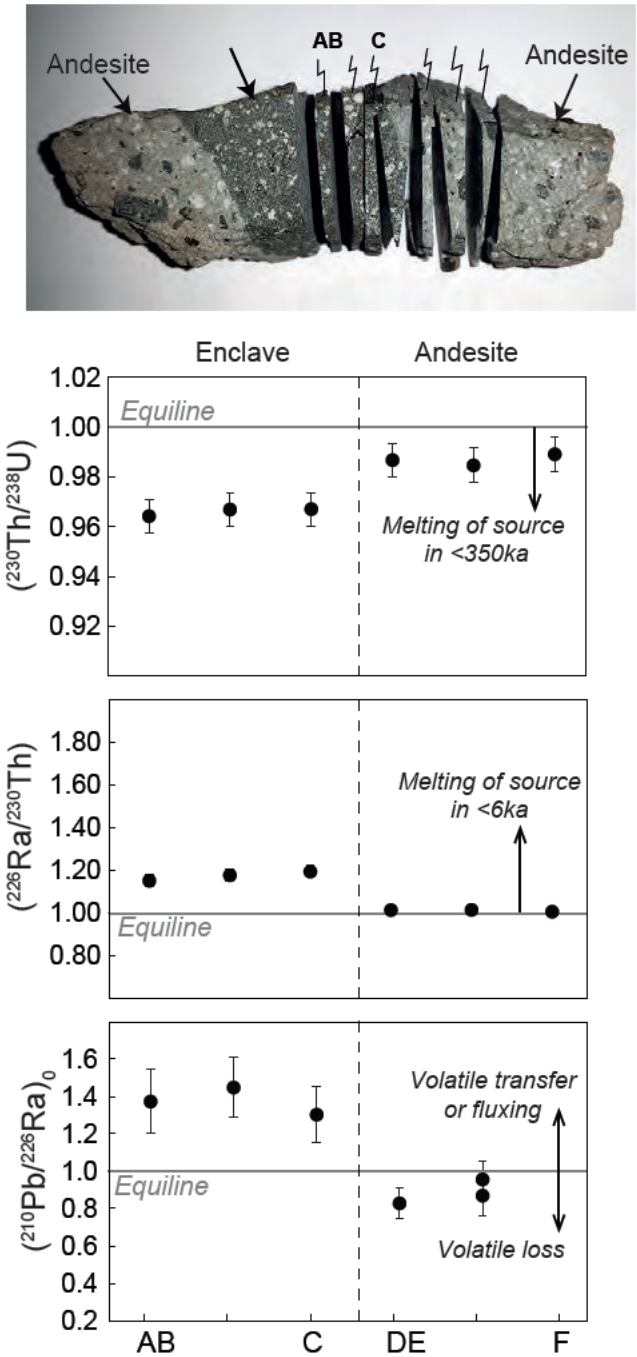

Figure 1: U-series data for sample MT35 from Phase V of the SHV eruption (January 2010).The dashed line denotes the interface of the enclave and host andesite as sectioned in the above photograph. Greater U-Th-Ra disequilibria in the enclave compared to the andesite indicates a younger magma, and excesses of ^{210}Pb show recent volatile aquisition in the magma giving rise to the enclaves.

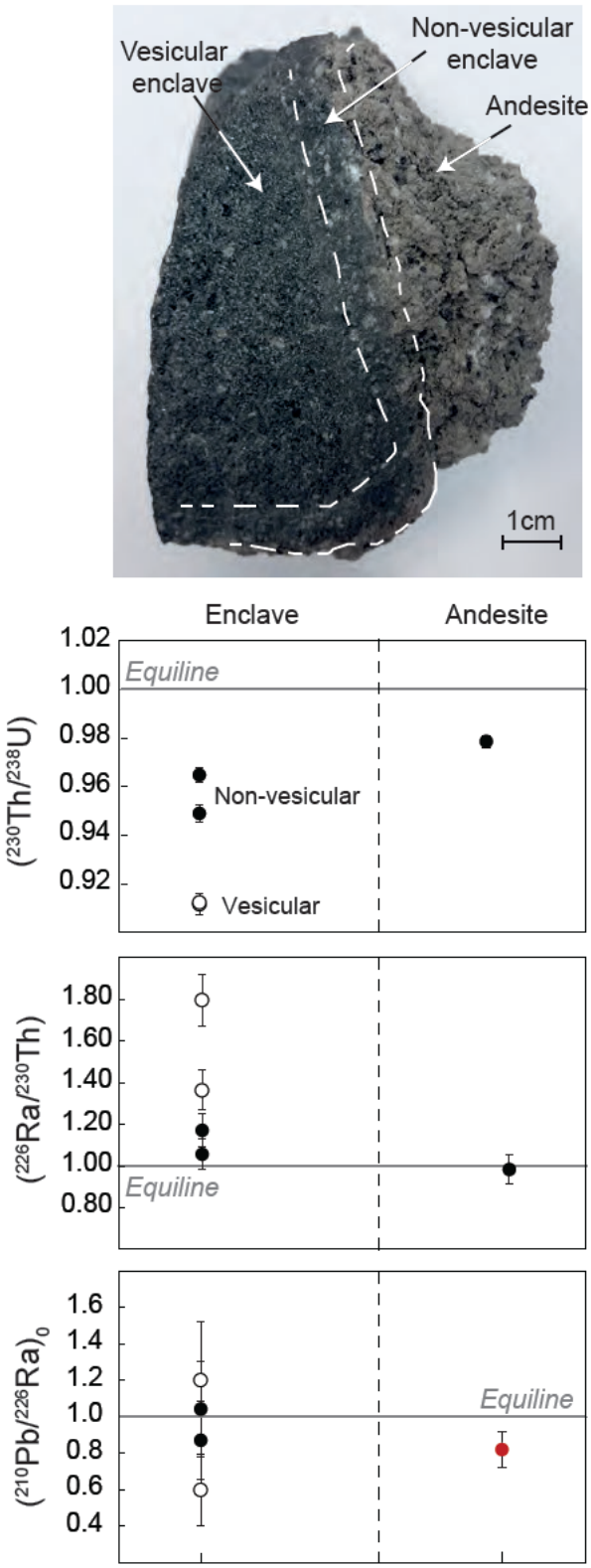

Figure 2: U-series data for sample MT75 from Phase V of the SHV eruption (January 2010).The dashed line denotes the interface of the enclave and host andesite, although note that the enclave has been sectioned into vesicular and non-vesicular regions as in the above photograph. As with MT35, greater U-Th-Ra disequilibria is observed in the enclave (especially the vesicular portion) compared to the andesite. The presence of both ^{210}Pb excess and deficit in the vesicular portion indicates its location at the volatile transfer interface, but these volatiles were not transferred beyond this region. Note that the y-axis scale on each plot is the same as for Figure 1.

recharge magma (Barclay et al., 2010).

Details of the eruptions and monitoring in addition to in-depth studies of the petrogenesis of the magmas are summarised in Sparks and Young (2002) and Wadge et al. (2014). A prominent feature of SHV is its large SO_2 plume and continued outgassing throughout the hiatuses and since January 2010, which may be caused by ponding of exsolved volatiles at shallow levels (Edmonds and Woods, 2018). A recent ^{210}Pb-^{226}Ra study of enclaves and andesites from the entire duration of the eruption inferred the cessation of mafic input (thus ceasing fresh volatile supply) towards the end of Phase II (McGee et al., In review).

Models for the formation and survival of mafic enclaves within silicic host rocks are unanimous in their need for overcoming the thermal and density contrast between two distinct magma compositions. This contrast is the reason why discrete domains of mafic material are preserved rather than hybridisation occurring, although disaggregation of enclaves is a common process (Coombs et al., 2003; Ubide et al., 2014) and indeed one that is observed at SHV (Humphreys et al., 2009). Two main mechanisms of formation and incorporation of mafic enclaves have been suggested: forced injection by dyking followed by convection (Bacon, 1986; Eichelberger and Izbekov, 2000) and development of gravitational instabilities due to accumulation of volatiles from the mafic magma (Bacon, 1986; Coombs et al., 2003; Kayzar et al., 2009; Thomas and Tait, 1997). In the latter model, the interface between the mafic and silicic magmas is a critical zone of interaction rarely seen in natural examples (Edmonds and Woods, 2018).

Here, we examine in detail two contrasting volcanic rock samples which are equally abundant (Plail et al., 2014) from the final eruption of January 2010. The two samples represent textural end-members and shed light on the nature of volatile interaction at the enclave-host interface and the physical process of enclave formation. One contains a non-vesicular enclave and was serially sectioned (enclave-andesite, Fig. 1), the other contains a highly vesicular enclave interior and was cut into representative sections (vesicular interior, non-vesicular enclave, andesite, Fig. 2). General enclave petrography is detailed in Plail et al. (2014) and the petrography and mineralogy of the studied samples are summarised below.

Table 1: New data and standards, method details

	$(^{234}U/^{238}U)$	$(^{238}U/^{232}Th)$	$(^{230}Th/^{232}Th)$	$(^{230}Th/^{238}U)$	U ppm	Th ppm	^{226}Ra fg/g	$(^{226}Ra/^{230}Th)$	$(^{210}Pb/^{226}Ra)_0$	^{210}Po dpm/g
MT35-A (Enclave)	1.002	0.936	0.903	0.964	0.38	1.22	143	1.153	1.374	0.408
MT35-B (Enclave)	1.004	0.963	0.931	0.967	0.36	1.14	141	1.179	1.448	0.421
MT35-C (Enclave)	1.004	0.962	0.930	0.967	0.39	1.24	155	1.196	1.303	0.424
MT35-D (Andesite)	1.003	0.945	0.933	0.987	0.75	2.42	258	1.015	0.829	0.488
MT35-E (Andesite)	0.998	0.953	0.938	0.985	0.73	2.34	251	1.016	0.870	0.493
MT35-F (Andesite)	1.009	0.941	0.931	0.989	0.76	2.44	257	1.007	-	-
MT75-A (Ves. enclave)	1.001	1.006	0.917	0.912	0.28	0.84	118	1.363	1.202	0.300
MT75-B (Ves. enclave)	0.999	1.012	0.923	0.912	0.34	1.03	192	1.798	0.598	0.289
MT75-C (Enclave)	0.997	0.978	0.928	0.949	0.47	1.46	161	1.057	1.043	0.366
MT75-D (Enclave)	1.003	0.965	0.931	0.965	0.48	1.51	185	1.172	0.871	0.365
MT75-E (Andesite)	1.002	0.956	0.935	0.979	0.87	2.75	284	0.983	xxx	xxx
BCR-2 (MT35)	0.998	0.872	0.867	0.995	1.71	5.96	561	0.967	-	-
BCR-2 (MT35 *rpt*)	1.007	0.870	0.872	1.003	1.71	5.95	-	-	-	-
RGM-2 (MT35 ^{210}Po)	-	-	-	-	-	-	-	-	-	4.14
BCR-2 (MT75, + ^{210}Po)	1.004	0.883	0.873	0.988	1.71	5.89	532	0.922	-	1.27
BCR-2 (MT75 *rpt*)	0.994	0.902	0.861	0.954	1.74	5.84	-	-	-	-

All U-Th-Ra data were obtained at MQGA, Macquarie University. ^{210}Po data for sample MT35 was obtained at MQGA and ^{210}Po data for sample MT75 was obtained at the University of Iowa. U-Th-Ra data for BCR-2 are compared to the compilation of Scott et al., 2018: $(^{238}U/^{232}Th) = 0.877$, $(^{230}Th/^{232}Th) = 0.879$, $(^{230}Th/^{238}U) = 1.003$, U ppm = 1.69, Th ppm = 5.83, ^{226}Ra fg/g = 566, $(^{226}Ra/^{230}Th) = 0.993$. ^{210}Po dpm/g are compared the analyses reported in Reagan et al., 2017 BCR-2 = 1.267, RGM-2 = 4.093.

5.4. Methods

Samples from dome collapse material emplaced in January and February 2010 by pyroclastic flows were cut with a precision diamond saw, cleaned in distilled water, dried, and crushed and powdered in an agate mill. Digestion and separation of spiked U-Th-Ra took place on the same sample aliquots, then U-Th were analysed by MC-ICP-MS on a Nu Instruments machine and Ra by TIMS on a Thermo Finnigan machine. ^{210}Pb was analysed using ^{210}Po as a proxy, digesting and separating a 2g aliquot of sample powder, plating Po onto silver discs and counting alpha radiation on an Ametek Alpha Counter for approximately 10 days. All U-Th-Ra and sample MT35 ^{210}Pb was analysed at Macquarie GeoAnalytical (MQGA), and MT75 ^{210}Pb was analysed at the University of Iowa. See Table S1 for all analyses including rock standards.

5.5. Petrography of MT35 and MT75

MT35 and MT75 rocks are erupted during the last eruption at Soufrière Hills Volcano (SHV) on 11th February 2010 and collected from deposits of the dome collapse. Detailed x-ray maps are in Appendix D2-3.

MT35 sample is characterized by andesitic host, which is porphyritic with fine-grained groundmass and contains basaltic andesitic enclaves (defined "Type A" by Plail, 2013). The sample displays a variety of textures and zoning patterns of plagioclase (plag) ±orthopyroxene (Opx) ±amphibole (Amph) ±quartz (qtz) and Fe-Ti oxides in lower of abundance. Plag is the most abundant phase and occurs as phenocrysts (up to ~ 4 mm in size), microphenocrysts (100-300 μm) and microlites (<100 μm) with a wide range of textures (patchy, oscillatory zoning and sieve-textured) and anorthite content (An) from approximately 45 to 90 mol % in the andesitic host and basaltic andesite enclave. Phenocrysts reveal low An (45-55 mol %) and the lowest MgO contents (0.01-0.015 wt.%). Moreover, phenocrysts show core composition with variable range of An (~An45-75) with a range of MgO contents from about 0.01 to 0.04 wt.%. Rims have higher An (> ~70 mol %) and also tend to have higher Mg than the cores.

In the andesitic host, single Opx crystals (> 300 μm) are unzoned (En57-59, Fs32-45, Wo_{19-2} and Mg# 56-60) or have a thin rim (<10 μm) of Cpx (Mg# 70-75 and $Wo1_{9-22}$). Amph is unreacted or sometime contain inclusions of plagioclase and oxides. Qtz has reaction rims of Cpx and magnetite, apatite and rare zircon are also present. The groundmass of the host andesite is dominated by plagioclase with a wide range in sizes that gives a seriate texture to the sample.

Microlites of Opx, Cpx, Fe-Ti oxides, and glass, with almost no vesicles are also present in the groundmass.

In the enclave, phenocrysts (crystals > 300 μm) of Opx are observed as single isolated crystals or as glomerocrysts (up to 8 mm), with reaction rims of clinopyroxene (Cpx), or unzoned with similar composition of the Opx found in the andesite. Moreover, reversely zoned (higher Mg/Fe in the rims than cores) are observed with En_{58-68}, Fs_{31-36}, $Wo_{1\ 3-2\ 8}$ and Mg# 60-73. Reacted large Amph, qtz and Fe-Ti oxides are in lower abundance. Amph (up to 5 mm in size) show reaction rims of Cpx, plag, oxides and glass. Phenocrysts of qtz, with or without, reaction rims of Cpx (up to 2 mm in size) are also observed. Magnetite is much more abundant than ilmenite but can be found with a rim of ilmenite. Accessory minerals are apatite and rare zircon. The groundmass of the enclave contains euhedral laths of plagioclase, amphibole, and pyroxenes as well as vesicles that are bounded by crystal margins.

MT75 sample exhibits andesite with enclaves, which are defined composite (Type C) by Plail (2013). Andesite is porphyritic with fine-grained groundmass and the mineral assemblage is Plag±Opx ± Amph±Fe-Ti oxides. Plag is the dominant phase with textures and compositions similar to MT35: phenocrysts (up to ~ 3 mm in size), with core composition of An50-55 and Mg 0.01-0.02 wt.% and with rim of An_{70-85} and Mg up to 0.1 wt.%. Opx crystals (> 100 μm) are unzoned with Mg# 60-70. Amph is unreacted and magnetite are also present. Qtz is not present in the host andesite. The groundmass is dominated by Plag, Opx, Cpx, Fe-Ti oxides and glass.

Enclaves show two different textural zones. One with high phenocrysts inherited from the host andesite that shows disequilibrium textures (e.g., plag sieve-textured, amph broken down rims) and low vesicularity. The diktytaxitic groundmass is composed of Plag, Opx, Cpx, Amph and glass, similar in texture and composition of the basaltic andesitic enclave in MT35. The other zone is characterized by rare inherited phenocrysts of Plag, Opx and Amph in a seriate groundmass of Plag, Cpx and Amph with a high vesicularity.

Plag are the most abundant phase and have two well-defined zones: an interior, often characterised by patchy, dusty and oscillatory zoning, and an overgrowth zone (rim) of a different composition. Some crystals contain an intermediate sieve-textured zone with abundant melt inclusions between the interior and overgrowth zones.

5.6. U-Th-Ra-Pb results

Analytical details, all data and rock standards analysed are presented in Table S1. Plotted error bars are the maximum accuracy error based on analyses of USGS rock standards BCR-2 and RGM-2.

The U-series data lie within the range of previous bulk andesite and enclave analyses from the entire 1995-2010 eruption (McGee et al., in review, Figure S1). The vesiculated interior of sample MT75 has the highest disequilibria in Th-Ra (extending up to ($^{226}Ra/^{230}Th$) ratios of 1.8), while the non-vesicular enclaves in each sample have similar ($^{230}Th/^{238}U$) and ($^{226}Ra/^{230}Th$) ratios (0.96 and 1.18 respectively) (Figs. 1 and 2). The host andesite is close to equilibrium (i.e. 1) in ($^{230}Th/^{238}U$) and ($^{226}Ra/^{230}Th$). The $(^{210}Pb/^{226}Ra)_0$ ratios of the two samples are rather different. All enclave slices from MT35 have ^{210}Pb-excesses (up to 1.4) and all andesite samples are in equilibrium or have a slight ^{210}Pb-deficit (Fig. 1). Enclaves samples from MT75, however, have $(^{210}Pb/^{226}Ra)_0$ ratios ranging from 0.6 to 1.2 i.e. display both ^{210}Pb-excesses and -deficits, although notably the extremes of this range are both 'vesicular' portions of the enclave while the non-vesicular portions are within error of equilibrium (Fig. 2). Andesite phenocryst residence times of 10s to up to 1200 years suggest that crystals are upwards of a few 100s of years old (Zellmer et al., 2003), therefore may have ($^{238}U/^{232}Th$) and ($^{226}Ra/^{230}Th$) disequilibria, but are too old to affect ($^{210}Pb/^{226}Ra$) ratios. Given the highly incompatible nature of U, Th and Ra in plagioclase and amphibole (the main phenocryst phases) incorporation of antecrysts would only act to dilute the observed disequilibrium.

5.7. Millennial-scale magma additions and decadal-scale volatile fluxes

The extent of disequilibria suggests a difference in the age between the magma bodies involved beneath SHV. The andesitic magma – which is close to U-Th-Ra equilibrium (Figs. 1 and 2) – is likely derived from a several 100s ka old highly crystalline mush network (c.f. (Cooper and Kent, 2014), being progressively thawed by the new, mafic melts responsible for the enclaves. In contrast, the denser (non-vesicular) enclave type (MT35) represents an older, more stagnated but recently reinvigorated reservoir while the vesiculated mafic material (MT75) represents magmatic volatile phase-rich magma brought into the system in the last few thousand years, hence its Th-Ra disequilibria (Fig. 2). ^{210}Pb tells of younger volatile exchange processes, as we now discuss.

The enclaves are not representative of primitive, mafic melts. This is shown by the presence of plagioclase and amphibole (see Supplement 1) and chemical characteristics such as SiO_2 up to 58 wt% and Cr and Ni contents >20 ppm (Christopher et al., 2014). It is therefore likely that they

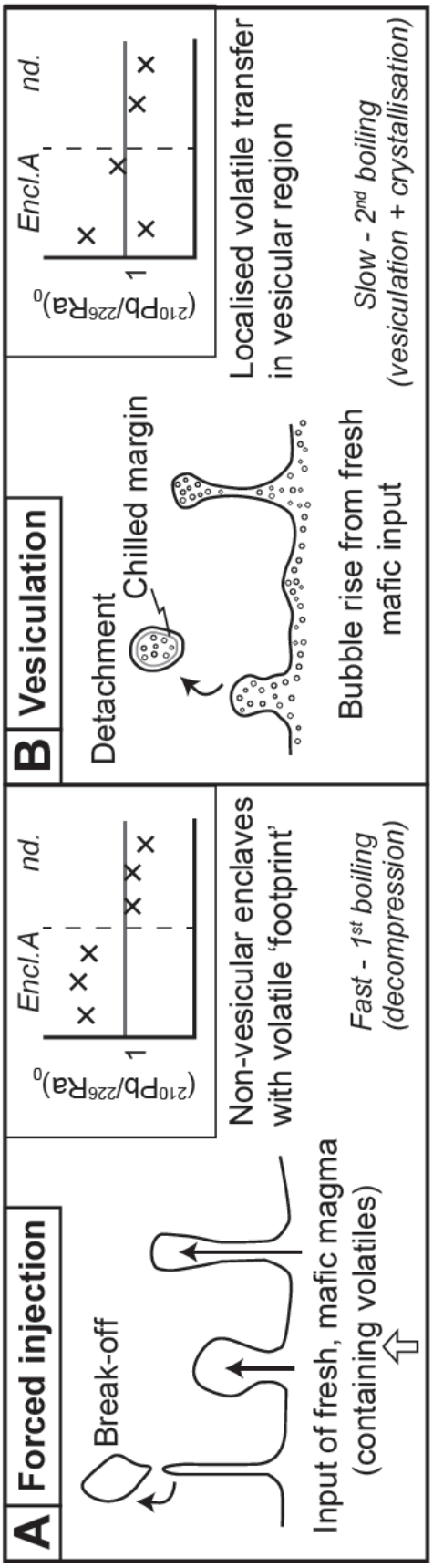

Figure 3: The $(^{210}Pb/^{226}Ra)_0$ signatures of the studied samples can be related to the formation mechanism of the enclaves. A: MT35 (non-vesicular type) may have been formed by forced injection of volatile-rich mafic magma, causing fast decompression-type movement and leading to the volatile 'footprint' of the mafic magma remaining as a ^{210}Pb excess in the enclave only. B: MT75 (vesicular type) may have been formed by the slower mechanism of vesiculation and crystallisation leading to detachment and ascent, due to the rise of volatiles from fresh mafic magma to the mafic-andesitic interface. This would explain the erratic volatile signature in the vesicular core of the enclave and equilibrium values in the rim and andesite.

represent samples of the hybrid zone between deeper mafic melts and the shallower andesitic reservoir beneath the currently active edifice (c.f. (Plail et al., 2018) and thus provide an excellent opportunity to investigate this important interface.

$(^{210}Pb/^{226}Ra)_0$ ratios of c. 1.4 in the enclave section of sample MT35 (Fig. 1) are consistent with recent (a few decades) fluxing or storing of fresh volatiles (containing ^{222}Rn) which have decayed to ^{210}Pb, either by diffusion from bubble walls back into the melt or accumulation of Pb-bearing fluids. The slight ^{210}Pb-deficits in the andesitic portion of this sample show that this reservoir was losing volatiles, consistent with the steady SO_2 plume from SHV throughout this time (e.g., Christopher et al., 2015). We define 'first boiling' a process where the melt can reach saturation of volatile phase during decompression and this process is reflected in the texture of enclave. The 'second boiling' process is evoke, when in the magmatic storage area, the melt exolved the magmatic volatile phase due to the isobaric pressure and crystallisation (Edmonds and Woods, 2018)). Forced injection is likely a fast enough process that no volatile transfer to the enclosing andesite occurs, although the 'footprint' of the volatile fluxing (in the form of a ^{210}Pb excess) remains in the enclave (Fig. 3). Thus, enclaves formed by forced injection are not the vehicle of volatile transfer to the enclosing andesite or the direct trigger of the eruption.

The vesiculated part of enclave MT75 has both ^{210}Pb excesses and deficits, while the non-vesicular part is within error of equilibrium (Fig. 2). This suggests that the latter enclave was in fact a chilled margin or rind forming a barrier to the interior, which witnessed volatile flux and loss on a local scale. We infer that the interior part of the enclave was formed directly at the interface of the andesitic reservoir and mafic recharge magma (a 'hybrid layer' as in Plail et al., 2018). The texture of this enclave is suggestive of crystallisation induced by vesiculation on ascent, the second boiling as discussed by Edmonds and Woods (2018). The abundance of vesicles suggests that these enclaves were formed by flotation, with the vapour phase contained in the vesicles being of low enough density to allow the enclaves to detach from the hybrid layer (Fig. 3). The non-vesicular enclave portion acting as a barrier means that, again, no transfer of volatiles occurred. Thus, such enclaves containing both vesiculated and non-vesiculated portions cannot be the medium by which volatiles are imparted to the host and are therefore not a direct trigger of the eruption.

Thus, the two samples studied here in detail relate to two mechanisms of enclave formation that may occur on different relative timescales: fast, forced injection and slower vesiculation and flotation (Fig. 3). The exact timescales (days, weeks, years) on which these are occurring may be reconcilable with crystal-scale studies. Both mechanisms preserve different textures in the erupted

enclaves (Supplement 1) which attest to variable volatile transfer and storage, however, the equilibrium and slight deficit ($^{210}Pb/^{226}Ra)_0$ ratios in the andesite (Figs. 1 & 2) shows that the host andesite now in contact with the enclaves has not gained volatiles. Although enclave formation by either mechanism may play a role in instigating convective overturn of the andesitic reservoir(s), we conclude that the transfer of volatiles from hybrid layer to andesitic reservoir is not a direct trigger of the eruption at SHV.

While enclaves have long been cited as evidence that heat and volatile transfer can trigger volcanic eruptions, the first detailed study of volatile behaviour between mafic enclaves and their host andesite shows no evidence that they themselves triggered the 1995-2010 eruption of Soufrière Hills Volcano. Rather, heat and volatile transfer from a deeper, more mafic recharge magma from which the enclaves themselves formed is implicated. Future studies could involve further geophysical imaging of this unseen part of the system and additional ^{210}Pb-^{226}Ra analyses of both types of enclaves.

Acknowledgements

This study was funded by an Australian Research Council (ARC) Discovery Project (DP150100328). We thank Melissa Plail for sharing her sample collection, and Yoann Greau at MQGA for his help with the MC-ICP-MS.

References

Bacon CR (1986) Magmatic inclusions in silicic and intermediate volcanic rocks. Journal of Geophysical Research: Solid Earth 91(B6):6091-6112 doi:doi:10.1029/JB091iB06p06091

Barclay J, Herd RA, Edwards BR, Christopher T, Kiddle EJ, Plail M, Donovan A (2010) Caught in the act: Implications for the increasing abundance of mafic enclaves during the recent eruptive episodes of the Soufrière Hills Volcano, Montserrat. Geophysical Research Letters 37(19)

Berlo K, Turner S (2010) 210Pb–226Ra disequilibria in volcanic rocks. Earth and Planetary Science Letters 296(3–4):155-164 doi:http://dx.doi.org/10.1016/j.epsl.2010.05.023

Bourdon B, Turner S, Henderson GM, Lundstrom CC (2003) Introduction to U-series Geochemistry. Reviews in Mineralogy and Geochemistry 52(1):1-21 doi:10.2113/0520001

Christopher T, Blundy J, Cashman K, Cole P, Edmonds M, Smith P, Sparks R, Stinton A (2015) Crustal-scale degassing due to magma system destabilization and magma-gas decoupling at

Soufrière Hills Volcano, Montserrat. Geochemistry, Geophysics, Geosystems 16(9):2797-2811

Christopher TE, Humphreys MC, Barclay J, Genareau K, De Angelis SM, Plail M, Donovan A (2014) Petrological and geochemical variation during the Soufriere Hills eruption, 1995 to 2010. Geological Society, London, Memoirs 39(1):317-342

Coombs ML, Eichelberger JC, Rutherford MJ (2003) Experimental and textural constraints on mafic enclave formation in volcanic rocks. Journal of Volcanology and Geothermal Research 119(1):125-144 doi:https://doi.org/10.1016/S0377-0273(02)00309-8

Cooper KM, Kent AJ (2014) Rapid remobilization of magmatic crystals kept in cold storage. Nature 506(7489):480

Edmonds M, Woods AW (2018) Exsolved volatiles in magma reservoirs. Journal of Volcanology and Geothermal Research

Eichelberger JC, Izbekov PE (2000) Eruption of andesite triggered by dyke injection: contrasting cases at Karymsky Volcano, Kamchatka and Mt Katmai, Alaska. Philosophical Transactions of the Royal Society of London Series A: Mathematical, Physical and Engineering Sciences 358(1770):1465-1485 doi:10.1098/rsta.2000.0599

Humphreys MS, Christopher T, Hards V (2009) Microlite transfer by disaggregation of mafic inclusions following magma mixing at Soufrière Hills volcano, Montserrat. Contributions to Mineralogy and Petrology 157(5):609-624 doi:10.1007/s00410-008-0356-3

Kayzar TM, Cooper KM, Reagan MK, Kent AJR (2009) Gas transport model for the magmatic system at Mount Pinatubo, Philippines: Insights from (210Pb)/(226Ra). Journal of Volcanology and Geothermal Research 181(1):124-140 doi:https://doi.org/10.1016/j.jvolgeores.2009.01.006

Martin VM, Morgan DJ, Jerram DA, Caddick MJ, Prior DJ, Davidson JP (2008) Bang! Month-Scale Eruption Triggering at Santorini Volcano. Science 321(5893):1178 doi:10.1126/science.1159584

McGee LE, Reagan M, Handley HK, Turner S, Sparks RSJ, Berlo K, Barclay J, Turner MB (In review) Volatile behaviour in the 1995-2010 eruption of the Soufrière Hills Volcano, Montserrat recorded by U-series disequilibria. Earth and Planetary Science Letters.

Molloy C, Shane P, Nairn I (2008) Pre-eruption thermal rejuvenation and stirring of a partly crystalline rhyolite pluton revealed by the Earthquake Flat Pyroclastics deposits, New Zealand.

Journal of the Geological Society 165(1):435-447 doi:10.1144/0016-76492007-071

Morgado E, Morgan DJ, Harvey J, Parada M-Á, Castruccio A, Brahm R, Gutiérrez F, Georgiev B, Hammond SJ (2019) Localised heating and intensive magmatic conditions prior to the 22–23 April 2015 Calbuco volcano eruption (Southern Chile). Bulletin of Volcanology 81(4):24 doi:10.1007/s00445-019-1280-2

Murphy MD, Sparks RSJ, Barclay J, Carroll MR, Brewer TS (2000) Remobilization of Andesite Magma by Intrusion of Mafic Magma at the Soufriere Hills Volcano, Montserrat, West Indies. Journal of Petrology 41(1):21-42 doi:10.1093/petrology/41.1.21

Pallister JS, Hoblitt RP, Reyes AG (1992) A basalt trigger for the 1991 eruptions of Pinatubo volcano? Nature 356:426 doi:10.1038/356426a0

Plail M, Barclay J, Humphreys MC, Edmonds M, Herd RA, Christopher TE (2014) Characterization of mafic enclaves in the erupted products of Soufrière Hills Volcano, Montserrat, 2009 to 2010. Geological Society, London, Memoirs 39(1):343-360

Plail M, Edmonds M, Woods AW, Barclay J, Humphreys MCS, Herd RA, Christopher T (2018) Mafic enclaves record syn-eruptive basalt intrusion and mixing. Earth and Planetary Science Letters 484:30-40 doi:https://doi.org/10.1016/j.epsl.2017.11.033

Reagan M, Turner S, Handley H, Turner M, Beier C, Caulfield J, Peate D (2017) 210Pb-226Ra disequilibria in young gas-laden magmas. Scientific Reports 7:45186

Ruprecht P, Bachmann O (2010) Pre-eruptive reheating during magma mixing at Quizapu volcano and the implications for the explosiveness of silicic arc volcanoes. Geology 38(10):919-922

Sigmarsson O, Vlastelic I, Andreasen R, Bindeman I, Devidal JL, Moune S, Keiding JK, Larsen G, Höskuldsson A, Thordarson T (2011) Remobilization of silicic intrusion by mafic magmas during the 2010 Eyjafjallajökull eruption. Solid Earth 2(2):271-281 doi:10.5194/se-2-271-2011

Sparks R, Young S (2002) The eruption of Soufriere Hills Volcano, Montserrat (1995-1999): overview of scientific results. Geological Society, London, Memoirs 21(1):45-69

Sparks SRJ, Sigurdsson H, Wilson L (1977) Magma mixing: a mechanism for triggering acid explosive eruptions. Nature 267:315 doi:10.1038/267315a0

Thomas N, Tait S (1997) The dimensions of magmatic inclusions as a constraint on the physical

mechanism of mixing. Journal of Volcanology and Geothermal Research 75(1-2):167-178

Ubide T, Galé C, Larrea P, Arranz E, Lago M, Tierz P (2014) The Relevance of Crystal Transfer to Magma Mixing: a Case Study in Composite Dykes from the Central Pyrenees. Journal of Petrology 55(8):1535-1559 doi:10.1093/petrology/egu033

Wadge G, Voight B, Sparks R, Cole P, Loughlin S, Robertson R (2014) An overview of the eruption of Soufriere Hills Volcano, Montserrat from 2000 to 2010. Geological Society, London, Memoirs 39(1):1-40

Zellmer GF, Sparks RSJ, Hawkesworth CJ, Wiedenbeck M (2003) Magma Emplacement and Remobilization Timescales Beneath Montserrat: Insights from Sr and Ba Zonation in Plagioclase Phenocrysts. Journal of Petrology 44(8):1413-1431 doi:10.1093/petrology/44.8.1413

Appendix D

Appendix D1: U-Th, Th-Ra and Ra-Pb plots of the studied serial sections (data in colour) compared to enclave and andesite data from 1995 to 2010 (data in black and white) from McGee et al., in review

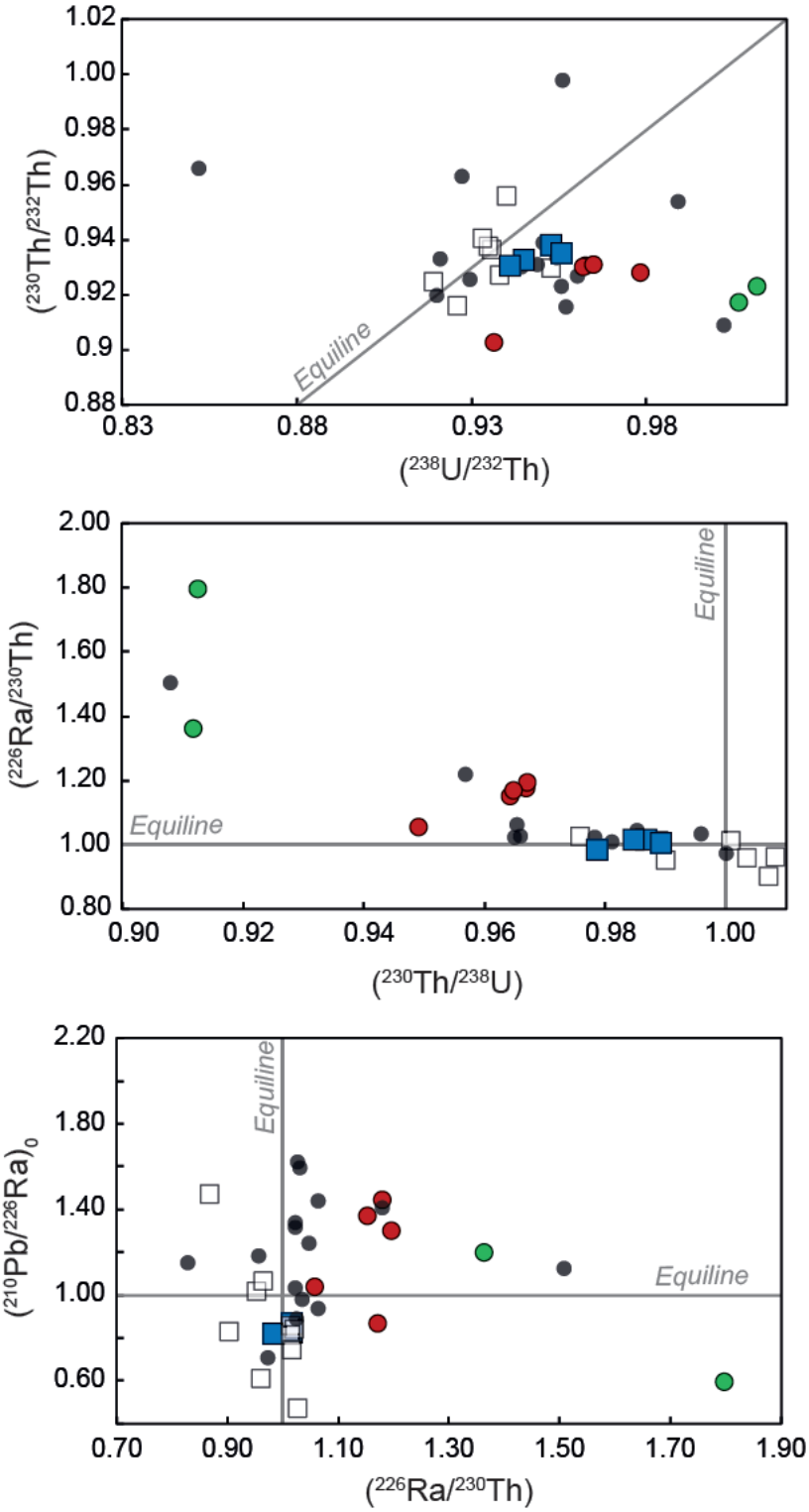

Previous work	*This study*
□ All andesites Phases I-V (1995-2010)	■ Andesite (MT35 & MT75)
● All enclaves Phases I-V (1995-2010)	● Enclave (normal, MT35 & MT75)
	● Enclave (vesicular, MT75 only)

Appendix D2: MT35 (rock from February 2010)X-ray map from Tornado.

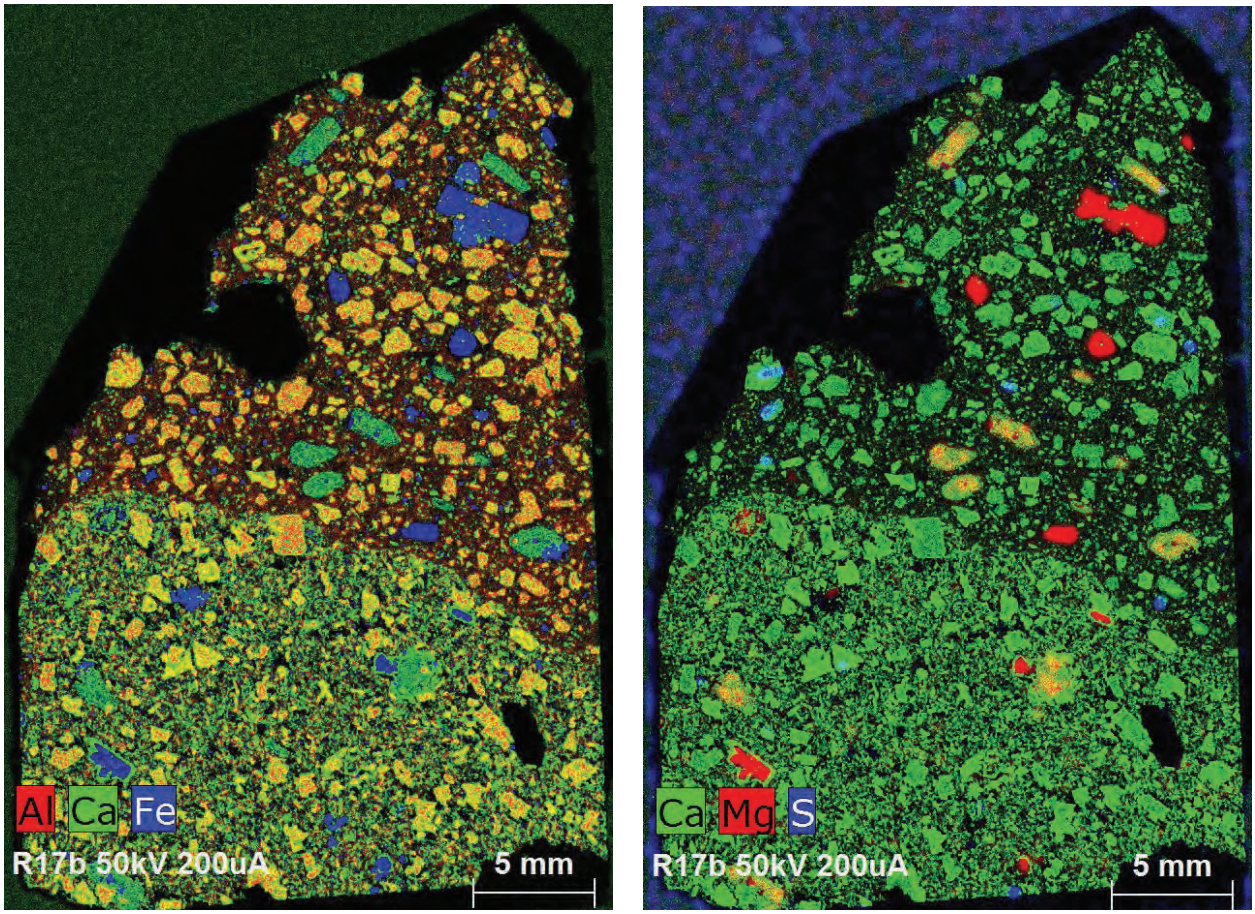

Appendix D2: MT75 (rock from February 2010)X-ray map from Tornado

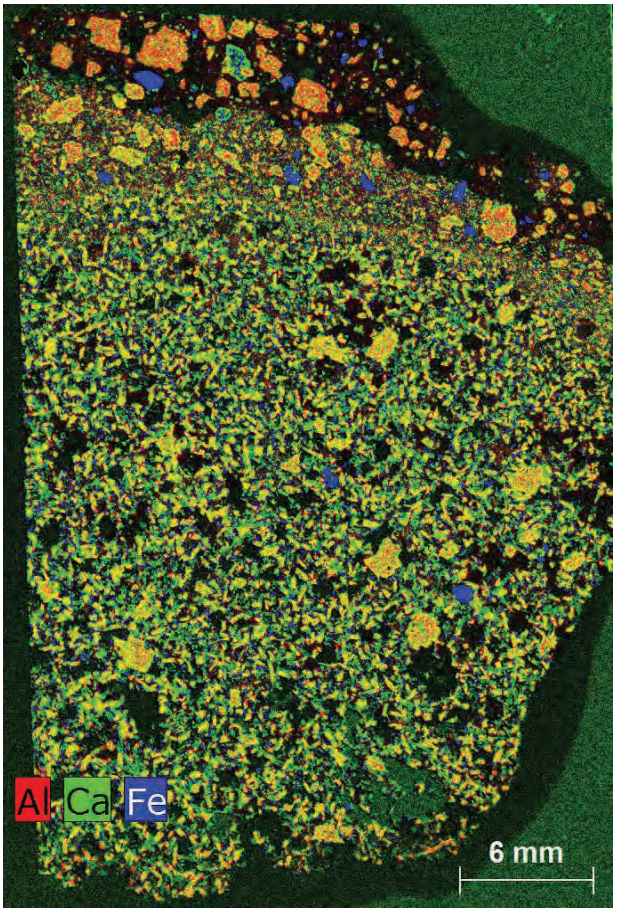

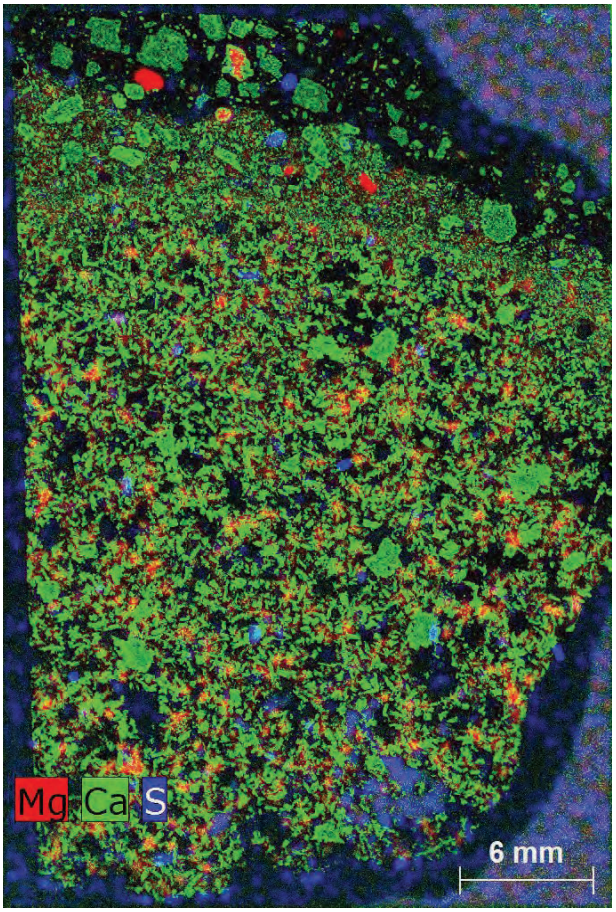

Chapter 6

Conclusions

6.1. Conclusions and future work

This thesis developed important constraints on nature and timing of the magmatic processes taking place in three different volcanic areas, making use of chemical and textural zoning patterns recorded in plagioclase and/or olivine crystals characterising the erupted volcanic rocks. This thesis was focused on achieving the following objectives:

1. Elucidate the timescales of mafic-silicic magma interactions at Soufrière Hills Volcano, through the modelling of the diffusive re-equilibration of Mg in plagioclase;
2. Unravel the nature and dynamics of the magmatic system at Gede volcano;
3. Constrain the magma ascent dynamics involved in the formation of Waitomokia volcano, through textural and compositional investigation of minerals;
4. Shed light on the level of complexity in sub-volcanic magmatic plumbing systems at different spatial and temporal scales, making use of detailed mineralogical studies.

6.2. Timescales of mafic-silicic magma interactions at Soufrière Hills volcano (Montserrat)

The sub-volcanic magmatic system of Soufrière Hills volcano has become a natural laboratory since its reawakening in 1995. A network of interdisciplinary volcanologists is still investigating the volcano after the eruption ceased in February 2010. Using implemented 1D numerical simulations of Mg diffusion in plagioclase, time ranges from a few hours up to two months were obtained for the typical timescales of magmatic interaction between host andesite and basaltic andesite, and for the eruption. This result, based on rock samples erupted during the last eruptive event, is consistent with previous works (e.g., Devine et al., 2003), in contrast with the time proposed by Zellmer et al., (2003) that is more than 100 years. These results provide an improved framework for interpreting current monitoring data, that is critical for hazard and eruption forecasting and risk mitigation.

6.3. Unravel the nature and dynamics of magmatic system at Gede volcano

The complexity of the magmatic system at Gede volcano is displayed by the different populations of plagioclase and pyroxene crystals that experienced multiple and different processes, such as fractional crystallisation and magma mingling/mixing. This study found no evidence for the crustal assimilation of carbonate material implicated at other Javanese volcanoes, and that was

suggested among the possible causes of the negative correlation between SiO_2 and Pb isotope ratios for the volcanic complex. Instead, it is suggested that the triggering mechanisms of eruptions are associated with multiple replenishments of more mafic magma (magma mixing). Considering that this volcano is close to the densely populated capital of Indonesia (Jakarta) it is of paramount importance to understand the processes that controlled its eruptive behaviour in the past, to enhance and make more effective the policies of hazard assessment and mitigation.

6.4. Constrain the magma ascent dynamics involved in the formation of Waitomokia Volcano

Waitomokia Volcano is one of over 50 volcanoes in the Auckland Volcanic Field (New Zealand) that have erupted in the last 250 ka. Relationships between crystal shape, texture and compositional zoning in olivine and clinopyroxene reveal relatively rapid ascent of the magma from its source in the upper mantle to the surface. Mineralogical complexity decreased from the initial phreatomagmatic to the final magmatic phases of the eruption. This study provides direct insight into the development of the architecture of the sub-volcanic magmatic system through time in intraplate basaltic volcanic fields. The increased understanding of magma dynamics and ascent timescales in an active field provides a useful insight into the fundamental questions about volcanic hazard mitigation. In particular, the answer to the question about how much time elapsed between the detection of the initial activity (e.g. earthquakes) and the eruption itself is likely very little.

6.5. Shed light on the level of complexity in sub-volcanic magmatic plumbing systems at different spatial and temporal scales

This work demonstrates through a detailed mineral-scale textural and chemical investigations that mineralogical complexity is present in all magmatic system analysed, disregarding the size of the volcano and the longevity of its eruption. In particular, this resulted true for the long-lived arc-volcanoes with repeated eruptions (Soufrière Hills and Gede Volcano) and the short-lived intraplate volcanoes with small-volume eruptions (Waitomokia Volcano). The sub-volcanic magmatic systems, taken into account in this study, are all characterised by open-system processes involving the interaction of distinct multiple batches of magma characterised by different depths and temperatures, which is consistent with the models discussed in Chapter 1 (see also Annen et al., 2006; Cashman et al., 2017).

6.6. Summary and broader implications of this work

This thesis provides a window into sub-volcanic magmatic systems by exploring three different volcanic areas. Magma injection, recharge, mingling, mixing, hybridization and eruption are all processes that can be incorporated into the large framework of processes occurring with variable evolution over time.

This work highlights that detailed studies of the main rock-forming minerals (such as plagioclase and olivine) are fundamental for understanding the sub-volcanic magmatic systems from the source to the surface, and reveals a complexity that may be otherwise missed by the whole-rock geochemical studies. Through the investigation of distinctly different volcanic systems (i.e. from a simple basaltic system with little crustal processing to larger, more complex and long-lived subduction zone volcanoes), this study shows that open-system magmatic processes are ubiquitous. Therefore, modelling magmatic processes within a closed-system framework should be performed with some caution.

Finally, our understanding of magma dynamics and ascent timescales, both at active volcanoes and in active volcanic fields, has been improved through the detailed investigation of mineral textures and compositions, and the diffusion modelling of these characteristics. This research, therefore, provides a context to interpret precursory volcanic activity and unrest situations in so supplying meaningful inputs for volcanic hazard mitigation policies that may affect millions of people living in volcanically active areas.

6.7. Future directions

Imminent future works are planned for each volcano studied in this thesis.

(1) Soufrière Hills Volcano. The investigation of magmatic interaction at Soufrière Hills Volcano (Chapters 1 and 4) was based on two volcanic rock samples belonging to the later phase of the eruptive episode of the (1995-2010). Therefore, it would be beneficial in future work to investigate representative enclave and host samples from additional phases of the eruption using the same approach. Analysis of deposits from the initial phase would provide insight into the mechanisms that trigger the beginning of the eruption and would enable to evaluate the changes in the sub-volcanic magmatic system during the whole eruptive episode, such as if there are temporal variations in magma mixing and ascent dynamics. Such results could be combined with the results gained in Chapter 4 and integrated with seismic records of the eruption.

(2) Gede Volcano. To fully understand the observed correlation between whole-rock isotopic ratios and indices that have been documented at Gede volcano by previous authors (Chapter 2),

in addition to the textural data it would be beneficial to conduct crystal $^{87}Sr/^{86}Sr$ isotopic profiling in plagioclase. This would provide an insight into the relative role and possible timing (relative to the crystallisation of plagioclase) of crustal assimilation processes, and into the character of the assimilant (carbonate crust or older mafic volcanic/plutonic material).

(3) Waitomokia Volcano. A relatively fast ascent rate has been suggested for Waitomokia volcano (Chapter 3) based both on the preservation of Mg-Fe zoning in olivine and on the skeletal texture of the olivine. The decrease in mineral compositional complexity observed throughout the eruption suggests that the ascent rate may have increased over the course of the eruption itself, following the opening of the conduit from source to surface. Therefore, future work to quantify the timescales of ascent would provide useful information to be further incorporated into future volcanic hazard and risk assessments for this volcanic field. This can be performed utilising the individual mineral Forsterite-zoning patterns already in hand and by collecting additional olivine crystallographic orientation data (by electron backscatter diffraction -EBSD- characterisation).

Supplementary Data

Table A1.1. *Plagioclase major element compositions obtained by electron microprobe and expressed in wt %. Data from the Soufrière Hills volcano (Montserrat, Lesser Antilles)*

Sample	Distance (μm)	SiO_2	Al_2O_3	CaO	Na_2O	MgO	K_2O	FeO	MnO	TiO_2	P_2O_5	Total
PL_EN_R2C_1_01	0	51.13	29.94	13.40	3.76	0.08	0.07	0.63	-0.00	0.03	0.01	99.06
PL_EN_R2C_1_02	1	50.46	30.37	14.03	3.54	0.08	0.07	0.63	-0.01	0.02	0.01	99.20
PL_EN_R2C_1_03	2	48.87	31.32	14.97	2.80	0.09	0.05	0.67	0.01	0.01	0.01	98.79
PL_EN_R2C_1_04	3	48.27	31.87	15.40	2.52	0.10	0.04	0.69	0.01	0.03	0.02	98.94
PL_EN_R2C_1_05	4	47.50	32.12	15.73	2.20	0.10	0.03	0.67	-0.00	0.03	0.02	98.41
PL_EN_R2C_1_06	5	47.04	32.27	15.98	2.15	0.12	0.03	0.64	0.01	0.02	0.01	98.27
PL_EN_R2C_1_07	6	45.90	33.31	16.84	1.59	0.09	0.02	0.57	0.01	0.01	-0.00	98.33
PL_EN_R2C_1_08	7	47.17	32.49	16.10	1.99	0.06	0.04	0.52	-0.00	0.00	0.00	98.37
PL_EN_R2C_1_09	8	52.70	29.12	11.90	4.43	0.04	0.09	0.34	-0.01	0.01	0.02	98.66
PL_EN_R2C_1_10	9	54.63	27.91	10.74	5.30	0.03	0.12	0.34	-0.01	0.00	0.01	99.08
PL_EN_R2C_1_11	10	54.04	28.07	10.93	4.90	0.04	0.11	0.34	0.01	-0.01	0.01	98.42
PL_EN_R2C_1_12	11	53.94	28.33	10.99	4.98	0.03	0.11	0.34	0.00	0.02	0.01	98.73
PL_EN_R2C_1_13	12	53.66	28.30	11.22	4.77	0.04	0.11	0.41	0.01	0.01	0.02	98.55
PL_EN_R2C_1_14	13	54.01	28.11	11.03	4.94	0.03	0.12	0.31	0.01	0.01	0.02	98.61
PL_EN_R2C_1_15	14	54.29	27.69	10.58	5.25	0.03	0.12	0.31	0.01	0.01	0.01	98.28
PL_EN_R2C_1_16	15	54.25	28.27	10.74	4.93	0.02	0.12	0.33	0.01	0.01	0.00	98.70
PL_EN_R2C_1_17	16	54.24	28.29	10.84	4.90	0.02	0.12	0.35	0.01	-0.00	0.02	98.77
PL_EN_R2C_1_18	17	54.09	28.43	11.13	4.91	0.02	0.11	0.32	-0.00	-0.00	0.02	99.02
PL_EN_R2C_1_19	18	53.28	28.82	11.35	4.75	0.03	0.10	0.32	-0.00	-0.00	0.01	98.65
PL_EN_R2C_1_20	19	52.46	29.15	12.03	4.40	0.03	0.10	0.32	0.00	0.00	0.06	98.56
PL_EN_R2C_1_21	20	52.10	29.49	12.31	4.16	0.02	0.09	0.33	0.00	0.02	-0.01	98.52
PL_EN_R2C_1_22	21	51.55	29.80	12.79	3.97	0.03	0.08	0.33	0.00	0.02	0.01	98.57
PL_EN_R2C_1_23	22	51.30	29.65	12.81	4.20	0.02	0.09	0.35	0.00	0.00	0.01	98.43
PL_EN_R2C_1_24	23	51.66	29.60	12.42	3.98	0.03	0.08	0.33	0.00	0.01	-0.00	98.11
PL_EN_R2C_1_25	24	51.64	29.67	12.33	4.15	0.02	0.08	0.38	0.02	0.01	0.02	98.32
PL_EN_R2C_1_26	25	51.82	29.60	12.46	4.09	0.03	0.09	0.33	0.01	-0.00	0.02	98.44
PL_EN_R2C_1_27	26	51.66	29.60	12.65	3.85	0.02	0.08	0.34	0.01	0.01	0.02	98.23
PL_EN_R2C_1_28	27	51.20	29.77	12.80	3.98	0.02	0.08	0.32	0.02	0.01	0.02	98.22
PL_EN_R2C_1_29	28	51.20	29.94	12.86	3.82	0.02	0.07	0.35	0.00	0.00	0.02	98.29
PL_EN_R2C_1_30	29	50.87	29.98	12.88	3.83	0.02	0.08	0.34	0.02	0.01	-0.01	98.02
PL_EN_R2C_1_31	30	50.93	30.09	13.22	3.70	0.02	0.08	0.36	0.00	0.02	-0.01	98.42
PL_EN_R2C_1_32	31	51.05	30.00	13.13	3.72	0.02	0.07	0.34	0.00	-0.00	-0.00	98.33
PL_EN_R2C_1_33	32	50.62	30.26	13.06	3.61	0.03	0.06	0.35	0.01	0.00	0.02	98.01
PL_EN_R2C_1_34	33	50.44	30.43	13.45	3.49	0.02	0.07	0.34	0.01	0.00	0.02	98.27
PL_EN_R2C_1_35	34	50.31	30.42	13.41	3.64	0.02	0.06	0.33	0.01	0.01	0.01	98.23
PL_EN_R2C_1_36	35	50.27	30.37	13.60	3.62	0.02	0.08	0.35	0.01	-0.01	0.01	98.32
PL_EN_R2C_1_37	36	50.50	30.37	13.40	3.49	0.02	0.07	0.35	0.01	0.02	0.01	98.23

Sample	Distance (μm)	SiO_2	Al_2O_3	CaO	Na_2O	MgO	K_2O	FeO	MnO	TiO_2	P_2O_5	Total
MT2E_PL_EN_R2C_2_21	20	55.18	27.77	10.23	5.15	0.02	0.14	0.29	0.01	0.00	0.04	98.84
MT2E_PL_EN_R2C_2_22	21	54.45	27.65	10.47	5.28	0.03	0.13	0.30	0.01	0.01	0.00	98.33
MT2E_PL_EN_R2C_2_23	22	55.05	27.63	10.60	5.17	0.03	0.13	0.31	0.00	-0.01	0.02	98.95
MT2E_PL_EN_R2C_2_24	23	54.91	27.69	10.39	5.33	0.02	0.13	0.31	0.01	0.01	0.01	98.81
MT2E_PL_EN_R2C_2_25	24	55.10	27.80	10.38	5.14	0.02	0.12	0.31	0.01	0.01	0.01	98.92
MT2E_PL_EN_R2C_2_26	25	54.73	27.87	10.56	5.22	0.03	0.12	0.30	0.01	0.02	0.02	98.88
MT2E_PL_EN_R2C_2_27	26	54.89	27.84	10.50	5.21	0.02	0.13	0.32	0.01	0.02	-0.00	98.94
MT2E_PL_EN_R2C_2_28	27	54.72	27.83	10.58	5.13	0.03	0.12	0.33	0.01	0.01	0.02	98.78
MT2E_PL_EN_R2C_2_29	28	54.64	27.63	10.60	5.10	0.03	0.13	0.32	0.01	0.02	0.00	98.48
MT2E_PL_EN_R2C_2_30	29	54.97	28.07	10.24	5.29	0.03	0.14	0.30	0.01	0.02	0.03	99.11
MT2E_PL_EN_R2C_2_31	30	54.93	27.84	10.61	5.23	0.03	0.13	0.33	-0.01	0.03	0.01	99.12
MT2E_PL_EN_R2C_2_32	31	54.61	28.03	10.28	5.18	0.03	0.14	0.31	0.00	0.02	0.03	98.62
MT2E_PL_EN_R2C_2_33	32	54.95	27.94	10.57	5.05	0.03	0.14	0.30	0.01	0.00	-0.00	98.98
MT2E_PL_EN_R2C_2_34	33	54.61	27.93	10.76	5.13	0.03	0.13	0.31	-0.01	0.02	0.03	98.93
MT2E_PL_EN_R2C_2_35	34	54.74	28.26	10.80	5.05	0.03	0.11	0.39	0.01	0.02	0.02	99.44
MT2E_PL_EN_R2C_2_36	35	54.25	28.03	10.90	5.05	0.03	0.12	0.32	0.01	0.01	0.01	98.75
MT2E_PL_EN_R2C_2_37	36	54.67	28.41	10.86	5.01	0.02	0.11	0.32	-0.00	0.01	0.02	99.44
MT2E_PL_EN_R2C_2_38	37	54.46	28.20	10.80	4.90	0.03	0.13	0.34	0.01	0.02	0.03	98.90
MT2E_PL_EN_R2C_2_39	38	54.26	28.12	11.05	5.05	0.03	0.12	0.33	0.01	0.01	0.03	99.01
MT2E_PL_EN_R2C_2_40	39	54.44	27.93	10.90	4.97	0.03	0.11	0.32	0.01	0.00	0.01	98.71
MT2E_PL_EN_R2C_2_41	40	54.21	28.04	10.93	5.14	0.03	0.11	0.34	0.00	0.02	0.01	98.83
MT2E_PL_EN_R2C_2_42	41	54.61	28.26	11.00	4.88	0.03	0.11	0.32	0.02	0.00	0.01	99.25
PL_EN_R2C_4_01	0	50.06	31.20	14.56	3.00	0.03	0.06	0.52	0.00	0.01	0.02	99.46
PL_EN_R2C_4_02	1	53.01	29.73	12.62	4.23	0.03	0.08	0.50	0.01	0.02	0.01	100.24
PL_EN_R2C_4_03	2	52.53	29.68	12.84	4.09	0.04	0.07	0.48	0.02	0.01	0.01	99.77
PL_EN_R2C_4_04	3	52.56	29.73	13.08	4.04	0.05	0.07	0.51	0.01	0.02	0.02	100.09
PL_EN_R2C_4_05	4	51.71	30.11	13.72	3.67	0.10	0.05	0.53	0.00	0.02	0.00	99.91
PL_EN_R2C_4_06	5	50.89	30.63	14.22	3.31	0.04	0.06	0.56	0.01	0.02	0.01	99.75
PL_EN_R2C_4_07	6	51.02	30.65	14.20	3.34	0.04	0.06	0.60	0.01	0.01	0.01	99.93
PL_EN_R2C_4_08	7	50.32	31.31	14.65	3.12	0.04	0.05	0.55	0.02	0.03	0.01	100.10
PL_EN_R2C_4_09	8	50.19	31.01	14.82	3.10	0.03	0.04	0.57	0.00	0.01	0.00	99.79
PL_EN_R2C_4_10	9	49.42	31.11	15.02	2.93	0.04	0.04	0.56	0.00	0.01	0.02	99.14
PL_EN_R2C_4_11	10	49.46	31.48	15.14	2.91	0.03	0.04	0.55	0.01	0.01	0.01	99.65
PL_EN_R2C_4_12	11	49.18	31.60	15.47	2.72	0.04	0.04	0.54	0.01	0.02	0.01	99.64
PL_EN_R2C_4_13	12	49.26	31.74	15.22	2.80	0.04	0.04	0.56	0.01	0.01	-0.00	99.67
PL_EN_R2C_4_14	13	50.37	30.65	14.11	3.13	0.04	0.05	0.46	0.01	-0.00	0.02	98.85
PL_EN_R2C_4_15	14	52.93	29.28	12.33	4.21	0.03	0.08	0.39	-0.00	0.02	0.01	99.27

Sample	Distance (μm)	SiO_2	Al_2O_3	CaO	Na_2O	MgO	K_2O	FeO	MnO	TiO_2	P_2O_5	Total
PL_EN_R2C_4_16	15	55.06	28.10	10.99	5.19	0.04	0.10	0.33	0.02	-0.00	0.01	99.83
PL_EN_R2C_4_17	16	53.66	28.81	11.68	4.71	0.03	0.09	0.34	0.00	0.01	0.01	99.36
PL_EN_R2C_4_18	17	53.90	28.73	11.50	4.54	0.03	0.09	0.31	0.00	0.00	0.01	99.12
PL_EN_R2C_4_19	18	54.26	28.58	11.53	4.69	0.04	0.10	0.36	-0.01	0.01	0.00	99.54
PL_EN_R2C_4_20	19	53.66	28.74	11.64	4.84	0.03	0.09	0.34	0.01	0.00	0.02	99.37
PL_EN_R2C_4_21	20	53.66	28.59	11.85	4.60	0.03	0.09	0.34	0.00	0.01	0.01	99.19
PL_EN_R2C_4_22	21	53.73	28.71	11.56	4.66	0.03	0.09	0.33	0.01	0.01	0.02	99.16
PL_EN_R2C_4_23	22	54.00	28.41	11.38	4.87	0.03	0.09	0.35	0.01	0.02	0.01	99.18
PL_EN_R2C_4_24	23	54.32	28.26	11.23	4.89	0.03	0.10	0.32	0.00	0.01	0.01	99.17
PL_EN_R2C_4_25	24	53.87	28.42	11.51	4.75	0.03	0.09	0.34	0.01	0.02	0.02	99.06
PL_EN_R2C_4_26	25	54.66	28.13	11.25	5.06	0.03	0.10	0.34	0.01	-0.01	0.02	99.59
PL_EN_R2C_4_27	26	55.53	27.95	10.74	5.22	0.03	0.11	0.30	0.01	0.02	0.00	99.92
PL_EN_R2C_4_28	27	55.10	28.25	11.02	5.05	0.03	0.11	0.31	-0.00	0.01	-0.00	99.88
PL_EN_R2C_4_29	28	54.02	28.79	11.94	4.78	0.03	0.09	0.34	0.01	0.01	0.02	100.04
PL_EN_R2C_4_30	29	53.75	28.88	12.03	4.52	0.03	0.09	0.33	0.00	0.02	0.02	99.68
PL_EN_R2C_4_31	30	53.67	28.81	11.89	4.58	0.03	0.08	0.34	0.01	0.00	-0.00	99.40
PL_EN_R2C_4_32	31	54.31	28.59	11.66	4.65	0.03	0.09	0.32	0.00	0.02	0.01	99.68
PL_EN_R2C_4_33	32	54.34	28.51	11.71	4.82	0.02	0.10	0.31	0.01	0.01	0.01	99.83
PL_EN_R2C_4_34	33	54.80	28.46	11.25	4.89	0.03	0.11	0.31	0.00	-0.00	0.01	99.85
PL_EN_R2C_4_35	34	55.12	28.35	11.08	4.99	0.03	0.11	0.29	-0.00	0.00	-0.01	99.96
PL_EN_R2C_4_36	35	55.23	27.89	11.03	5.18	0.02	0.12	0.31	-0.00	0.00	0.02	99.80
PL_EN_R2C_4_37	36	54.96	27.90	10.56	5.26	0.02	0.12	0.31	-0.01	0.01	-0.00	99.13
PL_EN_R2C_4_38	37	55.06	28.25	11.11	4.99	0.03	0.11	0.30	-0.00	0.01	0.03	99.89
PL_EN_R2C_4_39	38	54.50	28.50	11.17	4.90	0.02	0.09	0.31	0.02	0.01	-0.01	99.50
PL_EN_R2C_4_40	39	54.11	28.58	11.50	4.76	0.03	0.10	0.32	-0.01	-0.00	0.01	99.40
PL_EN_R2C_4_41	40	53.78	29.00	11.87	4.55	0.03	0.08	0.33	0.01	0.01	0.00	99.67
PL_EN_R2C_4_42	41	53.59	28.93	11.81	4.78	0.02	0.10	0.33	-0.00	0.01	0.00	99.56
PL_EN_R2C_4_43	42	54.38	28.55	11.64	4.67	0.03	0.11	0.33	0.01	-0.01	0.01	99.72
PL_EN_R2C_4_44	43	55.48	27.85	10.61	5.24	0.02	0.12	0.30	0.01	0.01	-0.00	99.65
PL_EN_R2C_4_45	44	55.04	27.92	10.90	5.15	0.02	0.12	0.31	0.01	-0.01	0.02	99.47
PL_EN_R2C_4_46	45	54.72	28.28	11.02	5.01	0.03	0.11	0.33	-0.00	0.03	0.00	99.53
PL_EN_R2C_4_47	46	53.93	28.67	11.50	4.83	0.03	0.09	0.32	0.01	0.04	0.01	99.43
PL_EN_R2C_4_48	47	54.17	28.51	11.39	4.69	0.02	0.10	0.31	-0.00	0.01	0.01	99.20
PL_EN_R2C_4_49	48	54.36	28.58	11.26	4.91	0.03	0.10	0.30	-0.00	0.02	0.03	99.58
PL_EN_R2C_4_50	49	55.21	27.83	10.74	5.20	0.03	0.12	0.31	0.01	0.00	0.01	99.46
PL_EN_R2C_4_51	50	55.43	27.60	10.49	5.29	0.03	0.11	0.29	-0.01	-0.01	0.02	99.24
PL_EN_R2C_4_52	51	55.57	27.66	10.37	5.24	0.03	0.12	0.29	0.01	-0.01	0.03	99.30
PL_EN_R2C_4_53	52	55.48	27.57	10.28	5.32	0.03	0.12	0.30	0.00	-0.01	0.01	99.11
PL_EN_R2C_4_54	53	55.67	27.58	10.19	5.56	0.03	0.13	0.29	0.01	0.02	0.01	99.47

Sample	Distance (μm)	SiO_2	Al_2O_3	CaO	Na_2O	MgO	K_2O	FeO	MnO	TiO_2	P_2O_5	Total
PL_EN_R2C_4_55	54	55.83	27.01	10.13	5.61	0.02	0.13	0.27	-0.00	0.01	0.00	99.01
PL_EN_R2C_4_56	55	55.74	27.40	10.23	5.40	0.02	0.13	0.28	0.01	0.01	0.01	99.23
PL_EN_R2C_4_57	56	55.73	27.48	10.18	5.44	0.02	0.12	0.28	0.02	0.02	-0.00	99.29
PL_EN_R2C_4_58	57	55.60	27.46	10.19	5.47	0.02	0.12	0.30	0.00	0.01	0.01	99.19
PL_EN_R2C_4_59	58	55.62	27.49	10.11	5.44	0.02	0.12	0.29	0.01	-0.00	0.01	99.11
PL_EN_R2C_4_60	59	55.84	27.45	10.40	5.38	0.03	0.12	0.32	-0.00	0.00	0.00	99.55
PL_EN_R2C_4_61	60	55.36	27.62	10.41	5.38	0.03	0.12	0.30	0.01	0.00	0.01	99.25
PL_EN_R2C_4_62	61	55.44	27.47	10.37	5.42	0.02	0.13	0.30	0.01	-0.00	0.02	99.17
PL_EN_R2C_4_63	62	55.89	27.71	10.37	5.40	0.02	0.13	0.30	0.00	0.01	0.01	99.83
PL_EN_R2C_4_64	63	55.98	27.46	10.19	5.49	0.03	0.13	0.29	0.01	0.01	0.02	99.60
PL_EN_R2C_4_65	64	55.97	27.56	10.26	5.39	0.03	0.13	0.27	0.01	0.01	0.01	99.63
PL_EN_R2C_4_66	65	55.71	27.26	10.61	5.46	0.02	0.14	0.30	0.01	0.00	-0.00	99.51
PL_EN_R2C_4_67	66	55.84	27.50	10.26	5.49	0.03	0.14	0.29	0.00	0.02	0.00	99.57
PL_EN_R2C_4_68	67	55.52	27.55	10.43	5.42	0.03	0.13	0.30	-0.01	-0.00	0.01	99.37
PL_EN_R2C_4_69	68	55.32	27.38	10.55	5.31	0.03	0.12	0.33	0.01	0.00	0.02	99.07
PL_EN_R2C_4_70	69	55.66	27.97	10.57	5.27	0.03	0.13	0.31	0.01	0.01	-0.00	99.97
PL_EN_R2C_4_71	70	55.28	27.90	10.64	5.26	0.02	0.11	0.31	0.00	-0.00	0.02	99.54
PL_EN_R2C_4_72	71	55.03	27.78	10.87	5.19	0.02	0.13	0.30	-0.01	0.00	0.01	99.34
PL_EN_R2C_4_73	72	55.15	28.07	10.82	5.09	0.03	0.11	0.29	0.00	0.01	0.02	99.58
PL_EN_R2C_4_74	73	55.00	28.23	11.17	5.06	0.03	0.12	0.31	0.01	0.01	0.01	99.95
PL_EN_R2C_4_75	74	54.69	28.03	11.10	5.08	0.02	0.10	0.29	0.01	-0.00	0.02	99.34
PL_EN_R2C_5_01	0	52.76	29.51	12.97	4.04	0.09	0.11	0.61	0.01	0.03	-0.00	100.11
PL_EN_R2C_5_02	1	50.99	30.15	14.33	3.55	0.09	0.07	0.68	0.00	0.02	0.01	99.89
PL_EN_R2C_5_03	2	49.06	31.54	15.81	2.67	0.09	0.05	0.72	0.00	0.02	-0.00	99.95
PL_EN_R2C_5_04	3	48.72	31.97	15.93	2.53	0.09	0.05	0.75	0.01	0.03	0.01	100.09
PL_EN_R2C_5_05	4	47.77	31.11	15.83	2.49	0.12	0.05	0.84	0.01	0.03	0.01	98.25
PL_EN_R2C_5_06	5	48.38	31.90	16.09	2.43	0.09	0.04	0.76	0.01	0.02	0.02	99.73
PL_EN_R2C_5_07	6	49.17	31.15	15.47	2.74	0.13	0.04	0.81	0.02	0.04	-0.01	99.54
PL_EN_R2C_5_08	7	48.61	31.59	15.90	2.46	0.09	0.03	0.72	-0.01	0.03	-0.01	99.41
PL_EN_R2C_5_09	8	48.73	31.60	16.07	2.41	0.09	0.04	0.70	0.01	0.03	0.01	99.68
PL_EN_R2C_5_10	9	48.60	31.74	16.26	2.47	0.10	0.04	0.67	-0.00	0.01	0.00	99.90
PL_EN_R2C_5_11	10	48.85	31.84	16.49	2.46	0.10	0.04	0.67	0.01	0.00	-0.00	100.46
PL_EN_R2C_5_12	11	48.36	31.62	16.00	2.51	0.09	0.04	0.67	0.02	0.03	-0.01	99.32
PL_EN_R2C_5_13	12	49.00	32.01	16.07	2.71	0.11	0.03	0.64	0.00	0.03	0.02	100.64
PL_EN_R2C_5_14	13	52.93	29.10	12.78	4.23	0.06	0.11	0.45	0.02	0.02	0.01	99.71
PL_EN_R2C_5_15	14	54.55	28.20	11.93	4.86	0.05	0.12	0.40	0.02	0.01	-0.00	100.14
PL_EN_R2C_5_16	15	54.80	28.05	11.22	5.15	0.04	0.13	0.35	0.02	0.01	-0.00	99.77
PL_EN_R2C_5_17	16	54.48	28.30	11.74	4.94	0.04	0.12	0.36	0.02	-0.00	0.01	100.01
PL_EN_R2C_5_18	17	55.45	27.66	10.69	5.48	0.04	0.12	0.32	0.01	0.03	0.01	99.81

Sample	Distance (μm)	SiO_2	Al_2O_3	CaO	Na_2O	MgO	K_2O	FeO	MnO	TiO_2	P_2O_5	Total
PL_EN_R2C_5_19	18	55.85	27.52	10.87	5.50	0.05	0.14	0.32	-0.00	0.00	0.00	100.24
PL_EN_R2C_5_20	19	55.62	27.67	10.83	5.37	0.04	0.14	0.30	0.01	-0.00	0.01	99.99
PL_EN_R2C_5_21	20	55.65	27.59	10.81	5.50	0.03	0.13	0.31	0.00	0.00	-0.00	100.03
PL_EN_R2C_5_22	21	55.41	27.52	10.70	5.39	0.04	0.12	0.30	0.01	0.01	0.02	99.51
PL_EN_R2C_5_23	22	55.17	28.01	11.08	5.15	0.04	0.14	0.33	0.01	0.00	0.01	99.93
PL_EN_R2C_5_24	23	55.23	27.91	10.95	5.25	0.03	0.13	0.32	-0.00	0.00	-0.00	99.80
PL_EN_R2C_5_25	24	55.28	27.54	10.79	5.50	0.02	0.13	0.29	-0.00	-0.01	0.01	99.53
PL_EN_R2C_5_26	25	55.54	27.53	10.94	5.42	0.03	0.13	0.29	0.01	0.01	-0.01	99.89
PL_EN_R2C_5_27	26	55.36	27.47	10.79	5.34	0.03	0.13	0.31	0.00	-0.01	0.01	99.44
PL_EN_R2C_5_28	27	55.55	27.73	10.70	5.46	0.03	0.13	0.30	0.00	0.01	0.01	99.93
PL_EN_R2C_5_29	28	55.20	27.74	10.86	5.34	0.03	0.14	0.30	0.02	-0.01	0.01	99.64
PL_EN_R2C_5_30	29	55.30	27.63	10.81	5.34	0.03	0.15	0.29	-0.00	-0.01	-0.00	99.53
PL_EN_R2C_5_31	30	55.77	27.52	10.87	5.40	0.03	0.13	0.27	0.00	0.01	0.01	100.02
PL_EN_R2C_5_32	31	55.30	27.68	10.95	5.50	0.03	0.15	0.29	0.01	0.03	0.01	99.94
PL_EN_R2C_5_33	32	55.67	27.57	10.88	5.51	0.03	0.13	0.31	0.00	0.02	-0.00	100.13
PL_EN_R2C_5_34	33	55.40	27.44	11.04	5.32	0.02	0.13	0.27	0.01	-0.00	0.02	99.65
PL_EN_R2C_5_35	34	55.29	27.64	11.14	5.42	0.02	0.14	0.29	-0.00	0.01	0.00	99.96
PL_EN_R2C_5_36	35	55.32	27.54	10.85	5.41	0.02	0.14	0.28	-0.00	0.01	0.01	99.57
PL_EN_R2C_5_37	36	55.28	27.50	10.83	5.42	0.03	0.13	0.28	0.01	0.01	0.01	99.50
PL_EN_R2C_5_38	37	55.20	27.61	10.66	5.19	0.03	0.13	0.28	-0.00	0.00	0.00	99.09
PL_EN_R2C_5_39	38	55.15	27.50	11.09	5.39	0.03	0.14	0.27	0.00	0.01	0.00	99.58
PL_EN_R2C_5_40	39	55.50	27.71	10.86	5.32	0.02	0.14	0.30	0.01	0.01	0.00	99.87

Sample	Distance (μm)	SiO_2	Al_2O_3	CaO	Na_2O	MgO	K_2O	FeO	MnO	TiO_2	P_2O_5	Total
MT2E_PL_EN_R2C_6_01	0	57.85	25.81	10.69	3.45	0.08	1.12	0.89	0.01	0.20	0.06	100.16
MT2E_PL_EN_R2C_6_02	1	50.76	30.60	14.52	3.36	0.09	0.09	0.65	0.00	0.04	-0.01	100.10
MT2E_PL_EN_R2C_6_03	2	50.70	30.51	14.50	3.40	0.10	0.08	0.63	-0.00	0.03	0.01	99.96
MT2E_PL_EN_R2C_6_04	3	49.71	30.82	14.72	3.15	0.10	0.08	0.66	-0.00	0.03	0.01	99.28
MT2E_PL_EN_R2C_6_05	4	50.00	30.70	14.56	3.12	0.11	0.08	0.65	-0.00	0.03	0.01	99.26
MT2E_PL_EN_R2C_6_06	5	48.95	31.41	15.17	2.71	0.09	0.06	0.61	-0.00	0.02	-0.01	99.01
MT2E_PL_EN_R2C_6_07	6	49.21	31.28	15.27	2.76	0.09	0.06	0.60	0.01	-0.00	-0.00	99.29
MT2E_PL_EN_R2C_6_08	7	49.38	31.73	16.04	2.68	0.11	0.07	0.63	0.01	0.03	-0.01	100.67
MT2E_PL_EN_R2C_6_09	8	48.24	31.84	16.01	2.41	0.09	0.05	0.59	0.01	0.00	0.01	99.24
MT2E_PL_EN_R2C_6_10	9	48.20	31.63	15.86	2.47	0.09	0.05	0.61	0.01	0.02	-0.00	98.94
MT2E_PL_EN_R2C_6_11	10	48.68	31.57	15.99	2.59	0.10	0.06	0.61	0.02	0.03	0.01	99.65
MT2E_PL_EN_R2C_6_12	11	48.12	32.00	16.42	2.33	0.10	0.06	0.64	-0.00	0.02	-0.00	99.68
MT2E_PL_EN_R2C_6_13	12	47.42	32.29	16.55	2.08	0.10	0.04	0.62	0.01	0.02	0.00	99.14
MT2E_PL_EN_R2C_6_14	13	47.42	32.54	16.69	2.02	0.10	0.04	0.59	-0.01	0.01	0.00	99.40
MT2E_PL_EN_R2C_6_15	14	47.22	32.38	16.61	2.11	0.11	0.04	0.58	0.00	0.02	0.01	99.08
MT2E_PL_EN_R2C_6_16	15	47.45	32.35	16.79	2.04	0.10	0.04	0.54	0.01	0.00	0.01	99.33
MT2E_PL_EN_R2C_6_17	16	47.36	32.34	16.72	2.10	0.11	0.03	0.55	-0.00	0.01	0.01	99.21
MT2E_PL_EN_R2C_6_18	17	47.31	32.50	17.00	1.97	0.11	0.02	0.54	0.01	0.02	0.01	99.50
MT2E_PL_EN_R2C_6_19	18	46.95	32.78	17.05	1.94	0.10	0.02	0.51	0.01	0.01	0.01	99.38
MT2E_PL_EN_R2C_6_20	19	46.89	33.00	17.23	1.86	0.10	0.03	0.55	0.00	0.01	-0.00	99.68
MT2E_PL_EN_R2C_6_21	20	45.94	32.15	17.30	1.96	0.11	0.03	0.53	0.01	0.02	0.01	98.06
MT2E_PL_EN_R2C_6_22	21	48.00	33.66	17.15	1.78	0.10	0.03	0.51	0.01	0.02	0.00	101.25
MT2E_PL_EN_R2C_6_23	22	46.68	33.09	17.86	1.76	0.10	0.02	0.50	0.01	0.02	0.01	100.06
MT2E_PL_EN_R2C_6_24	23	46.25	33.30	17.66	1.55	0.10	0.02	0.49	0.00	0.03	0.01	99.41
MT2E_PL_EN_R2C_6_25	24	46.09	33.23	17.84	1.58	0.10	0.02	0.49	0.01	0.03	0.02	99.42
MT2E_PL_EN_R2C_6_26	25	45.98	33.23	18.08	1.55	0.09	0.03	0.48	0.00	0.02	0.01	99.47
MT2E_PL_EN_R2C_6_27	26	46.01	33.33	17.79	1.45	0.09	0.02	0.48	0.01	0.02	0.01	99.22
MT2E_PL_EN_R2C_6_28	27	46.00	33.42	18.07	1.47	0.10	0.02	0.51	0.01	0.02	0.01	99.62
MT2E_PL_EN_R2C_6_29	28	46.08	33.49	17.85	1.47	0.10	0.02	0.49	0.00	0.02	0.00	99.51
MT2E_PL_EN_R2C_6_30	29	45.70	33.39	18.12	1.42	0.09	0.01	0.46	-0.01	0.02	-0.00	99.20
MT2E_PL_EN_R2C_6_31	30	45.76	33.81	18.56	1.37	0.09	0.02	0.45	0.01	0.01	0.01	100.08
MT2E_PL_EN_R2C_6_32	31	45.82	33.78	18.24	1.36	0.09	0.01	0.44	0.00	0.03	0.00	99.79
MT2E_PL_EN_R2C_6_33	32	45.83	33.50	18.19	1.37	0.09	0.02	0.46	0.01	0.03	-0.01	99.49
MT2E_PL_EN_R2C_6_34	33	45.66	33.67	18.24	1.34	0.09	0.02	0.43	0.01	0.03	0.00	99.49
MT2E_PL_EN_R2C_6_35	34	45.55	33.94	18.24	1.24	0.09	0.03	0.43	0.01	0.02	-0.00	99.54
MT2E_PL_EN_R2C_6_36	35	45.53	33.53	18.05	1.32	0.09	0.02	0.48	0.00	0.03	0.02	99.08
MT2E_PL_EN_R2C_6_37	36	45.49	33.82	18.73	1.32	0.08	0.01	0.48	-0.00	0.01	0.00	99.96
MT2E_PL_EN_R2C_6_38	37	46.34	32.94	17.69	1.67	0.09	0.03	0.47	0.00	0.02	0.01	99.27
MT2E_PL_EN_R2C_6_39	38	46.96	32.90	17.65	1.87	0.10	0.03	0.51	0.00	0.01	0.01	100.03

Sample	Distance (μm)	SiO_2	Al_2O_3	CaO	Na_2O	MgO	K_2O	FeO	MnO	TiO_2	P_2O_5	Total
MT2E_PL_EN_R2C_6_40	39	46.64	33.12	17.75	1.70	0.09	0.03	0.47	0.00	0.01	0.00	99.82
MT2E_PL_EN_R2C_6_41	40	46.39	32.83	17.40	1.66	0.09	0.02	0.49	0.00	0.00	-0.01	98.88
MT2E_PL_EN_R2C_6_42	41	46.94	32.70	17.50	1.85	0.07	0.05	0.54	0.01	0.03	0.01	99.71
MT2E_PL_EN_R2C_6_43	42	46.98	32.68	17.04	2.00	0.04	0.07	0.52	0.00	0.03	0.02	99.37
MT2E_PL_EN_R2C_6_44	43	47.16	32.61	17.40	1.82	0.03	0.09	0.55	0.01	0.02	0.02	99.72
MT2E_PL_EN_R2C_6_45	44	46.95	32.97	17.66	1.84	0.02	0.05	0.57	0.00	0.01	0.00	100.08
MT2E_PL_EN_R2C_6_46	45	49.81	31.81	16.19	2.40	0.03	0.14	0.53	-0.00	0.03	0.01	100.94
MT2E_PL_EN_R2C_6_47	46	45.43	28.15	13.88	2.37	0.02	0.13	0.61	-0.00	0.02	0.01	90.63
MT2E_PL_EN_R2C_6_48	47	50.92	30.42	14.40	3.38	0.03	0.08	0.44	0.01	0.01	0.02	99.71
MT2E_PL_EN_R2C_6_49	48	50.63	30.23	14.37	3.49	0.04	0.08	0.39	0.00	0.03	0.02	99.28
MT2E_PL_EN_R2C_6_50	49	50.54	30.53	14.44	3.30	0.02	0.06	0.40	0.02	0.03	0.00	99.34
MT2E_PL_EN_R2C_6_51	50	49.16	31.35	15.73	2.94	0.03	0.05	0.40	0.01	0.00	0.01	99.67
MT2E_PL_EN_R2C_6_52	51	51.17	30.12	14.02	3.75	0.03	0.07	0.38	0.02	0.01	0.01	99.58
MT2E_PL_EN_R2C_6_53	52	51.94	29.81	13.70	4.00	0.03	0.08	0.38	0.01	0.02	0.01	99.98
MT2E_PL_EN_R2C_6_54	53	51.62	29.70	13.87	3.98	0.03	0.07	0.38	0.01	0.03	0.01	99.69
MT2E_PL_EN_R2C_6_55	54	51.82	29.77	13.66	4.00	0.03	0.07	0.37	0.01	0.02	0.02	99.77
MT2E_PL_EN_R2C_6_56	55	51.30	30.03	14.14	3.61	0.03	0.07	0.37	0.01	0.02	0.00	99.57
MT2E_PL_EN_R2C_6_57	56	51.09	30.20	14.14	3.71	0.03	0.07	0.38	-0.00	0.02	0.00	99.64
MT2E_PL_EN_R2C_6_58	57	50.69	30.32	14.55	3.61	0.03	0.07	0.37	0.01	0.03	-0.00	99.66
MT2E_PL_EN_R2C_6_59	58	50.54	30.59	14.71	3.48	0.03	0.07	0.38	0.02	0.02	0.01	99.84
MT2E_PL_EN_R2C_6_60	59	50.97	30.16	14.25	3.65	0.02	0.07	0.39	0.00	0.03	0.01	99.55
MT2E_PL_EN_R2C_6_61	60	52.62	29.10	12.85	4.16	0.03	0.11	0.40	0.01	0.02	0.00	99.30
MT2E_PL_EN_R2C_6_62	61	54.72	27.80	11.59	5.04	0.04	0.14	0.43	0.01	0.02	0.05	99.84
MT2E_PL_EN_R2C_6_63	62	53.92	28.05	11.81	4.82	0.03	0.11	0.38	0.01	0.01	0.00	99.14
MT2E_PL_EN_R2C_6_64	63	54.65	27.98	11.42	5.07	0.02	0.12	0.30	0.00	0.02	0.03	99.60
MT2E_PL_EN_R2C_6_65	64	54.32	27.92	11.61	5.04	0.02	0.11	0.31	0.01	0.01	0.00	99.37
MT2E_PL_EN_R2C_6_66	65	53.86	28.27	12.03	4.96	0.02	0.11	0.32	0.01	0.01	0.00	99.60
MT2E_PL_EN_R2C_6_67	66	53.45	28.60	12.39	4.81	0.02	0.10	0.32	0.01	0.01	0.02	99.73
MT2E_PL_EN_R2C_6_68	67	54.44	28.08	11.80	5.07	0.02	0.10	0.30	0.00	0.00	0.02	99.83
MT2E_PL_EN_R2C_6_69	68	54.34	28.04	11.78	5.00	0.02	0.11	0.30	0.01	0.01	0.01	99.62
MT2E_PL_EN_R2C_6_70	69	54.43	27.98	11.47	5.04	0.03	0.11	0.32	0.01	0.01	0.03	99.42
MT2E_PL_EN_R2C_6_71	70	56.07	27.08	10.30	5.51	0.03	0.14	0.30	0.01	0.01	-0.00	99.44
MT2E_PL_EN_R2C_6_72	71	56.33	27.14	10.20	5.61	0.02	0.14	0.30	0.01	0.01	-0.01	99.74
MT2E_PL_EN_R2C_6_73	72	55.51	27.28	10.67	5.42	0.03	0.14	0.28	0.01	0.01	0.02	99.35
MT2E_PL_EN_R2C_6_74	73	55.45	27.69	11.16	5.30	0.02	0.12	0.30	0.00	0.01	0.01	100.07
MT2E_PL_EN_R2C_6_75	74	55.02	27.63	10.97	5.18	0.02	0.12	0.29	0.00	-0.00	0.01	99.24
MT2E_PL_EN_R2C_6_76	75	54.78	27.77	11.39	5.11	0.02	0.11	0.32	-0.00	0.01	0.02	99.52
MT2E_PL_EN_R2C_6_77	76	54.79	27.97	11.19	5.18	0.03	0.11	0.27	0.01	0.01	0.01	99.58
MT2E_PL_EN_R2C_6_78	77	54.35	28.18	11.58	4.83	0.02	0.11	0.28	-0.00	0.01	0.02	99.40

Sample	Distance (μm)	SiO_2	Al_2O_3	CaO	Na_2O	MgO	K_2O	FeO	MnO	TiO_2	P_2O_5	Total
MT2E_PL_EN_R2C_6_79	78	55.22	27.89	11.51	5.02	0.02	0.11	0.27	0.01	0.01	0.00	100.06
MT2E_PL_EN_R2C_6_80	79	54.53	27.90	11.34	5.00	0.02	0.11	0.27	0.01	0.01	0.00	99.19
MT2E_PL_EN_R2C_6_81	80	54.80	27.84	11.63	5.07	0.02	0.12	0.28	0.01	0.00	0.00	99.78
MT2E_PL_EN_R2C_6_82	81	54.89	28.09	11.25	5.15	0.02	0.11	0.27	0.00	-0.00	0.02	99.80
MT2E_PL_EN_R2C_6_83	82	55.11	27.54	10.97	5.28	0.02	0.12	0.27	0.00	0.01	-0.00	99.33
MT2E_PL_EN_R2C_6_84	83	56.19	28.22	11.14	5.14	0.03	0.12	0.27	0.00	0.01	0.01	101.14
MT2E_PL_EN_R2C_6_85	84	54.97	28.11	11.44	5.15	0.03	0.12	0.26	0.02	0.02	0.01	100.13
MT2E_PL_EN_R2C_6_86	85	54.56	27.93	11.39	5.04	0.02	0.10	0.27	0.00	0.02	0.00	99.35
MT2E_PL_EN_R2C_6_87	86	54.60	28.16	11.49	5.08	0.02	0.12	0.26	0.02	0.01	0.01	99.77
MT2E_PL_EN_R2C_6_88	87	53.66	28.54	12.41	4.70	0.02	0.09	0.27	0.01	0.00	0.01	99.72
MT2E_PL_EN_R2C_6_89	88	53.09	29.08	12.45	4.45	0.02	0.09	0.29	0.02	0.02	-0.00	99.51
MT2E_PL_EN_R2C_6_90	89	54.00	28.46	12.03	4.89	0.02	0.10	0.26	0.00	0.01	-0.00	99.77
MT2E_PL_EN_R2C_6_91	90	53.98	28.59	12.34	4.64	0.02	0.12	0.28	0.01	0.00	0.01	100.00
MT2E_PL_EN_R2C_6_92	91	53.33	29.02	12.30	4.51	0.02	0.09	0.28	0.02	0.01	0.02	99.58
MT2E_PL_EN_R2C_6_93	92	52.80	29.18	12.96	4.22	0.02	0.09	0.29	0.01	-0.00	0.00	99.57
MT2E_PL_EN_R2C_6_94	93	52.81	29.35	12.86	4.11	0.02	0.09	0.28	0.01	0.00	0.02	99.55
MT2E_PL_EN_R2C_6_95	94	53.57	28.99	12.48	4.61	0.03	0.10	0.28	0.02	0.01	0.01	100.09
MT2E_PL_EN_R2C_6_96	95	53.36	29.11	12.36	4.64	0.02	0.09	0.27	0.00	0.01	0.01	99.87
MT2E_PL_EN_R2C_6_97	96	52.49	29.59	12.98	4.34	0.02	0.09	0.29	0.02	0.02	0.03	99.85
MT2E_PL_EN_R2C_6_98	97	52.45	29.61	13.42	4.14	0.02	0.08	0.33	0.01	-0.00	-0.00	100.06
MT2E_PL_EN_R2C_6_99	98	50.72	28.73	13.26	3.98	0.02	0.09	0.82	0.01	0.01	0.02	97.67
MT2E_PL_EN_R2C_6_100	99	51.72	29.64	13.66	3.90	0.02	0.08	0.43	0.01	0.00	-0.01	99.47
MT2E_PL_EN_R2C_6_101	100	51.24	30.21	14.36	3.71	0.02	0.08	0.31	0.01	0.01	0.01	99.95
MT2E_PL_EN_R2C_6_102	101	51.21	29.88	14.02	3.71	0.02	0.07	0.32	-0.00	0.02	0.01	99.26
MT2E_PL_EN_R2C_6_103	102	50.69	29.84	13.84	3.62	0.02	0.07	0.30	0.00	-0.01	0.01	98.40
MT2E_PL_EN_R2C_6_104	103	51.26	30.10	13.92	3.74	0.03	0.08	0.29	-0.00	-0.00	0.01	99.42
MT2E_PL_EN_R2C_6_105	104	50.76	30.40	14.20	3.71	0.02	0.07	0.28	0.00	0.01	0.01	99.47
MT2E_PL_EN_R2C_6_106	105	50.61	30.66	14.76	3.44	0.02	0.07	0.30	0.01	-0.00	0.00	99.86
MT2E_PL_EN_R2C_6_107	106	50.24	30.96	15.21	3.39	0.02	0.06	0.28	0.01	-0.00	0.01	100.17
MT2E_PL_EN_R2C_6_108	107	50.08	31.18	14.76	3.16	0.02	0.06	0.27	0.01	0.01	0.01	99.54
MT2E_PL_EN_R2C_6_109	108	49.90	30.94	14.96	3.23	0.02	0.06	0.30	0.02	0.01	0.01	99.44
MT2E_PL_EN_R2C_6_110	109	51.04	30.43	14.23	3.63	0.02	0.07	0.30	0.00	0.01	0.01	99.76
MT2E_PL_EN_R2C_6_111	110	52.33	29.47	13.04	4.20	0.03	0.09	0.27	0.01	0.01	-0.00	99.44
MT2E_PL_EN_R2C_6_112	111	53.48	28.80	12.42	4.52	0.03	0.09	0.27	0.00	0.01	0.01	99.64
MT2E_PL_EN_R2C_6_113	112	52.83	27.76	12.05	4.54	0.02	0.10	0.32	0.01	0.00	0.00	97.63
MT2E_PL_EN_R2C_6_114	113	53.83	28.51	11.98	4.83	0.02	0.12	0.28	-0.00	0.00	-0.01	99.56
MT2E_PL_EN_R2C_6_115	114	53.84	28.45	12.22	4.78	0.01	0.09	0.29	0.01	-0.01	0.02	99.69
MT2E_PL_EN_R2C_6_116	115	53.38	28.74	12.14	4.63	0.03	0.10	0.30	-0.01	0.01	0.01	99.34
MT2E_PL_EN_R2C_6_117	116	53.19	28.88	12.62	4.48	0.02	0.10	0.30	0.01	0.00	0.01	99.62

Sample	Distance (μm)	SiO_2	Al_2O_3	CaO	Na_2O	MgO	K_2O	FeO	MnO	TiO_2	P_2O_5	Total
MT2E_PL_EN_R2C_6_118	117	53.28	28.98	12.45	4.51	0.02	0.09	0.25	0.00	0.00	0.01	99.60
MT2E_PL_EN_R2C_6_119	118	52.88	29.24	12.98	4.34	0.02	0.08	0.28	0.01	0.01	0.01	99.85
MT2E_PL_EN_R2C_6_120	119	52.36	29.41	13.17	4.23	0.02	0.09	0.27	0.02	0.01	0.02	99.60
MT2E_PL_EN_R2C_6_121	120	52.39	29.47	13.12	4.08	0.02	0.07	0.28	0.01	0.02	0.02	99.49
MT2E_PL_EN_R2C_6_122	121	52.35	29.58	13.35	4.10	0.03	0.08	0.27	0.01	0.01	0.01	99.79
MT2E_PL_EN_R2C_6_123	122	51.74	29.67	13.47	4.05	0.02	0.08	0.27	0.02	0.02	-0.00	99.34
MT2E_PL_EN_R2C_6_124	123	52.13	29.66	13.25	4.03	0.02	0.08	0.31	0.00	0.01	0.00	99.50
MT2E_PL_EN_R2C_6_125	124	52.42	29.63	12.99	4.23	0.02	0.08	0.29	0.01	0.02	-0.01	99.69
MT2E_PL_EN_R2C_6_126	125	51.99	29.80	13.34	4.02	0.03	0.08	0.33	-0.00	-0.00	0.01	99.58
MT2E_PL_EN_R2C_6_127	126	52.13	29.57	13.28	4.18	0.03	0.08	0.33	0.01	0.01	0.01	99.64
MT2E_PL_EN_R2C_6_128	127	54.66	27.78	11.09	5.30	0.03	0.13	0.32	0.01	0.02	0.02	99.34
MT2E_PL_EN_R2C_6_129	128	54.70	27.81	11.12	5.36	0.02	0.13	0.29	0.02	0.02	-0.00	99.46
MT2E_PL_EN_R2C_6_130	129	53.51	28.98	12.33	4.50	0.03	0.10	0.29	0.00	0.03	0.01	99.80
MT2E_PL_EN_R2C_6_131	130	52.49	29.45	13.06	4.31	0.03	0.09	0.29	0.00	-0.00	0.02	99.74
MT2E_PL_EN_R2C_6_132	131	52.67	29.92	13.56	4.27	0.03	0.08	0.32	0.01	0.02	0.01	100.89
MT2E_PL_EN_R2C_6_133	132	52.67	29.20	12.82	4.49	0.02	0.09	0.30	0.02	0.00	0.01	99.62
MT2E_PL_EN_R2C_6_134	133	52.00	29.75	13.63	4.12	0.03	0.09	0.31	-0.00	0.02	0.01	99.96
MT2E_PL_EN_R2C_6_135	134	52.19	29.76	13.56	4.11	0.03	0.08	0.30	0.02	0.02	0.01	100.07
MT2E_PL_EN_R2C_6_136	135	52.01	29.72	13.57	4.14	0.03	0.08	0.30	0.00	0.02	0.01	99.87
MT2E_PL_EN_R2C_6_137	136	52.50	29.28	13.14	4.20	0.02	0.09	0.31	0.00	-0.00	0.02	99.55
MT2E_PL_EN_R2C_6_138	137	52.77	29.22	12.60	4.35	0.02	0.09	0.31	0.01	0.00	0.01	99.37
MT2E_PL_EN_R2C_6_139	138	53.58	28.77	12.27	4.80	0.03	0.10	0.31	-0.00	0.02	0.01	99.87
MT2E_PL_EN_R2C_6_140	139	54.50	28.30	11.56	5.01	0.02	0.12	0.28	0.01	0.01	0.01	99.83
MT2E_PL_EN_R2C_6_141	140	54.12	28.50	12.11	4.80	0.02	0.11	0.29	0.01	0.00	-0.00	99.97
MT2E_PL_EN_R2C_6_142	141	54.33	28.24	11.65	4.93	0.03	0.11	0.30	0.01	0.01	0.01	99.62
MT2E_PL_EN_R2C_6_143	142	51.21	30.29	14.11	3.82	0.03	0.08	0.31	0.01	0.00	0.03	99.87
MT2E_PL_EN_R2C_6_144	143	51.00	30.17	14.01	3.74	0.03	0.08	0.33	0.01	0.01	0.01	99.38
MT2E_PL_EN_R2C_6_145	144	51.40	30.14	13.85	3.82	0.02	0.07	0.32	0.01	0.01	0.02	99.66
MT2E_PL_EN_R2C_6_146	145	51.80	29.44	13.23	3.96	0.02	0.07	0.32	0.01	0.01	0.01	98.87
MT2E_PL_EN_R2C_6_147	146	52.06	29.60	13.32	4.17	0.02	0.08	0.30	0.02	0.01	-0.00	99.58
MT2E_PL_EN_R2C_6_148	147	50.59	30.28	14.36	3.52	0.03	0.07	0.34	-0.01	0.02	0.00	99.20
MT2E_PL_EN_R2C_7_01	0	53.36	28.85	13.18	4.52	0.08	0.16	0.69	-0.00	0.05	0.02	100.93
MT2E_PL_EN_R2C_7_02	1	51.15	29.27	14.19	3.98	0.08	0.09	0.69	0.01	0.04	0.02	99.51
MT2E_PL_EN_R2C_7_03	2	50.77	29.63	14.48	3.89	0.08	0.08	0.63	0.01	0.03	0.00	99.60
MT2E_PL_EN_R2C_7_04	3	50.67	29.83	14.74	3.74	0.09	0.08	0.65	-0.00	0.05	0.02	99.86
MT2E_PL_EN_R2C_7_05	4	49.98	29.69	14.95	3.39	0.10	0.06	0.63	0.01	0.03	0.02	98.85
MT2E_PL_EN_R2C_7_06	5	49.88	30.17	15.11	3.46	0.11	0.07	0.68	0.01	0.03	-0.00	99.51
MT2E_PL_EN_R2C_7_07	6	49.66	30.10	15.59	3.27	0.09	0.06	0.70	0.01	0.04	-0.00	99.51
MT2E_PL_EN_R2C_7_08	7	48.92	30.74	16.15	2.97	0.12	0.06	0.67	0.00	0.02	0.02	99.66

Sample	Distance (μm)	SiO_2	Al_2O_3	CaO	Na_2O	MgO	K_2O	FeO	MnO	TiO_2	P_2O_5	Total
MT2E_PL_EN_R2C_7_09	8	48.31	31.24	16.51	2.64	0.20	0.05	0.64	0.01	0.02	0.01	99.62
MT2E_PL_EN_R2C_7_10	9	53.66	28.20	12.37	4.85	0.02	0.11	0.34	0.01	0.01	0.01	99.57
MT2E_PL_EN_R2C_7_11	10	53.64	28.05	12.02	5.08	0.02	0.12	0.30	0.01	0.02	-0.00	99.26
MT2E_PL_EN_R2C_7_12	11	54.44	27.78	11.42	5.31	0.02	0.13	0.28	0.02	0.02	0.01	99.43
MT2E_PL_EN_R2C_7_13	12	54.56	27.62	11.41	5.35	0.02	0.13	0.32	0.01	0.01	0.03	99.46
MT2E_PL_EN_R2C_7_14	13	54.31	27.70	11.59	5.38	0.03	0.13	0.31	-0.00	0.02	0.02	99.47
MT2E_PL_EN_R2C_7_15	14	53.25	28.51	12.31	4.88	0.03	0.12	0.31	0.01	0.00	0.01	99.43
MT2E_PL_EN_R2C_7_16	15	52.21	29.26	13.54	4.21	0.02	0.10	0.34	0.02	0.01	-0.01	99.71
MT2E_PL_EN_R2C_7_17	16	52.76	28.54	12.73	4.56	0.02	0.10	0.35	0.01	0.00	0.04	99.11
MT2E_PL_EN_R2C_7_18	17	53.48	28.44	12.33	4.79	0.02	0.12	0.33	-0.00	0.01	0.02	99.53
MT2E_PL_EN_R2C_7_19	18	54.00	27.95	12.09	4.93	0.02	0.13	0.32	0.00	0.01	0.00	99.48
MT2E_PL_EN_R2C_7_20	19	54.33	27.95	11.83	5.35	0.03	0.13	0.32	0.01	0.03	0.02	99.98
MT2E_PL_EN_R2C_7_21	20	53.70	28.21	12.36	4.92	0.02	0.12	0.31	0.01	0.01	-0.00	99.65
MT2E_PL_EN_R2C_7_22	21	53.73	27.97	12.07	4.87	0.02	0.12	0.32	0.02	0.00	-0.01	99.11
MT2E_PL_EN_R2C_7_23	22	54.23	27.74	11.65	5.14	0.02	0.12	0.31	0.02	0.03	-0.00	99.26
MT2E_PL_EN_R2C_7_24	23	54.52	27.79	11.53	5.34	0.02	0.12	0.31	0.00	0.01	0.01	99.66
MT2E_PL_EN_R2C_7_25	24	54.55	27.61	11.44	5.38	0.02	0.13	0.32	0.00	0.01	-0.00	99.46
MT2E_PL_EN_R2C_7_26	25	54.73	27.37	11.45	5.34	0.02	0.13	0.29	0.02	0.00	0.01	99.34
MT2E_PL_EN_R2C_7_27	26	54.91	27.53	11.57	5.44	0.03	0.13	0.31	0.01	0.01	-0.02	99.92
MT2E_PL_EN_R2C_7_28	27	54.97	27.26	11.22	5.51	0.02	0.14	0.31	0.00	0.01	0.02	99.46
MT2E_PL_EN_R2C_7_29	28	55.46	27.40	10.99	5.68	0.02	0.14	0.31	0.01	0.01	0.01	100.03
MT2E_PL_EN_R2C_7_30	29	55.59	26.99	10.59	5.77	0.03	0.15	0.29	-0.00	-0.00	0.02	99.43
MT2E_PL_EN_R2C_7_31	30	55.44	26.94	10.81	5.73	0.02	0.15	0.29	0.01	0.00	0.01	99.40
MT2E_PL_EN_R2C_7_32	31	55.38	27.13	10.95	5.67	0.03	0.14	0.30	0.02	0.02	-0.00	99.64
MT2E_PL_EN_R2C_7_33	32	55.14	27.07	10.95	5.46	0.02	0.13	0.32	0.01	0.00	0.00	99.10
MT2E_PL_EN_R2C_7_34	33	55.28	27.26	11.07	5.48	0.02	0.14	0.31	-0.00	0.02	0.02	99.60
MT2E_PL_EN_R2C_7_35	34	55.34	27.38	10.79	5.54	0.02	0.13	0.29	-0.00	0.01	-0.01	99.49
MT2E_PL_EN_R2C_7_36	35	55.35	27.09	11.10	5.60	0.02	0.13	0.30	0.02	0.00	-0.00	99.60

Sample	Distance (μm)	SiO_2	Al_2O_3	CaO	Na_2O	MgO	K_2O	FeO	MnO	TiO_2	P_2O_5	Total
MT2E_PL_HOST_8_01	0	54.34	27.34	11.52	4.66	0.06	0.29	0.66	0.01	0.06	0.14	99.07
MT2E_PL_HOST_8_02	1	51.78	29.40	13.58	3.99	0.09	0.09	0.61	-0.00	0.03	-0.01	99.55
MT2E_PL_HOST_8_03	2	50.85	30.06	14.51	3.36	0.08	0.07	0.65	0.01	0.03	-0.00	99.63
MT2E_PL_HOST_8_04	3	50.66	30.50	14.83	3.46	0.07	0.06	0.59	0.00	0.02	0.02	100.22
MT2E_PL_HOST_8_05	4	54.55	28.16	11.40	4.91	0.03	0.11	0.32	0.00	0.01	0.00	99.50
MT2E_PL_HOST_8_06	5	54.90	27.80	11.29	5.07	0.02	0.13	0.33	-0.00	0.01	-0.00	99.54
MT2E_PL_HOST_8_07	6	54.47	28.25	11.67	4.84	0.03	0.12	0.33	0.02	0.01	0.01	99.75
MT2E_PL_HOST_8_08	7	53.80	28.35	11.70	4.80	0.02	0.10	0.33	0.01	0.01	-0.00	99.13
MT2E_PL_HOST_8_09	8	53.77	28.77	12.33	4.71	0.03	0.10	0.34	0.01	0.01	0.01	100.08
MT2E_PL_HOST_8_10	9	53.24	29.01	12.34	4.49	0.02	0.10	0.32	0.02	0.03	0.02	99.58
MT2E_PL_HOST_8_11	10	52.85	29.22	12.65	4.38	0.02	0.09	0.32	-0.00	0.01	0.01	99.56
MT2E_PL_HOST_8_12	11	52.73	29.01	12.89	4.27	0.03	0.08	0.34	0.02	0.01	0.01	99.39
MT2E_PL_HOST_8_13	12	51.93	30.06	13.55	3.88	0.02	0.09	0.33	0.01	0.03	0.03	99.94
MT2E_PL_HOST_8_14	13	50.91	30.43	14.18	3.56	0.02	0.06	0.35	0.01	0.02	0.02	99.57
MT2E_PL_HOST_8_15	14	50.55	30.84	14.48	3.38	0.02	0.06	0.33	0.01	0.02	0.02	99.71
MT2E_PL_HOST_8_16	15	50.50	30.89	14.51	3.33	0.02	0.07	0.34	0.02	0.01	0.01	99.69
MT2E_PL_HOST_8_17	16	50.46	31.18	15.00	3.31	0.02	0.07	0.34	0.01	0.02	-0.01	100.39
MT2E_PL_HOST_8_18	17	49.88	31.27	14.96	3.16	0.02	0.06	0.36	0.00	0.01	0.02	99.74
MT2E_PL_HOST_8_19	18	49.52	31.20	15.35	3.06	0.02	0.06	0.33	0.00	0.02	0.01	99.58
MT2E_PL_HOST_8_20	19	49.89	31.35	15.34	3.02	0.02	0.06	0.36	0.02	0.02	0.02	100.11
MT2E_PL_HOST_8_21	20	49.63	31.29	15.19	2.82	0.02	0.06	0.36	0.01	-0.00	0.01	99.38
MT2E_PL_HOST_8_22	21	50.08	31.10	14.92	3.22	0.02	0.07	0.36	-0.00	0.01	0.02	99.80
MT2E_PL_HOST_8_23	22	50.30	31.32	14.75	3.20	0.02	0.05	0.35	0.01	0.00	0.01	100.01
MT2E_PL_HOST_8_24	23	51.40	30.45	13.86	3.61	0.02	0.07	0.34	0.01	0.02	0.01	99.79
MT2E_PL_HOST_8_25	24	51.02	30.82	14.50	3.52	0.02	0.08	0.31	0.00	0.02	0.02	100.32
MT2E_PL_HOST_8_26	25	54.98	28.68	11.77	4.84	0.02	0.15	0.30	0.00	0.01	0.01	100.78
MT2E_PL_HOST_8_27	26	53.70	28.58	11.88	4.74	0.02	0.15	0.30	0.01	0.02	0.02	99.42
MT2E_PL_HOST_8_28	27	53.93	29.46	12.54	4.54	0.03	0.13	0.29	-0.00	0.01	0.01	100.93
MT2E_PL_HOST_8_29	28	53.65	29.12	12.22	4.58	0.02	0.10	0.30	0.01	0.01	0.02	100.05
MT2E_PL_HOST_8_30	29	54.90	28.08	11.26	4.98	0.02	0.12	0.28	0.01	0.02	0.01	99.67
MT2E_PL_HOST_8_31	30	54.51	27.81	11.03	5.10	0.03	0.14	0.30	0.01	0.01	0.01	98.96
MT2E_PL_HOST_8_32	31	55.38	27.86	11.04	5.24	0.02	0.13	0.29	0.01	0.01	0.02	100.01
MT2E_PL_HOST_8_33	32	54.89	27.91	11.09	5.04	0.02	0.13	0.31	0.01	0.01	0.01	99.41
MT2E_PL_HOST_8_34	33	55.40	27.58	10.55	5.22	0.02	0.13	0.28	0.01	0.02	0.01	99.23
MT2E_PL_HOST_8_35	34	55.84	27.34	10.55	5.35	0.02	0.14	0.32	0.01	0.01	0.02	99.60
MT2E_PL_HOST_8_36	35	55.57	27.64	10.72	5.31	0.03	0.12	0.31	0.01	0.01	-0.00	99.73
MT2E_PL_HOST_8_37	36	55.35	27.90	10.87	5.16	0.02	0.13	0.31	0.02	0.01	0.02	99.79
MT2E_PL_HOST_8_38	37	55.05	27.95	10.95	5.08	0.02	0.13	0.30	0.01	-0.00	0.00	99.50
MT2E_PL_HOST_8_39	38	56.13	27.22	10.31	5.57	0.02	0.16	0.29	0.01	0.00	0.01	99.73

Sample	Distance (μm)	SiO_2	Al_2O_3	CaO	Na_2O	MgO	K_2O	FeO	MnO	TiO_2	P_2O_5	Total
MT2E_PL_HOST_8_40	39	56.07	27.25	10.23	5.60	0.02	0.15	0.29	-0.00	0.02	0.01	99.64
MT2E_PL_HOST_8_41	40	55.72	27.74	10.54	5.36	0.03	0.14	0.30	0.02	0.02	0.01	99.87
MT2E_PL_HOST_8_42	41	54.58	28.39	11.32	4.93	0.03	0.12	0.28	0.01	0.00	0.01	99.67
MT2E_PL_HOST_8_43	42	54.54	28.18	11.30	4.98	0.02	0.11	0.31	0.01	0.01	0.01	99.45
MT2E_PL_HOST_8_44	43	55.03	27.92	11.00	5.19	0.02	0.12	0.32	0.01	0.02	0.02	99.64
MT2E_PL_HOST_8_45	44	54.85	28.01	11.22	4.99	0.02	0.13	0.31	0.00	0.01	0.01	99.55
MT2E_PL_HOST_8_46	45	54.79	28.12	11.40	4.99	0.02	0.12	0.32	0.00	0.01	0.01	99.77
MT2E_PL_HOST_8_47	46	54.45	28.10	11.36	4.90	0.02	0.11	0.29	0.02	0.02	0.00	99.28
MT2E_PL_HOST_8_48	47	55.22	27.72	10.63	5.11	0.03	0.14	0.29	0.00	0.01	0.02	99.16
MT2E_PL_HOST_8_49	48	55.38	27.85	11.08	5.15	0.02	0.14	0.30	0.00	0.01	0.02	99.94
MT2E_PL_HOST_8_50	49	55.05	28.29	11.19	5.10	0.03	0.13	0.30	0.02	0.02	0.01	100.14
MT2E_PL_HOST_8_51	50	55.38	27.62	10.73	5.13	0.02	0.14	0.30	-0.00	0.03	-0.00	99.35
MT2E_PL_HOST_8_52	51	56.32	27.23	10.12	5.60	0.02	0.15	0.30	0.01	0.01	0.02	99.77
MT2E_PL_HOST_8_53	52	56.04	27.13	10.26	5.60	0.02	0.15	0.31	-0.01	0.01	0.01	99.52
MT2E_PL_HOST_8_54	53	55.47	27.76	11.00	5.25	0.02	0.13	0.30	0.01	0.01	0.01	99.97
MT2E_PL_HOST_8_55	54	54.94	27.93	11.32	5.19	0.02	0.12	0.30	0.01	0.01	0.00	99.85
MT2E_PL_HOST_8_56	55	55.04	27.82	10.73	5.16	0.02	0.14	0.29	0.01	0.00	-0.01	99.19
MT2E_PL_HOST_8_57	56	54.63	28.21	11.00	4.94	0.02	0.12	0.30	0.02	0.02	-0.02	99.23
MT2E_PL_HOST_8_58	57	53.77	29.12	11.84	4.59	0.02	0.11	0.32	-0.01	0.01	-0.00	99.78
MT2E_PL_HOST_8_59	58	54.38	28.56	11.52	4.74	0.03	0.12	0.30	0.01	0.01	0.01	99.68
MT2E_PL_HOST_8_60	59	54.32	28.47	11.58	4.95	0.03	0.11	0.31	0.02	0.01	0.02	99.81
MT2E_PL_HOST_8_61	60	53.92	28.56	11.74	4.80	0.03	0.11	0.32	0.01	0.02	0.01	99.51
MT2E_PL_HOST_8_62	61	53.68	28.93	12.28	4.50	0.02	0.10	0.32	0.00	0.01	0.02	99.87
MT2E_PL_HOST_8_63	62	54.67	28.33	11.53	5.03	0.02	0.12	0.29	0.01	0.02	0.00	100.02
MT2E_PL_HOST_8_64	63	55.68	27.74	10.60	5.41	0.02	0.13	0.31	0.00	0.01	0.02	99.94
MT2E_PL_HOST_8_65	64	55.28	28.02	10.89	5.14	0.02	0.14	0.31	-0.01	0.02	-0.00	99.81
MT2E_PL_HOST_8_66	65	54.92	28.32	11.29	5.11	0.03	0.12	0.30	0.01	0.02	0.01	100.13
MT2E_PL_HOST_8_67	66	54.71	28.21	11.07	4.94	0.03	0.13	0.30	0.01	0.02	0.01	99.42
MT2E_PL_HOST_8_68	67	54.71	28.27	11.18	4.98	0.02	0.12	0.30	-0.00	0.02	0.01	99.61
MT2E_PL_HOST_8_69	68	54.49	28.14	11.26	4.83	0.02	0.13	0.30	-0.00	0.00	0.01	99.18
MT2E_PL_HOST_8_70	69	54.65	28.30	11.04	4.91	0.02	0.12	0.30	0.01	-0.00	0.00	99.35
MT2E_PL_HOST_8_71	70	54.88	28.24	11.01	5.16	0.02	0.12	0.30	0.01	0.01	0.01	99.76
MT2E_PL_HOST_8_72	71	54.07	28.75	11.61	4.72	0.02	0.11	0.29	0.01	0.02	0.00	99.61
MT2E_PL_HOST_8_73	72	53.07	29.21	12.38	4.39	0.02	0.10	0.33	-0.00	0.01	0.01	99.53
MT2E_PL_HOST_8_74	73	52.62	29.77	12.79	4.19	0.03	0.09	0.35	-0.01	0.01	0.01	99.85
MT2E_PL_HOST_8_75	74	54.58	28.32	11.33	4.83	0.02	0.11	0.28	0.01	0.02	0.02	99.52
MT2E_PL_HOST_8_76	75	54.49	28.34	11.66	4.77	0.02	0.12	0.29	-0.00	0.01	0.01	99.70
MT2E_PL_HOST_8_77	76	53.56	28.80	11.91	4.50	0.02	0.10	0.30	-0.00	0.02	0.03	99.23
MT2E_PL_HOST_8_78	77	53.02	29.34	12.31	4.33	0.03	0.10	0.32	0.01	0.00	0.02	99.49

Sample	Distance (μm)	SiO_2	Al_2O_3	CaO	Na_2O	MgO	K_2O	FeO	MnO	TiO_2	P_2O_5	Total
MT2E_PL_HOST_8_79	78	53.34	29.16	12.30	4.49	0.03	0.10	0.32	-0.00	-0.00	0.02	99.75
MT2E_PL_HOST_8_80	79	54.25	28.50	11.50	4.72	0.03	0.11	0.31	0.00	0.01	0.02	99.44
MT2E_PL_HOST_8_81	80	54.27	28.64	11.44	4.73	0.02	0.11	0.30	0.01	0.02	0.00	99.54
MT2E_PL_HOST_8_82	81	53.70	28.83	11.73	4.71	0.03	0.10	0.32	0.01	0.00	0.02	99.45
MT2E_PL_HOST_8_83	82	52.94	29.39	12.65	4.28	0.03	0.09	0.31	0.01	0.01	0.00	99.70
MT2E_PL_HOST_8_84	83	52.65	29.31	12.68	4.36	0.02	0.10	0.35	0.02	0.03	0.00	99.52
MT2E_PL_HOST_8_85	84	51.70	29.92	13.27	3.79	0.03	0.08	0.36	0.01	0.01	0.01	99.18
MT2E_PL_HOST_8_86	85	51.28	30.45	13.75	3.66	0.03	0.06	0.33	0.01	0.03	0.01	99.61
MT2E_PL_HOST_8_87	86	49.88	31.52	15.01	2.94	0.02	0.07	0.35	0.01	0.01	0.00	99.81
MT2E_PL_HOST_9_01	0	79.41	9.82	0.80	2.23	0.09	3.87	1.38	0.03	0.57	0.06	98.26
MT2E_PL_HOST_9_02	1	84.83	8.94	1.91	2.69	0.05	1.96	0.75	0.00	0.31	0.60	102.05
MT2E_PL_HOST_9_03	2	78.43	11.07	1.38	3.35	0.44	2.94	1.88	0.06	0.44	0.08	100.08
MT2E_PL_HOST_9_04	3	58.49	26.22	11.01	4.50	0.07	0.40	0.51	0.00	0.04	0.02	101.25
MT2E_PL_HOST_9_05	4	52.58	29.64	13.05	4.07	0.03	0.10	0.44	0.01	0.02	0.03	99.96
MT2E_PL_HOST_9_06	5	51.62	30.15	14.02	3.83	0.03	0.07	0.41	0.01	0.00	0.00	100.15
MT2E_PL_HOST_9_07	6	49.52	31.48	15.53	2.91	0.03	0.05	0.40	0.02	0.03	0.02	99.99
MT2E_PL_HOST_9_08	7	49.17	31.92	15.94	2.69	0.02	0.04	0.42	0.01	0.04	0.00	100.24
MT2E_PL_HOST_9_09	8	48.73	31.95	16.38	2.46	0.03	0.03	0.39	0.01	0.01	0.01	99.99
MT2E_PL_HOST_9_10	9	49.05	32.02	15.75	2.75	0.03	0.04	0.40	0.02	0.01	0.01	100.07
MT2E_PL_HOST_9_11	10	51.99	29.85	13.72	3.85	0.02	0.07	0.39	0.01	0.03	0.01	99.94
MT2E_PL_HOST_9_12	11	51.59	29.59	13.38	3.77	0.03	0.06	0.35	-0.00	0.00	0.01	98.79
MT2E_PL_HOST_9_13	12	52.48	29.82	13.34	4.06	0.03	0.07	0.36	0.02	0.01	0.00	100.20
MT2E_PL_HOST_9_14	13	54.05	28.83	12.24	4.61	0.03	0.08	0.36	0.01	0.01	0.00	100.24
MT2E_PL_HOST_9_15	14	54.54	28.38	11.52	4.94	0.03	0.10	0.35	0.02	0.01	0.01	99.91
MT2E_PL_HOST_9_16	15	55.81	27.43	10.75	5.42	0.03	0.12	0.33	0.01	0.00	0.02	99.92
MT2E_PL_HOST_9_17	16	56.09	27.36	10.47	5.54	0.03	0.12	0.34	0.01	0.03	0.01	99.99
MT2E_PL_HOST_9_18	17	55.90	27.36	10.44	5.56	0.03	0.12	0.33	0.01	0.01	-0.00	99.76
MT2E_PL_HOST_9_19	18	56.48	27.32	10.94	5.56	0.03	0.12	0.33	0.01	0.01	0.02	100.81
MT2E_PL_HOST_9_20	19	55.96	27.45	10.58	5.48	0.03	0.13	0.34	0.00	0.01	0.01	99.99
MT2E_PL_HOST_9_21	20	54.13	28.31	11.64	4.83	0.03	0.11	0.33	0.01	0.01	0.01	99.41
MT2E_PL_HOST_9_22	21	52.57	29.56	13.03	4.13	0.03	0.07	0.34	0.01	0.01	0.01	99.76
MT2E_PL_HOST_9_23	22	53.96	28.60	12.23	4.77	0.03	0.10	0.31	0.01	0.01	0.01	100.04
MT2E_PL_HOST_9_24	23	54.36	28.33	11.89	4.91	0.02	0.11	0.31	0.01	-0.00	-0.00	99.93
MT2E_PL_HOST_9_25	24	52.25	30.01	13.41	3.93	0.03	0.08	0.34	-0.00	0.01	0.01	100.05
MT2E_PL_HOST_9_26	25	53.49	29.17	12.34	4.52	0.03	0.09	0.31	-0.00	0.02	-0.00	99.95
MT2E_PL_HOST_9_27	26	54.97	28.21	11.55	4.96	0.03	0.12	0.33	0.00	0.01	0.01	100.18
MT2E_PL_HOST_9_28	27	53.99	28.73	12.43	4.68	0.02	0.10	0.32	0.01	0.00	0.00	100.28
MT2E_PL_HOST_9_29	28	54.81	28.23	11.62	5.09	0.03	0.11	0.31	0.01	0.01	0.00	100.23
MT2E_PL_HOST_9_30	29	53.74	28.62	12.24	4.64	0.03	0.10	0.31	0.00	0.01	0.02	99.70

Sample	Distance (μm)	SiO_2	Al_2O_3	CaO	Na_2O	MgO	K_2O	FeO	MnO	TiO_2	P_2O_5	Total
MT2E_PL_HOST_9_31	30	54.93	28.04	11.47	4.90	0.03	0.11	0.32	0.00	0.02	0.00	99.82
MT2E_PL_HOST_9_32	31	55.20	27.74	11.26	5.27	0.02	0.10	0.31	0.02	-0.00	-0.00	99.92
MT2E_PL_HOST_9_33	32	54.87	28.33	11.56	4.88	0.03	0.11	0.31	0.00	0.02	0.00	100.11
MT2E_PL_HOST_9_34	33	54.28	28.56	11.93	4.72	0.02	0.10	0.31	0.01	0.02	0.01	99.96
MT2E_PL_HOST_9_35	34	54.42	28.52	11.91	4.69	0.03	0.09	0.30	0.01	0.02	0.02	100.01
MT2E_PL_HOST_9_36	35	55.16	28.09	11.66	5.09	0.03	0.11	0.31	0.01	0.02	0.01	100.48
MT2E_PL_HOST_9_37	36	55.77	27.86	10.80	5.24	0.03	0.11	0.31	0.00	0.01	0.00	100.15
MT2E_PL_HOST_9_38	37	55.52	27.63	11.06	5.19	0.03	0.12	0.32	0.02	0.01	0.01	99.91
MT2E_PL_HOST_9_39	38	55.86	27.84	11.04	5.34	0.03	0.12	0.32	0.01	0.01	0.01	100.59
MT2E_PL_HOST_9_40	39	55.33	28.14	11.10	5.09	0.02	0.11	0.31	0.00	-0.00	0.01	100.12
MT2E_PL_HOST_9_41	40	54.92	28.17	11.58	4.96	0.03	0.11	0.31	0.01	0.01	0.01	100.10
MT2E_PL_HOST_9_42	41	55.04	28.01	11.45	5.14	0.03	0.10	0.31	0.01	0.02	0.01	100.13
MT2E_PL_HOST_9_43	42	55.39	27.81	11.12	5.14	0.03	0.12	0.30	0.00	0.00	0.01	99.92
MT2E_PL_HOST_9_44	43	54.52	28.28	11.70	4.83	0.03	0.10	0.33	0.01	0.01	0.02	99.83
MT2E_PL_HOST_9_45	44	54.84	28.37	11.60	5.05	0.02	0.10	0.31	0.00	-0.00	0.01	100.30
MT2E_PL_HOST_9_46	45	55.16	27.85	11.30	4.93	0.03	0.11	0.32	-0.00	-0.01	0.02	99.71
MT2E_PL_HOST_9_47	46	55.04	28.09	11.32	5.10	0.03	0.11	0.32	0.01	0.02	0.01	100.03
MT2E_PL_HOST_9_48	47	54.65	28.20	11.36	4.95	0.02	0.11	0.30	-0.01	0.02	0.02	99.64
MT2E_PL_HOST_9_49	48	54.55	28.46	11.51	4.93	0.03	0.09	0.32	0.01	0.00	0.01	99.93
MT2E_PL_HOST_9_50	49	54.21	28.62	11.78	4.76	0.03	0.09	0.32	0.01	-0.00	0.02	99.84
MT2E_PL_HOST_9_51	50	54.34	28.83	11.99	4.64	0.03	0.09	0.34	0.00	0.01	0.00	100.27
MT2E_PL_HOST_9_52	51	54.09	28.84	12.04	4.68	0.02	0.10	0.32	0.02	0.01	0.02	100.14
MT2E_PL_HOST_9_53	52	53.43	29.23	12.52	4.40	0.03	0.08	0.33	-0.00	0.01	0.02	100.04
MT2E_PL_HOST_9_54	53	53.11	29.30	12.75	4.41	0.02	0.08	0.32	-0.00	0.00	0.01	99.99

Sample/ Distance (μm)	SiO_2	Al_2O_3	CaO	Na_2O	MgO	K_2O	FeO	MnO	TiO_2	P_2O_5	Total
PL_En_II_bis_01 0	69.43	18.86	3.47	5.89	0.08	1.70	0.96	NA	NA	NA	100.40
PL_En_II_bis_02 1	62.49	23.53	6.31	6.97	0.08	0.68	0.67	NA	NA	NA	100.74
PL_En_II_bis_03 2	58.09	26.04	9.11	6.21	0.08	0.31	0.69	NA	NA	NA	100.52
PL_En_II_bis_04 3	56.62	26.84	10.00	5.59	0.08	0.21	0.69	NA	NA	NA	100.03
PL_En_II_bis_05 4	54.92	27.75	11.26	5.00	0.08	0.15	0.70	NA	NA	NA	99.85
PL_En_II_bis_06 5	53.27	28.95	12.53	4.38	0.08	0.10	0.64	NA	NA	NA	99.95
PL_En_II_bis_07 6	52.35	29.72	13.32	3.92	0.08	0.08	0.65	NA	NA	NA	100.13
PL_En_II_bis_08 7	51.46	30.22	13.69	3.59	0.08	0.08	0.64	NA	NA	NA	99.76
PL_En_II_bis_09 8	51.03	30.51	13.82	3.45	0.08	0.05	0.62	NA	NA	NA	99.56
PL_En_II_bis_10 9	50.09	30.87	14.83	2.98	0.08	0.06	0.64	NA	NA	NA	99.55
PL_En_II_bis_11 10	49.33	31.49	15.46	2.64	0.09	0.04	0.74	NA	NA	NA	99.78
PL_En_II_bis_12 11	49.16	31.64	15.53	2.54	0.08	0.05	0.69	NA	NA	NA	99.69
PL_En_II_bis_13 12	49.11	31.76	15.43	2.46	0.09	0.04	0.70	NA	NA	NA	99.59
PL_En_II_bis_14 13	49.30	31.58	15.60	2.60	0.09	0.04	0.73	NA	NA	NA	99.94
PL_En_II_bis_15 14	49.01	31.56	15.57	2.50	0.10	0.04	0.71	NA	NA	NA	99.50
PL_En_II_bis_16 15	49.03	31.64	15.76	2.54	0.10	0.04	0.69	NA	NA	NA	99.80
PL_En_II_bis_17 16	49.09	31.61	15.53	2.50	0.10	0.04	0.70	NA	NA	NA	99.56
PL_En_II_bis_18 17	49.20	31.60	15.59	2.54	0.10	0.04	0.70	NA	NA	NA	99.76
PL_En_II_bis_19 18	48.85	31.85	15.86	2.56	0.11	0.03	0.70	NA	NA	NA	99.95
PL_En_II_bis_20 19	48.62	31.88	15.90	2.41	0.10	0.04	0.67	NA	NA	NA	99.61
PL_En_II_bis_21 20	48.48	31.82	15.80	2.42	0.10	0.03	0.65	NA	NA	NA	99.32
PL_En_II_bis_22 21	48.60	31.54	15.75	2.50	0.10	0.03	0.63	NA	NA	NA	99.15
PL_En_II_bis_23 22	48.61	31.73	15.65	2.34	0.09	0.03	0.65	NA	NA	NA	99.11
PL_En_II_bis_24 23	48.48	31.63	15.84	2.35	0.09	0.03	0.61	NA	NA	NA	99.04
PL_En_II_bis_25 24	48.23	31.81	15.98	2.23	0.08	0.03	0.64	NA	NA	NA	99.01
PL_En_II_bis_26 25	48.21	31.97	15.93	2.26	0.07	0.03	0.59	NA	NA	NA	99.06
PL_En_II_bis_27 26	48.09	32.12	16.26	2.14	0.04	0.02	0.61	NA	NA	NA	99.29
PL_En_II_bis_28 27	48.98	31.49	15.63	2.66	0.03	0.04	0.59	NA	NA	NA	99.42
PL_En_II_bis_29 28	49.09	31.36	15.26	2.86	0.02	0.04	0.65	NA	NA	NA	99.27
PL_En_II_bis_30 29	54.02	28.27	11.71	4.93	0.02	0.10	0.39	NA	NA	NA	99.45
PL_En_II_bis_31 30	55.37	27.77	10.67	5.47	0.02	0.12	0.35	NA	NA	NA	99.76
PL_En_II_bis_32 31	55.49	27.71	10.82	5.34	0.02	0.11	0.32	NA	NA	NA	99.81
PL_En_II_bis_33 32	54.71	28.45	11.20	5.16	0.02	0.11	0.37	NA	NA	NA	100.01
PL_En_II_bis_34 33	55.01	28.15	11.22	5.19	0.02	0.11	0.38	NA	NA	NA	100.08
PL_En_II_bis_35 34	55.70	27.93	10.90	5.20	0.02	0.11	0.36	NA	NA	NA	100.22
PL_En_II_bis_36 35	54.97	27.94	11.26	5.02	0.02	0.11	0.35	NA	NA	NA	99.68
PL_En_II_bis_37 36	54.42	28.73	11.82	4.80	0.01	0.10	0.35	NA	NA	NA	100.23
PL_En_II_bis_38 37	55.28	28.19	11.27	5.05	0.02	0.10	0.38	NA	NA	NA	100.29
PL_En_II_bis_39 38	55.18	27.89	11.29	5.18	0.02	0.11	0.34	NA	NA	NA	100.01

Sample/ Distance (μm)	SiO_2	Al_2O_3	CaO	Na_2O	MgO	K_2O	FeO	MnO	TiO_2	P_2O_5	Total
PL_En_II_bis_4039	55.54	27.91	10.90	5.26	0.02	0.10	0.36	NA	NA	NA	100.09
PL_En_II_bis_4140	55.63	28.06	10.87	5.22	0.02	0.10	0.36	NA	NA	NA	100.26
PL_En_II_bis_4241	55.82	27.74	10.78	5.25	0.02	0.12	0.35	NA	NA	NA	100.08
PL_En_II_bis_4342	55.64	27.74	10.80	5.35	0.01	0.12	0.35	NA	NA	NA	100.02
PL_En_II_bis_4443	56.14	27.54	10.68	5.34	0.02	0.12	0.34	NA	NA	NA	100.18
PL_En_II_bis_4544	56.01	27.74	10.64	5.34	0.02	0.13	0.36	NA	NA	NA	100.24
PL_En_II_bis_4645	55.67	27.64	10.93	5.24	0.01	0.12	0.34	NA	NA	NA	99.96
PL_En_II_bis_4746	54.87	28.38	11.45	4.91	0.01	0.09	0.37	NA	NA	NA	100.09
PL_En_II_bis_4847	53.96	28.78	12.08	4.72	0.02	0.09	0.35	NA	NA	NA	99.99
PL_En_II_bis_4948	54.60	28.13	11.32	5.04	0.02	0.11	0.34	NA	NA	NA	99.55
PL_En_II_bis_5049	55.93	27.56	10.40	5.47	0.02	0.13	0.35	NA	NA	NA	99.86
PL_En_II_bis_5150	56.47	27.30	10.28	5.67	0.02	0.13	0.34	NA	NA	NA	100.20
PL_En_II_bis_5251	56.48	27.18	10.19	5.72	0.02	0.13	0.34	NA	NA	NA	100.06
PL_En_II_bis_5352	56.26	27.05	10.05	5.55	0.02	0.13	0.34	NA	NA	NA	99.40
PL_En_II_bis_5453	56.37	27.09	10.11	5.72	0.02	0.13	0.32	NA	NA	NA	99.76
PL_En_II_bis_5554	56.89	27.17	10.30	5.76	0.02	0.14	0.31	NA	NA	NA	100.59
PL_En_II_bis_5655	56.93	27.25	10.17	5.69	0.02	0.13	0.33	NA	NA	NA	100.53
PL_En_II_bis_5756	56.62	27.13	10.20	5.68	0.01	0.13	0.35	NA	NA	NA	100.12
PL_En_II_bis_5857	56.91	27.25	10.19	5.63	0.02	0.12	0.34	NA	NA	NA	100.47
PL_En_II_bis_5958	56.68	27.16	10.17	5.58	0.02	0.14	0.30	NA	NA	NA	100.05
PL_En_II_bis_6059	56.72	27.16	10.07	5.71	0.02	0.12	0.32	NA	NA	NA	100.12
PL_En_II_bis_6160	56.48	27.28	10.30	5.66	0.02	0.13	0.32	NA	NA	NA	100.19

Sample	Distance (μm)	SiO_2	Al_2O_3	CaO	Na_2O	MgO	K_2O	FeO	MnO	TiO_2	P_2O_5	Total
PL_En_II_01	0	56.99	27.10	10.25	5.56	0.07	0.29	0.69	NA	NA	NA	100.95
PL_En_II_02	1	56.11	27.63	10.69	5.20	0.06	0.22	0.67	NA	NA	NA	100.58
PL_En_II_03	2	54.76	28.33	11.37	4.86	0.06	0.18	0.68	NA	NA	NA	100.24
PL_En_II_04	3	53.13	29.39	12.79	3.98	0.07	0.12	0.65	NA	NA	NA	100.13
PL_En_II_05	4	53.06	29.92	13.15	3.86	0.07	0.08	0.59	NA	NA	NA	100.74
PL_En_II_06	5	52.81	29.92	13.09	3.87	0.07	0.09	0.60	NA	NA	NA	100.44
PL_En_II_07	6	52.34	29.96	13.55	3.78	0.07	0.07	0.61	NA	NA	NA	100.38
PL_En_II_08	7	51.05	30.73	14.43	3.06	0.07	0.06	0.64	NA	NA	NA	100.05
PL_En_II_09	8	51.29	30.91	14.50	3.20	0.07	0.06	0.58	NA	NA	NA	100.60
PL_En_II_10	9	51.20	30.94	14.18	3.16	0.07	0.06	0.56	NA	NA	NA	100.18
PL_En_II_11	10	50.44	31.26	15.23	2.75	0.07	0.05	0.57	NA	NA	NA	100.37
PL_En_II_12	11	49.87	31.61	15.37	2.52	0.07	0.05	0.63	NA	NA	NA	100.13
PL_En_II_13	12	49.84	31.70	15.39	2.60	0.08	0.05	0.66	NA	NA	NA	100.31
PL_En_II_14	13	49.30	31.72	15.39	2.43	0.08	0.04	0.65	NA	NA	NA	99.62
PL_En_II_15	14	49.57	31.67	15.79	2.36	0.08	0.05	0.63	NA	NA	NA	100.15
PL_En_II_16	15	49.19	31.92	15.87	2.29	0.09	0.04	0.67	NA	NA	NA	100.06
PL_En_II_17	16	49.49	32.07	15.97	2.34	0.09	0.03	0.65	NA	NA	NA	100.64
PL_En_II_18	17	49.45	32.06	15.81	2.29	0.10	0.04	0.66	NA	NA	NA	100.41
PL_En_II_19	18	48.98	32.07	15.99	2.34	0.11	0.04	0.65	NA	NA	NA	100.19
PL_En_II_20	19	48.90	32.14	16.06	2.20	0.13	0.05	0.61	NA	NA	NA	100.09
PL_En_II_21	20	48.41	32.44	16.28	1.96	0.13	0.03	0.63	NA	NA	NA	99.87
PL_En_II_22	21	48.78	32.10	16.05	2.20	0.11	0.03	0.60	NA	NA	NA	99.86
PL_En_II_23	22	49.40	31.78	15.93	2.35	0.09	0.03	0.64	NA	NA	NA	100.22
PL_En_II_24	23	49.17	31.91	15.66	2.41	0.09	0.04	0.61	NA	NA	NA	99.89
PL_En_II_25	24	49.61	32.00	15.51	2.40	0.09	0.05	0.64	NA	NA	NA	100.31
PL_En_II_26	25	50.06	31.52	15.45	2.55	0.09	0.05	0.62	NA	NA	NA	100.34
PL_En_II_27	26	50.07	31.38	15.43	2.58	0.09	0.04	0.62	NA	NA	NA	100.21
PL_En_II_28	27	49.78	31.77	15.41	2.47	0.09	0.04	0.62	NA	NA	NA	100.18
PL_En_II_29	28	48.92	32.15	15.82	2.21	0.09	0.03	0.63	NA	NA	NA	99.86
PL_En_II_30	29	49.35	32.24	16.08	2.21	0.09	0.03	0.62	NA	NA	NA	100.62
PL_En_II_31	30	48.80	32.26	16.09	2.11	0.09	0.03	0.57	NA	NA	NA	99.96
PL_En_II_32	31	49.01	32.48	16.13	2.09	0.09	0.03	0.54	NA	NA	NA	100.37
PL_En_II_33	32	48.76	32.31	16.26	2.10	0.09	0.03	0.63	NA	NA	NA	100.19
PL_En_II_34	33	48.69	32.47	16.38	2.08	0.09	0.03	0.63	NA	NA	NA	100.36
PL_En_II_35	34	48.61	32.41	16.48	2.11	0.09	0.03	0.59	NA	NA	NA	100.32
PL_En_II_36	35	48.59	32.68	16.27	2.05	0.09	0.03	0.57	NA	NA	NA	100.29
PL_En_II_37	36	48.45	32.40	16.22	2.08	0.09	0.03	0.57	NA	NA	NA	99.83
PL_En_II_38	37	48.56	32.49	16.44	1.99	0.09	0.03	0.59	NA	NA	NA	100.17
PL_En_II_39	38	48.31	32.58	16.40	1.92	0.09	0.03	0.56	NA	NA	NA	99.89

Sample	Distance (μm)	SiO_2	Al_2O_3	CaO	Na_2O	MgO	K_2O	FeO	MnO	TiO_2	P_2O_5	Total
PL_En_II_40	39	48.68	32.58	16.47	2.04	0.08	0.02	0.56	NA	NA	NA	100.42
PL_En_II_41	40	48.59	32.42	16.41	2.03	0.08	0.03	0.58	NA	NA	NA	100.15
PL_En_II_42	41	48.39	32.56	16.43	2.00	0.07	0.03	0.54	NA	NA	NA	100.01
PL_En_II_43	42	47.74	32.37	16.36	1.80	0.07	0.02	0.57	NA	NA	NA	98.93
PL_En_II_44	43	50.95	31.30	14.76	2.94	0.05	0.04	0.51	NA	NA	NA	100.56
PL_En_II_45	44	53.27	29.76	12.94	3.90	0.04	0.07	0.40	NA	NA	NA	100.38
PL_En_II_46	45	55.65	28.31	11.03	5.13	0.04	0.11	0.32	NA	NA	NA	100.59
PL_En_II_47	46	56.77	27.66	10.56	5.45	0.03	0.13	0.31	NA	NA	NA	100.91
PL_En_II_48	47	56.81	27.73	10.58	5.40	0.03	0.11	0.27	NA	NA	NA	100.94
PL_En_II_49	48	56.27	28.17	10.79	5.29	0.03	0.11	0.28	NA	NA	NA	100.93
PL_En_II_50	49	55.68	28.30	11.46	4.98	0.02	0.10	0.30	NA	NA	NA	100.83
PL_En_II_51	50	55.63	28.42	11.21	4.83	0.02	0.09	0.32	NA	NA	NA	100.51
PL_En_II_52	51	55.17	28.48	11.36	4.87	0.02	0.10	0.34	NA	NA	NA	100.33
PL_En_II_53	52	55.23	28.64	11.62	4.78	0.02	0.11	0.30	NA	NA	NA	100.70
PL_En_II_54	53	54.88	29.16	11.66	4.67	0.01	0.10	0.31	NA	NA	NA	100.81
PL_En_II_55	54	55.06	28.39	11.62	4.83	0.01	0.09	0.34	NA	NA	NA	100.34
PL_En_II_56	55	55.58	28.45	11.35	4.87	0.02	0.10	0.30	NA	NA	NA	100.66
PL_En_II_57	56	55.37	28.56	11.38	4.86	0.02	0.10	0.29	NA	NA	NA	100.58
PL_En_II_58	57	55.22	28.13	11.22	4.97	0.02	0.11	0.30	NA	NA	NA	99.96
PL_En_II_59	58	55.83	28.21	10.93	5.11	0.02	0.11	0.33	NA	NA	NA	100.54
PL_En_II_60	59	55.90	28.34	10.91	5.10	0.01	0.12	0.30	NA	NA	NA	100.68
PL_En_II_61	60	56.04	28.19	11.03	5.25	0.02	0.12	0.32	NA	NA	NA	100.96
PL_En_II_62	61	55.87	28.43	10.96	5.19	0.02	0.11	0.31	NA	NA	NA	100.89
PL_En_II_63	62	55.91	28.46	10.98	5.21	0.02	0.10	0.30	NA	NA	NA	100.98
PL_En_II_64	63	56.08	28.20	10.92	5.23	0.01	0.11	0.28	NA	NA	NA	100.83
PL_En_II_65	64	56.03	28.01	10.91	5.15	0.02	0.11	0.34	NA	NA	NA	100.57
PL_En_II_66	65	55.80	28.17	11.09	5.01	0.01	0.11	0.28	NA	NA	NA	100.49
PL_En_II_67	66	55.52	28.18	11.00	5.02	0.02	0.11	0.27	NA	NA	NA	100.11
PL_En_II_68	67	55.58	28.21	11.21	5.07	0.02	0.11	0.31	NA	NA	NA	100.51
PL_En_II_69	68	55.21	28.52	11.33	4.92	0.01	0.10	0.32	NA	NA	NA	100.42
PL_En_II_70	69	55.44	28.52	11.59	4.75	0.02	0.10	0.36	NA	NA	NA	100.78
PL_En_II_71	70	55.12	28.83	11.74	4.61	0.01	0.10	0.30	NA	NA	NA	100.73
PL_En_II_72	71	55.06	28.78	11.84	4.76	0.01	0.10	0.29	NA	NA	NA	100.84
PL_En_II_73	72	54.81	28.78	11.75	4.59	0.02	0.10	0.31	NA	NA	NA	100.34
PL_En_II_74	73	54.78	28.82	11.71	4.64	0.01	0.10	0.30	NA	NA	NA	100.37
PL_En_II_75	74	54.58	28.77	11.90	4.59	0.01	0.10	0.32	NA	NA	NA	100.26
PL_En_II_76	75	54.50	28.72	11.74	4.67	0.01	0.09	0.30	NA	NA	NA	100.04
PL_En_II_77	76	54.92	28.91	12.02	4.60	0.01	0.10	0.29	NA	NA	NA	100.84
PL_En_II_78	77	54.34	28.62	11.80	4.42	0.02	0.09	0.34	NA	NA	NA	99.64

Sample	Distance (μm)	SiO_2	Al_2O_3	CaO	Na_2O	MgO	K_2O	FeO	MnO	TiO_2	P_2O_5	Total
PL_En_II_79	78	54.54	28.82	11.86	4.66	0.01	0.08	0.31	NA	NA	NA	100.29
PL_En_II_80	79	54.71	28.92	12.06	4.60	0.01	0.10	0.30	NA	NA	NA	100.70
PL_En_II_81	80	54.46	29.18	12.09	4.58	0.02	0.09	0.32	NA	NA	NA	100.73
PL_En_II_82	81	54.52	29.23	11.97	4.64	0.01	0.09	0.30	NA	NA	NA	100.76
PL_En_II_83	82	54.90	28.71	11.73	4.69	0.02	0.10	0.32	NA	NA	NA	100.48
PL_En_II_84	83	54.31	28.58	11.65	4.59	0.01	0.11	0.31	NA	NA	NA	99.57
PL_En_II_85	84	54.68	28.80	11.63	4.77	0.02	0.09	0.34	NA	NA	NA	100.34
PL_En_II_86	85	55.12	28.96	11.79	4.51	0.01	0.09	0.31	NA	NA	NA	100.79
PL_En_II_87	86	54.46	29.37	12.14	4.34	0.01	0.08	0.30	NA	NA	NA	100.72
PL_En_II_88	87	54.12	29.41	12.21	4.35	0.01	0.10	0.31	NA	NA	NA	100.51
PL_En_II_89	88	54.36	29.17	12.10	4.44	0.01	0.09	0.31	NA	NA	NA	100.48
PL_En_II_90	89	54.58	29.09	12.17	4.53	0.01	0.08	0.30	NA	NA	NA	100.76
PL_En_II_91	90	54.43	29.18	12.17	4.41	0.01	0.09	0.32	NA	NA	NA	100.61
PL_En_II_92	91	54.63	29.33	12.12	4.47	0.02	0.09	0.29	NA	NA	NA	100.95
PL_En_II_93	92	54.55	29.38	12.17	4.43	0.02	0.09	0.32	NA	NA	NA	100.96
PL_En_II_94	93	54.25	29.35	11.95	4.48	0.02	0.10	0.31	NA	NA	NA	100.46
PL_En_II_95	94	54.52	29.12	12.03	4.38	0.02	0.09	0.32	NA	NA	NA	100.47
PL_En_II_96	95	54.58	28.99	11.93	4.32	0.02	0.09	0.29	NA	NA	NA	100.22
PL_En_II_97	96	54.23	29.16	12.00	4.35	0.02	0.10	0.33	NA	NA	NA	100.18
PL_En_II_98	97	54.21	28.98	12.03	4.44	0.01	0.09	0.31	NA	NA	NA	100.08
PL_En_II_99	98	52.81	29.65	12.81	4.41	0.02	0.08	0.33	NA	NA	NA	100.11
PL_En_II_100	99	52.88	29.62	12.95	4.39	0.02	0.07	0.32	NA	NA	NA	100.26
PL_En_VI_01	0	52.86	28.85	12.99	3.63	0.11	0.07	0.91	NA	NA	NA	99.41
PL_En_VI_02	1	51.81	29.75	14.08	3.14	0.11	0.06	0.76	NA	NA	NA	99.69
PL_En_VI_03	2	51.47	30.91	14.25	3.09	0.11	0.05	0.64	NA	NA	NA	100.53
PL_En_VI_04	3	51.63	30.72	14.20	3.08	0.11	0.06	0.60	NA	NA	NA	100.39
PL_En_VI_05	4	51.17	31.34	14.88	2.88	0.11	0.05	0.61	NA	NA	NA	101.05
PL_En_VI_06	5	50.56	31.52	15.07	2.73	0.11	0.04	0.65	NA	NA	NA	100.69
PL_En_VI_07	6	49.87	31.74	15.30	2.55	0.12	0.05	0.63	NA	NA	NA	100.26
PL_En_VI_08	7	49.74	31.90	15.39	2.39	0.11	0.03	0.60	NA	NA	NA	100.17
PL_En_VI_09	8	49.75	31.94	15.67	2.28	0.11	0.03	0.63	NA	NA	NA	100.40
PL_En_VI_10	9	49.42	32.27	15.78	2.19	0.11	0.04	0.61	NA	NA	NA	100.41
PL_En_VI_11	10	49.45	32.31	15.90	2.18	0.12	0.04	0.59	NA	NA	NA	100.58
PL_En_VI_12	11	49.32	32.13	15.80	2.23	0.19	0.04	0.59	NA	NA	NA	100.31
PL_En_VI_13	12	49.13	32.30	15.87	2.19	0.29	0.03	0.57	NA	NA	NA	100.39
PL_En_VI_14	13	48.22	32.75	16.58	1.79	0.32	0.02	0.54	NA	NA	NA	100.23
PL_En_VI_15	14	48.09	32.96	16.71	1.73	0.26	0.03	0.57	NA	NA	NA	100.35
PL_En_VI_16	15	48.20	33.03	16.74	1.73	0.20	0.02	0.55	NA	NA	NA	100.47
PL_En_VI_17	16	47.98	33.20	16.74	1.68	0.12	0.02	0.52	NA	NA	NA	100.25

Sample	Distance (μm)	SiO_2	Al_2O_3	CaO	Na_2O	MgO	K_2O	FeO	MnO	TiO_2	P_2O_5	Total
PL_En_VI_18	17	47.98	32.62	16.85	1.61	0.08	0.03	0.65	NA	NA	NA	99.82
PL_En_VI_19	18	47.58	33.00	16.97	1.55	0.06	0.02	0.53	NA	NA	NA	99.71
PL_En_VI_20	19	47.99	33.05	16.65	1.58	0.06	0.02	0.50	NA	NA	NA	99.85
PL_En_VI_21	20	47.73	33.03	16.75	1.64	0.05	0.02	0.52	NA	NA	NA	99.74
PL_En_VI_22	21	48.10	32.57	16.22	1.78	0.05	0.03	0.50	NA	NA	NA	99.25
PL_En_VI_23	22	49.81	31.57	15.32	2.59	0.05	0.03	0.50	NA	NA	NA	99.87
PL_En_VI_24	23	50.89	30.74	14.40	3.07	0.05	0.04	0.52	NA	NA	NA	99.71
PL_En_VI_25	24	51.28	31.02	14.32	3.18	0.05	0.04	0.52	NA	NA	NA	100.40
PL_En_VI_26	25	51.18	30.80	14.33	3.16	0.05	0.05	0.56	NA	NA	NA	100.12
PL_En_VI_27	26	51.59	30.76	14.00	3.15	0.04	0.05	0.59	NA	NA	NA	100.18
PL_En_VI_28	27	51.24	30.94	14.23	3.17	0.05	0.04	0.53	NA	NA	NA	100.20
PL_En_VI_29	28	50.25	31.76	15.08	2.57	0.05	0.03	0.57	NA	NA	NA	100.31
PL_En_VI_30	29	49.80	31.79	15.35	2.39	0.05	0.04	0.54	NA	NA	NA	99.95
PL_En_VI_31	30	49.38	31.68	15.22	2.53	0.05	0.04	0.53	NA	NA	NA	99.43
PL_En_VI_32	31	49.48	31.95	15.32	2.33	0.06	0.03	0.54	NA	NA	NA	99.71
PL_En_VI_33	32	50.16	31.91	15.32	2.54	0.06	0.03	0.53	NA	NA	NA	100.54
PL_En_VI_34	33	50.15	32.02	15.44	2.55	0.06	0.03	0.61	NA	NA	NA	100.86
PL_En_VI_35	34	50.42	31.54	15.11	2.65	0.06	0.03	0.54	NA	NA	NA	100.35
PL_En_VI_36	35	49.95	31.52	14.93	2.70	0.06	0.04	0.53	NA	NA	NA	99.72
PL_En_VI_37	36	50.44	31.36	14.71	2.73	0.06	0.04	0.55	NA	NA	NA	99.89
PL_En_VI_38	37	50.37	31.24	14.76	2.79	0.06	0.04	0.53	NA	NA	NA	99.80
PL_En_VI_39	38	51.08	30.99	14.41	3.04	0.06	0.04	0.55	NA	NA	NA	100.18
PL_En_VI_40	39	50.99	30.86	14.26	3.05	0.06	0.04	0.57	NA	NA	NA	99.84
PL_En_VI_41	40	50.80	30.99	14.74	2.85	0.06	0.03	0.54	NA	NA	NA	100.01
PL_En_VI_42	41	51.70	30.65	14.29	3.37	0.06	0.04	0.57	NA	NA	NA	100.69
PL_En_VI_43	42	51.38	30.76	14.06	3.21	0.07	0.05	0.56	NA	NA	NA	100.08
PL_En_VI_44	43	51.20	30.57	14.19	3.25	0.07	0.04	0.55	NA	NA	NA	99.87
PL_En_VI_45	44	51.34	30.66	14.25	3.15	0.07	0.03	0.54	NA	NA	NA	100.03
PL_En_VI_46	45	51.42	30.78	14.03	3.32	0.07	0.04	0.55	NA	NA	NA	100.22
PL_En_VI_47	46	51.38	30.93	14.24	3.14	0.06	0.04	0.53	NA	NA	NA	100.33
PL_En_VI_48	47	51.61	30.75	14.22	3.07	0.06	0.04	0.56	NA	NA	NA	100.31
PL_En_VI_49	48	51.64	30.63	14.07	3.25	0.06	0.04	0.54	NA	NA	NA	100.23
PL_En_VI_50	49	51.55	30.71	13.97	3.44	0.06	0.03	0.56	NA	NA	NA	100.32
PL_En_VI_51	50	51.81	30.65	13.84	3.33	0.06	0.04	0.50	NA	NA	NA	100.23
PL_En_VI_52	51	52.03	30.49	14.02	3.38	0.06	0.04	0.56	NA	NA	NA	100.58
PL_En_VI_53	52	52.00	30.51	13.68	3.42	0.05	0.05	0.56	NA	NA	NA	100.28
PL_En_VI_54	53	51.58	30.56	14.12	3.45	0.05	0.05	0.56	NA	NA	NA	100.37
PL_En_VI_55	54	50.06	30.89	14.70	3.20	0.06	0.03	0.53	NA	NA	NA	99.47

Sample	Distance (μm)	SiO_2	Al_2O_3	CaO	Na_2O	MgO	K_2O	FeO	MnO	TiO_2	P_2O_5	Total
PL_H6Oct_VII_01	0	51.92	28.84	13.21	3.64	1.52	0.08	0.69	NA	NA	NA	99.92
PL_H6Oct_VII_02	1	51.15	30.32	13.97	3.19	1.26	0.07	0.66	NA	NA	NA	100.63
PL_H6Oct_VII_03	2	50.26	31.07	14.85	2.87	0.31	0.05	0.68	NA	NA	NA	100.09
PL_H6Oct_VII_04	3	49.57	31.55	15.03	2.61	0.07	0.04	0.68	NA	NA	NA	99.55
PL_H6Oct_VII_05	4	49.88	31.03	14.86	2.72	0.04	0.05	0.60	NA	NA	NA	99.17
PL_H6Oct_VII_06	5	53.81	29.07	11.93	4.12	0.03	0.10	0.44	NA	NA	NA	99.48
PL_H6Oct_VII_07	6	55.90	27.63	10.45	5.09	0.02	0.14	0.30	NA	NA	NA	99.52
PL_H6Oct_VII_08	7	56.46	27.40	10.20	5.45	0.02	0.13	0.28	NA	NA	NA	99.95
PL_H6Oct_VII_09	8	56.48	27.22	10.16	5.51	0.01	0.13	0.34	NA	NA	NA	99.86
PL_H6Oct_VII_10	9	56.70	27.72	10.34	5.41	0.02	0.14	0.35	NA	NA	NA	100.68
PL_H6Oct_VII_11	10	55.78	27.68	10.72	5.26	0.02	0.12	0.31	NA	NA	NA	99.89
PL_H6Oct_VII_12	11	54.32	28.90	11.65	4.60	0.01	0.10	0.31	NA	NA	NA	99.89
PL_H6Oct_VII_13	12	53.61	29.31	12.43	4.31	0.01	0.08	0.32	NA	NA	NA	100.07
PL_H6Oct_VII_14	13	53.92	29.29	12.32	4.24	0.01	0.09	0.34	NA	NA	NA	100.22
PL_H6Oct_VII_15	14	54.32	28.82	11.73	4.47	0.01	0.10	0.33	NA	NA	NA	99.79
PL_H6Oct_VII_16	15	55.04	28.45	11.26	4.92	0.02	0.12	0.32	NA	NA	NA	100.12
PL_H6Oct_VII_17	16	55.86	28.06	10.81	5.03	0.01	0.11	0.31	NA	NA	NA	100.19
PL_H6Oct_VII_18	17	55.96	27.84	10.71	5.28	0.02	0.13	0.31	NA	NA	NA	100.24
PL_H6Oct_VII_19	18	56.01	28.10	10.65	5.38	0.01	0.12	0.33	NA	NA	NA	100.60
PL_H6Oct_VII_20	19	56.17	27.77	10.59	5.33	0.01	0.13	0.33	NA	NA	NA	100.35
PL_H6Oct_VII_21	20	55.95	27.95	10.85	5.13	0.02	0.12	0.29	NA	NA	NA	100.30
PL_H6Oct_VII_22	21	55.81	27.86	10.84	5.15	0.01	0.11	0.32	NA	NA	NA	100.12
PL_H6Oct_VII_23	22	55.80	27.93	10.83	5.28	0.02	0.11	0.32	NA	NA	NA	100.28
PL_H6Oct_VII_24	23	56.11	27.94	10.72	5.36	0.01	0.13	0.32	NA	NA	NA	100.60
PL_H6Oct_VII_25	24	56.22	27.65	10.46	5.33	0.01	0.13	0.30	NA	NA	NA	100.12
PL_H6Oct_VII_26	25	56.63	27.66	10.39	5.61	0.01	0.14	0.32	NA	NA	NA	100.77
PL_H6Oct_VII_27	26	56.45	27.50	10.21	5.44	0.01	0.14	0.30	NA	NA	NA	100.05
PL_H6Oct_VII_28	27	56.45	27.56	10.31	5.53	0.01	0.13	0.30	NA	NA	NA	100.30
PL_H6Oct_VII_29	28	56.28	27.79	10.47	5.46	0.02	0.13	0.28	NA	NA	NA	100.42
PL_H6Oct_VII_30	29	55.88	28.05	10.85	5.20	0.02	0.12	0.31	NA	NA	NA	100.42
PL_H6Oct_VII_31	30	55.13	28.38	11.41	4.70	0.01	0.10	0.30	NA	NA	NA	100.04
PL_H6Oct_VII_32	31	54.68	28.78	11.62	4.71	0.01	0.11	0.32	NA	NA	NA	100.24
PL_H6Oct_VII_33	32	54.91	28.66	11.39	4.77	0.02	0.10	0.31	NA	NA	NA	100.17
PL_H6Oct_VII_34	33	55.23	28.57	11.20	4.99	0.01	0.11	0.29	NA	NA	NA	100.41
PL_H6Oct_VII_35	34	55.28	28.27	11.22	4.93	0.02	0.11	0.30	NA	NA	NA	100.13
PL_H6Oct_VII_36	35	55.10	28.37	11.14	4.96	0.02	0.12	0.28	NA	NA	NA	99.99
PL_H6Oct_VII_37	36	55.18	28.26	11.19	5.02	0.02	0.12	0.29	NA	NA	NA	100.06
PL_H6Oct_VII_38	37	55.21	28.37	11.11	5.07	0.01	0.11	0.30	NA	NA	NA	100.18
PL_H6Oct_VII_39	38	54.93	28.23	11.10	5.04	0.02	0.12	0.30	NA	NA	NA	99.73

Sample	Distance (μm)	SiO_2	Al_2O_3	CaO	Na_2O	MgO	K_2O	FeO	MnO	TiO_2	P_2O_5	Total
PL_H6Oct_VII_40	39	55.25	28.33	11.33	4.92	0.02	0.12	0.28	NA	NA	NA	100.24
PL_H6Oct_VII_41	40	55.32	28.44	11.34	4.89	0.02	0.11	0.29	NA	NA	NA	100.38
PL_H6Oct_VII_42	41	55.18	28.26	11.15	4.90	0.02	0.12	0.28	NA	NA	NA	99.91
PL_H6Oct_VII_43	42	55.17	28.45	11.13	4.97	0.01	0.11	0.33	NA	NA	NA	100.17
PL_H6Oct_VII_44	43	55.37	28.15	11.15	4.98	0.01	0.12	0.31	NA	NA	NA	100.08
PL_H6Oct_VII_45	44	55.16	28.24	10.83	5.01	0.01	0.12	0.31	NA	NA	NA	99.68
PL_H6Oct_VII_46	45	55.52	28.24	10.75	5.15	0.02	0.12	0.31	NA	NA	NA	100.10
PL_H6Oct_VII_47	46	55.66	28.03	10.78	5.09	0.02	0.12	0.31	NA	NA	NA	100.01
PL_H6Oct_VII_48	47	55.58	27.95	10.79	5.12	0.02	0.12	0.28	NA	NA	NA	99.86
PL_H6Oct_VII_49	48	56.23	27.85	10.49	5.35	0.02	0.13	0.30	NA	NA	NA	100.37
PL_H6Oct_VII_50	49	56.34	27.97	10.66	5.43	0.01	0.12	0.35	NA	NA	NA	100.89
PL_H6Oct_VII_51	50	56.01	27.98	10.58	5.37	0.02	0.12	0.30	NA	NA	NA	100.37
PL_H6Oct_VII_52	51	55.26	28.14	10.87	5.30	0.02	0.12	0.32	NA	NA	NA	100.04
PL_H6Oct_VII_53	52	55.43	28.04	10.93	5.26	0.02	0.13	0.31	NA	NA	NA	100.12
PL_H6Oct_VII_54	53	55.21	28.17	10.93	5.00	0.02	0.12	0.30	NA	NA	NA	99.75
PL_H6Oct_VII_55	54	55.07	28.33	11.12	4.97	0.02	0.11	0.28	NA	NA	NA	99.89
PL_H6Oct_VII_56	55	54.35	29.08	11.70	4.68	0.01	0.10	0.31	NA	NA	NA	100.24
PL_H6Oct_VII_57	56	53.86	29.23	12.08	4.48	0.02	0.10	0.29	NA	NA	NA	100.06
PL_H6Oct_VII_58	57	53.57	28.99	12.26	4.48	0.02	0.10	0.31	NA	NA	NA	99.72
PL_H6Oct_VII_59	58	53.20	29.22	12.16	4.32	0.01	0.10	0.38	NA	NA	NA	99.40
PL_H6Oct_VII_60	59	53.71	29.27	12.16	4.36	0.02	0.09	0.30	NA	NA	NA	99.91
PL_H6Oct_VII_61	60	53.65	29.09	12.12	4.59	0.01	0.09	0.31	NA	NA	NA	99.86
PL_H6Oct_VII_62	61	54.07	29.35	12.01	4.53	0.02	0.10	0.29	NA	NA	NA	100.37
PL_H6Oct_VII_63	62	54.04	29.17	11.92	4.58	0.02	0.09	0.29	NA	NA	NA	100.11
PL_H6Oct_VII_64	63	53.92	29.04	11.86	4.53	0.02	0.10	0.29	NA	NA	NA	99.74
PL_H6Oct_VII_65	64	54.03	29.24	12.07	4.45	0.02	0.10	0.28	NA	NA	NA	100.19
PL_H6Oct_VII_66	65	53.94	29.07	12.01	4.56	0.02	0.09	0.29	NA	NA	NA	99.97

Sample/ Distance (μm)	SiO_2	Al_2O_3	CaO	Na_2O	MgO	K_2O	FeO	MnO	TiO_2	P_2O_5	Total
PL_H6Oct_V_01 0	52.67	29.46	13.07	3.97	0.43	0.13	0.69	NA	NA	NA	100.42
PL_H6Oct_V_02 1	52.05	29.69	13.41	3.75	0.49	0.11	0.71	NA	NA	NA	100.22
PL_H6Oct_V_03 2	52.00	29.78	13.62	3.65	0.53	0.09	0.77	NA	NA	NA	100.45
PL_H6Oct_V_04 3	52.14	28.02	12.72	3.54	0.55	0.09	1.79	NA	NA	NA	98.84
PL_H6Oct_V_05 4	51.03	28.65	13.62	3.16	0.65	0.07	1.34	NA	NA	NA	98.52
PL_H6Oct_V_06 5	50.98	29.32	13.91	3.15	0.66	0.07	1.12	NA	NA	NA	99.21
PL_H6Oct_V_07 6	50.57	29.64	14.23	2.97	0.63	0.06	1.10	NA	NA	NA	99.21
PL_H6Oct_V_08 7	50.32	30.34	14.34	3.01	0.60	0.08	0.81	NA	NA	NA	99.50
PL_H6Oct_V_09 8	50.46	30.82	14.74	3.06	0.55	0.08	0.70	NA	NA	NA	100.43
PL_H6Oct_V_10 9	50.58	30.91	14.40	3.15	0.51	0.09	0.68	NA	NA	NA	100.32
PL_H6Oct_V_11 10	50.59	30.77	14.59	3.11	0.44	0.09	0.63	NA	NA	NA	100.21
PL_H6Oct_V_12 11	50.34	30.98	14.64	3.16	0.37	0.08	0.65	NA	NA	NA	100.23
PL_H6Oct_V_13 12	50.30	30.67	14.49	3.13	0.25	0.08	0.60	NA	NA	NA	99.52
PL_H6Oct_V_14 13	50.85	30.59	14.27	3.19	0.18	0.09	0.62	NA	NA	NA	99.80
PL_H6Oct_V_15 14	50.24	30.49	14.28	3.28	0.14	0.09	0.62	NA	NA	NA	99.14
PL_H6Oct_V_16 15	51.01	30.28	13.93	3.34	0.11	0.11	0.62	NA	NA	NA	99.40
PL_H6Oct_V_17 16	50.15	30.74	14.95	2.90	0.09	0.08	0.64	NA	NA	NA	99.54
PL_H6Oct_V_18 17	49.64	31.06	15.00	2.95	0.08	0.07	0.63	NA	NA	NA	99.42
PL_H6Oct_V_19 18	49.18	31.96	15.66	2.41	0.08	0.04	0.62	NA	NA	NA	99.94
PL_H6Oct_V_20 19	47.84	32.44	16.58	2.00	0.08	0.04	0.60	NA	NA	NA	99.58
PL_H6Oct_V_21 20	47.17	32.79	16.93	1.66	0.08	0.04	0.56	NA	NA	NA	99.23
PL_H6Oct_V_22 21	46.92	32.88	16.91	1.61	0.08	0.03	0.59	NA	NA	NA	99.01
PL_H6Oct_V_23 22	46.87	32.97	16.94	1.56	0.08	0.03	0.59	NA	NA	NA	99.03
PL_H6Oct_V_24 23	46.84	33.01	17.06	1.62	0.07	0.03	0.61	NA	NA	NA	99.24
PL_H6Oct_V_25 24	47.32	33.03	16.79	1.69	0.08	0.03	0.59	NA	NA	NA	99.53
PL_H6Oct_V_26 25	47.11	33.00	17.17	1.62	0.10	0.02	0.58	NA	NA	NA	99.61
PL_H6Oct_V_27 26	47.08	33.19	17.23	1.67	0.21	0.02	0.58	NA	NA	NA	99.99
PL_H6Oct_V_28 27	47.19	33.00	17.07	1.62	0.35	0.03	0.53	NA	NA	NA	99.80
PL_H6Oct_V_29 28	47.03	33.09	17.16	1.64	0.46	0.02	0.56	NA	NA	NA	99.97
PL_H6Oct_V_30 29	47.07	33.07	17.03	1.68	0.55	0.03	0.62	NA	NA	NA	100.05
PL_H6Oct_V_31 30	47.13	33.03	17.17	1.59	0.51	0.04	0.62	NA	NA	NA	100.09
PL_H6Oct_V_32 31	48.11	32.66	16.41	1.81	0.35	0.05	0.62	NA	NA	NA	100.01
PL_H6Oct_V_33 32	47.53	32.74	16.92	1.84	0.32	0.04	0.59	NA	NA	NA	99.98
PL_H6Oct_V_34 33	48.36	32.45	16.16	2.21	0.20	0.04	0.60	NA	NA	NA	100.04
PL_H6Oct_V_35 34	48.10	32.42	16.51	1.92	0.07	0.04	0.63	NA	NA	NA	99.68
PL_H6Oct_V_36 35	50.79	31.66	15.17	2.52	0.04	0.06	0.68	NA	NA	NA	100.91
PL_H6Oct_V_37 36	49.19	32.05	15.92	2.41	0.04	0.04	0.64	NA	NA	NA	100.29
PL_H6Oct_V_38 37	49.27	31.75	15.65	2.64	0.03	0.04	0.58	NA	NA	NA	99.96
PL_H6Oct_V_39 38	53.05	29.35	12.66	4.24	0.03	0.07	0.37	NA	NA	NA	99.77

Sample/ Distance (μm)	SiO_2	Al_2O_3	CaO	Na_2O	MgO	K_2O	FeO	MnO	TiO_2	P_2O_5	Total
PL_H6Oct_V_40 39	53.51	28.86	12.25	4.51	0.03	0.09	0.31	NA	NA	NA	99.56
PL_H6Oct_V_41 40	53.87	28.35	12.06	4.17	0.02	0.14	0.55	NA	NA	NA	99.17
PL_H6Oct_V_42 41	54.17	28.78	12.17	4.58	0.02	0.09	0.34	NA	NA	NA	100.16
PL_H6Oct_V_43 42	56.42	27.61	10.43	5.60	0.02	0.12	0.32	NA	NA	NA	100.52
PL_H6Oct_V_44 43	56.50	27.13	10.16	5.63	0.02	0.13	0.28	NA	NA	NA	99.86
PL_H6Oct_V_45 44	56.82	27.23	10.10	5.82	0.02	0.14	0.29	NA	NA	NA	100.41
PL_H6Oct_V_46 45	56.80	27.40	10.16	5.76	0.02	0.14	0.30	NA	NA	NA	100.57
PL_H6Oct_V_47 46	56.92	27.21	10.04	5.92	0.03	0.12	0.29	NA	NA	NA	100.53
PL_H6Oct_V_48 47	56.88	27.28	9.97	5.89	0.02	0.13	0.30	NA	NA	NA	100.47
PL_H6Oct_V_49 48	56.70	27.25	10.22	5.62	0.03	0.13	0.29	NA	NA	NA	100.24
PL_H6Oct_V_50 49	56.20	27.31	10.41	5.62	0.02	0.12	0.31	NA	NA	NA	99.98
PL_H6Oct_V_51 50	56.44	27.29	10.55	5.72	0.02	0.12	0.34	NA	NA	NA	100.48
PL_H6Oct_V_52 51	56.41	27.43	10.54	5.57	0.02	0.12	0.32	NA	NA	NA	100.41
PL_H6Oct_V_53 52	56.15	27.64	10.79	5.56	0.02	0.12	0.31	NA	NA	NA	100.58
PL_H6Oct_V_54 53	55.89	27.78	11.08	5.40	0.02	0.12	0.32	NA	NA	NA	100.61
PL_H6Oct_V_55 54	55.09	28.29	11.44	5.02	0.02	0.11	0.32	NA	NA	NA	100.29
PL_H6Oct_V_56 55	54.28	28.54	11.79	4.80	0.02	0.10	0.30	NA	NA	NA	99.82
PL_H6Oct_V_57 56	54.31	28.68	11.69	4.86	0.02	0.09	0.29	NA	NA	NA	99.95
PL_H6Oct_V_58 57	54.64	28.61	11.32	5.01	0.02	0.11	0.30	NA	NA	NA	100.01
PL_H6Oct_V_59 58	54.66	28.37	11.42	4.94	0.02	0.11	0.34	NA	NA	NA	99.87
PL_H6Oct_V_60 59	54.82	28.38	11.43	4.75	0.02	0.11	0.30	NA	NA	NA	99.81
PL_H6Oct_V_61 60	55.11	28.14	11.44	5.11	0.02	0.11	0.33	NA	NA	NA	100.25
PL_H6Oct_V_62 61	54.95	28.19	11.28	5.03	0.02	0.10	0.32	NA	NA	NA	99.89
PL_H6Oct_V_63 62	54.92	28.29	11.44	4.95	0.02	0.11	0.33	NA	NA	NA	100.07
PL_H6Oct_V_64 63	55.35	28.21	11.24	5.01	0.02	0.12	0.34	NA	NA	NA	100.29
PL_H6Oct_V_65 64	55.28	28.20	11.28	4.91	0.02	0.11	0.34	NA	NA	NA	100.14
PL_H6Oct_V_66 65	54.56	28.80	11.82	4.95	0.02	0.10	0.33	NA	NA	NA	100.58
PL_H6Oct_V_67 66	54.56	28.57	11.92	4.71	0.02	0.10	0.35	NA	NA	NA	100.23
PL_H6Oct_V_68 67	54.51	28.60	11.62	4.83	0.02	0.11	0.32	NA	NA	NA	99.99
PL_H6Oct_V_69 68	55.24	28.34	11.22	5.17	0.02	0.11	0.32	NA	NA	NA	100.41
PL_H6Oct_V_70 69	55.23	28.30	11.46	4.98	0.01	0.11	0.33	NA	NA	NA	100.41
PL_H6Oct_V_71 70	55.22	28.58	11.58	4.94	0.02	0.10	0.32	NA	NA	NA	100.76
PL_H6Oct_V_72 71	54.67	28.75	11.91	4.83	0.02	0.11	0.33	NA	NA	NA	100.60
PL_H6Oct_V_73 72	55.63	28.37	11.28	4.97	0.02	0.11	0.33	NA	NA	NA	100.71
PL_H6Oct_V_74 73	55.79	28.11	10.92	5.37	0.02	0.12	0.30	NA	NA	NA	100.62
PL_H6Oct_V_75 74	55.86	27.62	10.77	5.50	0.02	0.12	0.31	NA	NA	NA	100.20
PL_H6Oct_V_76 75	56.30	27.75	10.79	5.36	0.02	0.12	0.29	NA	NA	NA	100.63
PL_H6Oct_V_77 76	55.48	27.69	10.76	5.23	0.02	0.12	0.29	NA	NA	NA	99.58
PL_H6Oct_V_78 77	55.53	27.99	11.09	5.32	0.02	0.12	0.33	NA	NA	NA	100.40

Sample/ Distance (μm)	SiO_2	Al_2O_3	CaO	Na_2O	MgO	K_2O	FeO	MnO	TiO_2	P_2O_5	Total
PL_H6Oct_V_79 78	55.68	28.26	11.28	5.17	0.01	0.11	0.32	NA	NA	NA	100.83
PL_H6Oct_V_80 79	55.21	28.32	11.45	5.24	0.02	0.11	0.33	NA	NA	NA	100.68
PL_H6Oct_V_81 80	55.54	28.18	11.15	5.26	0.02	0.11	0.33	NA	NA	NA	100.58
PL_H6Oct_V_82 81	55.93	27.79	10.92	5.13	0.01	0.12	0.32	NA	NA	NA	100.21
PL_H6Oct_V_83 82	55.92	27.80	10.79	5.46	0.02	0.12	0.29	NA	NA	NA	100.40
PL_H6Oct_V_84 83	55.82	27.94	10.76	5.46	0.02	0.12	0.28	NA	NA	NA	100.40
PL_H6Oct_V_85 84	56.03	27.79	10.73	5.18	0.02	0.12	0.29	NA	NA	NA	100.15
PL_H6Oct_V_86 85	56.08	27.77	10.62	5.49	0.01	0.13	0.32	NA	NA	NA	100.42
PL_H6Oct_V_87 86	56.21	27.51	10.57	5.41	0.02	0.12	0.32	NA	NA	NA	100.17
PL_H6Oct_V_88 87	56.37	27.80	10.60	5.42	0.02	0.12	0.29	NA	NA	NA	100.62
PL_H6Oct_V_89 88	55.99	27.76	10.76	5.41	0.02	0.13	0.30	NA	NA	NA	100.36
PL_H6Oct_V_90 89	55.60	27.93	11.03	5.27	0.02	0.12	0.30	NA	NA	NA	100.26
PL_H6Oct_V_91 90	55.41	28.05	11.03	5.07	0.02	0.11	0.30	NA	NA	NA	99.98
PL_H6Oct_V_92 91	55.66	28.06	11.25	5.16	0.02	0.12	0.30	NA	NA	NA	100.57
PL_H6Oct_V_93 92	55.45	28.07	11.04	5.17	0.01	0.12	0.33	NA	NA	NA	100.20
PL_H6Oct_V_94 93	55.51	28.13	11.22	5.24	0.02	0.11	0.31	NA	NA	NA	100.54
PL_H6Oct_V_95 94	55.90	27.95	11.03	5.33	0.02	0.13	0.32	NA	NA	NA	100.68
PL_H6Oct_V_96 95	55.88	27.77	10.73	5.24	0.02	0.12	0.29	NA	NA	NA	100.05
PL_H6Oct_V_97 96	56.26	27.83	10.71	5.43	0.02	0.13	0.32	NA	NA	NA	100.70
PL_H6Oct_V_98 97	56.09	27.65	10.68	5.22	0.02	0.12	0.33	NA	NA	NA	100.12
PL_H6Oct_V_99 98	55.93	27.66	10.88	5.25	0.01	0.11	0.35	NA	NA	NA	100.19
PL_H6Oct_V_10099	55.78	27.85	10.99	5.27	0.01	0.12	0.31	NA	NA	NA	100.34
PL_H6Oct_V_101100	55.38	27.94	11.10	5.13	0.01	0.12	0.27	NA	NA	NA	99.96
PL_H6Oct_V_102101	55.90	28.18	10.92	5.34	0.02	0.12	0.28	NA	NA	NA	100.76
PL_H6Oct_V_103102	56.28	27.68	10.78	5.35	0.02	0.12	0.30	NA	NA	NA	100.53
PL_H6Oct_V_104103	56.29	27.91	10.46	5.40	0.01	0.12	0.29	NA	NA	NA	100.49
PL_H6Oct_V_105104	56.14	27.88	10.88	5.47	0.01	0.13	0.29	NA	NA	NA	100.81
PL_H6Oct_V_10 105	55.95	27.80	10.72	5.39	0.02	0.13	0.29	NA	NA	NA	100.29
PL_H6Oct_V_107106	55.77	27.80	10.80	5.26	0.02	0.12	0.31	NA	NA	NA	100.08
PL_H6Oct_V_108107	55.90	28.18	10.75	5.23	0.02	0.13	0.30	NA	NA	NA	100.50
PL_H6Oct_V_109108	56.02	27.71	10.92	5.44	0.02	0.12	0.29	NA	NA	NA	100.52
PL_H6Oct_V_110109	56.35	27.98	10.70	5.40	0.02	0.12	0.28	NA	NA	NA	100.86
PL_H6Oct_V_111110	56.23	27.68	10.56	5.37	0.03	0.12	0.28	NA	NA	NA	100.27
PL_H6Oct_V_112111	56.27	27.85	10.89	5.39	0.02	0.12	0.29	NA	NA	NA	100.83
PL_H6Oct_V_113112	56.09	27.81	10.57	5.32	0.02	0.13	0.30	NA	NA	NA	100.25
PL_H6Oct_V_114113	56.14	27.56	10.40	5.50	0.02	0.13	0.28	NA	NA	NA	100.03
PL_H6Oct_V_115114	56.78	27.51	10.29	5.70	0.03	0.13	0.28	NA	NA	NA	100.71
PL_H6Oct_V_116115	56.64	27.92	10.44	5.49	0.02	0.13	0.30	NA	NA	NA	100.95
PL_H6Oct_V_117116	55.65	28.04	11.03	5.25	0.02	0.11	0.32	NA	NA	NA	100.42

Sample	Distance (μm)	SiO_2	Al_2O_3	CaO	Na_2O	MgO	K_2O	FeO	MnO	TiO_2	P_2O_5	Total
PL_EN_I_01	0	10.01	3.41	1.04	2.13	-0.05	0.24	0.09	NA	NA	NA	16.85
PL_EN_I_02	1	27.31	9.45	2.70	5.10	-0.04	0.56	0.31	NA	NA	NA	45.38
PL_EN_I_03	2	57.67	19.85	4.40	8.84	-0.03	0.84	0.53	NA	NA	NA	92.09
PL_EN_I_04	3	62.48	22.39	5.40	8.63	-0.02	0.71	0.55	NA	NA	NA	100.15
PL_EN_I_05	4	61.58	23.71	6.46	7.65	-0.01	0.51	0.60	NA	NA	NA	100.50
PL_EN_I_06	5	58.81	25.73	8.58	6.62	0.01	0.29	0.63	NA	NA	NA	100.67
PL_EN_I_07	6	56.70	26.68	9.93	5.97	0.03	0.20	0.63	NA	NA	NA	100.14
PL_EN_I_08	7	55.88	27.36	10.59	5.39	0.03	0.16	0.66	NA	NA	NA	100.06
PL_EN_I_09	8	54.08	28.59	12.18	4.63	0.04	0.11	0.66	NA	NA	NA	100.29
PL_EN_I_10	9	53.47	28.77	12.56	4.30	0.05	0.09	0.58	NA	NA	NA	99.81
PL_EN_I_11	10	52.77	29.54	13.30	3.97	0.06	0.08	0.60	NA	NA	NA	100.31
PL_EN_I_12	11	52.37	29.88	13.50	3.82	0.06	0.07	0.58	NA	NA	NA	100.27
PL_EN_I_13	12	52.40	29.37	13.09	3.90	0.07	0.07	0.61	NA	NA	NA	99.50
PL_EN_I_14	13	52.54	29.42	13.33	3.99	0.07	0.07	0.59	NA	NA	NA	100.02
PL_EN_I_15	14	52.52	29.46	13.44	3.86	0.07	0.06	0.65	NA	NA	NA	100.05
PL_EN_I_16	15	51.65	29.79	13.83	3.66	0.07	0.06	0.63	NA	NA	NA	99.70
PL_EN_I_17	16	50.99	30.22	14.28	3.34	0.07	0.05	0.64	NA	NA	NA	99.59
PL_EN_I_18	17	50.97	30.23	14.18	3.28	0.07	0.05	0.65	NA	NA	NA	99.44
PL_EN_I_19	18	51.58	30.05	13.73	3.58	0.08	0.06	0.56	NA	NA	NA	99.63
PL_EN_I_20	19	51.05	30.50	14.35	3.40	0.07	0.04	0.55	NA	NA	NA	99.96
PL_EN_I_21	20	50.24	31.19	14.96	2.96	0.07	0.04	0.58	NA	NA	NA	100.05
PL_EN_I_22	21	50.15	30.86	15.05	2.78	0.07	0.04	0.60	NA	NA	NA	99.55
PL_EN_I_23	22	50.19	30.91	15.21	2.82	0.07	0.05	0.60	NA	NA	NA	99.85
PL_EN_I_24	23	50.02	30.79	15.05	2.88	0.07	0.05	0.61	NA	NA	NA	99.47
PL_EN_I_25	24	49.99	31.26	15.20	2.90	0.08	0.04	0.69	NA	NA	NA	100.15
PL_EN_I_26	25	49.73	31.15	15.27	2.76	0.08	0.04	0.65	NA	NA	NA	99.69
PL_EN_I_27	26	49.53	31.35	15.30	2.50	0.08	0.04	0.67	NA	NA	NA	99.47
PL_EN_I_28	27	49.35	31.30	15.64	2.51	0.08	0.03	0.67	NA	NA	NA	99.58
PL_EN_I_29	28	49.09	31.46	15.61	2.59	0.09	0.04	0.66	NA	NA	NA	99.53
PL_EN_I_30	29	48.95	31.56	16.04	2.39	0.09	0.03	0.61	NA	NA	NA	99.67
PL_EN_I_31	30	49.01	31.57	16.00	2.38	0.09	0.03	0.65	NA	NA	NA	99.74
PL_EN_I_32	31	48.76	31.71	15.88	2.32	0.09	0.03	0.63	NA	NA	NA	99.43
PL_EN_I_33	32	48.99	31.75	16.02	2.30	0.09	0.04	0.63	NA	NA	NA	99.83
PL_EN_I_34	33	48.57	31.64	15.80	2.34	0.10	0.04	0.65	NA	NA	NA	99.13
PL_EN_I_35	34	49.07	31.68	16.19	2.35	0.10	0.03	0.62	NA	NA	NA	100.04
PL_EN_I_36	35	48.69	31.79	16.16	2.33	0.10	0.04	0.61	NA	NA	NA	99.72
PL_EN_I_37	36	48.42	31.89	16.28	2.24	0.10	0.03	0.63	NA	NA	NA	99.59
PL_EN_I_38	37	48.13	32.02	16.20	2.03	0.11	0.03	0.60	NA	NA	NA	99.11
PL_EN_I_39	38	48.14	32.11	16.35	2.02	0.10	0.03	0.54	NA	NA	NA	99.28

Sample	Distance (μm)	SiO_2	Al_2O_3	CaO	Na_2O	MgO	K_2O	FeO	MnO	TiO_2	P_2O_5	Total
PL_EN_I_40	39	48.06	32.25	16.63	1.89	0.11	0.03	0.55	NA	NA	NA	99.52
PL_EN_I_41	40	47.70	32.45	16.71	1.91	0.10	0.03	0.57	NA	NA	NA	99.47
PL_EN_I_42	41	48.09	31.97	16.49	2.00	0.10	0.03	0.55	NA	NA	NA	99.22
PL_EN_I_43	42	48.08	32.34	16.45	2.02	0.10	0.03	0.56	NA	NA	NA	99.58
PL_EN_I_44	43	47.84	32.47	16.37	2.04	0.10	0.03	0.55	NA	NA	NA	99.39
PL_EN_I_45	44	47.79	32.63	16.95	1.77	0.10	0.02	0.57	NA	NA	NA	99.84
PL_EN_I_46	45	47.56	32.49	16.96	1.78	0.10	0.03	0.54	NA	NA	NA	99.46
PL_EN_I_47	46	47.41	32.73	16.69	1.79	0.10	0.02	0.57	NA	NA	NA	99.32
PL_EN_I_48	47	47.50	32.65	17.08	1.75	0.10	0.01	0.58	NA	NA	NA	99.68
PL_EN_I_49	48	46.89	32.87	17.34	1.61	0.10	0.02	0.55	NA	NA	NA	99.39
PL_EN_I_50	49	47.22	32.98	17.24	1.57	0.10	0.02	0.55	NA	NA	NA	99.67
PL_EN_I_51	50	47.22	32.76	17.07	1.57	0.10	0.01	0.54	NA	NA	NA	99.27
PL_EN_I_52	51	47.41	32.88	17.18	1.57	0.10	0.02	0.54	NA	NA	NA	99.69
PL_EN_I_53	52	47.01	32.88	17.36	1.55	0.10	0.01	0.50	NA	NA	NA	99.41
PL_EN_I_54	53	46.93	32.87	17.29	1.56	0.09	0.02	0.54	NA	NA	NA	99.30
PL_EN_I_55	54	47.15	32.87	17.27	1.54	0.10	0.02	0.51	NA	NA	NA	99.46
PL_EN_I_56	55	47.10	33.06	17.33	1.48	0.09	0.02	0.55	NA	NA	NA	99.63
PL_EN_I_57	56	46.51	32.94	17.37	1.53	0.10	0.02	0.54	NA	NA	NA	99.00
PL_EN_I_58	57	46.73	33.27	17.61	1.38	0.10	0.01	0.50	NA	NA	NA	99.61
PL_EN_I_59	58	46.86	33.10	17.36	1.43	0.10	0.01	0.51	NA	NA	NA	99.37
PL_EN_I_60	59	46.67	33.27	17.70	1.50	0.10	0.01	0.51	NA	NA	NA	99.75
PL_EN_I_61	60	46.49	33.08	17.37	1.41	0.10	0.02	0.49	NA	NA	NA	98.95
PL_EN_I_62	61	46.95	33.27	17.56	1.43	0.10	0.01	0.50	NA	NA	NA	99.81
PL_EN_I_63	62	46.73	33.23	17.43	1.37	0.10	0.01	0.51	NA	NA	NA	99.36
PL_EN_I_64	63	46.84	33.25	17.57	1.42	0.09	0.02	0.50	NA	NA	NA	99.68
PL_EN_I_65	64	47.30	33.39	17.34	1.43	0.09	0.02	0.49	NA	NA	NA	100.07
PL_EN_I_66	65	47.94	33.83	17.54	1.37	0.09	0.01	0.50	NA	NA	NA	101.30
PL_EN_I_67	66	42.08	30.42	16.72	1.01	0.09	0.01	0.96	NA	NA	NA	91.29
PL_EN_I_68	67	45.80	32.53	17.36	1.30	0.09	0.02	0.52	NA	NA	NA	97.62
PL_EN_I_69	68	46.54	32.97	17.38	1.46	0.08	0.02	0.51	NA	NA	NA	98.95
PL_EN_I_70	69	47.49	33.23	17.32	1.62	0.08	0.02	0.54	NA	NA	NA	100.29
PL_EN_I_71	70	47.44	33.15	17.23	1.57	0.09	0.02	0.52	NA	NA	NA	100.01
PL_EN_I_72	71	47.17	32.76	17.15	1.70	0.09	0.02	0.49	NA	NA	NA	99.37
PL_EN_I_73	72	47.57	32.60	16.98	1.68	0.09	0.02	0.56	NA	NA	NA	99.49
PL_EN_I_74	73	47.14	33.12	17.20	1.59	0.09	0.02	0.55	NA	NA	NA	99.71
PL_EN_I_75	74	46.96	33.20	17.48	1.44	0.08	0.01	0.53	NA	NA	NA	99.71
PL_EN_I_76	75	47.30	32.82	17.06	1.58	0.09	0.03	0.55	NA	NA	NA	99.42
PL_EN_I_77	76	47.65	31.92	16.47	1.82	0.10	0.03	0.79	NA	NA	NA	98.80
PL_EN_I_78	77	48.12	32.54	16.52	1.92	0.12	0.02	0.55	NA	NA	NA	99.79

Sample	Distance (μm)	SiO_2	Al_2O_3	CaO	Na_2O	MgO	K_2O	FeO	MnO	TiO_2	P_2O_5	Total
PL_EN_I_79	78	50.17	31.31	14.93	2.93	0.16	0.05	0.41	NA	NA	NA	99.95
PL_EN_I_80	79	50.85	30.62	14.60	3.25	0.18	0.05	0.39	NA	NA	NA	99.94
PL_EN_I_81	80	50.87	30.97	14.54	3.18	0.19	0.05	0.37	NA	NA	NA	100.16
PL_EN_I_82	81	50.63	31.14	14.88	2.89	0.19	0.05	0.40	NA	NA	NA	100.17
PL_EN_I_83	82	51.19	30.53	14.24	3.30	0.18	0.05	0.31	NA	NA	NA	99.81
PL_EN_I_84	83	51.12	30.76	14.45	3.40	0.16	0.05	0.34	NA	NA	NA	100.28
PL_EN_I_85	84	51.06	30.91	14.14	3.38	0.14	0.05	0.35	NA	NA	NA	100.02
PL_EN_I_86	85	51.40	30.55	13.92	3.59	0.09	0.05	0.36	NA	NA	NA	99.96
PL_EN_I_87	86	51.14	30.35	13.98	3.57	0.07	0.05	0.39	NA	NA	NA	99.55
PL_EN_I_88	87	51.70	30.75	13.99	3.53	0.05	0.05	0.36	NA	NA	NA	100.44
PL_EN_I_89	88	50.71	30.91	14.58	3.36	0.03	0.05	0.35	NA	NA	NA	100.00
PL_EN_I_90	89	50.44	30.94	14.66	3.01	0.03	0.04	0.38	NA	NA	NA	99.50
PL_EN_I_91	90	50.32	31.28	14.90	2.94	0.02	0.04	0.40	NA	NA	NA	99.90
PL_EN_I_92	91	49.94	31.20	15.01	2.76	0.02	0.04	0.43	NA	NA	NA	99.39
PL_EN_I_93	92	50.22	31.26	15.25	2.91	0.02	0.03	0.38	NA	NA	NA	100.08
PL_EN_I_94	93	49.88	31.29	15.33	2.81	0.02	0.04	0.40	NA	NA	NA	99.77
PL_EN_I_95	94	50.00	31.44	14.81	2.91	0.02	0.04	0.37	NA	NA	NA	99.59
PL_EN_I_96	95	50.14	31.36	14.97	2.87	0.02	0.04	0.40	NA	NA	NA	99.79
PL_EN_I_97	96	50.00	31.33	15.30	2.79	0.02	0.05	0.42	NA	NA	NA	99.91
PL_EN_I_98	97	50.09	31.42	14.99	2.98	0.01	0.05	0.39	NA	NA	NA	99.92
PL_EN_I_99	98	51.00	30.94	14.49	3.27	0.01	0.05	0.39	NA	NA	NA	100.16
PL_EN_I_100	99	50.74	30.87	14.53	3.21	0.02	0.06	0.39	NA	NA	NA	99.81
PL_EN_I_101	100	50.02	31.08	14.97	2.92	0.01	0.05	0.38	NA	NA	NA	99.44
PL_EN_I_102	101	49.99	31.68	15.15	2.89	0.01	0.04	0.46	NA	NA	NA	100.20
PL_EN_I_103	102	50.05	31.48	14.95	2.83	0.02	0.04	0.41	NA	NA	NA	99.77
PL_EN_I_104	103	50.28	31.38	15.02	2.94	0.02	0.04	0.38	NA	NA	NA	100.06
PL_EN_I_105	104	50.22	31.37	15.09	2.94	0.01	0.04	0.38	NA	NA	NA	100.05
PL_EN_I_106	105	50.36	31.50	15.09	2.98	0.02	0.04	0.38	NA	NA	NA	100.36
PL_EN_I_107	106	50.15	31.34	14.90	2.90	0.02	0.04	0.41	NA	NA	NA	99.76
PL_EN_I_108	107	50.06	31.24	15.02	2.93	0.01	0.04	0.41	NA	NA	NA	99.72
PL_EN_I_109	108	49.94	31.64	15.34	2.70	0.02	0.04	0.38	NA	NA	NA	100.05
PL_EN_I_110	109	49.27	32.19	15.55	2.64	0.01	0.03	0.40	NA	NA	NA	100.10
PL_EN_I_111	110	49.26	32.09	15.86	2.56	0.01	0.03	0.37	NA	NA	NA	100.19
PL_EN_I_112	111	49.39	31.79	15.53	2.55	0.01	0.04	0.43	NA	NA	NA	99.73
PL_EN_I_113	112	49.44	31.64	15.46	2.59	0.01	0.04	0.39	NA	NA	NA	99.56
PL_EN_I_114	113	49.64	31.75	15.49	2.77	0.01	0.04	0.38	NA	NA	NA	100.09
PL_EN_I_115	114	49.57	31.65	15.65	2.72	0.01	0.03	0.41	NA	NA	NA	100.04
PL_EN_I_116	115	49.17	32.12	15.66	2.49	0.01	0.03	0.39	NA	NA	NA	99.87
PL_EN_I_117	116	48.79	32.21	16.01	2.41	0.01	0.03	0.41	NA	NA	NA	99.89

Sample	Distance (μm)	SiO_2	Al_2O_3	CaO	Na_2O	MgO	K_2O	FeO	MnO	TiO_2	P_2O_5	Total
PL_H6Oct_IV_Mg_01	0	78.95	13.51	2.21	3.36	1.32	1.91	0.99	0.12	0.12	0.09	102.58
PL_H6Oct_IV_Mg_02	1	63.28	25.77	8.62	4.19	0.75	0.59	0.63	0.07	0.08	0.05	104.03
PL_H6Oct_IV_Mg_03	2	56.76	28.08	10.98	4.21	0.28	0.32	0.66	0.02	0.06	-0.01	101.36
PL_H6Oct_IV_Mg_04	3	53.02	29.59	12.70	3.77	0.11	0.21	0.69	-0.00	0.05	-0.02	100.11
PL_H6Oct_IV_Mg_05	4	52.88	29.53	12.94	3.86	0.09	0.18	0.64	-0.00	0.04	-0.03	100.13
PL_H6Oct_IV_Mg_06	5	52.94	29.65	12.89	3.73	0.09	0.15	0.68	-0.00	0.05	-0.03	100.14
PL_H6Oct_IV_Mg_07	6	51.60	29.99	13.57	3.53	0.09	0.09	0.67	0.00	0.04	-0.04	99.54
PL_H6Oct_IV_Mg_08	7	51.34	30.73	14.11	3.10	0.08	0.08	0.70	0.01	0.04	-0.04	100.15
PL_H6Oct_IV_Mg_09	8	50.57	31.01	14.78	2.73	0.07	0.06	0.69	0.01	0.03	-0.04	99.91
PL_H6Oct_IV_Mg_10	9	49.97	31.27	15.29	2.57	0.07	0.05	0.67	0.00	0.03	-0.04	99.88
PL_H6Oct_IV_Mg_11	10	49.80	31.32	15.21	2.48	0.06	0.05	0.68	0.00	0.03	-0.04	99.59
PL_H6Oct_IV_Mg_12	11	49.80	31.51	15.06	2.45	0.04	0.05	0.64	-0.00	0.02	-0.04	99.54
PL_H6Oct_IV_Mg_13	12	50.44	31.25	14.55	2.80	0.04	0.05	0.64	0.00	0.02	-0.04	99.74
PL_H6Oct_IV_Mg_14	13	54.33	28.78	11.57	4.54	0.03	0.10	0.40	-0.00	0.03	-0.04	99.74
PL_H6Oct_IV_Mg_15	14	54.82	28.40	11.20	4.84	0.02	0.11	0.33	0.00	0.03	-0.04	99.72
PL_H6Oct_IV_Mg_16	15	54.90	28.41	11.20	4.69	0.02	0.11	0.35	0.00	0.02	-0.04	99.67
PL_H6Oct_IV_Mg_17	16	53.88	28.87	12.06	4.44	0.02	0.09	0.37	0.00	0.02	-0.04	99.70
PL_H6Oct_IV_Mg_18	17	55.24	27.66	10.81	5.00	0.02	0.12	0.36	0.00	0.03	-0.02	99.21
PL_H6Oct_IV_Mg_19	18	56.52	27.60	10.39	5.28	0.02	0.13	0.34	0.00	0.03	-0.04	100.27
PL_H6Oct_IV_Mg_20	19	56.64	27.48	10.28	5.24	0.02	0.13	0.34	0.00	0.03	-0.03	100.12
PL_H6Oct_IV_Mg_21	20	56.51	27.63	10.36	5.05	0.02	0.13	0.34	0.00	0.03	-0.03	100.03
PL_H6Oct_IV_Mg_22	21	56.25	27.62	10.49	5.24	0.02	0.13	0.35	0.00	0.02	-0.03	100.10
PL_H6Oct_IV_Mg_23	22	56.01	27.94	10.80	5.27	0.02	0.12	0.30	-0.00	0.03	-0.03	100.47
PL_H6Oct_IV_Mg_24	23	55.84	27.94	10.86	5.18	0.02	0.12	0.37	0.01	0.03	-0.04	100.32
PL_H6Oct_IV_Mg_25	24	56.00	28.01	10.81	5.22	0.01	0.12	0.32	0.00	0.03	-0.04	100.49
PL_H6Oct_IV_Mg_26	25	56.43	27.60	10.49	5.35	0.01	0.12	0.34	-0.00	0.03	-0.03	100.34
PL_H6Oct_IV_Mg_27	26	56.50	27.57	10.31	5.36	0.02	0.13	0.36	-0.00	0.03	-0.03	100.25
PL_H6Oct_IV_Mg_28	27	56.75	27.47	10.23	5.44	0.02	0.13	0.35	-0.00	0.03	-0.04	100.37
PL_H6Oct_IV_Mg_29	28	56.86	27.35	10.35	5.41	0.02	0.14	0.34	-0.00	0.03	-0.03	100.46
PL_H6Oct_IV_Mg_30	29	56.81	27.23	10.27	5.28	0.02	0.14	0.33	-0.00	0.03	-0.04	100.08
PL_H6Oct_IV_Mg_31	30	56.69	27.44	10.22	5.18	0.02	0.13	0.32	-0.00	0.03	-0.04	99.99
PL_H6Oct_IV_Mg_32	31	56.59	27.57	10.44	5.29	0.02	0.13	0.32	0.00	0.03	-0.04	100.35
PL_H6Oct_IV_Mg_33	32	56.10	27.88	10.48	5.40	0.02	0.12	0.34	0.00	0.03	-0.03	100.35
PL_H6Oct_IV_Mg_34	33	56.17	27.59	10.35	5.25	0.02	0.12	0.34	0.00	0.03	-0.04	99.83
PL_H6Oct_IV_Mg_35	34	56.19	27.81	10.50	5.37	0.02	0.12	0.34	-0.00	0.03	-0.03	100.33
PL_H6Oct_IV_Mg_36	35	56.25	27.55	10.41	5.14	0.02	0.12	0.33	-0.00	0.03	-0.04	99.80
PL_H6Oct_IV_Mg_37	36	55.98	27.45	10.58	5.18	0.01	0.13	0.32	-0.00	0.03	-0.03	99.64
PL_H6Oct_IV_Mg_38	37	55.77	27.77	10.63	5.20	0.02	0.12	0.34	0.00	0.03	-0.04	99.83
PL_H6Oct_IV_Mg_39	38	55.88	27.64	10.55	5.27	0.02	0.12	0.32	-0.01	0.03	-0.04	99.79

Sample			Distance (μm)	SiO_2	Al_2O_3	CaO	Na_2O	MgO	K_2O	FeO	MnO	TiO_2	P_2O_5	Total
PL_H6Oct_IV, Un	39	MT2E_PL_H6Oct_IV_Mg_01	0	53.02	29.59	12.70	3.77	0.11	0.21	0.69	-0.00	0.05	-0.02	100.11
PL_H6Oct_IV, Un	39	MT2E_PL_H6Oct_IV_Mg_02	1	52.88	29.53	12.94	3.86	0.09	0.18	0.64	-0.00	0.04	-0.03	100.13
PL_H6Oct_IV, Un	39	MT2E_PL_H6Oct_IV_Mg_03	2	52.94	29.65	12.89	3.73	0.09	0.15	0.68	-0.00	0.05	-0.03	100.14
PL_H6Oct_IV, Un	39	MT2E_PL_H6Oct_IV_Mg_04	3	51.60	29.99	13.57	3.53	0.09	0.09	0.67	0.00	0.04	-0.04	99.54
PL_H6Oct_IV, Un	39	MT2E_PL_H6Oct_IV_Mg_05	4	51.34	30.73	14.11	3.10	0.08	0.08	0.70	0.01	0.04	-0.04	100.15
PL_H6Oct_IV, Un	39	MT2E_PL_H6Oct_IV_Mg_06	5	50.57	31.01	14.78	2.73	0.07	0.06	0.69	0.01	0.03	-0.04	99.91
PL_H6Oct_IV, Un	39	MT2E_PL_H6Oct_IV_Mg_07	6	49.97	31.27	15.29	2.57	0.07	0.05	0.67	0.00	0.03	-0.04	99.88
PL_H6Oct_IV, Un	39	MT2E_PL_H6Oct_IV_Mg_08	7	49.80	31.32	15.21	2.48	0.06	0.05	0.68	0.00	0.03	-0.04	99.59
PL_H6Oct_IV, Un	39	MT2E_PL_H6Oct_IV_Mg_09	8	49.80	31.51	15.06	2.45	0.04	0.05	0.64	-0.00	0.02	-0.04	99.54
PL_H6Oct_IV, Un	39	MT2E_PL_H6Oct_IV_Mg_10	9	50.44	31.25	14.55	2.80	0.04	0.05	0.64	0.00	0.02	-0.04	99.74
PL_H6Oct_IV, Un	39	MT2E_PL_H6Oct_IV_Mg_11	10	54.33	28.78	11.57	4.54	0.03	0.10	0.40	-0.00	0.03	-0.04	99.74
PL_H6Oct_IV, Un	39	MT2E_PL_H6Oct_IV_Mg_12	11	54.82	28.40	11.20	4.84	0.02	0.11	0.33	0.00	0.03	-0.04	99.72
PL_H6Oct_IV, Un	39	MT2E_PL_H6Oct_IV_Mg_13	12	54.90	28.41	11.20	4.69	0.02	0.11	0.35	0.00	0.02	-0.04	99.67
PL_H6Oct_IV, Un	39	MT2E_PL_H6Oct_IV_Mg_14	13	53.88	28.87	12.06	4.44	0.02	0.09	0.37	0.00	0.02	-0.04	99.70
PL_H6Oct_IV, Un	39	MT2E_PL_H6Oct_IV_Mg_15	14	55.24	27.66	10.81	5.00	0.02	0.12	0.36	0.00	0.03	-0.02	99.21
PL_H6Oct_IV, Un	39	MT2E_PL_H6Oct_IV_Mg_16	15	56.52	27.60	10.39	5.28	0.02	0.13	0.34	0.00	0.03	-0.04	100.27
PL_H6Oct_IV, Un	39	MT2E_PL_H6Oct_IV_Mg_17	16	56.64	27.48	10.28	5.24	0.02	0.13	0.34	0.00	0.03	-0.03	100.12
PL_H6Oct_IV, Un	39	MT2E_PL_H6Oct_IV_Mg_18	17	56.51	27.63	10.36	5.05	0.02	0.13	0.34	0.00	0.03	-0.03	100.03
PL_H6Oct_IV, Un	39	MT2E_PL_H6Oct_IV_Mg_19	18	56.25	27.62	10.49	5.24	0.02	0.13	0.35	0.00	0.02	-0.03	100.10
PL_H6Oct_IV, Un	39	MT2E_PL_H6Oct_IV_Mg_20	19	56.01	27.94	10.80	5.27	0.02	0.12	0.30	-0.00	0.03	-0.03	100.47
PL_H6Oct_IV, Un	39	MT2E_PL_H6Oct_IV_Mg_21	20	55.84	27.94	10.86	5.18	0.02	0.12	0.37	0.01	0.03	-0.04	100.32
PL_H6Oct_IV, Un	39	MT2E_PL_H6Oct_IV_Mg_22	21	56.00	28.01	10.81	5.22	0.01	0.12	0.32	0.00	0.03	-0.04	100.49
PL_H6Oct_IV, Un	39	MT2E_PL_H6Oct_IV_Mg_23	22	56.43	27.60	10.49	5.35	0.01	0.12	0.34	-0.00	0.03	-0.03	100.34
PL_H6Oct_IV, Un	39	MT2E_PL_H6Oct_IV_Mg_24	23	56.50	27.57	10.31	5.36	0.02	0.13	0.36	-0.00	0.03	-0.03	100.25
PL_H6Oct_IV, Un	39	MT2E_PL_H6Oct_IV_Mg_25	24	56.75	27.47	10.23	5.44	0.02	0.13	0.35	-0.00	0.03	-0.04	100.37
PL_H6Oct_IV, Un	39	MT2E_PL_H6Oct_IV_Mg_26	25	56.86	27.35	10.35	5.41	0.02	0.14	0.34	-0.00	0.03	-0.03	100.46
PL_H6Oct_IV, Un	39	MT2E_PL_H6Oct_IV_Mg_27	26	56.81	27.23	10.27	5.28	0.02	0.14	0.33	-0.00	0.03	-0.04	100.08
PL_H6Oct_IV, Un	39	MT2E_PL_H6Oct_IV_Mg_28	27	56.69	27.44	10.22	5.18	0.02	0.13	0.32	-0.00	0.03	-0.04	99.99
PL_H6Oct_IV, Un	39	MT2E_PL_H6Oct_IV_Mg_29	28	56.59	27.57	10.44	5.29	0.02	0.13	0.32	0.00	0.03	-0.04	100.35
PL_H6Oct_IV, Un	39	MT2E_PL_H6Oct_IV_Mg_30	29	56.10	27.88	10.48	5.40	0.02	0.12	0.34	0.00	0.03	-0.03	100.35
PL_H6Oct_IV, Un	39	MT2E_PL_H6Oct_IV_Mg_31	30	56.17	27.59	10.35	5.25	0.02	0.12	0.34	0.00	0.03	-0.04	99.83
PL_H6Oct_IV, Un	39	MT2E_PL_H6Oct_IV_Mg_32	31	56.19	27.81	10.50	5.37	0.02	0.12	0.34	-0.00	0.03	-0.03	100.33
PL_H6Oct_IV, Un	39	MT2E_PL_H6Oct_IV_Mg_33	32	56.25	27.55	10.41	5.14	0.02	0.12	0.33	-0.00	0.03	-0.04	99.80
PL_H6Oct_IV, Un	39	MT2E_PL_H6Oct_IV_Mg_34	33	55.98	27.45	10.58	5.18	0.01	0.13	0.32	-0.00	0.03	-0.03	99.64
PL_H6Oct_IV, Un	39	MT2E_PL_H6Oct_IV_Mg_35	34	55.77	27.77	10.63	5.20	0.02	0.12	0.34	0.00	0.03	-0.04	99.83
PL_H6Oct_IV, Un	39	MT2E_PL_H6Oct_IV_Mg_36	35	55.88	27.64	10.55	5.27	0.02	0.12	0.32	-0.01	0.03	-0.04	99.79
PL_H6Oct_IV, Un	39	MT2E_PL_H6Oct_IV_Mg_37	36	56.00	27.37	10.53	5.28	0.01	0.12	0.32	-0.00	0.02	-0.04	99.62
PL_H6Oct_IV, Un	39	MT2E_PL_H6Oct_IV_Mg_38	37	56.22	27.69	10.39	5.14	0.02	0.13	0.32	0.00	0.03	-0.03	99.91
PL_H6Oct_IV, Un	39	MT2E_PL_H6Oct_IV_Mg_39	38	55.99	27.77	10.69	5.20	0.02	0.13	0.32	0.00	0.02	-0.03	100.11

Sample	Distance (μm)	SiO_2	Al_2O_3	CaO	Na_2O	MgO	K_2O	FeO	MnO	TiO_2	P_2O_5	Total
PL_7-10_En_I_zoom_01	0	51.06	30.96	14.67	3.01	0.19	0.05	0.61	0.01	0.05	-0.04	100.58
PL_7-10_En_I_zoom_02	1	50.89	30.82	14.26	3.09	0.07	0.04	0.56	0.00	0.03	-0.03	99.74
PL_7-10_En_I_zoom_03	2	51.55	30.77	14.01	3.47	0.07	0.06	0.57	0.00	0.03	-0.03	100.50
PL_7-10_En_I_zoom_04	3	50.64	31.07	14.53	3.02	0.07	0.05	0.53	0.00	0.03	-0.03	99.91
PL_7-10_En_I_zoom_05	4	49.68	31.67	15.07	2.68	0.07	0.05	0.59	-0.00	0.03	-0.03	99.81
PL_7-10_En_I_zoom_06	5	50.04	31.77	15.21	2.73	0.07	0.05	0.63	0.00	0.03	-0.03	100.50
PL_7-10_En_I_zoom_07	6	49.50	31.42	15.35	2.59	0.07	0.05	0.65	-0.01	0.03	-0.04	99.61
PL_7-10_En_I_zoom_08	7	49.19	31.45	15.18	2.50	0.07	0.05	0.58	0.00	0.03	-0.04	99.01
PL_7-10_En_I_zoom_09	8	49.47	31.94	15.46	2.43	0.07	0.04	0.62	-0.01	0.04	-0.03	100.03
PL_7-10_En_I_zoom_10	9	49.64	31.64	15.60	2.45	0.08	0.05	0.68	-0.00	0.03	-0.04	100.11
PL_7-10_En_I_zoom_11	10	49.08	32.03	15.70	2.36	0.08	0.04	0.62	-0.00	0.03	-0.03	99.90
PL_7-10_En_I_zoom_12	11	49.11	32.09	15.75	2.38	0.08	0.03	0.61	-0.00	0.04	-0.03	100.05
PL_7-10_En_I_zoom_13	12	48.80	31.88	15.74	2.14	0.08	0.04	0.60	0.00	0.04	-0.04	99.29
PL_7-10_En_I_zoom_14	13	49.20	31.89	15.51	2.29	0.08	0.04	0.58	-0.01	0.04	-0.04	99.58
PL_7-10_En_I_zoom_15	14	49.01	31.85	15.65	2.36	0.09	0.04	0.61	0.00	0.03	-0.04	99.60
PL_7-10_En_I_zoom_16	15	49.05	32.20	15.88	2.42	0.09	0.04	0.57	-0.00	0.03	-0.04	100.23
PL_7-10_En_I_zoom_17	16	48.70	32.29	16.16	2.15	0.09	0.03	0.59	-0.00	0.04	-0.04	100.00
PL_7-10_En_I_zoom_18	17	48.63	32.50	16.30	1.97	0.08	0.04	0.57	-0.00	0.04	-0.03	100.09
PL_7-10_En_I_zoom_19	18	48.27	32.44	16.33	1.90	0.08	0.03	0.56	-0.01	0.04	-0.04	99.60
PL_7-10_En_I_zoom_20	19	48.14	32.55	16.35	1.91	0.08	0.03	0.53	0.00	0.04	-0.04	99.59
PL_7-10_En_I_zoom_21	20	48.71	32.41	16.24	1.95	0.09	0.03	0.55	0.01	0.04	-0.03	99.99
PL_7-10_En_I_zoom_22	21	48.17	32.73	16.35	1.91	0.09	0.03	0.56	-0.00	0.03	-0.03	99.83
PL_7-10_En_I_zoom_23	22	47.89	32.80	16.69	1.83	0.08	0.03	0.55	0.00	0.03	-0.04	99.85
PL_7-10_En_I_zoom_24	23	47.61	32.66	16.50	1.69	0.09	0.03	0.54	-0.00	0.04	-0.04	99.12
PL_7-10_En_I_zoom_25	24	47.41	33.01	16.72	1.67	0.09	0.04	0.52	-0.00	0.04	-0.04	99.44
PL_7-10_En_I_zoom_26	25	47.81	33.09	16.76	1.74	0.09	0.03	0.56	-0.00	0.04	-0.04	100.07
PL_7-10_En_I_zoom_27	26	47.57	33.44	17.07	1.65	0.09	0.03	0.55	-0.01	0.03	-0.03	100.40
PL_7-10_En_I_zoom_28	27	47.43	33.06	16.96	1.62	0.09	0.03	0.51	-0.01	0.03	-0.04	99.70
PL_7-10_En_I_zoom_29	28	47.22	33.12	17.19	1.58	0.09	0.02	0.53	-0.00	0.03	-0.03	99.75
PL_7-10_En_I_zoom_30	29	47.56	33.32	17.21	1.53	0.09	0.03	0.52	-0.01	0.03	-0.04	100.24
PL_7-10_En_I_zoom_31	30	47.47	33.11	17.04	1.56	0.08	0.03	0.55	-0.00	0.03	-0.04	99.83
PL_7-10_En_I_zoom_32	31	47.14	33.24	16.99	1.47	0.09	0.03	0.54	-0.01	0.04	-0.03	99.51
PL_7-10_En_I_zoom_33	32	46.95	33.47	17.27	1.42	0.09	0.03	0.53	0.00	0.03	-0.04	99.75
PL_7-10_En_I_zoom_34	33	47.16	33.39	17.20	1.47	0.08	0.02	0.53	-0.01	0.03	-0.03	99.85
PL_7-10_En_I_zoom_35	34	47.05	33.28	17.18	1.39	0.08	0.03	0.51	-0.00	0.03	-0.04	99.51
PL_7-10_En_I_zoom_36	35	47.26	33.62	17.05	1.38	0.08	0.02	0.53	-0.00	0.03	-0.03	99.94
PL_7-10_En_I_zoom_37	36	46.99	33.33	17.29	1.43	0.09	0.02	0.51	0.00	0.03	-0.04	99.66
PL_7-10_En_I_zoom_38	37	47.16	33.58	17.29	1.40	0.09	0.02	0.51	-0.01	0.03	-0.03	100.04
PL_7-10_En_I_zoom_39	38	46.96	33.56	17.43	1.44	0.08	0.03	0.50	-0.01	0.03	-0.04	99.98

Sample	Distance (μm)	SiO_2	Al_2O_3	CaO	Na_2O	MgO	K_2O	FeO	MnO	TiO_2	P_2O_5	Total
PL_7-10_En_I_zoom_40	39	46.85	33.51	17.31	1.41	0.09	0.02	0.48	0.00	0.03	-0.04	99.66
PL_7-10_En_I_zoom_41	40	47.07	33.42	17.27	1.42	0.08	0.03	0.50	0.00	0.03	-0.04	99.79
PL_7-10_En_I_zoom_42	41	46.90	33.54	17.41	1.36	0.08	0.02	0.50	-0.01	0.03	-0.04	99.79
PL_7-10_En_I_zoom_43	42	46.61	33.23	17.35	1.28	0.08	0.02	0.50	-0.00	0.03	-0.03	99.06
PL_7-10_En_I_zoom_44	43	47.10	33.46	17.35	1.48	0.08	0.02	0.48	-0.00	0.03	-0.04	99.97
PL_7-10_En_I_zoom_45	44	47.17	33.26	16.96	1.51	0.08	0.03	0.50	-0.01	0.03	-0.04	99.49
PL_7-10_En_I_zoom_46	45	47.32	33.16	16.93	1.44	0.08	0.03	0.53	-0.00	0.03	-0.03	99.48
PL_7-10_En_I_zoom_47	46	47.63	33.07	16.98	1.62	0.08	0.03	0.47	0.00	0.03	-0.04	99.88
PL_7-10_En_I_zoom_48	47	47.65	32.87	16.74	1.65	0.08	0.03	0.45	-0.01	0.03	-0.04	99.46
PL_7-10_En_I_zoom_49	48	47.11	33.57	17.10	1.51	0.08	0.02	0.46	-0.01	0.03	-0.04	99.83
PL_7-10_En_I_zoom_50	49	47.23	33.26	17.07	1.53	0.08	0.03	0.53	0.00	0.04	-0.03	99.73
PL_7-10_En_I_zoom_51	50	47.23	33.18	17.04	1.46	0.08	0.03	0.56	-0.00	0.03	-0.03	99.57
PL_7-10_En_I_zoom_52	51	47.11	33.26	17.09	1.47	0.08	0.04	0.58	-0.00	0.03	-0.04	99.61
PL_7-10_En_I_zoom_53	52	47.50	33.00	16.93	1.64	0.07	0.05	0.54	-0.00	0.03	-0.03	99.73
PL_7-10_En_I_zoom_54	53	49.32	31.44	14.89	2.50	0.07	0.06	0.43	-0.00	0.03	-0.04	98.70
PL_7-10_En_I_zoom_55	54	51.39	30.62	13.93	3.33	0.06	0.08	0.39	-0.00	0.03	-0.04	99.79
PL_7-10_En_I_zoom_56	55	51.10	30.84	13.98	3.32	0.05	0.08	0.38	-0.00	0.03	-0.03	99.74
PL_7-10_En_I_zoom_57	56	49.03	31.99	15.64	2.30	0.04	0.04	0.46	-0.00	0.02	-0.04	99.49
PL_7-10_En_I_zoom_58	57	50.55	30.99	14.41	3.22	0.03	0.06	0.37	-0.00	0.03	-0.03	99.64
PL_7-10_En_I_zoom_59	58	51.68	30.50	13.67	3.68	0.03	0.06	0.36	0.00	0.03	-0.04	99.96
PL_7-10_En_I_zoom_60	59	51.08	30.75	13.82	3.34	0.02	0.05	0.38	-0.01	0.03	-0.03	99.43
PL_7-10_En_I_zoom_61	60	50.80	31.01	14.29	3.23	0.02	0.05	0.35	0.00	0.03	-0.03	99.74
PL_7-10_En_I_zoom_62	61	50.29	31.37	14.71	2.95	0.02	0.05	0.38	-0.00	0.03	-0.04	99.76
PL_7-10_En_I_zoom_63	62	49.90	31.68	14.87	2.75	0.02	0.05	0.36	0.00	0.03	-0.03	99.63
PL_7-10_En_I_zoom_64	63	49.97	31.76	14.99	2.74	0.02	0.04	0.42	0.00	0.02	-0.03	99.94
PL_7-10_En_I_zoom_65	64	49.91	31.68	14.72	2.69	0.02	0.05	0.40	0.00	0.03	-0.04	99.45
PL_7-10_En_I_zoom_66	65	49.58	31.74	15.25	2.60	0.01	0.05	0.38	-0.00	0.03	-0.03	99.60
PL_7-10_En_I_zoom_67	66	49.81	31.55	15.03	2.65	0.01	0.05	0.39	0.00	0.03	-0.03	99.49
PL_7-10_En_I_zoom_68	67	49.89	31.55	14.96	2.88	0.01	0.06	0.38	0.00	0.03	-0.03	99.73
PL_7-10_En_I_zoom_69	68	50.00	31.48	14.72	2.86	0.02	0.06	0.36	-0.00	0.03	-0.03	99.49
PL_7-10_En_I_zoom_70	69	49.91	31.61	15.10	2.76	0.02	0.08	0.37	-0.00	0.03	-0.03	99.85
PL_7-10_En_I_zoom_71	70	50.08	31.43	14.88	2.73	0.04	0.08	0.39	-0.00	0.02	-0.04	99.61
PL_7-10_En_I_zoom_72	71	50.55	31.17	14.28	3.05	0.05	0.09	0.39	0.01	0.03	-0.04	99.59
PL_7-10_En_I_zoom_73	72	50.10	31.39	14.95	2.72	0.06	0.07	0.39	0.00	0.03	-0.03	99.69
PL_7-10_En_I_zoom_74	73	49.29	31.51	15.16	2.68	0.08	0.06	0.39	0.01	0.04	-0.03	99.18
PL_7-10_En_I_zoom_75	74	49.77	31.78	15.13	2.84	0.13	0.06	0.41	0.01	0.05	-0.03	100.14
PL_7-10_En_I_zoom_76	75	49.76	31.85	15.18	2.62	0.17	0.06	0.38	0.01	0.07	-0.03	100.07
PL_7-10_En_I_zoom_77	76	49.73	31.76	15.36	2.64	0.18	0.05	0.36	0.02	0.07	-0.03	100.14
PL_7-10_En_I_zoom_78	77	50.44	30.99	14.48	3.07	0.19	0.07	0.40	0.02	0.07	-0.03	99.70

Sample	Distance (μm)	SiO_2	Al_2O_3	CaO	Na_2O	MgO	K_2O	FeO	MnO	TiO_2	P_2O_5	Total
PL_7-10_En_I_zoom_79	78	50.43	31.35	14.69	3.04	0.22	0.07	0.42	0.02	0.09	-0.03	100.29
PL_7-10_En_I_zoom_80	79	49.61	31.76	15.19	2.40	0.24	0.08	0.49	0.03	0.11	-0.02	99.89
7-10_Plag 7_ EN_01	0	52.75	29.53	13.14	4.16	0.26	0.09	0.64	-0.00	0.05	-0.02	100.60
7-10_Plag 7_ EN_02	1	52.52	29.53	13.21	3.90	0.13	0.07	0.61	-0.01	0.05	-0.02	100.00
7-10_Plag 7_ EN_03	2	52.52	29.62	13.34	3.89	0.11	0.08	0.59	-0.01	0.05	-0.02	100.18
7-10_Plag 7_ EN_04	3	51.48	30.28	13.93	3.40	0.10	0.06	0.67	-0.00	0.05	-0.02	99.95
7-10_Plag 7_ EN_05	4	50.73	30.84	14.40	3.14	0.08	0.05	0.63	-0.00	0.05	-0.02	99.91
7-10_Plag 7_ EN_06	5	51.21	30.16	14.04	3.40	0.07	0.06	0.56	0.00	0.05	-0.03	99.52
7-10_Plag 7_ EN_07	6	51.68	30.16	13.71	3.64	0.07	0.06	0.60	-0.00	0.04	-0.03	99.93
7-10_Plag 7_ EN_08	7	51.24	30.19	13.91	3.49	0.07	0.06	0.62	-0.01	0.04	-0.02	99.60
7-10_Plag 7_ EN_09	8	51.27	30.08	14.11	3.33	0.07	0.06	0.62	-0.01	0.04	-0.03	99.53
7-10_Plag 7_ EN_10	9	50.46	30.80	14.43	3.21	0.07	0.05	0.62	0.00	0.04	-0.03	99.64
7-10_Plag 7_ EN_11	10	50.27	31.15	14.93	2.92	0.07	0.05	0.62	0.00	0.03	-0.04	100.00
7-10_Plag 7_ EN_12	11	49.82	31.29	15.08	2.84	0.07	0.05	0.65	-0.00	0.03	-0.03	99.79
7-10_Plag 7_ EN_13	12	49.93	31.18	15.07	2.82	0.07	0.05	0.63	0.00	0.04	-0.04	99.75
7-10_Plag 7_ EN_14	13	49.84	31.10	15.13	2.76	0.07	0.05	0.63	0.00	0.03	-0.04	99.57
7-10_Plag 7_ EN_15	14	49.91	31.40	15.11	2.73	0.07	0.04	0.66	-0.00	0.03	-0.04	99.90
7-10_Plag 7_ EN_16	15	49.54	31.58	15.13	2.63	0.07	0.04	0.66	-0.00	0.03	-0.03	99.64
7-10_Plag 7_ EN_17	16	49.61	31.29	15.16	2.57	0.07	0.04	0.72	0.00	0.03	-0.03	99.47
7-10_Plag 7_ EN_18	17	49.50	31.38	15.29	2.55	0.08	0.05	0.68	-0.01	0.04	-0.03	99.52
7-10_Plag 7_ EN_19	18	49.67	31.46	15.45	2.50	0.07	0.05	0.71	0.00	0.03	-0.04	99.92
7-10_Plag 7_ EN_20	19	49.01	31.46	15.70	2.52	0.07	0.05	0.70	-0.00	0.03	-0.04	99.51
7-10_Plag 7_ EN_21	20	49.12	31.59	15.72	2.57	0.08	0.03	0.67	0.00	0.03	-0.04	99.78
7-10_Plag 7_ EN_22	21	49.21	31.77	15.81	2.32	0.08	0.04	0.69	0.00	0.03	-0.04	99.91
7-10_Plag 7_ EN_23	22	48.77	31.77	15.74	2.27	0.08	0.04	0.71	-0.00	0.04	-0.04	99.36
7-10_Plag 7_ EN_24	23	48.90	32.03	15.99	2.35	0.08	0.04	0.67	-0.00	0.03	-0.04	100.06
7-10_Plag 7_ EN_25	24	48.86	31.84	16.00	2.18	0.08	0.03	0.66	-0.00	0.03	-0.04	99.65
7-10_Plag 7_ EN_26	25	48.50	31.68	15.87	2.23	0.08	0.04	0.70	0.00	0.03	-0.04	99.10
7-10_Plag 7_ EN_27	26	48.68	31.75	15.75	2.32	0.09	0.04	0.64	-0.00	0.03	-0.04	99.28
7-10_Plag 7_ EN_28	27	48.63	31.61	16.14	2.35	0.09	0.04	0.66	-0.00	0.03	-0.04	99.50
7-10_Plag 7_ EN_29	28	48.84	31.73	15.98	2.23	0.09	0.04	0.62	-0.00	0.04	-0.04	99.52
7-10_Plag 7_ EN_30	29	48.58	32.13	15.94	2.09	0.10	0.04	0.62	-0.00	0.04	-0.04	99.48
7-10_Plag 7_ EN_31	30	48.36	32.21	16.26	2.09	0.10	0.04	0.61	-0.00	0.03	-0.04	99.66
7-10_Plag 7_ EN_32	31	48.27	32.11	16.19	2.10	0.10	0.03	0.61	0.00	0.04	-0.04	99.40
7-10_Plag 7_ EN_33	32	48.46	32.21	16.15	2.02	0.10	0.04	0.63	-0.00	0.04	-0.04	99.61
7-10_Plag 7_ EN_34	33	48.06	32.33	16.57	2.02	0.10	0.03	0.60	-0.01	0.04	-0.04	99.70
7-10_Plag 7_ EN_35	34	47.85	32.33	16.55	2.03	0.10	0.03	0.60	-0.01	0.03	-0.04	99.49
7-10_Plag 7_ EN_36	35	47.74	32.57	16.36	1.94	0.09	0.04	0.56	-0.01	0.04	-0.04	99.29
7-10_Plag 7_ EN_37	36	47.97	32.36	16.55	1.97	0.09	0.03	0.62	-0.00	0.03	-0.04	99.60

Sample	Distance (μm)	SiO_2	Al_2O_3	CaO	Na_2O	MgO	K_2O	FeO	MnO	TiO_2	P_2O_5	Total
7-10_Plag 7_ EN_38	37	48.27	32.24	16.63	1.92	0.09	0.03	0.61	-0.01	0.04	-0.04	99.78
7-10_Plag 7_ EN_39	38	47.70	32.75	16.62	1.80	0.09	0.03	0.62	-0.00	0.03	-0.04	99.61
7-10_Plag 7_ EN_40	39	47.45	32.68	16.91	1.77	0.09	0.03	0.53	-0.01	0.04	-0.04	99.46
7-10_Plag 7_ EN_41	40	47.04	32.83	17.20	1.62	0.09	0.02	0.55	-0.00	0.03	-0.04	99.35
7-10_Plag 7_ EN_42	41	47.00	33.02	17.33	1.50	0.09	0.02	0.56	-0.02	0.03	-0.03	99.52
7-10_Plag 7_ EN_43	42	46.97	33.18	17.29	1.46	0.09	0.03	0.53	-0.01	0.03	-0.04	99.55
7-10_Plag 7_ EN_44	43	47.29	33.05	17.22	1.55	0.09	0.03	0.55	0.00	0.04	-0.04	99.76
7-10_Plag 7_ EN_45	44	47.39	33.05	17.01	1.64	0.10	0.03	0.56	-0.00	0.04	-0.04	99.78
7-10_Plag 7_ EN_46	45	46.91	33.11	17.43	1.51	0.09	0.02	0.51	-0.01	0.04	-0.04	99.58
7-10_Plag 7_ EN_47	46	46.83	33.42	17.36	1.51	0.10	0.02	0.55	-0.00	0.03	-0.04	99.77
7-10_Plag 7_ EN_48	47	46.67	33.33	17.40	1.40	0.10	0.02	0.52	-0.00	0.03	-0.04	99.43
7-10_Plag 7_ EN_49	48	46.93	33.37	17.31	1.48	0.10	0.03	0.50	-0.00	0.04	-0.04	99.71
7-10_Plag 7_ EN_50	49	46.83	33.39	17.41	1.44	0.09	0.02	0.48	-0.00	0.03	-0.04	99.65
7-10_Plag 7_ EN_51	50	46.86	33.49	17.67	1.40	0.09	0.03	0.52	-0.00	0.03	-0.04	100.06
7-10_Plag 7_ EN_52	51	46.59	33.45	17.54	1.31	0.09	0.02	0.55	-0.00	0.03	-0.04	99.54
7-10_Plag 7_ EN_53	52	46.42	33.32	17.58	1.30	0.09	0.02	0.46	-0.00	0.03	-0.04	99.19
7-10_Plag 7_ EN_54	53	46.42	33.50	17.55	1.41	0.09	0.02	0.51	-0.00	0.03	-0.04	99.50
7-10_Plag 7_ EN_55	54	46.49	33.51	17.81	1.39	0.09	0.02	0.49	-0.00	0.03	-0.03	99.81
7-10_Plag 7_ EN_56	55	45.80	33.63	18.10	1.11	0.09	0.02	0.52	-0.01	0.03	-0.04	99.26
7-10_Plag 7_ EN_57	56	45.84	33.79	17.92	1.03	0.09	0.02	0.53	-0.00	0.03	-0.03	99.22
7-10_Plag 7_ EN_58	57	45.84	33.76	17.95	1.07	0.09	0.02	0.54	-0.01	0.03	-0.03	99.26
7-10_Plag 7_ EN_59	58	45.59	34.00	18.06	1.01	0.09	0.02	0.48	-0.00	0.03	-0.03	99.25
7-10_Plag 7_ EN_60	59	45.66	33.88	18.24	0.92	0.09	0.02	0.48	-0.01	0.03	-0.04	99.29
7-10_Plag 7_ EN_61	60	45.50	34.14	17.93	0.96	0.09	0.01	0.48	-0.01	0.04	-0.03	99.12
7-10_Plag 7_ EN_62	61	45.54	34.09	18.27	0.88	0.09	0.01	0.48	-0.01	0.03	-0.04	99.34
7-10_Plag 7_ EN_63	62	46.11	33.75	18.16	1.03	0.08	0.02	0.51	-0.01	0.03	-0.04	99.64
7-10_Plag 7_ EN_64	63	47.99	32.47	16.70	1.89	0.08	0.03	0.56	-0.00	0.03	-0.04	99.71
7-10_Plag 7_ EN_65	64	49.24	31.50	15.49	2.63	0.08	0.05	0.58	-0.00	0.03	-0.04	99.56
7-10_Plag 7_ EN_66	65	49.24	31.49	15.53	2.48	0.08	0.04	0.59	-0.00	0.03	-0.03	99.44
7-10_Plag 7_ EN_67	66	49.42	31.59	15.65	2.50	0.08	0.04	0.55	-0.00	0.03	-0.04	99.82
7-10_Plag 7_ EN_68	67	48.15	32.08	16.00	2.13	0.08	0.04	0.60	0.01	0.03	-0.04	99.08
7-10_Plag 7_ EN_69	68	47.92	32.37	16.49	1.88	0.08	0.04	0.56	-0.00	0.03	-0.04	99.33
7-10_Plag 7_ EN_70	69	47.92	32.45	16.52	1.93	0.08	0.03	0.55	-0.01	0.03	-0.04	99.47
7-10_Plag 7_ EN_71	70	48.27	32.28	16.23	2.11	0.09	0.03	0.60	-0.00	0.04	-0.03	99.61
7-10_Plag 7_ EN_72	71	48.52	32.11	16.02	2.16	0.09	0.05	0.61	0.00	0.04	-0.04	99.56
7-10_Plag 7_ EN_73	72	48.21	32.01	16.24	2.12	0.09	0.04	0.61	-0.00	0.04	-0.04	99.32
7-10_Plag 7_ EN_74	73	47.63	32.55	16.40	1.98	0.09	0.04	0.58	-0.00	0.03	-0.03	99.26
7-10_Plag 7_ EN_75	74	47.71	32.58	16.61	1.91	0.08	0.03	0.61	-0.00	0.03	-0.03	99.52
7-10_Plag 7_ EN_76	75	47.72	32.52	16.80	1.90	0.09	0.03	0.56	-0.00	0.03	-0.04	99.62

Sample	Distance (μm)	SiO_2	Al_2O_3	CaO	Na_2O	MgO	K_2O	FeO	MnO	TiO_2	P_2O_5	Total
7-10_Plag 7_ EN_77	76	47.40	32.56	16.74	1.80	0.09	0.03	0.55	-0.00	0.03	-0.03	99.16
7-10_Plag 7_ EN_78	77	47.35	32.78	16.96	1.66	0.08	0.03	0.56	0.00	0.03	-0.04	99.42
7-10_Plag 7_ EN_79	78	47.22	32.84	16.90	1.77	0.08	0.03	0.58	0.00	0.04	-0.04	99.42
7-10_Plag 7_ EN_80	79	47.20	32.96	17.01	1.65	0.07	0.03	0.59	0.00	0.04	-0.04	99.52
7-10_Plag 7_ EN_81	80	47.15	32.99	17.23	1.58	0.07	0.02	0.55	-0.00	0.03	-0.03	99.60
7-10_Plag 7_ EN_82	81	46.93	32.94	17.12	1.64	0.07	0.03	0.58	-0.00	0.03	-0.04	99.30
7-10_Plag 7_ EN_83	82	47.22	33.20	17.11	1.65	0.07	0.03	0.62	0.00	0.03	-0.04	99.89
7-10_Plag 7_ EN_84	83	46.74	32.93	17.25	1.63	0.07	0.04	0.56	-0.00	0.04	-0.04	99.22
7-10_Plag 7_ EN_85	84	46.76	32.89	17.14	1.58	0.07	0.03	0.56	-0.00	0.03	-0.04	99.02
7-10_Plag 7_ EN_86	85	46.89	33.39	17.16	1.49	0.07	0.03	0.58	-0.00	0.03	-0.03	99.60
7-10_Plag 7_ EN_87	86	47.02	32.98	17.19	1.56	0.06	0.03	0.60	-0.00	0.03	-0.03	99.45
7-10_Plag 7_ EN_88	87	46.98	33.18	17.15	1.50	0.06	0.03	0.55	0.00	0.03	-0.03	99.45
7-10_Plag 7_ EN_89	88	47.29	32.93	16.98	1.60	0.06	0.04	0.54	-0.00	0.03	-0.03	99.44
7-10_Plag 7_ EN_90	89	47.73	32.54	16.59	1.85	0.06	0.07	0.57	-0.00	0.03	-0.03	99.41
7-10_Plag 7_ EN_91	90	48.54	32.06	16.40	1.83	0.06	0.10	0.57	-0.01	0.03	-0.04	99.55
7-10_Plag 7_ EN_92	91	49.21	31.52	15.98	2.02	0.06	0.16	0.74	-0.00	0.04	-0.04	99.69
7-10_Plag 7_ EN_93	92	47.49	32.58	16.84	1.72	0.05	0.08	0.64	0.00	0.03	-0.03	99.42
7-10_Plag 8_ EN_01	0	51.65	29.62	13.49	3.79	-0.05	0.10	0.65	-0.07	-0.11	-0.06	99.01
7-10_Plag 8_ EN_02	1	51.62	30.05	13.69	3.59	-0.04	0.08	0.62	-0.06	-0.08	-0.06	99.42
7-10_Plag 8_ EN_03	2	52.10	29.74	13.32	3.83	-0.02	0.08	0.56	-0.05	-0.06	-0.05	99.46
7-10_Plag 8_ EN_04	3	51.87	29.80	13.33	3.86	0.00	0.08	0.55	-0.03	-0.03	-0.05	99.37
7-10_Plag 8_ EN_05	4	51.25	29.97	13.47	3.64	0.02	0.07	0.54	-0.02	-0.00	-0.05	98.89
7-10_Plag 8_ EN_06	5	50.93	30.42	14.06	3.41	0.03	0.06	0.54	-0.01	0.02	-0.04	99.41
7-10_Plag 8_ EN_07	6	50.61	30.65	14.39	3.26	0.05	0.05	0.57	-0.01	0.03	-0.04	99.57
7-10_Plag 8_ EN_08	7	49.80	31.02	14.93	2.89	0.06	0.04	0.61	-0.00	0.04	-0.03	99.37
7-10_Plag 8_ EN_09	8	50.19	30.96	14.88	3.01	0.07	0.05	0.52	-0.01	0.04	-0.03	99.67
7-10_Plag 8_ EN_10	9	50.54	30.74	14.49	3.23	0.06	0.05	0.51	-0.00	0.04	-0.03	99.62
7-10_Plag 8_ EN_11	10	50.39	30.79	14.45	3.11	0.06	0.05	0.48	0.00	0.03	-0.03	99.33
7-10_Plag 8_ EN_12	11	50.47	31.15	14.79	3.33	0.06	0.05	0.52	-0.00	0.03	-0.03	100.36
7-10_Plag 8_ EN_13	12	50.45	30.73	14.46	3.15	0.06	0.05	0.51	0.00	0.03	-0.04	99.40
7-10_Plag 8_ EN_14	13	50.24	30.96	14.51	2.98	0.06	0.04	0.56	0.00	0.03	-0.03	99.35
7-10_Plag 8_ EN_15	14	49.74	31.28	15.13	2.97	0.06	0.04	0.61	0.01	0.03	-0.04	99.84
7-10_Plag 8_ EN_16	15	49.04	31.73	15.60	2.65	0.06	0.04	0.57	0.00	0.03	-0.03	99.69
7-10_Plag 8_ EN_17	16	48.74	31.77	15.81	2.44	0.06	0.03	0.58	-0.00	0.03	-0.03	99.42
7-10_Plag 8_ EN_18	17	49.20	32.08	15.82	2.49	0.06	0.04	0.58	-0.00	0.03	-0.04	100.24
7-10_Plag 8_ EN_19	18	48.91	31.87	15.73	2.49	0.06	0.03	0.57	0.00	0.03	-0.03	99.67
7-10_Plag 8_ EN_20	19	49.27	31.67	15.76	2.42	0.06	0.04	0.59	-0.00	0.03	-0.04	99.81
7-10_Plag 8_ EN_21	20	48.72	32.01	15.81	2.45	0.06	0.04	0.61	0.00	0.03	-0.04	99.69
7-10_Plag 8_ EN_22	21	48.48	31.86	15.81	2.38	0.06	0.03	0.65	-0.00	0.03	-0.03	99.27

Sample	Distance (μm)	SiO_2	Al_2O_3	CaO	Na_2O	MgO	K_2O	FeO	MnO	TiO_2	P_2O_5	Total
7-10_Plag 8_ EN_23	22	48.91	31.92	15.90	2.35	0.07	0.04	0.69	-0.00	0.03	-0.03	99.88
7-10_Plag 8_ EN_24	23	48.79	31.99	15.82	2.23	0.06	0.03	0.62	-0.00	0.03	-0.04	99.55
7-10_Plag 8_ EN_25	24	48.72	31.91	16.02	2.34	0.07	0.04	0.64	-0.00	0.03	-0.03	99.74
7-10_Plag 8_ EN_26	25	48.44	31.87	16.06	2.32	0.07	0.04	0.62	-0.01	0.03	-0.03	99.40
7-10_Plag 8_ EN_27	26	48.32	31.93	16.05	2.23	0.07	0.05	0.64	0.01	0.03	-0.04	99.28
7-10_Plag 8_ EN_28	27	48.71	32.02	16.12	2.33	0.07	0.03	0.66	0.00	0.03	-0.04	99.94
7-10_Plag 8_ EN_29	28	48.38	32.16	15.90	2.30	0.08	0.04	0.59	0.00	0.03	-0.04	99.44
7-10_Plag 8_ EN_30	29	48.40	32.07	16.26	2.15	0.07	0.03	0.61	0.00	0.03	-0.04	99.59
7-10_Plag 8_ EN_31	30	48.33	32.37	16.35	2.25	0.08	0.04	0.56	-0.00	0.03	-0.04	99.97
7-10_Plag 8_ EN_32	31	47.97	32.20	16.36	2.14	0.08	0.04	0.63	-0.00	0.04	-0.03	99.41
7-10_Plag 8_ EN_33	32	48.08	32.18	16.22	2.12	0.08	0.04	0.59	-0.00	0.03	-0.04	99.29
7-10_Plag 8_ EN_34	33	48.49	32.03	16.11	2.32	0.08	0.04	0.65	0.00	0.04	-0.03	99.72
7-10_Plag 8_ EN_35	34	48.47	32.05	16.05	2.34	0.08	0.03	0.58	-0.00	0.03	-0.03	99.60
7-10_Plag 8_ EN_36	35	48.33	32.01	15.99	2.47	0.09	0.04	0.60	-0.01	0.03	-0.03	99.52
7-10_Plag 8_ EN_37	36	47.97	32.33	16.10	2.19	0.09	0.04	0.59	0.00	0.03	-0.03	99.31
7-10_Plag 8_ EN_38	37	48.50	32.21	16.18	2.21	0.09	0.04	0.54	-0.00	0.04	-0.04	99.78
7-10_Plag 8_ EN_39	38	48.19	32.21	16.12	2.24	0.09	0.04	0.57	0.00	0.03	-0.03	99.47
7-10_Plag 8_ EN_40	39	47.90	32.42	16.37	2.08	0.09	0.03	0.55	-0.01	0.03	-0.04	99.43
7-10_Plag 8_ EN_41	40	48.00	32.28	16.48	1.98	0.09	0.03	0.54	0.01	0.04	-0.04	99.40
7-10_Plag 8_ EN_42	41	47.92	32.48	16.41	2.10	0.09	0.04	0.58	-0.00	0.03	-0.04	99.62
7-10_Plag 8_ EN_43	42	48.39	32.78	16.56	2.03	0.09	0.03	0.56	-0.00	0.04	-0.03	100.45
7-10_Plag 8_ EN_44	43	48.05	32.39	16.54	1.96	0.09	0.03	0.53	-0.00	0.03	-0.04	99.58
7-10_Plag 8_ EN_45	44	47.66	32.48	16.58	2.08	0.09	0.03	0.55	0.00	0.04	-0.03	99.48
7-10_Plag 8_ EN_46	45	47.86	32.73	16.76	1.98	0.09	0.03	0.59	-0.00	0.03	-0.04	100.04
7-10_Plag 8_ EN_47	46	47.82	32.38	16.61	1.95	0.09	0.03	0.55	0.00	0.03	-0.03	99.44
7-10_Plag 8_ EN_48	47	48.02	32.50	16.44	2.02	0.09	0.04	0.51	-0.00	0.03	-0.04	99.60
7-10_Plag 8_ EN_49	48	47.56	32.51	16.54	1.93	0.09	0.03	0.51	-0.00	0.03	-0.04	99.15
7-10_Plag 8_ EN_50	49	47.28	32.80	16.83	1.71	0.09	0.03	0.54	-0.01	0.03	-0.04	99.26
7-10_Plag 8_ EN_51	50	47.04	33.06	17.13	1.66	0.08	0.02	0.52	0.00	0.04	-0.04	99.51
7-10_Plag 8_ EN_52	51	47.08	33.30	17.30	1.55	0.08	0.02	0.51	-0.00	0.04	-0.03	99.84
7-10_Plag 8_ EN_53	52	46.85	32.88	17.29	1.56	0.08	0.02	0.52	-0.01	0.03	-0.03	99.21
7-10_Plag 8_ EN_54	53	47.00	33.16	17.17	1.55	0.08	0.02	0.53	-0.00	0.03	-0.04	99.51
7-10_Plag 8_ EN_55	54	46.90	33.23	17.35	1.64	0.09	0.02	0.47	0.00	0.03	-0.04	99.68
7-10_Plag 8_ EN_56	55	46.74	33.39	17.45	1.49	0.08	0.02	0.49	0.00	0.03	-0.04	99.67
7-10_Plag 8_ EN_57	56	46.86	33.05	17.17	1.57	0.08	0.02	0.51	-0.00	0.03	-0.04	99.25
7-10_Plag 8_ EN_58	57	46.95	33.15	17.50	1.53	0.08	0.02	0.51	-0.01	0.04	-0.05	99.73
7-10_Plag 8_ EN_59	58	47.13	33.38	17.45	1.47	0.08	0.03	0.52	-0.01	0.03	-0.04	100.03
7-10_Plag 8_ EN_60	59	46.91	33.19	17.40	1.45	0.08	0.03	0.49	-0.01	0.03	-0.04	99.54
7-10_Plag 8_ EN_61	60	46.75	33.46	17.32	1.54	0.08	0.02	0.50	-0.00	0.03	-0.04	99.65

Sample	Distance (μm)	SiO_2	Al_2O_3	CaO	Na_2O	MgO	K_2O	FeO	MnO	TiO_2	P_2O_5	Total
7-10_Plag 8_ EN_62	61	46.81	33.29	17.45	1.42	0.08	0.03	0.47	-0.00	0.03	-0.04	99.54
7-10_Plag 8_ EN_63	62	46.74	33.27	17.49	1.54	0.08	0.02	0.49	-0.00	0.03	-0.05	99.60
7-10_Plag 8_ EN_64	63	46.60	33.41	17.11	1.50	0.08	0.02	0.49	-0.00	0.03	-0.04	99.22
7-10_Plag 8_ EN_65	64	47.00	33.38	17.32	1.60	0.08	0.03	0.47	-0.00	0.03	-0.04	99.87
7-10_Plag 8_ EN_66	65	46.68	33.26	17.23	1.60	0.08	0.03	0.46	-0.00	0.04	-0.04	99.32
7-10_Plag 8_ EN_67	66	46.91	33.16	17.39	1.45	0.08	0.03	0.46	-0.00	0.04	-0.03	99.48
7-10_Plag 8_ EN_68	67	46.86	33.44	17.37	1.44	0.08	0.03	0.45	-0.01	0.03	-0.04	99.66
7-10_Plag 8_ EN_69	68	46.87	33.27	17.53	1.44	0.08	0.02	0.46	0.00	0.03	-0.03	99.67
7-10_Plag 8_ EN_70	69	46.66	33.37	17.25	1.55	0.08	0.02	0.44	0.00	0.03	-0.04	99.36
7-10_Plag 8_ EN_71	70	46.73	33.34	17.73	1.41	0.08	0.02	0.48	-0.00	0.03	-0.04	99.79
7-10_Plag 8_ EN_72	71	46.01	33.47	17.73	1.27	0.08	0.02	0.46	-0.01	0.03	-0.03	99.03
7-10_Plag 8_ EN_73	72	46.23	33.77	17.94	1.06	0.08	0.02	0.46	-0.00	0.03	-0.03	99.55
7-10_Plag 8_ EN_74	73	45.78	33.86	18.11	1.07	0.07	0.02	0.47	-0.00	0.03	-0.03	99.39
7-10_Plag 8_ EN_75	74	46.18	33.58	17.72	1.30	0.07	0.02	0.45	0.00	0.03	-0.04	99.30
7-10_Plag 8_ EN_76	75	47.06	33.72	17.76	1.34	0.07	0.05	0.47	0.00	0.03	-0.03	100.47
7-10_Plag 8_ EN_77	76	49.43	31.97	15.80	2.22	0.07	0.14	0.53	0.00	0.03	-0.03	100.15
7-10_Plag 8_ EN_78	77	49.93	31.13	16.03	1.76	0.06	0.33	0.76	-0.00	0.03	-0.03	100.00
7-10_Plag 8_ EN_79	78	55.04	27.36	13.30	2.14	0.08	0.96	1.32	0.00	0.05	-0.03	100.20
7-10_Plag 8_ EN_80	79	51.64	29.57	15.03	1.96	0.10	0.59	0.94	0.01	0.07	-0.03	99.87
7-10_Plag 8_ EN_81	80	47.70	32.80	16.90	1.63	0.13	0.14	0.54	0.01	0.09	-0.03	99.91
7-10_Plag 8_ EN_82	81	47.88	32.70	16.90	1.59	0.16	0.11	0.53	0.01	0.12	-0.02	99.96
7-10_Plag 8_ EN_83	82	47.70	32.68	16.90	1.75	0.17	0.12	0.51	0.01	0.13	-0.03	99.95
7-10_Plag 8_ EN_84	83	47.82	32.94	17.08	1.63	0.19	0.08	0.49	0.01	0.15	-0.02	100.37
7-10_Plag 8_ EN_85	84	49.80	30.76	14.60	2.93	0.20	0.14	0.53	0.02	0.15	-0.01	99.12
7-10_Plag 8_ EN_86	85	49.64	30.93	14.52	2.98	0.20	0.12	0.52	0.02	0.16	-0.03	99.07
7-10_Plag 8_ EN_87	86	48.09	32.35	16.43	1.82	0.16	0.10	0.46	0.01	0.13	-0.02	99.55
7-10_Plag 8_ EN_88	87	55.05	28.09	13.19	3.10	0.16	0.65	0.92	0.01	0.13	-0.02	101.29
7-10_Plag 8_ EN_89	88	52.44	29.15	14.36	2.03	0.18	0.66	0.91	0.01	0.15	-0.02	99.87
7-10_Plag 8_ EN_90	89	50.74	30.15	14.99	2.02	0.20	0.45	0.70	0.02	0.16	-0.02	99.41
7-10_Plag 8_ EN_91	90	48.39	32.04	16.12	1.92	0.22	0.19	0.53	0.01	0.18	-0.02	99.59
7-10_Plag 8_ EN_92	91	47.91	32.30	16.49	1.89	0.22	0.14	0.50	0.02	0.18	-0.01	99.64
7-10_Plag 8_ EN_93	92	49.50	31.43	15.94	1.89	0.22	0.28	0.64	0.02	0.17	-0.01	100.09
7-10_Plag 8_ EN_94	93	54.38	27.66	12.69	2.58	0.23	0.80	0.96	0.01	0.19	-0.01	99.49
7-10_Plag 8_ EN_95	94	54.65	27.27	12.10	2.89	0.22	0.73	0.93	0.02	0.17	-0.01	98.98
7-10_Plag 8_ EN_96	95	52.20	29.44	13.99	2.68	0.21	0.41	0.70	0.02	0.16	-0.02	99.79
7-10_Plag 8_ EN_97	96	53.60	28.82	12.89	3.86	0.19	0.42	0.71	0.02	0.14	-0.01	100.63
7-10_Plag 8_ EN_98	97	50.38	30.53	15.01	2.70	0.16	0.34	0.65	0.01	0.13	-0.02	99.89
7-10_Plag 8_ EN_99	98	49.60	31.16	15.85	1.94	0.16	0.32	0.62	0.01	0.12	-0.03	99.75
7-10_Plag 8_ EN_100	99	47.71	32.40	16.63	1.84	0.14	0.12	0.49	0.01	0.11	-0.02	99.43

Sample	Distance (μm)	SiO_2	Al_2O_3	CaO	Na_2O	MgO	K_2O	FeO	MnO	TiO_2	P_2O_5	Total
7-10_Plag 8_ EN_101	100	49.88	31.52	15.73	2.01	0.13	0.28	0.52	0.01	0.11	-0.03	100.15
7-10_Plag 8_ EN_102	101	55.06	27.86	12.69	2.52	0.12	0.82	0.97	0.01	0.10	-0.03	100.12
7-10_Plag 8_ EN_103	102	48.13	32.26	16.35	1.99	0.11	0.12	0.49	0.01	0.10	-0.02	99.53
7-10_Plag 8_ EN_104	103	47.99	32.75	16.62	1.92	0.11	0.09	0.45	0.01	0.10	-0.03	100.01
7-10_Plag 8_ EN_105	104	48.03	32.29	16.37	1.90	0.10	0.13	0.47	0.01	0.09	-0.03	99.37
7-10_Plag 8_ EN_106	105	51.63	30.40	15.32	2.09	0.10	0.41	0.60	0.01	0.09	-0.03	100.62
7-10_Plag 8_ EN_107	106	50.72	31.11	15.44	2.21	0.09	0.28	0.53	0.00	0.09	-0.03	100.45
7-10_Plag 8_ EN_108	107	50.58	31.14	15.49	2.13	0.09	0.31	0.53	0.01	0.09	-0.03	100.34
7-10_Plag 8_ EN_109	108	51.79	30.40	14.98	2.27	0.10	0.38	0.57	0.01	0.11	-0.02	100.59
7-10_Plag 8_ EN_110	109	54.32	28.52	13.64	2.40	0.11	0.71	0.78	0.00	0.12	-0.02	100.57
7-10_Plag 8_ EN_111	110	50.77	30.94	15.63	2.11	0.12	0.32	0.54	0.01	0.16	-0.01	100.59
7-10_Plag 8_ EN_112	111	50.34	30.95	15.38	2.16	0.13	0.33	0.57	0.01	0.18	-0.01	100.03
7-10_Plag 8_ EN_113	112	49.61	31.24	15.73	2.30	0.14	0.26	0.53	0.01	0.21	-0.01	100.01
7-10_Plag 8_ EN_114	113	50.26	30.80	14.94	2.88	0.15	0.23	0.56	0.01	0.21	-0.01	100.03
7-10_Plag 8_ EN_115	114	51.01	30.64	14.97	2.65	0.13	0.33	0.58	0.01	0.21	-0.01	100.52
7-10_Plag 8_ EN_116	115	49.43	30.85	15.60	2.12	0.12	0.29	0.64	0.01	0.19	-0.02	99.23
7-10_Plag 8_ EN_117	116	48.42	31.40	15.94	2.25	0.11	0.16	0.49	0.01	0.18	-0.01	98.93
7-10_Plag 8_ EN_118	117	53.61	28.04	12.97	2.57	0.11	0.75	0.91	-0.00	0.15	-0.02	99.09
7-10_Plag 8_ EN_119	118	53.43	28.21	13.10	2.80	0.11	0.66	0.83	0.00	0.14	-0.02	99.27
7-10_Plag 8_ EN_120	119	49.89	31.20	14.88	2.59	0.13	0.19	0.49	0.01	0.16	-0.02	99.51
7-10_Plag 8_ EN_121	120	48.96	32.03	15.73	2.28	0.13	0.12	0.49	0.01	0.16	-0.01	99.89
7-10_Plag 8_ EN_122	121	49.91	31.71	15.50	2.56	0.15	0.14	0.46	0.01	0.17	-0.01	100.59
7-10_Plag 8_ EN_123	122	53.88	28.95	13.83	2.65	0.17	0.60	0.77	0.01	0.18	-0.02	101.01
7-10_Plag 8_ EN_124	123	53.88	28.51	13.50	2.59	0.17	0.68	0.84	0.02	0.18	-0.01	100.36
7-10_Plag 8_ EN_125	124	55.52	26.63	12.27	2.51	0.18	1.00	1.10	0.02	0.18	-0.01	99.40
7-10_Plag 8_ EN_126	125	52.94	28.38	13.26	2.69	0.19	0.62	0.88	0.01	0.18	-0.01	99.16
7-10_Plag 8_ EN_127	126	50.94	30.49	14.32	2.84	0.20	0.25	0.54	0.02	0.19	-0.01	99.78
7-10_Plag 8_ EN_128	127	49.71	31.64	15.32	2.62	0.22	0.12	0.47	0.02	0.21	-0.00	100.34
7-10_Plag 8_ EN_129	128	50.05	31.31	15.17	2.79	0.23	0.13	0.46	0.02	0.20	-0.01	100.36
7-10_Plag 8_ EN_130	129	49.55	31.25	15.13	2.58	0.22	0.17	0.52	0.02	0.21	-0.01	99.63
7-10_Plag 8_ EN_131	130	49.92	31.30	15.14	2.69	0.21	0.15	0.48	0.01	0.20	-0.02	100.08

Sample	Distance (μm)	SiO_2	Al_2O_3	CaO	Na_2O	MgO	K_2O	FeO	MnO	TiO_2	P_2O_5	Total
7-10_Plag 6_EN_01	0	56.50	27.38	10.50	5.41	0.10	0.21	0.65	0.00	0.08	-0.03	100.80
7-10_Plag 6_EN_02	1	55.78	27.57	10.87	5.33	0.07	0.17	0.60	-0.00	0.08	-0.02	100.46
7-10_Plag 6_EN_03	2	54.66	28.22	11.52	4.71	0.07	0.13	0.62	-0.00	0.08	-0.02	99.97
7-10_Plag 6_EN_04	3	53.80	28.87	12.53	4.40	0.07	0.10	0.65	-0.00	0.07	-0.02	100.47
7-10_Plag 6_EN_05	4	53.21	29.28	12.70	4.05	0.08	0.09	0.63	-0.00	0.07	-0.03	100.08
7-10_Plag 6_EN_06	5	53.28	29.19	12.87	3.97	0.08	0.08	0.64	-0.00	0.07	-0.02	100.16
7-10_Plag 6_EN_07	6	52.99	29.39	12.98	4.14	0.08	0.08	0.60	-0.01	0.06	-0.03	100.28
7-10_Plag 6_EN_08	7	53.13	29.49	13.06	4.03	0.08	0.08	0.63	0.00	0.06	-0.03	100.52
7-10_Plag 6_EN_09	8	52.61	29.42	13.09	3.94	0.08	0.08	0.61	-0.00	0.05	-0.03	99.83
7-10_Plag 6_EN_10	9	52.45	29.82	13.29	3.72	0.08	0.08	0.59	-0.00	0.05	-0.03	100.04
7-10_Plag 6_EN_11	10	52.98	29.46	12.96	4.10	0.07	0.09	0.54	0.01	0.05	-0.04	100.23
7-10_Plag 6_EN_12	11	52.82	29.55	13.08	4.01	0.07	0.08	0.59	-0.01	0.05	-0.03	100.21
7-10_Plag 6_EN_13	12	52.60	29.59	13.08	3.71	0.08	0.08	0.57	-0.01	0.05	-0.03	99.70
7-10_Plag 6_EN_14	13	52.44	29.74	13.58	3.59	0.07	0.07	0.61	0.01	0.05	-0.03	100.13
7-10_Plag 6_EN_15	14	52.02	30.06	13.51	3.76	0.08	0.08	0.64	0.01	0.09	-0.00	100.25
7-10_Plag 6_EN_16	15	52.31	29.63	13.47	3.67	0.08	0.11	0.63	-0.00	0.13	0.00	100.02
7-10_Plag 6_EN_17	16	57.30	26.09	10.41	4.70	0.08	0.28	0.60	-0.00	0.20	0.01	99.67
7-10_Plag 6_EN_18	17	50.77	31.12	14.83	2.60	0.07	0.09	0.66	0.00	0.22	0.01	100.37
7-10_Plag 6_EN_19	18	49.27	31.47	15.30	2.56	0.07	0.05	0.69	-0.00	0.21	0.01	99.64
7-10_Plag 6_EN_20	19	49.36	31.56	15.32	2.43	0.07	0.06	0.68	0.00	0.19	0.01	99.69
7-10_Plag 6_EN_21	20	49.12	31.63	15.54	2.40	0.07	0.04	0.62	0.00	0.11	-0.01	99.53
7-10_Plag 6_EN_22	21	49.11	31.84	15.77	2.31	0.07	0.05	0.63	-0.01	0.07	-0.03	99.81
7-10_Plag 6_EN_23	22	48.99	31.66	15.68	2.26	0.08	0.04	0.59	0.00	0.03	-0.03	99.30
7-10_Plag 6_EN_24	23	49.29	31.70	15.53	2.35	0.08	0.05	0.61	0.00	0.04	-0.04	99.60
7-10_Plag 6_EN_25	24	48.94	31.81	15.71	2.38	0.08	0.04	0.61	-0.00	0.03	-0.04	99.56
7-10_Plag 6_EN_26	25	48.63	32.03	15.97	2.23	0.08	0.04	0.60	-0.01	0.03	-0.04	99.56
7-10_Plag 6_EN_27	26	48.57	32.06	16.05	2.08	0.07	0.04	0.61	-0.01	0.03	-0.03	99.48
7-10_Plag 6_EN_28	27	48.30	32.09	16.03	2.06	0.07	0.04	0.57	0.00	0.03	-0.04	99.15
7-10_Plag 6_EN_29	28	48.39	32.27	16.21	2.00	0.07	0.04	0.60	0.00	0.03	-0.04	99.57
7-10_Plag 6_EN_30	29	48.59	32.36	16.30	2.14	0.06	0.03	0.57	-0.00	0.03	-0.04	100.05
7-10_Plag 6_EN_31	30	49.20	31.75	15.53	2.46	0.06	0.05	0.58	0.00	0.03	-0.04	99.61
7-10_Plag 6_EN_32	31	52.42	29.67	13.04	3.90	0.05	0.09	0.39	-0.00	0.03	-0.04	99.54
7-10_Plag 6_EN_33	32	53.50	29.09	12.39	4.40	0.05	0.09	0.33	0.00	0.03	-0.03	99.85
7-10_Plag 6_EN_34	33	53.71	28.94	12.26	4.19	0.04	0.09	0.32	0.00	0.03	-0.03	99.57
7-10_Plag 6_EN_35	34	52.65	29.50	12.78	4.04	0.04	0.09	0.32	0.00	0.02	-0.03	99.41
7-10_Plag 6_EN_36	35	53.44	28.75	12.06	4.37	0.03	0.10	0.33	0.00	0.03	-0.03	99.09
7-10_Plag 6_EN_37	36	54.92	28.24	11.01	4.90	0.03	0.11	0.32	0.00	0.03	-0.03	99.53
7-10_Plag 6_EN_38	37	55.46	28.03	11.00	5.03	0.03	0.12	0.34	0.01	0.03	-0.03	100.02
7-10_Plag 6_EN_39	38	54.78	28.35	11.28	4.91	0.02	0.11	0.33	-0.00	0.03	-0.03	99.77

Sample	Distance (μm)	SiO_2	Al_2O_3	CaO	Na_2O	MgO	K_2O	FeO	MnO	TiO_2	P_2O_5	Total
7-10_Plag 6_EN_40	39	55.07	28.36	11.19	4.98	0.02	0.11	0.34	-0.00	0.03	-0.04	100.06
7-10_Plag 6_EN_41	40	55.24	28.24	11.11	4.95	0.02	0.11	0.34	0.00	0.03	-0.03	100.00
7-10_Plag 6_EN_42	41	55.71	28.07	10.90	4.91	0.02	0.12	0.34	-0.00	0.03	-0.04	100.06
7-10_Plag 6_EN_43	42	56.04	27.73	10.81	5.12	0.02	0.12	0.32	0.00	0.03	-0.04	100.14
7-10_Plag 6_EN_44	43	55.63	27.85	10.73	5.29	0.02	0.12	0.37	-0.00	0.03	-0.04	99.99
7-10_Plag 6_EN_45	44	56.22	27.69	10.71	5.27	0.02	0.12	0.33	0.00	0.03	-0.04	100.36
7-10_Plag 6_EN_46	45	55.84	28.13	10.63	5.21	0.02	0.12	0.33	-0.00	0.03	-0.04	100.27
7-10_Plag 6_EN_47	46	56.01	28.17	11.16	5.09	0.02	0.11	0.34	0.00	0.02	-0.03	100.89
7-10_Plag 6_EN_48	47	54.77	28.22	11.25	5.10	0.02	0.11	0.34	0.00	0.02	-0.04	99.79
7-10_Plag 6_EN_49	48	56.28	27.49	10.65	5.24	0.04	0.13	0.34	0.00	0.03	-0.04	100.15
7-10_Plag 6_EN_50	49	54.50	28.60	11.76	4.56	0.02	0.10	0.35	-0.00	0.03	-0.04	99.87
7-10_Plag 6_EN_51	50	54.19	28.92	11.99	4.53	0.02	0.11	0.33	0.00	0.03	-0.04	100.08
7-10_Plag 6_EN_52	51	54.78	28.38	11.45	4.82	0.02	0.12	0.31	-0.00	0.02	-0.04	99.86
7-10_Plag 6_EN_53	52	55.17	28.00	11.29	5.01	0.02	0.11	0.35	-0.00	0.03	-0.04	99.93
7-10_Plag 6_EN_54	53	55.00	28.51	11.24	5.02	0.02	0.11	0.33	0.00	0.03	-0.04	100.21
7-10_Plag 6_EN_55	54	54.82	28.58	11.47	4.81	0.02	0.11	0.32	0.00	0.03	-0.04	100.11
7-10_Plag 6_EN_56	55	54.78	28.55	11.52	4.84	0.02	0.11	0.33	-0.00	0.03	-0.03	100.13
7-10_Plag 6_EN_57	56	54.58	28.63	11.85	4.70	0.02	0.09	0.35	0.00	0.03	-0.04	100.22
7-10_Plag 6_EN_58	57	54.37	28.87	11.97	4.43	0.02	0.11	0.37	0.00	0.03	-0.04	100.13
7-10_Plag 6_EN_59	58	53.25	28.73	12.46	4.42	0.02	0.10	0.34	-0.00	0.03	-0.01	99.32
7-10_Plag 6_EN_60	59	53.49	28.99	12.69	4.21	0.02	0.10	0.37	-0.00	0.02	0.03	99.92
7-10_Plag 6_EN_61	60	53.26	29.26	12.60	4.23	0.02	0.09	0.35	-0.00	0.03	0.07	99.92
7-10_Plag 6_EN_62	61	53.42	29.37	12.61	4.40	0.02	0.08	0.36	0.00	0.02	0.02	100.30
7-10_Plag 6_EN_63	62	53.26	29.15	12.43	4.31	0.01	0.10	0.38	-0.00	0.02	0.01	99.67
7-10_Plag 6_EN_64	63	53.36	29.24	12.47	4.18	0.02	0.09	0.35	0.00	0.03	-0.01	99.72
7-10_Plag 6_EN_65	64	53.06	29.39	12.55	4.28	0.02	0.09	0.32	0.00	0.02	-0.03	99.69
7-10_Plag 6_EN_66	65	53.19	29.47	12.61	4.22	0.02	0.09	0.32	0.00	0.03	-0.03	99.91
7-10_Plag 6_EN_67	66	53.39	29.27	12.53	4.05	0.01	0.08	0.31	0.00	0.03	-0.03	99.66
7-10_Plag 6_EN_68	67	53.68	29.27	12.39	4.39	0.02	0.09	0.35	0.00	0.02	-0.03	100.18
7-10_Plag 6_EN_69	68	53.45	29.48	12.76	4.17	0.02	0.09	0.35	-0.00	0.03	-0.03	100.30
7-10_Plag 6_EN_70	69	53.24	29.22	12.52	4.23	0.02	0.09	0.36	0.00	0.03	-0.03	99.68
7-10_Plag 6_EN_71	70	53.42	29.60	12.79	4.22	0.02	0.08	0.35	-0.00	0.02	-0.03	100.47
7-10_Plag 6_EN_72	71	52.73	29.59	12.93	4.02	0.02	0.08	0.35	-0.00	0.03	-0.03	99.71
7-10_Plag 6_EN_73	72	52.56	29.97	13.16	3.89	0.02	0.07	0.30	0.00	0.02	-0.04	99.97
7-10_Plag 6_EN_74	73	52.56	29.94	12.99	3.99	0.01	0.09	0.34	0.01	0.02	-0.04	99.91
7-10_Plag 6_EN_75	74	53.00	29.76	12.79	4.14	0.01	0.09	0.33	0.00	0.03	-0.03	100.12
7-10_Plag 6_EN_76	75	52.93	29.45	12.90	4.17	0.02	0.08	0.31	-0.00	0.03	-0.03	99.86
7-10_Plag 6_EN_77	76	52.88	29.78	12.95	4.11	0.02	0.08	0.36	0.00	0.03	-0.03	100.18
7-10_Plag 6_EN_78	77	52.48	29.81	13.22	3.92	0.02	0.08	0.33	0.00	0.03	-0.03	99.85

Sample	Distance (μm)	SiO_2	Al_2O_3	CaO	Na_2O	MgO	K_2O	FeO	MnO	TiO_2	P_2O_5	Total
7-10_Plag 6_EN_79	78	52.16	30.36	13.49	3.67	0.02	0.07	0.35	0.00	0.03	-0.03	100.12
7-10_Plag 6_EN_80	79	51.74	30.33	13.81	3.47	0.02	0.07	0.37	0.00	0.02	-0.03	99.80
7-10_Plag 6_EN_81	80	51.66	30.48	14.00	3.36	0.02	0.07	0.38	0.00	0.03	-0.04	99.96
7-10_Plag 6_EN_82	81	51.94	30.65	13.85	3.41	0.01	0.07	0.36	0.00	0.03	-0.03	100.28
7-10_Plag 6_EN_83	82	51.64	30.66	13.96	3.55	0.02	0.06	0.37	0.00	0.03	-0.04	100.25
7-10_Plag 6_EN_84	83	51.23	30.53	14.14	3.22	0.01	0.06	0.35	0.00	0.02	-0.03	99.54
7-10_Plag 6_EN_85	84	51.08	30.86	14.28	3.28	0.01	0.06	0.38	0.00	0.02	-0.04	99.94
7-10_Plag 6_EN_86	85	50.75	30.99	14.41	3.29	0.01	0.06	0.33	0.00	0.03	-0.03	99.84
7-10_Plag 6_EN_87	86	50.89	31.09	14.57	3.04	0.01	0.05	0.33	-0.00	0.03	-0.04	99.97
7-10_Plag 6_EN_88	87	51.61	31.03	14.05	3.26	0.01	0.07	0.36	0.00	0.03	-0.04	100.39
7-10_Plag 6_EN_89	88	52.64	29.87	13.08	3.96	0.02	0.09	0.33	0.00	0.03	-0.03	99.99
7-10_Plag 6_EN_90	89	55.01	28.65	11.31	4.95	0.02	0.11	0.33	-0.00	0.03	-0.04	100.36
7-10_Plag 6_EN_91	90	56.05	27.94	10.66	5.35	0.02	0.12	0.33	0.00	0.03	-0.04	100.47
7-10_Plag 6_EN_92	91	56.20	27.63	10.56	5.36	0.02	0.14	0.30	0.00	0.03	-0.03	100.20
7-10_Plag 6_EN_93	92	56.11	27.74	10.68	5.32	0.01	0.13	0.31	-0.00	0.03	-0.04	100.29
7-10_Plag 6_EN_94	93	56.05	28.04	10.81	5.16	0.02	0.12	0.29	-0.00	0.03	-0.03	100.49
7-10_Plag 6_EN_95	94	56.05	28.03	10.93	5.19	0.02	0.12	0.32	0.00	0.02	-0.03	100.65
7-10_Plag 6_EN_96	95	51.79	30.55	13.78	3.43	0.02	0.07	0.34	0.00	0.03	-0.03	99.99
7-10_Plag 6_EN_97	96	56.31	27.85	10.69	5.36	0.02	0.13	0.30	0.00	0.03	-0.04	100.66
7-10_Plag 6_EN_98	97	56.00	27.56	10.49	5.41	0.02	0.13	0.31	-0.01	0.02	-0.04	99.91
7-10_Plag 6_EN_99	98	56.17	27.72	10.35	5.37	0.02	0.12	0.31	-0.00	0.02	-0.04	100.04
7-10_Plag 6_EN_100	99	56.50	27.62	10.42	5.47	0.02	0.14	0.29	-0.00	0.02	-0.04	100.46
7-10_Plag 6_EN_101	100	56.31	27.66	10.37	5.44	0.02	0.12	0.28	0.00	0.02	-0.03	100.20
7-10_Plag 6_EN_102	101	56.42	27.61	10.46	5.47	0.01	0.13	0.31	-0.01	0.02	-0.04	100.38
7-10_Plag 6_EN_103	102	56.66	27.93	10.40	5.40	0.02	0.13	0.31	-0.00	0.03	-0.04	100.83
7-10_Plag 6_EN_104	103	56.28	27.44	10.57	5.55	0.02	0.13	0.30	-0.00	0.02	-0.04	100.27
7-10_Plag 6_EN_105	104	56.28	27.82	10.49	5.56	0.02	0.12	0.28	0.00	0.02	-0.04	100.56
7-10_Plag 6_EN_106	105	56.38	27.64	10.45	5.57	0.02	0.13	0.31	-0.00	0.02	-0.04	100.48
7-10_Plag 6_EN_107	106	56.46	27.74	10.43	5.38	0.02	0.13	0.31	0.00	0.02	-0.03	100.45
7-10_Plag 6_EN_108	107	56.51	27.54	10.39	5.53	0.02	0.14	0.32	0.00	0.02	-0.04	100.43
7-10_Plag 6_EN_109	108	56.35	27.56	10.65	5.35	0.01	0.13	0.31	0.00	0.02	-0.03	100.35
7-10_Plag 6_EN_110	109	56.46	27.58	10.35	5.60	0.02	0.13	0.30	-0.01	0.02	-0.04	100.41
7-10_Plag 6_EN_111	110	56.55	27.60	10.46	5.70	0.02	0.13	0.30	0.00	0.02	-0.04	100.74
7-10_Plag 6_EN_112	111	56.58	27.82	10.57	5.44	0.02	0.13	0.30	-0.00	0.03	-0.04	100.84
7-10_Plag 6_EN_113	112	56.53	27.75	10.52	5.49	0.02	0.14	0.26	0.00	0.02	-0.03	100.71
7-10_Plag 6_EN_114	113	56.34	27.84	10.42	5.29	0.01	0.12	0.30	0.01	0.02	-0.04	100.32
7-10_Plag 6_EN_115	114	55.93	27.48	10.74	5.37	0.02	0.12	0.30	-0.00	0.02	-0.04	99.93
7-10_Plag 6_EN_116	115	56.03	28.15	10.71	5.27	0.01	0.12	0.31	0.01	0.02	-0.03	100.60
7-10_Plag 6_EN_117	116	55.73	28.11	10.99	5.32	0.02	0.11	0.31	0.00	0.03	-0.03	100.57

Sample	Distance (μm)	SiO_2	Al_2O_3	CaO	Na_2O	MgO	K_2O	FeO	MnO	TiO_2	P_2O_5	Total
7-10_Plag 6_EN_118	117	56.13	28.11	11.00	5.21	0.02	0.11	0.34	-0.00	0.03	-0.03	100.90
7-10_Plag 6_EN_119	118	54.56	28.93	11.63	4.73	0.02	0.10	0.33	0.00	0.03	-0.04	100.29
7-10_Plag 6_EN_120	119	54.27	29.10	12.05	4.61	0.01	0.08	0.33	-0.00	0.02	-0.03	100.44
7-10_Plag 6_EN_121	120	54.13	29.11	12.24	4.37	0.01	0.09	0.30	-0.01	0.02	-0.04	100.23
7-10_Plag 6_EN_122	121	53.91	29.06	12.25	4.45	0.01	0.10	0.32	0.00	0.03	-0.03	100.08
7-10_Plag 6_EN_123	122	54.68	28.51	11.66	4.72	0.01	0.12	0.30	0.00	0.03	-0.03	100.00
7-10_Plag 6_EN_124	123	54.22	28.36	11.62	4.69	0.02	0.11	0.29	0.00	0.03	-0.03	99.31
7-10_Plag 6_EN_125	124	54.01	28.73	11.85	4.75	0.02	0.10	0.31	-0.00	0.03	-0.03	99.77
7-10_Plag 6_EN_126	125	54.43	29.46	12.18	4.52	0.02	0.10	0.33	-0.00	0.03	-0.02	101.04
7-10_Plag 6_EN_127	126	52.94	29.62	13.05	4.02	0.02	0.08	0.33	0.01	0.03	-0.03	100.07
7-10_Plag 6_EN_128	127	52.18	30.03	13.44	3.61	0.01	0.08	0.33	0.00	0.03	-0.03	99.68
7-10_Plag 6_EN_129	128	51.83	30.71	14.02	3.47	0.01	0.07	0.33	0.00	0.02	-0.04	100.44
7-10_Plag 6_EN_130	129	51.46	30.63	14.04	3.35	0.01	0.07	0.32	-0.01	0.03	-0.03	99.88
7-10_Plag 6_EN_131	130	51.30	30.84	14.05	3.28	0.01	0.06	0.31	-0.00	0.03	-0.04	99.84
7-10_Plag 6_EN_132	131	52.63	29.96	13.17	3.80	0.01	0.07	0.31	0.00	0.03	-0.04	99.96
7-10_Plag 6_EN_133	132	55.05	28.52	11.26	4.82	0.01	0.11	0.30	0.00	0.03	-0.03	100.07
7-10_Plag 6_EN_134	133	55.47	28.03	10.91	5.16	0.02	0.12	0.28	0.01	0.03	-0.04	99.98
7-10_Plag 6_EN_135	134	55.88	28.14	11.03	5.36	0.02	0.12	0.29	0.01	0.03	-0.04	100.83
7-10_Plag 6_EN_136	135	55.19	28.37	11.33	4.93	0.02	0.10	0.30	0.00	0.03	-0.04	100.23
7-10_Plag 6_EN_137	136	55.44	28.10	11.27	5.03	0.01	0.12	0.28	0.00	0.03	-0.04	100.25
7-10_Plag 6_EN_138	137	55.91	28.04	10.87	5.17	0.02	0.11	0.27	0.00	0.03	-0.04	100.38
7-10_Plag 6_EN_139	138	55.93	28.06	10.77	5.25	0.02	0.12	0.32	0.00	0.02	-0.03	100.44
7-10_Plag 6_EN_140	139	55.68	27.99	10.98	5.13	0.02	0.11	0.29	-0.00	0.03	-0.04	100.18
7-10_Plag 6_EN_141	140	55.67	28.36	11.14	4.94	0.02	0.12	0.28	0.00	0.03	-0.04	100.52
7-10_Plag 6_EN_142	141	55.22	28.20	11.42	4.90	0.01	0.11	0.29	-0.00	0.03	-0.03	100.15
7-10_Plag 6_EN_143	142	55.14	28.61	11.41	4.86	0.02	0.11	0.30	-0.00	0.03	-0.04	100.43
7-10_Plag 6_EN_144	143	54.92	28.47	11.44	5.02	0.02	0.11	0.28	0.00	0.03	-0.03	100.25
7-10_Plag 6_EN_145	144	54.98	28.49	11.41	4.75	0.01	0.10	0.30	0.00	0.02	-0.03	100.04
7-10_Plag 6_EN_146	145	54.70	28.76	11.68	4.65	0.01	0.11	0.31	-0.00	0.02	-0.04	100.21
7-10_Plag 6_EN_147	146	54.95	28.47	11.68	4.91	0.01	0.09	0.29	-0.00	0.02	-0.04	100.40
7-10_Plag 6_EN_148	147	55.40	28.28	11.34	5.08	0.02	0.11	0.28	0.00	0.02	-0.04	100.49
7-10_Plag 6_EN_149	148	55.46	28.27	11.13	5.03	0.01	0.12	0.29	0.00	0.02	-0.04	100.31
7-10_Plag 6_EN_150	149	56.04	28.13	11.03	5.01	0.01	0.11	0.32	0.00	0.02	-0.03	100.65
7-10_Plag 6_EN_151	150	55.69	28.00	10.88	5.12	0.02	0.12	0.28	0.00	0.03	-0.04	100.09
7-10_Plag 6_EN_152	151	55.90	27.82	10.99	5.21	0.02	0.12	0.28	-0.00	0.02	-0.03	100.33
7-10_Plag 6_EN_153	152	56.09	28.08	10.98	5.32	0.02	0.11	0.29	-0.00	0.02	-0.03	100.89
7-10_Plag 6_EN_154	153	55.48	28.39	11.06	5.12	0.02	0.11	0.29	-0.00	0.03	-0.04	100.44
7-10_Plag 6_EN_155	154	54.80	28.79	11.64	4.61	0.01	0.10	0.28	0.00	0.03	-0.04	100.23
7-10_Plag 6_EN_156	155	53.29	29.45	12.64	4.16	0.02	0.09	0.30	-0.00	0.03	-0.04	99.93

Sample	Distance (μm)	SiO_2	Al_2O_3	CaO	Na_2O	MgO	K_2O	FeO	MnO	TiO_2	P_2O_5	Total
7-10_Plag 6_EN_157	156	53.75	29.24	12.43	4.23	0.01	0.09	0.31	-0.00	0.02	-0.03	100.05
7-10_Plag 6_EN_158	157	54.85	28.67	11.54	4.80	0.02	0.10	0.32	-0.00	0.02	-0.04	100.29
7-10_Plag 6_EN_159	158	55.65	27.97	11.07	5.10	0.02	0.11	0.31	0.00	0.03	-0.04	100.22
7-10_Plag 6_EN_160	159	55.69	28.15	11.05	5.19	0.02	0.11	0.29	-0.00	0.03	-0.03	100.50
7-10_Plag 6_EN_161	160	55.21	28.46	11.60	4.92	0.02	0.10	0.29	0.00	0.03	-0.03	100.61
7-10_Plag 6_EN_162	161	54.32	28.94	12.06	4.62	0.02	0.10	0.32	-0.00	0.03	-0.03	100.36
7-10_Plag 6_EN_163	162	55.24	28.44	11.36	5.00	0.01	0.11	0.28	0.01	0.02	-0.04	100.45
7-10_Plag 6_EN_164	163	55.19	28.18	10.99	5.14	0.02	0.12	0.30	0.00	0.03	-0.04	99.92
7-10_Plag 6_EN_165	164	55.44	28.11	11.01	5.18	0.02	0.10	0.32	-0.00	0.02	-0.03	100.16
7-10_Plag 6_EN_166	165	55.31	28.26	11.17	4.84	0.02	0.12	0.29	-0.00	0.02	-0.04	99.98
7-10_Plag 6_EN_167	166	54.78	28.60	11.76	4.88	0.01	0.10	0.31	-0.00	0.02	-0.03	100.44
7-10_Plag 6_EN_168	167	53.71	29.48	12.54	4.21	0.01	0.08	0.31	0.00	0.02	-0.03	100.34
7-10_Plag 6_EN_169	168	52.57	30.26	13.33	4.04	0.01	0.08	0.33	-0.01	0.02	-0.03	100.61
7-10_Plag 6_EN_170	169	54.25	28.82	11.97	4.59	0.02	0.10	0.30	-0.00	0.02	-0.04	100.02
7-10_Plag 6_EN_171	170	55.10	28.19	11.22	5.15	0.02	0.11	0.32	0.00	0.02	-0.03	100.09
7-10_Plag 6_EN_172	171	55.53	28.41	11.08	5.21	0.02	0.12	0.28	-0.00	0.03	-0.04	100.62
7-10_Plag 6_EN_173	172	55.55	28.35	11.13	5.02	0.02	0.11	0.28	-0.00	0.02	-0.03	100.46
7-10_Plag 6_EN_174	173	55.44	28.44	11.42	5.02	0.02	0.11	0.28	0.00	0.03	-0.03	100.72
7-10_Plag 6_EN_175	174	55.21	28.32	11.30	5.09	0.02	0.11	0.29	-0.00	0.02	-0.04	100.33
7-10_Plag 6_EN_176	175	55.09	28.47	11.48	5.07	0.01	0.11	0.27	-0.00	0.02	-0.03	100.50
7-10_Plag 6_EN_177	176	55.70	28.03	11.11	5.09	0.01	0.12	0.31	0.00	0.03	-0.03	100.38
7-10_Plag 6_EN_178	177	55.81	28.15	10.95	5.19	0.01	0.11	0.28	-0.00	0.02	-0.04	100.49
7-10_Plag 6_EN_179	178	55.77	27.97	10.82	5.16	0.01	0.11	0.24	0.00	0.03	-0.03	100.08
7-10_Plag 6_EN_180	179	55.85	27.90	10.71	5.30	0.02	0.12	0.26	-0.00	0.02	-0.03	100.14
7-10_Plag 6_EN_181	180	55.89	28.27	11.02	5.11	0.01	0.11	0.29	0.00	0.02	-0.04	100.68
7-10_Plag 6_EN_182	181	55.45	28.16	11.10	5.10	0.02	0.11	0.27	0.00	0.03	-0.04	100.20
7-10_Plag 6_EN_183	182	55.13	28.25	11.26	5.06	0.02	0.11	0.27	0.00	0.02	-0.04	100.09
7-10_Plag 6_EN_184	183	55.39	28.53	11.37	4.84	0.01	0.12	0.29	0.00	0.03	-0.04	100.55
7-10_Plag 6_EN_185	184	54.61	28.76	11.78	4.91	0.02	0.11	0.30	0.00	0.02	-0.03	100.48
7-10_Plag 6_EN_186	185	54.58	28.93	11.73	4.59	0.02	0.10	0.27	-0.00	0.02	-0.03	100.21
7-10_Plag 6_EN_187	186	54.44	28.67	11.81	4.55	0.02	0.10	0.31	0.01	0.02	-0.03	99.90
7-10_Plag 6_EN_188	187	54.50	28.92	11.69	4.78	0.01	0.10	0.27	0.00	0.02	-0.04	100.27
7-10_Plag 6_EN_189	188	55.03	28.83	11.72	4.93	0.02	0.10	0.30	0.01	0.02	-0.03	100.92
7-10_Plag 6_EN_190	189	54.62	28.80	11.87	4.70	0.02	0.10	0.27	-0.00	0.03	-0.04	100.36
7-10_Plag 6_EN_191	190	54.27	28.98	12.19	4.48	0.01	0.09	0.33	-0.00	0.03	-0.03	100.35
7-10_Plag 6_EN_192	191	53.75	29.47	12.30	4.44	0.01	0.10	0.29	0.00	0.02	-0.03	100.36
7-10_Plag 6_EN_193	192	53.68	29.36	12.55	4.32	0.01	0.09	0.28	-0.01	0.02	-0.04	100.28
7-10_Plag 6_EN_194	193	53.91	29.41	12.30	4.45	0.01	0.09	0.29	-0.00	0.02	-0.04	100.44
7-10_Plag 6_EN_195	194	53.37	29.75	12.81	4.19	0.01	0.08	0.28	-0.00	0.02	-0.03	100.49

Sample	Distance (μm)	SiO_2	Al_2O_3	CaO	Na_2O	MgO	K_2O	FeO	MnO	TiO_2	P_2O_5	Total
7-10_Plag 6_EN_196	195	53.29	29.66	12.73	4.09	0.01	0.08	0.31	0.01	0.02	-0.03	100.18
7-10_Plag 6_EN_197	196	53.10	29.63	12.70	4.17	0.02	0.09	0.31	0.01	0.03	-0.04	100.01
7-10_Plag 6_EN_198	197	53.51	29.45	12.49	4.50	0.01	0.09	0.28	0.00	0.03	-0.03	100.34
7-10_Plag 6_EN_199	198	54.33	29.06	12.34	4.52	0.01	0.10	0.29	-0.00	0.03	-0.03	100.64
7-10_Plag 6_EN_200	199	54.27	29.30	12.05	4.52	0.01	0.10	0.31	0.00	0.03	-0.04	100.56
7-10_Plag 6_EN_201	200	54.03	29.22	12.11	4.35	0.02	0.09	0.28	0.00	0.02	-0.03	100.07
7-10_Plag 6_EN_202	201	53.54	29.34	12.58	4.35	0.01	0.09	0.31	0.00	0.03	-0.03	100.21
7-10_Plag 6_EN_203	202	53.31	29.70	12.65	4.05	0.01	0.08	0.33	-0.01	0.03	-0.03	100.12
7-10_Plag 6_EN_204	203	52.56	29.86	13.24	3.89	0.01	0.08	0.32	-0.00	0.02	-0.03	99.96
7-10_Plag 6_EN_205	204	52.42	30.19	13.30	3.92	0.01	0.08	0.32	0.00	0.02	-0.03	100.22
7-10_Plag 6_EN_206	205	52.21	29.94	13.31	3.90	0.01	0.08	0.30	0.00	0.02	-0.03	99.73
7-10_Plag 6_EN_207	206	51.84	29.91	13.28	3.85	0.01	0.07	0.30	-0.00	0.02	-0.04	99.24
7-10_Plag 6_EN_208	207	52.00	30.16	13.36	3.72	0.01	0.07	0.30	-0.00	0.02	-0.04	99.60
7-10_Plag 6_EN_209	208	52.45	30.11	13.12	3.83	0.01	0.07	0.31	0.00	0.02	-0.03	99.90
7-10_Plag 6_EN_210	209	52.63	30.27	13.26	3.82	0.01	0.07	0.31	0.00	0.02	-0.03	100.37
7-10_Plag 6_EN_211	210	52.93	30.08	13.27	3.76	0.01	0.08	0.32	0.01	0.03	-0.03	100.45
7-10_Plag 6_EN_212	211	52.22	30.22	13.39	3.79	0.01	0.07	0.33	0.00	0.02	-0.03	100.03
7-10_Plag 6_EN_213	212	52.25	30.33	13.64	3.73	0.01	0.06	0.31	0.00	0.02	-0.03	100.32
7-10_Plag 6_EN_214	213	52.26	30.43	13.76	3.53	0.01	0.07	0.30	0.00	0.02	-0.03	100.34
7-10_Plag 6_EN_215	214	51.79	30.69	13.90	3.48	0.01	0.06	0.30	0.00	0.02	-0.03	100.21
7-10_Plag 6_EN_216	215	51.39	30.66	14.01	3.44	0.01	0.07	0.31	-0.00	0.02	-0.03	99.88
7-10_Plag 6_EN_217	216	51.61	30.76	14.04	3.54	0.01	0.06	0.31	-0.00	0.02	-0.03	100.31
7-10_Plag 6_EN_218	217	51.95	30.79	13.80	3.42	0.01	0.07	0.32	-0.00	0.02	-0.04	100.34
7-10_Plag 6_EN_219	218	54.75	28.59	11.56	4.75	0.02	0.11	0.27	0.00	0.03	-0.04	100.04
7-10_Plag 6_EN_220	219	55.66	27.86	10.96	5.08	0.01	0.13	0.29	0.00	0.02	-0.03	99.98
7-10_Plag 6_EN_221	220	56.26	27.79	10.79	5.44	0.02	0.12	0.28	0.00	0.03	-0.03	100.69
7-10_Plag 6_EN_222	221	56.83	27.45	10.16	5.48	0.01	0.14	0.28	-0.00	0.02	-0.04	100.34
7-10_Plag 6_EN_223	222	56.93	27.47	10.27	5.69	0.02	0.13	0.30	-0.00	0.03	-0.04	100.79
7-10_Plag 6_EN_224	223	56.93	27.14	9.92	5.69	0.02	0.14	0.28	-0.00	0.03	-0.03	100.10
7-10_Plag 6_EN_225	224	57.40	27.33	10.09	5.75	0.02	0.13	0.30	-0.00	0.03	-0.04	101.00
7-10_Plag 6_EN_226	225	57.16	27.23	9.87	5.85	0.02	0.14	0.26	0.00	0.03	-0.03	100.52
7-10_Plag 6_EN_227	226	57.00	27.13	10.03	5.66	0.02	0.14	0.28	0.00	0.03	-0.04	100.25
7-10_Plag 6_EN_228	227	57.31	27.19	9.96	5.77	0.01	0.15	0.26	0.00	0.03	-0.03	100.65
7-10_Plag 6_EN_229	228	57.31	27.11	9.93	5.72	0.02	0.15	0.30	-0.00	0.03	-0.04	100.52
7-10_Plag 6_EN_230	229	56.88	26.99	9.82	5.48	0.02	0.16	0.30	0.00	0.02	-0.04	99.63
7-10_Plag 6_EN_231	230	57.19	27.23	10.04	5.68	0.02	0.14	0.27	-0.00	0.02	-0.03	100.55
7-10_Plag 6_EN_232	231	56.77	27.31	10.29	5.60	0.02	0.15	0.27	-0.00	0.03	-0.04	100.39
7-10_Plag 6_EN_233	232	56.86	27.51	10.11	5.55	0.02	0.13	0.28	-0.00	0.02	-0.03	100.45
7-10_Plag 6_EN_234	233	56.61	27.62	10.35	5.68	0.01	0.13	0.26	0.00	0.02	-0.04	100.64

Sample	Distance (μm)	SiO_2	Al_2O_3	CaO	Na_2O	MgO	K_2O	FeO	MnO	TiO_2	P_2O_5	Total
7-10_Plag 6_EN_235	234	56.49	27.89	10.42	5.46	0.01	0.12	0.27	-0.00	0.03	-0.04	100.66
7-10_Plag 6_EN_236	235	56.73	27.79	10.40	5.59	0.02	0.14	0.28	0.00	0.03	-0.04	100.93
7-10_Plag 6_EN_237	236	56.30	27.72	10.65	5.25	0.02	0.13	0.28	-0.00	0.03	-0.04	100.33
7-10_Plag 6_EN_238	237	56.43	27.88	10.64	5.25	0.01	0.12	0.26	0.00	0.02	-0.04	100.59
7-10_Plag 6_EN_239	238	56.40	27.91	10.62	5.40	0.01	0.13	0.26	0.00	0.02	-0.04	100.72
7-10_Plag 6_EN_240	239	56.48	28.31	10.75	5.18	0.01	0.12	0.30	0.00	0.03	-0.04	101.16
7-10_Plag 6_EN_241	240	56.03	27.88	10.80	5.19	0.02	0.13	0.29	0.00	0.02	-0.04	100.33
7-10_Plag 6_EN_242	241	55.70	27.73	10.73	5.44	0.02	0.12	0.28	0.00	0.02	-0.04	100.01
7-10_Plag 6_EN_243	242	56.26	27.93	10.67	5.40	0.02	0.12	0.28	0.00	0.02	-0.04	100.64
7-10_Plag 6_EN_244	243	56.07	27.79	10.67	5.43	0.02	0.12	0.31	0.00	0.02	-0.04	100.41
7-10_Plag 6_EN_245	244	56.36	27.42	10.41	5.38	0.02	0.12	0.26	0.00	0.02	-0.04	99.96
7-10_Plag 6_EN_246	245	56.59	27.72	10.42	5.40	0.02	0.13	0.26	-0.00	0.02	-0.03	100.53
7-10_Plag 6_EN_247	246	56.77	27.56	10.30	5.56	0.02	0.14	0.28	-0.00	0.02	-0.04	100.63
7-10_Plag 6_EN_248	247	56.88	27.58	10.25	5.51	0.01	0.13	0.26	-0.00	0.02	-0.03	100.62
7-10_Plag 6_EN_249	248	56.76	27.58	10.31	5.52	0.01	0.13	0.26	0.00	0.03	-0.04	100.57
7-10_Plag 6_EN_250	249	57.04	27.63	10.22	5.57	0.02	0.12	0.29	-0.00	0.02	-0.04	100.87
7-10_Plag 6_EN_251	250	56.79	27.55	10.35	5.89	0.02	0.12	0.30	-0.00	0.03	-0.04	101.00
7-10_Plag 6_EN_252	251	56.45	27.42	10.53	5.55	0.02	0.14	0.25	0.00	0.03	-0.04	100.35
7-10_Plag 6_EN_253	252	56.12	27.67	10.42	5.48	0.02	0.13	0.27	0.00	0.02	-0.03	100.10
7-10_Plag 6_EN_254	253	56.62	27.79	10.26	5.54	0.02	0.13	0.25	-0.00	0.02	-0.04	100.59
7-10_Plag 6_EN_255	254	56.58	27.80	10.39	5.54	0.01	0.13	0.30	-0.01	0.02	-0.04	100.72
7-10_Plag 6_EN_256	255	56.44	27.82	10.37	5.45	0.01	0.13	0.29	-0.00	0.03	-0.04	100.51
7-10_Plag 6_EN_257	256	56.19	27.82	10.81	5.20	0.01	0.13	0.29	0.00	0.02	-0.04	100.45
7-10_Plag 6_EN_258	257	56.75	27.88	10.55	5.29	0.01	0.11	0.26	-0.00	0.02	-0.04	100.85
7-10_Plag 6_EN_259	258	56.65	27.75	10.60	5.35	0.01	0.12	0.29	0.00	0.03	-0.04	100.77
7-10_Plag 6_EN_260	259	56.29	27.81	10.66	5.34	0.01	0.12	0.26	-0.00	0.02	-0.04	100.46
7-10_Plag 6_EN_261	260	56.10	27.86	10.73	5.31	0.02	0.12	0.26	0.00	0.02	-0.04	100.38
7-10_Plag 6_EN_262	261	55.94	27.82	10.63	5.39	0.01	0.13	0.30	0.00	0.02	-0.04	100.21
7-10_Plag 6_EN_263	262	56.17	27.99	10.82	5.16	0.02	0.12	0.28	0.01	0.02	-0.04	100.53
7-10_Plag 6_EN_264	263	55.94	28.02	10.80	5.25	0.02	0.11	0.28	-0.00	0.02	-0.04	100.38
7-10_Plag 6_EN_265	264	55.67	28.15	11.01	5.11	0.01	0.11	0.27	-0.00	0.02	-0.04	100.31
7-10_Plag 6_EN_266	265	55.57	27.99	10.94	5.14	0.02	0.12	0.27	-0.00	0.02	-0.04	100.02
7-10_Plag 6_EN_267	266	55.45	28.28	10.92	5.10	0.01	0.11	0.30	0.00	0.02	-0.04	100.16
7-10_Plag 6_EN_268	267	55.71	28.15	10.97	5.12	0.01	0.11	0.27	-0.00	0.02	-0.04	100.33
7-10_Plag 6_EN_269	268	55.79	28.06	11.05	5.11	0.01	0.12	0.28	0.01	0.02	-0.04	100.41
7-10_Plag 6_EN_270	269	55.79	27.96	10.87	5.20	0.02	0.12	0.27	-0.00	0.03	-0.03	100.22
7-10_Plag 6_EN_271	270	55.88	27.90	10.72	5.21	0.02	0.12	0.27	-0.00	0.02	-0.03	100.12
7-10_Plag 6_EN_272	271	55.86	28.01	10.78	5.28	0.01	0.12	0.28	-0.00	0.02	-0.04	100.33
7-10_Plag 6_EN_273	272	55.87	27.92	10.83	5.40	0.02	0.13	0.29	-0.00	0.02	-0.04	100.43

Sample	Distance (μm)	SiO_2	Al_2O_3	CaO	Na_2O	MgO	K_2O	FeO	MnO	TiO_2	P_2O_5	Total
PLAG_A_01	0	53.31	29.46	12.71	4.20	0.08	0.16	0.56	0.00	0.04	-0.03	100.50
PLAG_A_02	1	53.32	29.28	12.40	4.17	0.08	0.15	0.58	0.00	0.04	-0.04	99.98
PLAG_A_03	2	52.81	29.57	12.81	4.10	0.08	0.12	0.58	-0.00	0.04	-0.03	100.08
PLAG_A_04	3	52.13	29.84	13.42	3.55	0.08	0.09	0.63	0.00	0.04	-0.04	99.74
PLAG_A_05	4	51.93	29.90	13.76	3.59	0.09	0.08	0.65	0.00	0.04	-0.04	100.00
PLAG_A_06	5	50.66	30.80	14.60	3.08	0.09	0.06	0.63	-0.01	0.04	-0.03	99.91
PLAG_A_07	6	50.41	30.97	14.68	3.13	0.09	0.06	0.69	-0.00	0.04	-0.04	100.02
PLAG_A_08	7	49.91	30.86	14.99	2.88	0.09	0.05	0.69	-0.00	0.04	-0.03	99.47
PLAG_A_09	8	49.61	31.50	15.47	2.48	0.09	0.05	0.64	-0.00	0.04	-0.04	99.84
PLAG_A_10	9	49.07	31.51	15.56	2.47	0.08	0.04	0.63	-0.00	0.04	-0.04	99.37
PLAG_A_11	10	48.78	32.04	15.85	2.40	0.09	0.04	0.64	-0.00	0.03	-0.04	99.83
PLAG_A_12	11	49.15	31.84	16.01	2.30	0.08	0.04	0.61	0.00	0.03	-0.03	100.03
PLAG_A_13	12	48.95	31.90	15.74	2.53	0.09	0.05	0.66	0.01	0.03	-0.04	99.92
PLAG_A_14	13	48.97	31.91	15.83	2.27	0.09	0.04	0.60	0.00	0.03	-0.04	99.71
PLAG_A_15	14	48.05	32.66	16.41	1.96	0.08	0.03	0.60	-0.00	0.03	-0.03	99.79
PLAG_A_16	15	47.90	32.36	16.66	1.98	0.08	0.03	0.57	-0.01	0.03	-0.04	99.58
PLAG_A_17	16	48.05	32.48	16.40	1.96	0.07	0.04	0.60	-0.01	0.03	-0.04	99.58
PLAG_A_18	17	48.08	32.31	16.44	2.08	0.07	0.04	0.58	-0.00	0.04	-0.03	99.60
PLAG_A_19	18	48.33	32.25	16.29	2.11	0.06	0.04	0.60	0.01	0.04	-0.04	99.69
PLAG_A_20	19	48.37	32.46	16.54	2.08	0.06	0.03	0.58	0.00	0.05	-0.03	100.14
PLAG_A_21	20	48.00	32.73	16.69	1.98	0.06	0.05	0.57	0.00	0.06	-0.04	100.10
PLAG_A_22	21	48.83	31.99	16.06	2.19	0.06	0.06	0.56	0.01	0.08	-0.03	99.81
PLAG_A_23	22	49.65	31.71	15.44	2.68	0.09	0.08	0.60	0.01	0.10	-0.03	100.34
PLAG_A_24	23	49.13	31.97	15.81	2.38	0.29	0.11	0.61	0.02	0.11	-0.03	100.40
PLAG_A_25	24	50.67	30.60	14.61	2.47	0.67	0.38	0.68	0.02	0.13	-0.03	100.19
PLAG_A_26	25	50.98	30.56	14.84	2.28	0.93	0.46	0.69	0.04	0.12	-0.03	100.88
PLAG_A_27	26	51.94	29.40	13.60	2.64	1.19	0.60	0.68	0.06	0.12	-0.03	100.20
PLAG_A_28	27	49.38	31.69	15.39	2.44	1.20	0.13	0.52	0.05	0.08	-0.03	100.85
PLAG_A_29	28	49.17	31.81	15.85	2.28	0.49	0.14	0.54	0.02	0.07	-0.04	100.34
PLAG_A_30	29	54.18	27.61	12.30	2.67	0.44	0.98	0.88	0.02	0.07	-0.03	99.11
PLAG_A_31	30	57.82	26.12	10.52	3.51	0.61	1.25	0.90	0.03	0.08	-0.03	100.80
PLAG_A_32	31	50.77	29.80	14.07	2.87	0.50	0.31	0.69	0.02	0.10	-0.03	99.08
PLAG_A_33	32	51.73	30.23	13.83	3.57	0.23	0.19	0.48	0.01	0.09	-0.03	100.33
PLAG_A_34	33	50.61	30.83	14.75	2.88	0.19	0.18	0.55	0.01	0.10	-0.03	100.06
PLAG_A_35	34	51.41	30.36	13.81	3.46	0.41	0.19	0.48	0.04	0.10	-0.03	100.22
PLAG_A_36	35	52.54	29.66	13.24	3.59	0.62	0.33	0.52	0.05	0.10	-0.04	100.61
PLAG_A_37	36	50.36	31.29	14.73	2.98	0.50	0.13	0.45	0.05	0.07	-0.03	100.54
PLAG_A_38	37	52.80	29.64	13.48	3.33	0.16	0.44	0.61	0.02	0.08	-0.03	100.54
PLAG_A_39	38	52.11	30.08	13.56	3.58	0.19	0.19	0.42	0.02	0.11	-0.02	100.23

Sample	Distance (μm)	SiO_2	Al_2O_3	CaO	Na_2O	MgO	K_2O	FeO	MnO	TiO_2	P_2O_5	Total
PLAG_A_40	39	53.23	29.39	12.73	4.27	0.20	0.21	0.39	0.02	0.13	-0.02	100.56
PLAG_A_41	40	53.72	28.87	11.99	4.62	0.20	0.21	0.34	0.02	0.13	-0.03	100.06
PLAG_A_42	41	54.22	28.94	12.25	4.50	0.18	0.27	0.37	0.02	0.11	-0.04	100.84
PLAG_A_43	42	53.61	28.69	12.67	3.97	0.17	0.42	0.50	0.01	0.11	-0.03	100.12
PLAG_A_44	43	54.19	28.41	12.64	3.49	0.16	0.61	0.62	0.01	0.10	-0.03	100.20
PLAG_A_45	44	52.00	29.98	13.79	3.40	0.15	0.30	0.49	0.01	0.10	-0.03	100.18
PLAG_A_46	45	51.04	30.68	14.34	3.40	0.13	0.16	0.39	0.01	0.10	-0.04	100.20
PLAG_A_47	46	52.93	29.00	13.04	3.90	0.11	0.37	0.51	0.01	0.09	-0.02	99.94
PLAG_A_48	47	56.85	27.30	9.87	5.84	0.09	0.21	0.25	0.01	0.07	-0.03	100.44
PLAG_A_49	48	57.27	27.01	9.75	5.93	0.08	0.20	0.26	0.01	0.07	-0.03	100.55
PLAG_A_50	49	56.98	26.89	9.73	5.85	0.07	0.19	0.28	0.01	0.06	-0.03	100.02
PLAG_A_51	50	56.84	26.86	9.71	5.76	0.05	0.19	0.23	0.00	0.05	-0.04	99.66
PLAG_A_52	51	57.07	27.04	9.96	5.95	0.04	0.20	0.24	0.01	0.03	-0.03	100.50
PLAG_A_53	52	56.98	27.05	9.97	5.95	0.03	0.23	0.25	-0.00	0.02	-0.03	100.45
PLAG_A_54	53	56.79	27.21	10.00	5.56	0.03	0.27	0.29	0.00	0.03	-0.04	100.15
PLAG_A_55	54	57.74	25.62	9.93	4.99	0.02	0.69	0.65	-0.00	0.02	-0.03	99.62
PLAG_A_56	55	56.92	27.33	10.12	5.66	0.02	0.31	0.23	-0.00	0.02	-0.03	100.57
PLAG_A_57	56	56.76	27.25	10.28	5.77	0.01	0.22	0.25	0.00	0.02	-0.04	100.53
PLAG_A_58	57	56.61	27.30	10.28	5.61	0.01	0.19	0.26	-0.01	0.03	-0.03	100.24
PLAG_A_59	58	56.25	27.34	10.22	5.62	0.01	0.16	0.28	0.00	0.02	-0.04	99.86
PLAG_A_60	59	56.10	27.26	10.38	5.63	0.01	0.16	0.29	0.00	0.02	-0.04	99.81
PLAG_A_61	60	56.38	27.62	10.44	5.55	0.01	0.14	0.29	0.00	0.03	-0.03	100.42
PLAG_A_62	61	56.34	27.34	10.42	5.81	0.01	0.14	0.30	0.00	0.02	-0.03	100.35
PLAG_A_63	62	56.18	27.42	10.36	5.53	0.01	0.14	0.27	-0.01	0.02	-0.04	99.89
PLAG_A_B_01	0	53.44	29.17	12.66	4.00	0.37	0.21	0.71	-0.01	0.06	-0.03	100.58
PLAG_A_B_02	1	52.48	29.95	13.37	3.52	0.42	0.17	0.72	-0.01	0.05	-0.03	100.63
PLAG_A_B_03	2	52.06	30.19	13.75	3.46	0.45	0.12	0.75	0.00	0.07	-0.03	100.81
PLAG_A_B_04	3	51.49	30.43	13.99	3.38	0.48	0.09	0.71	0.01	0.06	-0.03	100.62
PLAG_A_B_05	4	51.40	30.35	13.92	3.42	0.48	0.07	0.73	0.02	0.06	-0.04	100.40
PLAG_A_B_06	5	52.29	30.11	13.80	3.51	0.42	0.08	0.68	0.01	0.06	-0.03	100.93
PLAG_A_B_07	6	51.81	30.21	13.84	3.45	0.26	0.08	0.70	0.01	0.05	-0.04	100.37
PLAG_A_B_08	7	50.83	31.06	14.81	2.69	0.15	0.06	0.71	0.00	0.04	-0.03	100.31
PLAG_A_B_09	8	50.09	31.00	15.18	2.77	0.10	0.05	0.70	0.00	0.05	-0.03	99.91
PLAG_A_B_10	9	49.80	31.56	15.30	2.66	0.09	0.05	0.68	-0.00	0.05	-0.04	100.16
PLAG_A_B_11	10	49.71	31.57	15.60	2.44	0.09	0.04	0.68	0.00	0.04	-0.04	100.15
PLAG_A_B_12	11	49.23	31.86	15.64	2.35	0.09	0.05	0.66	0.00	0.04	-0.03	99.87
PLAG_A_B_13	12	49.19	31.97	15.73	2.35	0.09	0.05	0.67	-0.00	0.05	-0.03	100.05
PLAG_A_B_14	13	49.19	32.04	15.70	2.36	0.09	0.04	0.61	-0.00	0.04	-0.04	100.02
PLAG_A_B_15	14	49.27	32.06	15.66	2.26	0.09	0.04	0.63	0.00	0.04	-0.04	100.02

Sample/	Distance (μm)	SiO_2	Al_2O_3	CaO	Na_2O	MgO	K_2O	FeO	MnO	TiO_2	P_2O_5	Total
PLAG_A_B_16	15	49.29	31.97	15.96	2.29	0.09	0.05	0.66	-0.00	0.04	-0.04	100.31
PLAG_A_B_17	16	49.29	32.01	16.01	2.42	0.09	0.05	0.62	0.00	0.04	-0.04	100.49
PLAG_A_B_18	17	49.14	31.96	15.89	2.21	0.09	0.04	0.63	-0.00	0.03	-0.03	99.96
PLAG_A_B_19	18	49.36	32.18	15.94	2.21	0.09	0.04	0.63	-0.00	0.04	-0.03	100.43
PLAG_A_B_20	19	49.13	31.85	15.71	2.37	0.09	0.04	0.68	-0.00	0.04	-0.04	99.87
PLAG_A_B_21	20	49.13	32.05	15.86	2.34	0.09	0.05	0.67	-0.00	0.04	-0.04	100.17
PLAG_A_B_22	21	48.97	32.03	15.91	2.22	0.09	0.04	0.65	0.00	0.04	-0.03	99.92
PLAG_A_B_23	22	48.65	32.08	16.11	2.15	0.09	0.04	0.66	-0.00	0.03	-0.03	99.77
PLAG_A_B_24	23	49.32	32.06	15.97	2.25	0.10	0.04	0.63	0.00	0.04	-0.04	100.37
PLAG_A_B_25	24	48.93	31.99	15.83	2.21	0.09	0.04	0.64	0.00	0.04	-0.04	99.73
PLAG_A_B_26	25	49.22	31.86	15.83	2.31	0.09	0.05	0.65	-0.00	0.04	-0.04	100.02
PLAG_A_B_27	26	49.48	31.74	15.86	2.30	0.09	0.04	0.64	-0.00	0.04	-0.04	100.16
PLAG_A_B_28	27	49.00	31.95	15.76	2.39	0.09	0.04	0.62	-0.00	0.04	-0.03	99.85
PLAG_A_B_29	28	49.37	31.96	15.84	2.23	0.10	0.04	0.64	0.00	0.04	-0.03	100.19
PLAG_A_B_30	29	48.97	32.08	15.96	2.19	0.14	0.05	0.61	0.00	0.05	-0.04	100.01
PLAG_A_B_31	30	50.05	31.48	15.24	2.62	0.13	0.05	0.65	0.00	0.05	-0.04	100.21
PLAG_A_B_32	31	50.36	31.49	15.05	2.61	0.13	0.07	0.64	0.01	0.05	-0.04	100.37
PLAG_A_B_33	32	54.27	28.13	11.82	4.69	0.13	0.12	0.85	0.01	0.05	-0.04	100.04
PLAG_A_B_34	33	55.62	28.22	11.06	4.97	0.13	0.13	0.31	0.01	0.05	-0.03	100.47
PLAG_A_B_35	34	55.15	28.30	11.41	5.00	0.03	0.11	0.33	-0.01	0.03	-0.04	100.31
PLAG_A_B_36	35	54.90	28.24	11.43	5.00	0.02	0.10	0.31	0.00	0.03	-0.04	99.99
PLAG_A_B_37	36	55.28	28.48	11.41	5.05	0.02	0.10	0.35	0.00	0.03	-0.03	100.69
PLAG_A_B_38	37	55.64	28.39	11.23	5.00	0.02	0.10	0.29	-0.01	0.03	-0.04	100.66
PLAG_A_B_39	38	55.78	28.24	11.09	5.19	0.02	0.12	0.32	0.00	0.03	-0.03	100.74
PLAG_A_B_40	39	56.32	27.97	10.73	5.36	0.02	0.11	0.28	0.00	0.03	-0.04	100.79
PLAG_A_B_41	40	55.97	28.01	10.89	5.35	0.02	0.11	0.30	0.00	0.03	-0.04	100.65
PLAG_A_B_42	41	55.90	28.13	11.18	5.10	0.01	0.11	0.33	0.00	0.02	-0.04	100.76
PLAG_A_B_43	42	55.28	28.45	11.24	5.04	0.02	0.11	0.33	-0.00	0.03	-0.04	100.46
PLAG_A_B_44	43	56.03	28.17	11.17	5.10	0.02	0.11	0.31	-0.00	0.03	-0.04	100.89
PLAG_A_B_45	44	56.56	27.45	10.44	5.58	0.02	0.13	0.31	0.00	0.03	-0.03	100.48
PLAG_A_B_46	45	57.18	27.19	9.90	5.64	0.02	0.14	0.30	0.00	0.03	-0.04	100.35
PLAG_A_B_47	46	57.39	27.16	10.00	5.85	0.02	0.15	0.29	-0.01	0.03	-0.04	100.83
PLAG_A_B_48	47	57.71	26.94	9.94	5.77	0.02	0.13	0.28	0.00	0.03	-0.03	100.78
PLAG_A_B_49	48	57.81	26.94	9.73	5.93	0.01	0.14	0.32	-0.00	0.03	-0.04	100.87
PLAG_A_B_50	49	57.88	26.92	9.71	5.88	0.02	0.15	0.26	0.00	0.03	-0.03	100.83
PLAG_A_B_51	50	57.98	26.88	9.74	5.87	0.01	0.14	0.29	-0.00	0.03	-0.04	100.90
PLAG_A_B_52	51	57.72	27.11	9.76	5.94	0.01	0.14	0.30	0.00	0.03	-0.03	100.99
PLAG_A_B_53	52	57.22	26.92	9.78	5.97	0.02	0.14	0.27	0.00	0.03	-0.03	100.33

Sample	Distance (μm)	SiO_2	Al_2O_3	CaO	Na_2O	MgO	K_2O	FeO	MnO	TiO_2	P_2O_5	Total
PLAG_C_01	0	81.15	11.34	1.96	3.64	3.48	1.57	0.88	0.23	0.45	0.12	104.82
PLAG_C_02	1	77.93	13.12	2.78	4.35	2.27	1.12	0.57	0.16	0.35	0.11	102.76
PLAG_C_03	2	71.77	17.01	4.65	4.39	1.24	0.75	0.49	0.10	0.27	0.02	100.70
PLAG_C_04	3	58.09	26.52	9.68	5.52	0.16	0.37	0.47	0.02	0.17	-0.02	100.97
PLAG_C_05	4	56.50	27.47	10.48	5.50	0.04	0.27	0.47	0.00	0.10	-0.03	100.80
PLAG_C_06	5	55.60	28.15	11.11	5.14	0.03	0.19	0.44	0.00	0.05	-0.04	100.67
PLAG_C_07	6	54.60	28.64	11.86	4.86	0.03	0.13	0.47	0.00	0.04	-0.04	100.59
PLAG_C_08	7	54.60	28.52	11.70	4.76	0.03	0.12	0.50	-0.00	0.03	-0.03	100.22
PLAG_C_09	8	54.36	29.06	12.15	4.52	0.03	0.09	0.52	0.01	0.03	-0.04	100.73
PLAG_C_10	9	53.75	29.19	12.47	4.30	0.03	0.08	0.52	-0.00	0.03	-0.04	100.32
PLAG_C_11	10	54.15	28.99	12.30	4.48	0.02	0.09	0.48	0.00	0.03	-0.04	100.51
PLAG_C_12	11	54.50	28.64	11.94	4.75	0.02	0.09	0.44	-0.00	0.03	-0.04	100.38
PLAG_C_13	12	54.63	28.88	12.09	4.58	0.02	0.10	0.39	-0.00	0.03	-0.04	100.69
PLAG_C_14	13	54.39	28.83	12.07	4.44	0.02	0.09	0.39	0.00	0.03	-0.03	100.25
PLAG_C_15	14	54.57	28.95	12.21	4.60	0.02	0.09	0.40	-0.00	0.03	-0.03	100.83
PLAG_C_16	15	54.24	29.29	12.56	4.39	0.02	0.09	0.42	-0.00	0.03	-0.03	101.01
PLAG_C_17	16	53.37	29.64	12.64	4.24	0.02	0.09	0.41	0.01	0.03	-0.03	100.43
PLAG_C_18	17	53.76	29.70	12.84	4.25	0.02	0.07	0.39	0.00	0.03	-0.03	101.04
PLAG_C_19	18	52.98	29.76	13.19	4.08	0.02	0.07	0.40	0.00	0.03	-0.04	100.50
PLAG_C_20	19	53.08	29.90	13.14	3.89	0.02	0.08	0.41	0.00	0.04	-0.03	100.52
PLAG_C_21	20	53.01	29.87	13.16	3.95	0.02	0.07	0.39	0.01	0.03	-0.03	100.47
PLAG_C_22	21	53.20	29.70	12.93	4.02	0.02	0.08	0.42	0.00	0.03	-0.03	100.38
PLAG_C_23	22	53.42	29.39	12.91	4.12	0.03	0.08	0.40	-0.00	0.03	-0.04	100.35
PLAG_C_24	23	53.36	29.77	12.91	4.08	0.02	0.08	0.42	-0.00	0.03	-0.03	100.66
PLAG_C_25	24	53.08	30.09	13.43	4.00	0.02	0.07	0.42	-0.00	0.03	-0.04	101.11
PLAG_C_26	25	52.23	30.45	13.86	3.59	0.02	0.07	0.43	0.01	0.03	-0.03	100.66
PLAG_C_27	26	52.08	30.58	14.00	3.59	0.02	0.07	0.44	0.00	0.03	-0.03	100.78
PLAG_C_28	27	51.42	30.82	14.24	3.23	0.02	0.06	0.46	0.00	0.03	-0.04	100.23
PLAG_C_29	28	51.01	31.23	14.81	3.16	0.02	0.06	0.48	0.00	0.03	-0.04	100.75
PLAG_C_30	29	50.92	31.10	14.90	3.10	0.02	0.05	0.49	-0.00	0.03	-0.03	100.59
PLAG_C_31	30	51.26	30.91	14.40	3.20	0.02	0.06	0.48	-0.00	0.03	-0.03	100.32
PLAG_C_32	31	51.05	31.14	14.75	2.91	0.02	0.04	0.49	-0.00	0.03	-0.04	100.40
PLAG_C_33	32	50.85	31.24	14.85	2.93	0.02	0.05	0.46	-0.00	0.04	-0.04	100.39
PLAG_C_34	33	50.88	30.92	14.59	3.18	0.02	0.05	0.46	0.01	0.03	-0.04	100.10
PLAG_C_35	34	50.81	31.20	14.71	3.01	0.02	0.05	0.49	0.00	0.03	-0.04	100.29
PLAG_C_36	35	50.40	31.79	15.05	2.82	0.02	0.04	0.49	0.00	0.03	-0.04	100.62
PLAG_C_37	36	50.45	31.60	15.00	2.85	0.02	0.05	0.50	-0.00	0.03	-0.03	100.48
PLAG_C_38	37	50.60	31.17	15.05	2.90	0.02	0.06	0.50	0.00	0.03	-0.03	100.30
PLAG_C_39	38	53.95	28.95	12.60	4.02	0.02	0.17	0.54	0.00	0.03	-0.03	100.24

Sample	Distance (μm)	SiO_2	Al_2O_3	CaO	Na_2O	MgO	K_2O	FeO	MnO	TiO_2	P_2O_5	Total
PLAG_C_40	39	54.05	29.30	12.50	4.14	0.02	0.10	0.44	-0.00	0.03	-0.03	100.55
PLAG_C_41	40	53.41	29.59	12.89	4.14	0.02	0.09	0.43	0.00	0.03	-0.04	100.57
PLAG_C_42	41	53.73	29.42	12.93	4.21	0.02	0.09	0.43	-0.00	0.03	-0.03	100.81
PLAG_C_43	42	53.54	29.55	12.99	4.18	0.02	0.08	0.38	0.00	0.03	-0.03	100.73
PLAG_C_44	43	53.02	30.03	13.29	3.83	0.02	0.07	0.42	-0.01	0.03	-0.03	100.67
PLAG_C_45	44	52.90	29.68	13.26	3.85	0.02	0.07	0.42	0.01	0.03	-0.03	100.20
PLAG_C_46	45	52.98	29.80	13.02	3.97	0.02	0.07	0.45	0.01	0.03	-0.03	100.32
PLAG_C_47	46	53.06	29.83	13.13	3.98	0.02	0.07	0.42	0.00	0.03	-0.04	100.51
PLAG_C_48	47	52.78	29.76	13.38	3.90	0.02	0.07	0.44	-0.00	0.03	-0.03	100.34
PLAG_C_49	48	52.31	29.94	13.76	3.79	0.02	0.07	0.45	-0.00	0.03	-0.03	100.32
PLAG_C_50	49	52.54	30.14	13.54	3.68	0.02	0.07	0.46	0.00	0.03	-0.04	100.45
PLAG_C_51	50	52.64	30.00	13.17	3.80	0.02	0.08	0.45	0.00	0.03	-0.03	100.16
PLAG_C_52	51	52.85	29.93	13.20	3.88	0.02	0.07	0.42	0.00	0.04	-0.04	100.38
PLAG_C_53	52	52.27	30.43	13.76	3.41	0.02	0.06	0.42	0.00	0.03	-0.03	100.37
PLAG_C_54	53	51.82	30.47	13.88	3.46	0.02	0.07	0.44	0.00	0.03	-0.03	100.17
PLAG_C_55	54	51.63	30.47	13.90	3.51	0.02	0.06	0.42	-0.00	0.03	-0.03	99.99
PLAG_C_56	55	51.91	30.41	13.82	3.70	0.02	0.06	0.43	-0.00	0.03	-0.04	100.35
PLAG_C_57	56	51.97	30.37	13.81	3.40	0.02	0.06	0.45	-0.00	0.04	-0.03	100.08
PLAG_C_58	57	51.56	30.62	14.10	3.31	0.02	0.06	0.42	0.00	0.04	-0.04	100.10
PLAG_C_59	58	51.65	30.81	14.19	3.35	0.02	0.06	0.39	0.01	0.03	-0.04	100.47
PLAG_C_60	59	51.43	30.85	14.11	3.31	0.02	0.05	0.43	0.00	0.03	-0.03	100.21
PLAG_C_61	60	51.64	30.81	14.12	3.41	0.02	0.07	0.40	0.00	0.03	-0.04	100.46
PLAG_C_62	61	52.01	30.80	13.94	3.44	0.02	0.06	0.39	0.00	0.04	-0.04	100.67
PLAG_C_63	62	51.54	30.81	13.95	3.30	0.02	0.06	0.41	0.01	0.03	-0.04	100.10
PLAG_C_64	63	51.59	30.66	14.27	3.41	0.02	0.06	0.42	0.00	0.04	-0.04	100.42
PLAG_C_65	64	51.54	30.72	14.01	3.30	0.02	0.06	0.40	0.00	0.04	-0.04	100.03
PLAG_C_66	65	51.46	30.60	14.28	3.33	0.02	0.06	0.41	0.00	0.04	-0.04	100.16
PLAG_C_67	66	51.69	30.92	14.29	3.18	0.02	0.06	0.41	0.00	0.03	-0.03	100.55
PLAG_C_68	67	51.50	30.83	14.24	3.15	0.02	0.06	0.42	-0.00	0.03	-0.04	100.22
PLAG_C_69	68	51.70	30.78	14.06	3.29	0.02	0.06	0.40	-0.00	0.03	-0.03	100.32
PLAG_C_70	69	50.92	30.92	14.23	3.22	0.02	0.05	0.42	0.00	0.04	-0.04	99.78
PLAG_C_71	70	51.20	30.95	14.59	3.16	0.03	0.05	0.39	0.00	0.04	-0.02	100.39
PLAG_D_01	0	67.15	19.55	5.66	5.65	0.67	0.74	0.54	0.05	0.13	-0.03	100.11
PLAG_D_02	1	57.92	26.43	9.76	5.93	0.68	0.41	0.58	0.05	0.15	-0.02	101.90
PLAG_D_03	2	56.83	27.20	10.09	5.65	0.79	0.36	0.53	0.06	0.15	-0.02	101.64
PLAG_D_04	3	55.12	28.32	11.23	5.04	0.47	0.28	0.56	0.03	0.16	-0.01	101.20
PLAG_D_05	4	52.70	29.63	13.14	3.90	0.24	0.15	0.62	0.01	0.15	-0.01	100.53
PLAG_D_06	5	51.38	30.62	14.07	3.29	0.11	0.11	0.55	-0.01	0.15	-0.00	100.27
PLAG_D_07	6	51.10	31.11	14.61	3.31	0.10	0.08	0.47	0.00	0.13	-0.00	100.91

Sample	Distance (μm)	SiO_2	Al_2O_3	CaO	Na_2O	MgO	K_2O	FeO	MnO	TiO_2	P_2O_5	Total
PLAG_D_08	7	52.66	30.27	13.24	3.86	0.11	0.08	0.46	0.00	0.12	-0.01	100.78
PLAG_D_09	8	52.16	30.48	13.73	3.73	0.12	0.07	0.45	-0.00	0.09	-0.00	100.82
PLAG_D_10	9	52.42	30.59	13.48	3.86	0.13	0.08	0.37	0.00	0.06	-0.01	100.96
PLAG_D_11	10	53.29	29.82	12.83	4.13	0.11	0.08	0.40	0.01	0.05	-0.02	100.69
PLAG_D_12	11	53.89	29.45	12.54	4.41	0.07	0.08	0.39	0.00	0.04	-0.02	100.85
PLAG_D_13	12	53.67	29.55	12.81	4.11	0.04	0.08	0.40	-0.00	0.04	-0.03	100.67
PLAG_D_14	13	52.76	30.18	13.45	4.03	0.04	0.07	0.39	0.00	0.04	-0.03	100.92
PLAG_D_15	14	52.90	29.96	13.18	4.05	0.03	0.07	0.38	0.00	0.04	-0.03	100.58
PLAG_D_16	15	53.77	29.26	12.41	4.26	0.03	0.08	0.40	0.01	0.03	-0.03	100.21
PLAG_D_17	16	53.71	29.30	12.53	4.38	0.03	0.09	0.39	0.00	0.04	-0.03	100.43
PLAG_D_18	17	53.73	29.52	12.52	4.45	0.02	0.09	0.40	0.00	0.03	-0.03	100.74
PLAG_D_19	18	53.89	29.35	12.45	4.29	0.02	0.09	0.38	0.01	0.04	-0.03	100.46
PLAG_D_20	19	53.21	29.85	12.68	4.15	0.02	0.08	0.39	0.00	0.04	-0.03	100.38
PLAG_D_21	20	53.29	30.01	13.06	4.20	0.03	0.08	0.39	0.00	0.04	-0.03	101.07
PLAG_D_22	21	52.87	30.01	13.27	3.81	0.03	0.07	0.38	0.00	0.05	-0.03	100.46
PLAG_D_23	22	52.46	30.34	13.51	3.94	0.02	0.07	0.39	0.00	0.04	-0.03	100.75
PLAG_D_24	23	52.35	30.40	13.71	3.61	0.02	0.07	0.43	0.00	0.04	-0.03	100.61
PLAG_D_25	24	52.21	30.76	13.63	3.61	0.02	0.06	0.41	0.00	0.04	-0.03	100.71
PLAG_D_26	25	51.54	30.87	14.15	3.51	0.02	0.06	0.44	0.01	0.03	-0.03	100.60
PLAG_D_27	26	51.91	30.67	13.63	3.54	0.11	0.07	0.42	0.01	0.05	-0.03	100.38
PLAG_D_28	27	51.73	31.02	14.22	3.28	0.03	0.06	0.41	-0.00	0.03	-0.03	100.75
PLAG_D_29	28	55.54	27.48	12.10	3.08	0.03	0.36	0.85	-0.00	0.03	-0.03	99.43
PLAG_D_30	29	54.34	26.57	11.78	3.03	0.02	0.36	0.91	0.00	0.03	-0.04	97.00
PLAG_D_31	30	52.07	31.24	14.26	3.34	0.02	0.08	0.40	0.00	0.03	-0.03	101.40
PLAG_D_32	31	52.31	31.76	14.55	3.20	0.02	0.06	0.39	0.00	0.04	-0.03	102.30
PLAG_D_33	32	52.07	31.88	14.79	3.11	0.02	0.05	0.40	0.00	0.04	-0.04	102.31
PLAG_D_34	33	51.32	31.56	14.75	2.95	0.02	0.05	0.41	0.00	0.04	-0.03	101.06
PLAG_D_35	34	51.24	31.67	14.73	3.14	0.02	0.05	0.38	0.00	0.04	-0.03	101.24
PLAG_D_36	35	51.02	31.36	14.57	3.26	0.02	0.05	0.38	0.00	0.04	-0.04	100.67
PLAG_D_37	36	50.91	31.10	14.66	3.16	0.02	0.06	0.41	0.00	0.04	-0.03	100.33
PLAG_D_38	37	51.02	31.53	14.57	3.21	0.02	0.06	0.41	0.00	0.05	-0.03	100.84
PLAG_D_39	38	51.37	31.51	14.86	3.08	0.02	0.06	0.41	0.00	0.05	-0.03	101.33
PLAG_D_40	39	52.53	32.31	14.61	3.10	0.02	0.06	0.39	0.00	0.05	-0.04	103.03
PLAG_D_41	40	54.13	32.85	14.71	3.17	0.02	0.05	0.42	-0.00	0.04	-0.03	105.37
PLAG_D_42	41	52.94	32.26	14.89	3.12	0.03	0.06	0.39	-0.00	0.05	-0.03	103.71
PLAG_D_43	42	52.87	32.54	14.81	3.04	0.03	0.05	0.41	0.01	0.07	-0.03	103.80
PLAG_D_44	43	51.31	32.25	15.10	2.93	0.03	0.05	0.41	0.00	0.08	-0.03	102.13
PLAG_D_45	44	51.50	32.22	14.98	2.85	0.04	0.05	0.39	-0.00	0.07	-0.04	102.07
PLAG_D_46	45	51.37	32.16	15.01	3.04	0.04	0.05	0.40	0.00	0.08	-0.03	102.13

Sample	Distance (μm)	SiO_2	Al_2O_3	CaO	Na_2O	MgO	K_2O	FeO	MnO	TiO_2	P_2O_5	Total
PLAG_D_47	46	52.22	32.45	14.81	2.96	0.03	0.06	0.42	0.00	0.06	-0.03	102.97
PLAG_D_48	47	51.71	32.19	15.03	3.13	0.04	0.05	0.40	0.01	0.05	-0.04	102.56
PLAG_D_49	48	51.43	31.82	14.81	2.98	0.04	0.05	0.43	-0.01	0.05	-0.04	101.57
PLAG_D_50	49	51.50	31.75	15.19	3.16	0.03	0.05	0.40	-0.00	0.05	-0.03	102.11
PLAG_D_51	50	50.55	31.94	14.92	3.07	0.03	0.06	0.43	-0.00	0.05	-0.04	100.99
PLAG_D_52	51	50.72	31.30	14.84	2.87	0.03	0.06	0.39	-0.00	0.05	-0.03	100.22
PLAG_D_53	52	53.58	28.95	13.32	2.83	0.04	0.31	0.79	0.00	0.06	-0.03	99.84
PLAG_D_54	53	51.79	26.13	12.09	2.84	0.04	0.43	0.91	-0.00	0.07	-0.03	94.27
PLAG_D_55	54	50.71	31.65	15.10	2.84	0.04	0.06	0.40	0.00	0.08	-0.04	100.85
PLAG_D_56	55	49.95	31.78	15.38	2.72	0.03	0.04	0.35	-0.00	0.08	-0.03	100.30
PLAG_D_57	56	50.15	31.68	15.35	2.70	0.04	0.04	0.43	-0.00	0.08	-0.03	100.44
PLAG_D_58	57	49.82	32.08	15.47	2.64	0.04	0.04	0.39	-0.00	0.08	-0.03	100.53
PLAG_D_59	58	49.80	31.77	15.41	2.60	0.03	0.04	0.40	0.00	0.08	-0.04	100.10
PLAG_D_60	59	50.03	32.05	15.31	2.55	0.03	0.04	0.40	0.00	0.06	-0.04	100.43
PLAG_D_61	60	49.32	32.11	15.75	2.58	0.02	0.04	0.38	0.00	0.04	-0.03	100.21
PLAG_D_62	61	49.45	32.33	15.80	2.47	0.02	0.04	0.39	0.01	0.04	-0.04	100.52
PLAG_D_63	62	49.79	32.12	15.74	2.54	0.02	0.05	0.39	0.01	0.04	-0.04	100.66
PLAG_D_64	63	49.69	32.20	15.60	2.62	0.02	0.04	0.38	0.00	0.04	-0.04	100.55
PLAG_D_65	64	49.62	32.22	15.61	2.63	0.02	0.04	0.45	0.01	0.03	-0.04	100.58
PLAG_D_66	65	49.27	32.03	15.67	2.53	0.01	0.04	0.36	0.01	0.04	-0.04	99.92
PLAG_D_67	66	49.07	32.40	15.83	2.42	0.01	0.04	0.38	0.01	0.04	-0.04	100.16
PLAG_D_68	67	48.90	32.38	16.02	2.33	0.01	0.04	0.40	0.00	0.04	-0.04	100.09
PLAG_D_69	68	49.39	32.56	16.09	2.39	0.01	0.04	0.39	-0.00	0.03	-0.04	100.87
PLAG_D_70	69	49.73	32.20	15.70	2.53	0.01	0.04	0.43	0.00	0.03	-0.03	100.64
PLAG_D_71	70	49.46	32.24	15.56	2.50	0.01	0.04	0.42	-0.00	0.04	-0.04	100.23
PLAG_D_72	71	49.43	32.07	15.65	2.64	0.01	0.04	0.40	0.01	0.03	-0.04	100.24
PLAG_D_73	72	49.15	32.25	15.63	2.50	0.01	0.04	0.39	0.01	0.03	-0.04	99.97
PLAG_D_74	73	49.75	32.20	15.76	2.67	0.01	0.04	0.39	0.01	0.03	-0.04	100.82
PLAG_D_75	74	49.52	32.11	15.71	2.44	0.01	0.04	0.38	0.00	0.03	-0.04	100.21
PLAG_D_76	75	49.64	32.41	15.72	2.39	0.01	0.04	0.41	0.01	0.03	-0.03	100.63
PLAG_D_77	76	49.57	32.21	15.88	2.45	0.01	0.04	0.41	0.00	0.04	-0.04	100.58
PLAG_D_78	77	49.25	32.02	15.59	2.44	0.01	0.05	0.39	0.00	0.03	-0.03	99.74
PLAG_D_79	78	49.76	32.03	15.63	2.48	0.01	0.04	0.37	0.01	0.03	-0.04	100.32
PLAG_D_80	79	49.47	32.08	15.92	2.40	0.01	0.05	0.40	0.00	0.03	-0.03	100.34
PLAG_D_81	80	49.35	32.30	15.82	2.44	0.01	0.04	0.45	-0.00	0.03	-0.04	100.40
PLAG_D_82	81	49.19	32.36	15.74	2.56	0.01	0.04	0.38	0.01	0.04	-0.04	100.28
PLAG_D_83	82	49.14	32.46	16.03	2.36	0.01	0.04	0.44	-0.00	0.03	-0.03	100.49
PLAG_D_84	83	49.52	32.31	15.65	2.47	0.02	0.03	0.38	0.00	0.03	-0.03	100.38
PLAG_D_85	84	49.14	32.47	16.04	2.31	0.01	0.04	0.40	-0.00	0.03	-0.04	100.40

Sample	Distance (μm)	SiO_2	Al_2O_3	CaO	Na_2O	MgO	K_2O	FeO	MnO	TiO_2	P_2O_5	Total
PLAG_D_86	85	49.23	32.45	15.78	2.33	0.01	0.04	0.38	0.01	0.03	-0.04	100.24
PLAG_D_87	86	48.78	32.61	16.17	2.23	0.01	0.04	0.41	0.01	0.03	-0.04	100.25
PLAG_D_88	87	48.84	32.67	16.02	2.19	0.01	0.03	0.43	-0.00	0.03	-0.03	100.18
PLAG_D_89	88	48.90	32.51	16.24	2.23	0.01	0.04	0.43	-0.00	0.03	-0.03	100.35
PLAG_D_90	89	48.77	32.51	16.12	2.10	0.01	0.03	0.41	-0.00	0.04	-0.04	99.96
PLAG_D_91	90	48.87	32.66	16.23	2.24	0.01	0.04	0.43	0.01	0.03	-0.04	100.47
PLAG_D_92	91	49.15	32.61	16.30	2.15	0.01	0.04	0.41	0.00	0.03	-0.04	100.67
PLAG_D_93	92	49.06	32.68	16.07	2.35	0.01	0.04	0.42	0.00	0.03	-0.03	100.63
PLAG_D_94	93	48.93	32.67	16.13	2.19	0.01	0.04	0.40	0.01	0.03	-0.03	100.39
PLAG_D_95	94	48.85	32.69	16.04	2.10	0.01	0.03	0.40	0.00	0.03	-0.04	100.13
PLAG_D_96	95	49.09	32.52	16.21	2.25	0.01	0.04	0.41	0.01	0.03	-0.04	100.53
PLAG_D_97	96	48.97	32.54	16.20	2.24	0.01	0.04	0.41	0.00	0.03	-0.04	100.40
PLAG_D_98	97	49.25	32.69	16.13	2.24	0.01	0.04	0.40	0.00	0.03	-0.04	100.76
PLAG_D_99	98	49.26	32.60	15.97	2.26	0.01	0.03	0.39	0.00	0.03	-0.03	100.52
PLAG_D_100	99	47.91	31.67	15.63	2.26	0.01	0.03	0.39	0.01	0.04	-0.03	97.93
PLAG_D_101	100	49.40	32.22	15.76	2.49	0.01	0.05	0.39	0.01	0.03	-0.04	100.32
PLAG_D_102	101	50.19	31.91	15.44	2.70	0.01	0.04	0.41	0.00	0.03	-0.04	100.70
PLAG_D_103	102	51.29	31.46	14.68	3.10	0.01	0.05	0.38	0.00	0.04	-0.04	100.96
PLAG_D_104	103	52.18	30.59	14.03	3.61	0.01	0.06	0.35	0.01	0.03	-0.04	100.85
PLAG_D_105	104	52.67	30.37	13.61	3.75	0.01	0.08	0.39	-0.00	0.03	-0.04	100.88
PLAG_D_106	105	52.81	30.11	13.23	3.97	0.01	0.08	0.35	0.00	0.03	-0.03	100.58
PLAG_D_107	106	53.27	30.12	13.18	4.13	0.02	0.08	0.37	-0.00	0.03	-0.03	101.16
PLAG_D_108	107	53.31	29.78	13.09	4.20	0.02	0.07	0.38	0.01	0.03	-0.03	100.87
PLAG_D_109	108	53.22	29.54	12.81	4.11	0.02	0.09	0.70	0.00	0.04	-0.03	100.48
PLAG_D_110	109	53.02	29.73	13.00	4.04	0.02	0.08	0.52	-0.00	0.04	-0.04	100.41
PLAG_D_111	110	52.80	30.19	13.55	3.80	0.02	0.07	0.38	0.00	0.04	-0.04	100.81
PLAG_D_112	111	52.60	30.22	13.40	3.77	0.02	0.08	0.35	0.01	0.04	-0.03	100.46
PLAG_D_113	112	52.72	30.05	13.47	3.83	0.02	0.08	0.37	0.01	0.05	-0.04	100.55
PLAG_D_114	113	52.92	29.67	12.87	4.02	0.02	0.10	0.36	0.00	0.04	-0.03	99.97
PLAG_D_115	114	52.38	30.11	13.24	3.74	0.02	0.09	0.38	0.00	0.05	-0.04	99.97
PLAG_D_116	115	52.11	30.36	13.69	3.37	0.02	0.08	0.40	0.00	0.05	-0.04	100.04
PLAG_D_117	116	51.55	30.71	14.07	3.33	0.02	0.09	0.40	0.00	0.05	-0.03	100.19
PLAG_D_118	117	51.70	30.57	14.02	3.42	0.02	0.07	0.42	-0.00	0.05	-0.03	100.24
PLAG_D_119	118	51.97	30.68	13.85	3.53	0.02	0.08	0.42	0.00	0.04	-0.03	100.57
PLAG_D_120	119	52.35	30.64	13.69	3.59	0.03	0.07	0.45	-0.00	0.04	-0.03	100.82
PLAG_D_121	120	52.53	30.12	13.47	3.59	0.03	0.07	0.41	0.00	0.03	-0.04	100.21
PLAG_D_122	121	53.27	29.71	12.95	4.00	0.03	0.08	0.38	-0.00	0.03	-0.03	100.41
PLAG_D_123	122	54.44	29.09	12.28	4.40	0.03	0.09	0.38	-0.01	0.03	-0.03	100.69
PLAG_D_124	123	54.78	28.73	11.89	4.79	0.03	0.09	0.36	0.00	0.03	-0.03	100.68

Sample	Distance (μm)	SiO_2	Al_2O_3	CaO	Na_2O	MgO	K_2O	FeO	MnO	TiO_2	P_2O_5	Total
PLAG_D_125	124	55.82	28.30	11.34	4.97	0.03	0.12	0.32	0.00	0.03	-0.03	100.89
PLAG_D_126	125	56.23	27.90	10.93	5.28	0.03	0.12	0.29	0.00	0.04	-0.04	100.79
PLAG_D_127	126	56.57	27.79	10.76	5.42	0.03	0.13	0.33	0.00	0.03	-0.03	101.02
PLAG_D_128	127	56.67	27.81	10.49	5.51	0.02	0.13	0.31	0.00	0.03	-0.03	100.96
PLAG_D_129	128	56.58	27.89	10.71	5.32	0.02	0.13	0.30	-0.00	0.03	-0.04	100.95
PLAG_D_130	129	55.77	28.21	10.98	5.09	0.02	0.11	0.31	-0.00	0.03	-0.03	100.49
PLAG_D_131	130	55.90	28.21	11.23	5.19	0.02	0.11	0.30	-0.00	0.03	-0.04	100.95
PLAG_D_132	131	55.81	28.14	11.29	5.19	0.02	0.11	0.29	-0.00	0.03	-0.04	100.84
PLAG_D_133	132	55.38	28.48	11.20	4.99	0.02	0.11	0.29	-0.00	0.03	-0.04	100.45
PLAG_D_134	133	54.97	28.90	11.70	4.85	0.02	0.10	0.31	-0.00	0.03	-0.04	100.83
PLAG_D_135	134	55.18	28.47	11.62	4.83	0.02	0.10	0.32	0.00	0.03	-0.04	100.53
PLAG_D_136	135	55.48	28.36	11.16	4.94	0.02	0.10	0.32	0.00	0.03	-0.03	100.38
PLAG_D_137	136	55.29	28.61	11.39	4.75	0.02	0.10	0.33	-0.00	0.03	-0.03	100.48
PLAG_D_138	137	55.27	28.72	11.47	5.02	0.02	0.10	0.36	0.00	0.03	-0.04	100.95
PLAG_D_139	138	56.16	27.70	10.67	5.12	0.02	0.11	0.33	-0.00	0.03	-0.04	100.11
PLAG_D_140	139	56.55	27.46	10.42	5.50	0.02	0.12	0.34	0.01	0.03	-0.04	100.41
PLAG_D_141	140	56.66	27.59	10.54	5.40	0.02	0.12	0.31	-0.00	0.03	-0.04	100.64
PLAG_D_142	141	56.87	27.74	10.55	5.53	0.02	0.12	0.36	-0.00	0.03	-0.04	101.18
PLAG_D_143	142	56.41	27.71	10.57	5.50	0.02	0.12	0.31	0.00	0.03	-0.03	100.64
PLAG_D_144	143	56.36	27.86	10.63	5.36	0.02	0.12	0.31	0.01	0.04	-0.03	100.67
PLAG_D_145	144	56.44	27.72	10.74	5.35	0.02	0.12	0.29	0.00	0.03	-0.04	100.67
PLAG_D_146	145	56.65	27.60	10.39	5.29	0.02	0.13	0.35	-0.00	0.03	-0.04	100.42
PLAG_D_147	146	56.30	27.72	10.66	5.39	0.02	0.13	0.34	-0.00	0.03	-0.04	100.55
PLAG_D_148	147	56.69	27.46	10.54	5.36	0.02	0.12	0.32	0.00	0.03	-0.04	100.49
PLAG_D_149	148	56.47	27.77	10.52	5.26	0.02	0.12	0.32	-0.00	0.03	-0.03	100.47
PLAG_D_150	149	56.88	27.71	10.49	5.50	0.02	0.12	0.32	0.01	0.03	-0.04	101.03

Table A1.2. Orthopyroxene major element compositions obtained by electron microprobe and expressed in wt %.
Data from the Soufrière Hills volcano (Montserrat, Lesser Antilles)

Sample	Distance (μm)	SiO_2	Al_2O_3	CaO	K_2O	MgO	Na_2O	TiO_2	Cr_2O_3	FeO	MnO	Total
MT-1D_B_R2C_01	0	52.86	0.26	3.57	-0.00	12.60	0.06	0.14	-0.02	29.90	0.95	100.32
MT-1D_B_R2C_02	1	51.38	0.26	3.45	0.00	12.85	0.05	0.17	-0.01	30.88	0.97	100.01
MT-1D_B_R2C_03	2	50.78	0.27	3.34	0.00	12.60	0.05	0.17	0.00	31.31	0.99	99.51
MT-1D_B_R2C_04	3	50.26	0.33	3.41	0.04	12.86	0.06	0.18	0.01	31.58	1.00	99.73
MT-1D_B_R2C_05	4	50.65	1.06	11.54	0.02	13.93	0.21	0.26	-0.00	21.72	0.76	100.16
MT-1D_B_R2C_06	5	51.74	1.72	18.42	0.00	15.55	0.20	0.33	-0.01	11.14	0.53	99.63
MT-1D_B_R2C_07	6	52.04	2.06	19.04	0.02	15.85	0.19	0.30	0.00	10.06	0.50	100.07
MT-1D_B_R2C_08	7	51.96	2.07	19.07	-0.00	15.93	0.19	0.28	-0.00	10.07	0.48	100.05
MT-1D_B_R2C_09	8	51.58	1.86	19.07	0.00	15.88	0.18	0.23	-0.01	9.49	0.49	98.77
MT-1D_B_R2C_10	9	52.51	2.04	19.41	-0.00	16.17	0.17	0.28	-0.01	9.21	0.43	100.21
MT-1D_B_R2C_11	10	52.13	2.67	19.59	-0.01	15.73	0.19	0.36	0.01	9.42	0.41	100.51
MT-1D_B_R2C_12	11	51.54	2.67	20.25	-0.01	15.20	0.19	0.41	0.00	9.03	0.42	99.70
MT-1D_B_R2C_13	12	51.98	2.40	20.37	0.00	15.40	0.22	0.30	0.00	9.01	0.43	100.12
MT-1D_B_R2C_14	13	50.79	3.91	21.12	0.02	14.58	0.21	0.53	0.01	8.91	0.37	100.44
MT-1D_B_R2C_15	14	48.79	5.73	21.49	0.01	13.59	0.23	0.89	0.01	8.98	0.25	99.97
MT-1D_B_R2C_16	15	48.20	6.34	21.53	-0.01	13.43	0.22	0.98	-0.01	9.05	0.20	99.94
MT-1D_B_R2C_17	16	47.84	6.46	21.58	0.01	13.45	0.23	1.00	-0.01	9.00	0.22	99.77
MT-1D_B_R2C_18	17	47.49	6.67	21.69	-0.00	13.32	0.23	1.06	0.01	9.02	0.21	99.70
MT-1D_B_R2C_19	18	47.95	6.32	21.81	0.01	13.39	0.24	0.97	0.01	8.82	0.22	99.74
MT-1D_B_R2C_20	19	48.01	6.23	21.87	-0.00	13.35	0.24	0.96	-0.00	8.94	0.22	99.81
MT-1D_B_R2C_21	20	48.20	6.15	21.77	0.01	13.47	0.22	0.89	0.00	8.83	0.22	99.76
MT-1D_B_R2C_22	21	48.55	6.01	21.69	0.00	13.71	0.23	0.89	-0.00	8.72	0.21	100.00
MT-1D_B_R2C_23	22	48.75	5.59	21.69	-0.00	13.86	0.22	0.84	0.00	8.81	0.23	99.99
MT-1D_B_R2C_24	23	49.65	4.45	21.63	-0.01	14.12	0.19	0.62	-0.02	8.67	0.24	99.55
MT-1D_B_R2C_25	24	48.43	5.88	21.70	0.02	13.38	0.23	0.90	0.00	9.30	0.24	100.09
MT-1D_B_R2C_26	25	49.20	5.14	21.96	0.01	13.73	0.22	0.79	-0.01	8.90	0.24	100.20
MT-1D_B_R2C_27	26	48.62	5.79	21.92	-0.01	13.41	0.23	0.83	0.01	9.02	0.22	100.05
MT-1D_B_R2C_28	27	47.79	6.60	22.00	-0.00	12.95	0.25	0.97	0.00	9.33	0.23	100.12
MT-1D_B_R2C_29	28	47.60	6.77	21.98	0.00	12.90	0.24	1.07	0.00	9.30	0.23	100.10
MT-1D_B_R2C_30	29	47.23	6.87	21.93	0.01	12.79	0.24	1.08	-0.01	9.37	0.23	99.74
MT-1D_B_R2C_31	30	47.44	6.66	21.77	-0.00	12.95	0.24	1.02	-0.00	9.21	0.24	99.53
MT-1D_B_R2C_32	31	47.37	6.70	22.01	0.02	12.83	0.22	1.03	-0.01	9.34	0.21	99.71
MT-1D_B_R2C_33	32	46.94	6.98	22.08	0.00	12.64	0.23	1.19	-0.00	9.49	0.22	99.75
MT-1D_B_R2C_34	33	46.09	6.73	21.85	0.01	12.33	0.23	1.17	-0.01	9.23	0.23	97.86

Sample	Distance (μm)	SiO_2	Al_2O_3	CaO	K_2O	MgO	Na_2O	TiO_2	Cr_2O_3	FeO	MnO	Total
MT-1D_B_R2C_35	34	46.92	7.05	21.98	-0.02	12.65	0.23	1.14	0.01	9.45	0.23	99.65
MT-1D_B_R2C_36	35	46.61	7.16	21.26	0.02	12.88	0.22	1.14	0.02	9.71	0.25	99.26
MT-1D_B_R2C_37	36	47.17	7.15	22.00	0.01	12.64	0.24	1.18	-0.01	9.41	0.24	100.03
MT-1D_B_R2C_38	37	46.96	7.12	21.78	0.00	12.60	0.25	1.18	-0.00	9.37	0.23	99.50
MT-1D_B_R2C_39	38	46.84	7.15	21.72	-0.00	12.56	0.26	1.25	-0.00	9.53	0.23	99.54
MT-1D_B_R2C_40	39	47.03	7.18	21.80	-0.00	12.64	0.24	1.23	0.00	9.45	0.24	99.82
MT-1D_B_R2C_41	40	47.11	7.12	21.73	-0.01	12.69	0.25	1.19	0.01	9.74	0.24	100.06
MT-1D_B_R2C_42	41	47.48	7.12	21.98	-0.00	12.91	0.25	1.24	0.01	9.64	0.25	100.88
MT-1D_B_R2C_43	42	47.29	6.90	21.44	0.00	12.84	0.24	1.19	-0.00	9.46	0.23	99.58
MT-1D_B_R2C_44	43	46.91	6.93	21.52	-0.01	12.83	0.25	1.18	0.01	9.67	0.24	99.54
MT-1D_B_R2C_45	44	46.93	6.82	21.45	-0.00	12.87	0.27	1.20	0.01	9.47	0.26	99.27
MT-1D_B_R2C_46	45	47.29	6.77	21.37	0.00	12.96	0.26	1.16	0.00	9.48	0.23	99.53
MT-1D_B_R2C_47	46	47.88	6.39	20.61	0.01	13.20	0.25	1.10	0.01	9.91	0.28	99.65
MT-1D_B_R2C_48	47	49.78	4.17	17.41	-0.01	15.13	0.22	0.62	0.00	11.69	0.45	99.44
MT-1D_B_R2C_49	48	52.30	1.41	4.04	0.01	20.33	0.03	0.23	0.01	21.15	1.06	100.58
MT-1D_B_R2C_50	49	51.16	2.63	16.37	0.00	15.88	0.17	0.36	0.01	11.98	0.51	99.06
MT-1D_B_R2C_51	50	51.79	2.52	10.70	0.01	17.47	0.14	0.31	-0.01	16.03	0.80	99.77
MT-1D_B_R2C_52	51	53.32	1.27	2.80	0.00	20.31	0.04	0.16	0.00	21.24	1.15	100.30
MT-1D_B_R2C_53	52	51.75	1.77	1.82	0.03	19.19	0.15	0.18	0.01	23.31	1.15	99.36
MT-1D_B_R2C_54	53	55.77	2.82	1.53	0.11	17.36	0.35	0.13	-0.01	18.78	1.18	98.01
MT-1D_B_R2C_55	54	54.31	1.36	1.39	0.04	20.71	0.35	0.11	-0.00	20.44	1.36	100.07
MT-1D_B_R2C_56	55	53.07	0.53	1.49	0.01	21.44	0.03	0.12	-0.01	21.36	1.42	99.47
MT-1D_B_R2C_57	56	52.43	0.48	1.53	-0.00	21.09	0.02	0.12	-0.01	21.36	1.34	98.35
MT-1D_B_R2C_58	57	52.69	0.46	1.58	-0.02	20.93	0.01	0.13	0.01	22.07	1.35	99.21
MT-1D_B_R2C_59	58	52.94	0.49	1.60	-0.02	20.75	0.02	0.12	-0.00	22.36	1.33	99.58
MT-1D_B_R2C_60	59	52.65	0.50	1.58	-0.00	20.70	0.03	0.12	0.01	22.55	1.36	99.49
MT-1D_B_R2C_61	60	52.74	0.53	1.56	0.01	20.50	0.01	0.11	-0.00	22.77	1.36	99.58
MT-1D_B_R2C_62	61	52.79	0.50	1.56	-0.01	20.27	0.00	0.11	0.00	23.07	1.35	99.65
MT-1D_B_R2C_63	62	52.41	0.47	1.56	0.00	20.15	0.01	0.12	0.01	23.26	1.35	99.34
MT-1D_B_R2C_64	63	52.74	0.43	1.48	-0.00	20.24	0.00	0.08	-0.01	23.37	1.40	99.71
MT-1D_B_R2C_65	64	52.58	0.41	1.45	0.01	20.07	0.01	0.11	0.01	23.32	1.40	99.36
MT-1D_B_R2C_66	65	52.44	0.41	1.39	0.01	20.18	0.02	0.10	0.01	23.52	1.40	99.48
MT-1D_B_R2C_67	66	52.75	0.38	1.34	-0.01	20.15	0.02	0.08	0.00	23.36	1.43	99.49
MT-1D_B_R2C_68	67	52.77	0.40	1.26	0.01	20.05	0.01	0.08	-0.01	23.63	1.44	99.65
MT-1D_B_R2C_69	68	52.44	0.47	1.19	0.01	20.04	0.01	0.08	0.01	23.73	1.43	99.41
MT-1D_B_R2C_70	69	52.24	0.61	1.12	-0.01	19.83	0.01	0.10	0.00	23.88	1.45	99.24
MT-1D_B_R2C_71	70	52.15	0.63	1.06	0.02	19.93	0.02	0.12	-0.00	24.00	1.46	99.39
MT-1D_B_R2C_72	71	52.24	0.68	1.03	-0.01	19.91	0.02	0.09	-0.01	24.17	1.46	99.58
MT-1D_B_R2C_73	72	52.16	0.66	1.02	-0.03	19.91	0.01	0.08	-0.00	24.14	1.52	99.47

Sample	Distance (μm)	SiO_2	Al_2O_3	CaO	K_2O	MgO	Na_2O	TiO_2	Cr_2O_3	FeO	MnO	Total
MT-1D_B_R2C_74	73	51.83	0.69	0.96	0.01	19.88	0.01	0.11	-0.00	24.10	1.49	99.06
MT-1D_B_R2C_75	74	51.86	0.70	0.96	-0.01	19.79	0.01	0.10	-0.00	24.18	1.54	99.12
MT-1D_B_R2C_76	75	51.99	0.71	0.97	0.01	19.77	0.01	0.09	0.00	24.18	1.55	99.29
MT-1D_B_R2C_77	76	51.94	0.70	0.96	-0.00	19.71	0.02	0.09	0.00	24.24	1.57	99.23
MT-1D_B_R2C_78	77	51.94	0.74	0.97	-0.01	19.67	0.00	0.09	0.00	24.31	1.53	99.24
MT-1D_B_R2C_79	78	52.22	0.71	0.99	-0.01	19.70	0.01	0.11	-0.02	24.31	1.61	99.64
MT-1D_B_R2C_80	79	52.18	0.64	0.96	-0.01	19.66	0.02	0.09	0.00	24.24	1.64	99.41
MT-1D_B_R2C_81	80	52.27	0.58	0.97	0.01	19.81	0.02	0.08	-0.01	24.15	1.60	99.47
MT-1D_B_R2C_82	81	52.41	0.52	0.98	-0.00	19.93	0.01	0.10	-0.00	24.22	1.63	99.79
MT-1D_B_R2C_83	82	52.36	0.51	0.98	-0.00	19.88	0.01	0.11	-0.01	24.49	1.62	99.95
MT-1D_B_R2C_84	83	52.29	0.55	1.00	0.00	19.87	0.01	0.09	-0.01	24.49	1.65	99.94
MT-1D_B_R2C_85	84	52.33	0.52	1.00	-0.00	19.68	0.02	0.09	-0.00	24.49	1.71	99.82
MT-1D_B_R2C_86	85	52.58	0.50	0.98	-0.00	19.64	0.01	0.07	-0.00	24.22	1.65	99.66
MT-1D_B_R2C_87	86	52.57	0.49	0.99	-0.00	19.77	0.02	0.09	-0.01	24.42	1.66	100.01
MT-1D_B_R2C_88	87	52.46	0.49	0.99	0.01	19.64	0.01	0.08	-0.00	24.24	1.67	99.58
MT-1D_B_R2C_89	88	52.51	0.52	0.99	-0.01	19.77	0.03	0.08	0.01	24.56	1.69	100.14
MT-1D_B_R2C_90	89	52.19	0.56	1.00	0.03	19.45	0.00	0.06	-0.00	24.56	1.66	99.51
MT-1D_B_R2C_91	90	52.29	0.61	0.98	0.01	19.59	0.01	0.09	-0.01	24.72	1.67	99.96
MT-1D_B_R2C_92	91	52.18	0.62	1.00	-0.02	19.50	0.01	0.08	0.00	24.59	1.74	99.71
MT-1D_B_R2C_93	92	51.87	0.66	0.97	-0.01	19.44	0.02	0.09	-0.00	24.85	1.73	99.61
MT-1D_B_R2C_94	93	52.31	0.66	0.98	-0.00	19.52	0.01	0.09	-0.00	24.62	1.70	99.87
MT-1D_B_R2C_95	94	52.01	0.67	0.96	-0.01	19.41	0.01	0.08	-0.01	24.82	1.69	99.62
MT-1D_B_R2C_96	95	52.11	0.69	0.94	0.01	19.44	0.00	0.06	0.00	24.72	1.70	99.68
MT-1D_B_R2C_97	96	51.91	0.64	0.97	-0.01	19.36	0.01	0.09	0.00	24.50	1.73	99.20
MT-1D_B_R2C_98	97	51.88	0.64	0.95	-0.00	19.44	0.00	0.09	0.01	24.72	1.75	99.48
MT-1D_B_R2C_99	98	56.05	0.71	1.06	0.02	21.01	0.03	0.12	0.02	26.68	1.83	107.51
MT-1D_B_R2C_100	99	51.75	0.62	0.95	0.00	19.37	0.00	0.11	-0.02	24.86	1.67	99.31
MT-1D_B_R2C_101	100	51.71	0.61	0.95	-0.02	19.30	0.01	0.07	-0.00	24.77	1.67	99.08
MT-1D_B_R2C_102	101	52.02	0.61	0.98	0.01	19.45	0.02	0.11	0.00	24.90	1.70	99.81
MT-1D_B_R2C_103	102	51.71	0.63	0.95	-0.01	19.36	0.01	0.09	0.01	25.05	1.74	99.54
MT-1D_B_R2C_104	103	50.95	0.58	0.97	-0.00	19.76	0.03	0.08	0.01	24.83	1.72	98.93
MT-1D_B_R2C_105	104	47.23	0.50	0.94	0.00	19.40	0.01	0.09	-0.00	24.70	1.72	94.58
MT-1D_B_R2C_106	105	46.35	0.47	0.95	0.00	19.47	0.02	0.07	0.01	24.64	1.73	93.71
MT-1D_B_R2C_107	106	46.37	0.46	0.93	-0.00	19.13	0.01	0.11	-0.00	24.47	1.69	93.16
MT-1D_B_R2C_108	107	46.68	0.44	0.94	-0.01	18.31	0.02	0.08	0.01	23.67	1.65	91.80
MT-1D_B_R2C_109	108	47.17	0.47	0.91	-0.02	14.80	-0.04	0.08	-0.02	23.98	1.67	88.99
MT-1D_B_R2C_110	109	34.79	0.38	0.57	-0.02	8.01	-0.03	0.05	-0.03	12.04	0.80	56.56
MT-1D_B_R2C_111	110	49.71	0.51	0.91	0.00	9.36	-0.07	0.08	-0.01	24.25	1.63	86.37
MT-1D_B_R2C_112	111	53.61	0.58	0.96	-0.02	16.88	0.00	0.09	-0.01	24.29	1.67	98.05

Sample	Distance (μm)	SiO_2	Al_2O_3	CaO	K_2O	MgO	Na_2O	TiO_2	Cr_2O_3	FeO	MnO	Total
MT-1D_B_R2C_113	112	53.06	0.53	0.97	0.01	19.72	0.02	0.09	-0.00	24.96	1.69	101.04
MT-1D_B_R2C_114	113	54.68	0.55	0.98	0.03	19.15	0.02	0.10	0.00	24.78	1.71	102.01
MT-1D_B_R2C_115	114	51.54	0.51	0.95	-0.00	21.18	0.05	0.08	-0.00	24.75	1.70	100.77
MT-1D_B_R2C_116	115	51.81	0.54	1.02	0.01	19.34	0.05	0.09	0.02	24.70	1.70	99.27
MT-1D_B_R2C_117	116	53.52	0.50	1.00	-0.00	19.43	0.02	0.10	0.00	25.05	1.70	101.32
MT-1D_B_R2C_118	117	52.61	0.48	0.98	0.01	19.31	0.00	0.08	0.00	24.85	1.73	100.05
MT-1D_B_R2C_119	118	52.19	0.46	0.98	-0.01	19.34	0.00	0.10	-0.00	24.92	1.72	99.69
MT-1D_B_R2C_120	119	52.11	0.48	0.96	0.00	19.42	0.03	0.09	-0.01	24.86	1.70	99.65
MT-1D_B_R2C_121	120	52.35	0.48	0.96	0.00	19.38	0.02	0.10	-0.00	25.07	1.70	100.08
MT-1D_B_R2C_122	121	52.10	0.47	0.98	0.01	19.45	0.01	0.09	-0.00	25.08	1.71	99.89
MT-1D_B_R2C_123	122	52.41	0.45	0.97	-0.00	19.34	0.01	0.10	-0.01	24.96	1.72	99.95
MT-1D_B_R2C_124	123	51.79	0.44	1.00	0.00	19.24	0.02	0.11	-0.01	24.90	1.73	99.21
MT-1D_B_R2C_125	124	51.92	0.45	1.00	-0.00	19.22	0.01	0.11	0.00	24.56	1.71	98.97
MT-1D_B_R2C_126	125	51.72	0.42	0.98	0.01	19.29	0.01	0.10	0.01	24.62	1.69	98.85
MT-1D_B_R2C_127	126	52.28	0.43	0.96	-0.00	19.27	0.02	0.08	-0.01	24.60	1.71	99.34
MT-1D_B_R2C_128	127	52.02	0.45	0.99	-0.00	19.43	0.01	0.10	0.01	24.99	1.70	99.70
MT-1D_B_R2C_129	128	52.30	0.48	1.01	-0.01	19.26	0.00	0.11	-0.00	24.91	1.71	99.78
MT-1D_B_R2C_130	129	52.12	0.49	0.99	-0.00	19.35	0.01	0.10	-0.00	24.76	1.72	99.54
MT-1D_B_R2C_131	130	52.09	0.48	1.03	0.01	19.24	0.02	0.12	-0.01	24.99	1.68	99.66
MT-1D_B_R2C_132	131	51.77	0.47	1.01	0.00	19.28	0.00	0.12	-0.01	24.92	1.67	99.23
MT-1D_B_R2C_133	132	52.01	0.47	1.03	0.01	19.21	0.00	0.10	-0.01	24.91	1.73	99.46
MT-1D_B_R2C_134	133	51.96	0.48	1.03	-0.01	19.21	0.02	0.10	0.02	24.87	1.71	99.39
MT-1D_B_R2C_135	134	52.09	0.45	1.02	-0.00	19.32	0.02	0.08	0.00	25.01	1.72	99.70
MT-1D_B_R2C_136	135	51.63	0.49	1.02	0.00	19.32	0.01	0.10	0.00	24.97	1.72	99.25
MT-1D_B_R2C_137	136	52.05	0.47	1.02	-0.01	19.19	0.02	0.13	-0.01	24.94	1.70	99.50
MT-1D_B_R2C_138	137	51.99	0.48	1.03	-0.00	19.38	0.02	0.11	-0.00	24.84	1.67	99.51
MT-1D_B_R2C_139	138	51.83	0.47	1.02	-0.01	19.32	0.01	0.11	-0.00	25.01	1.68	99.44
MT-1D_B_R2C_140	139	52.14	0.45	1.04	0.01	19.24	0.02	0.12	0.00	24.65	1.72	99.38
MT-1D_B_R2C_141	140	51.97	0.46	1.06	-0.01	19.20	0.01	0.11	0.01	24.88	1.72	99.40
MT-1D_B_R2C_142	141	52.16	0.43	1.04	-0.01	19.25	0.01	0.11	0.01	24.76	1.69	99.44
MT-1D_B_R2C_143	142	52.08	0.43	1.04	0.01	19.32	0.01	0.12	0.01	25.00	1.73	99.75
MT-1D_B_R2C_144	143	52.41	0.43	1.03	0.01	19.36	0.01	0.08	-0.01	24.92	1.70	99.94
MT-1D_B_R2C_145	144	52.09	0.43	1.05	-0.00	19.32	0.01	0.11	-0.00	24.95	1.67	99.62
MT-1D_B_R2C_146	145	52.14	0.44	1.04	0.00	19.42	0.02	0.11	-0.01	24.92	1.67	99.74
MT-1D_B_R2C_147	146	52.34	0.43	1.05	-0.01	19.48	0.01	0.11	-0.01	24.89	1.67	99.95
MT-1D_B_R2C_148	147	52.20	0.44	1.05	-0.01	19.33	0.01	0.10	-0.01	24.77	1.68	99.56
MT-1D_B_R2C_149	148	52.07	0.43	1.02	-0.00	19.41	0.01	0.11	-0.00	24.90	1.72	99.65
MT-1D_B_R2C_150	149	51.98	0.44	1.07	-0.02	19.55	0.01	0.10	-0.01	24.84	1.70	99.65
MT-1D_B_R2C_151	150	52.05	0.40	1.06	0.00	19.51	0.01	0.10	0.01	25.01	1.72	99.88

Sample	Distance (μm)	SiO_2	Al_2O_3	CaO	K_2O	MgO	Na_2O	TiO_2	Cr_2O_3	FeO	MnO	Total
MT-1D_B_R2C_152	151	51.86	0.43	1.04	0.01	19.46	0.02	0.10	-0.01	24.80	1.68	99.39
MT-1D_B_R2C_153	152	51.91	0.40	1.02	-0.01	19.36	0.01	0.09	0.01	24.61	1.71	99.12
MT-1D_B_R2C_154	153	51.90	0.42	1.03	-0.02	19.35	0.02	0.12	-0.01	24.67	1.68	99.16
MT-1D_B_R2C_155	154	51.70	0.42	1.04	-0.02	19.50	0.01	0.11	-0.00	24.90	1.75	99.39
MT-1D_B_R2C_156	155	51.63	0.44	1.03	-0.02	19.26	0.01	0.08	0.00	24.68	1.68	98.80
MT-1D_B_R2C_157	156	52.01	0.42	1.01	-0.00	19.33	0.02	0.10	-0.01	24.81	1.68	99.37
MT-1D_B_R2C_158	157	51.76	0.44	1.02	-0.00	19.24	0.02	0.07	-0.01	24.98	1.69	99.22
MT-1D_B_R2C_159	158	52.03	0.44	1.04	-0.01	19.33	0.02	0.07	-0.01	24.85	1.70	99.46
MT-1D_B_R2C_160	159	51.68	0.43	1.00	0.02	19.39	0.00	0.11	0.01	24.72	1.69	99.05
MT-1D_B_R2C_161	160	51.87	0.47	0.97	-0.01	19.34	0.02	0.09	-0.01	24.78	1.66	99.18
MT-1D_B_R2C_162	161	51.50	0.45	1.01	-0.00	19.28	0.02	0.08	-0.01	24.83	1.69	98.85
MT-1D_B_R2C_163	162	52.07	0.43	1.04	0.01	19.42	0.01	0.10	-0.00	24.82	1.66	99.56
MT-1D_B_R2C_164	163	51.84	0.40	1.02	-0.01	19.53	0.01	0.09	-0.00	24.67	1.68	99.23
MT-1D_B_R2C_165	164	51.65	0.40	1.02	-0.01	19.51	0.01	0.08	0.01	24.74	1.70	99.11
MT-1D_B_R2C_166	165	51.95	0.37	1.00	0.00	19.42	0.00	0.08	0.01	24.70	1.67	99.20
MT-1D_B_R2C_167	166	51.94	0.38	0.99	0.01	19.52	0.01	0.08	-0.00	24.64	1.72	99.28
MT-1D_B_R2C_168	167	52.00	0.33	1.00	-0.00	19.58	0.01	0.09	-0.00	24.84	1.66	99.50
MT-1D_B_R2C_169	168	51.92	0.33	1.00	-0.00	19.53	0.01	0.05	-0.02	24.61	1.70	99.13
MT-1D_B_R2C_170	169	51.93	0.33	1.00	-0.01	19.39	0.01	0.08	-0.01	24.67	1.67	99.07
MT-1D_B_R2C_171	170	52.17	0.34	1.02	-0.01	19.45	0.00	0.08	0.01	24.70	1.65	99.42
MT-1D_B_R2C_172	171	51.88	0.33	0.98	0.00	19.52	0.01	0.07	0.00	24.61	1.72	99.13
MT-1D_B_R2C_173	172	51.94	0.34	0.98	-0.00	19.44	0.02	0.07	0.00	24.68	1.68	99.15
MT-1D_B_R2C_174	173	51.85	0.35	1.00	0.00	19.33	0.02	0.08	-0.00	24.74	1.68	99.04
MT-1D_B_R2C_175	174	52.05	0.37	1.00	-0.00	19.55	0.00	0.10	0.02	24.72	1.68	99.48
MT-1D_B_R2C_176	175	52.32	0.37	1.02	-0.01	19.43	0.01	0.08	-0.01	24.75	1.71	99.67
MT-1D_B_R2C_177	176	52.11	0.36	0.99	0.01	19.56	0.01	0.10	-0.01	24.71	1.72	99.56
MT-1D_B_R2C_178	177	52.22	0.40	0.97	0.01	19.54	0.01	0.10	0.00	24.63	1.69	99.58
MT-1D_B_R2C_179	178	52.13	0.41	0.98	-0.00	19.44	0.01	0.09	0.01	24.86	1.69	99.62
MT-1D_B_R2C_180	179	51.99	0.43	1.00	0.00	19.42	0.02	0.08	-0.00	24.83	1.65	99.41
MT-1D_B_R2C_181	180	51.76	0.44	0.98	0.00	19.48	0.01	0.07	0.02	24.55	1.69	99.02
MT-1D_B_R2C_182	181	52.05	0.45	0.98	0.00	19.64	0.02	0.09	0.00	24.77	1.69	99.69
MT-1D_B_R2C_183	182	51.73	0.46	0.97	-0.01	19.41	0.01	0.10	-0.01	25.06	1.65	99.38
MT-1D_B_R2C_184	183	51.92	0.48	0.98	-0.01	19.48	0.02	0.10	-0.00	24.55	1.69	99.21
MT-1D_B_R2C_185	184	51.77	0.52	0.99	0.00	19.44	0.01	0.09	-0.02	24.70	1.66	99.16
MT-1D_B_R2C_186	185	51.91	0.57	1.00	-0.01	19.47	0.02	0.10	0.01	24.74	1.65	99.45
MT-1D_B_R2C_187	186	51.55	0.61	0.98	0.00	19.33	0.02	0.11	-0.00	24.89	1.65	99.13
MT-1D_B_R2C_188	187	51.82	0.60	0.99	-0.02	19.29	0.01	0.09	0.01	24.88	1.65	99.32
MT-1D_B_R2C_189	188	51.48	0.64	0.98	-0.02	19.41	0.01	0.09	0.00	24.89	1.66	99.14
MT-1D_B_R2C_190	189	51.82	0.62	1.01	0.01	19.26	0.01	0.11	0.00	24.86	1.66	99.37

Sample	Distance (μm)	SiO_2	Al_2O_3	CaO	K_2O	MgO	Na_2O	TiO_2	Cr_2O_3	FeO	MnO	Total
MT-1D_B_R2C_191	190	51.96	0.63	0.97	-0.01	19.19	0.01	0.11	-0.00	24.77	1.68	99.29
MT-1D_B_R2C_192	191	51.69	0.57	0.96	-0.01	19.30	0.02	0.09	-0.01	24.70	1.70	99.01
MT-1D_B_R2C_193	192	51.95	0.56	1.02	-0.01	19.41	0.02	0.10	-0.00	24.75	1.66	99.44
MT-1D_B_R2C_194	193	52.10	0.51	0.96	0.01	19.49	0.01	0.05	0.00	24.72	1.68	99.56
MT-1D_B_R2C_195	194	52.18	0.50	1.00	-0.01	19.50	0.02	0.09	0.02	24.81	1.63	99.73
MT-1D_B_R2C_196	195	52.12	0.44	0.97	0.02	19.47	0.01	0.07	0.01	24.76	1.69	99.55
MT-1D_B_R2C_197	196	52.51	0.44	0.99	-0.00	19.55	0.02	0.09	-0.01	24.91	1.67	100.15
MT-1D_B_R2C_198	197	52.13	0.43	1.01	0.00	19.43	0.01	0.10	-0.01	24.60	1.64	99.35
MT-1D_B_R2C_199	198	52.17	0.42	0.97	0.01	19.49	0.01	0.10	-0.02	24.83	1.65	99.62
MT-1D_B_R2C_200	199	52.21	0.41	0.99	-0.00	19.37	0.01	0.09	0.01	24.56	1.70	99.34
MT-1D_B_R2C_201	200	52.55	0.40	1.00	-0.00	19.49	0.02	0.08	-0.00	24.84	1.66	100.04
MT-1D_B_R2C_202	201	52.30	0.42	1.00	0.01	19.58	0.00	0.10	-0.00	24.47	1.71	99.59
MT-1D_B_R2C_203	202	52.38	0.42	1.00	0.01	19.57	0.01	0.09	0.01	24.55	1.65	99.69
MT-1D_B_R2C_204	203	52.05	0.42	0.97	0.01	19.51	0.02	0.10	-0.01	24.60	1.69	99.36
MT-1D_B_R2C_205	204	52.38	0.42	1.03	0.02	19.61	0.02	0.10	-0.00	24.78	1.67	100.01
MT-1D_B_R2C_206	205	52.33	0.41	0.99	-0.01	19.55	0.01	0.08	0.00	24.57	1.68	99.61
MT-1D_B_R2C_207	206	52.50	0.39	0.98	0.01	19.47	0.02	0.12	0.01	24.70	1.68	99.88
MT-1D_B_R2C_208	207	52.46	0.38	0.98	-0.01	19.53	0.02	0.09	0.00	24.61	1.65	99.71
MT-1D_B_R2C_209	208	52.33	0.37	0.99	0.01	19.61	0.01	0.10	-0.01	24.67	1.67	99.75
MT-1D_B_R2C_210	209	52.38	0.36	1.00	-0.00	19.66	0.02	0.08	-0.01	24.45	1.67	99.62
MT-1D_B_R2C_211	210	52.30	0.37	1.00	-0.01	19.60	0.01	0.09	-0.01	24.88	1.66	99.89
MT-1D_B_R2C_212	211	52.43	0.35	1.02	-0.01	19.48	0.01	0.09	0.01	24.56	1.67	99.59
MT-1D_B_R2C_213	212	52.15	0.36	1.05	0.01	19.57	0.01	0.07	0.01	24.55	1.66	99.43
MT-1D_B_R2C_214	213	52.31	0.38	1.01	0.00	19.65	0.01	0.05	-0.01	24.62	1.70	99.72
MT-1D_B_R2C_215	214	52.24	0.40	1.01	-0.00	19.43	0.01	0.08	-0.00	24.70	1.67	99.53
MT-1D_E_R2C_01	0	72.90	15.78	4.45	0.82	0.03	2.39	0.18	-0.01	0.86	0.02	97.43
MT-1D_E_R2C_02	1	72.29	15.25	4.38	0.55	0.02	1.61	0.15	-0.01	0.79	0.02	95.05
MT-1D_E_R2C_03	2	61.28	22.42	8.60	0.47	0.04	4.15	0.10	-0.00	0.85	0.02	97.93
MT-1D_E_R2C_04	3	76.81	12.35	2.18	0.91	0.03	1.75	0.31	0.01	0.88	0.02	95.24
MT-1D_E_R2C_05	4	64.30	22.90	7.86	0.69	0.09	2.94	0.09	0.01	0.96	0.02	99.86
MT-1D_E_R2C_06	5	62.26	23.45	8.30	0.52	0.21	2.92	0.07	-0.02	1.06	0.02	98.80
MT-1D_E_R2C_07	6	75.15	12.88	2.75	0.60	0.59	1.65	0.17	-0.00	1.03	0.04	94.84
MT-1D_E_R2C_08	7	69.01	8.77	1.98	0.50	7.87	0.72	0.27	0.00	12.86	0.54	102.54
MT-1D_E_R2C_09	8	54.34	1.50	1.53	0.08	21.11	0.06	0.26	0.00	21.01	0.87	100.76
MT-1D_E_R2C_10	9	52.94	1.07	1.57	0.01	22.82	0.03	0.24	0.00	19.82	0.78	99.27
MT-1D_E_R2C_11	10	52.90	1.76	1.77	0.01	23.77	0.03	0.28	0.01	18.47	0.63	99.62
MT-1D_E_R2C_12	11	51.65	2.91	1.95	0.01	23.91	0.02	0.27	-0.01	17.35	0.55	98.62
MT-1D_E_R2C_13	12	52.62	1.30	1.50	0.01	22.19	0.02	0.15	0.01	21.00	1.24	100.03
MT-1D_E_R2C_14	13	51.97	0.82	0.93	0.02	19.47	0.02	0.13	-0.00	24.77	1.73	99.84

Sample	Distance (μm)	SiO_2	Al_2O_3	CaO	K_2O	MgO	Na_2O	TiO_2	Cr_2O_3	FeO	MnO	Total
MT-1D_E_R2C_15	14	51.95	0.78	0.88	0.02	19.13	0.02	0.09	-0.00	24.81	1.68	99.34
MT-1D_E_R2C_16	15	51.99	0.75	0.86	0.00	19.17	0.03	0.11	0.00	25.12	1.75	99.77
MT-1D_E_R2C_17	16	51.76	0.77	0.89	0.02	19.05	0.02	0.11	0.00	25.27	1.70	99.59
MT-1D_E_R2C_18	17	51.84	0.73	0.88	0.01	18.95	0.02	0.09	0.02	24.98	1.71	99.23
MT-1D_E_R2C_19	18	52.00	0.68	0.92	0.01	19.12	0.03	0.11	-0.00	25.13	1.72	99.70
MT-1D_E_R2C_20	19	51.87	0.66	0.93	0.00	19.07	0.01	0.12	0.01	25.16	1.72	99.56
MT-1D_E_R2C_21	20	51.86	0.57	0.94	0.00	19.21	0.02	0.12	0.00	24.86	1.74	99.33
MT-1D_E_R2C_22	21	52.10	0.56	0.97	0.00	19.17	0.02	0.12	-0.01	24.95	1.70	99.57
MT-1D_E_R2C_23	22	52.16	0.54	0.97	-0.00	18.93	0.03	0.12	-0.01	24.98	1.71	99.43
MT-1D_E_R2C_24	23	52.01	0.54	0.97	0.01	19.12	0.03	0.12	0.00	24.94	1.72	99.46
MT-1D_E_R2C_25	24	52.18	0.52	0.98	0.02	19.24	0.02	0.11	-0.01	25.03	1.71	99.79
MT-1D_E_R2C_26	25	51.89	0.52	1.00	-0.01	19.10	0.02	0.10	0.00	25.11	1.70	99.43
MT-1D_E_R2C_27	26	52.05	0.53	1.00	-0.01	19.10	0.02	0.10	-0.00	25.04	1.76	99.58
MT-1D_E_R2C_28	27	51.71	0.51	1.03	0.01	19.12	0.02	0.10	-0.00	25.03	1.75	99.28
MT-1D_E_R2C_29	28	52.02	0.52	1.02	0.00	19.04	0.03	0.12	-0.01	24.97	1.71	99.42
MT-1D_E_R2C_30	29	52.10	0.53	1.04	0.01	19.06	0.02	0.11	-0.01	25.00	1.70	99.55
MT-1D_E_R2C_31	30	52.15	0.54	1.02	-0.00	19.22	0.02	0.10	-0.01	25.26	1.64	99.92
MT-1D_E_R2C_32	31	51.92	0.57	1.02	0.01	19.20	0.02	0.09	-0.01	25.03	1.71	99.56
MT-1D_E_R2C_33	32	52.02	0.55	1.03	-0.00	19.06	0.02	0.11	-0.01	25.03	1.72	99.53
MT-1D_E_R2C_34	33	52.04	0.56	1.02	0.01	19.20	0.02	0.11	0.00	25.24	1.70	99.91
MT-1D_E_R2C_35	34	52.07	0.58	1.04	0.01	19.15	0.03	0.10	-0.01	25.07	1.69	99.73
MT-1D_E_R2C_36	35	51.97	0.58	1.03	0.00	19.11	0.02	0.10	0.02	25.18	1.69	99.71
MT-1D_E_R2C_37	36	51.65	0.58	0.99	-0.00	19.15	0.02	0.10	-0.01	24.98	1.68	99.14
MT-1D_E_R2C_38	37	51.95	0.58	1.02	0.01	19.14	0.01	0.09	0.00	25.19	1.67	99.66
MT-1D_E_R2C_39	38	51.75	0.60	1.01	0.01	19.18	0.02	0.11	-0.01	25.20	1.70	99.57
MT-1D_E_R2C_40	39	51.76	0.61	1.00	-0.00	19.10	0.03	0.09	0.00	25.09	1.70	99.38
MT-1D_E_R2C_41	40	51.76	0.62	1.05	0.00	19.21	0.02	0.11	0.01	25.02	1.73	99.54
MT-1D_E_R2C_42	41	51.87	0.63	1.01	-0.01	19.14	0.02	0.11	-0.01	25.19	1.71	99.68
MT-1D_E_R2C_43	42	51.98	0.66	0.98	-0.00	19.23	0.02	0.12	0.00	25.03	1.69	99.70
MT-1D_E_R2C_44	43	51.81	0.67	0.99	0.01	19.07	0.01	0.09	0.01	25.10	1.71	99.48
MT-1D_E_R2C_45	44	52.02	0.66	0.98	-0.01	19.21	0.02	0.12	-0.01	25.25	1.69	99.93
MT-1D_E_R2C_46	45	51.89	0.67	0.99	-0.00	19.06	0.02	0.11	-0.00	25.18	1.69	99.60
MT-1D_E_R2C_47	46	51.85	0.67	0.98	-0.00	19.17	0.02	0.10	-0.01	25.16	1.68	99.61
MT-1D_E_R2C_48	47	51.85	0.68	0.98	-0.02	19.06	0.02	0.12	-0.00	25.51	1.71	99.90
MT-1D_E_R2C_49	48	52.02	0.69	0.96	0.01	19.11	0.02	0.12	-0.01	25.09	1.68	99.67
MT-1D_E_R2C_50	49	52.13	0.72	0.97	-0.00	19.14	0.03	0.08	-0.01	25.37	1.67	100.11
MT-1D_E_R2C_51	50	51.83	0.70	0.98	0.01	19.21	0.01	0.11	0.01	25.26	1.66	99.77
MT-1D_E_R2C_52	51	52.09	0.67	0.96	-0.01	19.16	0.02	0.11	-0.00	25.49	1.66	100.15
MT-1D_E_R2C_53	52	51.90	0.64	0.94	0.01	19.19	0.03	0.11	-0.01	25.07	1.70	99.58

Sample	Distance (μm)	SiO_2	Al_2O_3	CaO	K_2O	MgO	Na_2O	TiO_2	Cr_2O_3	FeO	MnO	Total
MT-1D_E_R2C_54	53	52.04	0.61	0.97	0.01	19.27	0.02	0.10	-0.00	25.32	1.72	100.04
MT-1D_E_R2C_55	54	51.90	0.56	0.96	0.01	19.22	0.02	0.11	-0.00	25.11	1.68	99.56
MT-1D_E_R2C_56	55	52.31	0.51	0.97	0.00	19.34	0.02	0.13	-0.01	25.05	1.66	99.97
MT-1D_E_R2C_57	56	52.07	0.49	0.98	0.02	19.26	0.02	0.12	-0.00	25.11	1.71	99.78
MT-1D_E_R2C_58	57	51.99	0.49	0.99	0.00	19.19	0.02	0.08	0.00	25.00	1.69	99.44
MT-1D_E_R2C_59	58	52.15	0.51	1.02	-0.01	19.08	0.04	0.12	-0.01	24.81	1.69	99.41
MT-1D_E_R2C_60	59	52.51	0.50	1.03	-0.01	19.31	0.02	0.11	-0.01	25.06	1.66	100.19
MT-1D_E_R2C_61	60	52.14	0.50	1.07	-0.00	19.20	0.02	0.09	0.00	25.19	1.66	99.87
MT-1D_E_R2C_62	61	52.23	0.50	1.04	-0.01	19.21	0.02	0.10	0.01	24.92	1.68	99.70
MT-1D_E_R2C_63	62	51.05	0.52	2.38	-0.00	18.54	0.03	0.11	-0.00	24.72	1.70	99.04
MT-1D_E_R2C_64	63	51.60	0.56	3.07	0.00	18.11	0.03	0.10	-0.01	24.34	1.67	99.47
MT-1D_E_R2C_65	64	52.92	0.58	1.23	0.01	19.15	0.01	0.13	0.00	25.16	1.67	100.86
MT-1D_E_R2C_66	65	52.57	0.63	1.08	0.01	19.25	0.03	0.10	-0.01	25.04	1.67	100.37
MT-1D_E_R2C_67	66	52.27	0.67	1.05	-0.01	19.15	0.02	0.11	-0.02	25.23	1.67	100.14
MT-1D_E_R2C_68	67	51.95	0.71	1.03	0.02	19.10	0.02	0.14	0.00	25.10	1.65	99.74
MT-1D_E_R2C_69	68	51.91	0.75	1.06	0.01	19.21	0.03	0.13	0.00	24.97	1.67	99.75
MT-1D_E_R2C_70	69	52.09	0.73	1.07	-0.00	19.18	0.02	0.12	-0.01	25.01	1.67	99.89
MT-1D_E_R2C_71	70	52.06	0.71	1.05	0.00	19.23	0.03	0.12	-0.01	25.13	1.66	99.98
MT-1D_E_R2C_72	71	51.99	0.69	1.05	-0.02	19.13	0.02	0.13	-0.00	25.16	1.69	99.83
MT-1D_E_R2C_73	72	52.43	0.65	1.05	-0.00	19.32	0.04	0.10	-0.02	25.18	1.72	100.47
MT-1D_E_R2C_74	73	51.99	0.60	1.04	0.03	19.35	0.03	0.13	0.01	24.95	1.72	99.83
MT-1D_E_R2C_75	74	52.27	0.60	1.02	0.01	19.30	0.03	0.10	-0.00	25.16	1.71	100.18
MT-1D_E_R2C_76	75	52.53	0.58	1.04	-0.01	19.50	0.03	0.10	0.02	25.03	1.70	100.50
MT-1D_E_R2C_77	76	52.28	0.59	1.00	-0.01	19.45	0.02	0.08	-0.00	25.15	1.68	100.24
MT-1D_E_R2C_78	77	52.16	0.58	1.01	0.00	19.35	0.02	0.11	-0.00	24.97	1.71	99.90
MT-1D_E_R2C_79	78	52.03	0.60	0.99	-0.00	19.32	0.02	0.08	-0.01	24.83	1.71	99.57
MT-1D_E_R2C_80	79	52.00	0.59	0.98	-0.01	19.48	0.02	0.11	-0.01	24.92	1.70	99.78
MT-1D_E_R2C_81	80	52.02	0.62	1.01	-0.02	19.48	0.03	0.10	0.00	25.03	1.71	99.98
MT-1D_E_R2C_82	81	52.12	0.61	1.00	0.00	19.34	0.03	0.10	0.01	24.97	1.67	99.85
MT-1D_E_R2C_83	82	52.25	0.64	0.98	0.00	19.38	0.03	0.10	-0.00	24.91	1.69	99.98
MT-1D_E_R2C_84	83	52.17	0.63	0.96	0.01	19.35	0.02	0.09	-0.01	24.97	1.70	99.89
MT-1D_E_R2C_85	84	52.11	0.65	0.95	0.01	19.32	0.02	0.10	-0.00	25.05	1.64	99.85
MT-1D_E_R2C_86	85	52.11	0.65	0.96	0.02	19.52	0.02	0.10	0.00	25.07	1.69	100.15
MT-1D_E_R2C_87	86	52.03	0.69	0.95	0.01	19.37	0.03	0.08	-0.00	24.91	1.73	99.80
MT-1D_E_R2C_88	87	65.46	18.35	6.53	0.45	1.72	2.21	0.15	0.00	4.50	0.24	99.61
MT-1D_E_R2C_89	88	60.04	26.05	10.14	0.30	0.13	3.12	0.06	-0.01	1.17	0.03	101.03
MT-1D_E_R2C_90	89	54.65	28.00	11.67	0.29	0.09	3.65	0.03	-0.01	1.19	0.03	99.57
MT-1D_E_R2C_91	90	54.86	26.12	10.93	0.34	0.78	3.81	0.03	0.00	1.59	0.06	98.52
MT-1D_E_R2C_92	91	53.98	6.99	3.08	0.30	15.90	1.27	0.22	0.00	20.15	0.95	102.85

Sample	Distance (μm)	SiO_2	Al_2O_3	CaO	K_2O	MgO	Na_2O	TiO_2	Cr_2O_3	FeO	MnO	Total
MT-1D_E_R2C_93	92	52.55	1.09	1.35	0.06	20.51	0.11	0.16	-0.01	22.73	1.22	99.77
MT-1D_E_R2C_94	93	51.94	0.71	0.90	0.02	19.21	0.02	0.10	-0.01	25.03	1.72	99.65
MT-1D_E_R2C_95	94	51.78	0.77	0.85	0.01	19.08	0.02	0.12	0.00	25.11	1.72	99.46
MT-1D_E_R2C_96	95	51.69	0.79	0.84	0.01	19.03	0.02	0.11	0.00	25.02	1.70	99.22
MT-1D_E_R2C_97	96	51.50	0.78	0.83	0.01	18.94	0.02	0.11	-0.01	25.21	1.74	99.13
MT-1D_E_R2C_98	97	51.79	0.80	0.81	-0.00	18.96	0.02	0.10	-0.00	25.20	1.75	99.41
MT-1D_E_R2C_99	98	50.96	0.77	0.80	0.00	18.81	0.02	0.10	-0.02	24.84	1.72	98.01
MT-1D_E_R2C_100	99	51.80	0.74	0.78	0.00	18.96	0.03	0.11	-0.00	25.34	1.71	99.47
MT-1D_E_R2C_101	100	56.03	0.78	0.87	0.01	20.67	0.03	0.10	0.02	27.51	1.91	107.94
MT-1D_E_R2C_102	101	51.73	0.72	0.78	-0.00	19.08	0.03	0.08	0.01	25.10	1.69	99.21
MT-1D_E_R2C_103	102	51.70	0.73	0.81	0.01	19.09	0.03	0.11	-0.00	25.54	1.75	99.76
MT-1D_E_R2C_104	103	50.83	0.76	0.82	0.00	18.72	0.03	0.11	0.00	25.01	1.69	97.99
MT-1D_E_R2C_105	104	51.59	0.78	0.87	0.01	18.84	0.03	0.11	-0.00	25.42	1.74	99.39
MT-1D_E_R2C_106	105	51.29	0.77	0.84	0.01	18.91	0.05	0.10	-0.01	24.99	1.74	98.67
MT-1D_E_R2C_107	106	51.69	0.76	0.84	0.00	19.01	0.04	0.13	-0.00	25.52	1.79	99.77
MT-1D_E_R2C_108	107	51.58	0.77	0.89	-0.02	18.92	0.03	0.10	0.00	25.52	1.74	99.54
MT-1D_E_R2C_109	108	51.61	0.76	0.83	0.01	18.76	0.03	0.10	0.02	25.45	1.73	99.29
MT-1D_E_R2C_110	109	51.69	0.76	0.85	0.00	18.99	0.05	0.08	0.02	25.44	1.74	99.64
MT-1D_E_R2C_111	110	51.97	0.74	0.91	0.01	18.75	0.04	0.13	0.01	25.53	1.72	99.81
MT-1D_E_R2C_112	111	51.60	0.75	0.86	0.01	18.92	0.02	0.09	-0.00	25.39	1.75	99.40
MT-1D_E_R2C_113	112	51.70	0.77	0.88	-0.02	18.91	0.03	0.07	-0.01	25.39	1.77	99.51
MT-1D_E_R2C_114	113	51.88	0.76	0.88	-0.01	18.95	0.03	0.12	0.00	25.37	1.77	99.75
MT-1D_E_R2C_115	114	51.80	0.71	0.90	-0.00	19.10	0.03	0.10	-0.00	25.44	1.75	99.81
MT-1D_E_R2C_116	115	52.09	0.72	0.88	0.02	18.88	0.05	0.13	0.01	25.36	1.75	99.87
MT-1D_E_R2C_117	116	52.13	0.65	0.91	-0.00	18.91	0.02	0.13	0.00	25.47	1.75	99.97
MT-1D_E_R2C_118	117	51.90	0.66	0.93	0.00	18.86	0.04	0.10	0.01	25.39	1.75	99.63
MT-1D_E_R2C_119	118	52.01	0.66	0.91	-0.00	19.01	0.03	0.13	-0.01	25.55	1.73	100.01
MT-1D_E_R2C_120	119	52.05	0.66	0.93	-0.00	19.05	0.04	0.11	-0.00	25.29	1.73	99.87
MT-1D_E_R2C_121	120	53.12	0.66	1.22	0.01	18.65	0.48	0.09	-0.01	23.83	1.61	99.66
MT-1D_E_R2C_122	121	51.91	0.65	0.93	0.00	18.90	0.05	0.12	-0.00	25.22	1.72	99.51
MT-1D_E_R2C_123	122	52.25	0.69	0.92	-0.00	19.16	0.03	0.10	-0.02	25.28	1.77	100.18
MT-1D_E_R2C_124	123	51.79	0.72	0.91	0.02	19.05	0.03	0.13	-0.01	25.27	1.73	99.63
MT-1D_E_R2C_125	124	51.99	0.73	0.92	0.01	19.20	0.03	0.09	-0.01	25.30	1.69	99.95
MT-1D_E_R2C_126	125	52.26	0.72	0.89	-0.02	19.08	0.02	0.12	0.00	25.26	1.72	100.05
MT-1D_E_R2C_127	126	52.00	0.72	0.91	-0.00	19.22	0.04	0.14	-0.01	25.04	1.71	99.77
MT-1D_E_R2C_128	127	52.17	0.72	0.88	0.01	19.13	0.04	0.10	-0.01	25.31	1.71	100.06
MT-1D_E_R2C_129	128	52.22	0.74	0.89	0.02	19.20	0.05	0.09	-0.00	25.36	1.72	100.28
MT-1D_E_R2C_130	129	51.94	0.75	0.90	-0.00	19.14	0.05	0.11	0.00	25.33	1.72	99.93
MT-1D_E_R2C_131	130	52.01	0.72	0.87	0.01	19.22	0.04	0.09	-0.00	25.40	1.69	100.05

Sample	Distance (μm)	SiO_2	Al_2O_3	CaO	K_2O	MgO	Na_2O	TiO_2	Cr_2O_3	FeO	MnO	Total
MT-1D_E_R2C_132	131	51.87	0.71	0.90	-0.00	19.17	0.03	0.11	0.01	25.14	1.73	99.66
MT-1D_E_R2C_133	132	52.18	0.70	0.91	0.00	19.18	0.03	0.10	-0.00	25.19	1.73	100.02
MT-1D_E_R2C_134	133	52.07	0.68	0.91	0.01	19.23	0.03	0.10	-0.01	25.05	1.68	99.74
MT-3L_P4_R2C_01	0	53.07	1.00	1.60	-0.00	22.06	0.04	0.21	0.00	20.64	0.89	99.51
MT-3L_P4_R2C_02	1	52.99	0.80	1.31	-0.00	21.67	0.02	0.15	-0.00	21.73	1.19	99.86
MT-3L_P4_R2C_03	2	52.37	0.74	1.21	0.00	21.08	0.01	0.14	0.00	22.84	1.29	99.69
MT-3L_P4_R2C_04	3	52.60	0.75	1.25	-0.00	21.25	0.02	0.15	0.00	22.23	1.22	99.47
MT-3L_P4_R2C_05	4	52.96	0.55	1.08	0.01	20.94	0.01	0.12	0.01	22.81	1.38	99.88
MT-3L_P4_R2C_06	5	52.74	0.52	1.04	0.00	20.63	0.01	0.08	0.00	23.37	1.47	99.86
MT-3L_P4_R2C_07	6	52.77	0.52	1.04	-0.00	20.53	0.01	0.10	-0.01	23.49	1.47	99.92
MT-3L_P4_R2C_08	7	52.80	0.52	1.04	-0.00	20.62	0.02	0.11	-0.01	23.35	1.45	99.89
MT-3L_P4_R2C_09	8	52.38	0.52	1.05	-0.01	20.46	0.02	0.08	-0.01	23.35	1.47	99.32
MT-3L_P4_R2C_10	9	52.30	0.52	1.03	-0.00	20.35	0.02	0.11	0.01	23.45	1.48	99.27
MT-3L_P4_R2C_11	10	52.56	0.51	1.04	0.02	20.33	0.01	0.07	0.01	23.41	1.49	99.46
MT-3L_P4_R2C_12	11	52.63	0.51	1.06	0.01	20.35	0.01	0.10	-0.01	23.47	1.47	99.61
MT-3L_P4_R2C_13	12	52.95	0.54	1.08	0.00	20.20	0.01	0.13	-0.01	23.34	1.47	99.71
MT-3L_P4_R2C_14	13	51.66	0.54	1.08	0.01	20.12	0.01	0.12	-0.01	23.72	1.51	98.74
MT-3L_P4_R2C_15	14	52.59	0.53	1.05	0.00	20.24	0.01	0.11	-0.00	23.70	1.54	99.77
MT-3L_P4_R2C_16	15	52.41	0.50	1.05	-0.00	20.30	0.01	0.09	0.01	23.71	1.57	99.65
MT-3L_P4_R2C_17	16	52.52	0.54	1.05	-0.01	20.18	0.02	0.10	0.01	23.78	1.55	99.75
MT-3L_P4_R2C_18	17	52.63	0.55	1.05	0.01	20.11	0.00	0.11	-0.01	23.85	1.53	99.84
MT-3L_P4_R2C_19	18	52.84	0.56	1.07	-0.02	19.99	0.01	0.12	0.01	23.83	1.55	99.95
MT-3L_P4_R2C_20	19	52.70	0.56	1.07	0.01	20.02	0.03	0.09	-0.01	24.13	1.59	100.18
MT-3L_P4_R2C_21	20	52.30	0.61	1.04	0.01	19.75	0.01	0.12	-0.00	24.35	1.59	99.77
MT-3L_P4_R2C_22	21	52.28	0.64	1.07	0.01	19.62	0.02	0.11	0.00	24.04	1.64	99.41
MT-3L_P4_R2C_23	22	52.39	0.61	1.09	0.01	19.67	0.02	0.10	0.00	24.04	1.68	99.60
MT-3L_P4_R2C_24	23	56.49	0.66	1.16	0.00	21.29	0.01	0.13	0.00	26.14	1.81	107.69
MT-3L_P4_R2C_25	24	51.98	0.57	1.02	-0.00	19.53	0.01	0.12	0.00	24.00	1.65	98.88
MT-3L_P4_R2C_26	25	52.22	0.56	1.03	-0.02	19.63	0.02	0.09	-0.01	24.29	1.64	99.45
MT-3L_P4_R2C_27	26	52.13	0.62	1.02	-0.00	19.65	0.01	0.11	-0.02	24.35	1.69	99.56
MT-3L_P4_R2C_28	27	52.36	0.62	1.01	0.02	19.48	0.01	0.10	0.01	24.62	1.69	99.92
MT-3L_P4_R2C_29	28	52.15	0.58	1.04	-0.02	19.63	0.02	0.10	0.00	24.77	1.70	99.97
MT-3L_P4_R2C_30	29	52.87	0.61	1.00	-0.01	19.69	0.02	0.10	-0.01	24.68	1.69	100.64
MT-3L_P4_R2C_31	30	52.16	0.59	1.02	0.00	19.63	0.01	0.11	0.00	24.75	1.70	99.98
MT-3L_P4_R2C_32	31	51.98	0.56	1.01	0.02	19.70	0.01	0.11	-0.01	24.58	1.72	99.68
MT-3L_P4_R2C_33	32	52.15	0.55	1.04	-0.00	19.66	0.01	0.11	-0.00	24.60	1.68	99.80
MT-3L_P4_R2C_34	33	52.22	0.55	1.02	0.00	19.71	0.01	0.10	0.01	24.68	1.72	100.02
MT-3L_P4_R2C_35	34	52.15	0.52	1.00	-0.01	19.73	0.02	0.09	-0.00	24.49	1.67	99.65
MT-3L_P4_R2C_36	35	52.47	0.51	1.00	-0.02	19.79	0.02	0.12	-0.01	24.51	1.72	100.10

Sample	Distance (μm)	SiO_2	Al_2O_3	CaO	K_2O	MgO	Na_2O	TiO_2	Cr_2O_3	FeO	MnO	Total
MT-3L_P4_R2C_37	36	51.92	0.51	1.00	0.00	19.56	0.01	0.11	0.00	24.74	1.71	99.57
MT-3L_P4_R2C_38	37	52.28	0.54	0.98	0.00	19.70	0.01	0.10	-0.00	24.68	1.72	100.01
MT-3L_P4_R2C_39	38	52.12	0.52	0.99	0.00	19.50	0.02	0.09	-0.01	24.86	1.68	99.78
MT-3L_P4_R2C_40	39	52.03	0.59	0.96	-0.00	19.43	0.02	0.11	-0.01	24.66	1.71	99.50
MT-3L_P4_R2C_41	40	52.08	0.60	0.94	-0.00	19.54	0.01	0.12	0.01	24.78	1.72	99.80
MT-3L_P4_R2C_42	41	51.81	0.59	0.91	0.00	19.26	0.01	0.11	-0.02	24.77	1.74	99.19
MT-3L_P4_R2C_43	42	52.24	0.62	0.92	0.00	19.39	0.02	0.10	0.00	24.75	1.80	99.84
MT-3L_P4_R2C_44	43	52.03	0.60	0.90	0.00	19.41	0.02	0.09	-0.00	24.92	1.71	99.69
MT-3L_P4_R2C_45	44	52.14	0.62	0.90	-0.00	19.29	0.02	0.09	-0.01	25.03	1.75	99.83
MT-3L_P4_R2C_46	45	51.81	0.64	0.91	-0.00	18.92	0.00	0.10	0.00	24.99	1.73	99.10
MT-3L_P4_R2C_47	46	51.77	0.67	0.88	0.01	18.99	0.01	0.11	-0.00	25.20	1.78	99.42
MT-3L_P4_R2C_48	47	51.65	0.62	0.88	0.01	18.88	0.00	0.06	-0.00	25.19	1.81	99.10
MT-3L_P4_R2C_49	48	52.10	0.53	0.91	-0.01	19.05	0.00	0.08	-0.02	25.21	1.78	99.65
MT-3L_P4_R2C_50	49	56.21	0.52	1.03	0.00	20.62	0.03	0.12	0.01	27.11	1.90	107.55
MT-3L_P4_R2C_51	50	52.09	0.48	0.98	0.00	19.19	0.02	0.08	-0.00	24.97	1.76	99.56
MT-3L_P4_R2C_52	51	51.92	0.46	1.01	-0.00	18.90	0.01	0.10	0.01	24.91	1.73	99.05
MT-3L_P4_R2C_53	52	52.03	0.50	1.03	0.01	19.18	0.02	0.08	-0.01	24.84	1.73	99.39
MT-3L_P4_R2C_54	53	52.06	0.49	1.02	0.01	19.14	0.01	0.10	0.01	24.98	1.72	99.54
MT-3L_P4_R2C_55	54	52.00	0.53	1.04	0.00	19.10	0.01	0.08	0.00	24.91	1.73	99.42
MT-3L_P4_R2C_56	55	52.31	0.52	1.04	0.00	19.58	0.01	0.11	0.00	24.94	1.73	100.24
MT-3L_P4_R2C_57	56	51.60	0.49	1.01	0.00	19.36	0.01	0.10	0.00	24.81	1.71	99.11
MT-3L_P4_R2C_58	57	51.95	0.52	1.02	-0.01	19.41	0.01	0.10	-0.02	24.74	1.67	99.39
MT-3L_P4_R2C_59	58	52.40	0.54	1.00	-0.01	19.48	0.02	0.10	-0.01	24.76	1.68	99.95
MT-3L_P4_R2C_60	59	51.71	0.54	1.03	-0.01	19.40	0.02	0.11	-0.00	24.83	1.69	99.31
MT-3L_P4_R2C_61	60	51.99	0.54	1.04	-0.00	19.31	0.02	0.09	-0.01	24.62	1.68	99.29
MT-3L_P4_R2C_62	61	52.14	0.55	1.04	-0.00	19.43	0.02	0.11	-0.01	24.67	1.70	99.64
MT-3L_P4_R2C_63	62	52.17	0.58	1.03	-0.01	19.55	0.01	0.11	-0.01	24.68	1.69	99.79
MT-3L_P4_R2C_64	63	52.06	0.58	1.05	-0.01	19.57	0.02	0.12	-0.01	24.67	1.70	99.75
MT-3L_P4_R2C_65	64	52.15	0.58	1.03	-0.00	19.58	0.02	0.11	0.00	24.68	1.72	99.86
MT-3L_P4_R2C_66	65	52.04	0.58	1.03	-0.01	19.83	0.01	0.12	-0.00	24.55	1.67	99.81
MT-3L_P4_R2C_67	66	52.00	0.60	1.06	0.01	19.51	0.00	0.11	0.01	24.55	1.67	99.53
MT-3L_P4_R2C_68	67	52.29	0.61	1.02	-0.01	19.67	0.01	0.10	0.01	24.74	1.67	100.11
MT-3L_P4_R2C_69	68	51.86	0.61	1.05	0.00	19.67	0.02	0.10	-0.00	24.78	1.66	99.76
MT-3L_P4_R2C_70	69	52.19	0.61	1.04	-0.00	19.59	0.02	0.09	0.01	24.73	1.68	99.96
MT-3L_P4_R2C_71	70	51.92	0.66	1.04	-0.00	19.63	0.01	0.09	-0.02	24.69	1.68	99.69
MT-3L_P4_R2C_72	71	51.80	0.56	1.02	-0.00	19.65	0.01	0.12	0.00	24.77	1.69	99.62
MT-3L_P4_R2C_73	72	52.40	0.55	1.01	0.00	19.83	0.02	0.09	-0.01	24.65	1.71	100.25
MT-3L_P4_R2C_74	73	52.10	0.55	0.97	-0.01	19.77	0.02	0.08	0.01	24.79	1.64	99.93
MT-3L_P4_R2C_75	74	52.40	0.54	0.96	0.01	19.86	0.01	0.10	0.01	24.51	1.65	100.04

Sample	Distance (μm)	SiO_2	Al_2O_3	CaO	K_2O	MgO	Na_2O	TiO_2	Cr_2O_3	FeO	MnO	Total
MT-3L_P4_R2C_76	75	51.86	0.51	0.93	0.01	19.48	0.02	0.10	0.00	24.49	1.68	99.09
MT-3L_P4_R2C_77	76	51.81	0.52	0.93	-0.00	19.47	0.02	0.09	-0.00	24.65	1.69	99.16
MT-3L_P4_R2C_78	77	52.10	0.53	0.92	0.00	19.68	0.01	0.07	0.00	24.58	1.65	99.53
MT-3L_P4_R2C_79	78	52.07	0.51	0.88	-0.01	19.61	0.01	0.12	-0.01	24.79	1.68	99.64
MT-3L_P4_R2C_80	79	51.99	0.49	0.86	-0.00	19.55	0.01	0.11	-0.00	24.79	1.69	99.49
MT-3L_P4_R2C_81	80	52.17	0.51	0.83	-0.00	19.72	0.02	0.10	0.01	24.85	1.68	99.88
MT-3L_P4_R2C_82	81	52.56	0.52	0.82	0.00	19.93	0.00	0.08	-0.01	24.90	1.71	100.51
MT-3L_P4_R2C_83	82	52.00	0.50	0.81	-0.01	19.86	0.01	0.08	-0.00	24.80	1.74	99.79
MT-3L_P4_R2C_84	83	52.13	0.51	0.79	-0.01	19.50	0.01	0.11	-0.00	25.05	1.76	99.85
MT-3L_P4_R2C_85	84	52.11	0.51	0.76	0.00	19.36	0.01	0.08	0.01	25.10	1.76	99.71
MT-3L_P4_R2C_86	85	52.00	0.53	0.75	-0.01	19.51	0.01	0.12	-0.01	25.40	1.82	100.11
MT-3L_P4_R2C_87	86	52.02	0.53	0.78	-0.01	19.68	0.01	0.11	0.01	25.28	1.78	100.18
MT-3L_P4_R2C_88	87	52.00	0.54	0.77	0.00	19.68	0.02	0.10	-0.01	25.23	1.80	100.12
MT-3L_P4_R2C_89	88	52.04	0.58	0.77	-0.01	19.18	0.01	0.08	-0.03	25.40	1.78	99.80
MT-3L_P4_R2C_90	89	51.66	0.60	0.77	0.02	19.19	0.02	0.10	0.01	25.40	1.79	99.56
MT-3L_P4_R2C_91	90	51.95	0.67	0.78	0.01	19.28	0.02	0.08	-0.01	25.65	1.78	100.22
MT-3L_P4_R2C_92	91	51.80	0.71	0.79	0.02	19.15	0.01	0.08	0.01	25.48	1.81	99.84
MT-3L_P4_R2C_93	92	51.71	0.65	0.80	-0.02	18.98	0.01	0.09	-0.00	25.53	1.79	99.54
MT-3L_P4_R2C_94	93	50.49	0.60	2.44	0.01	17.81	0.01	0.08	-0.00	24.59	1.74	97.77
MT-3L_P4_R2C_95	94	40.49	0.51	12.49	-0.01	14.22	0.03	0.07	-0.00	19.41	1.50	88.70
MT-3L_P4_R2C_96	95	35.45	0.44	16.21	-0.02	12.90	0.05	0.08	-0.00	17.29	1.35	83.76
MT-3L_P4_R2C_97	96	45.74	0.55	6.55	0.00	17.04	0.03	0.05	-0.02	23.23	1.66	94.83
MT-3L_P4_R2C_98	97	47.69	0.57	4.44	-0.01	17.77	0.03	0.06	-0.00	24.25	1.72	96.51
MT-3L_P4_R2C_99	98	50.25	0.60	2.40	0.01	18.63	0.02	0.08	-0.01	25.15	1.78	98.91
MT-3L_P4_R2C_100	99	51.22	0.62	1.42	-0.01	18.98	0.02	0.09	-0.02	25.38	1.81	99.51
MT-3L_P4_R2C_101	100	52.17	0.61	0.86	0.00	19.23	0.02	0.09	-0.01	25.40	1.81	100.18
MT-3L_P4_R2C_102	101	51.99	0.63	0.79	-0.00	19.22	0.02	0.08	-0.00	25.55	1.78	100.06
MT-3L_P4_R2C_103	102	52.27	0.65	0.74	0.01	19.21	0.02	0.07	-0.02	25.26	1.81	100.00
MT-3L_P4_R2C_104	103	51.86	0.65	0.78	0.00	19.11	0.02	0.10	0.00	25.63	1.78	99.93
MT-3L_P4_R2C_105	104	52.13	0.66	0.74	-0.01	19.23	0.02	0.08	-0.02	25.44	1.78	100.03
MT-3L_P4_R2C_106	105	51.95	0.67	0.75	0.01	19.34	0.02	0.08	-0.01	25.46	1.78	100.04
MT-3L_P4_R2C_107	106	52.20	0.71	0.73	0.01	19.15	0.01	0.11	-0.01	25.29	1.79	99.97
MT-3L_P4_R2C_108	107	52.50	0.75	0.72	-0.01	19.29	0.01	0.08	0.01	25.36	1.81	100.53
MT-3L_P4_R2C_109	108	51.39	0.74	0.75	0.00	19.11	0.02	0.09	0.00	25.31	1.74	99.15
MT-3L_P4_R2C_110	109	51.88	0.79	0.71	-0.00	19.25	0.02	0.09	0.00	25.35	1.74	99.83
MT-3L_P4_R2C_111	110	52.12	0.81	0.74	0.02	19.35	0.01	0.08	0.00	25.34	1.75	100.24
MT-3L_P4_R2C_112	111	51.80	0.78	0.75	0.01	18.93	0.01	0.09	0.01	25.38	1.74	99.50
MT-3L_P4_R2C_113	112	52.13	0.80	0.76	-0.01	19.20	0.01	0.10	-0.00	25.60	1.73	100.33
MT-3L_P4_R2C_114	113	51.56	0.83	0.75	-0.01	19.29	0.02	0.08	-0.00	25.38	1.75	99.65

Sample	Distance (μm)	SiO_2	Al_2O_3	CaO	K_2O	MgO	Na_2O	TiO_2	Cr_2O_3	FeO	MnO	Total
MT-3L_P4_R2C_115	114	51.83	0.81	0.76	0.01	19.27	0.02	0.10	-0.01	25.43	1.75	99.97
MT-3L_P4_R2C_116	115	51.99	0.82	0.75	0.01	19.40	0.02	0.10	-0.02	25.32	1.75	100.14
MT-3L_P4_R2C_117	116	51.81	0.80	0.75	-0.00	19.20	0.02	0.08	0.00	25.48	1.72	99.86
MT-3L_P4_R2C_118	117	51.92	0.77	0.76	-0.00	19.43	0.01	0.07	-0.00	25.41	1.74	100.10
MT-3L_P4_R2C_119	118	51.92	0.76	0.76	0.01	19.33	0.02	0.09	-0.00	25.38	1.72	99.98
MT-3L_P4_R2C_120	119	51.96	0.74	0.75	0.00	19.38	0.01	0.11	-0.00	25.26	1.73	99.95
MT-3L_P4_R2C_121	120	52.16	0.72	0.76	0.01	19.21	0.01	0.08	0.00	25.23	1.75	99.91
MT-3L_P4_R2C_122	121	51.98	0.77	0.74	0.01	19.44	0.02	0.11	-0.00	25.21	1.73	100.01
MT-3L_P4_R2C_123	122	52.11	0.77	0.74	0.00	19.33	0.02	0.09	0.01	25.13	1.72	99.93
MT-3L_P4_R2C_124	123	51.76	0.78	0.74	-0.01	19.28	0.02	0.09	-0.01	25.15	1.70	99.49
MT-3L_P4_R2C_125	124	51.90	0.74	0.77	0.01	19.58	0.02	0.09	-0.00	25.11	1.69	99.91
MT-3L_P4_R2C_126	125	56.18	0.75	0.86	-0.00	21.11	0.03	0.08	0.02	27.00	1.82	107.84
MT-3L_P4_R2C_127	126	52.28	0.64	0.83	-0.01	19.50	0.02	0.10	0.00	25.11	1.72	100.21
MT-3L_P4_R2C_128	127	52.36	0.59	0.89	-0.00	19.49	0.01	0.12	-0.01	24.93	1.70	100.07
MT-3L_P4_R2C_129	128	52.31	0.52	0.94	-0.00	19.59	0.02	0.09	0.00	24.93	1.70	100.09
MT-3L_P4_R2C_130	129	52.25	0.52	1.01	-0.01	19.71	0.01	0.12	-0.01	24.75	1.65	99.99
MT-3L_P4_R2C_131	130	52.42	0.52	1.01	0.01	19.77	0.01	0.09	0.01	24.81	1.65	100.30
MT-3L_P4_R2C_132	131	52.44	0.51	1.03	0.00	19.89	0.02	0.12	-0.01	24.61	1.67	100.27
MT-3L_P4_R2C_133	132	52.42	0.52	1.03	-0.00	19.79	0.01	0.11	-0.01	24.51	1.64	100.02
MT-3L_P4_R2C_134	133	51.98	0.51	1.05	-0.00	19.76	0.03	0.09	0.01	24.54	1.63	99.60
MT-3L_P4_R2C_135	134	52.56	0.51	1.08	0.00	19.59	0.02	0.11	0.01	24.63	1.62	100.13
MT-3L_P4_R2C_136	135	52.39	0.50	1.06	-0.01	19.83	0.03	0.11	-0.01	24.67	1.66	100.24
MT-3L_P4_R2C_137	136	52.15	0.49	1.07	0.00	19.69	0.01	0.10	0.01	24.36	1.65	99.52
MT-3L_P4_R2C_138	137	52.58	0.50	1.07	0.00	19.67	0.01	0.09	-0.00	24.40	1.67	100.00
MT-3L_P4_R2C_139	138	52.46	0.51	1.13	-0.01	19.84	0.01	0.11	-0.02	24.71	1.64	100.39
MT-3L_P4_R2C_140	139	52.23	0.49	1.06	0.00	19.81	0.02	0.11	0.00	24.59	1.63	99.96
MT-3L_P4_R2C_141	140	51.68	0.47	1.12	0.01	19.60	-0.00	0.10	0.01	24.55	1.63	99.14
MT-3L_P4_R2C_142	141	52.39	0.50	1.10	-0.03	19.92	0.01	0.12	-0.01	24.38	1.66	100.05
MT-3L_P4_R2C_143	142	51.74	0.50	1.11	-0.01	19.84	0.01	0.12	0.02	24.02	1.64	98.98
MT-3L_P4_R2C_144	143	52.20	0.50	1.15	0.01	19.81	0.02	0.12	-0.01	24.39	1.61	99.77
MT-3L_P4_R2C_145	144	52.24	0.50	1.12	-0.01	19.95	0.03	0.12	-0.02	24.28	1.64	99.85
MT-3L_P4_R2C_146	145	52.00	0.50	1.13	0.01	19.65	0.02	0.13	-0.00	24.30	1.66	99.40
MT-3L_P4_R2C_147	146	52.30	0.54	1.14	-0.01	19.97	0.02	0.11	-0.01	24.43	1.66	100.17
MT-3L_P4_R2C_148	147	52.33	0.58	1.15	-0.00	19.91	0.02	0.09	-0.01	24.47	1.64	100.18
MT-3L_P4_R2C_149	148	51.97	0.61	1.11	0.01	19.63	0.02	0.12	-0.00	24.23	1.67	99.36
MT-3L_P4_R2C_150	149	51.93	0.66	1.14	-0.02	19.75	0.01	0.09	0.01	24.45	1.65	99.67
MT-3L_P4_R2C_151	150	52.13	0.69	1.14	0.00	19.71	0.03	0.08	0.00	24.33	1.65	99.76
MT-3L_P4_R2C_152	151	51.96	0.75	1.13	0.00	19.72	0.02	0.10	0.01	24.47	1.68	99.84
MT-3L_P4_R2C_153	152	52.07	0.76	1.10	-0.00	19.72	0.00	0.13	-0.01	24.53	1.67	99.99

Sample	Distance (μm)	SiO_2	Al_2O_3	CaO	K_2O	MgO	Na_2O	TiO_2	Cr_2O_3	FeO	MnO	Total
MT-3L_P4_R2C_154	153	51.97	0.76	1.12	-0.00	19.78	0.02	0.12	-0.01	24.43	1.69	99.86
MT-3L_P4_R2C_155	154	52.24	0.76	1.11	0.01	19.45	0.02	0.12	-0.01	24.48	1.62	99.81
MT-3L_P4_R2C_156	155	52.29	0.72	1.06	-0.01	19.59	0.01	0.13	-0.00	24.58	1.70	100.09
MT-3L_P4_R2C_157	156	51.63	0.72	1.06	0.00	19.57	0.01	0.09	-0.00	24.62	1.67	99.37
MT-3L_P4_R2C_158	157	52.21	0.71	1.07	-0.00	19.73	0.02	0.11	-0.00	24.46	1.66	99.95
MT-3L_P4_R2C_159	158	51.54	0.71	1.06	-0.01	19.65	0.02	0.12	-0.00	24.69	1.66	99.43
MT-3L_P4_R2C_160	159	52.23	0.69	1.06	-0.00	19.55	0.03	0.09	-0.01	24.32	1.63	99.59
MT-3L_P4_R2C_161	160	52.28	0.67	1.04	-0.00	19.89	0.02	0.10	-0.01	24.32	1.68	99.99
MT-3L_P4_R2C_162	161	52.09	0.73	1.07	0.00	19.87	0.02	0.08	-0.00	24.25	1.67	99.78
MT-3L_P4_R2C_163	162	52.12	0.80	1.08	0.02	19.95	0.02	0.14	-0.01	24.34	1.60	100.05
MT-3L_P4_R2C_164	163	51.97	0.85	1.08	0.01	19.66	0.02	0.13	0.01	24.49	1.64	99.86
MT-3L_P4_R2C_165	164	51.70	0.89	1.10	0.01	19.36	0.01	0.13	-0.01	24.58	1.65	99.42
MT-3L_P4_R2C_166	165	52.21	0.91	1.08	-0.01	19.74	0.02	0.10	0.00	24.43	1.65	100.13
MT-3L_P4_R2C_167	166	51.78	0.87	1.09	-0.01	19.83	0.00	0.12	-0.00	24.36	1.66	99.70
MT-3L_P4_R2C_168	167	51.94	0.81	1.12	0.01	19.88	0.02	0.11	0.00	24.44	1.59	99.94
MT-3L_P4_R2C_169	168	51.75	0.75	1.11	-0.02	19.71	0.03	0.15	0.00	24.02	1.65	99.16
MT-3L_P4_R2C_170	169	52.14	0.68	1.08	0.01	19.68	0.02	0.12	0.01	24.47	1.62	99.83
MT-3L_P4_R2C_171	170	51.92	0.60	1.09	0.01	19.75	0.02	0.11	-0.02	24.37	1.63	99.49
MT-3L_P4_R2C_172	171	52.16	0.56	1.09	0.03	19.82	0.00	0.11	0.00	24.15	1.64	99.57
MT-3L_P4_R2C_173	172	52.32	0.53	1.07	0.01	19.99	0.02	0.11	0.01	24.42	1.61	100.08
MT-3L_P4_R2C_174	173	52.28	0.50	1.05	0.00	20.17	0.01	0.13	0.02	24.34	1.64	100.15
MT-3L_P4_R2C_175	174	52.29	0.51	1.04	-0.01	19.93	0.02	0.10	-0.01	24.51	1.66	100.04
MT-3L_P4_R2C_176	175	52.30	0.53	1.02	0.00	19.80	0.01	0.11	-0.01	24.28	1.62	99.67
MT-3L_P4_R2C_177	176	52.09	0.54	1.03	-0.00	19.85	0.01	0.11	0.00	24.30	1.63	99.57
MT-3L_P4_R2C_178	177	52.79	0.57	1.00	-0.00	19.92	0.01	0.11	-0.01	24.56	1.63	100.59
MT-3L_P4_R2C_179	178	52.05	0.55	0.98	0.01	19.86	0.01	0.08	-0.01	24.61	1.63	99.78
MT-3L_P4_R2C_180	179	52.27	0.55	0.96	-0.02	19.94	0.01	0.10	-0.00	24.58	1.71	100.10
MT-3L_P4_R2C_181	180	52.12	0.56	0.98	-0.01	19.71	0.01	0.11	-0.00	24.55	1.68	99.70
MT-3L_P4_R2C_182	181	52.35	0.55	0.95	0.00	19.79	0.01	0.09	-0.01	24.57	1.70	100.00
MT-3L_P4_R2C_183	182	52.30	0.54	0.94	-0.01	19.81	0.02	0.11	-0.02	24.68	1.66	100.03
MT-3L_P4_R2C_184	183	52.36	0.51	0.91	0.00	19.81	0.01	0.05	-0.01	24.50	1.69	99.83
MT-3L_P4_R2C_185	184	52.33	0.52	0.91	0.02	19.81	0.01	0.06	-0.01	24.84	1.67	100.17
MT-3L_P4_R2C_186	185	52.08	0.52	0.91	0.01	19.76	0.01	0.09	0.00	24.59	1.69	99.67
MT-3L_P4_R2C_187	186	52.31	0.54	0.91	-0.00	19.76	0.02	0.12	-0.01	24.85	1.69	100.18
MT-3L_P4_R2C_188	187	52.24	0.58	0.91	-0.01	19.80	0.01	0.10	-0.00	24.82	1.69	100.12
MT-3L_P4_R2C_189	188	52.20	0.64	0.94	-0.00	19.62	0.02	0.10	-0.02	24.96	1.69	100.15
MT-3L_P4_R2C_190	189	51.70	0.65	0.92	-0.01	19.71	0.01	0.11	-0.00	24.84	1.68	99.61
MT-3L_P4_R2C_191	190	51.79	0.69	0.91	0.02	19.68	0.02	0.12	-0.01	24.63	1.69	99.53
MT-3L_P4_R2C_192	191	51.71	0.68	0.91	0.01	19.98	0.02	0.10	-0.01	24.92	1.68	100.01

Sample	Distance (μm)	SiO_2	Al_2O_3	CaO	K_2O	MgO	Na_2O	TiO_2	Cr_2O_3	FeO	MnO	Total
MT-3L_P4_R2C_193	192	52.03	0.67	0.93	-0.01	20.01	0.02	0.10	0.01	24.76	1.70	100.21
MT-3L_P4_R2C_194	193	51.89	0.66	0.93	-0.02	19.85	0.00	0.11	0.00	24.98	1.67	100.08
MT-3L_P4_R2C_195	194	51.87	0.64	0.94	0.01	19.48	0.01	0.09	0.02	24.63	1.73	99.41
MT-3L_P4_R2C_196	195	52.11	0.61	0.94	-0.00	19.92	0.03	0.09	0.01	24.94	1.67	100.30
MT-3L_P4_R2C_197	196	51.95	0.59	0.95	-0.01	19.72	0.01	0.10	0.01	24.94	1.69	99.95
MT-3L_P4_R2C_198	197	52.30	0.56	0.93	0.01	20.07	0.01	0.12	0.01	24.95	1.71	100.67
MT-3L_P4_R2C_199	198	52.12	0.54	0.97	0.00	19.83	0.02	0.08	-0.01	24.72	1.72	99.97
MT-3L_P4_R2C_200	199	51.60	0.56	0.97	0.00	19.21	0.00	0.09	-0.00	24.87	1.69	99.01
MT-3L_P4_R2C_201	200	52.26	0.53	1.00	0.01	19.73	0.01	0.10	0.01	24.79	1.69	100.14
MT-3L_P4_R2C_202	201	52.05	0.52	1.00	-0.00	19.64	0.01	0.07	-0.01	24.54	1.71	99.54
MT-3L_P4_R2C_203	202	51.36	0.54	0.98	0.00	19.02	0.01	0.13	0.02	24.71	1.67	98.45
MT-3L_P4_R2C_204	203	52.31	0.51	1.00	0.02	19.77	0.02	0.11	-0.01	24.73	1.71	100.17
MT-3L_P4_R2C_205	204	51.67	0.51	1.02	0.01	19.37	0.02	0.11	0.01	24.64	1.73	99.09
MT-3L_P4_R2C_206	205	52.27	0.52	1.00	-0.00	19.80	0.01	0.09	0.00	24.90	1.67	100.28
MT-3L_P4_R2C_207	206	52.14	0.51	1.03	-0.00	19.71	0.01	0.11	0.00	24.64	1.67	99.83
MT-3L_P4_R2C_208	207	52.29	0.52	1.02	-0.00	19.74	0.02	0.11	-0.00	24.76	1.67	100.13
MT-3L_P4_R2C_209	208	51.93	0.51	1.01	0.00	19.81	0.02	0.09	-0.01	24.77	1.69	99.83
MT-3L_P4_R2C_210	209	51.99	0.52	1.06	-0.01	19.79	0.02	0.09	-0.01	24.78	1.68	99.91
MT-3L_P4_R2C_211	210	52.22	0.50	1.08	0.00	19.94	0.01	0.11	-0.01	24.99	1.67	100.51
MT-3L_P4_R2C_212	211	51.49	0.48	1.08	-0.01	19.72	0.02	0.09	0.00	24.87	1.66	99.41
MT-3L_P4_R2C_213	212	52.14	0.50	1.07	-0.00	19.73	0.01	0.13	-0.01	24.69	1.67	99.93
MT-3L_P4_R2C_214	213	52.15	0.51	1.05	-0.01	19.64	0.02	0.13	-0.01	24.67	1.70	99.84
MT-3L_P4_R2C_215	214	51.73	0.51	1.07	-0.00	19.58	0.01	0.12	-0.00	24.62	1.70	99.32
MT-3L_P4_R2C_216	215	51.80	0.53	1.05	0.00	19.36	0.00	0.10	-0.00	24.90	1.70	99.44
MT-3L_P4_R2C_217	216	52.39	0.54	1.08	0.01	19.62	0.01	0.11	0.01	24.76	1.74	100.26
MT-3L_P4_R2C_218	217	52.46	0.55	1.08	0.02	19.62	0.03	0.10	-0.00	24.70	1.73	100.29
MT-3L_P4_R2C_219	218	51.17	0.54	1.07	0.02	19.41	0.00	0.12	0.01	24.81	1.71	98.85
MT-3L_P4_R2C_220	219	51.91	0.59	1.09	0.02	19.69	0.02	0.14	0.01	24.61	1.73	99.81
MT-3L_P4_R2C_221	220	52.06	0.59	1.08	0.01	19.76	0.01	0.10	0.00	24.75	1.69	100.05
MT-3L_P4_R2C_222	221	52.19	0.61	1.09	0.01	19.84	0.01	0.10	-0.00	24.69	1.70	100.24
MT-3L_P4_R2C_223	222	51.95	0.63	1.10	-0.00	19.44	0.01	0.12	0.01	25.07	1.70	100.02
MT-3L_P4_R2C_224	223	52.12	0.63	1.10	-0.00	19.60	0.01	0.11	-0.01	24.65	1.71	99.91
MT-3L_P4_R2C_225	224	51.94	0.64	1.08	-0.00	19.66	0.03	0.09	-0.01	24.93	1.68	100.04
MT-3L_P4_R2C_226	225	51.91	0.65	1.05	-0.01	19.43	0.02	0.12	0.00	24.95	1.67	99.79
MT-3L_P4_R2C_227	226	51.86	0.62	1.07	-0.00	19.68	0.02	0.14	-0.01	24.85	1.69	99.94
MT-3L_P4_R2C_228	227	51.92	0.62	1.10	0.00	19.33	0.01	0.12	-0.00	24.92	1.74	99.76
MT-3L_P4_R2C_229	228	51.75	0.59	1.11	-0.00	19.35	0.00	0.12	-0.01	24.87	1.74	99.52
MT-3L_P4_R2C_230	229	51.93	0.60	1.08	-0.00	19.55	0.02	0.11	0.00	24.86	1.78	99.93
MT-3L_P4_R2C_231	230	51.85	0.58	1.12	-0.01	19.57	0.01	0.10	-0.00	24.84	1.72	99.77

Sample	Distance (μm)	SiO_2	Al_2O_3	CaO	K_2O	MgO	Na_2O	TiO_2	Cr_2O_3	FeO	MnO	Total
MT-3L_P4_R2C_232	231	52.17	0.55	1.06	-0.01	19.71	0.01	0.10	0.01	24.74	1.74	100.10
MT-3L_P4_R2C_233	232	52.04	0.54	1.04	0.02	19.52	0.02	0.12	-0.01	24.76	1.71	99.75
MT-3L_P4_R2C_234	233	52.36	0.55	1.09	-0.01	19.52	0.01	0.10	-0.00	24.88	1.69	100.19
MT-3L_P1_R2C_01	0	56.21	1.72	2.21	0.15	14.33	0.30	0.18	0.02	26.97	1.46	103.56
MT-3L_P1_R2C_02	1	50.89	0.46	1.22	0.02	17.67	0.06	0.12	-0.01	25.84	1.39	97.65
MT-3L_P1_R2C_03	2	54.22	1.01	1.83	0.07	16.57	0.19	0.15	0.02	27.31	1.37	102.73
MT-3L_P1_R2C_04	3	52.52	0.34	1.16	-0.00	19.92	0.01	0.09	-0.00	23.12	1.42	98.57
MT-3L_P1_R2C_05	4	52.87	0.31	1.22	-0.00	20.14	0.01	0.10	-0.01	23.32	1.54	99.48
MT-3L_P1_R2C_06	5	53.20	0.36	1.15	0.01	20.88	0.02	0.13	0.03	23.32	1.51	100.60
MT-3L_P1_R2C_07	6	52.33	0.33	0.89	0.02	19.85	0.01	0.08	0.01	24.20	1.67	99.38
MT-3L_P1_R2C_08	7	52.16	0.31	0.88	-0.01	20.02	0.01	0.08	-0.00	24.41	1.77	99.62
MT-3L_P1_R2C_09	8	52.50	0.32	0.84	0.00	19.21	0.00	0.09	0.01	24.85	1.77	99.60
MT-3L_P1_R2C_10	9	52.17	0.32	0.90	0.02	19.71	0.01	0.10	0.00	24.60	1.77	99.60
MT-3L_P1_R2C_11	10	52.34	0.33	0.80	0.01	19.70	0.02	0.06	0.00	24.98	1.81	100.05
MT-3L_P1_R2C_12	11	52.15	0.32	0.85	0.01	19.25	0.00	0.08	-0.02	25.04	1.81	99.49
MT-3L_P1_R2C_13	12	52.21	0.32	0.84	-0.00	19.18	0.01	0.07	-0.01	24.97	1.87	99.46
MT-3L_P1_R2C_14	13	51.80	0.35	0.77	0.01	19.09	0.01	0.06	-0.00	25.19	1.83	99.11
MT-3L_P1_R2C_15	14	52.23	0.42	0.84	0.01	18.98	0.01	0.08	-0.01	24.94	1.86	99.35
MT-3L_P1_R2C_16	15	51.94	0.44	0.85	-0.01	19.21	0.01	0.08	0.00	25.24	1.80	99.57
MT-3L_P1_R2C_17	16	52.04	0.43	0.85	0.01	19.03	0.02	0.09	-0.02	24.98	1.81	99.24
MT-3L_P1_R2C_18	17	51.86	0.49	0.95	-0.00	19.13	0.01	0.10	-0.01	25.29	1.83	99.64
MT-3L_P1_R2C_19	18	51.76	0.46	0.97	-0.00	18.98	0.00	0.08	0.00	25.21	1.81	99.28
MT-3L_P1_R2C_20	19	52.12	0.37	0.95	0.01	19.37	0.01	0.08	0.01	25.19	1.82	99.94
MT-3L_P1_R2C_21	20	52.02	0.32	0.96	-0.00	19.25	0.02	0.08	-0.00	25.24	1.80	99.68
MT-3L_P1_R2C_22	21	52.22	0.30	0.93	0.00	19.35	0.01	0.06	0.01	25.37	1.80	100.05
MT-3L_P1_R2C_23	22	52.22	0.31	0.96	-0.02	19.20	0.01	0.06	-0.01	25.02	1.79	99.53
MT-3L_P1_R2C_24	23	52.24	0.33	0.97	0.00	19.32	0.00	0.07	0.00	25.41	1.79	100.13
MT-3L_P1_R2C_25	24	51.96	0.34	0.96	0.00	19.32	0.02	0.09	0.00	24.98	1.78	99.46
MT-3L_P1_R2C_26	25	52.17	0.32	0.97	0.02	19.35	0.01	0.09	-0.01	25.08	1.78	99.77
MT-3L_P1_R2C_27	26	51.85	0.32	0.96	-0.00	19.51	0.01	0.07	-0.00	25.27	1.75	99.73
MT-3L_P1_R2C_28	27	52.09	0.34	0.94	-0.01	19.44	0.01	0.04	0.01	25.20	1.75	99.81
MT-3L_P1_R2C_29	28	52.09	0.37	0.98	-0.01	19.24	0.01	0.10	0.00	25.06	1.80	99.65
MT-3L_P1_R2C_30	29	51.87	0.41	1.01	-0.01	19.23	0.01	0.07	-0.01	24.98	1.74	99.29
MT-3L_P1_R2C_31	30	52.06	0.42	1.00	0.00	19.49	0.02	0.08	-0.01	24.93	1.78	99.77
MT-3L_P1_R2C_32	31	52.17	0.37	0.99	-0.00	19.33	0.01	0.08	0.01	25.14	1.80	99.89
MT-3L_P1_R2C_33	32	51.76	0.36	1.00	-0.00	19.23	-0.00	0.11	0.01	24.98	1.75	99.19
MT-3L_P1_R2C_34	33	51.75	0.36	0.98	0.02	19.26	0.02	0.10	0.00	25.17	1.76	99.43
MT-3L_P1_R2C_35	34	51.75	0.41	0.99	-0.00	19.11	0.02	0.06	0.00	25.30	1.74	99.38
MT-3L_P1_R2C_36	35	52.04	0.56	0.99	-0.00	19.36	0.02	0.08	-0.00	24.92	1.74	99.70

Sample	Distance (μm)	SiO_2	Al_2O_3	CaO	K_2O	MgO	Na_2O	TiO_2	Cr_2O_3	FeO	MnO	Total
MT-3L_P1_R2C_37	36	51.69	0.63	1.04	-0.00	19.23	0.03	0.09	0.01	25.34	1.77	99.81
MT-3L_P1_R2C_38	37	51.66	0.62	1.03	-0.00	19.27	0.02	0.09	0.00	24.99	1.76	99.43
MT-3L_P1_R2C_39	38	51.43	0.64	1.00	0.00	19.23	0.02	0.08	-0.01	25.26	1.80	99.45
MT-3L_P1_R2C_40	39	51.66	0.63	1.02	-0.01	19.12	0.01	0.08	-0.00	25.29	1.78	99.56
MT-3L_P1_R2C_41	40	52.12	0.64	1.00	0.01	19.05	0.01	0.06	-0.01	25.06	1.73	99.68
MT-3L_P1_R2C_42	41	51.67	0.65	0.99	0.01	19.39	0.03	0.08	-0.00	25.19	1.73	99.75
MT-3L_P1_R2C_43	42	51.61	0.64	0.96	0.02	18.96	0.00	0.08	-0.02	25.09	1.79	99.14
MT-3L_P1_R2C_44	43	51.78	0.64	1.01	0.00	19.01	0.02	0.12	0.01	25.10	1.75	99.45
MT-3L_P1_R2C_45	44	51.52	0.69	0.97	-0.01	18.98	0.00	0.08	-0.01	25.21	1.78	99.20
MT-3L_P1_R2C_46	45	51.70	0.73	0.97	-0.00	19.36	0.01	0.10	-0.00	25.25	1.77	99.89
MT-3L_P1_R2C_47	46	51.65	0.65	0.97	0.02	19.19	0.02	0.09	0.00	25.18	1.77	99.55
MT-3L_P1_R2C_48	47	51.59	0.55	0.97	0.01	19.32	0.01	0.10	0.01	24.98	1.71	99.24
MT-3L_P1_R2C_49	48	52.04	0.53	0.99	0.01	19.41	0.02	0.09	-0.02	25.55	1.74	100.36
MT-3L_P1_R2C_50	49	51.72	0.53	1.00	0.02	19.30	0.02	0.10	0.02	25.07	1.74	99.52
MT-3L_P1_R2C_51	50	51.86	0.53	0.99	0.01	19.44	0.01	0.08	-0.00	24.84	1.73	99.49
MT-3L_P1_R2C_52	51	51.53	0.50	1.01	0.00	19.05	0.00	0.10	0.00	25.21	1.75	99.17
MT-3L_P1_R2C_53	52	51.89	0.52	1.01	-0.02	19.15	0.02	0.10	-0.00	25.04	1.72	99.44
MT-3L_P1_R2C_54	53	51.72	0.49	0.99	0.01	18.90	0.01	0.10	0.01	25.18	1.72	99.12
MT-3L_P1_R2C_55	54	52.06	0.49	1.01	-0.01	19.02	0.01	0.09	-0.01	25.14	1.78	99.59
MT-3L_P1_R2C_56	55	52.08	0.49	1.03	0.00	19.21	0.00	0.09	-0.00	25.10	1.70	99.70
MT-3L_P1_R2C_57	56	52.02	0.46	1.02	-0.01	19.45	0.02	0.10	-0.01	25.20	1.72	99.96
MT-3L_P1_R2C_58	57	52.03	0.48	1.00	0.00	19.49	0.01	0.08	-0.01	25.26	1.75	100.10
MT-3L_P1_R2C_59	58	55.92	0.51	1.10	0.01	20.81	0.02	0.11	0.01	27.18	1.88	107.57
MT-3L_P1_R2C_60	59	51.93	0.49	1.04	-0.01	19.37	0.01	0.11	0.00	25.01	1.75	99.71
MT-3L_P1_R2C_61	60	51.87	0.50	1.04	-0.01	19.16	0.01	0.10	-0.01	25.36	1.75	99.75
MT-3L_P1_R2C_62	61	51.73	0.50	1.00	0.00	19.44	0.01	0.11	-0.01	24.95	1.72	99.46
MT-3L_P1_R2C_63	62	51.87	0.50	1.00	-0.00	19.51	0.02	0.14	0.02	25.34	1.72	100.11
MT-3L_P1_R2C_64	63	51.66	0.47	1.01	0.01	19.10	0.00	0.11	-0.01	25.15	1.75	99.26
MT-3L_P1_R2C_65	64	52.01	0.49	1.01	-0.01	19.21	0.02	0.12	-0.00	25.08	1.74	99.68
MT-3L_P1_R2C_66	65	56.35	0.54	1.12	-0.01	20.70	0.03	0.10	0.03	27.13	1.84	107.82
MT-3L_P1_R2C_67	66	51.81	0.47	0.99	-0.00	19.24	0.01	0.09	-0.00	25.15	1.76	99.52
MT-3L_P1_R2C_68	67	51.32	0.46	1.05	-0.00	18.98	0.01	0.08	-0.01	24.91	1.72	98.53
MT-3L_P1_R2C_69	68	52.08	0.47	1.01	-0.01	19.45	0.02	0.12	-0.00	25.08	1.78	99.99
MT-3L_P1_R2C_70	69	51.95	0.47	1.01	0.02	19.46	0.02	0.12	-0.00	25.29	1.71	100.04
MT-3L_P1_R2C_71	70	51.62	0.47	1.04	0.01	19.68	0.02	0.09	0.01	25.04	1.74	99.72
MT-3L_P1_R2C_72	71	52.09	0.47	0.97	-0.01	19.12	0.01	0.10	-0.01	25.12	1.75	99.59
MT-3L_P1_R2C_73	72	51.95	0.47	1.03	0.01	19.26	0.01	0.09	0.00	25.09	1.71	99.62
MT-3L_P1_R2C_74	73	52.22	0.49	1.01	-0.00	19.26	0.01	0.06	0.01	25.14	1.68	99.87
MT-3L_P1_R2C_75	74	51.74	0.49	1.03	-0.00	19.50	0.02	0.11	-0.01	25.32	1.68	99.86

Sample	Distance (μm)	SiO_2	Al_2O_3	CaO	K_2O	MgO	Na_2O	TiO_2	Cr_2O_3	FeO	MnO	Total
MT-3L_P1_R2C_76	75	52.17	0.48	1.04	0.01	19.18	0.01	0.18	0.03	25.21	1.76	100.05
MT-3L_P1_R2C_77	76	52.11	0.50	1.01	-0.00	19.07	0.00	0.11	0.00	25.23	1.70	99.74
MT-3L_P1_R2C_78	77	51.69	0.51	1.04	0.02	19.56	0.02	0.10	0.00	25.15	1.72	99.81
MT-3L_P1_R2C_79	78	51.83	0.49	1.03	-0.01	19.22	0.01	0.11	0.00	25.20	1.73	99.61
MT-3L_P1_R2C_80	79	51.95	0.49	1.02	-0.01	19.55	0.01	0.13	0.01	25.12	1.70	99.97
MT-3L_P1_R2C_81	80	51.90	0.46	1.01	-0.01	19.27	0.01	0.08	-0.01	25.12	1.73	99.55
MT-3L_P1_R2C_82	81	52.13	0.45	0.99	0.00	19.58	0.02	0.08	-0.02	25.24	1.77	100.24
MT-3L_P1_R2C_83	82	51.89	0.42	1.02	0.00	19.37	0.01	0.08	-0.00	25.06	1.70	99.56
MT-3L_P1_R2C_84	83	52.00	0.41	1.00	0.01	19.52	0.02	0.10	-0.01	24.92	1.71	99.68
MT-3L_P1_R2C_85	84	51.89	0.39	1.01	0.01	19.48	0.02	0.11	-0.00	25.41	1.74	100.06
MT-3L_P1_R2C_86	85	52.11	0.40	0.98	0.00	19.24	0.00	0.08	0.01	25.16	1.72	99.70
MT-3L_P1_R2C_87	86	51.85	0.40	1.02	-0.01	19.25	-0.00	0.08	-0.02	25.05	1.73	99.34
MT-3L_P1_R2C_88	87	51.95	0.40	0.97	0.00	19.33	0.01	0.09	0.00	25.05	1.68	99.49
MT-3L_P1_R2C_89	88	52.01	0.40	0.96	0.02	19.36	0.01	0.11	0.01	25.05	1.73	99.66
MT-3L_P1_R2C_90	89	52.08	0.40	0.97	-0.03	19.48	0.02	0.07	-0.02	24.93	1.71	99.62
MT-3L_P1_R2C_91	90	51.82	0.40	0.98	0.00	19.43	0.01	0.08	-0.01	25.17	1.74	99.62
MT-3L_P1_R2C_92	91	51.88	0.42	0.98	-0.00	19.31	0.01	0.06	0.01	25.04	1.71	99.42
MT-3L_P1_R2C_93	92	51.67	0.43	0.94	-0.01	19.52	0.01	0.05	-0.01	24.99	1.66	99.26
MT-3L_P1_R2C_94	93	51.95	0.45	0.95	-0.01	19.51	0.00	0.07	-0.00	25.21	1.69	99.81
MT-3L_P1_R2C_95	94	51.91	0.48	0.92	-0.01	19.43	0.00	0.08	-0.01	25.36	1.68	99.85
MT-3L_P1_R2C_96	95	52.00	0.50	0.92	0.01	19.46	0.00	0.09	0.01	25.18	1.70	99.87
MT-3L_P1_R2C_97	96	51.82	0.54	0.93	0.02	19.58	0.01	0.10	-0.01	25.26	1.73	100.00
MT-3L_P1_R2C_98	97	51.68	0.57	0.91	0.00	19.26	0.01	0.08	-0.01	25.38	1.68	99.57
MT-3L_P1_R2C_99	98	51.63	0.60	0.90	-0.00	19.22	0.00	0.07	0.00	25.13	1.71	99.27
MT-3L_P1_R2C_100	99	51.74	0.59	0.90	0.01	19.78	0.01	0.06	-0.02	25.17	1.70	99.94
MT-3L_P1_R2C_101	100	51.79	0.61	0.90	0.00	19.37	0.00	0.07	-0.01	25.14	1.68	99.55
MT-3L_P1_R2C_102	101	51.65	0.61	0.88	0.01	19.10	0.02	0.11	0.00	25.12	1.72	99.22
MT-3L_P1_R2C_103	102	51.83	0.65	0.88	0.03	19.25	0.00	0.09	-0.00	25.27	1.68	99.67
MT-3L_P1_R2C_104	103	51.56	0.64	0.90	-0.01	19.35	0.02	0.08	-0.00	25.38	1.68	99.59
MT-3L_P1_R2C_105	104	51.80	0.70	0.87	0.00	19.47	0.01	0.09	-0.01	25.21	1.70	99.85
MT-3L_P1_R2C_106	105	51.50	0.72	0.86	-0.01	18.96	0.00	0.09	-0.00	25.33	1.67	99.11
MT-3L_P1_R2C_107	106	51.42	0.78	0.90	-0.01	19.41	0.01	0.08	0.01	25.40	1.68	99.67
MT-3L_P1_R2C_108	107	51.59	0.79	0.89	-0.01	19.14	0.01	0.08	-0.00	25.24	1.70	99.42
MT-3L_P1_R2C_109	108	51.66	0.79	0.88	-0.01	19.24	0.01	0.09	0.00	25.38	1.70	99.73
MT-3L_P1_R2C_110	109	51.44	0.76	0.87	-0.01	19.38	0.01	0.09	-0.00	25.26	1.69	99.49
MT-3L_P1_R2C_111	110	51.42	0.74	0.87	0.01	19.21	0.01	0.09	0.01	25.35	1.67	99.40
MT-3L_P1_R2C_112	111	51.58	0.72	0.86	0.02	19.44	0.02	0.09	-0.01	25.03	1.67	99.42
MT-3L_P1_R2C_113	112	51.61	0.72	0.91	-0.01	19.34	0.01	0.10	0.01	25.29	1.69	99.66
MT-3L_P1_R2C_114	113	50.75	0.73	0.85	0.00	18.88	0.02	0.10	-0.00	24.86	1.64	97.83

Sample	Distance (μm)	SiO_2	Al_2O_3	CaO	K_2O	MgO	Na_2O	TiO_2	Cr_2O_3	FeO	MnO	Total
MT-3L_P1_R2C_115	114	51.74	0.73	0.91	-0.01	19.06	0.01	0.09	0.00	25.20	1.71	99.43
MT-3L_P1_R2C_116	115	51.49	0.72	0.91	-0.00	19.28	0.00	0.08	0.00	25.37	1.67	99.52
MT-3L_P1_R2C_117	116	51.71	0.71	0.89	0.01	19.19	0.02	0.11	0.02	25.31	1.72	99.68
MT-3L_P1_R2C_118	117	51.67	0.70	0.95	0.01	19.54	0.02	0.07	0.01	25.25	1.65	99.87
MT-3L_P1_R2C_119	118	51.38	0.70	0.91	-0.01	19.39	0.01	0.07	0.01	25.43	1.68	99.57
MT-3L_P1_R2C_120	119	51.52	0.71	0.90	-0.01	19.09	0.01	0.08	0.00	25.38	1.70	99.38
MT-3L_P1_R2C_121	120	51.50	0.70	0.96	-0.01	19.21	0.00	0.12	0.02	25.08	1.74	99.32
MT-3L_P1_R2C_122	121	51.83	0.72	0.93	-0.01	19.28	0.01	0.08	0.00	25.08	1.69	99.62
MT-3L_P1_R2C_123	122	52.14	0.70	0.89	-0.00	19.26	0.01	0.08	-0.00	25.13	1.69	99.89
MT-3L_P1_R2C_124	123	51.59	0.71	0.96	-0.01	19.48	0.01	0.08	-0.01	25.33	1.70	99.85
MT-3L_P1_R2C_125	124	51.94	0.69	0.94	0.00	19.26	0.01	0.09	-0.00	25.26	1.68	99.88
MT-3L_P1_R2C_126	125	56.00	0.77	1.05	0.01	20.91	0.02	0.13	0.00	27.27	1.86	108.02
MT-3L_P1_R2C_127	126	51.70	0.70	0.93	-0.01	19.35	0.01	0.09	-0.01	25.39	1.68	99.82
MT-3L_P1_R2C_128	127	51.79	0.70	0.93	-0.01	19.37	0.01	0.11	0.02	25.20	1.68	99.81
MT-3L_P1_R2C_129	128	51.50	0.68	0.94	-0.01	19.27	0.01	0.10	0.00	25.27	1.70	99.48
MT-3L_P1_R2C_130	129	51.89	0.68	0.94	-0.01	19.29	0.01	0.10	0.02	25.32	1.68	99.93
MT-3L_P1_R2C_131	130	51.75	0.69	0.99	0.02	19.52	0.02	0.11	-0.01	25.15	1.68	99.90
MT-3L_P1_R2C_132	131	51.66	0.68	0.99	-0.02	19.21	0.01	0.13	0.01	25.23	1.71	99.61
MT-3L_P1_R2C_133	132	51.49	0.65	0.97	0.00	19.69	0.01	0.09	-0.01	25.04	1.70	99.64
MT-3L_P1_R2C_134	133	51.90	0.70	0.99	-0.01	19.13	0.01	0.08	-0.01	25.14	1.73	99.65
MT-3L_P1_R2C_135	134	52.15	0.71	0.97	-0.00	19.00	0.02	0.11	-0.00	25.35	1.69	100.01
MT-3L_P1_R2C_136	135	51.91	0.69	1.00	0.01	19.28	0.01	0.11	0.00	25.13	1.71	99.85
MT-3L_P1_R2C_137	136	51.85	0.70	1.00	0.01	19.42	0.02	0.11	0.00	25.25	1.72	100.07
MT-3L_P1_R2C_138	137	51.90	0.71	0.98	-0.00	19.50	0.01	0.10	-0.01	25.12	1.73	100.05
MT-3L_P1_R2C_139	138	51.81	0.72	1.01	0.01	19.47	0.01	0.10	0.01	25.30	1.67	100.10
MT-3L_P1_R2C_140	139	51.71	0.72	1.00	-0.00	19.65	0.01	0.09	0.02	25.20	1.71	100.11
MT-3L_P1_R2C_141	140	52.06	0.69	1.01	-0.01	19.20	0.02	0.10	-0.01	25.18	1.70	99.93
MT-3L_P1_R2C_142	141	51.47	0.71	1.02	0.00	19.45	0.02	0.08	-0.02	24.91	1.68	99.33
MT-3L_P1_R2C_143	142	51.84	0.71	1.00	0.00	19.31	0.02	0.12	-0.01	25.09	1.70	99.77
MT-3L_P1_R2C_144	143	51.66	0.71	1.02	0.01	19.19	0.03	0.14	0.00	24.92	1.68	99.37
MT-3L_P1_R2C_145	144	51.73	0.72	1.01	-0.02	18.68	0.00	0.13	-0.00	25.06	1.71	99.03
MT-3L_P1_R2C_146	145	51.89	0.69	1.00	-0.00	19.13	0.01	0.12	-0.02	25.17	1.69	99.68
MT-3L_P1_R2C_147	146	51.68	0.70	1.00	0.00	19.01	0.03	0.11	-0.00	25.05	1.69	99.25
MT-3L_P1_R2C_148	147	51.75	0.70	1.02	-0.00	18.95	0.01	0.08	-0.00	25.03	1.72	99.25
MT-3L_P1_R2C_149	148	51.72	0.72	1.02	-0.00	19.30	0.01	0.11	0.01	25.14	1.72	99.73
MT-3L_P1_R2C_150	149	51.63	0.69	1.03	0.01	19.40	0.01	0.11	0.01	25.12	1.70	99.72
MT-3L_P1_R2C_151	150	52.03	0.72	1.02	0.00	19.37	0.01	0.12	-0.00	25.15	1.71	100.15
MT-3L_P1_R2C_152	151	51.92	0.72	1.06	0.01	19.31	0.01	0.10	0.01	25.07	1.69	99.91
MT-3L_P1_R2C_153	152	52.06	0.71	1.04	-0.02	19.43	0.01	0.10	0.00	25.26	1.70	100.30

Sample	Distance (μm)	SiO_2	Al_2O_3	CaO	K_2O	MgO	Na_2O	TiO_2	Cr_2O_3	FeO	MnO	Total
MT-3L_P1_R2C_154	153	51.79	0.70	1.00	0.02	19.37	0.02	0.12	-0.03	25.00	1.70	99.70
MT-3L_P1_R2C_155	154	51.67	0.72	1.03	-0.01	19.29	0.01	0.13	0.01	25.21	1.65	99.70
MT-3L_P1_R2C_156	155	51.74	0.70	1.01	0.00	19.33	0.01	0.10	-0.00	25.19	1.66	99.75
MT-3L_P1_R2C_157	156	51.61	0.70	1.02	-0.00	19.16	0.01	0.11	-0.00	25.06	1.70	99.36
MT-3L_P1_R2C_158	157	51.68	0.69	1.01	0.00	19.22	0.01	0.12	-0.00	25.12	1.70	99.55
MT-3L_P1_R2C_159	158	51.69	0.72	1.02	-0.00	19.13	0.01	0.11	0.01	25.29	1.70	99.66
MT-3L_P1_R2C_160	159	51.83	0.71	0.99	-0.02	19.49	0.00	0.10	-0.01	25.22	1.67	99.99
MT-3L_P1_R2C_161	160	51.77	0.74	1.02	-0.00	19.56	0.02	0.12	0.01	25.16	1.69	100.09
MT-3L_P1_R2C_162	161	51.80	0.72	1.04	-0.00	19.25	0.01	0.11	0.01	25.21	1.66	99.81
MT-3L_P1_R2C_163	162	51.63	0.72	1.02	0.01	19.18	0.01	0.10	-0.01	25.25	1.70	99.61
MT-3L_P1_R2C_164	163	51.80	0.72	0.98	-0.00	19.29	0.00	0.13	-0.01	25.19	1.65	99.74
MT-3L_P1_R2C_165	164	51.50	0.71	1.02	0.01	19.26	0.01	0.08	0.00	24.87	1.70	99.16
MT-3L_P1_R2C_166	165	51.77	0.72	1.01	-0.00	19.37	0.01	0.12	-0.01	25.13	1.72	99.83
MT-3L_P1_R2C_167	166	51.70	0.70	1.03	-0.01	19.18	0.02	0.11	-0.00	25.27	1.70	99.70
MT-3L_P1_R2C_168	167	51.66	0.71	1.04	-0.01	19.05	0.01	0.10	0.00	25.31	1.69	99.56
MT-3L_P1_R2C_169	168	51.60	0.72	1.01	0.01	19.32	0.02	0.10	0.01	25.20	1.70	99.68
MT-3L_P1_R2C_170	169	51.72	0.74	0.98	-0.01	19.33	0.02	0.10	-0.02	25.14	1.67	99.67
MT-3L_P1_R2C_171	170	51.57	0.72	1.00	0.01	19.08	0.01	0.12	0.00	25.38	1.66	99.55
MT-3L_P1_R2C_172	171	51.56	0.73	1.01	0.01	19.45	0.02	0.11	-0.01	24.96	1.67	99.51
MT-3L_P1_R2C_173	172	51.49	0.73	1.01	-0.00	19.21	0.00	0.11	-0.00	25.15	1.69	99.38
MT-3L_P1_R2C_174	173	51.78	0.72	1.02	0.00	19.42	0.02	0.10	-0.01	25.30	1.70	100.04
MT-3L_P1_R2C_175	174	51.75	0.73	1.03	0.00	19.41	0.02	0.11	0.00	25.22	1.67	99.95
MT-3L_P1_R2C_176	175	52.03	0.71	1.02	-0.00	19.31	0.02	0.07	0.01	25.33	1.68	100.19
MT-3L_P1_R2C_177	176	52.16	0.72	1.00	-0.00	19.28	0.02	0.14	0.01	25.12	1.67	100.11
MT-3L_P1_R2C_178	177	51.82	0.73	1.01	-0.01	19.22	0.01	0.11	0.00	25.32	1.64	99.86
MT-3L_P1_R2C_179	178	52.01	0.74	1.00	0.00	19.17	0.01	0.12	0.00	24.94	1.66	99.65
MT-3L_P1_R2C_180	179	51.06	0.67	1.01	0.01	19.31	0.01	0.06	-0.01	25.16	1.70	98.99
MT-3L_P1_R2C_181	180	52.18	0.74	1.00	-0.01	19.57	0.02	0.09	0.00	25.21	1.68	100.48
MT-3L_P1_R2C_182	181	51.74	0.73	0.96	-0.00	19.14	0.01	0.10	-0.02	25.30	1.69	99.66
MT-3L_P1_R2C_183	182	51.15	0.74	1.00	0.01	19.28	0.02	0.11	-0.01	25.27	1.63	99.20
MT-3L_P1_R2C_184	183	51.41	0.71	0.99	-0.00	19.29	0.02	0.12	-0.01	25.41	1.67	99.61
MT-3L_P1_R2C_185	184	51.78	0.73	1.01	0.02	19.34	0.02	0.11	0.02	25.09	1.74	99.85
MT-3L_P1_R2C_186	185	51.26	0.72	1.00	-0.00	19.06	0.02	0.12	0.01	25.20	1.74	99.12
MT-3L_P1_R2C_187	186	51.51	0.71	1.00	-0.01	19.13	0.01	0.12	-0.01	25.13	1.68	99.29
MT-3L_P1_R2C_188	187	51.79	0.73	1.00	0.02	19.52	0.02	0.13	-0.02	25.20	1.64	100.02
MT-3L_P1_R2C_189	188	51.78	0.71	0.99	0.02	19.17	0.01	0.11	-0.01	25.17	1.66	99.62
MT-3L_P1_R2C_190	189	51.61	0.71	0.99	-0.00	19.34	0.01	0.13	0.01	25.20	1.65	99.65
MT-3L_P1_R2C_191	190	51.50	0.69	0.99	-0.00	19.24	0.01	0.11	-0.01	25.18	1.67	99.38
MT-3L_P1_R2C_192	191	51.76	0.71	0.97	0.00	19.54	0.02	0.12	0.00	25.28	1.66	100.06

Sample	Distance (μm)	SiO_2	Al_2O_3	CaO	K_2O	MgO	Na_2O	TiO_2	Cr_2O_3	FeO	MnO	Total
MT-3L_P1_R2C_193	192	51.64	0.72	0.96	-0.02	19.37	0.01	0.10	-0.01	25.22	1.64	99.62
MT-3L_P1_R2C_194	193	51.52	0.71	1.01	-0.01	19.22	0.00	0.09	0.01	25.21	1.64	99.39
MT-3L_P1_R2C_195	194	51.44	0.71	1.00	-0.01	19.14	0.01	0.09	0.00	24.78	1.64	98.81
MT-3L_P1_R2C_196	195	51.66	0.73	1.00	-0.00	19.17	0.01	0.09	-0.00	25.25	1.68	99.59
MT-3L_P1_R2C_197	196	51.54	0.72	0.99	0.01	19.38	0.02	0.12	0.01	25.14	1.66	99.60
MT-3L_P1_R2C_198	197	51.58	0.73	1.00	0.01	19.36	0.01	0.13	0.01	25.07	1.67	99.56
MT-3L_P1_R2C_199	198	51.82	0.75	1.02	0.00	19.44	0.03	0.09	0.00	25.13	1.67	99.95
MT-3L_P1_R2C_200	199	51.76	0.74	0.99	0.00	19.49	0.01	0.10	-0.02	25.29	1.70	100.08
MT-3L_P1_R2C_201	200	51.70	0.72	0.98	-0.01	19.31	0.01	0.11	0.01	25.00	1.64	99.48
MT-3L_P1_R2C_202	201	51.61	0.74	1.00	0.01	19.59	0.01	0.13	-0.00	25.11	1.68	99.87
MT-3L_P1_R2C_203	202	51.59	0.74	1.01	0.00	19.09	0.02	0.12	-0.01	25.38	1.65	99.58
MT-3L_P1_R2C_204	203	51.97	0.73	0.99	-0.01	19.40	0.01	0.10	-0.01	25.25	1.65	100.09
MT-3L_P1_R2C_205	204	51.73	0.72	1.00	-0.01	19.16	0.00	0.11	-0.00	25.14	1.66	99.50
MT-3L_P1_R2C_206	205	51.86	0.70	0.99	-0.02	19.23	0.02	0.09	-0.01	25.22	1.61	99.69
MT-3L_P1_R2C_207	206	51.36	0.72	0.99	-0.01	18.37	-0.00	0.08	-0.01	25.09	1.73	98.31
MT-3L_P1_R2C_208	207	48.87	0.68	0.97	0.02	18.49	0.03	0.11	-0.01	24.15	1.57	94.87
MT-3L_P1_R2C_209	208	51.50	0.71	0.97	-0.01	18.97	0.01	0.11	-0.01	25.22	1.69	99.17
MT-3L_P1_R2C_210	209	51.60	0.69	1.01	-0.00	19.31	0.02	0.10	-0.00	25.14	1.65	99.52
MT-3L_P1_R2C_211	210	51.71	0.70	0.98	0.00	19.40	0.02	0.11	0.00	25.36	1.66	99.94
MT-3L_P1_R2C_212	211	51.91	0.69	0.99	-0.01	19.29	0.01	0.10	0.00	25.19	1.65	99.83
MT-3L_P1_R2C_213	212	51.91	0.70	0.96	0.00	19.23	0.01	0.14	-0.00	25.23	1.61	99.78
MT-3L_P1_R2C_214	213	51.97	0.65	0.96	-0.01	19.32	0.03	0.10	-0.01	25.33	1.62	99.96
MT-3L_P1_R2C_215	214	51.84	0.67	1.03	-0.00	19.31	0.01	0.10	-0.01	25.17	1.68	99.80
MT-3L_P1_R2C_216	215	51.82	0.67	0.99	0.01	19.48	0.01	0.11	-0.01	25.12	1.63	99.84
MT-3L_P1_R2C_217	216	51.91	0.64	1.00	-0.00	19.35	0.01	0.11	-0.01	25.47	1.62	100.10
MT-3L_P1_R2C_218	217	52.17	0.64	1.01	0.01	19.29	0.00	0.10	-0.00	25.15	1.58	99.96
MT-3L_P1_R2C_219	218	51.86	0.63	0.98	0.01	19.26	0.00	0.12	-0.01	25.16	1.63	99.66
MT-3L_P1_R2C_220	219	51.70	0.62	1.01	-0.00	19.38	0.02	0.12	0.01	25.21	1.69	99.75
MT-3L_P1_R2C_221	220	52.07	0.60	0.98	-0.01	19.43	0.01	0.12	0.01	25.25	1.64	100.10
MT-3L_P1_R2C_222	221	51.92	0.60	1.01	0.01	19.30	0.01	0.08	-0.00	25.04	1.65	99.62
MT-3L_P1_R2C_223	222	51.76	0.62	0.99	0.01	19.47	0.01	0.10	0.00	25.14	1.64	99.73
MT-3L_P1_R2C_224	223	52.05	0.60	0.98	-0.01	19.35	0.01	0.11	0.00	25.17	1.66	99.93
MT-3L_P1_R2C_225	224	52.05	0.60	0.99	-0.00	19.51	0.01	0.10	-0.01	25.26	1.67	100.18
MT-3L_P1_R2C_226	225	52.01	0.58	1.00	0.02	19.74	0.01	0.09	-0.01	25.06	1.67	100.19
MT-3L_P1_R2C_227	226	52.24	0.60	0.99	0.00	19.42	0.01	0.08	0.01	25.11	1.65	100.12
MT-3L_P1_R2C_228	227	51.96	0.60	0.99	-0.01	19.53	0.01	0.11	-0.01	25.26	1.67	100.12
MT-3L_P1_R2C_229	228	51.89	0.59	1.02	0.01	19.37	0.00	0.11	-0.02	25.11	1.67	99.74
MT-3L_P1_R2C_230	229	52.07	0.60	0.98	-0.01	19.40	0.00	0.13	0.01	25.05	1.62	99.84
MT-3L_P1_R2C_231	230	52.04	0.62	0.97	0.02	19.34	0.00	0.11	-0.01	25.10	1.62	99.82

Sample	Distance (μm)	SiO_2	Al_2O_3	CaO	K_2O	MgO	Na_2O	TiO_2	Cr_2O_3	FeO	MnO	Total
MT-3L_P1_R2C_232	231	51.70	0.62	1.01	-0.01	19.41	0.00	0.11	0.01	25.21	1.63	99.69
MT-3L_P1_R2C_233	232	51.82	0.62	0.99	0.01	19.53	0.02	0.14	-0.00	25.12	1.63	99.88
MT-3L_P1_R2C_234	233	51.70	0.62	1.01	-0.00	19.16	0.02	0.11	0.00	25.21	1.64	99.48
MT-3L_P1_R2C_235	234	51.94	0.62	0.98	0.02	19.40	0.01	0.13	-0.00	25.10	1.62	99.81
MT-3L_P1_R2C_236	235	51.80	0.62	0.98	0.00	19.34	0.02	0.14	0.00	25.08	1.63	99.62
MT-3L_P1_R2C_237	236	52.00	0.64	1.00	-0.00	19.26	0.01	0.13	0.01	25.06	1.59	99.68
MT-3L_P1_R2C_238	237	51.96	0.61	0.97	-0.00	19.50	0.01	0.12	-0.00	25.05	1.62	99.83
MT-3L_P1_R2C_239	238	51.86	0.63	1.01	-0.01	19.54	0.01	0.12	-0.02	25.21	1.66	100.00
MT-3L_P1_R2C_240	239	52.01	0.61	1.01	-0.00	19.49	0.01	0.11	-0.00	25.06	1.61	99.91
MT-3L_P1_R2C_241	240	51.95	0.61	0.98	-0.01	19.34	0.01	0.12	-0.00	25.08	1.63	99.71
MT-3L_P1_R2C_242	241	51.88	0.60	1.00	0.01	19.27	0.01	0.12	-0.00	25.15	1.64	99.69
MT-3L_P1_R2C_243	242	51.55	0.61	0.97	-0.01	19.11	0.01	0.11	-0.00	25.26	1.62	99.24
MT-3L_P1_R2C_244	243	51.98	0.61	1.01	0.02	19.47	0.01	0.12	-0.01	25.27	1.62	100.09
MT-3L_P1_R2C_245	244	52.04	0.61	1.00	-0.01	19.47	0.01	0.11	-0.00	24.95	1.62	99.79
MT-3L_P1_R2C_246	245	51.96	0.62	0.99	-0.01	19.67	0.01	0.10	0.00	24.82	1.67	99.84
MT-3L_P1_R2C_247	246	52.03	0.59	0.96	0.00	19.70	0.02	0.11	-0.00	25.29	1.61	100.32
MT-3L_P1_R2C_248	247	51.89	0.61	0.96	0.00	19.67	0.01	0.10	-0.00	25.11	1.63	99.99
MT-3L_P1_R2C_249	248	51.21	0.59	0.98	0.00	18.67	0.01	0.11	-0.01	24.45	1.60	97.62
MT-3L_P1_R2C_250	249	52.18	0.59	1.02	-0.00	19.20	0.01	0.11	-0.01	24.99	1.64	99.74
MT-3L_P1_R2C_251	250	52.06	0.62	1.02	0.01	19.50	0.01	0.11	-0.00	25.07	1.65	100.05
MT-3L_P1_R2C_252	251	52.35	0.60	0.97	-0.01	19.50	0.00	0.14	-0.01	25.07	1.62	100.24
MT-3L_P1_R2C_253	252	52.46	0.61	0.98	0.02	19.50	0.02	0.10	0.01	25.09	1.64	100.44
MT-3L_P1_R2C_254	253	51.83	0.59	0.99	0.01	19.65	0.01	0.11	0.00	25.02	1.67	99.88
MT-3L_P1_R2C_255	254	51.84	0.58	1.00	0.01	19.56	0.02	0.11	-0.00	25.11	1.62	99.84
MT-3L_P1_R2C_256	255	51.65	0.59	1.01	0.00	19.28	0.02	0.14	-0.01	25.08	1.64	99.39
MT-3L_P1_R2C_257	256	51.73	0.60	1.00	0.01	19.17	0.01	0.11	-0.00	24.71	1.62	98.96
MT-3L_P1_R2C_258	257	51.76	0.58	0.99	-0.01	19.43	0.02	0.11	-0.01	24.99	1.64	99.51
MT-3L_P1_R2C_259	258	51.60	0.60	0.97	-0.01	19.50	0.01	0.13	-0.01	25.14	1.61	99.53
MT-3L_P1_R2C_260	259	51.80	0.57	0.99	-0.01	19.43	0.00	0.12	0.00	25.11	1.66	99.67
MT-3L_P1_R2C_261	260	51.93	0.59	1.00	-0.00	19.75	0.02	0.11	0.00	24.99	1.63	100.02
MT-3L_P1_R2C_262	261	52.01	0.59	1.00	0.00	20.00	0.02	0.11	0.00	25.07	1.64	100.42
MT-3L_P1_R2C_263	262	51.96	0.57	0.97	-0.01	19.31	0.02	0.13	-0.01	25.00	1.62	99.56
MT-3L_P1_R2C_264	263	52.08	0.57	0.97	0.00	19.30	0.02	0.12	-0.02	24.97	1.63	99.64
MT-3L_P1_R2C_265	264	51.82	0.54	0.98	-0.00	19.69	0.02	0.11	-0.01	24.96	1.61	99.73
MT-3L_P1_R2C_266	265	51.90	0.55	1.01	0.00	19.26	0.01	0.12	0.00	25.15	1.62	99.63
MT-3L_P1_R2C_267	266	51.80	0.54	1.01	0.01	19.36	0.01	0.11	0.00	24.97	1.62	99.43
MT-3L_P1_R2C_268	267	51.98	0.53	1.01	-0.00	19.55	0.01	0.12	0.01	25.05	1.64	99.88
MT-3L_P1_R2C_269	268	51.83	0.53	0.99	0.00	19.34	0.00	0.11	-0.01	24.81	1.64	99.24
MT-3L_P1_R2C_270	269	51.99	0.54	1.00	-0.01	19.56	0.01	0.13	0.00	24.84	1.59	99.66

Sample	Distance (μm)	SiO_2	Al_2O_3	CaO	K_2O	MgO	Na_2O	TiO_2	Cr_2O_3	FeO	MnO	Total
MT-3L_P1_R2C_271	270	51.95	0.50	0.98	0.01	19.57	0.01	0.09	-0.01	25.04	1.62	99.77
MT-3L_P1_R2C_272	271	52.08	0.50	0.99	-0.00	19.55	0.02	0.11	0.01	24.81	1.59	99.65
MT-3L_P1_R2C_273	272	52.26	0.50	0.98	-0.00	19.46	0.01	0.10	-0.01	25.05	1.61	99.95
MT-3L_P1_R2C_274	273	51.83	0.49	0.99	0.00	19.56	0.02	0.09	0.01	24.75	1.61	99.37
MT-3L_P1_R2C_275	274	51.88	0.48	1.00	-0.01	19.65	0.01	0.13	-0.02	24.91	1.67	99.71
MT-3L_P1_R2C_276	275	51.94	0.49	0.99	-0.00	19.34	0.01	0.08	0.01	24.70	1.62	99.18
MT-3L_P1_R2C_277	276	52.02	0.49	0.97	0.02	19.87	0.01	0.14	-0.01	25.06	1.68	100.25
MT-3L_P1_R2C_278	277	51.80	0.49	1.00	-0.00	19.74	0.02	0.10	-0.01	24.85	1.67	99.65
MT-3L_P1_R2C_279	278	51.82	0.50	0.99	-0.00	19.53	0.01	0.10	0.01	24.89	1.64	99.49
MT-3L_P1_R2C_280	279	51.70	0.49	0.98	-0.01	19.60	0.01	0.11	-0.01	25.11	1.58	99.56
MT-3L_P1_R2C_281	280	52.26	0.49	0.98	0.00	19.66	0.01	0.11	-0.02	24.94	1.63	100.07
MT-3L_P1_R2C_282	281	52.17	0.51	1.01	0.00	19.63	0.01	0.13	-0.01	24.97	1.62	100.05
MT-3M_P1_R2C_01	0	57.05	19.03	5.59	1.22	0.07	1.55	0.26	0.00	1.40	0.02	86.19
MT-3M_P1_R2C_02	1	43.50	28.96	13.89	0.11	0.07	2.36	0.01	0.01	1.09	0.04	90.03
MT-3M_P1_R2C_03	2	43.55	29.53	14.48	0.09	0.13	2.43	0.04	0.00	1.11	0.02	91.38
MT-3M_P1_R2C_04	3	42.59	25.04	13.41	0.05	2.05	2.24	0.03	-0.00	1.87	0.06	87.35
MT-3M_P1_R2C_05	4	44.50	15.22	8.07	0.07	11.05	1.33	0.13	-0.00	8.61	0.25	89.21
MT-3M_P1_R2C_06	5	47.96	2.57	1.52	0.00	24.62	0.02	0.19	-0.00	16.60	0.51	93.99
MT-3M_P1_R2C_07	6	48.05	2.46	1.52	-0.01	24.72	0.02	0.23	0.00	16.78	0.52	94.28
MT-3M_P1_R2C_08	7	48.31	2.15	1.58	0.00	24.92	0.02	0.18	0.01	16.29	0.49	93.94
MT-3M_P1_R2C_09	8	48.51	1.99	1.46	0.01	24.88	0.01	0.17	-0.01	16.57	0.53	94.13
MT-3M_P1_R2C_10	9	48.39	1.97	1.65	0.01	24.39	0.02	0.20	-0.01	17.12	0.56	94.31
MT-3M_P1_R2C_11	10	47.91	1.45	1.49	0.00	22.27	0.02	0.18	-0.01	19.74	0.96	94.02
MT-3M_P1_R2C_12	11	47.66	0.61	0.96	0.01	19.42	0.01	0.10	-0.01	24.02	1.64	94.43
MT-3M_P1_R2C_13	12	47.57	0.56	0.94	-0.00	19.10	0.00	0.12	-0.01	24.55	1.62	94.43
MT-3M_P1_R2C_14	13	47.66	0.57	0.90	-0.00	19.23	0.02	0.10	0.01	24.55	1.63	94.67
MT-3M_P1_R2C_15	14	47.56	0.56	0.92	0.02	19.26	0.02	0.09	0.01	24.37	1.63	94.44
MT-3M_P1_R2C_16	15	47.48	0.59	0.88	-0.01	19.25	0.01	0.09	-0.00	24.53	1.70	94.51
MT-3M_P1_R2C_17	16	47.58	0.63	0.87	0.00	19.12	0.01	0.12	-0.00	24.62	1.67	94.62
MT-3M_P1_R2C_18	17	47.61	0.66	0.90	-0.00	19.28	0.03	0.11	-0.00	24.65	1.65	94.87
MT-3M_P1_R2C_19	18	47.64	0.66	0.88	0.01	19.18	0.01	0.12	-0.01	24.69	1.71	94.89
MT-3M_P1_R2C_20	19	47.72	0.61	0.91	0.01	19.01	0.02	0.12	0.01	24.68	1.69	94.77
MT-3M_P1_R2C_21	20	47.89	0.56	0.92	-0.00	19.25	0.01	0.12	-0.01	24.68	1.67	95.09
MT-3M_P1_R2C_22	21	51.66	0.61	0.99	0.01	20.75	0.02	0.12	0.01	26.46	1.85	102.48
MT-3M_P1_R2C_23	22	47.59	0.51	0.88	-0.01	19.24	0.01	0.11	-0.01	24.65	1.67	94.64
MT-3M_P1_R2C_24	23	47.67	0.53	0.94	0.00	19.28	0.02	0.10	-0.00	24.70	1.62	94.86
MT-3M_P1_R2C_25	24	47.74	0.52	0.92	-0.01	19.09	0.03	0.10	-0.01	24.68	1.66	94.70
MT-3M_P1_R2C_26	25	47.62	0.48	0.93	0.00	19.13	0.01	0.11	-0.01	24.53	1.65	94.46
MT-3M_P1_R2C_27	26	47.67	0.48	0.92	0.01	19.22	0.00	0.11	-0.01	24.53	1.66	94.60

Sample	Distance (μm)	SiO_2	Al_2O_3	CaO	K_2O	MgO	Na_2O	TiO_2	Cr_2O_3	FeO	MnO	Total
MT-3M_P1_R2C_28	27	47.90	0.50	0.95	-0.01	19.23	0.02	0.12	0.00	24.66	1.65	95.03
MT-3M_P1_R2C_29	28	47.60	0.48	0.94	0.01	19.26	0.01	0.14	0.01	24.54	1.68	94.66
MT-3M_P1_R2C_30	29	47.73	0.49	0.93	-0.01	19.06	0.02	0.11	-0.00	24.56	1.67	94.56
MT-3M_P1_R2C_31	30	47.93	0.49	0.98	0.00	18.99	0.02	0.08	-0.01	24.47	1.65	94.61
MT-3M_P1_R2C_32	31	47.51	0.48	0.92	0.02	19.22	0.01	0.10	0.00	24.67	1.64	94.57
MT-3M_P1_R2C_33	32	47.86	0.50	0.97	0.01	19.17	0.01	0.11	-0.00	24.65	1.65	94.93
MT-3M_P1_R2C_34	33	47.64	0.49	0.95	-0.01	19.29	0.01	0.14	-0.01	24.58	1.65	94.75
MT-3M_P1_R2C_35	34	47.74	0.49	0.99	-0.02	19.32	0.02	0.12	-0.01	24.45	1.64	94.72
MT-3M_P1_R2C_36	35	47.68	0.53	0.99	0.00	19.28	0.01	0.09	-0.01	24.72	1.64	94.94
MT-3M_P1_R2C_37	36	47.83	0.52	0.96	0.01	19.16	0.01	0.10	0.01	24.47	1.65	94.72
MT-3M_P1_R2C_38	37	47.65	0.51	0.98	0.01	19.24	0.01	0.12	-0.00	24.50	1.69	94.70
MT-3M_P1_R2C_39	38	47.76	0.49	0.98	-0.00	19.31	0.01	0.08	-0.00	24.60	1.65	94.89
MT-3M_P1_R2C_40	39	47.86	0.49	0.97	0.00	19.31	0.01	0.10	-0.01	24.39	1.64	94.78
MT-3M_P1_R2C_41	40	47.73	0.48	1.00	0.00	19.27	0.01	0.11	-0.01	24.35	1.60	94.55
MT-3M_P1_R2C_42	41	47.57	0.47	0.97	-0.00	19.34	0.02	0.11	-0.01	24.59	1.67	94.73
MT-3M_P1_R2C_43	42	47.71	0.49	1.00	-0.02	19.40	0.02	0.12	0.00	24.60	1.62	94.93
MT-3M_P1_R2C_44	43	47.78	0.52	0.99	-0.00	19.37	0.01	0.09	-0.01	24.41	1.65	94.82
MT-3M_P1_R2C_45	44	47.78	0.53	1.01	0.00	19.32	0.02	0.11	-0.02	24.35	1.62	94.72
MT-3M_P1_R2C_46	45	47.62	0.56	0.96	0.00	19.26	0.01	0.09	-0.00	24.62	1.63	94.75
MT-3M_P1_R2C_47	46	47.66	0.59	1.00	0.00	19.27	0.01	0.13	-0.01	24.51	1.64	94.81
MT-3M_P1_R2C_48	47	47.63	0.58	0.99	0.02	19.26	0.01	0.11	-0.01	24.47	1.61	94.67
MT-3M_P1_R2C_49	48	47.48	0.60	1.00	-0.01	19.31	0.01	0.11	-0.00	24.38	1.61	94.50
MT-3M_P1_R2C_50	49	47.42	0.61	1.00	0.00	19.29	0.00	0.13	-0.01	24.33	1.70	94.47
MT-3M_P1_R2C_51	50	47.14	0.62	0.97	-0.00	19.18	0.01	0.11	-0.01	24.29	1.63	93.94
MT-3M_P1_R2C_52	51	47.54	0.61	0.98	0.01	19.18	0.02	0.12	0.00	24.15	1.60	94.23
MT-3M_P1_R2C_53	52	47.51	0.64	1.00	0.01	19.25	0.01	0.09	-0.00	24.37	1.57	94.45
MT-3M_P1_R2C_54	53	47.55	0.65	0.97	-0.01	19.35	0.01	0.09	-0.01	24.54	1.67	94.83
MT-3M_P1_R2C_55	54	47.32	0.62	0.98	-0.00	19.20	0.02	0.12	0.00	24.48	1.67	94.39
MT-3M_P1_R2C_56	55	47.31	0.64	0.97	0.00	19.29	0.02	0.12	-0.00	24.45	1.66	94.45
MT-3M_P1_R2C_57	56	47.29	0.62	0.95	-0.01	19.31	0.00	0.11	0.01	24.47	1.65	94.39
MT-3M_P1_R2C_58	57	47.19	0.62	0.96	0.01	19.31	0.00	0.11	-0.00	24.43	1.65	94.27
MT-3M_P1_R2C_59	58	47.32	0.62	0.96	-0.01	19.29	0.01	0.10	0.01	24.27	1.68	94.25
MT-3M_P1_R2C_60	59	47.27	0.61	0.93	-0.01	19.27	0.02	0.09	-0.00	24.36	1.62	94.15
MT-3M_P1_R2C_61	60	47.02	0.62	0.94	0.00	19.31	0.01	0.09	0.00	24.22	1.63	93.84
MT-3M_P1_R2C_62	61	47.22	0.63	0.92	0.00	19.38	0.01	0.11	-0.01	24.27	1.67	94.19
MT-3M_P1_R2C_63	62	47.27	0.60	0.94	-0.01	19.37	0.01	0.11	0.01	24.34	1.66	94.32
MT-3M_P1_R2C_64	63	47.34	0.60	0.93	0.01	19.47	0.01	0.11	-0.02	24.51	1.66	94.62
MT-3M_P1_R2C_65	64	47.30	0.56	0.94	-0.00	19.35	0.01	0.09	-0.02	24.34	1.62	94.19
MT-3M_P1_R2C_66	65	47.08	0.60	0.94	-0.01	19.27	0.01	0.08	0.01	24.07	1.65	93.72

Sample	Distance (μm)	SiO_2	Al_2O_3	CaO	K_2O	MgO	Na_2O	TiO_2	Cr_2O_3	FeO	MnO	Total
MT-3M_P1_R2C_2_01	0	47.74	2.58	1.50	0.11	18.75	0.24	0.19	-0.01	20.56	0.88	92.55
MT-3M_P1_R2C_2_02	1	47.61	2.03	1.75	0.02	22.93	0.03	0.29	0.00	18.83	0.65	94.15
MT-3M_P1_R2C_2_03	2	48.30	2.01	1.56	0.01	24.57	0.02	0.21	-0.00	16.75	0.50	93.91
MT-3M_P1_R2C_2_04	3	48.06	2.14	1.68	-0.02	24.58	0.01	0.22	-0.01	16.93	0.49	94.08
MT-3M_P1_R2C_2_05	4	48.17	1.96	1.55	0.00	24.68	0.01	0.20	0.00	16.40	0.50	93.49
MT-3M_P1_R2C_2_06	5	48.58	1.81	1.55	-0.01	24.86	0.02	0.16	0.01	16.22	0.55	93.75
MT-3M_P1_R2C_2_07	6	48.11	1.47	1.52	0.01	23.15	0.02	0.20	-0.00	18.60	0.73	93.80
MT-3M_P1_R2C_2_08	7	47.78	1.45	1.54	0.01	22.66	0.02	0.18	-0.01	19.46	0.76	93.85
MT-3M_P1_R2C_2_09	8	48.17	1.36	1.46	-0.00	23.09	0.01	0.17	-0.00	18.58	0.71	93.55
MT-3M_P1_R2C_2_10	9	47.91	1.42	1.54	-0.00	22.37	0.02	0.19	-0.02	19.48	0.79	93.70
MT-3M_P1_R2C_2_11	10	48.80	1.31	1.42	0.01	23.79	0.02	0.15	0.00	18.16	0.71	94.37
MT-3M_P1_R2C_2_12	11	48.58	1.30	1.40	-0.00	23.94	0.02	0.14	-0.02	17.97	0.71	94.03
MT-3M_P1_R2C_2_13	12	48.22	1.37	1.31	0.00	23.17	0.01	0.11	-0.01	18.88	0.78	93.84
MT-3M_P1_R2C_2_14	13	51.60	1.94	1.45	0.01	24.15	0.02	0.19	0.02	21.53	0.84	101.73
MT-3M_P1_R2C_2_15	14	47.52	2.05	1.39	0.00	22.42	0.01	0.21	-0.01	19.84	0.70	94.13
MT-3M_P1_R2C_2_16	15	47.87	2.20	1.41	-0.02	22.77	0.01	0.20	0.01	19.71	0.66	94.81
MT-3M_P1_R2C_2_17	16	47.67	2.28	1.51	0.00	23.18	0.02	0.20	0.01	18.83	0.59	94.28
MT-3M_P1_R2C_2_18	17	47.60	2.29	1.61	0.02	23.43	0.03	0.23	-0.01	17.89	0.55	93.63
MT-3M_P1_R2C_2_19	18	48.40	2.04	1.49	0.01	24.66	0.01	0.17	-0.00	16.99	0.54	94.31
MT-3M_P1_R2C_2_20	19	48.23	2.12	1.49	-0.01	24.50	0.01	0.22	-0.01	16.77	0.49	93.82
MT-3M_P1_R2C_2_21	20	47.99	1.49	1.33	0.02	21.65	0.01	0.14	0.01	20.57	1.06	94.27
MT-3M_P1_R2C_2_22	21	47.76	0.70	0.90	0.02	19.53	0.01	0.12	-0.01	24.21	1.60	94.84
MT-3M_P1_R2C_2_23	22	47.67	0.65	0.89	0.01	19.26	0.01	0.14	-0.00	24.48	1.68	94.78
MT-3M_P1_R2C_2_24	23	47.51	0.74	0.85	-0.00	19.04	0.01	0.10	-0.01	25.02	1.68	94.93
MT-3M_P1_R2C_2_25	24	47.58	0.73	0.81	0.01	18.81	0.01	0.10	-0.01	24.84	1.70	94.58
MT-3M_P1_R2C_2_26	25	47.36	0.69	0.81	-0.03	18.86	0.02	0.12	0.00	24.71	1.68	94.22
MT-3M_P1_R2C_2_27	26	49.12	1.92	0.94	0.34	18.98	0.12	0.13	0.00	21.99	1.33	94.85
MT-3M_P1_R2C_2_28	27	47.47	0.67	0.84	-0.00	19.00	0.01	0.14	0.01	24.88	1.73	94.74
MT-3M_P1_R2C_2_29	28	47.65	0.67	0.85	0.01	19.06	0.01	0.08	-0.01	24.90	1.72	94.92
MT-3M_P1_R2C_2_30	29	47.29	0.64	0.88	-0.00	18.97	0.01	0.08	0.01	24.83	1.74	94.45
MT-3M_P1_R2C_2_31	30	47.31	0.62	0.89	0.00	18.85	0.01	0.11	-0.01	24.84	1.67	94.31
MT-3M_P1_R2C_2_32	31	47.56	0.57	0.92	-0.01	18.98	0.01	0.12	0.00	24.86	1.69	94.71
MT-3M_P1_R2C_2_33	32	47.80	0.57	0.89	-0.01	18.96	0.02	0.14	-0.01	24.86	1.68	94.91
MT-3M_P1_R2C_2_34	33	47.60	0.54	0.91	-0.02	19.07	0.01	0.13	0.00	24.60	1.69	94.52
MT-3M_P1_R2C_2_35	34	47.53	0.53	0.91	0.01	18.99	0.02	0.12	-0.01	24.83	1.69	94.61
MT-3M_P1_R2C_2_36	35	47.61	0.54	0.95	0.00	19.14	0.02	0.12	-0.00	24.85	1.69	94.92
MT-3M_P1_R2C_2_37	36	48.24	0.52	0.98	0.00	19.39	0.01	0.12	0.01	24.89	1.72	95.87
MT-3M_P1_R2C_2_38	37	47.98	0.54	0.98	0.03	18.82	0.02	0.10	-0.00	24.65	1.69	94.81

Sample	Distance (μm)	SiO_2	Al_2O_3	CaO	K_2O	MgO	Na_2O	TiO_2	Cr_2O_3	FeO	MnO	Total
MT-3M_P1_R2C_2_39	38	47.79	0.56	0.93	-0.01	19.10	0.01	0.12	-0.00	24.90	1.73	95.13
MT-3M_P1_R2C_2_40	39	47.65	0.57	0.98	-0.00	19.16	0.01	0.12	0.01	24.82	1.67	94.97
MT-3M_P1_R2C_2_41	40	47.72	0.60	0.98	0.01	19.17	0.01	0.10	-0.01	24.97	1.72	95.26
MT-3M_P1_R2C_2_42	41	47.74	0.59	0.96	0.01	18.94	0.02	0.14	-0.00	24.83	1.71	94.93
MT-3M_P1_R2C_2_43	42	47.74	0.60	0.99	-0.00	19.04	0.01	0.09	-0.00	24.79	1.69	94.93
MT-3M_P1_R2C_2_44	43	47.71	0.61	0.95	-0.00	19.13	0.00	0.12	0.00	24.93	1.70	95.14
MT-3M_P1_R2C_2_45	44	47.59	0.59	0.96	0.00	19.05	0.01	0.12	-0.01	24.76	1.71	94.81
MT-3M_P1_R2C_2_46	45	47.61	0.62	0.95	0.01	19.09	0.02	0.12	0.00	24.93	1.67	95.01
MT-3M_P1_R2C_2_47	46	47.52	0.63	0.95	0.01	19.03	0.01	0.08	-0.00	24.73	1.73	94.68
MT-3M_P1_R2C_2_48	47	47.64	0.63	0.96	-0.00	19.05	0.01	0.13	0.00	24.81	1.69	94.91
MT-3M_P1_R2C_2_49	48	47.60	0.64	0.97	-0.00	19.08	0.02	0.11	-0.01	24.96	1.70	95.06
MT-3M_P1_R2C_2_50	49	47.51	0.66	0.94	0.01	19.08	0.01	0.13	0.00	24.84	1.73	94.91
MT-3M_P1_R2C_2_51	50	47.46	0.66	0.92	0.01	18.99	0.02	0.12	0.01	24.85	1.68	94.72
MT-3M_P1_R2C_2_52	51	47.36	0.65	0.94	0.00	18.98	0.02	0.11	-0.01	25.04	1.71	94.80
MT-3M_P1_R2C_2_53	52	47.44	0.65	0.91	0.00	19.08	0.01	0.11	0.00	24.76	1.72	94.67
MT-3M_P1_R2C_2_54	53	47.78	0.64	0.90	-0.01	19.08	0.01	0.11	0.00	24.93	1.68	95.13
MT-3M_P1_R2C_2_55	54	47.48	0.64	0.90	0.01	18.97	0.02	0.10	0.01	24.77	1.71	94.61
MT-3M_P1_R2C_2_56	55	47.72	0.62	0.89	0.02	19.12	0.01	0.09	-0.01	24.97	1.74	95.17
MT-3M_P1_R2C_2_57	56	47.47	0.62	0.86	0.00	19.11	0.01	0.09	0.00	24.93	1.72	94.82
MT-3M_P1_R2C_2_58	57	47.32	0.61	0.87	0.00	19.04	0.01	0.12	-0.00	24.90	1.70	94.58
MT-3M_P1_R2C_2_59	58	47.40	0.59	0.88	0.01	19.11	0.02	0.09	0.00	24.88	1.70	94.67
MT-3M_P1_R2C_2_60	59	47.40	0.56	0.88	0.00	19.18	0.02	0.11	0.02	24.84	1.71	94.71
MT-3M_P1_R2C_2_61	60	47.49	0.59	0.87	0.01	19.03	0.01	0.08	-0.01	24.77	1.71	94.56
MT-3M_P1_R2C_2_62	61	51.46	0.61	0.96	0.01	20.78	0.03	0.09	0.02	26.84	1.87	102.67
MT-3M_P1_R2C_2_63	62	47.58	0.60	0.88	0.02	19.11	0.01	0.10	0.01	24.94	1.77	95.02
MT-3M_P1_R2C_2_64	63	47.41	0.57	0.87	0.01	19.03	0.02	0.11	0.00	24.97	1.76	94.76
MT-3M_P1_R2C_2_65	64	47.64	0.55	0.87	-0.00	19.14	0.01	0.10	0.00	24.94	1.72	94.96
MT-3M_P1_R2C_2_66	65	47.58	0.56	0.90	0.01	19.06	0.01	0.10	-0.02	24.69	1.75	94.64
MT-3M_P1_R2C_2_67	66	47.41	0.56	0.87	0.01	19.24	0.01	0.11	-0.01	24.85	1.76	94.81
MT-3M_P1_R2C_2_68	67	47.32	0.57	0.87	0.02	19.12	0.01	0.11	-0.00	24.78	1.73	94.53
MT-3M_P1_R2C_2_69	68	47.27	0.60	0.90	-0.00	19.03	0.01	0.11	-0.01	24.73	1.70	94.35
MT-3M_P1_R2C_2_70	69	47.30	0.63	0.90	0.01	19.02	0.01	0.13	0.00	24.94	1.68	94.61
MT-3M_P1_R2C_2_71	70	46.95	0.64	0.90	0.00	18.88	0.01	0.10	-0.00	24.91	1.68	94.09
MT-3M_P1_R2C_2_72	71	46.80	0.67	0.87	-0.00	19.07	0.01	0.11	-0.01	24.98	1.71	94.22
MT-3M_P1_R2C_2_73	72	46.89	0.68	0.93	0.02	18.94	0.01	0.14	-0.01	24.84	1.67	94.12
MT-3M_P1_R2C_2_74	73	46.90	0.72	0.88	-0.01	19.01	0.01	0.10	0.00	25.16	1.67	94.44
MT-3M_P1_R2C_2_75	74	46.96	0.69	0.91	-0.01	18.98	0.00	0.09	-0.00	25.05	1.75	94.42
MT-3M_P1_R2C_2_76	75	46.65	0.69	0.86	-0.01	19.04	0.02	0.10	0.00	25.00	1.72	94.07
MT-3M_P1_R2C_2_77	76	46.76	0.70	0.87	0.00	19.01	0.00	0.11	0.00	24.80	1.67	93.92

Sample	Distance (μm)	SiO_2	Al_2O_3	CaO	K_2O	MgO	Na_2O	TiO_2	Cr_2O_3	FeO	MnO	Total
MT-3M_P4_R2C_01	0	56.57	25.13	10.59	0.82	0.43	3.25	0.16	-0.02	1.52	0.03	98.49
MT-3M_P4_R2C_02	1	63.86	8.51	1.12	2.04	4.64	0.72	0.60	-0.01	4.98	0.18	86.64
MT-3M_P4_R2C_03	2	56.87	3.96	1.28	0.71	15.69	0.20	0.41	-0.00	14.78	0.59	94.47
MT-3M_P4_R2C_04	3	52.10	0.92	1.58	0.02	24.04	0.02	0.13	-0.01	18.41	0.59	97.80
MT-3M_P4_R2C_05	4	52.34	0.78	1.43	0.00	25.91	0.02	0.13	-0.01	16.61	0.51	97.72
MT-3M_P4_R2C_06	5	52.56	0.79	1.48	0.00	26.20	0.02	0.16	-0.02	15.85	0.51	97.56
MT-3M_P4_R2C_07	6	52.49	0.83	1.52	-0.01	25.99	0.03	0.14	0.00	16.10	0.49	97.57
MT-3M_P4_R2C_08	7	52.21	0.95	1.64	0.01	25.71	0.01	0.12	0.00	16.33	0.53	97.50
MT-3M_P4_R2C_09	8	52.29	1.01	1.69	0.00	25.82	0.02	0.15	-0.01	16.43	0.51	97.89
MT-3M_P4_R2C_10	9	52.20	0.90	1.68	-0.00	25.74	0.02	0.15	-0.00	16.35	0.53	97.56
MT-3M_P4_R2C_11	10	52.00	0.96	1.69	0.01	25.62	0.01	0.14	-0.02	16.32	0.49	97.22
MT-3M_P4_R2C_12	11	52.15	0.80	1.74	0.00	24.53	0.00	0.13	-0.01	17.96	0.61	97.91
MT-3M_P4_R2C_13	12	51.46	0.47	1.34	0.01	22.96	0.02	0.09	0.00	20.95	1.10	98.41
MT-3M_P4_R2C_14	13	51.42	0.50	1.02	0.00	21.53	0.01	0.11	0.00	22.34	1.32	98.24
MT-3M_P4_R2C_15	14	50.85	0.49	1.00	0.01	21.07	0.02	0.06	-0.00	22.86	1.41	97.76
MT-3M_P4_R2C_16	15	50.99	0.48	0.96	-0.01	20.78	0.01	0.09	-0.02	23.37	1.38	98.03
MT-3M_P4_R2C_17	16	50.93	0.46	0.97	-0.00	20.59	0.02	0.11	0.00	23.42	1.37	97.87
MT-3M_P4_R2C_18	17	50.61	0.55	0.98	0.03	20.42	0.02	0.13	-0.01	23.59	1.36	97.66
MT-3M_P4_R2C_19	18	50.55	0.52	0.99	0.01	20.45	0.02	0.10	0.00	23.62	1.36	97.62
MT-3M_P4_R2C_20	19	54.57	0.60	1.06	0.02	22.18	0.02	0.12	-0.00	25.73	1.49	105.78
MT-3M_P4_R2C_21	20	50.66	0.51	1.00	0.00	20.57	0.02	0.09	0.00	23.67	1.33	97.85
MT-3M_P4_R2C_22	21	50.70	0.49	1.00	-0.02	20.54	0.01	0.10	-0.00	23.77	1.36	97.96
MT-3M_P4_R2C_23	22	50.83	0.50	1.00	0.02	20.44	0.01	0.12	-0.00	23.48	1.34	97.73
MT-3M_P4_R2C_24	23	50.74	0.51	1.01	-0.02	20.52	0.02	0.12	-0.02	23.35	1.34	97.58
MT-3M_P4_R2C_25	24	50.89	0.52	1.01	-0.00	20.61	0.01	0.11	-0.01	23.56	1.34	98.03
MT-3M_P4_R2C_26	25	51.05	0.49	1.03	-0.02	20.56	0.01	0.13	0.01	23.53	1.33	98.12
MT-3M_P4_R2C_27	26	50.94	0.51	1.05	-0.01	20.67	0.02	0.12	-0.03	23.56	1.41	98.25
MT-3M_P4_R2C_28	27	50.83	0.46	1.07	-0.01	20.52	0.01	0.11	-0.01	23.46	1.41	97.85
MT-3M_P4_R2C_29	28	51.39	0.47	1.04	0.01	20.45	0.01	0.11	-0.01	23.59	1.47	98.52
MT-3M_P4_R2C_30	29	51.33	0.46	1.03	-0.01	20.44	0.01	0.10	-0.00	23.70	1.44	98.50
MT-3M_P4_R2C_31	30	51.22	0.39	1.04	0.00	20.47	0.01	0.09	-0.01	23.53	1.49	98.24
MT-3M_P4_R2C_32	31	51.11	0.32	1.06	0.00	20.41	0.01	0.08	0.01	23.52	1.47	97.98
MT-3M_P4_R2C_33	32	51.49	0.30	1.05	-0.00	20.41	0.01	0.07	0.01	23.51	1.49	98.33
MT-3M_P4_R2C_34	33	51.35	0.31	1.07	0.00	20.51	0.01	0.07	0.01	23.49	1.54	98.36
MT-3M_P4_R2C_35	34	51.42	0.31	1.08	-0.00	20.60	0.01	0.07	-0.01	23.67	1.49	98.63
MT-3M_P4_R2C_36	35	51.47	0.33	1.09	0.00	20.53	0.01	0.08	0.01	23.36	1.51	98.39
MT-3M_P4_R2C_37	36	51.34	0.32	1.09	-0.00	20.43	0.01	0.07	-0.02	23.58	1.50	98.32
MT-3M_P4_R2C_38	37	51.34	0.34	1.10	-0.01	20.41	0.02	0.07	0.00	23.53	1.54	98.33

Sample	Distance (μm)	SiO_2	Al_2O_3	CaO	K_2O	MgO	Na_2O	TiO_2	Cr_2O_3	FeO	MnO	Total
MT-3M_P4_R2C_39	38	51.24	0.33	1.10	-0.00	20.35	0.01	0.06	0.01	23.40	1.55	98.03
MT-3M_P4_R2C_40	39	51.47	0.33	1.08	0.02	20.52	0.01	0.07	-0.01	23.72	1.52	98.71
MT-3M_P4_R2C_41	40	50.90	0.33	1.09	0.03	20.51	0.01	0.06	-0.01	23.58	1.58	98.07
MT-3M_P4_R2C_42	41	51.20	0.33	1.09	0.01	20.27	0.01	0.07	-0.01	23.59	1.54	98.08
MT-3M_P4_R2C_43	42	51.26	0.32	1.10	0.01	20.36	0.02	0.08	-0.00	23.64	1.60	98.39
MT-3M_P4_R2C_44	43	51.35	0.32	1.06	0.00	20.31	0.01	0.09	-0.00	23.75	1.55	98.43
MT-3M_P4_R2C_45	44	51.18	0.32	1.07	-0.01	20.21	0.01	0.07	-0.00	23.70	1.61	98.17
MT-3M_P4_R2C_46	45	51.25	0.33	1.09	-0.01	20.18	0.02	0.08	-0.01	23.97	1.60	98.49
MT-3M_P4_R2C_47	46	51.33	0.33	1.05	-0.01	20.13	0.01	0.08	-0.01	23.77	1.60	98.28
MT-3M_P4_R2C_48	47	51.08	0.32	1.04	-0.00	20.19	0.02	0.06	-0.00	23.97	1.59	98.26
MT-3M_P4_R2C_49	48	51.19	0.32	1.05	0.00	20.11	0.02	0.07	-0.01	23.85	1.62	98.23
MT-3M_P4_R2C_50	49	51.38	0.32	1.02	0.00	20.18	0.00	0.08	0.00	24.05	1.62	98.66
MT-3M_P4_R2C_51	50	51.14	0.35	1.04	-0.01	20.05	0.02	0.07	0.00	23.81	1.62	98.08
MT-3M_P4_R2C_52	51	51.10	0.35	1.01	0.00	20.12	0.00	0.09	-0.01	23.97	1.65	98.30
MT-3M_P4_R2C_53	52	50.95	0.37	1.01	0.01	20.08	0.01	0.07	-0.01	24.09	1.62	98.21
MT-3M_P4_R2C_54	53	50.96	0.48	0.99	0.00	20.10	0.01	0.10	-0.00	24.10	1.64	98.36
MT-3M_P4_R2C_55	54	50.98	0.50	0.95	-0.02	19.92	0.02	0.08	0.00	24.15	1.62	98.19
MT-3M_P4_R2C_56	55	50.93	0.54	0.93	-0.01	19.82	0.01	0.07	0.00	24.53	1.61	98.43
MT-3M_P4_R2C_57	56	50.83	0.57	0.94	-0.00	19.65	0.01	0.08	-0.02	24.44	1.68	98.20
MT-3M_P4_R2C_58	57	50.74	0.62	0.93	-0.01	19.83	0.01	0.09	-0.01	24.49	1.63	98.32
MT-3M_P4_R2C_59	58	50.56	0.63	0.92	-0.01	19.64	0.03	0.09	-0.01	24.52	1.66	98.03
MT-3M_P4_R2C_60	59	50.50	0.60	0.91	0.01	19.82	0.02	0.10	-0.01	24.52	1.64	98.12
MT-3M_P4_R2C_61	60	50.81	0.56	0.92	0.02	19.65	0.01	0.08	-0.01	24.31	1.66	98.02
MT-3M_P4_R2C_62	61	50.61	0.57	0.89	0.01	19.73	0.02	0.08	-0.01	24.78	1.68	98.34
MT-3M_P4_R2C_63	62	50.58	0.60	0.91	0.02	19.68	0.02	0.10	0.00	24.62	1.66	98.19
MT-3M_P4_R2C_64	63	50.61	0.64	0.91	0.01	19.68	0.01	0.08	0.00	24.67	1.70	98.31
MT-3M_P4_R2C_65	64	50.68	0.65	0.90	-0.01	19.60	0.02	0.10	-0.01	24.71	1.70	98.34
MT-3M_P4_R2C_66	65	50.65	0.67	0.92	-0.01	19.51	0.02	0.10	-0.00	24.89	1.66	98.41
MT-3M_P4_R2C_67	66	50.18	0.65	0.90	-0.01	19.45	0.02	0.10	0.00	24.76	1.67	97.71
MT-3M_P4_R2C_68	67	50.32	0.65	0.91	0.00	19.34	0.01	0.11	-0.01	24.57	1.68	97.58
MT-3M_P4_R2C_69	68	50.42	0.62	0.90	0.00	19.34	0.01	0.11	0.01	24.69	1.71	97.81
MT-3M_P4_R2C_70	69	50.48	0.62	0.92	0.01	19.57	0.01	0.12	-0.01	24.75	1.66	98.14
MT-3M_P4_R2C_71	70	50.56	0.60	0.94	0.02	19.56	0.01	0.09	-0.00	24.73	1.68	98.19
MT-3M_P4_R2C_72	71	50.39	0.59	0.93	0.01	19.61	0.01	0.08	-0.01	24.69	1.66	97.96
MT-3M_P4_R2C_73	72	50.32	0.59	0.92	0.01	19.49	0.02	0.11	-0.02	24.65	1.64	97.73
MT-3M_P4_R2C_74	73	50.38	0.55	0.96	-0.02	19.37	0.01	0.11	0.01	24.49	1.69	97.56
MT-3M_P4_R2C_75	74	50.58	0.55	0.94	0.01	19.49	0.00	0.10	0.00	24.59	1.68	97.94
MT-3M_P4_R2C_76	75	54.56	0.57	1.02	0.01	21.04	0.04	0.09	0.01	26.80	1.80	105.95
MT-3M_P4_R2C_77	76	50.23	0.51	0.95	0.01	19.30	0.02	0.10	-0.02	24.58	1.67	97.36

Sample	Distance (μm)	SiO_2	Al_2O_3	CaO	K_2O	MgO	Na_2O	TiO_2	Cr_2O_3	FeO	MnO	Total
MT-3M_P4_R2C_78	77	50.78	0.48	0.94	-0.00	19.47	0.00	0.09	0.00	24.61	1.65	98.02
MT-3M_P4_R2C_79	78	50.81	0.40	0.99	0.02	19.26	0.02	0.08	-0.01	24.71	1.71	98.00
MT-3M_P4_R2C_80	79	50.81	0.39	0.95	-0.00	19.52	0.01	0.07	0.01	24.63	1.66	98.05
MT-3M_P4_R2C_81	80	50.97	0.37	0.99	0.01	19.57	0.01	0.09	0.00	24.52	1.70	98.23
MT-3M_P4_R2C_82	81	51.01	0.36	0.96	0.00	19.53	0.00	0.08	0.00	24.55	1.67	98.17
MT-3M_P4_R2C_83	82	50.99	0.35	0.97	0.02	19.53	0.01	0.07	-0.01	24.36	1.68	97.97
MT-3M_P4_R2C_84	83	51.01	0.34	0.98	-0.00	19.38	0.02	0.07	-0.00	24.57	1.66	98.03
MT-3M_P4_R2C_85	84	50.81	0.34	0.98	-0.00	19.59	0.01	0.07	-0.00	24.52	1.65	97.97
MT-3M_P4_R2C_86	85	51.15	0.35	0.99	0.01	19.63	0.01	0.09	0.00	24.76	1.68	98.67
MT-3M_P4_R2C_87	86	51.19	0.34	0.98	-0.01	19.69	0.01	0.05	-0.01	24.74	1.66	98.65
MT-3M_P4_R2C_88	87	51.30	0.36	1.00	-0.01	19.55	0.02	0.10	0.02	24.76	1.68	98.77
MT-3M_P4_R2C_89	88	51.31	0.39	1.00	-0.00	19.66	0.01	0.08	-0.00	24.73	1.65	98.81
MT-3M_P4_R2C_90	89	51.22	0.40	0.98	-0.02	19.62	0.01	0.09	-0.00	24.44	1.65	98.41
MT-3M_P4_R2C_91	90	51.33	0.43	0.98	-0.01	19.63	0.01	0.09	-0.01	24.69	1.69	98.82
MT-3M_P4_R2C_92	91	51.11	0.47	0.99	-0.00	19.48	0.03	0.07	-0.00	24.55	1.71	98.40
MT-3M_P4_R2C_93	92	51.57	0.56	0.98	-0.00	19.46	0.01	0.10	-0.01	24.99	1.64	99.31
MT-3M_P4_R2C_94	93	51.64	0.57	0.99	-0.00	19.53	0.01	0.10	-0.01	25.03	1.68	99.54
MT-3M_P4_R2C_95	94	51.57	0.54	0.96	-0.01	19.91	0.01	0.10	-0.01	24.80	1.68	99.56
MT-3M_P4_R2C_96	95	51.58	0.53	0.97	0.01	20.00	0.02	0.07	0.01	24.92	1.64	99.75
MT-3M_P4_R2C_97	96	51.35	0.51	1.01	0.01	19.97	0.02	0.08	0.00	24.62	1.63	99.20
MT-3M_P4_R2C_98	97	51.31	0.50	0.92	-0.00	19.71	0.01	0.08	-0.00	24.71	1.64	98.88
MT-3M_P4_R2C_99	98	51.12	0.47	0.93	0.00	19.65	0.01	0.10	0.01	24.76	1.65	98.72

Sample	Distance (μm)	SiO_2	Al_2O_3	CaO	K_2O	MgO	Na_2O	TiO_2	Cr_2O_3	FeO	MnO	Total
MT-3M_P4_R2C_2_01	0	51.69	1.41	1.52	0.00	21.54	0.02	0.27	0.01	20.07	0.80	97.34
MT-3M_P4_R2C_2_02	1	51.57	0.97	1.32	0.03	20.12	0.02	0.15	0.01	21.45	1.05	96.68
MT-3M_P4_R2C_2_03	2	49.41	1.51	1.45	0.10	19.22	0.08	0.21	0.00	21.41	0.97	94.37
MT-3M_P4_R2C_2_04	3	52.05	1.40	1.30	-0.00	22.57	0.01	0.18	-0.01	18.91	0.75	97.15
MT-3M_P4_R2C_2_05	4	51.69	1.68	1.44	0.01	24.12	0.02	0.18	0.01	18.32	0.64	98.10
MT-3M_P4_R2C_2_06	5	55.57	2.27	1.66	-0.00	26.80	0.03	0.31	0.02	18.23	0.57	105.46
MT-3M_P4_R2C_2_07	6	51.12	2.40	1.74	0.01	24.65	0.01	0.24	0.01	17.04	0.54	97.76
MT-3M_P4_R2C_2_08	7	51.56	2.42	1.98	0.00	24.68	0.01	0.24	-0.01	16.20	0.51	97.60
MT-3M_P4_R2C_2_09	8	52.09	1.45	2.02	0.02	23.74	0.02	0.16	0.01	17.10	0.65	97.26
MT-3M_P4_R2C_2_10	9	51.98	2.20	1.98	0.01	24.80	0.03	0.23	0.00	16.26	0.52	98.01
MT-3M_P4_R2C_2_11	10	51.31	0.68	1.00	0.01	20.68	0.01	0.12	0.00	23.26	1.30	98.36
MT-3M_P4_R2C_2_12	11	51.26	0.69	1.00	0.00	20.68	0.02	0.11	-0.00	22.90	1.27	97.95
MT-3M_P4_R2C_2_13	12	51.39	0.69	1.00	-0.01	20.79	0.01	0.12	0.00	23.32	1.26	98.56
MT-3M_P4_R2C_2_14	13	51.11	0.77	1.05	-0.01	20.71	0.01	0.13	0.00	23.24	1.28	98.29
MT-3M_P4_R2C_2_15	14	51.24	0.68	1.02	0.00	20.65	0.02	0.15	0.00	23.08	1.35	98.20
MT-3M_P4_R2C_2_16	15	51.23	0.53	0.99	-0.00	20.63	0.02	0.11	-0.02	23.25	1.38	98.11
MT-3M_P4_R2C_2_17	16	50.94	0.52	1.00	0.01	20.55	0.01	0.14	-0.01	23.26	1.41	97.84
MT-3M_P4_R2C_2_18	17	51.26	0.55	1.01	-0.01	20.44	0.01	0.13	0.00	23.27	1.46	98.13
MT-3M_P4_R2C_2_19	18	51.01	0.56	1.01	-0.00	20.30	0.01	0.11	-0.00	23.23	1.47	97.70
MT-3M_P4_R2C_2_20	19	50.93	0.67	1.02	-0.00	20.19	0.00	0.14	0.01	23.60	1.53	98.09
MT-3M_P4_R2C_2_21	20	50.66	0.75	1.08	0.01	19.88	0.02	0.11	0.00	23.52	1.54	97.58
MT-3M_P4_R2C_2_22	21	50.64	0.86	1.08	0.00	19.93	0.02	0.11	-0.01	23.84	1.58	98.06
MT-3M_P4_R2C_2_23	22	50.69	0.87	1.07	-0.00	20.07	0.01	0.13	0.00	23.44	1.53	97.80
MT-3M_P4_R2C_2_24	23	50.82	0.76	1.06	0.00	20.10	0.01	0.13	-0.01	23.60	1.58	98.04
MT-3M_P4_R2C_2_25	24	50.42	0.84	1.09	-0.01	20.04	0.02	0.11	0.01	23.66	1.59	97.77
MT-3M_P4_R2C_2_26	25	50.60	0.81	1.07	-0.00	20.16	0.02	0.10	-0.00	23.57	1.53	97.86
MT-3M_P4_R2C_2_27	26	50.57	0.79	1.04	-0.01	20.06	0.01	0.11	0.01	23.63	1.58	97.80
MT-3M_P4_R2C_2_28	27	50.41	0.82	1.00	-0.00	19.96	0.02	0.12	0.01	23.64	1.55	97.52
MT-3M_P4_R2C_2_29	28	50.70	0.73	0.98	0.01	19.66	0.02	0.10	0.00	24.58	1.63	98.41
MT-3M_P4_R2C_2_30	29	50.46	0.63	0.90	0.01	19.44	0.02	0.11	0.01	24.58	1.71	97.88
MT-3M_P4_R2C_2_31	30	50.65	0.56	0.95	-0.01	19.34	0.01	0.11	0.01	24.63	1.71	97.96
MT-3M_P4_R2C_2_32	31	51.53	2.01	1.92	0.00	24.52	0.02	0.21	-0.00	16.38	0.52	97.12
MT-3M_P4_R2C_2_33	32	50.62	0.56	0.97	-0.01	19.44	0.04	0.10	0.01	25.05	1.66	98.45
MT-3M_P4_R2C_2_34	33	50.38	0.61	0.99	-0.00	19.40	0.01	0.10	-0.01	24.65	1.68	97.80
MT-3M_P4_R2C_2_35	34	50.46	0.65	1.01	-0.01	19.52	0.01	0.11	0.01	24.45	1.67	97.88
MT-3M_P4_R2C_2_36	35	50.53	0.67	1.02	0.01	19.37	0.02	0.10	0.00	24.64	1.64	98.00
MT-3M_P4_R2C_2_37	36	50.59	0.69	0.98	0.00	19.39	0.01	0.13	0.00	24.50	1.68	97.97
MT-3M_P4_R2C_2_38	37	50.26	0.77	1.01	-0.01	19.38	0.02	0.13	0.00	24.57	1.68	97.81

Sample	Distance (μm)	SiO_2	Al_2O_3	CaO	K_2O	MgO	Na_2O	TiO_2	Cr_2O_3	FeO	MnO	Total
MT-3M_P4_R2C_2_39	38	50.44	0.81	0.99	0.01	19.33	0.02	0.12	-0.00	24.50	1.68	97.91
MT-3M_P4_R2C_2_40	39	50.37	0.81	0.99	0.00	19.27	0.01	0.11	-0.01	24.65	1.66	97.88
MT-3M_P4_R2C_2_41	40	50.47	0.80	0.98	0.02	19.12	0.04	0.11	-0.01	24.57	1.62	97.72
MT-3M_P4_R2C_2_42	41	50.61	0.69	1.01	-0.00	19.42	0.02	0.12	-0.00	24.52	1.62	98.00
MT-3M_P4_R2C_2_43	42	50.72	0.58	0.94	0.01	19.50	0.02	0.09	-0.01	24.49	1.70	98.03
MT-3M_P4_R2C_2_44	43	50.63	0.54	0.96	0.01	19.57	0.01	0.10	-0.01	24.49	1.68	97.97
MT-3M_P4_R2C_2_45	44	50.69	0.54	0.98	0.01	19.65	0.01	0.13	0.01	24.67	1.64	98.31
MT-3M_P4_R2C_2_46	45	50.77	0.53	0.98	-0.01	19.52	0.02	0.12	0.00	24.50	1.65	98.07
MT-3M_P4_R2C_2_47	46	50.82	0.54	0.97	0.00	19.50	0.02	0.10	-0.01	24.33	1.66	97.94
MT-3M_P4_R2C_2_48	47	51.09	0.53	1.00	0.01	19.65	0.01	0.11	-0.02	24.56	1.65	98.60
MT-3M_P4_R2C_2_49	48	50.84	0.56	0.99	-0.02	19.33	0.01	0.09	-0.01	24.43	1.60	97.81
MT-3M_P4_R2C_2_50	49	50.94	0.58	1.02	-0.01	19.52	0.02	0.12	0.00	24.44	1.62	98.25
MT-3M_P4_R2C_2_51	50	51.42	0.55	1.05	0.00	19.70	0.01	0.13	-0.02	24.49	1.62	98.95
MT-3M_P4_R2C_2_52	51	51.15	0.56	1.03	0.00	19.43	0.01	0.09	0.01	24.37	1.63	98.28
MT-3M_P4_R2C_2_53	52	50.90	0.60	1.04	0.00	19.57	0.00	0.11	-0.01	24.51	1.61	98.34
MT-3M_P4_R2C_2_54	53	50.79	0.66	1.07	0.01	19.48	0.02	0.12	-0.01	24.51	1.68	98.32
MT-3M_P4_R2C_2_55	54	50.75	0.68	1.04	0.01	19.43	0.02	0.09	-0.02	24.57	1.62	98.19
MT-3M_P4_R2C_2_56	55	50.85	0.65	1.05	0.01	19.50	0.01	0.15	0.02	24.47	1.68	98.39
MT-3M_P4_R2C_2_57	56	50.73	0.73	1.12	0.00	19.35	0.02	0.10	0.00	24.48	1.59	98.12
MT-3M_P4_R2C_2_58	57	51.10	0.76	1.09	-0.01	19.32	0.02	0.12	0.01	24.59	1.67	98.67
MT-3M_P4_R2C_2_59	58	50.87	0.56	1.08	-0.01	19.69	0.00	0.10	-0.01	24.52	1.64	98.44
MT-3M_P4_R2C_2_60	59	51.09	0.48	1.09	-0.01	19.65	0.02	0.10	0.00	24.34	1.62	98.37
MT-3M_P4_R2C_2_61	60	51.07	0.45	1.08	0.00	19.67	0.01	0.07	-0.00	24.28	1.61	98.24
MT-3M_P4_R2C_2_62	61	51.15	0.46	1.07	0.00	19.59	0.02	0.07	-0.01	24.41	1.62	98.38
MT-3M_P4_R2C_2_63	62	51.24	0.45	1.04	-0.02	19.67	0.02	0.09	0.01	24.29	1.65	98.45
MT-3M_P4_R2C_2_64	63	51.39	0.46	1.06	0.02	19.73	0.00	0.07	0.00	24.36	1.64	98.74
MT-3M_P4_R2C_2_65	64	51.20	0.44	1.04	-0.00	19.64	0.01	0.08	-0.00	24.36	1.66	98.42
MT-3M_P4_R2C_2_66	65	51.11	0.46	1.06	-0.03	19.45	0.01	0.08	-0.01	24.62	1.66	98.42
MT-3M_P4_R2C_2_67	66	50.86	0.52	1.04	0.01	19.46	0.02	0.11	-0.01	24.10	1.60	97.72
MT-3M_P4_R2C_2_68	67	51.14	0.53	1.05	0.01	19.67	0.02	0.07	-0.01	24.43	1.63	98.55
MT-3M_P4_R2C_2_69	68	51.00	0.53	1.04	0.01	19.68	0.02	0.11	0.01	24.28	1.57	98.26
MT-3M_P4_R2C_2_70	69	50.99	0.53	1.04	-0.01	19.57	0.01	0.09	0.00	24.12	1.63	97.97
MT-3M_P4_R2C_2_71	70	51.60	0.53	1.06	0.00	19.80	0.01	0.11	0.00	24.62	1.61	99.32
MT-3M_P4_R2C_2_72	71	50.99	0.53	0.99	0.01	19.65	0.01	0.10	-0.01	24.47	1.59	98.32
MT-3M_P4_R2C_2_73	72	51.02	0.51	1.01	0.02	19.73	0.01	0.08	0.00	24.46	1.64	98.48
MT-3M_P4_R2C_2_74	73	51.39	0.54	1.00	0.01	19.72	0.00	0.11	0.00	24.33	1.63	98.74
MT-3M_P4_R2C_2_75	74	50.75	0.53	1.02	0.00	19.69	0.01	0.08	-0.02	24.22	1.65	97.94
MT-3M_P4_R2C_2_76	75	51.16	0.54	0.99	0.02	19.66	0.01	0.07	-0.01	24.33	1.57	98.36
MT-3M_P4_R2C_2_77	76	50.88	0.51	1.01	0.00	19.66	0.01	0.10	0.00	24.25	1.64	98.08

Sample	Distance (μm)	SiO_2	Al_2O_3	CaO	K_2O	MgO	Na_2O	TiO_2	Cr_2O_3	FeO	MnO	Total
MT-3M_P4_R2C_2_78	77	50.93	0.52	0.99	0.02	19.70	0.02	0.13	-0.02	24.46	1.61	98.35
MT-3M_P4_R2C_2_79	78	51.02	0.51	1.00	-0.01	19.72	0.02	0.10	-0.01	24.56	1.57	98.47
MT-3M_P4_R2C_2_80	79	51.32	0.51	1.00	-0.01	19.63	0.01	0.07	-0.00	24.58	1.64	98.76
MT-3M_P4_R2C_2_81	80	50.93	0.50	1.01	0.00	19.60	0.01	0.11	0.01	24.39	1.60	98.15
MT-3M_P4_R2C_2_82	81	50.03	0.49	1.02	-0.01	19.08	0.01	0.09	-0.01	23.67	1.60	95.97
MT-3M_P4_R2C_2_83	82	48.72	0.47	1.07	-0.01	19.16	0.02	0.06	-0.01	22.44	1.52	93.45
MT-3M_P4_R2C_2_84	83	50.88	0.49	0.98	0.01	19.74	0.02	0.12	-0.01	24.37	1.59	98.18
MT-3M_P4_R2C_2_85	84	51.02	0.48	1.01	-0.02	19.78	0.01	0.09	-0.01	24.29	1.66	98.31
MT-3M_P4_R2C_2_86	85	50.88	0.48	1.00	0.01	19.60	0.01	0.10	-0.00	24.11	1.62	97.80
MT-3M_P4_R2C_2_87	86	51.12	0.49	1.00	-0.01	19.67	0.01	0.10	0.01	24.23	1.60	98.23
MT-3M_P4_R2C_2_88	87	50.94	0.49	0.99	-0.00	19.72	0.01	0.11	0.01	24.47	1.64	98.36
MT-3M_P4_R2C_2_89	88	50.96	0.48	0.99	-0.02	19.65	0.01	0.11	-0.02	24.21	1.60	97.97
MT-3M_P4_R2C_2_90	89	50.97	0.45	0.99	-0.02	19.65	0.02	0.08	0.00	24.25	1.60	97.99
MT-3M_P4_R2C_2_91	90	50.95	0.46	1.01	0.00	19.68	0.03	0.11	-0.01	24.21	1.61	98.06
MT-3M_P4_R2C_2_92	91	50.99	0.46	1.00	-0.01	19.72	0.02	0.11	0.01	24.10	1.64	98.04
MT-3M_P4_R2C_2_93	92	54.95	0.50	1.08	0.01	21.39	0.03	0.14	0.01	26.28	1.75	106.14
MT-3M_P4_R2C_2_94	93	51.07	0.44	0.97	0.01	19.64	0.02	0.10	0.00	24.38	1.65	98.27
MT-3M_P4_R2C_2_95	94	50.74	0.43	0.97	0.01	19.63	0.02	0.08	-0.01	24.44	1.63	97.94
MT-3M_P4_R2C_2_96	95	50.63	0.44	0.99	-0.01	19.59	0.01	0.09	-0.02	24.24	1.61	97.59
MT-3M_P4_R2C_2_97	96	51.01	0.45	1.00	-0.01	19.69	0.01	0.09	-0.00	24.50	1.63	98.37
MT-3M_P4_R2C_2_98	97	50.73	0.45	0.98	-0.00	19.74	0.02	0.09	0.00	24.64	1.62	98.27
MT-3M_P4_R2C_2_99	98	50.71	0.47	1.00	-0.01	19.69	0.01	0.10	-0.01	24.49	1.61	98.05
MT-3M_P4_R2C_2_100	99	50.99	0.45	0.98	0.02	19.74	0.02	0.10	0.01	24.56	1.64	98.50
MT-3M_P4_R2C_2_101	100	50.83	0.46	0.99	0.00	19.63	0.01	0.10	-0.01	24.59	1.63	98.22
MT-3M_P4_R2C_2_102	101	50.65	0.47	0.96	-0.00	19.63	0.02	0.09	0.01	24.43	1.66	97.92
MT-3M_P4_R2C_2_103	102	50.73	0.48	1.00	-0.01	19.63	0.02	0.07	-0.01	24.35	1.64	97.90
MT-3M_P4_R2C_2_104	103	50.66	0.46	0.99	0.01	19.67	0.02	0.07	-0.01	24.58	1.62	98.07
MT-3M_P4_R2C_2_105	104	50.59	0.47	0.98	0.01	19.56	0.02	0.11	-0.01	24.31	1.67	97.71
MT-3M_P4_R2C_2_106	105	50.68	0.47	0.98	-0.00	19.61	0.01	0.10	-0.00	24.28	1.63	97.76
MT-3M_P4_R2C_2_107	106	50.75	0.46	0.97	-0.01	19.65	0.03	0.09	0.00	24.53	1.62	98.10
MT-3M_P4_R2C_2_108	107	50.83	0.47	0.97	0.01	19.59	0.00	0.11	0.01	24.45	1.60	98.04
MT-3M_P4_R2C_2_109	108	50.62	0.48	0.98	0.01	19.56	0.00	0.09	-0.00	24.58	1.64	97.96
MT-3M_P4_R2C_2_110	109	50.86	0.50	0.96	-0.00	19.58	0.01	0.10	0.01	24.29	1.63	97.94
MT-3M_P4_R2C_2_111	110	50.95	0.47	0.99	-0.00	19.63	0.01	0.07	-0.00	24.63	1.62	98.38
MT-3M_P4_R2C_2_112	111	50.65	0.50	0.98	0.01	19.56	0.02	0.10	0.00	24.55	1.63	98.00
MT-3M_P4_R2C_2_113	112	50.54	0.49	0.95	-0.01	19.58	0.01	0.07	-0.01	24.53	1.65	97.81
MT-3M_P4_R2C_2_114	113	50.64	0.51	0.96	-0.01	19.66	0.02	0.09	-0.00	24.59	1.59	98.05
MT-3M_P4_R2C_2_115	114	50.84	0.51	0.96	-0.02	19.70	0.01	0.10	-0.02	24.65	1.62	98.36
MT-3M_P4_R2C_2_116	115	50.80	0.51	1.00	-0.01	19.55	0.01	0.09	0.00	24.55	1.64	98.15

Sample	Distance (μm)	SiO_2	Al_2O_3	CaO	K_2O	MgO	Na_2O	TiO_2	Cr_2O_3	FeO	MnO	Total
MT-3M_P4_R2C_2_117	116	50.56	0.50	0.99	0.00	19.52	0.01	0.08	0.00	24.34	1.65	97.65
MT-3M_P4_R2C_2_118	117	50.85	0.51	1.00	-0.01	19.66	0.01	0.08	-0.01	24.48	1.62	98.20
MT-3M_P4_R2C_2_119	118	50.74	0.50	0.97	0.01	19.70	0.02	0.09	0.01	24.46	1.63	98.11
MT-3M_P4_R2C_2_120	119	55.17	0.56	1.09	0.00	21.24	0.03	0.10	0.02	26.48	1.80	106.49
MT-3M_P4_R2C_2_121	120	50.64	0.51	1.00	-0.01	19.52	0.01	0.08	0.00	24.31	1.61	97.68
MT-3M_P4_R2C_2_122	121	50.74	0.49	0.99	0.03	19.48	0.01	0.11	-0.00	24.26	1.62	97.73
MT-3M_P4_R2C_2_123	122	54.67	0.53	1.10	0.02	21.18	0.03	0.12	0.03	26.55	1.79	106.02
MT-3M_P4_R2C_2_124	123	50.85	0.50	0.98	0.00	19.60	0.02	0.07	-0.00	24.64	1.62	98.28
MT-3M_P4_R2C_2_125	124	51.03	0.50	0.97	0.01	19.63	0.01	0.11	0.00	24.57	1.67	98.49
MT-3M_P4_R2C_2_126	125	50.90	0.49	1.02	0.01	19.68	0.01	0.08	-0.01	24.58	1.63	98.40
MT-3M_P4_R2C_2_127	126	50.90	0.50	1.01	0.00	19.73	0.01	0.09	-0.00	24.64	1.64	98.53
MT-3M_P4_R2C_2_128	127	50.93	0.48	0.96	0.01	19.61	0.01	0.10	-0.02	24.35	1.63	98.08
MT-3M_P4_R2C_2_129	128	51.01	0.50	1.01	-0.00	19.75	0.02	0.11	0.00	24.52	1.62	98.53
MT-3M_P4_R2C_2_130	129	50.99	0.50	0.98	-0.01	19.68	0.02	0.12	-0.01	24.60	1.60	98.48
MT-3M_P4_R2C_2_131	130	51.08	0.49	1.00	0.00	19.71	0.01	0.09	0.01	24.48	1.65	98.51
MT-3M_P4_R2C_2_132	131	51.05	0.51	0.97	-0.00	19.64	0.00	0.09	-0.00	24.45	1.62	98.32
MT-3M_P4_R2C_2_133	132	51.05	0.50	0.99	-0.01	19.64	0.02	0.08	0.00	24.55	1.67	98.47
MT-3M_P4_R2C_2_134	133	51.01	0.51	0.96	0.00	19.64	0.02	0.10	-0.00	24.48	1.68	98.40
MT-3M_P4_R2C_2_135	134	50.97	0.50	0.95	0.01	19.54	0.00	0.09	-0.01	24.32	1.63	98.01
MT-3M_P4_R2C_2_136	135	50.95	0.50	1.02	0.00	19.78	0.02	0.10	-0.00	24.36	1.66	98.38
MT-3M_P4_R2C_2_137	136	50.96	0.51	0.99	0.00	19.67	0.02	0.11	-0.01	24.43	1.64	98.32
MT-3M_P4_R2C_2_138	137	50.95	0.51	0.94	0.00	19.60	0.01	0.11	0.01	24.40	1.63	98.18
MT-3M_P4_R2C_2_139	138	50.67	0.52	1.01	-0.01	19.60	0.01	0.12	0.01	24.58	1.65	98.16
MT-3M_P4_R2C_2_140	139	50.93	0.50	1.01	0.02	19.73	0.01	0.12	0.00	24.32	1.62	98.25
MT-3M_P4_R2C_2_141	140	50.85	0.51	0.96	0.01	19.74	0.01	0.07	-0.01	24.26	1.63	98.01
MT-3M_P4_R2C_2_142	141	50.81	0.53	1.00	-0.01	19.63	0.01	0.10	-0.01	24.33	1.63	98.01
MT-3M_P4_R2C_2_143	142	50.88	0.51	1.01	-0.01	19.64	0.01	0.08	0.00	24.61	1.62	98.35
MT-3M_P4_R2C_2_144	143	50.73	0.50	1.00	-0.00	19.63	0.01	0.11	-0.01	24.39	1.60	97.96
MT-3M_P4_R2C_2_145	144	50.73	0.51	0.99	0.03	19.62	0.02	0.08	0.01	24.31	1.63	97.92
MT-3M_P4_R2C_2_146	145	50.79	0.51	0.96	0.01	19.60	0.01	0.09	0.02	24.46	1.64	98.11
MT-3M_P4_R2C_2_147	146	50.64	0.52	1.02	0.00	19.55	0.01	0.09	-0.00	24.29	1.64	97.76
MT-3M_P4_R2C_2_148	147	50.98	0.51	0.98	0.01	19.65	0.00	0.10	-0.01	24.40	1.61	98.22
MT-3M_P4_R2C_2_149	148	50.83	0.50	0.99	-0.01	19.73	0.01	0.09	0.02	24.50	1.66	98.32
MT-3M_P4_R2C_2_150	149	51.46	0.51	1.01	-0.01	19.92	0.01	0.08	0.00	24.90	1.60	99.47
MT-3M_P4_R2C_2_151	150	50.82	0.54	0.98	0.01	19.81	0.01	0.11	0.02	24.52	1.72	98.54
MT-3M_P4_R2C_2_152	151	50.84	0.52	0.99	-0.00	19.57	0.01	0.11	-0.01	24.43	1.63	98.09
MT-3M_P4_R2C_2_153	152	50.81	0.51	0.99	0.01	19.68	0.01	0.09	-0.00	24.39	1.62	98.10
MT-3M_P4_R2C_2_154	153	50.87	0.52	0.96	-0.00	19.75	0.01	0.10	0.00	24.50	1.65	98.37
MT-3M_P4_R2C_2_155	154	50.85	0.50	0.94	0.01	19.57	0.02	0.11	0.01	24.46	1.65	98.12

Sample	Distance (μm)	SiO_2	Al_2O_3	CaO	K_2O	MgO	Na_2O	TiO_2	Cr_2O_3	FeO	MnO	Total
MT-3M_P4_R2C_2_156	155	50.97	0.52	1.02	0.01	19.77	0.02	0.09	0.01	24.49	1.66	98.55
MT-3M_P4_R2C_2_157	156	50.88	0.52	0.97	0.00	19.57	0.01	0.09	-0.01	24.14	1.64	97.82
MT-3M_P4_R2C_2_158	157	51.02	0.50	0.98	0.01	19.60	-0.00	0.11	-0.01	24.61	1.63	98.44
MT-3M_P4_R2C_2_159	158	50.60	0.50	0.99	0.01	19.65	0.02	0.10	0.01	24.45	1.64	97.97
MT-3M_P4_R2C_2_160	159	50.99	0.51	0.97	-0.01	19.72	0.01	0.12	0.01	24.57	1.63	98.51
MT-3M_P4_R2C_2_161	160	50.82	0.50	0.98	-0.01	19.70	0.01	0.11	-0.00	24.39	1.63	98.12
MT-3M_P4_R2C_2_162	161	50.90	0.53	0.99	0.01	19.66	0.02	0.10	0.01	24.47	1.66	98.33
MT-3M_P4_R2C_2_163	162	50.76	0.51	1.01	0.00	19.68	0.02	0.12	-0.01	24.59	1.64	98.32
MT-3M_P4_R2C_2_164	163	50.58	0.50	0.98	-0.00	19.63	0.01	0.11	0.00	24.45	1.66	97.93
MT-3M_P4_R2C_2_165	164	50.81	0.50	1.01	-0.00	19.66	0.01	0.09	-0.02	24.33	1.59	97.99
MT-3M_P4_R2C_2_166	165	50.61	0.50	1.00	0.01	19.74	0.01	0.09	-0.00	24.44	1.63	98.02
MT-3M_P4_R2C_2_167	166	50.86	0.51	1.01	-0.00	19.87	0.01	0.10	-0.02	24.54	1.61	98.49
MT-3M_P4_R2C_2_168	167	50.99	0.53	1.01	0.03	19.51	0.02	0.10	-0.01	24.17	1.63	97.98
MT-3M_P4_R2C_2_169	168	50.76	0.53	0.99	-0.00	19.46	0.02	0.10	-0.02	24.19	1.62	97.64
MT-3M_P4_R2C_2_170	169	50.84	0.54	1.00	-0.01	19.43	0.02	0.08	0.00	24.48	1.63	98.01
MT-3M_P4_R2C_2_171	170	50.54	0.54	0.96	0.00	19.77	0.01	0.09	-0.02	24.49	1.66	98.05
MT-3M_P4_R2C_2_172	171	50.67	0.51	0.97	0.01	19.44	0.01	0.10	0.00	24.33	1.64	97.70
MT-3M_P4_R2C_2_173	172	50.41	0.53	0.99	-0.01	19.55	0.02	0.09	0.01	24.46	1.64	97.70
MT-3M_P4_R2C_2_174	173	50.72	0.52	0.97	0.01	19.56	0.02	0.13	0.00	24.36	1.68	97.98
MT-3M_P4_R2C_2_175	174	50.44	0.55	0.97	0.01	19.53	0.02	0.10	-0.00	24.46	1.61	97.68
MT-3M_P4_R2C_2_176	175	50.42	0.53	0.96	-0.00	19.68	0.01	0.11	-0.00	24.46	1.66	97.83
MT-3M_P4_R2C_2_177	176	50.39	0.53	0.98	-0.01	19.74	0.00	0.11	0.00	24.46	1.65	97.87
MT-3M_P4_R2C_2_178	177	50.76	0.53	0.98	0.01	19.58	0.01	0.08	-0.01	24.57	1.65	98.15
MT-3M_P4_R2C_2_179	178	50.55	0.54	0.95	0.01	19.60	0.01	0.11	0.00	24.56	1.65	97.97
MT-3M_P4_R2C_2_180	179	50.57	0.54	0.96	0.01	19.65	0.01	0.10	-0.00	24.46	1.61	97.90
MT-3M_P4_R2C_2_181	180	50.56	0.54	0.98	0.00	19.74	0.01	0.09	0.00	24.57	1.63	98.13
MT-3M_P4_R2C_2_182	181	50.35	0.52	0.96	0.01	19.58	0.01	0.11	-0.01	24.48	1.63	97.65
MT-3M_P4_R2C_2_183	182	50.19	0.56	0.99	0.01	19.50	0.01	0.09	-0.00	24.49	1.66	97.49
MT-3M_P4_R2C_2_184	183	50.31	0.53	0.99	0.02	19.67	0.01	0.10	-0.00	24.45	1.67	97.76
MT-3M_P4_R2C_2_185	184	50.54	0.52	0.95	0.02	19.58	0.01	0.11	0.00	24.32	1.65	97.69
MT-3M_P4_R2C_2_186	185	50.28	0.53	0.98	-0.01	19.55	0.01	0.10	-0.00	24.46	1.65	97.55
MT-3M_P4_R2C_2_187	186	50.59	0.54	1.00	0.00	19.59	-0.00	0.13	0.00	24.31	1.67	97.82
MT-3M_P4_R2C_2_188	187	50.68	0.54	0.96	-0.00	19.59	0.01	0.12	-0.01	24.59	1.64	98.11
MT-3M_P4_R2C_2_189	188	50.47	0.54	0.97	-0.00	19.57	0.01	0.12	-0.02	24.28	1.64	97.59
MT-3M_P4_R2C_2_190	189	50.33	0.54	0.97	0.00	19.54	-0.00	0.11	-0.00	24.36	1.65	97.49
MT-3M_P4_R2C_2_191	190	50.46	0.54	0.98	-0.00	19.47	0.01	0.09	-0.02	24.38	1.65	97.55
MT-3M_P4_R2C_2_192	191	50.39	0.54	0.96	-0.00	19.35	0.01	0.12	0.01	24.29	1.66	97.32
MT-3M_P4_R2C_2_193	192	50.44	0.54	0.96	0.00	19.54	0.01	0.11	-0.00	24.37	1.62	97.59
MT-3M_P4_R2C_2_194	193	50.67	0.52	0.96	0.01	19.57	0.00	0.10	-0.01	24.47	1.68	97.97

Sample	Distance (μm)	SiO_2	Al_2O_3	CaO	K_2O	MgO	Na_2O	TiO_2	Cr_2O_3	FeO	MnO	Total
MT-3M_P10_R2C_01	0	42.81	10.40	2.64	0.72	0.08	2.09	0.02	-0.03	0.50	-0.01	59.24
MT-3M_P10_R2C_02	1	58.68	20.56	5.65	0.92	0.05	4.89	0.06	0.00	0.69	0.00	91.51
MT-3M_P10_R2C_03	2	55.19	24.33	8.84	0.62	0.06	5.15	0.05	-0.01	0.81	0.01	95.04
MT-3M_P10_R2C_04	3	54.02	28.22	11.93	0.33	0.10	4.47	0.02	0.00	0.83	0.01	99.93
MT-3M_P10_R2C_05	4	52.79	29.67	13.08	0.27	0.11	4.14	0.03	-0.00	0.85	0.02	100.96
MT-3M_P10_R2C_06	5	51.64	29.75	13.66	0.18	0.11	4.10	0.03	-0.00	0.87	0.00	100.33
MT-3M_P10_R2C_07	6	51.36	29.10	13.09	0.27	0.12	3.78	0.04	0.00	0.93	0.01	98.69
MT-3M_P10_R2C_08	7	51.61	29.50	13.50	0.20	0.10	3.59	0.06	-0.01	0.98	0.02	99.55
MT-3M_P10_R2C_09	8	51.62	29.83	13.66	0.16	0.10	3.62	0.03	0.00	0.89	0.01	99.92
MT-3M_P10_R2C_10	9	51.39	29.82	13.72	0.14	0.14	3.55	0.04	0.00	0.87	0.01	99.67
MT-3M_P10_R2C_11	10	50.74	26.66	14.60	0.16	2.08	2.94	0.08	-0.00	1.90	0.07	99.21
MT-3M_P10_R2C_12	11	53.08	6.89	16.58	0.04	14.36	0.71	0.31	0.01	10.25	0.41	102.65
MT-3M_P10_R2C_13	12	52.86	1.79	17.50	0.01	16.56	0.16	0.30	-0.02	10.66	0.43	100.26
MT-3M_P10_R2C_14	13	52.52	1.83	18.72	0.02	16.61	0.14	0.30	-0.01	9.42	0.36	99.91
MT-3M_P10_R2C_15	14	52.65	2.07	19.42	0.01	16.26	0.15	0.33	0.02	8.94	0.29	100.15
MT-3M_P10_R2C_16	15	52.09	2.29	19.92	0.01	16.08	0.16	0.33	0.00	8.67	0.28	99.82
MT-3M_P10_R2C_17	16	51.87	3.11	20.49	0.01	15.83	0.15	0.47	0.01	8.43	0.26	100.63
MT-3M_P10_R2C_18	17	48.69	6.19	21.21	-0.01	13.73	0.22	1.03	-0.00	8.92	0.22	100.21
MT-3M_P10_R2C_19	18	47.94	6.67	21.37	0.01	13.35	0.24	1.05	-0.00	9.10	0.22	99.96
MT-3M_P10_R2C_20	19	47.68	6.79	21.33	0.02	13.35	0.24	1.07	0.01	9.04	0.22	99.74
MT-3M_P10_R2C_21	20	47.79	6.87	21.49	0.01	13.29	0.25	1.09	0.01	9.00	0.21	100.00
MT-3M_P10_R2C_22	21	47.87	6.84	21.43	0.00	13.16	0.25	1.03	0.02	8.94	0.20	99.76
MT-3M_P10_R2C_23	22	47.94	7.01	21.55	0.00	13.22	0.26	1.18	0.01	9.16	0.21	100.54
MT-3M_P10_R2C_24	23	47.76	6.99	21.42	0.02	13.05	0.25	1.16	0.03	9.01	0.23	99.91
MT-3M_P10_R2C_25	24	47.56	6.92	21.38	0.01	13.11	0.24	1.10	0.02	9.03	0.23	99.59
MT-3M_P10_R2C_26	25	47.66	6.94	21.46	0.02	13.15	0.26	1.11	-0.01	8.92	0.21	99.72
MT-3M_P10_R2C_27	26	47.68	6.93	21.48	0.01	13.11	0.23	1.15	0.00	9.04	0.20	99.83
MT-3M_P10_R2C_28	27	47.74	6.94	21.48	0.01	13.25	0.24	1.05	-0.01	8.97	0.19	99.86
MT-3M_P10_R2C_29	28	47.82	6.96	21.46	0.00	13.25	0.24	1.16	0.03	8.97	0.24	100.12
MT-3M_P10_R2C_30	29	47.76	6.91	21.55	0.02	13.20	0.25	1.02	0.00	8.95	0.21	99.87
MT-3M_P10_R2C_31	30	47.74	6.85	21.51	0.02	13.18	0.24	1.07	0.01	8.92	0.20	99.74
MT-3M_P10_R2C_32	31	47.85	6.81	21.73	0.02	13.26	0.25	1.05	-0.01	8.90	0.21	100.08
MT-3M_P10_R2C_33	32	47.80	6.77	21.69	0.01	13.15	0.24	0.97	0.01	8.66	0.23	99.53
MT-3M_P10_R2C_34	33	47.90	6.63	21.54	0.03	13.34	0.25	0.94	0.00	8.80	0.20	99.65
MT-3M_P10_R2C_35	34	48.47	5.96	21.62	0.03	13.66	0.23	0.91	-0.01	8.81	0.22	99.91
MT-3M_P10_R2C_36	35	51.17	3.57	21.32	-0.01	15.14	0.19	0.41	0.00	7.86	0.22	99.88
MT-3M_P10_R2C_37	36	51.70	3.12	21.37	0.01	15.59	0.18	0.43	0.00	7.61	0.23	100.23
MT-3M_P10_R2C_38	37	52.11	2.98	21.51	0.02	15.73	0.18	0.37	-0.01	7.43	0.22	100.54
MT-3M_P10_R2C_39	38	51.77	3.20	21.33	0.00	15.47	0.17	0.40	-0.01	7.59	0.25	100.16

Sample	Distance (μm)	SiO_2	Al_2O_3	CaO	K_2O	MgO	Na_2O	TiO_2	Cr_2O_3	FeO	MnO	Total
MT-3M_P10_R2C_40	39	51.37	3.85	21.29	-0.02	15.24	0.17	0.48	0.01	7.89	0.22	100.52
MT-3M_P10_R2C_41	40	49.54	5.87	22.10	0.01	13.97	0.22	0.68	-0.01	7.90	0.19	100.46
MT-3M_P10_R2C_42	41	49.08	6.45	22.11	0.03	13.63	0.23	0.75	-0.01	7.82	0.18	100.27
MT-3M_P10_R2C_43	42	48.31	6.74	22.30	0.01	13.36	0.24	0.73	0.01	7.88	0.17	99.76
MT-3M_P10_R2C_44	43	48.43	6.81	22.55	0.01	13.39	0.23	0.71	0.01	7.76	0.17	100.07
MT-3M_P10_R2C_45	44	48.44	6.90	22.41	0.02	13.34	0.23	0.74	0.01	7.71	0.17	99.97
MT-3M_P10_R2C_46	45	48.35	6.91	22.50	0.00	13.37	0.23	0.75	0.01	7.66	0.15	99.92
MT-3M_P10_R2C_47	46	48.42	6.82	22.43	-0.01	13.40	0.22	0.78	-0.00	7.61	0.16	99.83
MT-3M_P10_R2C_48	47	48.51	6.76	22.56	0.01	13.41	0.24	0.72	0.01	7.67	0.17	100.06
MT-3M_P10_R2C_49	48	48.40	6.74	22.50	0.02	13.42	0.22	0.77	0.00	7.56	0.16	99.80
MT-3M_P10_R2C_50	49	48.55	6.78	22.68	-0.00	13.52	0.22	0.76	0.01	7.60	0.16	100.26
MT-3M_P10_R2C_51	50	48.45	6.55	22.49	-0.00	13.47	0.23	0.71	-0.00	7.62	0.16	99.67
MT-3M_P10_R2C_52	51	48.30	6.59	22.55	-0.01	13.51	0.24	0.73	0.00	7.50	0.15	99.57
MT-3M_P10_R2C_53	52	48.24	6.58	22.36	-0.01	13.61	0.22	0.71	-0.00	7.55	0.17	99.43
MT-3M_P10_R2C_54	53	47.85	6.52	22.14	0.01	13.50	0.22	0.78	-0.00	7.24	0.14	98.41
MT-3M_P10_R2C_55	54	46.33	6.23	21.61	-0.00	12.66	0.20	0.70	0.01	7.04	0.15	94.94
MT-3M_P10_R2C_56	55	46.06	6.25	21.59	0.00	12.32	0.18	0.70	-0.00	6.89	0.15	94.14
MT-3M_P10_R2C_57	56	49.19	6.73	22.69	0.03	13.49	0.21	0.74	0.02	7.26	0.16	100.52
MT-3M_P10_R2C_58	57	49.13	6.76	22.58	0.01	13.65	0.23	0.76	0.02	7.14	0.18	100.44
MT-3M_P10_R2C_59	58	48.52	6.65	22.74	0.01	13.61	0.21	0.74	0.00	7.22	0.16	99.85
MT-3M_P10_R2C_60	59	36.62	4.89	18.98	-0.00	9.56	0.12	0.67	-0.02	6.27	0.12	77.21
MT-3M_P10_R2C_61	60	42.93	6.18	20.33	0.05	12.20	0.23	0.72	0.00	6.55	0.12	89.31
MT-3M_P10_R2C_62	61	48.90	6.93	22.69	0.01	13.80	0.23	0.75	0.01	7.22	0.16	100.69
MT-3M_P10_R2C_63	62	48.68	6.88	22.67	0.02	13.72	0.21	0.70	-0.00	7.14	0.15	100.15
MT-3M_P10_R2C_64	63	48.62	6.85	22.75	0.01	13.69	0.21	0.71	0.00	7.20	0.17	100.21
MT-3M_P10_R2C_65	64	48.63	6.85	22.79	-0.00	13.50	0.20	0.77	0.00	7.16	0.15	100.06
MT-3M_P10_R2C_66	65	48.53	6.82	22.81	-0.00	13.69	0.22	0.72	0.01	7.28	0.16	100.25
MT-3M_P10_R2C_67	66	48.70	6.81	22.68	0.01	13.71	0.22	0.68	0.00	7.34	0.17	100.34
MT-3M_P10_R2C_68	67	48.79	6.64	22.36	-0.00	13.78	0.23	0.63	0.00	7.31	0.18	99.92
MT-3M_P10_R2C_69	68	49.08	6.44	22.40	0.01	13.89	0.23	0.59	0.01	7.56	0.20	100.41
MT-3M_P10_R2C_70	69	49.12	6.27	22.00	0.00	14.12	0.24	0.56	-0.02	7.58	0.20	100.09
MT-3M_P10_R2C_71	70	49.32	5.96	21.58	0.03	14.50	0.24	0.51	0.01	7.65	0.23	100.01
MT-3M_P10_R2C_72	71	49.75	5.74	21.21	0.04	14.58	0.23	0.49	0.00	7.95	0.25	100.25
MT-3M_P10_R2C_73	72	49.67	5.79	21.08	0.00	14.65	0.25	0.58	0.01	7.98	0.22	100.23
MT-3M_P10_R2C_74	73	49.69	5.68	20.72	0.02	14.81	0.25	0.50	-0.01	8.17	0.26	100.09
MT-3M_P10_R2C_75	74	51.34	5.07	19.65	0.22	14.05	0.39	0.52	-0.01	8.69	0.33	100.25
MT-3M_P10_R2C_76	75	52.65	3.91	19.49	0.32	13.96	0.37	0.57	0.00	8.93	0.40	100.61
MT-3M_P10_R2C_77	76	52.55	1.09	3.73	0.03	20.47	0.08	0.21	0.00	21.29	1.45	100.92
MT-3M_P10_R2C_78	77	53.18	7.60	17.29	0.56	11.57	0.39	0.72	0.02	8.35	0.31	99.98

Sample	Distance (μm)	SiO_2	Al_2O_3	CaO	K_2O	MgO	Na_2O	TiO_2	Cr_2O_3	FeO	MnO	Total
MT-3M_P10_R2C_79	78	62.51	12.09	4.62	1.92	3.53	0.38	0.49	-0.00	3.71	0.18	89.42
MT-3M_P10_R2C_80	79	63.44	9.55	5.73	1.67	7.74	0.50	0.43	-0.02	6.58	0.40	96.03
MT-3M_P10_R2C_81	80	58.05	4.48	10.30	0.61	15.09	0.53	0.42	-0.01	11.04	0.67	101.19
MT-3M_P10_R2C_82	81	54.93	3.21	14.28	0.28	15.72	0.49	0.42	-0.00	11.27	0.62	101.23
MT-3M_P10_R2C_83	82	51.01	4.57	15.52	0.05	15.71	0.27	0.56	0.00	11.76	0.56	100.01
MT-3M_P10_R2C_84	83	51.59	2.87	8.70	0.03	17.59	0.18	0.36	0.00	17.50	1.04	99.87
MT-3M_P10_R2C_85	84	52.88	0.48	1.36	-0.01	20.18	0.04	0.11	-0.00	23.78	1.60	100.41
MT-3M_P10_R2C_86	85	52.60	0.39	1.11	-0.00	20.11	0.02	0.08	-0.01	24.23	1.61	100.13
MT-3M_P10_R2C_87	86	51.99	0.47	1.12	0.02	19.40	0.03	0.14	0.00	24.52	1.66	99.35
MT-3M_P10_R2C_88	87	49.55	0.55	1.05	-0.00	15.99	0.01	0.48	0.00	27.52	1.56	96.71
MT-3M_P10_R2C_89	88	51.79	0.45	1.07	0.02	17.71	0.02	0.12	0.01	24.89	1.64	97.72
MT-3M_P10_R2C_90	89	52.65	0.54	1.08	0.08	19.13	0.04	0.13	-0.01	24.89	1.65	100.18
MT-3M_P10_R2C_91	90	52.64	0.48	1.07	0.03	19.98	0.03	0.08	-0.01	24.97	1.63	100.88
MT-3M_P10_R2C_92	91	52.40	0.48	1.09	0.02	19.78	0.03	0.09	-0.02	24.89	1.62	100.38
MT-3M_P10_R2C_93	92	52.55	0.40	1.06	0.01	19.94	0.02	0.09	0.00	25.00	1.64	100.71
MT-3M_P10_R2C_94	93	52.46	0.38	1.07	-0.01	19.45	0.02	0.11	0.00	24.81	1.61	99.89
MT-3M_P10_R2C_95	94	52.46	0.39	1.10	0.01	19.59	0.01	0.08	0.00	24.72	1.64	99.99
MT-3M_P10_R2C_96	95	52.29	0.41	1.04	0.01	19.53	0.02	0.08	-0.02	24.81	1.63	99.79
MT-3M_P10_R2C_97	96	52.52	0.42	1.07	0.01	19.43	0.01	0.11	0.01	24.91	1.64	100.14
MT-3M_P10_R2C_98	97	52.27	0.44	1.03	0.00	19.35	0.01	0.08	0.00	24.81	1.59	99.59
MT-3M_P10_R2C_99	98	52.35	0.46	1.04	-0.01	19.42	0.01	0.12	-0.01	24.86	1.69	99.93
MT-3M_P10_R2C_100	99	52.23	0.46	1.03	0.03	19.45	0.01	0.10	-0.02	24.82	1.61	99.73
MT-3M_P10_R2C_101	100	52.24	0.49	1.04	0.00	19.35	0.02	0.12	0.00	24.86	1.64	99.75
MT-3M_P10_R2C_102	101	52.00	0.49	1.05	0.03	19.52	0.01	0.09	-0.01	24.86	1.64	99.68
MT-3M_P10_R2C_103	102	52.02	0.48	1.04	-0.00	19.45	0.01	0.11	0.01	24.92	1.62	99.66
MT-3M_P10_R2C_104	103	50.89	0.47	1.04	0.01	18.90	0.01	0.08	0.00	24.43	1.61	97.44
MT-3M_P10_R2C_105	104	52.55	0.50	1.04	0.01	19.59	0.02	0.11	-0.00	25.02	1.64	100.48
MT-3M_P10_R2C_106	105	52.19	0.48	1.03	0.01	19.50	0.02	0.10	0.01	24.80	1.64	99.78
MT-3M_P10_R2C_107	106	52.26	0.48	1.05	0.01	19.42	0.01	0.09	-0.00	24.83	1.64	99.79
MT-3M_P10_R2C_108	107	52.46	0.47	1.01	0.03	19.55	0.02	0.11	0.00	24.76	1.61	100.01
MT-3M_P10_R2C_109	108	52.49	0.49	1.05	0.01	19.44	0.01	0.09	0.00	24.73	1.65	99.96
MT-3M_P10_R2C_110	109	52.58	0.47	1.05	0.02	19.61	0.01	0.11	-0.02	24.92	1.62	100.37
MT-3M_P10_R2C_111	110	52.44	0.48	1.03	0.01	19.50	0.02	0.12	-0.00	24.72	1.62	99.94
MT-3M_P10_R2C_112	111	52.25	0.47	1.03	0.02	19.57	0.02	0.10	-0.00	24.65	1.64	99.75
MT-3M_P10_R2C_113	112	52.39	0.50	1.04	0.02	19.58	0.02	0.09	-0.00	24.97	1.62	100.21
MT-3M_P10_R2C_114	113	52.13	0.50	1.04	0.01	19.51	0.02	0.11	0.00	24.81	1.64	99.76
MT-3M_P10_R2C_115	114	52.07	0.48	1.03	0.00	19.51	0.01	0.11	0.00	24.69	1.60	99.52
MT-3M_P10_R2C_116	115	52.25	0.49	1.03	0.02	19.56	0.02	0.09	0.01	24.70	1.66	99.83
MT-3M_P10_R2C_117	116	52.45	0.49	1.03	0.01	19.69	0.02	0.09	-0.02	24.85	1.61	100.23

Sample	Distance (μm)	SiO_2	Al_2O_3	CaO	K_2O	MgO	Na_2O	TiO_2	Cr_2O_3	FeO	MnO	Total
MT-3M_P10_R2C_118	117	52.39	0.49	1.06	0.03	19.51	0.02	0.12	0.01	24.94	1.63	100.19
MT-3M_P10_R2C_119	118	52.39	0.48	1.05	0.03	19.70	0.01	0.09	-0.01	25.02	1.65	100.42
MT-3M_P10_R2C_120	119	52.20	0.45	1.06	0.02	19.65	0.01	0.11	-0.01	24.85	1.64	99.97
MT-3M_P10_R2C_121	120	52.43	0.46	1.11	0.00	19.57	0.01	0.10	-0.01	24.94	1.63	100.25
MT-3M_P10_R2C_122	121	52.49	0.43	1.04	0.00	19.61	0.02	0.07	0.00	24.60	1.62	99.88
MT-3M_P10_R2C_123	122	52.21	0.42	1.06	-0.00	19.67	0.01	0.08	-0.01	24.51	1.61	99.57
MT-3M_P10_R2C_124	123	52.43	0.42	1.07	0.01	19.51	0.01	0.09	-0.00	24.58	1.65	99.77
MT-3M_P10_R2C_125	124	52.63	0.40	1.06	0.03	19.58	0.02	0.09	-0.00	24.89	1.62	100.32
MT-3M_P10_R2C_126	125	52.48	0.40	1.07	0.01	19.70	0.02	0.10	-0.01	24.75	1.66	100.16
MT-3M_P10_R2C_127	126	52.41	0.38	1.05	0.01	19.71	0.02	0.07	0.00	24.63	1.63	99.91
MT-3M_P10_R2C_128	127	52.26	0.37	1.08	0.00	19.58	0.02	0.07	0.00	24.66	1.63	99.69
MT-3M_P10_R2C_129	128	52.56	0.36	1.08	0.01	19.91	0.02	0.06	-0.01	24.75	1.64	100.39
MT-3M_P10_R2C_130	129	52.33	0.34	1.05	0.02	19.63	0.02	0.07	0.00	24.58	1.67	99.71
MT-3M_P10_R2C_131	130	52.78	0.35	1.05	0.02	19.78	0.02	0.11	0.00	24.52	1.66	100.28
MT-3M_P10_R2C_132	131	52.48	0.37	1.05	0.00	19.80	0.02	0.10	-0.01	24.71	1.65	100.17
MT-3M_P10_R2C_133	132	52.33	0.38	1.08	0.01	19.73	0.03	0.12	-0.00	24.71	1.68	100.07
MT-3M_P10_R2C_134	133	52.53	0.37	1.10	0.01	19.79	0.02	0.10	-0.01	24.77	1.65	100.33
MT-3M_P10_R2C_135	134	52.53	0.39	1.07	0.00	19.54	0.03	0.10	-0.00	24.61	1.67	99.95
MT-3M_P10_R2C_136	135	52.44	0.37	1.09	-0.00	19.74	0.02	0.09	0.01	24.57	1.63	99.96
MT-3M_P10_R2C_137	136	52.21	0.37	1.04	-0.00	19.79	0.01	0.07	0.01	24.67	1.64	99.81
MT-3M_P10_R2C_138	137	52.38	0.37	1.07	-0.01	19.70	0.01	0.09	0.00	24.60	1.62	99.82
MT-3M_P10_R2C_139	138	52.33	0.36	1.07	-0.02	19.66	0.03	0.08	0.01	24.61	1.65	99.78
MT-3M_P10_R2C_140	139	52.37	0.37	1.10	0.02	19.77	0.02	0.09	0.00	24.67	1.68	100.10
MT-3M_P10_R2C_141	140	52.29	0.35	1.08	0.01	19.80	0.01	0.08	-0.00	24.70	1.62	99.94
MT-3M_P10_R2C_142	141	52.46	0.35	1.05	-0.00	19.86	0.02	0.08	-0.00	24.79	1.64	100.24
MT-3M_P10_R2C_143	142	52.41	0.36	1.07	0.00	19.84	0.02	0.09	-0.02	24.63	1.64	100.05
MT-3M_P10_R2C_144	143	52.42	0.36	1.09	0.01	19.58	0.01	0.07	0.01	24.70	1.64	99.89
MT-3M_P10_R2C_145	144	52.56	0.37	1.08	0.01	19.73	0.02	0.08	-0.00	24.65	1.64	100.13
MT-3M_P10_R2C_146	145	52.22	0.37	1.06	0.01	19.69	0.03	0.06	0.02	24.64	1.62	99.72
MT-3M_P10_R2C_147	146	52.49	0.38	1.07	0.02	19.76	0.02	0.07	-0.01	24.70	1.63	100.12
MT-3M_P10_R2C_148	147	52.38	0.39	1.08	0.01	19.78	0.01	0.08	0.01	24.63	1.59	99.96
MT-3M_P10_R2C_149	148	52.39	0.40	1.08	0.02	19.69	0.02	0.05	0.01	24.68	1.66	99.99
MT-3M_P10_R2C_150	149	52.10	0.40	1.06	0.01	19.60	0.01	0.06	-0.01	24.46	1.65	99.35
MT-3M_P10_R2C_151	150	52.06	0.40	1.07	0.01	19.59	0.01	0.08	-0.01	24.51	1.63	99.35

Table B1.1. Plagioclase major element compositions obtained by electron microprobe, expressed in %. Data from Gede Volcano (West Java, Indonesia).

Abbreviations: Grain: P, phenocryst; GM, groundmass.
Spot position: C, core; M, mid point; R, rim.

An, anorthite; Ab, albite; Or, orthoclase.

Sample	Position	Distance (μm)	SiO_2	Al_2O_3	MgO	CaO	FeO	Na_2O	K_2O	TiO_2	Total	An	Ab	Or
G23_1P_B_01	C	0	47.66	31.51	0.08	16.71	0.65	2.14	0.04	0.00	98.79	81.00	18.77	0.23
G23_1P_B_02	C	21.94	48.65	31.56	0.08	16.71	0.59	2.33	0.09	0.05	100.06	79.44	20.05	0.51
G23_1P_B_03	C	43.89	48.75	31.29	0.08	16.46	0.56	2.25	0.08	0.03	99.50	79.80	19.74	0.46
G23_1P_B_04	M	65.83	47.95	31.42	0.07	16.52	0.67	2.40	0.06	0.03	99.12	78.91	20.75	0.34
G23_1P_B_05	M	87.78	46.94	32.30	0.06	17.71	0.59	1.65	0.06	0.00	99.31	85.28	14.38	0.34
G23_1P_B_06	M	109.72	47.97	31.69	0.07	16.98	0.71	1.92	0.08	0.00	99.42	82.63	16.91	0.46
G23_1P_B_07	M	131.66	47.10	28.73	1.31	16.04	3.48	1.97	0.10	0.36	99.17	81.32	18.07	0.60
G23_1P_B_09	R	175.55	47.49	31.80	0.06	17.14	0.81	1.86	0.07	0.00	99.23	83.25	16.35	0.40
G23_1P_B_10	R	197.5	58.24	21.23	0.30	8.11	2.83	4.40	1.32	0.96	97.49	45.96	45.13	8.91
G23_3P_A_01	C	39.97	47.35	30.91	0.08	16.38	0.54	2.46	0.05	0.00	97.77	78.41	21.31	0.28
G23_3P_A_02	C	59.96	46.55	31.35	0.04	16.80	0.54	2.20	0.05	0.00	97.53	80.61	19.10	0.29
G23_3P_A_03	C	99.93	47.64	31.59	0.07	16.53	0.56	2.31	0.08	0.00	98.78	79.45	20.09	0.46
G23_3P_A_04	M	119.92	46.74	31.22	0.07	16.82	0.67	2.22	0.06	0.00	97.80	80.44	19.21	0.34
G23_3P_A_05	M	139.91	44.96	32.26	0.09	17.70	0.65	1.47	0.08	0.00	97.21	86.53	13.00	0.47
G23_3P_A_06	R	259.83	44.92	31.97	0.06	17.99	0.64	1.55	0.05	0.00	97.18	86.26	13.45	0.29
G23_3P_B_01	C	0.00	47.13	31.64	0.09	16.99	0.60	2.00	0.05	0.00	98.50	82.20	17.51	0.29
G23_3P_B_02	C	22.01	47.04	31.77	0.07	17.10	0.58	2.01	0.05	0.00	98.62	82.22	17.49	0.29
G23_3P_B_03	C	66.03	50.31	30.09	0.09	14.86	0.58	3.21	0.11	0.00	99.25	71.44	27.93	0.63
G23_3P_B_04	C	88.03	48.73	31.58	0.05	16.68	0.65	2.23	0.05	0.00	99.97	80.29	19.42	0.29
G23_3P_B_05	M	110.04	48.59	31.52	0.06	16.77	0.69	2.03	0.04	0.00	99.70	81.84	17.93	0.23
G23_3P_B_06	M	132.05	49.26	30.68	0.16	15.78	0.94	2.34	0.07	0.00	99.23	78.52	21.07	0.41
G23_3P_B_07	M	154.06	47.57	31.80	0.08	17.09	0.63	1.87	0.05	0.00	99.09	83.23	16.48	0.29
G23_3P_B_08	M	176.07	48.63	31.05	0.08	16.39	0.71	2.28	0.07	0.00	99.21	79.57	20.03	0.40
G23_3P_B_09	M	198.08	47.70	31.17	0.10	16.06	0.57	2.44	0.07	0.03	98.14	78.12	21.48	0.41
G23_3P_B_10	M	220.09	48.79	30.62	0.07	15.79	0.56	2.62	0.10	0.04	98.59	76.46	22.96	0.58
G23_3P_B_11	R	242.09	48.43	30.81	0.08	16.04	0.67	2.68	0.07	0.00	98.78	76.48	23.12	0.40
G23_3P_B_12	R	286.11	46.85	31.70	0.09	17.05	0.70	1.91	0.05	0.04	98.39	82.90	16.81	0.29
G23_3P_B_13	R	308.12	46.72	31.84	0.07	17.27	0.70	2.00	0.07	0.00	98.67	82.35	17.26	0.40
G23_4P_B_01	C	0.00	46.19	33.15	0.06	18.52	0.68	1.09	0.05	0.00	99.74	90.11	9.60	0.29
G23_4P_B_02	C	19.96	44.81	33.86	0.00	19.05	0.69	0.76	0.05	0.00	99.22	93.00	6.71	0.29
G23_4P_B_03	C	39.91	45.66	33.26	0.08	18.69	0.65	1.04	0.05	0.00	99.43	90.59	9.12	0.29

Sample	Position	Distance (μm)	SiO_2	Al_2O_3	MgO	CaO	FeO	Na_2O	K_2O	TiO_2	Total	An	Ab	Or
G23_4P_B_04	C	59.87	45.15	33.75	0.03	19.05	0.56	0.87	0.00	0.00	99.41	92.37	7.63	0.00
G23_4P_B_05	M	79.82	49.41	31.17	0.08	15.86	0.72	2.67	0.09	0.04	100.04	76.25	23.23	0.52
G23_4P_B_06	M	99.78	48.21	32.01	0.08	16.71	0.67	2.11	0.04	0.00	99.83	81.21	18.56	0.23
G23_4P_B_07	M	119.73	53.84	22.77	1.83	11.16	5.36	3.18	1.03	0.72	100.03	61.52	31.72	6.76
G23_4P_B_08	M	139.69	48.44	31.59	0.09	16.50	0.67	2.31	0.09	0.00	99.69	79.38	20.11	0.52
G23_4P_B_09	R	159.65	48.56	31.71	0.07	16.49	0.68	2.40	0.06	0.00	99.97	78.88	20.78	0.34
G23_4P_B_10	R	199.56	48.96	31.25	0.12	15.96	0.63	2.62	0.10	0.03	99.67	76.66	22.77	0.57
G23_4P_B_11	R	219.51	45.44	32.98	0.07	18.06	0.55	1.37	0.04	0.00	98.51	87.73	12.04	0.23
G23_4P_B_13	R	259.42	47.65	32.03	0.08	17.03	0.70	1.88	0.06	0.03	99.46	83.06	16.59	0.35
G23_5P_01	C	0.00	44.31	33.95	0.07	19.09	0.56	0.71	0.00	0.00	98.69	93.69	6.31	0.00
G23_5P_02	M	60.02	46.73	30.62	0.12	15.90	0.70	2.44	0.11	0.03	96.65	77.76	21.60	0.64
G23_5P_03	M	80.03	46.99	32.43	0.00	16.90	0.58	1.92	0.08	0.03	98.93	82.56	16.97	0.47
G23_5P_04	R	100.04	45.83	32.79	0.07	17.65	0.53	1.63	0.04	0.03	98.57	85.48	14.29	0.23
G23_5P_05	C	140.06	46.82	32.64	0.07	17.42	0.53	2.02	0.06	0.03	99.59	82.38	17.29	0.34
G23_5P_06	C	160.07	46.77	32.65	0.03	17.29	0.53	1.68	0.06	0.00	99.01	84.75	14.90	0.35
G23_5P_07	C	180.07	46.19	32.72	0.06	17.39	0.59	1.86	0.06	0.00	98.87	83.50	16.16	0.34
G23_5P_08	C	200.08	47.08	32.43	0.06	17.24	0.53	1.90	0.05	0.03	99.32	83.13	16.58	0.29
G23_5P_09	M	240.10	46.56	32.44	0.05	17.28	0.54	1.80	0.08	0.04	98.79	83.75	15.79	0.46
G23_5P_10	M	260.11	47.24	31.91	0.06	16.56	0.56	2.36	0.07	0.03	98.79	79.18	20.42	0.40
G23_5P_11	M	280.11	46.85	32.65	0.05	17.14	0.62	1.96	0.04	0.00	99.31	82.66	17.11	0.23
G23_5P_12	M	300.12	46.61	32.64	0.05	17.38	0.54	1.74	0.04	0.03	99.03	84.47	15.30	0.23
G23_5P_13	M	320.13	44.89	33.67	0.00	18.59	0.50	1.12	0.00	0.00	98.77	90.17	9.83	0.00
G23_5P_14	M	340.14	45.35	33.94	0.05	18.77	0.51	1.08	0.03	0.00	99.73	90.41	9.41	0.17
G23_5P_15	R	360.15	46.61	32.59	0.06	17.22	0.53	1.85	0.06	0.03	98.95	83.43	16.22	0.35
G23_5P_16	R	380.15	47.48	30.67	0.54	16.14	1.36	2.15	0.16	0.10	98.60	79.82	19.24	0.94
G23_5P_17	R	420.17	46.91	32.13	0.14	17.17	0.78	1.90	0.07	0.03	99.13	82.98	16.62	0.40
G23_5P_18	C	440.18	45.87	32.81	0.05	17.43	0.55	1.67	0.06	0.00	98.44	84.93	14.72	0.35
G23_5P_19	M	460.19	45.84	33.57	0.03	18.25	0.56	1.27	0.04	0.00	99.56	88.61	11.16	0.23
G23_5P_20	M	520.21	46.51	32.70	0.07	17.37	0.55	1.98	0.05	0.00	99.23	82.66	17.05	0.28
G23_5P_21	M	540.22	46.07	32.73	0.04	17.51	0.60	1.77	0.09	0.00	98.81	84.10	15.38	0.51
G23_5P_22	M	560.23	45.75	33.10	0.06	17.88	0.64	1.52	0.06	0.03	99.04	86.37	13.29	0.35
G23_5P_23	M	580.24	46.51	32.57	0.04	17.31	0.63	1.80	0.07	0.00	98.93	83.82	15.77	0.40
G23_5P_24	R	600.24	45.88	32.82	0.10	17.69	0.71	1.58	0.07	0.04	98.89	85.74	13.86	0.40
G23_5P_25	R	640.26	45.35	33.26	0.06	18.05	0.63	1.48	0.08	0.00	98.91	86.68	12.86	0.46
G23_5P_26	R	680.28	46.15	32.76	0.09	17.46	0.71	1.83	0.10	0.00	99.10	83.58	15.85	0.57
G23_5P_27	R	700.29	45.86	33.17	0.05	17.75	0.59	1.63	0.08	0.00	99.13	85.36	14.18	0.46
G23_6P_01	C	20.01	46.10	32.15	0.05	17.56	0.60	1.71	0.06	0.03	98.26	84.72	14.93	0.34
G23_6P_02	M	79.93	45.38	32.01	0.07	16.71	0.62	1.98	0.07	0.00	96.84	82.01	17.58	0.41
G23_6P_03	M	179.83	45.89	32.17	0.14	17.66	0.68	1.63	0.08	0.03	98.28	85.29	14.25	0.46

Sample	Position	Distance (μm)	SiO_2	Al_2O_3	MgO	CaO	FeO	Na_2O	K_2O	TiO_2	Total	An	Ab	Or
G23_6P_04	M	259.76	45.60	32.62	0.06	17.79	0.64	1.51	0.04	0.00	98.26	86.48	13.28	0.23
G23_6P_05	M	359.66	47.96	31.84	0.12	17.68	0.66	1.81	0.21	0.00	100.28	83.37	15.45	1.18
G23_6P_06	R	519.51	50.00	24.38	2.18	13.13	3.98	2.97	0.92	0.56	98.23	66.99	27.42	5.59
G23_RACH3_01	C	22.00	45.89	32.74	0.05	18.34	0.52	1.24	0.03	0.00	98.81	88.94	10.88	0.17
G23_RACH3_02	C	44.01	46.06	32.51	0.05	17.56	0.59	1.63	0.00	0.00	98.40	85.62	14.38	0.00
G23_RACH3_03	M	66.01	45.65	33.14	0.04	18.63	0.43	1.12	0.00	0.00	99.01	90.19	9.81	0.00
G23_RACH3_04	M	88.02	46.16	32.52	0.04	17.94	0.48	1.46	0.03	0.00	98.63	87.01	12.81	0.17
G23_RACH3_05	M	110.02	46.40	32.56	0.03	17.74	0.49	1.60	0.03	0.00	98.85	85.82	14.01	0.17
G23_RACH3_06	M	132.03	45.89	32.51	0.05	17.85	0.40	1.51	0.04	0.00	98.25	86.52	13.25	0.23
G23_RACH3_07	M	154.03	45.90	32.82	0.06	18.02	0.55	1.41	0.05	0.00	98.81	87.34	12.37	0.29
G23_RACH3_08	R	198.04	45.44	33.26	0.04	18.61	0.56	0.99	0.00	0.00	98.90	91.22	8.78	0.00
G23_RACH3_09	R	220.05	45.55	32.57	0.06	18.22	0.61	1.32	0.00	0.00	98.33	88.41	11.59	0.00
G25_1P_A_01	C	0	47.45	31.72	0.06	16.62	0.60	2.34	0.09	0.00	98.88	79.29	20.20	0.51
G25_1P_A_02	M	20.01	47.43	31.62	0.05	16.57	0.61	2.31	0.11	0.00	98.70	79.35	20.02	0.63
G25_1P_A_03	M	80.03	47.89	31.43	0.05	16.33	0.59	2.32	0.09	0.00	98.70	79.14	20.35	0.52
G25_1P_A_04	M	120.04	47.41	31.55	0.06	16.23	0.56	2.29	0.09	0.04	98.23	79.24	20.23	0.52
G25_1P_A_05	M	160.06	46.63	31.81	0.04	16.84	0.56	2.11	0.07	0.00	98.06	81.19	18.41	0.40
G25_1P_A_06	R	200.07	46.39	32.07	0.00	17.28	0.59	1.89	0.06	0.03	98.31	83.19	16.47	0.34
G25_1P_A_07	R	260.09	47.73	31.28	0.05	16.27	0.54	2.47	0.09	0.00	98.43	78.05	21.44	0.51
G25_2P_D_01	C	0	46.29	32.08	0.04	17.05	0.52	2.03	0.07	0.00	98.08	81.94	17.66	0.40
G25_2P_D_02	C	21.55	47.06	31.86	0.05	16.87	0.63	2.07	0.08	0.00	98.62	81.45	18.09	0.46
G25_2P_D_03	C	43.11	45.82	32.68	0.03	17.63	0.58	1.73	0.06	0.00	98.53	84.63	15.03	0.34
G25_2P_D_04	M	64.66	46.26	32.16	0.05	17.42	0.56	1.88	0.06	0.05	98.44	83.38	16.28	0.34
G25_2P_D_05	M	86.21	47.24	32.64	0.06	17.48	0.61	1.77	0.11	0.00	99.91	83.98	15.39	0.63
G25_2P_D_06	M	107.77	45.48	32.88	0.05	17.95	0.53	1.56	0.06	0.00	98.51	86.11	13.54	0.34
G25_2P_D_07	M	129.32	49.85	30.82	0.10	14.52	0.72	2.90	0.16	0.00	99.07	72.75	26.29	0.95
G25_2P_D_08	M	172.43	49.25	30.82	0.06	15.50	0.55	2.83	0.13	0.00	99.14	74.61	24.65	0.75
G25_2P_D_09	M	193.98	48.65	30.65	0.05	15.38	0.57	2.99	0.13	0.00	98.42	73.43	25.83	0.74
G25_2P_D_10	R	215.53	48.31	30.78	0.05	15.70	0.55	2.90	0.10	0.03	98.42	74.52	24.91	0.57
G25_2P_D_11	R	237.09	52.64	28.11	0.05	12.22	0.57	4.62	0.24	0.00	98.45	58.56	40.07	1.37
G25_2P_D_12	R	258.64	53.79	27.18	0.05	10.92	0.59	5.25	0.40	0.03	98.21	52.26	45.46	2.28
G25_3P_F_01	C	29.87	44.29	33.35	0.00	18.86	0.50	1.00	0.06	0.00	98.06	90.93	8.72	0.34
G25_3P_F_02	M	39.83	46.32	31.87	0.05	17.40	0.61	2.15	0.12	0.00	98.52	81.18	18.15	0.67
G25_3P_F_03	M	49.79	45.09	32.99	0.00	18.56	0.57	1.18	0.05	0.00	98.44	89.42	10.29	0.29
G25_3P_F_04	M	59.75	44.99	32.81	0.00	18.16	0.55	1.47	0.00	0.00	97.98	87.22	12.78	0.00
G25_3P_F_05	M	69.7	45.66	32.29	0.03	17.44	0.59	1.88	0.06	0.00	97.95	83.39	16.27	0.34
G25_3P_F_06	M	89.62	48.81	30.42	0.03	15.29	0.49	2.97	0.13	0.00	98.14	73.44	25.82	0.74
G25_3P_F_07	R	99.58	49.46	29.70	0.04	14.44	0.64	3.43	0.20	0.04	97.95	69.14	29.72	1.14
G25_3P_F_08	R	109.53	52.53	27.72	0.05	11.80	0.56	4.83	0.30	0.04	97.83	56.47	41.83	1.71

Sample	Position	Distance (μm)	SiO_2	Al_2O_3	MgO	CaO	FeO	Na_2O	K_2O	TiO_2	Total	An	Ab	Or
G25_4P_G_01	R	25.03	56.42	25.22	0.03	8.87	0.45	6.63	0.55	0.00	98.17	41.21	55.74	3.04
G25_4P_G_02	R	50.02	54.12	26.72	0.00	10.61	0.48	5.55	0.32	0.00	97.80	50.44	47.75	1.81
G25_4P_G_03	R	75.03	54.19	27.17	0.04	11.18	0.49	5.40	0.36	0.00	98.83	52.29	45.70	2.00
G25_4P_G_04	M	100.03	52.72	27.85	0.04	12.15	0.48	4.63	0.29	0.00	98.16	58.21	40.14	1.65
G25_4P_G_05	M	150.05	54.24	26.86	0.04	10.63	0.53	5.56	0.34	0.00	98.20	50.39	47.69	1.92
G25_4P_G_06	M	175.05	54.94	26.61	0.03	10.40	0.48	5.71	0.41	0.03	98.61	49.01	48.69	2.30
G25_4P_G_07	M	200.06	54.07	27.15	0.03	11.06	0.52	5.51	0.38	0.00	98.72	51.48	46.41	2.11
G25_4P_G_08	M	250.07	51.97	28.50	0.03	12.72	0.49	4.29	0.26	0.00	98.26	61.17	37.34	1.49
G25_4P_G_09	M	275.08	51.65	28.46	0.05	12.87	0.50	4.48	0.28	0.04	98.33	60.39	38.04	1.56
G25_4P_G_10	M	300.08	49.64	29.73	0.05	14.42	0.51	3.60	0.19	0.04	98.18	68.14	30.79	1.07
G25_4P_G_11	M	325.09	46.74	31.70	0.04	16.80	0.56	2.06	0.11	0.00	98.01	81.32	18.04	0.63
G25_4P_G_12	M	350.1	48.38	31.05	0.04	16.01	0.52	2.68	0.11	0.00	98.79	76.27	23.10	0.62
G25_4P_G_13	M	375.11	48.59	30.77	0.04	15.43	0.59	2.96	0.13	0.00	98.51	73.68	25.58	0.74
G25_4P_G_14	M	400.11	48.59	30.66	0.03	15.33	0.55	3.10	0.13	0.00	98.39	72.67	26.59	0.73
G25_4P_G_15	M	425.12	48.11	31.66	0.00	16.37	0.52	2.39	0.13	0.00	99.18	78.51	20.74	0.74
G25_4P_G_16	M	450.13	46.57	32.50	0.00	17.44	0.53	1.76	0.08	0.03	98.91	84.17	15.37	0.46
G25_4P_G_17	M	475.14	48.01	30.81	0.03	15.65	0.49	2.91	0.12	0.03	98.05	74.32	25.01	0.68
G25_4P_G_18	M	500.14	49.57	30.16	0.00	14.69	0.53	3.55	0.15	0.00	98.65	68.99	30.17	0.84
G25_4P_G_19	M	525.15	51.45	28.94	0.03	13.29	0.56	4.23	0.29	0.00	98.79	62.42	35.95	1.62
G25_4P_G_20	M	550.16	51.59	28.49	0.03	12.86	0.50	4.35	0.26	0.00	98.08	61.12	37.41	1.47
G25_4P_G_21	M	575.16	52.54	28.34	0.06	12.55	0.52	4.54	0.28	0.03	98.86	59.48	38.94	1.58
G25_4P_G_22	M	600.17	51.85	28.43	0.04	12.62	0.48	4.38	0.26	0.03	98.09	60.51	38.00	1.48
G25_4P_G_23	M	625.18	52.31	28.55	0.00	12.53	0.51	4.54	0.25	0.05	98.74	59.54	39.04	1.41
G25_4P_G_24	M	700.2	52.71	27.98	0.05	12.03	0.51	4.78	0.28	0.05	98.39	57.25	41.16	1.59
G25_4P_G_25	M	725.2	53.15	27.83	0.05	11.88	0.52	4.68	0.30	0.05	98.46	57.37	40.90	1.73
G25_4P_G_26	C	775.22	52.76	28.19	0.04	12.41	0.58	4.67	0.28	0.03	98.96	58.55	39.87	1.57
G25_4P_G_27	C	800.22	53.43	27.88	0.05	12.07	0.52	4.66	0.33	0.04	98.98	57.76	40.36	1.88
G25_4P_G_28	C	825.23	52.58	28.14	0.04	12.12	0.50	4.77	0.35	0.03	98.53	57.25	40.78	1.97
G25_4P_G_29	C	850.24	53.27	28.38	0.05	12.42	0.55	4.64	0.24	0.03	99.58	58.86	39.79	1.35
G25_4P_G_30	C	875.24	54.42	27.40	0.03	11.10	0.43	5.31	0.35	0.00	99.04	52.54	45.48	1.97
G25_4P_G_31	C	900.25	53.67	27.49	0.04	11.39	0.48	5.00	0.32	0.04	98.43	54.71	43.46	1.83
G25_4P_H_01	C	20.01	47.61	31.26	0.03	15.75	0.54	2.65	0.11	0.00	97.95	76.17	23.19	0.63
G25_4P_H_02	C	39.99	47.27	31.67	0.03	16.47	0.58	2.22	0.10	0.04	98.38	79.93	19.50	0.58
G25_4P_H_03	C	59.97	50.40	30.05	0.03	14.97	0.60	3.47	0.19	0.03	99.74	69.71	29.24	1.05
G25_4P_H_04	M	79.96	46.16	32.09	0.04	17.08	0.52	2.02	0.06	0.03	98.00	82.09	17.57	0.34
G25_4P_H_05	M	119.93	48.27	31.34	0.04	16.06	0.59	2.62	0.12	0.03	99.07	76.68	22.64	0.68
G25_4P_H_06	M	139.92	47.95	31.06	0.05	15.84	0.54	2.57	0.12	0.03	98.16	76.77	22.54	0.69
G25_4P_H_07	M	199.88	47.18	31.54	0.05	16.26	0.56	2.38	0.09	0.03	98.09	78.65	20.83	0.52
G25_4P_H_08	M	239.87	44.51	32.84	0.00	18.40	0.56	1.20	0.04	0.03	97.58	89.24	10.53	0.23

Sample	Position	Distance (μm)	SiO_2	Al_2O_3	MgO	CaO	FeO	Na_2O	K_2O	TiO_2	Total	An	Ab	Or
G25_4P_H_09	M	259.85	44.62	32.91	0.04	18.44	0.51	1.35	0.04	0.00	97.91	88.10	11.67	0.23
G25_4P_H_10	M	279.84	49.13	30.15	0.06	15.07	0.60	3.26	0.10	0.03	98.40	71.46	27.97	0.56
G25_4P_H_11	M	299.83	47.75	30.92	0.07	15.86	0.58	2.58	0.12	0.00	97.88	76.72	22.59	0.69
G25_4P_H_12	M	319.82	51.60	25.60	0.50	12.21	1.90	4.19	0.69	0.19	96.88	59.23	36.78	3.99
G25_4P_H_13	M	339.8	45.63	32.22	0.06	17.46	0.57	1.70	0.05	0.00	97.69	84.77	14.94	0.29
G25_4P_H_14	M	359.79	46.60	31.28	0.06	16.88	0.58	2.04	0.19	0.03	97.66	81.16	17.75	1.09
G25_4P_H_15	M	379.78	44.98	32.05	0.03	17.94	0.54	1.65	0.08	0.00	97.27	85.34	14.20	0.45
G25_4P_H_16	R	399.77	48.76	30.15	0.05	15.00	0.59	3.14	0.13	0.03	97.85	71.99	27.27	0.74
G25_4P_H_17	R	419.75	50.28	28.99	0.06	13.75	0.59	3.93	0.20	0.00	97.80	65.17	33.71	1.13
G25_4P_I_01	C	20.02	46.36	31.92	0.05	16.91	0.53	1.99	0.07	0.00	97.83	82.11	17.49	0.40
G25_4P_I_02	C	30.03	47.69	31.28	0.06	16.06	0.61	2.58	0.06	0.00	98.34	77.21	22.45	0.34
G25_4P_I_03	C	40.04	48.25	30.78	0.04	15.93	0.59	2.79	0.12	0.00	98.50	75.42	23.90	0.68
G25_4P_I_04	C	50.05	48.34	30.78	0.05	15.64	0.61	2.91	0.09	0.00	98.42	74.43	25.06	0.51
G25_4P_I_05	M	60.06	46.69	32.08	0.00	16.96	0.60	2.12	0.06	0.00	98.51	81.27	18.38	0.34
G25_4P_I_06	M	70.07	48.56	30.95	0.04	15.77	0.61	2.76	0.08	0.00	98.77	75.60	23.94	0.46
G25_4P_I_07	M	80.08	51.25	29.19	0.06	13.71	0.58	3.93	0.15	0.00	98.87	65.28	33.87	0.85
G25_4P_I_08	M	90.09	51.35	28.97	0.05	13.38	0.59	3.96	0.17	0.04	98.51	64.49	34.54	0.98
G25_4P_I_09	M	100.10	50.65	29.51	0.06	14.25	0.56	3.60	0.17	0.04	98.84	67.96	31.07	0.97
G25_4P_I_10	M	110.11	52.82	28.19	0.06	12.40	0.51	4.60	0.22	0.03	98.83	59.09	39.67	1.25
G25_4P_I_11	M	120.12	51.57	28.40	0.09	12.85	0.70	4.41	0.21	0.05	98.28	60.96	37.86	1.19
G25_4P_I_12	M	130.13	51.16	28.84	0.07	13.25	0.56	4.24	0.18	0.03	98.33	62.69	36.30	1.01
G25_4P_I_13	M	140.14	52.20	28.43	0.07	12.62	0.62	4.63	0.20	0.03	98.80	59.43	39.45	1.12
G25_4P_I_14	R	150.15	55.08	26.97	0.07	10.60	0.62	5.46	0.28	0.05	99.13	50.93	47.47	1.60
G25_4P_I_15	R	160.17	54.27	27.56	0.05	11.53	0.59	4.95	0.37	0.03	99.35	55.09	42.80	2.11
G25_6P_L_01	R	0	53.50	27.83	0.05	11.79	0.60	4.98	0.29	0.00	99.04	55.75	42.62	1.63
G25_6P_L_02	R	20	53.78	27.71	0.05	11.74	0.57	4.94	0.26	0.00	99.05	55.93	42.59	1.47
G25_6P_L_03	R	40	51.88	28.61	0.06	12.96	0.57	4.02	0.23	0.00	98.37	63.19	35.47	1.34
G25_6P_L_04	R	60	52.13	28.41	0.06	12.54	0.50	4.58	0.22	0.00	98.44	59.46	39.30	1.24
G25_6P_L_05	R	80	49.22	28.88	0.10	14.21	1.11	3.49	0.16	0.08	97.25	68.59	30.49	0.92
G25_6P_L_06	M	100	47.58	31.32	0.06	16.14	0.59	2.53	0.09	0.00	98.31	77.50	21.98	0.51
G25_6P_L_07	M	120	47.58	31.14	0.06	16.12	0.64	2.49	0.12	0.03	98.18	77.62	21.70	0.69
G25_6P_L_08	M	160	47.33	31.85	0.04	16.61	0.57	2.29	0.11	0.00	98.80	79.53	19.84	0.63
G25_6P_L_09	M	180	48.10	31.36	0.08	16.19	0.62	2.55	0.19	0.00	99.09	76.98	21.94	1.08
G25_6P_L_10	M	200	48.47	30.50	0.08	15.63	0.64	2.50	0.19	0.00	98.01	76.69	22.20	1.11
G25_6P_L_11	M	240	49.35	30.69	0.06	15.51	0.54	2.81	0.18	0.00	99.14	74.53	24.44	1.03
G25_6P_L_12	M	260	48.53	31.13	0.04	15.77	0.54	2.74	0.12	0.00	98.87	75.56	23.76	0.68
G25_6P_L_13	M	280	48.31	30.89	0.05	15.76	0.57	2.68	0.12	0.00	98.38	75.94	23.37	0.69
G25_6P_L_14	M	340	48.42	30.82	0.06	15.35	0.51	2.97	0.14	0.03	98.30	73.48	25.73	0.80
G25_6P_L_15	M	360	49.16	29.46	0.10	14.21	0.61	3.53	0.18	0.03	97.28	68.28	30.69	1.03

Sample	Position	Distance (μm)	SiO_2	Al_2O_3	MgO	CaO	FeO	Na_2O	K_2O	TiO_2	Total	An	Ab	Or
G25_6P_L_16	M	380	49.24	30.06	0.08	14.74	0.61	3.35	0.16	0.00	98.24	70.21	28.88	0.91
G25_6P_L_17	M	400	48.72	31.73	0.12	15.95	0.88	2.14	0.13	0.05	99.72	79.84	19.38	0.77
G25_6P_L_18	M	419.99	49.19	30.46	0.07	15.22	0.51	3.05	0.15	0.00	98.65	72.76	26.39	0.85
G25_6P_L_19	M	439.99	49.09	30.56	0.03	15.21	0.53	2.94	0.14	0.00	98.50	73.49	25.71	0.81
G25_6P_L_20	M	460	49.63	29.89	0.07	14.71	0.58	3.10	0.25	0.05	98.28	71.35	27.21	1.44
G25_6P_L_21	M	479.99	49.23	29.73	0.07	14.43	0.63	3.23	0.13	0.03	97.48	70.63	28.61	0.76
G25_6P_L_22	M	499.99	50.12	30.51	0.07	14.92	0.65	2.74	0.26	0.03	99.30	73.91	24.56	1.53
G25_6P_L_23	M	539.99	48.59	31.15	0.04	16.03	0.52	2.73	0.09	0.03	99.18	76.05	23.44	0.51
G25_6P_L_24	M	559.99	46.14	32.40	0.03	17.66	0.51	1.77	0.05	0.00	98.56	84.41	15.31	0.28
G25_6P_L_25	C	579.99	49.10	29.99	0.05	14.80	0.60	3.23	0.21	0.00	97.98	70.83	27.97	1.20
G25_RH1_01	C	0.00	52.80	28.89	0.06	12.79	0.53	4.14	0.29	0.05	99.55	62.01	36.32	1.67
G25_RH1_02	C	25.00	51.92	29.23	0.05	13.44	0.53	3.87	0.25	0.03	99.32	64.80	33.77	1.44
G25_RH1_03	C	50.00	51.06	30.14	0.03	14.35	0.52	3.40	0.21	0.04	99.75	69.15	29.65	1.20
G25_RH1_04	C	74.99	51.14	29.67	0.07	14.09	0.54	3.42	0.21	0.00	99.14	68.63	30.15	1.22
G25_RH1_05	C	99.99	52.91	28.83	0.06	12.93	0.58	3.88	0.29	0.04	99.52	63.71	34.59	1.70
G25_RH1_06	C	124.99	52.68	28.88	0.04	13.00	0.48	4.12	0.32	0.05	99.57	62.39	35.78	1.83
G25_RH1_07	M	149.99	52.92	28.77	0.06	12.92	0.51	4.12	0.28	0.03	99.61	62.39	36.00	1.61
G25_RH1_08	M	174.98	52.98	28.75	0.07	13.01	0.51	4.00	0.29	0.03	99.64	63.17	35.15	1.68
G25_RH1_09	M	199.98	52.51	28.84	0.04	12.93	0.53	4.31	0.26	0.04	99.46	61.46	37.07	1.47
G25_RH1_10	M	249.98	52.85	28.76	0.05	12.79	0.43	3.98	0.30	0.04	99.20	62.85	35.39	1.76
G25_RH1_11	M	274.97	52.75	28.75	0.04	12.93	0.49	3.99	0.29	0.00	99.24	63.09	35.23	1.68
G25_RH1_12	M	299.97	52.40	28.81	0.03	12.93	0.50	4.02	0.29	0.04	99.02	62.92	35.40	1.68
G25_RH1_13	M	324.97	52.90	28.85	0.03	12.88	0.52	4.12	0.28	0.05	99.63	62.32	36.07	1.61
G25_RH1_14	M	349.97	52.16	28.77	0.04	12.97	0.47	4.29	0.26	0.00	98.96	61.64	36.89	1.47
G25_RH1_15	M	374.97	53.43	28.67	0.03	12.89	0.52	4.05	0.24	0.04	99.87	62.86	35.74	1.39
G25_RH1_16	M	399.96	52.65	28.77	0.05	12.92	0.47	3.96	0.26	0.04	99.12	63.35	35.14	1.52
G25_RH1_17	M	424.96	51.62	27.39	0.08	12.31	0.46	4.52	0.27	0.04	96.69	59.15	39.30	1.54
G25_RH1_18	M	449.96	53.72	28.35	0.04	12.64	0.46	4.21	0.27	0.04	99.73	61.42	37.02	1.56
G25_RH1_19	M	474.96	53.35	28.86	0.03	12.76	0.48	4.21	0.28	0.00	99.97	61.61	36.78	1.61
G25_RH1_20	M	499.95	52.75	28.46	0.05	12.71	0.49	4.17	0.27	0.03	98.93	61.77	36.67	1.56
G25_RH1_21	M	524.95	52.67	28.50	0.04	12.76	0.53	4.29	0.25	0.00	99.04	61.28	37.29	1.43
G25_RH1_22	M	549.95	52.96	28.23	0.05	12.31	0.43	4.51	0.32	0.00	98.81	59.03	39.14	1.83
G25_RH1_23	M	574.95	53.17	28.22	0.03	12.49	0.48	4.22	0.29	0.03	98.93	61.01	37.30	1.69
G25_RH1_24	M	624.94	52.31	28.46	0.04	12.76	0.47	4.26	0.27	0.04	98.61	61.37	37.08	1.55
G25_RH1_25	M	674.94	51.32	29.41	0.00	13.94	0.54	3.55	0.23	0.03	99.02	67.55	31.13	1.33
G25_RH1_26	M	699.94	52.29	28.48	0.03	12.86	0.45	3.97	0.26	0.03	98.37	63.18	35.30	1.52
G25_RH1_27	M	724.93	52.14	29.05	0.04	13.48	0.48	3.72	0.23	0.04	99.18	65.80	32.86	1.34
G25_RH1_28	M	749.93	52.85	28.68	0.05	12.91	0.45	4.33	0.30	0.03	99.60	61.18	37.13	1.69
G25_RH1_29	M	774.93	52.69	28.54	0.05	13.01	0.52	4.01	0.27	0.04	99.13	63.19	35.25	1.56

Sample	Position	Distance (μm)	SiO_2	Al_2O_3	MgO	CaO	FeO	Na_2O	K_2O	TiO_2	Total	An	Ab	Or
G25_RH1_30	M	799.93	52.27	28.60	0.00	12.82	0.46	4.17	0.26	0.03	98.61	62.01	36.50	1.50
G25_RH1_31	M	824.92	52.68	28.69	0.03	12.96	0.50	4.02	0.25	0.00	99.13	63.12	35.43	1.45
G25_RH1_32	M	849.92	52.74	28.61	0.06	12.90	0.49	4.05	0.27	0.04	99.16	62.77	35.66	1.56
G25_RH1_33	M	874.92	52.02	28.53	0.00	12.80	0.46	4.28	0.29	0.05	98.43	61.27	37.08	1.65
G25_RH1_34	M	899.92	52.21	28.76	0.03	12.91	0.49	4.00	0.25	0.00	98.65	63.14	35.40	1.46
G25_RH1_35	R	924.92	52.52	28.75	0.05	12.93	0.51	4.14	0.28	0.03	99.21	62.30	36.10	1.61
G25_RH1_36	R	949.91	52.84	28.51	0.04	12.90	0.50	4.17	0.27	0.00	99.23	62.12	36.34	1.55
G25_RH1_37	R	974.91	52.46	28.65	0.04	12.96	0.50	4.11	0.22	0.03	98.97	62.73	36.00	1.27
G25_RH1_38	R	999.91	51.61	28.77	0.03	13.22	0.49	3.84	0.23	0.00	98.19	64.67	33.99	1.34
G25_RH1_39	R	1024.91	52.90	28.44	0.04	12.90	0.48	4.11	0.25	0.00	99.12	62.51	36.04	1.44
G25_RH1_40	R	1049.90	52.89	27.83	0.00	12.03	0.47	4.41	0.27	0.00	97.90	59.17	39.25	1.58
G25_RH1_41	R	1074.90	54.02	27.45	0.03	11.72	0.46	4.79	0.31	0.00	98.78	56.46	41.76	1.78
G25_RH2_01	C	0.00	54.60	26.90	0.05	11.22	0.53	4.82	0.34	0.06	98.52	55.14	42.87	1.99
G25_RH2_02	C	19.99	54.74	26.83	0.04	11.20	0.47	4.91	0.42	0.04	98.65	54.41	43.16	2.43
G25_RH2_03	C	39.97	54.53	26.89	0.05	11.16	0.51	5.03	0.37	0.05	98.59	53.91	43.97	2.13
G25_RH2_04	M	59.96	55.07	26.79	0.05	11.17	0.57	4.71	0.33	0.04	98.73	55.61	42.43	1.96
G25_RH2_05	M	79.95	54.55	27.09	0.03	11.10	0.53	5.01	0.39	0.04	98.74	53.80	43.95	2.25
G25_RH2_06	M	99.94	54.51	26.81	0.05	11.13	0.55	5.04	0.36	0.03	98.48	53.82	44.10	2.07
G25_RH2_07	M	119.93	54.84	26.79	0.05	11.09	0.53	5.11	0.40	0.04	98.85	53.28	44.43	2.29
G25_RH2_08	M	139.92	54.89	26.75	0.05	11.02	0.49	4.73	0.36	0.03	98.32	55.08	42.78	2.14
G25_RH2_09	M	159.90	54.25	26.95	0.04	11.22	0.51	5.04	0.33	0.04	98.38	54.12	43.99	1.90
G25_RH2_10	M	179.89	54.39	27.41	0.04	11.52	0.58	4.93	0.32	0.03	99.22	55.32	42.85	1.83
G25_RH2_11	M	199.88	54.26	27.24	0.04	11.40	0.58	4.89	0.34	0.04	98.79	55.20	42.84	1.96
G25_RH2_12	R	219.87	55.16	26.65	0.05	10.82	0.52	5.28	0.33	0.03	98.84	52.10	46.01	1.89
G25_RH2_13	R	239.86	55.52	26.67	0.04	10.45	0.53	5.29	0.39	0.03	98.92	51.01	46.73	2.27
G25_RH2_14	R	259.84	56.30	26.49	0.04	10.34	0.49	5.55	0.37	0.03	99.61	49.65	48.23	2.12
G20_1P_A_01	R	0	48.35	32.41	0.07	16.39	0.69	2.38	0.07	0.00	100.36	78.87	20.73	0.40
G20_1P_A_02	R	21.16	49.66	30.78	0.07	14.85	0.63	3.02	0.12	0.00	99.13	72.59	26.71	0.70
G20_1P_A_03	R	63.47	47.59	32.26	0.07	15.96	0.59	2.33	0.08	0.00	98.88	78.73	20.80	0.47
G20_1P_A_04	M	84.63	48.01	32.34	0.07	16.32	0.65	2.56	0.08	0.00	100.03	77.54	22.01	0.45
G20_1P_A_05	M	105.79	49.64	31.43	0.06	15.25	0.62	3.27	0.13	0.00	100.40	71.52	27.75	0.73
G20_1P_A_06	M	126.94	47.79	32.00	0.05	16.27	0.62	2.45	0.13	0.03	99.34	78.00	21.26	0.74
G20_1P_A_07	M	190.42	48.09	31.97	0.00	16.35	0.72	2.47	0.15	0.00	99.75	77.86	21.29	0.85
G20_1P_A_08	M	253.89	47.52	32.35	0.06	16.56	0.68	2.17	0.12	0.04	99.50	80.27	19.03	0.69
G20_1P_A_09	M	296.2	48.65	31.32	0.05	15.88	0.60	2.65	0.07	0.03	99.25	76.50	23.10	0.40
G20_1P_A_10	M	317.36	47.14	31.38	0.11	16.03	0.75	2.43	0.09	0.03	97.96	78.06	21.41	0.52
G20_1P_A_11	M	338.52	48.24	31.96	0.05	16.11	0.65	2.46	0.09	0.03	99.59	77.94	21.54	0.52
G20_1P_A_12	M	359.67	45.48	32.52	0.05	17.43	0.73	1.63	0.09	0.03	97.96	85.08	14.40	0.52
G20_1P_A_13	M	380.83	49.09	31.36	0.04	15.47	0.61	2.80	0.14	0.03	99.54	74.72	24.47	0.81

Sample	Position	Distance (μm)	SiO_2	Al_2O_3	MgO	CaO	FeO	Na_2O	K_2O	TiO_2	Total	An	Ab	Or
G20_1P_A_14	M	423.14	47.32	32.43	0.03	16.70	0.62	2.15	0.10	0.00	99.35	80.64	18.79	0.57
G20_1P_A_15	M	444.3	46.67	33.12	0.00	17.53	0.62	1.76	0.07	0.00	99.77	84.29	15.31	0.40
G20_1P_A_16	M	486.62	47.87	32.00	0.03	16.26	0.67	2.45	0.10	0.04	99.42	78.13	21.30	0.57
G20_1P_A_17	M	507.77	47.65	32.25	0.04	16.64	0.59	2.17	0.07	0.00	99.41	80.58	19.02	0.40
G20_1P_A_18	M	528.93	48.04	33.05	0.04	16.78	0.63	2.15	0.11	0.00	100.80	80.67	18.70	0.63
G20_1P_A_19	M	550.09	49.01	31.03	0.06	15.16	0.61	3.00	0.13	0.00	99.00	73.08	26.17	0.75
G20_1P_A_20	M	592.4	49.07	31.25	0.03	15.36	0.64	2.91	0.13	0.03	99.42	73.91	25.34	0.74
G20_1P_A_21	C	613.56	49.09	31.39	0.07	15.55	0.68	2.85	0.09	0.04	99.76	74.71	24.78	0.51
G20_1P_A_22	C	634.72	48.02	31.82	0.05	15.92	0.64	2.81	0.11	0.05	99.42	75.32	24.06	0.62
G20_1P_A_23	C	655.87	49.37	31.38	0.04	15.52	0.65	2.92	0.15	0.04	100.07	73.97	25.18	0.85
G20_1P_A_24	C	719.34	48.63	31.44	0.06	15.59	0.59	2.78	0.11	0.04	99.24	75.13	24.24	0.63
G20_1P_B_01	R	0	48.26	31.79	0.04	16.07	0.64	2.47	0.10	0.00	99.37	77.79	21.64	0.58
G20_1P_B_02	R	22.05	48.49	30.74	0.05	15.46	0.68	2.52	0.16	0.03	98.13	76.49	22.56	0.94
G20_1P_B_03	R	44.1	47.02	32.40	0.00	16.85	0.66	2.30	0.09	0.00	99.32	79.78	19.71	0.51
G20_1P_B_04	R	88.2	46.76	32.52	0.03	16.85	0.64	2.00	0.14	0.00	98.94	81.65	17.54	0.81
G20_1P_B_05	M	110.24	47.52	33.11	0.10	16.55	0.97	1.73	0.08	0.03	100.09	83.69	15.83	0.48
G20_1P_B_06	M	176.39	47.07	32.68	0.03	16.99	0.58	1.87	0.09	0.00	99.31	82.95	16.52	0.52
G20_1P_B_07	M	198.44	51.38	29.29	0.08	13.36	0.82	3.04	0.35	0.04	98.36	69.30	28.54	2.16
G20_1P_B_08	M	220.49	49.20	31.57	0.05	15.95	0.70	2.94	0.36	0.05	100.82	73.51	24.52	1.98
G20_1P_B_09	M	242.53	47.68	31.42	0.09	16.04	0.71	2.69	0.10	0.03	98.76	76.28	23.15	0.57
G20_1P_B_10	M	330.73	49.50	31.15	0.06	15.17	0.59	2.89	0.10	0.04	99.50	73.93	25.49	0.58
G20_1P_B_11	M	396.88	48.75	31.52	0.05	15.60	0.67	2.74	0.09	0.03	99.45	75.49	23.99	0.52
G20_1P_B_12	M	418.92	46.81	31.73	0.05	16.25	0.65	2.27	0.08	0.03	97.87	79.45	20.08	0.47
G20_1P_B_13	M	463.02	47.79	32.06	0.05	16.36	0.63	2.45	0.13	0.00	99.47	78.10	21.16	0.74
G20_1P_B_14	M	485.07	48.41	31.82	0.06	15.73	0.70	2.25	0.12	0.00	99.09	78.87	20.41	0.72
G20_1P_B_15	M	507.12	49.33	31.81	0.05	15.86	0.65	2.72	0.14	0.00	100.56	75.71	23.50	0.80
G20_1P_B_16	M	529.17	47.50	32.26	0.00	16.41	0.70	2.39	0.11	0.03	99.40	78.64	20.73	0.63
G20_1P_B_17	C	573.26	46.19	32.91	0.00	17.24	0.65	1.99	0.07	0.00	99.05	82.39	17.21	0.40
G20_1P_B_18	C	595.31	46.99	32.66	0.03	17.10	0.57	2.11	0.13	0.00	99.59	81.15	18.12	0.73
G20_2P_D_01	R	0	46.21	33.56	0.05	17.78	0.63	1.71	0.06	0.00	100.00	84.89	14.77	0.34
G20_2P_D_02	M	110.28	46.67	32.57	0.05	17.03	0.64	2.00	0.07	0.00	99.03	82.14	17.46	0.40
G20_2P_D_03	M	132.34	46.33	32.98	0.04	17.19	0.63	1.96	0.05	0.00	99.18	82.66	17.06	0.29
G20_2P_D_04	M	154.39	46.33	33.60	0.05	17.88	0.62	1.67	0.00	0.03	100.18	85.54	14.46	0.00
G20_2P_D_05	M	198.5	45.20	32.62	0.14	17.02	1.08	1.34	0.07	0.04	97.51	87.16	12.42	0.43
G20_2P_D_06	M	308.78	46.06	33.52	0.04	17.87	0.64	1.46	0.05	0.00	99.64	86.87	12.84	0.29
G20_2P_D_07	M	330.84	46.27	33.17	0.05	17.67	0.60	1.63	0.05	0.00	99.44	85.45	14.26	0.29
G20_2P_D_08	M	463.18	46.05	33.34	0.00	17.89	0.58	1.69	0.04	0.00	99.59	85.21	14.57	0.23
G20_2P_D_09	C	507.29	45.33	33.37	0.03	17.68	0.63	1.45	0.07	0.04	98.60	86.72	12.87	0.41
G20_2P_D_10	C	573.46	48.61	33.44	0.05	16.70	0.74	1.78	0.08	0.03	101.43	83.43	16.09	0.48

Sample	Position	Distance (μm)	SiO_2	Al_2O_3	MgO	CaO	FeO	Na_2O	K_2O	TiO_2	Total	An	Ab	Or
G20_4P_F(A-B)_01		0	52.14	29.04	0.07	12.85	0.71	4.19	0.21	0.04	99.25	62.13	36.66	1.21
G20_4P_F(A-B)_02		6.67	52.23	28.96	0.09	12.84	0.70	4.27	0.17	0.03	99.29	61.82	37.20	0.97
G20_4P_F(A-B)_03		13.34	53.58	27.66	0.06	11.63	0.70	4.82	0.26	0.04	98.75	56.29	42.21	1.50
G20_4P_F(A-B)_04		20.01	53.64	27.86	0.08	11.53	0.62	4.86	0.23	0.05	98.87	55.97	42.70	1.33
G20_4P_F(A-B)_05	M	26.68	52.85	28.27	0.17	12.06	0.83	4.55	0.23	0.04	99.00	58.64	40.03	1.33
G20_4P_F(A-B)_06	M	33.35	52.87	28.98	0.07	12.77	0.70	4.19	0.17	0.04	99.79	62.13	36.89	0.98
G20_4P_F(A-B)_07	M	40.02	52.50	28.87	0.09	12.73	0.74	4.20	0.22	0.05	99.40	61.82	36.91	1.27
G20_4P_F(A-B)_08	M	46.69	51.44	29.52	0.09	13.51	0.71	4.17	0.17	0.05	99.66	63.55	35.50	0.95
G20_4P_F(A-B)_09	M	53.36	51.41	29.30	0.33	13.21	0.84	3.87	0.18	0.05	99.19	64.67	34.28	1.05
G20_4P_F(A-B)_10	M	60.03	49.10	31.93	0.15	15.55	0.87	2.36	0.10	0.05	100.11	77.98	21.42	0.60
G20_4P_F(B-C)_01	M	22.22	47.72	31.80	0.06	16.50	0.67	2.21	0.11	0.03	99.10	79.98	19.39	0.63
G20_4P_F(B-C)_02	M	44.43	46.04	33.11	0.03	17.75	0.66	1.66	0.05	0.03	99.33	85.28	14.43	0.29
G20_4P_F(B-C)_03	M	66.65	58.25	24.67	0.18	8.42	1.11	6.38	0.86	0.07	99.94	40.12	55.01	4.88
G20_4P_F(B-C)_04	M	88.86	46.41	32.81	0.05	17.20	0.72	1.93	0.08	0.00	99.20	82.74	16.80	0.46
G20_4P_F(B-C)_05	C	111.08	47.95	32.06	0.06	16.27	0.67	2.44	0.12	0.00	99.57	78.11	21.20	0.69
G20_4P_F(B-C)_06	C	133.3	50.55	32.12	0.05	15.01	0.87	2.59	0.16	0.03	101.38	75.47	23.57	0.96
G20_4P_F(B-C)_07	C	199.96	53.17	28.53	0.08	12.13	0.73	4.57	0.38	0.05	99.64	58.17	39.66	2.17
G35_1P_A_01	C	25	45.52	32.74	0.03	18.69	0.58	1.44	0.05	0.00	99.05	87.52	12.20	0.28
G35_1P_A_02	C	49.99	46.60	32.53	0.03	18.33	0.61	1.56	0.08	0.03	99.78	86.25	13.30	0.46
G35_1P_A_03	C	74.99	47.24	32.25	0.03	17.88	0.61	1.66	0.06	0.03	99.76	85.29	14.36	0.35
G35_1P_A_04	C	99.99	47.22	32.00	0.04	17.80	0.62	1.72	0.05	0.03	99.49	84.83	14.88	0.29
G35_1P_A_05	C	124.98	46.75	32.33	0.00	18.01	0.54	1.64	0.04	0.00	99.32	85.63	14.14	0.23
G35_1P_A_06	C	174.98	45.97	32.83	0.03	18.50	0.56	1.39	0.07	0.00	99.35	87.69	11.90	0.40
G35_1P_A_07	C	199.97	46.44	32.56	0.03	18.03	0.56	1.51	0.06	0.03	99.22	86.53	13.12	0.35
G35_1P_A_08	C	224.97	46.17	33.09	0.00	18.65	0.57	1.35	0.04	0.00	99.88	88.24	11.53	0.23
G35_1P_A_09	M	274.96	45.26	32.84	0.00	18.82	0.57	1.13	0.05	0.03	98.70	89.92	9.79	0.29
G35_1P_A_10	M	299.96	47.12	32.09	0.03	17.75	0.68	1.85	0.09	0.03	99.64	83.72	15.77	0.52
G35_1P_A_11	M	324.96	46.89	32.42	0.05	17.96	0.59	1.57	0.06	0.00	99.55	86.03	13.62	0.35
G35_1P_A_12	M	349.95	47.42	31.83	0.04	17.55	0.59	1.81	0.05	0.00	99.29	84.06	15.65	0.29
G35_1P_A_13	M	399.95	46.70	32.52	0.05	18.00	0.56	1.60	0.03	0.03	99.50	85.98	13.85	0.17
G35_1P_A_14	M	424.94	46.22	32.77	0.03	18.35	0.55	1.36	0.03	0.00	99.31	88.04	11.78	0.17
G35_1P_A_15	M	449.94	45.48	32.87	0.00	18.67	0.57	1.22	0.07	0.00	98.89	89.02	10.57	0.41
G35_1P_A_16	M	474.94	46.21	32.66	0.00	18.53	0.70	1.42	0.05	0.00	99.57	87.58	12.13	0.29
G35_1P_A_17	M	499.93	48.35	31.50	0.04	17.00	0.61	2.30	0.09	0.03	99.92	79.95	19.54	0.51
G35_1P_A_18	M	524.93	46.61	32.68	0.04	18.47	0.65	1.37	0.06	0.04	99.93	87.88	11.77	0.35
G35_1P_A_19	M	549.93	46.19	32.73	0.00	18.52	0.71	1.21	0.04	0.04	99.45	89.18	10.58	0.23
G35_1P_A_20	M	574.92	45.82	32.94	0.00	18.73	0.60	1.27	0.05	0.00	99.41	88.85	10.86	0.29
G35_1P_A_21	M	599.92	45.94	32.62	0.00	18.41	0.61	1.30	0.05	0.00	98.93	88.44	11.27	0.29
G35_1P_A_22	M	624.92	47.37	31.98	0.03	17.54	0.57	1.93	0.07	0.00	99.50	83.07	16.53	0.40

Sample	Position	Distance (μm)	SiO_2	Al_2O_3	MgO	CaO	FeO	Na_2O	K_2O	TiO_2	Total	An	Ab	Or
G35_1P_A_23	M	649.91	46.35	32.68	0.04	18.07	0.60	1.48	0.03	0.00	99.26	86.94	12.88	0.18
G35_1P_A_24	M	674.91	46.91	32.61	0.03	17.89	0.66	1.61	0.05	0.00	99.77	85.73	13.98	0.29
G35_1P_A_25	M	699.91	47.62	31.88	0.04	17.36	0.58	1.84	0.07	0.03	99.42	83.58	16.01	0.41
G35_1P_A_26	M	724.9	46.25	33.05	0.00	18.55	0.57	1.20	0.04	0.00	99.67	89.28	10.49	0.23
G35_1P_A_27	M	749.9	47.33	32.11	0.00	17.46	0.65	2.08	0.11	0.00	99.75	81.74	17.64	0.63
G35_1P_A_28	M	774.89	46.67	32.72	0.00	18.23	0.64	1.34	0.06	0.00	99.65	87.97	11.68	0.35
G35_1P_A_29	M	799.89	47.77	31.71	0.00	17.45	0.68	1.87	0.09	0.00	99.57	83.34	16.14	0.52
G35_1P_A_30	R	824.89	46.36	32.76	0.03	18.26	0.69	1.51	0.08	0.03	99.72	86.58	12.96	0.46
G35_1P_A_31	R	849.89	48.04	32.44	0.04	17.50	0.74	1.86	0.08	0.04	100.75	83.50	16.04	0.46
G35_1P_A_32	R	874.88	47.11	32.28	0.03	17.85	0.61	1.63	0.05	0.00	99.56	85.55	14.16	0.29
G35_1P_A_33	R	924.88	50.52	29.66	0.07	14.70	0.64	3.38	0.13	0.04	99.14	70.09	29.16	0.75
G35_1P_A_34	R	949.87	51.38	29.73	0.06	14.79	0.66	3.41	0.16	0.04	100.23	69.92	29.16	0.92
G35_1P_A_35	R	974.87	50.17	30.61	0.05	15.61	0.79	2.91	0.11	0.04	100.29	74.31	25.05	0.64
G35_1P_A_36	R	999.87	49.15	30.64	0.04	15.86	0.81	2.69	0.15	0.03	99.37	75.82	23.31	0.87
G35_1P_B_01	C	0	45.71	32.12	0.03	18.39	0.60	1.45	0.00	0.00	98.31	87.52	12.48	0.00
G35_1P_B_02	C	25.06	46.02	32.15	0.04	18.19	0.65	1.55	0.07	0.04	98.72	86.28	13.32	0.40
G35_1P_B_03	M	50.12	46.14	32.14	0.08	18.37	0.62	1.50	0.08	0.00	98.94	86.72	12.82	0.46
G35_1P_B_04	M	75.18	46.44	32.03	0.06	18.08	0.59	1.67	0.04	0.03	98.94	85.45	14.32	0.23
G35_1P_B_05	M	100.24	46.66	31.62	0.03	17.62	0.67	1.90	0.07	0.00	98.57	83.34	16.25	0.40
G35_1P_B_06	M	125.3	48.49	30.86	0.05	16.31	0.70	2.66	0.14	0.03	99.25	76.57	22.63	0.80
G35_1P_B_07	R	150.36	49.98	29.31	0.05	14.96	0.83	3.41	0.20	0.05	98.80	70.00	28.86	1.14
G35_1P_C_01	C	0.00	46.27	33.03	0.03	18.70	0.61	1.23	0.06	0.00	99.94	89.02	10.63	0.35
G35_1P_C_02	C	50.03	47.62	32.24	0.04	17.54	0.62	1.90	0.06	0.00	100.03	83.34	16.32	0.35
G35_1P_C_03	M	100.06	47.83	32.32	0.06	17.54	0.73	1.97	0.08	0.00	100.54	82.73	16.81	0.46
G35_1P_C_04	M	150.09	52.13	29.35	0.09	14.36	0.67	3.73	0.16	0.05	100.55	67.37	31.71	0.91
G35_1P_C_05	M	200.12	52.43	28.97	0.10	13.84	0.70	3.91	0.26	0.06	100.26	65.23	33.34	1.43
G35_1P_C_06	M	250.14	48.11	32.25	0.06	17.40	0.62	1.92	0.09	0.00	100.45	82.93	16.55	0.52
G35_1P_C_07	R	300.17	47.97	32.18	0.04	17.45	0.71	1.93	0.08	0.00	100.36	82.95	16.59	0.46
G35_1P_C_08	R	350.20	52.30	29.54	0.04	14.34	0.79	3.68	0.21	0.05	100.95	67.46	31.34	1.20
G35_1P_D_01	C	0	45.90	33.44	0.00	19.06	0.56	1.00	0.00	0.00	99.96	91.33	8.67	0.00
G35_1P_D_02	C	170.64	47.91	33.59	0.03	18.02	0.61	1.52	0.08	0.00	101.77	86.36	13.18	0.47
G35_1P_D_03	M	255.96	45.74	33.54	0.00	19.07	0.44	1.13	0.00	0.00	99.92	90.30	9.70	0.00
G35_1P_D_04	M	298.62	46.15	33.03	0.00	18.88	0.64	1.22	0.04	0.00	99.97	89.29	10.48	0.23
G35_1P_D_05	M	341.28	44.76	32.99	0.03	18.75	0.66	0.92	0.04	0.00	98.16	91.64	8.12	0.24
G35_1P_D_06	M	383.93	45.55	32.88	0.04	18.52	0.60	1.36	0.05	0.00	99.01	88.04	11.67	0.29
G35_1P_D_07	M	426.59	46.72	32.17	0.04	18.03	0.59	1.63	0.08	0.00	99.27	85.52	14.01	0.46
G35_1P_D_08	M	469.25	46.73	32.21	0.06	17.89	0.69	1.77	0.07	0.03	99.45	84.51	15.09	0.40
G35_1P_D_09	M	511.91	46.41	32.12	0.06	17.81	0.72	1.66	0.04	0.00	98.83	85.34	14.43	0.23
G35_1P_D_10	M	554.57	46.52	32.33	0.04	18.00	0.76	1.67	0.06	0.00	99.38	85.30	14.35	0.35

Sample	Position	Distance (μm)	SiO_2	Al_2O_3	MgO	CaO	FeO	Na_2O	K_2O	TiO_2	Total	An	Ab	Or
G35_1P_D_11	M	597.23	47.46	31.53	0.04	17.45	0.76	1.90	0.23	0.00	99.37	82.45	16.23	1.32
G35_1P_D_12	R	639.89	46.62	32.51	0.05	18.33	0.79	1.61	0.05	0.03	99.99	86.02	13.69	0.29
G35_1P_D_13	R	682.55	49.38	30.04	0.10	15.46	0.77	2.87	0.14	0.05	98.81	74.26	24.92	0.82
G35_1P_E_01	C	55.56	56.63	25.76	0.07	10.04	0.81	5.53	1.12	0.10	100.07	46.95	46.80	6.25
G35_1P_E_02	M	111.12	47.36	31.80	0.06	17.55	0.71	1.93	0.08	0.04	99.54	83.03	16.51	0.46
G35_1P_E_03	M	166.68	52.20	28.83	0.10	13.70	0.76	4.05	0.18	0.07	99.89	64.48	34.49	1.03
G35_1P_E_04	M	222.23	51.33	29.23	0.08	14.31	0.80	3.56	0.14	0.04	99.49	68.38	30.80	0.81
G35_1P_E_05	M	277.79	50.08	30.00	0.08	15.05	0.77	3.13	0.13	0.06	99.31	72.09	27.15	0.76
G35_1P_E_06	R	333.35	51.84	29.10	0.08	14.03	0.86	3.83	0.20	0.07	100.01	66.19	32.67	1.15
G35_1P_E_07	R	388.91	56.37	25.72	0.05	10.00	1.02	5.78	0.47	0.09	99.50	47.60	49.74	2.66
G35_4P_C_01	C	0	45.78	32.12	0.00	18.03	0.64	1.48	0.07	0.04	98.17	86.71	12.88	0.41
G35_4P_C_02	C	53.77	46.29	31.39	0.05	17.49	0.69	1.65	0.08	0.12	97.77	84.98	14.54	0.47
G35_4P_C_03	C	107.54	46.18	32.42	0.00	18.67	0.60	1.44	0.05	0.00	99.36	87.51	12.21	0.28
G35_4P_C_04	C	161.31	45.71	32.28	0.06	18.21	0.58	1.52	0.07	0.03	98.46	86.52	13.08	0.40
G35_4P_C_05	C	215.07	45.70	32.53	0.05	18.34	0.53	1.38	0.05	0.03	98.61	87.78	11.93	0.29
G35_4P_C_06	M	268.84	46.36	32.15	0.06	18.05	0.61	1.74	0.09	0.03	99.09	84.75	14.74	0.51
G35_4P_C_07	M	322.61	45.15	32.80	0.03	18.50	0.59	1.28	0.05	0.04	98.43	88.64	11.07	0.29
G35_4P_C_08	M	376.38	45.64	32.73	0.04	18.61	0.53	1.38	0.04	0.03	99.00	87.98	11.79	0.23
G35_4P_C_09	M	430.15	45.80	32.88	0.04	18.72	0.65	1.25	0.03	0.00	99.37	89.10	10.73	0.17
G35_4P_C_10	M	483.92	45.61	32.69	0.05	18.62	0.61	1.16	0.05	0.00	98.80	89.58	10.13	0.29
G35_4P_C_11	M	537.68	46.94	31.02	0.04	17.13	0.69	1.93	0.09	0.04	97.89	82.63	16.84	0.53
G35_4P_C_12	M	591.45	48.02	31.36	0.07	17.07	0.73	2.11	0.06	0.03	99.46	81.42	18.23	0.35
G35_4P_C_13	M	645.22	48.49	31.08	0.08	16.45	0.67	2.48	0.10	0.03	99.38	78.11	21.31	0.58
G35_4P_C_14	M	698.99	49.97	30.41	0.09	15.72	0.63	2.91	0.11	0.05	99.90	74.45	24.92	0.63
G35_4P_C_15	R	752.76	50.29	30.23	0.08	15.47	0.62	3.22	0.12	0.04	100.09	72.12	27.20	0.68
G35_4P_C_16	R	860.3	50.75	29.57	0.08	14.91	0.66	3.32	0.14	0.05	99.49	70.72	28.47	0.81
G35_4P_C_17	R	914.06	51.26	29.51	0.09	14.32	0.67	3.70	0.14	0.06	99.76	67.56	31.63	0.80
G35_4P_C_18	R	967.83	51.80	28.80	0.11	13.89	0.78	3.82	0.21	0.07	99.48	65.98	32.81	1.21
G35_4P_C_19	R	1021.6	61.63	23.47	0.04	6.33	0.62	7.58	1.10	0.10	100.87	29.62	64.24	6.14

Table B1.2. Orthopyroxene major element compositions obtained by electron microprobe, expressed in %. Values below detection limit are shown as “<dl”. Data from Gede Volcano (Indonesia).

Sample	SiO_2	TiO_2	Al_2O_3	FeO	MnO	MgO	CaO	Na_2O	TOTAL
G25_2O_B_01	55.61	0.25	1.51	19.4	0.63	20.75	1.36	<dl	99.51
G25_2O_B_02	52.64	0.19	0.97	19.4	0.7	25.11	1.41	<dl	100.42
G25_2O_B_03	51.83	0.24	1.31	19.94	0.67	24.55	1.44	<dl	99.98
G25_2O_B_04	52.14	0.23	1.02	19.36	0.78	25.1	1.52	<dl	100.15
G25_2O_B_05	51.35	0.36	2.19	19.02	0.64	24.88	1.59	<dl	100.03
G25_2O_B_06	52.43	0.28	1.76	18.33	0.6	25.68	1.52	<dl	100.6
G25_4C_E_01	52.2	0.57	2.84	20.53	0.9	23.83	1.63	<dl	102.5
G25_4C_E_02	51.29	0.51	1.6	19.54	0.75	23.95	1.62	0.07	99.33
G25_4C_E_03	50.93	0.44	1.68	20.74	0.8	23.44	1.68	<dl	99.71
G25_4C_E_04	49.25	0.44	1.63	19.07	0.7	24.82	1.48	<dl	97.39
G25_4C_E_05	51.11	0.56	2.57	20.99	0.86	23.76	1.57	<dl	101.42
G25_4C_E_06	51.45	0.37	1.73	19.81	0.75	24.86	1.56	<dl	100.53
G25_4C_E_07	51.78	0.4	1.79	14.37	0.6	17.31	17.33	0.09	103.67
G25_2C_B_01	54.58	0.21	1.98	10.87	0.25	29.73	1.76	0.03	100.46
G25_2C_B_02	52.62	0.23	0.77	19.09	0.65	25.66	1.6	<dl	100.62
G25_2C_B_03	52.48	0.24	1.21	18.85	0.6	25.71	1.48	0.07	100.64
G25_2C_B_04	52.64	0.18	0.74	18.21	0.61	26.31	1.5	<dl	100.19
G25_2C_B_05	53.05	0.18	0.86	17.94	0.61	26.42	1.53	<dl	100.59
G25_2C_B_06	52.99	0.22	0.7	17.73	0.59	26.38	1.59	<dl	100.2
G25_2C_B_07	51.74	0.25	1.39	18.17	0.66	25.83	1.43	<dl	99.47
G25_2C_B_08	53.08	0.2	0.8	18.16	0.62	26.14	1.52	0.06	100.58
G25_2C_B_09	52.67	0.21	0.7	18.9	0.67	25.57	1.49	<dl	100.21
G25_2C_B_10	51.78	0.2	0.78	19.97	0.72	24.72	1.42	<dl	99.59
G25_2C_B_11	51.74	0.19	0.77	20.49	0.79	24.59	1.43	<dl	100
G25_2C_B_12	51.36	0.24	1.01	20.08	0.77	24.36	1.42	<dl	99.24
G25_2C_B_13	52.1	0.19	0.95	19.1	0.72	25.35	1.63	<dl	100.04
G25_2C_B_14	52.46	0.18	0.77	17.68	0.65	26.35	1.44	<dl	99.53
G25_2C_B_15	48.22	0.18	0.42	21.32	0.92	24.38	1.58	0.11	97.13
G25_OPX_H_01	54.42	0.24	2.05	10.94	0.21	29.16	1.69	0.03	100.46
G25_OPX_H_02	53.1	0.22	1.05	18.46	0.67	24.24	1.39	<dl	99.13
G25_OPX_H_03	52.61	0.25	1.32	18.49	0.69	23.83	1.39	0.07	98.65
G25_OPX_H_04	52.84	0.25	1.19	18.5	0.67	23.9	1.4	<dl	98.75
G25_OPX_H_05	52.88	0.24	1.16	18.49	0.7	24.75	1.49	<dl	99.71
G25_OPX_H_06	52.26	0.25	1.3	18.37	0.7	24.03	1.39	0.08	98.38
G25_OPX_H_07	53.21	0.2	1.04	18.49	0.63	24.25	1.37	<dl	99.19
G25_OPX_H_08	53.23	0.26	1.34	18.2	0.65	23.95	1.4	<dl	99.03
G25_OPX_H_09	48.29	0.23	1.15	17.79	0.65	24.15	1.3	<dl	93.56

Table B1.3. Clinopyroxene major element compositions obtained by electron microprobe, expressed in %. Values below detection limit are shown as "<dl". Data from Gede Volcano (West Java, Indonesia).

Sample	SiO_2	TiO_2	Al_2O_3	Cr_2O_3	Fe_2O_3	FeO	NiO	MnO	MgO	CaO	Na_2O	TOTAL
201C1py	52.51	0.70	3.13	0.00	0.00	9.82	<dl	0.41	13.49	19.44	0.36	99.87
201C2py	53.94	0.60	2.77	0.00	0.00	9.64	<dl	0.41	13.73	19.39	0.37	100.84
233Cpy2	51.70	0.63	2.71	0.00	0.00	7.49	<dl	0.34	14.12	19.27	0.28	96.55
233Cpy1	53.23	0.48	2.11	0.00	0.00	7.03	<dl	0.32	14.91	19.25	0.26	97.60
23DBpy1	51.89	0.66	2.96	0.00	0.00	7.78	<dl	0.35	14.22	20.20	0.29	98.36
23DApy2	47.73	0.61	2.70	0.00	0.00	6.95	<dl	0.31	13.17	18.72	0.27	90.47
233C3py	54.17	0.51	2.86	0.00	0.00	7.19	<dl	0.34	15.14	19.00	0.37	99.57
233C4py	54.69	0.48	1.89	0.00	0.91	7.40	<dl	0.39	14.99	19.33	0.28	100.36
23DB2py	56.04	0.76	3.64	0.00	0.00	8.22	<dl	0.36	15.44	20.22	0.30	104.98
35C4py	51.64	0.64	3.22	0.00	0.00	8.32	<dl	0.31	14.83	19.40	0.37	98.73
35C5py	51.68	0.59	2.47	0.00	0.00	8.31	<dl	0.32	15.05	19.43	0.29	98.15
35C6py	48.32	0.88	4.06	0.00	0.00	8.10	<dl	0.27	13.57	19.43	0.37	95.01
35C7py	53.51	0.72	3.28	0.00	0.00	9.39	<dl	0.36	15.40	19.37	0.37	102.39
355C5py	51.45	0.80	3.58	0.02	0.00	7.44	<dl	0.25	13.29	19.07	0.39	96.29
355C3py	50.44	0.63	3.62	0.01	0.00	6.46	<dl	0.22	14.32	19.28	0.29	95.28

Table B1.4. Olivine major element compositions obtained by electron microprobe, expressed in %. Data from Gede Volcano (West Java, Indonesia).

Sample	SiO_2	TiO_2	Al_2O_3	Cr_2O_3	FeO	MnO	MgO	NiO	CaO	TOTAL	Fo
G35_OL_4C_C_1	51.25	0.66	2.38	0	9.81	0.34	15.4	0	19.57	99.41	73.001
G35_OL_4C_C_2	36.87	0	0.03	0	29.07	0.69	32.47	0	0.24	99.37	66.040
G35_OL_4C_C_3	50.71	0.94	3.48	0	9.69	0.32	14.46	0	20.22	99.82	72.023
G35_OL_4C_C_4	35.45	0.03	0.04	0	36.7	0.86	25.65	0	0.26	98.99	54.898
G35_OL_4C_A_1	37.3	0	0	0	30.43	0.7	31.92	0	0.23	100.58	64.634
G35_OL_4C_A_2	37.51	0	0.03	0	28.55	0.66	33.49	0	0.2	100.44	67.143
G35_OL_4C_A_3	37.39	0	0.03	0	30.03	0.68	32.59	0	0.2	100.92	65.416
G35_OL_4C_B_1	50.66	0.69	2.51	0	9.11	0.32	15.4	0	20.41	99.1	74.427
G35_OL_4C_B_2	48.72	1.18	4.64	0	10.22	0.28	13.77	0	20.26	99.07	70.036
G35_OL_4C_B_3	50.97	0.77	1.67	0	12.1	0.54	15.57	0	17.34	98.96	68.701
G35_OL_4C_B_4	34.9	0.03	0.05	0	33.49	0.81	28.73	0	0.28	98.29	59.886

Table B2.Trace element composition of plagioclase from Gede volcano, expressed in ppm. Values below detection limit are presented as “<dl”. Data obtained by LA-ICP-MS.

Sample	Li	Be	B	Na	Mg	Al	Si	P	K	Ca	Sc	Ti	V	Cr	Mn	Fe	Co
234B1	7.28	0.304	18.3	13200	1670	161000	211000	101	1330	111000	2.84	613	15.2	<dl	161	7200	2.46
234B2	4.93	0.232	5.00	10900	385	165000	212000	30.7	357	111000	0.977	157	5.08	0.720	55.0	4150	0.534
233A2	17.1	0.101	7.25	17700	519	170000	250000	63.4	737	105000	1.12	188	3.70	<dl	65.4	4810	0.768
236P3	23.6	0.370	8.86	15000	845	192000	265000	95.3	1160	122000	1.83	324	6.45	<dl	145	6100	1.41
233C2	3.80	0.061	5.07	2100	85200	14300	242000	31.6	2.25	137000	166	3760	328	10.1	2610	58200	43.6
233C1	3.57	0.069	5.00	1900	89900	11200	249000	23.3	3.14	137000	135	2860	272	21.4	2500	54700	42.7
23DB1	4.49	0.190	5.62	2170	85800	15700	242000	36.9	6.59	144000	172	3950	341	13.0	2690	60500	43.6
23DA2	3.35	0.132	4.77	1980	79500	14300	223000	32.7	4.20	133000	172	3670	335	6.52	2380	54000	37.5
231B2	13.3	1.040	6.08	17600	654	172000	233000	46.6	846	114000	1.11	206	3.16	<dl	68.3	4840	0.774
351A2	16.5	<dl	5.83	11800	1260	176000	217000	42.6	925	123000	3.19	752	34.5	10.5	142	8160	1.66
351A3	5.81	<dl	5.55	11500	397	179000	224000	29.2	571	123000	0.993	176	3.84	<dl	79.3	4210	0.347
351C2	7.29	0.220	7.09	18700	452	176000	245000	124	1210	114000	1.05	219	2.56	0.620	69.6	5120	0.411
351D2	4.14	<dl	11.9	8410	331	169000	184000	26.7	758	118000	0.805	138	2.34	1.02	59.9	3960	0.449
354C1	15.1	0.450	12.2	36100	835	253000	370000	55.8	2270	153000	1.48	458	4.09	0.990	107	7370	0.780
354C3	5.74	0.340	9.83	13400	1270	179000	246000	99.2	1400	115000	2.71	540	15.9	0.710	176	8590	1.24
355C1	22.7	0.214	6.40	3060	88900	22900	254000	54.4	146	153000	248	5680	569	24.3	2270	67900	43.1
25H2	22.7	0.092	3.42	1030	52700	4990	143000	231	60.5	81500	71.6	1230	102	1.40	1970	37000	26.0
25H3	24.9	<dl	4.80	186	124000	5800	236000	168	4.31	9080	42.4	1160	79.2	7.65	4340	113000	88.9
25R1B	14.7	0.790	5.94	30300	307	160000	259000	60.3	2610	90100	0.812	209	1.06	<dl	50.3	3740	0.419
25R1C	13.8	0.660	5.83	29900	319	161000	253000	60.5	2630	90100	0.773	218	1.14	<dl	50.6	3760	0.402
25R1M	14.8	0.820	5.62	29900	291	160000	251000	55.0	2450	90100	0.712	198	0.888	0.490	47.7	3620	0.375
25R2C	15.7	0.790	5.92	34600	295	150000	253000	63.4	3030	78600	0.739	203	0.952	<dl	39.9	3780	0.373
25R2M	16.7	1.010	6.34	35900	315	153000	257000	65.2	3150	78600	0.807	211	1.00	0.540	38.7	3850	0.565
256C1	11.0	0.082	2.79	1050	53800	8540	141000	30.4	58.6	81500	77.1	1680	158	39.5	1420	35000	27.3
35C1	28.8	0.089	4.61	2370	77300	24400	212000	18.3	14.2	136000	156	4570	444	225	1470	50800	35.2
35C2	13.1	0.444	7.23	38500	934	234000	358000	46.6	2340	136000	1.39	389	3.97	<dl	63.2	6310	0.633

Sample	Li	Be	B	Na	Mg	Al	Si	P	K	Ca	Sc	Ti	V	Cr	Mn	Fe	Co
35C3	16.8	0.104	4.23	2370	82100	20200	220000	19.5	1.67	136000	148	3610	407	81.8	1580	51200	37.5
35C4	27.4	0.090	5.59	2900	90300	17200	245000	35.5	202	136000	182	3870	426	22.9	2400	65200	43.1
35C5	31.4	0.084	4.36	2250	91600	13100	245000	26.3	1.52	136000	192	3570	404	17.0	2500	65600	43.6
35C6	32.0	0.125	4.79	2760	82500	21600	228000	25.6	34.1	136000	209	5280	519	25.9	2120	63200	39.7
35C7	33.1	0.110	5.04	2780	93200	17500	251000	28.9	28.2	136000	207	4370	485	14.9	2750	72900	45.7
35C8	15.1	0.053	4.73	2700	79600	24400	221000	24.3	0.770	136000	191	5170	507	26.0	1870	58800	38.0
35C9	1090	3.020	542	5050	<dl	20300	<dl	6740	549	136000	1300	7570	1180	197	419000	<dl	19800
25R1	11.4	0.910	37.2	30600	291	155000	253000	63.8	1880	90100	0.828	198	0.784	<dl	45.2	3450	0.346
25R2R	17.3	2.500	42.4	43900	402	163000	292000	62.0	3700	78600	0.923	152	0.668	<dl	56.3	3500	0.461
25H1	3.66	0.133	2.83	1100	51200	6110	140000	16.5	4.67	81500	70.0	1600	137	3.77	1540	31100	24.2
25CF	24.9	0.126	28.2	1700	51100	9270	151000	90.6	832	81500	82.4	2220	173	5.63	1740	35100	24.6
234B3	6.82	<dl	65.4	14500	616	169000	221000	46.8	496	111000	1.03	186	2.67	1.53	52.2	4750	0.805
233B	10.3	<dl	8.41	13700	551	183000	228000	24.0	429	111000	0.810	186	1.98	3.11	53.9	4400	0.574
233A1	11.0	0.530	27.8	12600	685	162000	207000	43.9	514	105000	0.878	201	4.14	<dl	60.5	4620	0.652
231B1	3.18	0.490	8.09	5870	209	182000	188000	30.9	210	114000	0.558	93.8	1.15	<dl	53.1	2680	0.305
235P4	6.86	0.580	9.44	15000	876	187000	213000	77.6	838	117000	1.31	410	8.11	<dl	105	5150	1.47
236P1	13.2	<dl	12.1	11500	513	197000	212000	62.0	401	122000	0.730	145	1.47	<dl	59.8	4190	0.505
236P2	50.9	0.520	27.0	15500	1370	192000	252000	97.4	1350	122000	2.39	636	12.7	4.52	144	7500	1.60
23R31	6.54	<dl	51.4	14400	902	189000	227000	70.2	472	114000	0.490	183	4.11	<dl	66.9	5810	1.64
23R32	11.1	<dl	8.04	9160	347	182000	208000	31.5	264	114000	0.657	101	1.59	2.18	58.2	3930	0.409
233C3	4.22	0.170	8.54	2720	91300	15100	253000	53.5	409	137000	127	3060	276	9.08	2610	55900	42.8
233C4	4.26	<dl	56.9	2090	90400	9990	256000	32.6	27.8	137000	121	2860	280	4.33	2990	63900	49.5
23DB2	2.95	<dl	52.9	2240	93100	19200	262000	42.0	51.0	144000	194	4570	419	10.1	2810	63900	41.7
23DA1	2.93	0.223	37.6	2050	84200	15400	236000	42.9	31.1	133000	172	3860	352	6.66	2600	58100	40.5
355C2	5.72	<dl	4.23	1980	84000	18600	228000	22.5	11.7	136000	159	3880	405	68.6	1580	46900	35.3

Sample	Li	Be	B	Na	Mg	Al	Si	P	K	Ca	Sc	Ti	V	Cr	Mn	Fe	Co
355C3	5.15	<dl	3.83	2120	86400	19200	236000	19.0	10.1	136000	147	3760	418	61.2	1700	50300	37.3
202D2	7.32	<dl	8.31	10500	310	196000	209000	53.9	405	119000	0.563	122	0.938	5.27	62.2	4140	0.311
201B1	12.7	<dl	17.1	21900	1180	214000	267000	118	1250	123000	1.70	512	8.92	5.15	126	7910	1.24
201B2	6.75	<dl	9.35	10300	335	195000	225000	98.0	359	123000	0.640	170	2.56	3.54	56.5	3980	0.280
355C4	9.63	0.078	4.77	2180	77400	20400	220000	22.8	4.77	136000	146	3900	392	91.7	1460	45900	34.6
355C5	15.0	0.156	32.5	2930	80200	18900	240000	239	781	136000	190	4800	454	94.5	1940	57800	37.6
201C1	22.6	0.245	6.69	2660	81400	16600	245000	35.8	1.80	139000	137	4220	350	13.1	3160	76400	47.8
201C2	5.82	0.295	6.46	2720	82800	14600	252000	39.9	1.51	139000	140	3580	319	15.4	3170	74900	49.1
201A1	9.64	0.580	5.02	17700	406	169000	236000	56.4	783	111000	0.533	153	1.36	<dl	59.3	4360	0.248
201A2	11.0	0.570	5.92	20200	573	175000	256000	62.2	1130	111000	0.737	222	2.83	<dl	80.4	5210	0.463
202D1	9.52	0.260	6.95	16000	529	184000	262000	54.8	872	119000	0.685	142	1.74	<dl	80.2	5100	0.360
204C1	11.6	<dl	3.35	1230	53500	10300	149000	14.6	0.930	87900	71.4	2260	148	18.7	1430	34100	23.3
204C2	12.8	<dl	5.19	190	153000	8200	281000	23.2	<0.52	10400	41.0	1460	83.1	6.84	4200	113000	90.0
204C3	7.80	<dl	4.70	193	124000	6520	226000	18.6	0.810	10400	33.5	1270	70.0	5.26	3290	88500	69.7
204C4	2.41	0.103	3.77	1280	55700	7790	160000	25.7	1.09	87900	82.5	3380	212	7.94	1880	49800	30.3
235P1	3.00	<dl	6.15	9620	357	170000	223000	43.9	438	117000	0.600	138	2.73	0.700	67.4	3930	0.429
235P2	4.58	0.290	10.9	14400	1730	181000	247000	84.7	1400	117000	2.08	517	13.6	<dl	180	8840	1.65
233BC	3.37	<dl	6.78	11500	488	169000	230000	39.8	447	111000	0.782	147	2.59	<dl	62.6	4610	0.495
351BC	5.71	0.187	6.70	11500	350	169000	220000	75.9	567	114000	0.705	173	2.84	<dl	64.9	4140	0.217
1PA1	13.4	0.600	5.54	24800	420	196000	293000	59.7	1110	118000	1.31	163	1.02	<dl	66.8	4570	0.493
1CA1	10.5	0.215	3.91	2410	90800	13900	249000	29.3	3.41	143000	122	3190	257	5.82	2610	64100	44.4
2CB1	12.0	<dl	3.12	173	142000	4460	255000	309	29.3	10700	36.4	1120	63.8	2.95	5130	128000	87.2
2CB2	24.9	<dl	3.41	205	153000	9070	285000	57.6	41.2	10700	61.0	1730	130	12.0	4720	131000	96.4
2OP1	64.8	0.173	2.85	207	144000	6910	265000	30.3	15.3	10000	49.9	1440	96.4	6.09	4830	131000	93.8
4PH1	7.99	0.231	2.82	10900	235	172000	227000	32.1	398	114000	0.804	92.8	1.22	<dl	62.1	3650	0.287
4PG1	19.3	1.290	5.50	39100	332	179000	309000	81.7	2760	96500	1.09	259	1.06	<dl	45.7	4190	0.383

Sample	Li	Be	B	Na	Mg	Al	Si	P	K	Ca	Sc	Ti	V	Cr	Mn	Fe	Co
4PG2	9.79	0.627	3.97	17900	202	155000	221000	78.7	961	96500	0.784	147	0.561	0.440	48.4	3410	0.225
4PG3	19.2	1.070	5.47	39900	286	181000	313000	70.5	2790	96500	1.16	233	0.948	0.400	44.9	3900	<0.161
1PA2	10.7	0.460	3.52	20000	377	183000	256000	52.5	974	118000	1.01	168	1.09	<dl	61.5	4190	0.445
1PA3	11.2	0.280	2.79	20000	378	184000	252000	41.0	893	118000	1.05	163	1.48	<dl	62.0	4220	0.408
4PH2	9.26	<dl	2.14	15000	287	176000	231000	36.0	633	114000	1.06	125	1.43	<dl	55.9	3590	0.243
4PH3	15.0	0.710	3.43	22700	412	188000	252000	60.5	1040	114000	0.845	169	1.48	<dl	56.0	4270	0.453
4PI1	12.8	0.910	2.33	26100	393	161000	237000	52.4	1400	92900	0.839	181	0.909	<dl	52.8	3740	0.517
6PL1	14.0	1.470	3.87	26400	411	165000	244000	66.1	1260	96500	0.870	157	0.399	1.43	46.6	3590	0.337
6PL2	4.48	0.280	3.29	8360	171	143000	167000	9.12	288	96500	0.576	87.5	0.769	<dl	46.2	2480	0.093

Sample	Ni	Cu	Zn	Ga	Rb	Sr	Y	Zr	Nb	Cs	Ba	La	Ce	Pr	Nd	Sm	Eu
234B1	0.335	10.1	12.8	24.8	4.78	566	2.76	11.1	0.492	0.321	48.9	3.18	7.33	0.803	3.30	0.584	0.581
234B2	0.126	2.79	3.54	20.8	0.198	520	0.242	0.463	0.023	0.014	22.6	0.899	1.52	0.176	0.680	0.108	0.280
233A2	0.222	7.61	5.66	28.4	0.677	594	0.385	0.747	0.062	<dl	38.4	1.57	2.79	0.346	1.11	0.280	0.513
236P3	<dl	47.8	6.68	28.5	4.17	612	1.13	4.96	0.283	0.203	47.6	2.55	5.04	0.607	1.90	0.150	0.649
233C2	11.0	2.13	65.6	6.88	0.128	16.1	32.3	26.5	0.033	<dl	0.067	1.73	7.57	1.71	10.5	4.17	1.17
233C1	12.0	1.96	60.1	5.19	0.017	16.8	20.4	14.6	0.018	<dl	0.058	1.00	4.65	1.05	6.55	2.54	0.790
23DB1	11.1	2.68	73.3	7.10	0.015	21.0	34.1	29.0	0.035	<dl	0.179	1.85	8.15	1.85	11.5	4.49	1.25
23DA2	8.63	2.00	58.5	6.53	0.125	21.8	29.6	24.4	0.029	<dl	0.118	1.54	7.02	1.58	9.81	3.99	1.11
231B2	0.149	16.3	7.90	25.8	0.646	633	0.475	1.20	0.055	0.052	38.0	1.52	2.57	0.300	1.07	0.188	0.597
351A2	2.32	85.4	20.9	23.5	1.83	471	1.14	2.94	0.140	0.066	34.7	1.23	2.35	0.279	1.20	0.334	0.437
351A3	0.113	19.8	7.74	23.3	0.440	460	0.348	0.518	0.024	0.029	20.4	0.708	1.50	0.146	0.614	0.087	0.289
351C2	0.108	13.7	6.04	28.8	0.738	508	0.743	1.26	0.062	0.032	43.0	1.44	2.86	0.367	1.35	0.400	0.635
351D2	0.405	36.7	216	22.6	0.360	462	0.381	0.408	0.029	0.079	21.2	0.957	4.97	0.191	0.720	0.091	0.289

Sample	Ni	Cu	Zn	Ga	Rb	Sr	Y	Zr	Nb	Cs	Ba	La	Ce	Pr	Nd	Sm	Eu
354C1	<dl	15.9	9.95	42.0	0.940	741	0.545	0.603	0.023	0.036	68.5	1.74	3.03	0.331	1.26	0.230	0.742
354C3	0.126	36.7	9.10	26.2	2.58	456	2.32	6.27	0.162	0.103	35.4	2.02	4.43	0.548	2.19	0.382	0.510
355C1	13.8	15.8	60.8	10.9	0.786	20.0	34.8	31.7	0.114	<dl	1.07	2.37	8.85	1.69	11.4	4.61	1.38
25H2	4.64	2.34	53.8	2.92	0.195	8.73	24.6	16.1	0.023	0.024	1.24	2.50	8.87	1.69	9.90	3.70	0.778
25H3	19.1	1.57	253	3.98	0.017	<dl	5.95	2.64	0.005	<dl	0.059	0.241	0.676	0.104	0.612	0.263	0.075
25R1B	0.047	2.56	7.07	30.2	0.773	561	0.517	0.044	<dl	<dl	95.3	2.91	5.05	0.530	2.07	0.302	0.904
25R1C	0.069	2.13	6.90	28.7	0.720	565	0.476	0.027	0.003	<dl	91.0	2.84	4.83	0.521	1.97	0.343	0.897
25R1M	1.14	2.24	6.89	29.5	0.702	570	0.550	0.032	0.109	<dl	101	3.23	5.49	0.585	2.33	0.357	0.933
25R2C	2.43	2.54	8.15	32.0	0.912	525	0.508	0.033	<dl	<dl	123	3.83	6.24	0.625	2.58	0.351	1.08
25R2M	0.635	2.93	9.42	33.1	1.15	537	0.520	0.398	0.006	0.011	130	3.83	6.23	0.649	2.34	0.344	1.12
256C1	11.6	3.09	38.3	3.80	0.233	9.86	15.7	15.2	0.030	0.014	0.849	1.02	4.25	0.872	5.57	2.22	0.627
35C1	70.0	11.7	36.6	8.65	0.009	17.3	17.4	16.4	0.041	<dl	0.015	0.798	3.54	0.751	5.26	2.29	0.844
35C2	0.196	8.89	7.58	39.2	0.745	707	0.331	0.036	<dl	0.091	58.6	1.43	2.43	0.251	1.14	0.189	0.582
35C3	19.6	12.6	38.9	7.32	0.017	16.8	15.5	13.3	0.013	0.005	0.071	0.674	3.03	0.671	4.52	2.09	0.721
35C4	14.0	33.8	63.6	7.79	0.858	18.0	22.0	17.0	0.079	0.076	3.31	1.15	4.44	0.897	5.94	2.60	0.871
35C5	12.6	14.7	66.2	6.35	0.006	15.2	21.5	15.1	0.014	<dl	<dl	0.898	4.06	0.872	5.85	2.66	0.875
35C6	12.6	17.3	55.7	9.66	0.136	17.7	25.8	23.0	0.030	0.009	0.438	1.18	5.11	1.09	7.58	3.38	1.12
35C7	12.4	18.1	74.0	8.26	0.105	15.3	26.4	20.0	0.024	<dl	0.279	1.04	4.76	0.990	6.76	3.22	1.03
35C8	13.2	8.61	46.6	9.67	0.011	17.9	24.6	20.8	0.023	<dl	0.017	1.13	5.03	1.07	7.55	3.16	1.06
35C9	9260	2420	26500	35.6	3.97	<dl	79.1	23.8	1.26	<dl	222	11.1	310	2.12	7.61	1.53	0.580
25R1	0.304	2.10	14.2	25.5	0.765	541	0.570	0.102	0.003	<dl	106	3.63	6.65	0.683	2.38	0.409	0.985
25R2R	0.860	8.57	35.4	37.5	0.834	667	0.807	0.558	0.006	<dl	219	8.81	13.0	1.27	4.54	0.655	1.85
25H1	5.95	0.972	47.0	2.67	0.012	9.16	18.4	15.1	0.006	<dl	0.043	0.963	4.80	1.02	6.06	2.67	0.529
25CF	5.32	3.42	58.4	4.54	4.24	10.6	25.4	31.6	0.214	0.252	7.26	2.50	9.43	1.83	10.4	3.74	0.819
234B3	0.710	8.71	7.61	21.5	0.506	564	0.207	0.551	0.053	0.043	34.5	1.24	2.20	0.274	0.870	<dl	0.269
233B	0.210	6.79	5.74	19.9	0.281	595	0.419	0.559	<dl	<dl	32.5	1.37	2.38	0.248	1.33	0.172	0.428

Sample	Ni	Cu	Zn	Ga	Rb	Sr	Y	Zr	Nb	Cs	Ba	La	Ce	Pr	Nd	Sm	Eu
233A1	0.260	19.1	5.00	19.8	0.803	532	0.379	0.790	0.109	<dl	29.0	1.29	2.08	0.217	0.960	<dl	0.239
231B1	0.299	3.84	2.97	14.5	<dl	532	0.360	0.046	<dl	<dl	24.8	1.18	2.09	0.249	0.900	0.108	0.349
235P4	0.361	27.3	9.61	19.9	1.57	581	1.57	5.68	0.282	0.064	44.7	2.33	4.46	0.557	1.99	0.363	0.618
236P1	1.44	12.2	7.05	19.8	0.316	664	0.286	0.372	<dl	<dl	32.0	1.29	2.19	0.310	1.16	<dl	0.428
236P2	0.700	94.4	10.1	22.7	3.70	624	1.95	9.76	0.486	0.147	52.9	2.78	5.66	0.709	2.74	0.420	0.621
23R31	7.51	11.8	7.97	24.0	0.390	590	0.465	0.450	<dl	0.069	35.6	1.88	2.86	0.309	1.07	<dl	0.397
23R32	0.448	11.0	4.81	19.3	0.193	572	0.194	0.154	0.047	<dl	21.8	1.08	1.77	0.199	0.785	<dl	0.298
233C3	11.2	7.28	70.6	5.88	1.73	31.2	19.8	17.6	0.187	0.123	8.76	1.36	5.07	1.10	6.49	2.68	0.777
233C4	14.8	3.19	88.0	5.23	0.024	15.2	26.4	17.5	0.026	<dl	0.160	1.36	6.21	1.35	8.59	3.40	0.969
23DB2	7.42	3.29	76.7	7.96	0.253	27.7	30.7	26.6	0.074	<dl	1.78	1.54	7.49	1.57	9.72	4.04	1.11
23DA1	9.37	2.42	72.7	6.66	0.073	23.1	32.9	26.5	0.037	<dl	0.966	1.80	7.67	1.73	11.2	4.16	1.26
355C2	16.9	100	184	6.31	0.170	16.6	16.1	13.5	0.010	<dl	0.151	0.618	2.85	0.674	4.56	1.98	0.710
355C3	19.3	101	238	6.13	0.047	14.9	16.3	13.2	0.017	<dl	0.091	0.592	3.19	0.697	4.41	1.98	0.696
202D2	0.550	14.4	21.3	20.8	0.237	615	0.399	0.406	0.038	<dl	35.7	1.59	2.95	0.374	1.66	0.470	0.424
201B1	1.13	56.7	21.4	24.1	1.36	681	1.80	4.36	0.142	0.250	54.8	2.72	5.34	0.603	2.77	0.450	0.890
201B2	0.590	10.6	10.5	20.7	0.146	617	0.568	0.185	0.009	<dl	47.5	2.90	5.03	0.608	2.23	0.360	0.599
355C4	18.2	10.2	38.5	6.65	<dl	21.3	15.7	12.8	0.021	<dl	0.130	0.634	2.91	0.667	4.75	2.14	0.658
355C5	17.0	163	83.5	9.19	21.8	26.4	26.3	33.5	0.490	17.2	14.6	4.21	11.4	1.84	9.63	3.74	1.02
201C1	18.4	5.06	99.8	8.28	<dl	17.3	49.7	38.1	0.056	<dl	<dl	2.56	11.4	2.56	16.3	6.45	1.38
201C2	19.1	4.48	95.2	7.69	0.022	16.3	54.3	40.7	0.047	<dl	<dl	2.60	11.9	2.74	17.9	7.18	1.31
201A1	<dl	26.6	4.17	25.9	1.06	624	0.415	0.621	0.022	0.112	44.8	1.90	3.46	0.399	1.68	0.310	0.579
201A2	0.134	72.6	5.59	27.9	2.28	630	0.688	1.32	0.073	0.269	56.5	2.72	4.80	0.501	2.08	0.390	0.603
202D1	<dl	56.1	4.43	28.1	1.59	626	0.436	1.03	0.046	0.067	35.8	1.62	3.06	0.373	1.42	0.207	0.524
204C1	16.2	2.82	28.8	3.91	<dl	11.4	15.7	12.8	0.015	<dl	<dl	0.695	3.34	0.790	5.38	2.15	0.584
204C2	43.3	4.82	181	3.87	<dl	<dl	3.75	1.60	<dl	<dl	<dl	0.005	0.049	0.018	0.176	0.108	0.042
204C3	34.3	4.09	141	3.14	<dl	1.07	3.29	1.53	0.005	<dl	<dl	0.017	0.124	0.031	0.250	0.110	0.032

Sample	Ni	Cu	Zn	Ga	Rb	Sr	Y	Zr	Nb	Cs	Ba	La	Ce	Pr	Nd	Sm	Eu
204C4	17.4	1.79	51.6	4.47	<dl	12.3	25.9	16.4	0.091	<dl	0.029	1.41	6.28	1.42	9.12	3.74	0.840
235P1	<dl	7.72	3.31	21.7	1.00	525	0.354	0.531	0.048	<dl	23.5	0.880	1.65	0.196	0.754	0.110	0.302
235P2	0.149	49.2	8.25	27.4	4.35	584	1.72	4.41	0.371	0.256	47.8	2.28	4.46	0.537	2.07	0.193	0.645
233BC	0.211	14.3	3.59	23.0	0.547	546	0.350	0.563	0.095	0.050	27.5	0.907	1.64	0.198	0.590	0.111	0.375
351BC	<dl	6.29	6.50	22.4	0.559	468	0.891	0.504	0.058	0.023	22.9	1.45	2.56	0.331	1.46	0.380	0.313
1PA1	0.124	5.23	5.62	30.3	0.367	692	0.364	0.205	<dl	0.038	57.4	2.19	3.67	0.392	1.50	0.309	0.559
1CA1	12.7	5.06	71.6	6.65	0.049	18.5	28.9	26.2	0.020	<dl	<dl	1.65	7.58	1.75	10.6	4.19	1.08
2CB1	16.4	52.0	280	2.96	0.108	1.31	6.93	2.75	0.016	<dl	0.551	1.10	2.81	0.390	1.98	0.553	0.077
2CB2	19.9	2.32	252	5.54	0.199	<dl	7.02	4.71	0.014	0.016	0.479	0.086	0.395	0.045	0.395	0.276	0.061
2OP1	18.5	3.07	248	4.11	0.074	<dl	6.74	3.35	<dl	0.005	<dl	0.014	0.076	0.043	0.228	0.187	0.032
4PH1	0.133	0.236	3.05	20.1	0.132	532	0.208	0.040	0.009	<dl	28.4	0.830	1.41	0.165	0.714	0.119	0.351
4PG1	<dl	1.12	9.08	31.4	0.605	613	0.866	0.413	0.816	<dl	145	5.68	9.71	1.05	3.95	0.590	1.30
4PG2	<dl	0.638	4.47	21.6	0.190	467	0.890	0.054	0.003	<dl	78.3	4.04	7.65	0.895	3.34	0.603	0.905
4PG3	<dl	1.06	8.32	32.8	0.447	654	0.806	0.038	<dl	<dl	160	5.50	9.54	1.08	3.73	0.541	1.46
1PA2	0.240	4.63	6.54	25.8	0.729	676	0.490	1.50	0.038	0.020	60.0	2.55	4.39	0.399	1.85	0.470	0.800
1PA3	0.270	2.81	6.14	25.7	0.590	662	0.372	0.544	0.045	0.043	59.2	2.50	4.40	0.539	1.73	0.208	0.559
4PH2	<dl	0.980	5.84	20.7	0.241	588	0.353	0.142	0.017	<dl	41.5	1.54	2.84	0.277	0.990	0.160	0.481
4PH3	<dl	1.18	5.33	24.0	0.393	718	0.417	0.218	<dl	<dl	69.7	3.20	4.86	0.535	1.57	0.358	0.751
4PI1	0.520	2.69	8.05	23.1	0.552	647	0.260	0.103	0.020	<dl	91.4	3.22	5.19	0.560	2.46	0.241	1.03
6PL1	<dl	0.810	5.33	26.3	0.340	657	0.381	<0.055	<dl	<dl	82.3	3.40	5.57	0.582	2.34	0.260	0.920
6PL2	0.150	1.59	2.26	15.0	0.085	470	0.497	0.099	0.007	<dl	41.0	1.67	3.82	0.377	2.06	0.250	0.508
51C1Pl1A	0.121	5.00	3.32	21.8	0.093	600	0.126	<dl	<dl	<dl	24.1	0.701	1.09	0.137	0.585	0.056	0.202
51C1Pl1B	<dl	16.1	3.92	23.7	0.158	560	0.204	0.105	<dl	<dl	24.8	0.816	1.43	0.142	0.534	0.097	0.300
51C2Pl1A	0.144	3.96	2.84	22.8	0.145	558	0.134	0.101	<dl	0.016	21.0	0.694	1.11	0.128	0.556	0.079	0.258
51C2Pl1C	<dl	6.45	3.15	25.7	0.214	604	0.217	0.189	<dl	<dl	27.5	1.06	1.89	0.220	0.739	0.140	0.395

Sample	Ni	Cu	Zn	Ga	Rb	Sr	Y	Zr	Nb	Cs	Ba	La	Ce	Pr	Nd	Sm	Eu
51C2Pl1B	0.158	12.5	4.10	25.0	0.196	590	0.176	0.085	0.005	<dl	30.7	0.943	1.72	0.175	0.709	0.118	0.313
51C3Pl1A	0.099	5.60	3.30	24.2	0.227	619	0.166	0.085	<dl	<dl	24.7	1.10	1.81	0.215	0.798	0.083	0.373
51C4Pl1A	0.153	4.86	8.95	26.6	0.625	587	0.688	0.057	<dl	<dl	134	5.27	8.82	0.924	3.39	0.421	1.20
51C4Pl1C	<dl	6.48	9.04	29.9	0.784	688	0.521	0.066	0.002	<dl	213	6.08	9.43	0.970	3.22	0.480	1.73
51C5Pl1A	0.108	3.55	6.78	23.6	0.564	569	0.753	0.123	<dl	<dl	98.9	4.07	7.22	0.790	3.11	0.537	0.869
51C5Pl1B	<dl	3.37	6.70	25.3	0.432	582	0.769	0.066	0.003	<dl	109	4.13	7.28	0.831	3.11	0.478	1.23
51C5Pl1C	<dl	4.26	8.63	26.7	0.591	580	0.602	0.041	<dl	<dl	115	3.57	6.20	0.659	2.56	0.441	1.05
51C6Pl1A	<dl	4.08	7.51	26.6	0.657	557	0.787	0.079	0.005	<dl	116	3.87	7.26	0.819	3.05	0.495	1.04
51C6Pl1B	0.127	3.84	7.57	26.9	0.838	563	0.646	0.216	0.011	<dl	120	3.67	6.49	0.771	2.68	0.585	1.06
51C6Pl1C	<dl	4.63	8.27	26.4	0.801	586	0.537	0.325	0.006	<dl	132	3.18	5.57	0.619	2.26	0.346	1.14
51C6Pl2A	0.106	6.94	8.96	27.6	0.644	588	0.650	0.039	0.006	<dl	157	4.94	8.51	0.920	3.30	0.433	1.50
51C6Pl2B	0.105	4.83	9.02	29.1	0.790	640	0.739	0.061	<dl	<dl	168	6.27	9.93	1.03	4.06	0.444	1.53
51C6Pl3A	<dl	4.91	7.60	29.4	0.876	540	0.789	<dl	0.010	<dl	115	4.32	7.17	0.765	2.78	0.393	1.00
51C7Pl2A	0.589	2.67	2.09	18.7	0.076	568	0.110	0.025	<dl	<dl	21.6	0.448	0.755	0.092	0.421	0.062	0.153
51C7Pl2B	0.191	6.87	2.94	26.8	0.069	632	0.230	<dl	0.008	<dl	29.9	1.25	1.99	0.216	0.791	0.101	0.372
51C8Pl1B	0.088	5.05	3.19	26.8	0.060	623	0.165	<dl	<dl	<dl	26.5	1.15	2.00	0.258	0.844	0.167	0.411
51C8Pl2A	0.250	4.06	7.25	27.9	0.868	605	0.367	0.093	0.008	<dl	77.1	0.977	1.82	0.258	0.880	0.148	1.24
51C8Pl2B	0.210	3.89	9.08	21.2	0.696	587	0.601	0.162	0.064	<dl	60.7	1.59	3.20	0.376	1.67	0.360	1.09
51C8Pl2C	1.05	5.83	17.1	26.3	2.80	561	0.990	0.327	0.084	0.14	107	2.77	7.68	0.897	2.59	0.320	1.42
51C4Pl1B_R	<dl	7.09	8.48	26.4	0.719	656	0.552	0.041	<dl	<dl	164	4.43	7.10	0.776	2.77	0.494	1.49
51C5Pl1D_R	<dl	8.34	10.2	25.2	1.18	726	0.545	0.504	0.034	0.06	217	6.80	11.2	0.950	3.14	0.430	1.71
13C1Pl1A	0.144	7.79	7.45	28.4	0.749	583	0.754	0.101	<dl	<dl	119	4.43	7.35	0.779	2.86	0.426	0.999
13C1Pl1B	<dl	16.9	6.75	25.9	0.187	617	0.282	0.043	0.007	<dl	41.5	1.75	2.93	0.304	1.16	0.126	0.501
13C1Pl2A	0.134	6.31	6.11	23.9	0.325	604	1.08	0.196	<dl	<dl	102	5.44	9.45	1.02	4.01	0.582	1.05
13C1Pl2B	0.102	6.30	7.49	27.1	0.644	608	0.617	0.071	0.004	0.00	138	4.80	7.69	0.759	2.66	0.339	1.09
13C1Pl3A	0.147	5.00	7.71	28.2	0.694	594	0.619	0.130	0.009	<dl	121	4.00	6.47	0.697	2.64	0.394	1.16

Sample	Gd	Tb	Dy	Ho	Er	Tm	Yb	Lu	Hf	Ta	Pb	Th	U
234B1	0.496	0.091	0.464	0.088	0.203	0.040	0.268	0.051	0.248	0.031	2.82	0.464	0.404
234B2	<dl	0.015	0.063	0.012	0.025	<dl	<dl	<dl	<dl	<dl	1.04	0.026	<dl
233A2	0.287	0.014	0.077	0.010	<dl	0.029	<dl	<dl	0.031	0.009	1.85	<dl	<dl
236P3	0.150	0.007	0.375	0.119	0.041	0.035	0.153	0.042	0.176	0.017	2.96	0.245	<dl
233C2	5.37	0.948	6.25	1.36	3.63	0.474	2.88	0.461	1.32	0.005	0.085	0.028	<dl
233C1	3.43	0.588	3.98	0.857	2.30	0.296	1.86	0.285	0.735	<dl	0.084	0.014	<dl
23DB1	5.72	1.02	6.64	1.46	3.69	0.531	3.22	0.463	1.45	0.008	0.130	0.040	<dl
23DA2	5.08	0.896	5.86	1.21	3.19	0.437	2.63	0.386	1.17	0.005	0.178	0.050	0.005
231B2	0.143	0.021	0.092	0.024	0.042	0.008	<dl	<dl	0.042	0.009	1.47	0.040	0.025
351A2	0.228	0.025	0.191	0.056	0.070	0.025	0.108	0.012	0.540	0.012	3.57	0.181	0.064
351A3	0.170	<dl	0.064	0.022	<dl	<dl	0.036	<dl	0.035	0.008	1.04	0.021	<dl
351C2	0.395	0.046	0.196	0.024	0.085	0.011	0.129	<dl	0.020	<dl	2.32	0.102	0.020
351D2	0.122	0.015	0.153	0.039	0.056	<dl	<dl	<dl	0.380	0.023	7.50	0.034	0.096
354C1	0.200	0.022	0.108	0.020	<dl	<dl	<dl	<dl	<dl	<dl	2.71	<dl	<dl
354C3	0.323	0.086	0.399	0.093	0.176	0.045	0.198	0.062	0.156	<dl	2.01	0.295	0.089
355C1	5.77	1.14	6.83	1.54	3.81	0.512	3.24	0.448	1.68	0.014	0.279	0.182	0.076
25H2	4.41	0.808	5.03	1.02	2.64	0.374	2.31	0.316	0.735	<dl	0.168	0.129	0.017
25H3	0.469	0.104	0.842	0.226	0.766	0.136	1.20	0.203	0.088	<dl	0.029	<dl	<dl
25R1B	0.228	0.026	0.134	0.024	0.035	0.009	0.034	0.005	0.005	<dl	4.65	<dl	0.005
25R1C	0.189	0.020	0.111	0.026	0.023	<dl	0.047	<dl	<dl	<dl	4.16	<dl	<dl
25R1M	0.236	0.032	0.119	0.023	0.040	0.008	0.053	<dl	<dl	<dl	4.45	<dl	<dl
25R2C	0.212	0.021	0.114	0.013	0.029	<dl	<dl	<dl	<dl	<dl	4.70	<dl	<dl
25R2M	0.218	0.027	0.093	0.023	0.029	0.049	0.026	<dl	<dl	<dl	5.00	<dl	<dl
256C1	2.76	0.499	3.16	0.667	1.76	0.234	1.62	0.220	0.772	0.014	0.134	0.047	0.006
35C1	2.97	0.538	3.56	0.724	1.92	0.237	1.66	0.215	0.866	0.004	0.052	0.029	0.006
35C2	0.143	0.016	0.071	0.013	<dl	<dl	<dl	0.009	<dl	<dl	2.32	<dl	<dl

Sample	Gd	Tb	Dy	Ho	Er	Tm	Yb	Lu	Hf	Ta	Pb	Th	U
35C3	2.67	0.507	3.27	0.658	1.69	0.248	1.53	0.214	0.661	0.019	0.077	0.021	0.007
35C4	3.43	0.644	4.39	0.909	2.52	0.330	2.21	0.312	0.861	0.010	0.269	0.075	0.019
35C5	3.55	0.669	4.37	0.923	2.32	0.325	2.24	0.319	0.770	0.003	0.120	0.023	0.006
35C6	4.26	0.783	5.09	1.06	2.76	0.379	2.48	0.363	1.20	0.005	0.131	0.033	0.008
35C7	4.09	0.767	5.12	1.05	2.93	0.399	2.59	0.381	1.10	0.006	0.153	0.031	0.006
35C8	4.29	0.765	4.90	1.08	2.75	0.371	2.45	0.312	1.14	0.007	0.437	0.037	0.008
35C9	2.65	0.990	8.02	3.08	10.9	1.61	21.4	3.60	<dl	<dl	57.6	<dl	0.830
25R1	0.353	0.021	0.278	0.038	<dl	0.017	<dl	<dl	<dl	<dl	4.08	<dl	<dl
25R2R	0.303	0.032	0.105	0.034	0.050	<dl	<dl	<dl	<dl	0.026	8.10	<dl	<dl
25H1	3.04	0.509	3.36	0.726	1.81	0.241	1.69	0.218	0.702	<dl	0.241	0.013	0.012
25CF	4.33	0.760	4.82	0.976	2.59	0.344	2.29	0.329	1.41	0.022	0.763	0.349	0.097
234B3	0.218	0.025	<dl	<dl	<dl	<dl	0.056	0.018	<dl	<dl	1.82	<dl	<dl
233B	0.142	0.044	0.155	<dl	0.075	<dl	<dl	0.040	<dl	<dl	1.12	<dl	<dl
233A1	0.112	<dl	<dl	<dl	<dl	<dl	0.097	<dl	<dl	<dl	1.17	<dl	<dl
231B1	<dl	0.032	<dl	0.028	<dl	<dl	0.016	<dl	<dl	<dl	1.30	<dl	<dl
235P4	0.580	0.040	0.434	0.068	0.155	0.028	0.133	<dl	0.157	<dl	2.02	0.192	0.078
236P1	<dl	0.039	0.175	<dl	1.88	0.023	<dl	<dl	<dl	0.084	2.14	<dl	<dl
236P2	0.740	0.071	0.388	0.122	0.183	<dl	0.340	0.040	0.280	<dl	2.33	0.512	0.119
23R31	0.270	<dl	0.189	<dl	<dl	0.038	0.060	<dl	<dl	<dl	1.52	0.085	<dl
23R32	<dl	0.031	<dl	<dl	<dl	0.028	<dl	<dl	<dl	<dl	2.05	<dl	0.048
233C3	3.34	0.571	3.99	0.814	2.25	0.277	1.95	0.277	0.884	0.024	1.08	0.191	0.060
233C4	4.46	0.715	5.32	1.04	2.90	0.380	2.55	0.367	0.873	<dl	0.632	0.031	<dl
23DB2	5.50	0.864	5.79	1.16	3.22	0.476	2.91	0.415	1.32	<dl	0.596	0.073	0.013
23DA1	5.47	1.00	6.49	1.37	3.71	0.506	3.12	0.455	1.27	0.015	0.329	0.044	0.018
355C2	2.59	0.480	3.17	0.639	1.84	0.228	1.51	0.196	0.744	0.012	16.9	0.020	<dl
355C3	2.79	0.466	3.27	0.718	1.71	0.218	1.39	0.215	0.733	0.017	19.3	0.021	<dl

Sample	Gd	Tb	Dy	Ho	Er	Tm	Yb	Lu	Hf	Ta	Pb	Th	
202D2	0.390	<dl	0.145	0.062	<dl	<dl	0.093	<dl	<dl	<dl	4.35	<dl	<dl
201B1	0.630	0.092	<dl	0.064	0.320	0.056	<dl	0.067	<dl	<dl	4.63	0.230	<dl
201B2	<dl	0.038	0.132	<dl	0.080	<dl	<dl	0.023	<dl	0.025	4.02	0.063	<dl
355C4	2.73	0.454	3.29	0.641	1.76	0.228	1.54	0.210	0.730	<dl	0.321	0.014	0.006
355C5	4.64	0.763	5.36	1.07	2.96	0.376	2.66	0.362	1.53	0.056	6.47	2.71	0.563
201C1	8.44	1.38	9.47	1.97	5.49	0.733	5.18	0.731	1.90	0.006	0.219	0.072	0.022
201C2	9.23	1.53	10.6	2.16	5.98	0.802	5.26	0.777	2.33	0.007	0.200	0.062	0.024
201A1	0.077	<dl	0.133	0.013	0.046	0.005	<dl	<dl	0.058	0.015	1.75	0.024	0.049
201A2	0.232	0.025	<dl	0.016	0.106	<dl	0.066	0.008	<dl	<dl	2.37	0.089	<dl
202D1	0.162	<dl	0.032	0.038	0.083	0.015	<dl	<dl	0.035	<dl	1.58	0.047	0.018
204C1	2.71	0.470	3.09	0.668	1.72	0.242	1.45	0.201	0.813	<dl	0.069	0.023	0.005
204C2	0.178	0.059	0.534	0.141	0.544	0.088	0.731	0.152	0.104	<dl	<dl	<dl	<dl
204C3	0.252	0.055	0.451	0.141	0.478	0.088	0.630	0.117	0.098	<dl	<dl	<dl	<dl
204C4	4.63	0.759	5.06	1.01	2.72	0.391	2.40	0.352	1.05	0.010	0.088	0.029	0.009
235P1	0.148	0.020	0.063	0.024	0.042	<dl	<dl	<dl	<dl	<dl	1.45	0.039	0.019
235P2	0.231	0.053	0.430	0.095	0.172	<dl	0.102	<dl	0.128	0.021	3.23	0.228	0.126
233BC	0.223	0.014	0.124	<dl	<dl	<dl	<dl	<dl	<dl	<dl	1.22	0.072	0.020
351BC	0.265	0.038	0.180	0.027	0.072	0.010	<dl	0.013	0.043	<dl	1.40	0.118	0.032
1PA1	0.137	0.014	0.083	0.009	0.033	<dl	<dl	<dl	<dl	0.005	3.15	<dl	0.005
1CA1	5.10	0.856	5.85	1.18	3.31	0.438	2.78	0.417	1.17	<dl	0.123	0.053	0.009
2CB1	0.725	0.142	1.18	0.265	0.876	0.152	1.05	0.181	0.152	<dl	0.024	0.072	0.017
2CB2	0.484	0.112	0.908	0.244	0.903	0.178	1.39	0.263	0.190	<dl	0.051	0.018	0.010
2OP1	0.312	0.076	0.917	0.223	0.898	0.201	1.49	0.187	0.154	<dl	<dl	<dl	<dl
4PH1	0.084	<dl	<dl	<dl	<dl	0.005	<dl	0.003	<dl	<dl	1.63	<dl	<dl
4PG1	0.346	0.037	0.225	0.026	0.082	<dl	0.045	<dl	<dl	<dl	6.52	<dl	<dl
4PG2	0.346	0.043	0.220	0.035	0.051	0.005	0.025	<dl	<dl	0.004	4.46	<dl	<dl

Sample	Gd	Tb	Dy	Ho	Er	Tm	Yb	Lu	Hf	Ta	Pb	Th	U
4PG3	0.339	<dl	0.142	0.028	0.073	<dl	0.026	0.006	<dl	<dl	7.02	<dl	<dl
1PA2	0.083	0.012	0.169	0.034	<dl	0.008	0.088	<dl	<dl	0.019	2.79	<dl	0.021
1PA3	<dl	0.022	0.054	0.028	0.061	0.013	<dl	0.002	0.008	0.016	2.55	0.032	<dl
4PH2	0.258	0.018	0.070	0.011	0.059	<dl	0.016	0.007	<dl	<dl	2.35	<dl	<dl
4PH3	0.232	0.031	0.053	<dl	0.040	<dl	<dl	<dl	<dl	0.022	2.83	<dl	<dl
4PI1	0.231	0.028	<dl	<dl	<dl	0.010	<dl	<dl	<dl	<dl	3.38	<dl	<dl
6PL1	0.184	<dl	0.041	<dl	0.073	<dl	0.019	<dl	<dl	<dl	2.55	0.022	<dl
6PL2	0.163	0.021	0.089	<dl	<dl	0.023	<dl	<dl	0.046	<dl	2.34	<dl	<dl
51C1Pl1A	<dl	<dl	<dl	<dl	0.018	<dl	<dl	<dl	0.085	<dl	0.730	<dl	0.001
51C1Pl1B	<dl	0.007	0.064	<dl	<dl	0.005	<dl	<dl	<dl	<dl	0.939	<dl	0.008
51C2Pl1A	<dl	<dl	0.050	0.009	<dl	<dl	0.029	0.006	0.020	0.009	0.818	<dl	<dl
51C2Pl1C	0.047	0.012	0.031	0.007	0.029	0.009	<dl	0.007	<dl	<dl	1.22	0.017	<dl
51C2Pl1B	<dl	0.008	0.035	0.011	0.018	<dl	<dl	0.006	<dl	<dl	1.14	<dl	<dl
51C3Pl1A	<dl	0.011	<dl	<dl	0.033	<dl	<dl	0.002	0.014	<dl	1.12	<dl	<dl
51C4Pl1A	0.347	0.022	0.068	0.020	<dl	0.011	0.063	<dl	<dl	<dl	5.95	<dl	<dl
51C4Pl1C	0.160	0.033	0.135	0.011	0.061	<dl	<dl	0.005	<dl	0.004	7.37	<dl	0.006
51C5Pl1A	0.191	0.033	0.131	0.027	0.037	<dl	0.026	<dl	<dl	<dl	4.75	0.006	<dl
51C5Pl1B	0.383	0.029	0.185	0.036	0.035	0.014	0.048	<dl	0.012	0.013	5.63	<dl	<dl
51C5Pl1C	0.261	0.022	0.154	0.023	0.047	<dl	<dl	<dl	0.007	<dl	5.67	0.004	0.003
51C6Pl1A	0.312	0.029	0.150	0.018	0.058	0.006	0.022	0.007	0.013	<dl	5.24	0.007	<dl
51C6Pl1B	0.315	0.032	0.122	0.031	0.063	<dl	<dl	0.006	0.005	<dl	5.05	0.012	0.006
51C6Pl1C	0.234	0.029	0.148	0.016	0.052	<dl	0.037	<dl	<dl	<dl	5.32	0.004	0.004
51C6Pl2A	0.406	0.025	0.188	0.022	0.051	0.014	0.055	<dl	0.043	0.001	6.57	<dl	<dl
51C6Pl2B	0.500	0.044	0.187	0.033	0.054	<dl	0.045	<dl	0.004	0.001	6.18	0.015	<dl
51C6Pl3A	0.282	0.043	0.165	0.027	0.049	0.017	<dl	<dl	<dl	0.006	4.91	0.009	<dl

Sample	Gd	Tb	Dy	Ho	Er	Tm	Yb	Lu	Hf	Ta	Pb	Th	U
51C7Pl2A	0.057	<dl	0.025	<dl	<dl	<dl	0.017	<dl	0.008	<dl	0.477	0.004	<dl
51C7Pl2B	0.086	0.006	0.079	0.007	<dl	0.003	<dl	<dl	<dl	<dl	1.07	<dl	0.001
51C8Pl1B	0.107	0.006	0.036	<dl	0.019	<dl	<dl	0.007	<dl	0.003	1.35	<dl	<dl
51C8Pl2A	0.203	<dl	<dl	<dl	0.042	0.018	0.083	0.033	<dl	<dl	6.89	<dl	0.014
51C8Pl2B	0.210	0.068	0.129	0.040	0.032	<dl	0.122	<dl	<dl	<dl	5.38	0.038	0.038
51C8Pl2C	0.270	0.050	0.325	0.046	0.080	0.036	0.048	0.011	0.052	<dl	8.48	0.062	0.108
13C1Pl1A	0.411	0.030	0.228	0.022	0.052	0.016	<dl	0.010	0.003	<dl	4.87	0.012	<dl
13C1Pl1B	0.150	0.012	0.082	0.009	<dl	<dl	<dl	<dl	<dl	<dl	1.67	<dl	4.770
13C1Pl2A	0.457	0.029	0.181	0.029	0.091	0.008	0.066	<dl	<dl	0.004	5.12	<dl	<dl
13C1Pl2B	0.214	0.025	0.147	0.026	0.069	0.007	0.033	0.007	<dl	<dl	5.60	0.017	<dl
13C1Pl3A	0.129	0.028	0.115	0.026	0.044	0.009	0.030	0.004	<dl	<dl	5.19	<dl	0.023
13C1Pl3C	0.211	0.025	0.146	0.016	0.040	0.007	0.031	0.007	<dl	0.002	5.25	0.005	0.016
13C1Pl3D	0.251	0.030	0.170	0.036	0.058	0.005	0.019	<dl	<dl	<dl	5.18	0.011	<dl
13C1Pl3B	0.228	0.028	0.148	0.013	0.058	<dl	<dl	0.010	0.176	<dl	5.15	<dl	<dl
13C1Pl3F	0.309	0.038	0.170	0.018	0.034	0.009	<dl	0.013	0.179	0.007	5.46	0.014	<dl
13C1Pl4B	0.087	0.022	0.073	0.011	0.024	<dl	<dl	0.007	<dl	<dl	1.94	0.006	<dl
13C2Pl1A	0.218	0.027	0.146	0.024	0.057	<dl	0.033	0.005	<dl	<dl	5.75	0.003	<dl
13C2Pl1C	0.206	0.037	0.143	0.021	0.042	0.007	0.036	<dl	<dl	<dl	5.77	0.012	0.003
13C2Pl1D	0.456	0.055	0.204	0.025	0.066	<dl	0.049	0.010	<dl	<dl	7.02	0.008	<dl
13C2Pl2A	0.242	0.031	0.146	0.036	0.043	0.013	0.039	<dl	<dl	<dl	5.43	0.009	<dl
13C3Pl1A	0.297	0.035	0.160	0.023	0.073	<dl	0.025	0.006	<dl	0.001	4.83	<dl	0.005
13C3Pl1B	0.351	0.033	0.147	0.030	0.054	0.007	<dl	0.007	<dl	<dl	5.49	<dl	<dl
13C3Pl1C	0.260	0.035	0.122	0.028	0.043	0.010	<dl	0.005	<dl	<dl	5.72	<dl	<dl
13C4Pl1A	0.256	0.038	0.196	0.032	0.055	0.011	<dl	<dl	<dl	<dl	4.85	<dl	0.004
13C4Pl1B	0.412	0.049	0.219	0.038	0.066	<dl	0.077	0.008	<dl	<dl	5.06	<dl	<dl
13C4Pl1C	0.300	0.040	0.162	0.027	0.069	0.007	0.030	<dl	<dl	<dl	5.78	<dl	0.006

Table B3. Sr-Ba melt composition surrounding plagioclase from Gede volcano (West Java, Indonesia)

Sample G23	Melt Sr	Melt Ba
234B2	393.955	414.860
233A2	298.182	391.161
PL3	296.404	674.057
233A1	341.725	420.435
231B1	310.387	312.852
236P1	429.329	469.019
R1	217.807	190.712
23R31	423.234	605.429
23R32	376.065	326.433
XPL1	122.303	264.730
XPL4	255.853	404.115
235P1	294.078	281.156
233BC	308.825	332.167
234B3	323.977	426.658
233B	298.767	332.188

Sample G25	Melt Sr	Melt Ba
25R1B	165.398	453.832
25R1C	173.263	458.167
25R1M	185.944	557.137
25R2C	122.133	417.286
25R2M	125.705	445.803
25R1	164.751	527.749
25R2R	135.771	615.319
1PA1	343.133	575.897
4PH1	361.570	446.801
4PG1	160.865	583.738
4PG2	280.647	1034.420
4PG3	136.407	463.399
1PA3	328.522	593.455
4PH2	237.266	309.562
4PH3	237.620	391.994
4PI1	215.079	517.224
6PL1	259.737	596.962
6PL2	246.485	446.221

Sample G35	Melt Sr	Melt Ba
351A3	292.009	290.749
351D2	326.156	352.104
3510	157.939	124.764
354C1	173.470	309.482
351A1	441.359	891.994
351B1	254.893	372.498
351C1	245.544	414.155
351D1	290.731	450.823
35102	244.304	337.230
354C2	288.394	352.047

Sample G20	Melt Sr	Melt Ba
202D2	400.675	529.420
201B2	350.906	579.297
201A1	287.663	404.922

Table C1.1. Clinopyroxene major element compositions, obtained by electron microprobe and expressed in %. Data from the Waitomokia volcano (New Zealand).

Sample	Na_2O	MgO	Al_2O_3	SiO_2	P_2O_5	K_2O	CaO	TiO_2	Cr_2O_3	MnO	FeO	NiO	Total
VMA1_09_a core	0.41	14.07	4.3	49.03	0.27	0.01	22.76	1.95	0.4	0.12	6.77	0	100.09
VMA1_09_b core	0.59	10.46	10.1	41.55	0.23	0.02	22.8	4.73	0.12	0.11	8.24	-0.03	98.93
VMA1_09_c rim	0.46	11.34	7.98	43.98	0.26	0.02	22.44	4.13	0.05	0.1	8.5	0.02	99.27
VMA1_09_d	0.51	10.77	9.24	43.01	0.29	0.01	22.72	4.44	0.02	0.15	8.3	0.03	99.5
VMA1_09_e rim	0.51	11.44	7.63	44.21	0.23	0.01	22.86	3.74	0.19	0.11	7.73	-0.02	98.63
VMA1_09_f rim	0.5	12	6.9	45.55	0.22	0.01	22.87	3.42	0.27	0.13	7.5	-0.02	99.34
VMA1_09_g core	0.38	13.7	4.54	48.41	0.27	0	22.8	2.2	0.25	0.14	7.27	0.02	99.98
VMA1_09_h core	0.38	14.29	4.15	48.93	0.22	0	22.93	1.91	0.38	0.15	6.62	0.04	99.99
VMA1_09_ m	0.49	12.82	7.1	46.39	0.24	0.01	22.79	3.04	0.58	0.12	7.11	-0.01	100.68
VMA1_09_ n	0.53	10.62	9.46	42.29	0.28	0.03	22.25	4.87	0.02	0.1	9.02	0.01	99.48
VMA1_09_ o core	0.43	12.73	5.28	47.71	0.33	0	22.38	2.6	-0.01	0.15	8.7	0.03	100.33
VMA1_09_ p core	0.5	12.24	6.75	45.35	0.29	0	22.43	3.16	0.13	0.12	8	0.01	98.99
VMA1_09_ q rim	2.01	5.48	12.7	44.1	1.14	1.25	13.68	4.03	0.01	0.29	12.56	-0.01	97.25
VMA1_09_ r core	0.61	13.98	3.24	50.35	0.19	0.01	20.44	0.87	0.03	0.38	10.44	0	100.53
VMA1_09_ s core	0.6	11.86	7.78	44.92	0.29	0	22.34	3.21	0.1	0.11	7.96	0.02	99.21
VMA1_09_ t rim	0.61	9.45	11.02	40.56	0.29	0.04	22.15	5.63	0.02	0.18	8.96	-0.01	98.9
VMA1_09_ u rim	1.94	5.84	14.43	41.62	0.99	1.1	15.42	4.42	-0.01	0.17	11	-0.01	96.92
VMA1_12_a core	0.46	14.13	4.09	49.17	0.25	0.02	21.97	1.5	0.32	0.19	7.15	0	99.25
VMA1_12_b core	0.51	11.95	7.64	45.83	0.26	0.01	22.75	3.33	0.23	0.14	7.73	0.02	100.41
VMA1_12_c core	0.61	11.03	9.06	42.62	0.22	0.01	22.43	4.81	0.13	0.13	8.59	0.02	99.65
VMC3_01_a core	0.39	13.68	4.78	48.57	0.26	0	22.58	2.24	0.23	0.11	7.22	0.02	100.07
VMC3_01_b rim	0.59	10.34	9.67	42.05	0.28	0.02	22.41	4.7	0.02	0.12	8.77	-0.01	98.96
VMC3_01_c core	0.5	11.93	6.85	44.87	0.33	0	22.42	3.52	0.15	0.11	8.25	0.03	98.95
VMC3_01_d rim	0.51	11.39	6.96	44.89	0.31	0.02	22.43	3.55	0	0.18	8.66	0	98.91
VMC3_01_e	0.43	13.8	4.34	48.35	0.24	0.01	22.66	2.14	0.18	0.14	7.16	0.01	99.44
VMC3_01_f core	0.5	9.62	7.68	44.06	0.32	0.14	21.86	3.9	0.03	0.17	8.69	0.02	96.97
VMC3_12_a core	0.4	13.53	4.92	47.84	0.31	0.01	22.14	2.38	0.24	0.18	7.7	0.01	99.66
VMC3_12_b rim	0.55	12.17	7.64	44.85	0.25	0.02	22.78	3.28	0.23	0.06	7.74	0.02	99.6
VMC3_12_ c core	0.52	11.75	8.37	43.48	0.25	0.01	22.62	4.06	0.32	0.1	7.88	-0.02	99.34
VMC3_12_ d rim	0.58	10.4	9.14	42.43	0.27	0.02	22.55	4.8	0.01	0.12	8.62	-0.01	98.93
VMC3_12_ e	1.25	8.83	11.65	42.28	0.61	0.34	21	4.38	0.05	0.11	9.62	-0.01	100.11
WQE3_Pic 00_1	0.61	11.6	8.43	43.03	0.26	0	22.44	4.25	0.33	0.1	8.04	0.02	99.1
WQE3_Pic 00_2	0.59	11.81	7.94	44.31	0.23	0.01	22.54	3.58	0.3	0.1	7.65	-0.01	99.06
WQE3_Pic 00_3	2.06	6.48	14.26	43.55	0.91	1.3	16.32	4.51	0	0.21	11.14	0.03	100.77
WQE3_Pic 00_4	0.56	10.16	10.35	40.81	0.24	0.04	22.34	5.32	0.03	0.09	8.9	0	98.85
WQE3_Pic 00_5	0.41	12.67	5.85	45.97	0.3	0.01	22.58	2.95	0.02	0.17	8.68	0.01	99.63

Sample	Na_2O	MgO	Al_2O_3	SiO_2	P_2O_5	K_2O	CaO	TiO_2	Cr_2O_3	MnO	FeO	NiO	Total
WQE3_Pic 00_6	0.54	12.04	7.35	44.76	0.28	0.02	22.59	3.44	0.48	0.1	7.55	0	99.15
WQE3_Pic 00_7	0.58	11.3	8.12	43.68	0.35	0.02	22.42	3.68	0.01	0.13	8.48	0.02	98.78
WQE3_Pic 00_8	0.62	11.23	8.47	43.09	0.29	0.02	22.22	4.15	0.11	0.14	8.48	0	98.81
WQE3_Pic 00_9	0.48	12.86	5.43	46.72	0.3	0.01	22.59	2.56	0.06	0.13	7.78	0.02	98.95
WQE3_Pic 00_10	0.57	10.71	9.72	41.7	0.24	0	22.7	4.72	0.12	0.09	8.29	-0.01	98.86
WQE3_Pic 00_11	0.57	10.68	9.72	41.56	0.25	0.01	22.68	4.73	0.08	0.11	8.4	-0.01	98.78

Table C1.2. Olivine major element compositions from the Waitomokia volcano (New Zealand), obtained by electron microprobe and expressed in %. NA stands for “not analysed”. Data from the Waitomokia volcano (New Zealand).

Sample	Dist (μm)	Na_2O	SiO_2	MgO	Al_2O_3	MnO	FeO	Cr_2O_3	K_2O	TiO_2	CaO	NiO	P_2O_5	Total	Mg#
AVF 100_01	0	0	47.31	9.06	12.78	0.14	9.05	0.02	0	0	18.87	0	NA	97.23	64.09
AVF 100_02	10	0	43.44	8.72	11.5	0.15	9.04	0	0	0	18.38	0	NA	91.24	63.23
AVF 100_03	20	0	48.83	4.21	19.9	0.09	4.39	0	0	0	15.22	0.01	NA	92.64	63.09
AVF 100_04	30	0	48.35	1.95	18.7	0.2	9.34	0	0	0	5.23	0	NA	83.77	27.12
AVF 100_05	40	0	46.91	4.04	16.67	0.19	11.84	0.01	0	0	8.26	0	NA	87.92	37.82
AVF 100_06	50	0	38.79	41.2	0.05	0.27	18.64	0.02	0	0	0.43	0.11	NA	99.51	79.76
AVF 100_07	60	0	39.19	43.01	0.04	0.24	17.41	0.03	0	0	0.38	0.14	NA	100.45	81.49
AVF 100_08	70	0	39.15	43.37	0.04	0.23	16.83	0.04	0	0	0.34	0.16	NA	100.16	82.12
AVF 100_09	80	0	39.3	43.19	0.04	0.22	16.85	0.03	0	0	0.33	0.17	NA	100.14	82.04
AVF 100_10	90	0	39.1	42.56	0.05	0.21	17.02	0.03	0	0	0.32	0.15	NA	99.44	81.68
AVF 100_11	100	0	39.1	42.37	0.05	0.21	17.3	0.03	0	0	0.25	0.17	NA	99.48	81.36
AVF 100_12	110	0	39.01	42.82	0.05	0.2	16.76	0.04	0	0	0.21	0.21	NA	99.3	82.00
AVF 100_13	120	0	39.3	43.46	0.05	0.2	16.02	0.03	0	0	0.21	0.21	NA	99.49	82.86
AVF 100_14	130	0	39.24	43.95	0.07	0.17	15.18	0.04	0	0	0.21	0.24	NA	99.1	83.77
AVF 100_15	140	0	39.54	44	0.06	0.16	14.81	0.04	0	0	0.22	0.23	NA	99.06	84.12
AVF 100_16	150	0	39.62	45.32	0.07	0.16	14.62	0.04	0	0	0.22	0.25	NA	100.3	84.68
AVF 100_17	160	0	39.5	44.55	0.05	0.16	14.48	0.04	0	0	0.2	0.26	NA	99.25	84.58
AVF 100_18	170	0	39.56	44.52	0.05	0.15	14.31	0.04	0	0	0.21	0.26	NA	99.12	84.72
AVF 100_19	180	0	39.5	44.5	0.07	0.16	14.37	0.04	0	0	0.21	0.26	NA	99.11	84.66
AVF 100_20	190	0	39.47	44.63	0.07	0.15	14.31	0.05	0	0	0.2	0.28	NA	99.15	84.75
AVF 100_21	200	0	38.84	43.27	0.08	0.15	14.2	0.04	0	0	0.22	0.27	NA	97.08	84.45
AVF 100_22	210	0	39.69	44.67	0.06	0.16	14.19	0.04	0	0	0.2	0.29	NA	99.29	84.87
AVF 100_23	220	0	39.48	44.69	0.06	0.16	14.08	0.04	0	0	0.19	0.28	NA	98.97	84.98
AVF 100_24	230	0	39.48	44.8	0.07	0.15	13.96	0.04	0	0	0.2	0.31	NA	99	85.12
AVF 100_25	240	0	39.63	44.92	0.07	0.15	13.91	0.04	0	0	0.21	0.29	NA	99.21	85.20

Sample	Dist (μm)	Na_2O	SiO_2	MgO	Al_2O_3	MnO	FeO	Cr_2O_3	K_2O	TiO_2	CaO	NiO	P_2O_5	Total	Mg#
AVF 100_26	250	0	39.71	44.87	0.09	0.14	13.73	0.03	0	0	0.19	0.32	NA	99.08	85.35
AVF 100_27	260	0	39.51	44.99	0.08	0.14	13.69	0.03	0	0	0.19	0.31	NA	98.95	85.42
AVF 100_28	270	0	39.46	44.81	0.08	0.14	13.63	0.05	0	0	0.19	0.32	NA	98.68	85.42
AVF 100_29	280	0	39.57	45.11	0.07	0.14	13.54	0.05	0	0	0.19	0.32	NA	98.99	85.59
AVF 100_30	290	0	39.64	45.26	0.08	0.14	13.52	0.04	0	0	0.2	0.32	NA	99.19	85.65
AVF 100_31	300	0	39.47	45.18	0.07	0.15	13.61	0.04	0	0	0.19	0.32	NA	99.03	85.54
AVF 100_32	310	0	39.47	45.14	0.08	0.14	13.51	0.04	0	0	0.18	0.3	NA	98.86	85.62
AVF 100_33	320	0	37.32	42.72	0.22	0.14	13.46	0.04	0	0	0.2	0.31	NA	94.4	84.98
AVF 100_34	330	0	39.72	45.21	0.08	0.15	13.59	0.04	0	0	0.18	0.32	NA	99.28	85.57
AVF 100_35	340	0	39.72	45.23	0.08	0.14	13.48	0.04	0	0	0.2	0.33	NA	99.22	85.68
AVF 100_36	350	0	39.69	45.27	0.08	0.14	13.56	0.02	0	0	0.19	0.32	NA	99.27	85.61
AVF 100_37	360	0	39.73	45.35	0.07	0.15	13.69	0.04	0	0	0.2	0.31	NA	99.54	85.52
AVF 100_38	370	0	39.66	45.13	0.06	0.16	13.55	0.04	0	0	0.19	0.31	NA	99.09	85.58
AVF 100_39	380	0	39.76	45.39	0.07	0.15	13.63	0.03	0	0	0.19	0.31	NA	99.53	85.58
AVF 100_40	390	0	39.77	45.45	0.07	0.15	13.69	0.04	0	0	0.19	0.32	NA	99.67	85.54
AVF 100_41	400	0	39.75	45.33	0.07	0.14	13.64	0.05	0	0	0.2	0.31	NA	99.47	85.56
AVF 100_42	410	0	39.78	45.08	0.07	0.14	13.67	0.04	0	0	0.2	0.32	NA	99.3	85.46
AVF 100_43	420	0	39.88	45.36	0.06	0.15	13.58	0.03	0	0	0.2	0.32	NA	99.59	85.62
AVF 100_44	430	0	39.69	45.22	0.08	0.14	13.56	0.03	0	0	0.19	0.32	NA	99.24	85.60
AVF 100_45	440	0	39.95	45.28	0.08	0.14	13.56	0.04	0	0	0.19	0.32	NA	99.56	85.62
AVF 100_46	450	0	39.74	45.1	0.06	0.14	13.55	0.03	0	0	0.2	0.32	NA	99.15	85.58
AVF 100_47	460	0	39.75	45.17	0.08	0.14	13.59	0.03	0	0	0.2	0.32	NA	99.28	85.56
AVF 100_48	470	0	39.73	45.11	0.07	0.14	13.66	0.04	0	0	0.2	0.32	NA	99.27	85.48
AVF 100_49	480	0	39.83	45.24	0.08	0.14	13.62	0.04	0	0	0.19	0.32	NA	99.45	85.55
AVF 100_50	490	0	39.63	45.09	0.06	0.14	13.66	0.04	0	0	0.19	0.32	NA	99.13	85.47
AVF 100_51	500	0	39.73	45.26	0.06	0.15	13.55	0.04	0	0	0.2	0.33	NA	99.33	85.62
AVF 100_52	510	0	39.85	45.26	0.07	0.15	13.49	0.04	0	0	0.19	0.32	NA	99.36	85.67
AVF 100_53	520	0	39.62	45.18	0.07	0.14	13.47	0.04	0	0	0.19	0.32	NA	99.03	85.67
AVF 100_54	530	0	39.92	45.42	0.08	0.15	13.5	0.04	0	0	0.19	0.31	NA	99.61	85.71
AVF 100_55	540	0	39.68	45.25	0.08	0.15	13.59	0.03	0	0	0.2	0.31	NA	99.29	85.58
AVF_100_01_01	0	0	47.61	11.13	6.49	0.2	8.94	0	0	0	20.17	0.01	NA	94.55	68.94
AVF_100_01_02	10	0	46.34	6.36	13.49	0.22	14.63	0.01	0	0	12.48	0.01	NA	93.53	43.66
AVF_100_01_03	20	0	46.09	8.7	11.83	0.18	9.34	0	0	0	18.56	0	NA	94.71	62.41
AVF_100_01_04	30	0	48.81	9	12.56	0.12	7.24	0	0	0	19.37	0	NA	97.11	68.90
AVF_100_01_05	40	0	47.49	6.23	14.35	0.15	8.61	0.01	0	0	14.18	0.01	NA	91.03	56.33
AVF_100_01_06	50	0	49.67	1.55	18.74	0.17	8.77	-0.01	0	0	6.53	0	NA	85.42	23.96
AVF_100_01_07	60	0	51.67	0.15	27.4	0	1.09	0.01	0	0	11.11	-0.01	NA	91.43	19.70
AVF_100_01_08	70	0	43.95	18.69	10.21	0.48	24.78	0.01	0	0	1.71	0.02	NA	99.86	57.35
AVF_100_01_09	80	0	38.39	39.53	0.04	0.3	20.36	0.01	0	0	0.48	0.08	NA	99.2	77.58

Sample	Dist (μm)	Na_2O	SiO_2	MgO	Al_2O_3	MnO	FeO	Cr_2O_3	K_2O	TiO_2	CaO	NiO	P_2O_5	Total	Mg#
AVF_100_01_10	90	0	38.67	40.89	0.03	0.28	19.11	0.02	0	0	0.42	0.11	NA	99.54	79.23
AVF_100_01_11	100	0	39.01	41.67	0.04	0.27	18.47	0.03	0	0	0.38	0.13	NA	100	80.09
AVF_100_01_12	110	0	39.06	42.33	0.01	0.25	17.62	0.03	0	0	0.36	0.14	NA	99.81	81.07
AVF_100_01_13	120	0	38.99	42.59	0.04	0.24	17.21	0.04	0	0	0.36	0.15	NA	99.6	81.52
AVF_100_01_14	130	0	39.31	42.88	0.04	0.24	17.1	0.03	0	0	0.33	0.16	NA	100.11	81.72
AVF_100_01_15	140	0	39.08	42.93	0.04	0.23	17.16	0.03	0	0	0.34	0.15	NA	99.97	81.68
AVF_100_01_16	150	0	39.18	42.76	0.03	0.24	17.17	0.03	0	0	0.34	0.17	NA	99.93	81.62
AVF_100_01_17	160	0	39.16	42.67	0.05	0.24	17.07	0.04	0	0	0.34	0.17	NA	99.73	81.67
AVF_100_01_18	170	0	39.06	42.81	0.03	0.24	17.18	0.02	0	0	0.34	0.17	NA	99.86	81.62
AVF_100_01_19	180	0	39.02	42.42	0.04	0.23	17.38	0.03	0	0	0.27	0.18	NA	99.58	81.31
AVF_100_01_20	190	0	38.96	42.49	0.05	0.22	17.57	0.03	0	0	0.26	0.18	NA	99.76	81.17
AVF_100_01_21	200	0	39.14	42.44	0.05	0.2	17.45	0.02	0	0	0.23	0.19	NA	99.73	81.26
AVF_100_01_22	210	0	39.14	42.97	0.05	0.21	17.16	0.03	0	0	0.23	0.21	NA	100.01	81.70
AVF_100_01_23	220	0	39.22	42.9	0.05	0.2	16.83	0.03	0	0	0.21	0.22	NA	99.67	81.96
AVF_100_01_24	230	0	39.42	43.47	0.07	0.18	16.2	0.04	0	0	0.22	0.23	NA	99.84	82.71
AVF_100_01_25	240	0	39.39	43.76	0.06	0.17	15.71	0.04	0	0	0.22	0.24	NA	99.59	83.24
AVF_100_01_26	250	0	39.58	44.43	0.07	0.18	15.08	0.04	0	0	0.21	0.24	NA	99.82	84.00
AVF_100_01_27	260	0	39.54	44.71	0.07	0.16	14.83	0.05	0	0	0.21	0.25	NA	99.81	84.31
AVF_100_01_28	270	0	39.57	44.55	0.07	0.16	14.73	0.04	0	0	0.21	0.26	NA	99.59	84.35
AVF_100_01_29	280	0	39.5	44.68	0.07	0.16	14.69	0.04	0	0	0.21	0.24	NA	99.6	84.43
AVF_100_01_30	290	0	39.68	44.76	0.08	0.16	14.59	0.05	0	0	0.21	0.25	NA	99.79	84.54
AVF_100_01_31	300	0	39.57	44.6	0.07	0.16	14.66	0.04	0	0	0.2	0.27	NA	99.57	84.43
AVF_100_01_32	310	0	39.51	44.88	0.06	0.17	14.64	0.03	0	0	0.2	0.26	NA	99.76	84.53
AVF_100_01_33	320	0	39.64	44.56	0.07	0.16	14.58	0.04	0	0	0.2	0.26	NA	99.5	84.49
AVF_100_01_34	330	0	39.45	44.66	0.09	0.16	14.58	0.05	0	0	0.21	0.27	NA	99.47	84.52
AVF_100_01_35	340	0	39.54	44.46	0.06	0.16	14.66	0.04	0	0	0.2	0.27	NA	99.4	84.39
AVF_100_01_36	350	0	39.36	44.56	0.08	0.17	14.54	0.05	0	0	0.2	0.27	NA	99.22	84.53
AVF_100_01_37	360	0	39.13	44.07	0.06	0.15	14.48	0.03	0	0	0.2	0.26	NA	98.38	84.44
AVF_100_01_38	370	0	39.46	44.37	0.07	0.15	14.6	0.03	0	0	0.2	0.28	NA	99.16	84.42
AVF_100_01_39	380	0	39.39	44.34	0.07	0.15	14.54	0.03	0	0	0.2	0.29	NA	99.01	84.46
AVF_100_01_40	390	0	39.1	44.01	0.06	0.16	14.42	0.04	0	0	0.2	0.29	NA	98.29	84.47
AVF_100_01_41	400	0	38.2	43.09	0.06	0.14	14.4	0.03	0	0	0.2	0.28	NA	96.41	84.21
AV_100_22_01	0	0	51.98	0.38	25.34	0.03	3.5	0	0	0	9.36	0.01	NA	90.6	16.22
AV_100_22_02	10	0	48.56	2.03	20.14	0.11	5.25	0.01	0	0	11.06	0	NA	87.16	40.80
AV_100_22_03	20	0	44.98	7.81	11.17	0.14	8.68	0.01	0	0	17.68	0.01	NA	90.48	61.60
AV_100_22_04	30	0	46.47	4.93	14.26	0.16	8.01	0.01	0	0	9.91	0	NA	83.75	52.32
AV_100_22_05	40	0	49.84	2.47	18.39	0.17	9.43	-0.01	0	0	6.75	0.01	NA	87.06	31.83
AV_100_22_06	50	0	38.4	39.19	0.04	0.32	21.54	0.02	0	0	0.44	0.13	NA	100.08	76.43
AV_100_22_07	60	0	39.39	42.66	0.04	0.23	17.33	0.03	0	0	0.34	0.17	NA	100.19	81.44

Sample	Dist (μm)	Na_2O	SiO_2	MgO	Al_2O_3	MnO	FeO	Cr_2O_3	K_2O	TiO_2	CaO	NiO	P_2O_5	Total	Mg#
AV_100_22_08	70	0	39.13	42.31	0.03	0.21	17.86	0.03	0	0	0.28	0.19	NA	100.04	80.85
AV_100_22_09	80	0	39.17	42.35	0.04	0.22	17.78	0.03	0	0	0.27	0.19	NA	100.04	80.94
AV_100_22_10	90	0	39.3	42.47	0.04	0.21	17.62	0.04	0	0	0.25	0.2	NA	100.14	81.12
AV_100_22_11	100	0	39.29	42.81	0.04	0.21	17.55	0.02	0	0	0.25	0.2	NA	100.37	81.30
AV_100_22_12	110	0	39.36	42.78	0.04	0.21	17.38	0.02	0	0	0.24	0.21	NA	100.25	81.44
AV_100_22_13	120	0	39.46	42.97	0.05	0.21	17.21	0.04	0	0	0.23	0.2	NA	100.39	81.65
AV_100_22_14	130	0	39.36	42.83	0.06	0.2	16.96	0.04	0	0	0.23	0.21	NA	99.89	81.82
AV_100_22_15	140	0	39.7	43.39	0.07	0.19	16.99	0.02	0	0	0.24	0.21	NA	100.81	81.99
AV_100_22_16	150	0	39.31	42.98	0.05	0.19	17	0.03	0	0	0.23	0.2	NA	99.99	81.84
AV_100_22_17	160	0	39.31	42.87	0.05	0.2	17.09	0.03	0	0	0.23	0.21	NA	99.99	81.72
AV_100_22_18	170	0	39.33	42.9	0.04	0.21	17.1	0.03	0	0	0.25	0.22	NA	100.08	81.73
AV_100_22_19	180	0	39.47	42.74	0.06	0.21	17.2	0.03	0	0	0.24	0.21	NA	100.16	81.58
AV_100_22_20	190	0	39.32	42.56	0.06	0.2	17.25	0.04	0	0	0.24	0.21	NA	99.87	81.47
AV_100_22_21	200	0	40.59	43.99	0.03	0.22	17.6	0.04	0	0	0.25	0.2	NA	102.92	81.67
AV_100_22_22	210	0	39.34	42.41	0.05	0.22	17.48	0.03	0	0	0.27	0.18	NA	99.99	81.22
AV_100_22_23	220	0	39.17	42.44	0.04	0.22	17.47	0.03	0	0	0.28	0.17	NA	99.83	81.24
AV_100_22_24	230	0	39.11	42.17	0.04	0.22	17.72	0.02	0	0	0.32	0.17	NA	99.77	80.92
AV_100_22_25	240	0	37.46	34.53	0.03	0.48	26.79	0.01	0	0	0.49	0.07	NA	99.88	69.67
AV_100_22_26	250	0	49.75	1.5	19.41	0.19	8.83	0.01	0	0	5.52	-0.01	NA	85.21	23.24
AVF_100_Pc04_01	0	0	50.16	0.08	27.3	0.01	1.03	0.01	0	0	11.46	0	NA	90.04	12.16
AVF_100_Pc04_02	10	0	50.95	1.65	20.23	0.21	10.44	0	0	0	4.38	0	NA	87.85	21.98
AVF_100_Pc04_03	20	0	27.34	2.47	18.59	0.32	36.94	0.02	0	0	4.11	0	NA	89.78	10.65
AVF_100_Pc04_04	30	0	51.21	0.72	23.99	0.12	5.39	0	0	0	8.74	0.01	NA	90.18	19.23
AVF_100_Pc04_05	40	0	52.5	0.29	25.76	0.06	3.56	0.01	0	0	9.64	0	NA	91.81	12.68
AVF_100_Pc04_06	50	0	50.06	2.27	18.55	0.17	9.36	0	0	0	6.36	0	NA	86.78	30.18
AVF_100_Pc04_07	60	0	48.95	3.51	17.46	0.2	9.18	0.01	0	0	10.93	0.01	NA	90.25	40.53
AVF_100_Pc04_08	70	0	52.43	0.29	27.46	0.03	2.98	0	0	0	10.24	0	NA	93.43	14.78
AVF_100_Pc04_09	80	0	52.85	0.09	28.28	0.01	0.86	0	0	0	11.6	0.01	NA	93.71	15.72
AVF_100_Pc04_10	90	0	51.61	0.11	28.88	0.02	1.73	0	0	0	12.16	0	NA	94.5	10.18
AVF_100_Pc04_11	100	0	47.04	11.24	7.77	0.19	9.27	0	0	0	22.3	0	NA	97.8	68.37
AVF_100_Pc04_12	110	0	39.19	42.73	0.05	0.25	18.35	0.03	0	0	0.3	0.19	NA	101.11	80.59
AVF_100_Pc04_13	120	0	39.57	43.56	0.05	0.19	16.03	0.03	0	0	0.24	0.25	NA	99.92	82.89
AVF_100_Pc04_14	130	0	39.81	44.17	0.06	0.17	15.51	0.04	0	0	0.22	0.26	NA	100.25	83.54
AVF_100_Pc04_15	140	0	39.85	44.66	0.07	0.17	14.98	0.03	0	0	0.21	0.29	NA	100.26	84.16
AVF_100_Pc04_16	150	0	39.04	43.2	0.3	0.16	14.57	0.04	0	0	0.22	0.29	NA	97.83	84.09
AVF_100_Pc04_17	160	0	41.07	46.16	0.18	0.15	14.63	0.03	0	0	0.22	0.31	NA	102.76	84.90
AVF_100_Pc04_18	170	0	40.67	45.56	0.08	0.16	14.36	0.03	0	0	0.22	0.32	NA	101.4	84.97
AVF_100_Pc04_19	180	0	39.91	45.23	0.07	0.16	14.51	0.03	0	0	0.22	0.33	NA	100.46	84.75
AVF_100_Pc04_20	190	0	39.92	45.07	0.07	0.16	14.33	0.03	0	0	0.2	0.32	NA	100.12	84.86

Sample	Dist (μm)	Na_2O	SiO_2	MgO	Al_2O_3	MnO	FeO	Cr_2O_3	K_2O	TiO_2	CaO	NiO	P_2O_5	Total	Mg#
AVF_100_Pc04_21	200	0	39.68	44.88	0.07	0.16	14.19	0.02	0	0	0.24	0.33	NA	99.57	84.93
AVF_100_Pc04_22	210	0	39.97	45.17	0.08	0.16	14.27	0.03	0	0	0.22	0.34	NA	100.24	84.95
AVF_100_Pc04_23	220	0	39.84	45.1	0.08	0.15	14.46	0.03	0	0	0.21	0.34	NA	100.2	84.76
AVF_100_Pc04_24	230	0	39.85	44.85	0.07	0.15	14.29	0.03	0	0	0.22	0.33	NA	99.79	84.84
AVF_100_Pc04_25	240	0	39.95	45.01	0.09	0.16	14.29	0.03	0	0	0.21	0.32	NA	100.07	84.88
AVF_100_Pc04_26	250	0	39.91	45.04	0.08	0.16	14.14	0.03	0	0	0.2	0.33	NA	99.9	85.03
AVF_100_Pc04_27	260	0	39.94	44.92	0.07	0.15	14.25	0.03	0	0	0.21	0.34	NA	99.91	84.89
AVF_100_Pc04_28	270	0	40.02	45.31	0.08	0.15	14.36	0.03	0	0	0.2	0.34	NA	100.5	84.90
AVF_100_Pc04_29	280	0	39.78	44.85	0.08	0.16	14.33	0.02	0	0	0.22	0.33	NA	99.77	84.80
AVF_100_Pc04_30	290	0	39.89	44.95	0.08	0.15	14.2	0.03	0	0	0.21	0.33	NA	99.84	84.95
AVF_100_Pc04_31	300	0	39.87	44.82	0.07	0.15	14.36	0.04	0	0	0.21	0.34	NA	99.85	84.76
AVF_100_Pc04_32	310	0	39.98	45	0.09	0.15	14.33	0.04	0	0	0.21	0.33	NA	100.14	84.84
AVF_100_Pc04_33	320	0	39.97	45	0.09	0.15	14.27	0.03	0	0	0.21	0.33	NA	100.06	84.90
AVF_100_Pc04_34	330	0	39.99	44.81	0.08	0.16	14.21	0.03	0	0	0.21	0.33	NA	99.82	84.90
AVF_100_Pc04_35	340	0	39.89	45.11	0.09	0.16	14.32	0.04	0	0	0.21	0.33	NA	100.14	84.88
AVF_100_Pc04_36	350	0	40.13	45.01	0.07	0.16	14.29	0.02	0	0	0.21	0.34	NA	100.23	84.88
AVF_100_Pc04_37	360	0	39.91	45.19	0.08	0.15	14.26	0.04	0	0	0.2	0.34	NA	100.17	84.96
AVF_100_Pc04_38	370	0	35.38	37.04	0.3	0.15	14.09	0.03	0	0	0.25	0.34	NA	87.58	82.41
AVF_100_Pc04_39	380	0	34.9	36.52	0.89	0.14	13.86	0.02	0	0	0.29	0.3	NA	86.93	82.45
AVF_100_Pc04_40	390	0	32.53	36.16	0.26	0.15	14.33	0.03	0	0	0.25	0.33	NA	84.05	81.81
AVF_100_Pc04_41	400	0	39.65	44.58	0.08	0.17	14.23	0.05	0	0	0.21	0.33	NA	99.3	84.81
AVF_100_Pc04_42	410	0	40.52	46.53	0.09	0.15	14.2	0.03	0	0	0.21	0.32	NA	102.06	85.38
AVF_100_Pc04_43	420	0	39.94	45.03	0.09	0.16	14.4	0.04	0	0	0.2	0.33	NA	100.19	84.79
AVF_100_Pc04_44	430	0	39.91	45.1	0.07	0.15	14.31	0.03	0	0	0.2	0.32	NA	100.1	84.89
AVF_100_Pc04_45	440	0	39.9	44.9	0.08	0.15	14.28	0.03	0	0	0.21	0.33	NA	99.87	84.86
AVF_100_Pc04_46	450	0	39.93	45.28	0.08	0.16	14.3	0.03	0	0	0.2	0.34	NA	100.33	84.95
AVF_100_Pc04_47	460	0	39.81	45.17	0.07	0.16	14.24	0.03	0	0	0.22	0.33	NA	100.02	84.97
AVF_100_Pc04_48	470	0	39.87	45.1	0.07	0.15	14.2	0.05	0	0	0.2	0.34	NA	99.98	84.99
AVF_100_Pc04_49	480	0	40.02	45.06	0.08	0.15	14.36	0.03	0	0	0.21	0.34	NA	100.25	84.83
AVF_100_Pc04_50	490	0	39.68	45.06	0.09	0.15	14.33	0.03	0	0	0.21	0.34	NA	99.88	84.86
AVF_100_Pc04_51	500	0	39.92	44.98	0.07	0.15	14.26	0.03	0	0	0.21	0.32	NA	99.95	84.90
AVF_100_Pc04_52	510	0	40	45.11	0.08	0.16	14.25	0.03	0	0	0.2	0.32	NA	100.16	84.95
AVF_100_Pc04_53	520	0	39.9	45.17	0.08	0.15	14.23	0.03	0	0	0.2	0.33	NA	100.08	84.98
AVF_100_Pc04_54	530	0	39.95	45.44	0.06	0.15	14.21	0.04	0	0	0.21	0.33	NA	100.39	85.07
AVF_100_Pc04_55	540	0	39.72	45.09	0.11	0.15	14.4	0.04	0	0	0.22	0.33	NA	100.05	84.81
AVF_100_Pc04_56	550	0	39.8	45.2	0.09	0.14	14.37	0.03	0	0	0.21	0.33	NA	100.17	84.86
AVF_100_Pc04_57	560	0	39.69	44.83	0.07	0.14	14.23	0.03	0	0	0.2	0.32	NA	99.51	84.88
AVF_100_Pc04_58	570	0	39.6	45.06	0.12	0.15	14.22	0.03	0	0	0.2	0.33	NA	99.71	84.96
AVF_100_Pc04_59	580	0	39.77	44.83	0.07	0.15	14.2	0.03	0	0	0.2	0.33	NA	99.57	84.91

Sample	Dist (μm)	Na_2O	SiO_2	MgO	Al_2O_3	MnO	FeO	Cr_2O_3	K_2O	TiO_2	CaO	NiO	P_2O_5	Total	Mg#
AVF_100_Pc04_60	590	0	39.84	45.28	0.07	0.15	14.25	0.03	0	0	0.21	0.33	NA	100.16	84.99
AVF_100_Pc04_61	600	0	39.61	45.17	0.12	0.13	14.07	0.03	0	0	0.23	0.32	NA	99.68	85.12
AVF_100_Pc04_62	610	0	32.43	35.32	0.11	0.16	14.23	0.03	0	0	0.21	0.33	NA	82.81	81.56
AVF_100_Pc04_63	620	0	39.43	44.77	0.06	0.16	14.19	0.03	0	0	0.21	0.34	NA	99.19	84.90
AVF_100_Pc04_64	630	0	39.7	44.81	0.09	0.15	14.22	0.03	0	0	0.22	0.32	NA	99.53	84.89
AVF_100_Pc04_65	640	0	39.87	45.28	0.07	0.16	14.41	0.03	0	0	0.2	0.34	NA	100.36	84.85
AVF_100_Pc04_66	650	0	40.26	43.17	0.6	0.14	14.73	0.04	0	0	0.28	0.32	NA	99.54	83.93
AVF_100_Pc04_67	660	0	39.64	44.89	0.08	0.15	14.28	0.03	0	0	0.19	0.34	NA	99.6	84.86
AVF_100_Pc04_68	670	0	39.64	45.02	0.07	0.15	14.27	0.03	0	0	0.2	0.32	NA	99.69	84.90
AVF_100_Pc04_69	680	0	39.54	44.81	0.09	0.16	14.18	0.03	0	0	0.21	0.32	NA	99.34	84.92
AVF_100_Pc04_70	690	0	39.76	44.97	0.09	0.15	14.21	0.02	0	0	0.2	0.33	NA	99.72	84.94
AVF_100_Pc04_71	700	0	39.63	44.99	0.06	0.14	14.3	0.02	0	0	0.2	0.33	NA	99.68	84.87
AVF_100_Pc04_72	710	0	39.62	45.08	0.08	0.16	14.46	0.03	0	0	0.21	0.33	NA	99.97	84.75
AVF_100_Pc04_73	720	0	39.51	44.99	0.07	0.15	14.41	0.03	0	0	0.2	0.34	NA	99.69	84.77
AVF_100_Pc04_74	730	0	39.57	44.9	0.07	0.15	14.27	0.03	0	0	0.2	0.34	NA	99.54	84.87
AVF_100_Pc04_75	740	0	39.61	44.97	0.06	0.15	14.4	0.03	0	0	0.2	0.33	NA	99.75	84.77
AVF_100_Pc04_76	750	0	39.49	43.87	0.1	0.14	14.31	0.03	0	0	0.21	0.33	NA	98.48	84.53
AVF_100_Pc04_77	760	0	39.42	44.81	0.06	0.14	14.32	0.04	0	0	0.19	0.34	NA	99.33	84.80
AVF_100_Pc04_78	770	0	39.35	44.83	0.06	0.15	14.26	0.03	0	0	0.21	0.33	NA	99.23	84.86
AVF_100_Pc04_79	780	0	39.5	44.9	0.1	0.16	14.25	0.03	0	0	0.21	0.34	NA	99.48	84.89
AVF_100_Pc04_80	790	0	39.64	45.17	0.05	0.15	14.32	0.04	0	0	0.2	0.34	NA	99.91	84.90
AVF_100_Pc04_81	800	0	39.61	45.07	0.05	0.16	14.21	0.03	0	0	0.2	0.34	NA	99.67	84.97
AVF_100_Pc04_82	810	0	40	45.86	0.07	0.15	14.25	0.03	0	0	0.21	0.32	NA	100.9	85.16
AVF_100_Pc04_83	820	0	39.31	44.87	0.06	0.15	14.25	0.03	0	0	0.2	0.33	NA	99.2	84.88
AVF_100_Pc04_84	830	0	39.27	44.53	0.11	0.16	14.21	0.04	0	0	0.21	0.33	NA	98.86	84.82
AVF_100_Pc04_85	840	0	39.22	44.11	0.71	0.14	14.22	0.03	0	0	0.22	0.32	NA	98.97	84.68
AVF_100_Pc04_86	850	0	39.46	45.06	0.09	0.15	14.36	0.03	0	0	0.2	0.31	NA	99.66	84.83
AVF_100_Pc04_87	860	0	39.5	45	0.09	0.15	14.35	0.04	0	0	0.2	0.31	NA	99.64	84.83
AVF_100_Pc04_88	870	0	39.64	45.18	0.08	0.15	14.29	0.04	0	0	0.2	0.31	NA	99.89	84.93
AVF_100_Pc04_89	880	0	39.64	45.28	0.05	0.16	14.36	0.03	0	0	0.2	0.3	NA	100.03	84.90
AVF_100_Pc04_90	890	0	39.66	45.09	0.06	0.15	14.4	0.04	0	0	0.2	0.3	NA	99.9	84.81
AVF_100_Pc04_91	900	0	39.34	45	0.06	0.17	14.46	0.04	0	0	0.2	0.28	NA	99.54	84.73
AVF_100_Pc04_92	910	0	39.4	44.88	0.05	0.16	14.52	0.04	0	0	0.19	0.31	NA	99.54	84.64
AVF_100_Pc04_93	920	0	39.3	44.77	0.14	0.15	14.56	0.04	0	0	0.21	0.29	NA	99.45	84.57
AVF_100_Pc04_94	930	0	39.32	44.85	0.05	0.17	14.66	0.04	0	0	0.2	0.27	NA	99.56	84.50
AVF_100_Pc04_95	940	0	39.37	44.56	0.06	0.15	14.64	0.04	0	0	0.2	0.27	NA	99.28	84.44
AVF_100_Pc04_96	950	0	39.29	44.6	0.08	0.16	14.69	0.03	0	0	0.21	0.26	NA	99.31	84.40
AVF_100_Pc04_97	960	0	39.26	44.52	0.07	0.15	14.94	0.04	0	0	0.21	0.26	NA	99.47	84.16
AVF_100_Pc04_98	970	0	39.27	44.09	0.06	0.17	15.29	0.04	0	0	0.21	0.25	NA	99.38	83.71

Sample	Dist (μm)	Na_2O	SiO_2	MgO	Al_2O_3	MnO	FeO	Cr_2O_3	K_2O	TiO_2	CaO	NiO	P_2O_5	Total	Mg#
AVF_100_Pc04_99	980	0	38.89	43.32	0.05	0.19	16.03	0.04	0	0	0.22	0.22	NA	98.95	82.81
AVF_100_Pc04_100	990	0	38.76	43.06	0.05	0.19	16.58	0.05	0	0	0.22	0.21	NA	99.12	82.24
AVF_100_Pc04_101	1000	0	39	42.75	0.06	0.19	17.04	0.04	0	0	0.23	0.2	NA	99.52	81.73
AVF_100_Pc04_102	1010	0	38.62	42.47	0.04	0.2	17.32	0.05	0	0	0.24	0.19	NA	99.13	81.38
AVF_100_Pc04_103	1020	0	38.62	42.14	0.04	0.21	17.51	0.04	0	0	0.26	0.18	NA	98.99	81.10
AVF_100_Pc04_104	1030	0	38.61	41.09	0.79	0.22	17.18	0.03	0	0	0.31	0.17	NA	98.4	81.00
AVF_100_Pc04_105	1040	0	38.21	41.45	0.03	0.25	17.57	0.03	0	0	0.36	0.15	NA	98.04	80.79
AVF_100_Pc04_106	1050	0	37.75	40.36	0.03	0.25	18.61	0.03	0	0	0.39	0.12	NA	97.55	79.45
AVF_100_Pc04_107	1060	0	40.11	25.92	5.22	0.49	28.73	0.01	0	0	1.55	0.04	NA	102.06	61.66
AVF_100_Pc04_108	1070	0	48.58	2.12	18.59	0.18	12.13	0.02	0	0	4.7	0.01	NA	86.33	23.75
AVF_100_Pc04_109	1080	0	42.27	10.28	9.4	0.12	9.09	0	0	0	21.58	0.01	NA	92.76	66.84
AVF 100_Pc07_1		0	39.13	41.33	0.05	0.29	19.18	0.02	0	0	0.46	0.13	NA	100.57	79.34
AVF 100_Pc07_2		0	38.69	40.58	0.06	0.3	19.28	0.02	0	0	0.37	0.12	NA	99.41	78.96
AVF 100_Pc07_3		0	39.35	43.21	0.03	0.2	16.52	0.03	0	0	0.23	0.22	NA	99.79	82.34
AVF 100_Pc07_4		0	41.11	9.86	10.82	0.12	9.04	0.02	0	0	22.52	0.01	NA	93.5	66.04
AVF 100_Pc07_5		0	39.81	44.66	0.06	0.15	14.87	0.04	0	0	0.21	0.29	NA	100.1	84.26
AVF 100_Pc07_6		0	39.01	41.39	0.03	0.27	18.66	0.03	0	0	0.42	0.13	NA	99.94	79.81
AVF 100_Pc07_7		0	41.81	10.52	9.81	0.1	8.55	0.16	0	0	22.56	0.01	NA	93.52	68.68
AVF 100_Pc07_8		0	39.46	43.29	0.05	0.19	16.47	0.03	0	0	0.23	0.24	NA	99.94	82.41
AVF 100_Pc07_9		0	38.3	39.25	0.03	0.32	22.29	0.01	0	0	0.38	0.12	NA	100.7	75.84
VMA1_Ol 01_01	0	1.23	43.68	8.94	12.44	0.14	9.46	0.02	0.3	4.59	20.95	-0.01	0.35	102.08	62.75
VMA1_Ol 01_02	4	0.53	44.27	11.91	7.92	0.09	7.92	0.27	0.01	3.7	22.85	0.01	0.25	99.72	72.83
VMA1_Ol 01_03	8	0.08	42.09	35.25	0.91	0.27	18.24	0.05	0	0.4	4.87	0.08	0.09	102.33	77.50
VMA1_Ol 01_04	12	0.01	39.13	41.25	0.04	0.26	19.01	0.02	0	0.06	0.47	0.12	0.02	100.4	79.46
VMA1_Ol 01_05	16	0.02	39.78	41.48	0.03	0.27	18.38	0.01	-0.01	0.05	0.44	0.09	0.03	100.57	80.09
VMA1_Ol 01_06	20	0.02	39.12	42.17	0.02	0.31	18.03	0.03	0	0.04	0.4	0.12	0.01	100.26	80.65
VMA1_Ol 01_07	24	0.01	39.18	42.73	0.02	0.27	17.68	0.03	0	0.04	0.38	0.12	0.03	100.5	81.16
VMA1_Ol 01_08	28	0.03	39.26	42.95	0.02	0.23	17.1	0.05	0.01	0.02	0.36	0.19	0.04	100.25	81.74
VMA1_Ol 01_09	32	0	40.12	43.04	0.04	0.27	16.95	0.04	0	0.03	0.34	0.16	0.05	101.03	81.90
VMA1_Ol 01_10	36	0.01	39.66	43.09	0.01	0.24	16.71	0.03	0	0.03	0.35	0.19	0.05	100.38	82.13
VMA1_Ol 01_11	40	0.03	39.39	43.37	0.06	0.25	16.74	0.03	0	0.02	0.32	0.16	0	100.38	82.20
VMA1_Ol 01_12	44	0	39.46	42.98	0.03	0.22	17.13	0.04	0	0.03	0.24	0.2	0.01	100.34	81.73
VMA1_Ol 01_13	48	0.01	39.56	42.72	-0.01	0.23	17.21	0.03	0.01	0.01	0.23	0.22	0.02	100.25	81.57
VMA1_Ol 01_14	52	0.02	39.17	43.25	0.07	0.2	17.42	0.04	-0.01	0.03	0.25	0.22	0.03	100.68	81.57
VMA1_Ol 01_15	56	0.02	39.58	43.06	0.08	0.23	16.9	0.05	-0.01	0.03	0.23	0.24	0.03	100.44	81.96
VMA1_Ol 01_16	60	0.01	39.66	43.45	0.06	0.25	16.67	0.07	0.01	0.02	0.22	0.21	0.03	100.66	82.29
VMA1_Ol 01_17	64	0.01	39.54	43.95	0.08	0.2	16.37	0.03	0	0.02	0.21	0.19	0	100.6	82.72
VMA1_Ol 01_18	68	0.02	40.01	44.15	0.06	0.23	15.81	0.06	0	0.01	0.23	0.28	0.01	100.85	83.27
VMA1_Ol 01_19	72	0.01	40.23	44.22	0.03	0.2	15.5	0.04	0.01	0.02	0.23	0.24	0.03	100.75	83.57

Sample	Dist (μm)	Na_2O	SiO_2	MgO	Al_2O_3	MnO	FeO	Cr_2O_3	K_2O	TiO_2	CaO	NiO	P_2O_5	Total	Mg#
VMA1_Ol 01_20	76	0.01	39.71	44.54	0.07	0.21	15.37	0.04	0	0.02	0.23	0.24	0.02	100.46	83.78
VMA1_Ol 01_21	80	0.02	40.3	45	0.07	0.19	15.09	0.04	0	0.01	0.21	0.25	-0.01	101.18	84.17
VMA1_Ol 01_22	84	0.02	40.3	42.8	0.31	0.19	14.49	0.06	0.01	0.13	0.22	0.23	0.02	98.79	84.04
VMA1_Ol 01_23	88	0.01	40.11	45.15	0.06	0.19	14.54	0.03	0	0.01	0.24	0.24	0	100.58	84.70
VMA1_Ol 01_24	92	0.01	40.14	45.49	0.05	0.17	14.5	0.03	0	0.01	0.21	0.25	0.01	100.87	84.83
VMA1_Ol 01_25	96	0.01	40.31	45.49	0.06	0.2	14.18	0.04	0	0.01	0.2	0.25	0.01	100.78	85.12
VMA1_Ol 01_26	100	0.03	40.01	45.67	0.03	0.16	14.13	0.03	0	0.01	0.22	0.34	0.02	100.63	85.21
VMA1_Ol 01_27	104	0.03	39.59	45.67	0.43	0.18	13.98	0.05	0.01	0.11	0.26	0.31	0.03	100.65	85.34
VMA1_Ol 01_28	108	0.01	39.99	45.79	0.05	0.17	13.96	0.06	0	0.01	0.2	0.3	-0.02	100.53	85.39
VMA1_Ol 01_29	112	0.01	40.27	45.6	0.06	0.16	13.86	0.04	0	0.02	0.2	0.34	0.03	100.59	85.43
VMA1_Ol 01_30	116	0.02	39.7	45.86	0.07	0.18	13.86	0.06	0	0	0.22	0.26	0.01	100.24	85.50
VMA1_Ol 01_31	120	0.02	39.95	45.82	0.05	0.16	13.8	0.04	0	0.01	0.22	0.27	0.03	100.38	85.55
VMA1_Ol 01_32	124	0.03	39.02	43.67	0.39	0.14	13.62	0.03	0.01	0.34	0.3	0.26	0.01	97.82	85.11
VMA1_Ol 01_33	128	0	40.03	46.01	0.04	0.17	13.68	0.04	0	0.02	0.2	0.33	0.02	100.54	85.70
VMA1_Ol 01_34	132	0.02	40.11	45.92	0.05	0.17	13.63	0.03	0	0.02	0.21	0.29	0.01	100.46	85.73
VMA1_Ol 01_35	136	0.02	40.29	45.75	0.08	0.18	13.67	0.05	0	0.01	0.21	0.24	0.02	100.53	85.64
VMA1_Ol 01_36	140	0.02	39.97	46.17	0.06	0.17	13.81	0.06	0	0.02	0.21	0.3	0.01	100.8	85.63
VMA1_Ol 01_37	144	0.02	40.28	46.24	0.07	0.17	13.76	0.04	0	0.01	0.2	0.28	0.02	101.09	85.69
VMA1_Ol 01_38	148	0.01	40.3	46.09	0.05	0.17	13.75	0.05	0	0.01	0.21	0.27	0.02	100.93	85.66
VMA1_Ol 01_39	152	0.04	40.02	45.88	0.17	0.16	13.65	0.05	0	0.02	0.2	0.28	0.01	100.47	85.70
VMA1_Ol 01_40	156	0.02	39.92	46.05	0.06	0.17	13.74	0.05	0	0.01	0.2	0.32	0.05	100.58	85.66
VMA1_Ol 01_41	160	0.01	40.1	45.88	0.1	0.22	13.69	0.03	0.01	0.01	0.2	0.27	0.06	100.59	85.66
VMA1_Ol 01_42	164	0	40.25	46.25	0.05	0.16	13.68	0.05	0	0.01	0.2	0.29	0.05	101.02	85.77
VMA1_Ol 01_43	168	0.03	40.35	45.98	0.04	0.16	13.78	0.04	0	0	0.22	0.3	0.01	100.91	85.61
VMA1_Ol 01_44	172	0.02	40.04	46.17	0.04	0.19	13.75	0.07	0	0.01	0.19	0.29	0.01	100.79	85.68
VMA1_Ol 01_45	176	0.01	40	46.21	0.04	0.15	13.77	0.04	0.01	0.01	0.21	0.3	0.01	100.75	85.68
VMA1_Ol 01_46	180	0.02	40.12	45.99	0.05	0.18	13.87	0.04	0	0	0.21	0.28	-0.01	100.75	85.53
VMA1_Ol 01_47	184	0.01	40.12	45.78	0.04	0.2	14	0.07	0	0.02	0.21	0.33	0	100.78	85.36
VMA1_Ol 01_48	188	0.02	39.97	45.64	0.05	0.21	14.18	0.06	-0.01	0.02	0.2	0.33	0	100.66	85.16
VMA1_Ol 01_49	192	0.02	39.93	45.62	0.05	0.19	14.29	0.05	0	0.01	0.21	0.3	0	100.67	85.05
VMA1_Ol 01_50	196	0.01	39.99	45.2	0.04	0.16	14.83	0.05	0	0.02	0.21	0.31	-0.02	100.78	84.46
VMA1_Ol 01_51	200	0.01	39.7	44.95	0.08	0.21	15.33	0.05	0	0	0.23	0.23	-0.01	100.78	83.94
VMA1_Ol 01_52	204	0.01	39.28	44.23	0.03	0.21	15.89	0.03	0	0.01	0.23	0.24	0	100.16	83.23
VMA1_Ol 01_53	208	0.02	39.23	43.46	0.04	0.22	16.77	0.02	0	0.01	0.22	0.2	0.01	100.2	82.20
VMA1_Ol 01_54	212	0.02	38.92	42.37	0.03	0.3	18.49	0.02	-0.01	0.02	0.32	0.13	-0.01	100.61	80.33
VMA1_Ol 01_55	216	0.5	24.8	15.96	5.05	0.3	15.26	-0.01	0.48	0.67	2.84	0.02	0.43	66.31	65.09
VMA1_Ol 06_01	0	0.57	45.04	11.61	7.92	0.16	8.4	0.07	0.01	3.43	22.34	-0.01	0.28	99.84	71.13
VMA1_Ol 06_02	4	0.54	44.84	11.94	7.46	0.11	8.1	0.18	0.02	3.23	22.61	0.02	0.28	99.33	72.43
VMA1_Ol 06_03	8	0.39	49	14.1	4.18	0.09	7.47	0.32	0.01	1.98	22.4	0.01	0.27	100.2	77.09

Sample	Dist (μm)	Na_2O	SiO_2	MgO	Al_2O_3	MnO	FeO	Cr_2O_3	K_2O	TiO_2	CaO	NiO	P_2O_5	Total	Mg#
VMA1_Ol 06_04	12	0.08	39.75	39.04	0.96	0.34	18.87	0.04	0	0.36	0.86	0.05	0.04	100.39	78.67
VMA1_Ol 06_05	16	0.03	39.27	40.55	0.07	0.31	19.91	0.02	0	0.04	0.47	0.11	0.03	100.81	78.40
VMA1_Ol 06_06	20	0.02	38.63	40.91	-0.01	0.34	19.52	0.03	0	0.03	0.47	0.1	0.04	100.08	78.88
VMA1_Ol 06_07	24	0.01	38.77	40.71	0.02	0.29	19.18	0.02	0	0.03	0.44	0.07	0.02	99.56	79.09
VMA1_Ol 06_08	28	0.01	39.04	41.28	0.04	0.26	19.2	0.04	0	0.02	0.41	0.1	0.02	100.42	79.31
VMA1_Ol 06_09	32	0.02	38.97	41.06	0.04	0.34	19.36	0.04	0	0.05	0.39	0.1	0.03	100.41	79.08
VMA1_Ol 06_10	36	0.02	38.6	41.66	0.02	0.26	18.84	0.02	0	0.03	0.38	0.1	0.04	99.96	79.76
VMA1_Ol 06_11	40	0.02	39.26	41.91	0.03	0.31	18.26	0.03	0	0.04	0.38	0.16	0.02	100.42	80.36
VMA1_Ol 06_12	44	0.01	38.91	42.08	0.02	0.25	18.09	0.02	0	0.02	0.37	0.15	0.01	99.94	80.57
VMA1_Ol 06_13	48	0.02	39.19	42.21	0.02	0.29	17.89	0.02	0	0.02	0.39	0.14	0.05	100.23	80.79
VMA1_Ol 06_14	52	0.01	39.37	42.56	-0.01	0.27	17.77	0.04	0	0.02	0.34	0.11	0.01	100.5	81.02
VMA1_Ol 06_15	56	0	39.47	42.37	0.01	0.26	17.66	0.03	0.01	0.03	0.34	0.14	0.04	100.36	81.05
VMA1_Ol 06_16	60	0.02	39.37	42.92	0.02	0.29	17.27	0.02	0	0.02	0.34	0.15	0.02	100.45	81.58
VMA1_Ol 06_17	64	0.01	39.39	43.28	0.04	0.22	17.2	0.03	0	0.03	0.34	0.16	0.01	100.72	81.77
VMA1_Ol 06_18	68	0.02	39.2	43.13	0.06	0.28	17.02	0.02	0.01	0.02	0.33	0.19	0.04	100.32	81.87
VMA1_Ol 06_19	72	0.03	39.45	42.99	0.04	0.24	17.23	0.03	0	0.03	0.28	0.16	0.06	100.55	81.64
VMA1_Ol 06_20	76	0.01	39.29	42.65	0.05	0.25	17.32	0.06	-0.01	0.01	0.28	0.18	0.02	100.11	81.45
VMA1_Ol 06_21	80	0.01	39.48	42.71	0.07	0.23	17.34	0.03	0	0.04	0.26	0.16	0	100.31	81.45
VMA1_Ol 06_22	84	0.03	39.4	42.83	0.06	0.22	17.27	0.04	0	0.02	0.27	0.2	0.03	100.37	81.55
VMA1_Ol 06_23	88	0.06	38.48	36.4	1.51	0.21	16.98	0	0.09	0.73	0.33	0.18	0.01	94.99	79.26
VMA1_Ol 06_24	92	0.03	39.48	42.92	0.07	0.26	17.28	0.03	-0.01	0.03	0.24	0.22	0.02	100.58	81.58
VMA1_Ol 06_25	96	0.01	39.66	42.85	0.06	0.2	17.26	0.05	0	0.03	0.23	0.19	0.02	100.55	81.57
VMA1_Ol 06_26	100	0.02	39.07	42.93	0.08	0.24	17.13	0.06	-0.01	0.01	0.22	0.19	0.01	99.96	81.71
VMA1_Ol 06_27	104	0.01	39.39	43.01	0.04	0.21	17.08	0.04	0	0.02	0.22	0.2	0.03	100.26	81.78
VMA1_Ol 06_28	108	0.02	39.24	43.02	0.06	0.22	17.15	0.03	0.01	0.02	0.23	0.22	0.04	100.25	81.72
VMA1_Ol 06_29	112	0.03	39.73	43.21	0.06	0.22	16.87	0.02	0	0.01	0.21	0.24	0.02	100.63	82.03
VMA1_Ol 06_30	116	0.02	39.58	43.29	0.03	0.19	16.73	0.03	0	0.02	0.21	0.21	-0.01	100.31	82.18
VMA1_Ol 06_31	120	0.04	39.36	43.49	0.06	0.17	16.53	0.06	0	0.01	0.21	0.22	0.01	100.15	82.42
VMA1_Ol 06_32	124	0.02	39.6	43.99	0.05	0.22	16.22	0.05	0	0.01	0.22	0.21	0.04	100.62	82.86
VMA1_Ol 06_33	128	0.01	39.74	43.98	0.06	0.2	16.05	0.04	0	0.01	0.21	0.21	0.01	100.51	83.01
VMA1_Ol 06_34	132	0.02	39.82	44.08	0.06	0.21	15.72	0.03	0	0.01	0.21	0.24	0	100.4	83.33
VMA1_Ol 06_35	136	0.03	39.8	44.24	0.04	0.2	15.42	0.06	-0.01	0.01	0.2	0.25	0.03	100.27	83.64
VMA1_Ol 06_36	140	0.02	39.73	44.74	0.09	0.2	15.33	0.03	0.01	0.02	0.21	0.28	0.03	100.66	83.88
VMA1_Ol 06_37	144	0.01	40.05	44.49	0.06	0.18	14.99	0.04	0	0.01	0.2	0.25	0	100.29	84.10
VMA1_Ol 06_38	148	0.01	39.85	44.98	0.04	0.2	14.89	0.03	0.01	0.02	0.22	0.23	0.02	100.49	84.34
VMA1_Ol 06_39	152	0.02	40.19	44.97	0.1	0.21	14.66	0.04	0	0.01	0.19	0.25	0.02	100.68	84.54
VMA1_Ol 06_40	156	0	39.92	45.06	0.07	0.15	14.48	0.04	0	0	0.2	0.25	0	100.16	84.73
VMA1_Ol 06_41	160	0.02	40.34	45.26	0.04	0.17	14.47	0.03	0	0.01	0.19	0.26	0.01	100.8	84.79
VMA1_Ol 06_42	164	0.02	39.93	45.53	0.04	0.19	14.5	0.02	0	0.01	0.2	0.32	-0.01	100.74	84.84

Sample	Dist (μm)	Na_2O	SiO_2	MgO	Al_2O_3	MnO	FeO	Cr_2O_3	K_2O	TiO_2	CaO	NiO	P_2O_5	Total	Mg#
VMA1_Ol 06_43	168	0.01	39.98	45.32	0.05	0.18	14.22	0.05	0	0.01	0.2	0.27	0.02	100.31	85.03
VMA1_Ol 06_44	172	0.02	39.77	45.48	0.06	0.19	14.26	0.05	0	0.03	0.2	0.29	0.04	100.4	85.04
VMA1_Ol 06_45	176	0.03	40.08	45.33	0.07	0.21	14.21	0.03	-0.01	0.01	0.19	0.25	0.01	100.42	85.04
VMA1_Ol 06_46	180	0.02	39.78	45.64	0.07	0.2	14.23	0.04	0	0.01	0.22	0.24	-0.02	100.42	85.11
VMA1_Ol 06_47	184	0.02	39.76	45.25	0.04	0.2	14.1	0.04	-0.01	0.02	0.21	0.26	0.02	99.91	85.12
VMA1_Ol 06_48	188	0.02	39.77	45.49	0.07	0.2	14.24	0.04	0	0.02	0.19	0.3	0.03	100.36	85.06
VMA1_Ol 06_49	192	0.01	39.94	45.54	0.07	0.2	14.32	0.04	0	0.01	0.21	0.25	0.01	100.6	85.00
VMA1_Ol 06_50	196	0.01	39.79	45.87	0.03	0.18	13.94	0.04	0	0.02	0.21	0.29	0	100.38	85.43
VMA1_Ol 06_51	200	0.03	40.11	45.65	0.04	0.16	14.24	0.02	0	0.02	0.21	0.27	0.01	100.75	85.11
VMA1_Ol 06_52	204	0.02	39.93	45.42	0.09	0.2	14.13	0.03	0	0.01	0.21	0.28	0.01	100.34	85.14
VMA1_Ol 06_53	208	0	40.16	45.35	0.06	0.17	14.03	0.04	0	0.01	0.21	0.26	0	100.28	85.21
VMA1_Ol 06_54	212	0.03	40.16	45.5	0.08	0.15	14.23	0.05	-0.01	0.02	0.2	0.28	0.01	100.72	85.07
VMA1_Ol 06_55	216	0.02	40.1	45.6	0.06	0.16	14.24	0.04	0.01	0.02	0.21	0.28	0	100.75	85.09
VMA1_Ol 06_56	220	0.01	39.85	45.53	0.03	0.19	14.18	0.03	0	0.01	0.22	0.29	0.01	100.35	85.13
VMA1_Ol 06_57	224	0.02	39.87	45.49	0.04	0.16	14.2	0.04	-0.01	0.01	0.21	0.28	0.01	100.34	85.10
VMA1_Ol 06_58	228	0.02	40.15	45.7	0.06	0.16	14.15	0.03	0	0.01	0.2	0.25	0.03	100.75	85.20
VMA1_Ol 06_59	232	0.02	40.09	45.74	0.06	0.19	14.25	0.04	0	0.01	0.21	0.29	0.01	100.92	85.12
VMA1_Ol 06_60	236	-0.01	40	45.77	0.05	0.21	14.19	0.02	-0.01	0.01	0.22	0.28	0	100.73	85.18
VMA1_Ol 06_61	240	0.01	40.05	45.42	0.07	0.16	14.06	0.05	0	0.01	0.21	0.28	0.02	100.34	85.20
VMA1_Ol 06_62	244	0.02	39.98	45.43	0.07	0.15	14.04	0.05	0	0	0.21	0.3	0.01	100.26	85.22
VMA1_Ol 06_63	248	0.02	40.08	45.77	0.04	0.17	14.21	0.04	0	0.01	0.21	0.25	0.01	100.82	85.17
VMA1 ol 07_01	0	0.68	42.56	10.67	9.83	0.12	8.43	0.04	0.05	4.32	22.29	0	0.28	99.28	69.29
VMA1 ol 07_02	4	0.53	44.59	11.93	8.04	0.13	8.08	0.12	0	3.56	22.51	0.03	0.25	99.77	72.47
VMA1 ol 07_03	8	0	38.67	40.78	0.04	0.31	19.47	0.04	0	0.07	0.49	0.13	0.02	100.03	78.87
VMA1 ol 07_04	12	0.01	38.76	41.47	0.02	0.29	18.59	0.03	0	0.05	0.43	0.12	0.04	99.8	79.91
VMA1 ol 07_05	16	0.01	39.19	41.65	0.03	0.27	18	0.02	0	0.04	0.42	0.1	0.06	99.78	80.49
VMA1 ol 07_06	20	0.02	39.22	42.56	0.03	0.27	17.52	0.06	0	0.03	0.35	0.12	0.02	100.2	81.24
VMA1 ol 07_07	24	0	39.51	43.05	0.05	0.25	17.29	0.05	0	0.04	0.35	0.16	0.04	100.8	81.61
VMA1 ol 07_08	28	0.01	39.45	42.96	0.07	0.28	17.15	0.05	0	0.03	0.33	0.15	0.07	100.56	81.70
VMA1 ol 07_09	32	0.01	39.35	42.72	0.07	0.22	17.31	0.02	0	0.02	0.27	0.16	0.03	100.18	81.48
VMA1 ol 07_10	36	0	39.49	42.93	0.05	0.22	17.49	0.03	-0.01	0.03	0.25	0.19	0.05	100.72	81.40
VMA1 ol 07_11	40	0.02	39.33	43.02	0.01	0.23	17.36	0.03	0	0.02	0.25	0.2	0.03	100.48	81.54
VMA1 ol 07_12	44	0.01	39.43	42.75	0.06	0.25	17.41	0.03	0	0.02	0.24	0.18	0.03	100.4	81.40
VMA1 ol 07_13	48	0.02	39.37	42.95	0.06	0.21	17.27	0.04	0	0.02	0.25	0.24	0.05	100.47	81.59
VMA1 ol 07_14	52	0.02	39.8	43.01	0.04	0.21	17.01	0.03	0	0.01	0.22	0.22	0	100.58	81.84
VMA1 ol 07_15	56	0.02	39.64	43.43	0.06	0.22	16.8	0.05	0	0.02	0.21	0.25	0.03	100.72	82.17
VMA1 ol 07_16	60	0.02	39.53	43.52	0.03	0.26	16.5	0.05	0	0.01	0.23	0.2	0.02	100.36	82.46
VMA1 ol 07_17	64	0.02	39.84	43.84	0.06	0.18	16.41	0.05	0	0.01	0.22	0.23	-0.01	100.84	82.65
VMA1 ol 07_18	68	0.01	39.61	43.73	0.03	0.23	16.24	0.04	0	0.01	0.21	0.18	0.02	100.29	82.76

Sample	Dist (μm)	Na_2O	SiO_2	MgO	Al_2O_3	MnO	FeO	Cr_2O_3	K_2O	TiO_2	CaO	NiO	P_2O_5	Total	Mg#
VMA1 ol 07_19	73	0.02	39.45	43.92	0.07	0.15	16.2	0.05	0	0.03	0.21	0.22	0.04	100.34	82.86
VMA1 ol 07_20	77	0.02	39.8	43.87	0.04	0.18	15.95	0.05	0	0.02	0.22	0.23	-0.01	100.38	83.06
VMA1 ol 07_21	81	0.02	39.8	44.45	0.05	0.21	15.77	0.02	0	0.01	0.21	0.27	0	100.81	83.40
VMA1 ol 07_22	85	0.03	40.03	44.32	0.07	0.18	15.47	0.02	0	0.02	0.22	0.26	0.03	100.64	83.62
VMA1 ol 07_23	89	0.01	39.58	44.53	0.04	0.19	15.36	0.03	0	0.02	0.22	0.25	0.05	100.29	83.79
VMA1 ol 07_24	93	0.03	39.93	44.54	0.15	0.19	14.97	0.03	-0.01	0.01	0.22	0.28	0.02	100.35	84.14
VMA1 ol 07_25	97	0	39.92	45.26	0.06	0.15	14.57	0.07	0	0	0.2	0.28	0.02	100.54	84.70
VMA1 ol 07_26	101	0.01	39.95	45.32	0.06	0.16	14.34	0.03	0.01	0.02	0.2	0.31	0.03	100.42	84.93
VMA1 ol 07_27	105	0.01	39.88	45.54	0.07	0.18	14.18	0.04	0	0.01	0.21	0.26	0.03	100.4	85.13
VMA1 ol 07_28	109	0.01	40.27	45.61	0.06	0.17	14.26	0.03	0	0.02	0.18	0.3	0	100.9	85.08
VMA1 ol 07_29	113	0.03	39.93	45.72	0.09	0.15	13.93	0.04	0	0.02	0.21	0.3	0.03	100.46	85.40
VMA1 ol 07_30	117	0.01	40.36	45.9	0.09	0.17	13.93	0.04	0	0.01	0.19	0.29	0.03	101.01	85.45
VMA1 ol 07_31	121	0	40.02	45.92	0.07	0.16	13.93	0.02	0	0.01	0.2	0.28	0.01	100.64	85.46
VMA1 ol 07_32	125	0.02	40.12	45.95	0.06	0.14	13.56	0.03	-0.01	0.02	0.18	0.31	0	100.39	85.80
VMA1 ol 07_33	129	0.03	40.01	45.79	0.05	0.16	13.77	0.02	-0.01	0.01	0.2	0.32	0.01	100.37	85.56
VMA1 ol 07_34	133	-0.01	40.18	45.81	0.09	0.18	13.71	0.03	0	0.01	0.21	0.33	0.02	100.56	85.62
VMA1 ol 07_35	137	0.03	40.16	45.94	0.06	0.16	13.75	0.03	0	-0.01	0.21	0.33	0.01	100.69	85.62
VMA1 ol 07_36	141	0.02	40.36	45.89	0.09	0.17	13.61	0.03	0	0	0.21	0.31	0.01	100.7	85.74
VMA1 ol 07_37	145	0.03	40.13	46.18	0.09	0.17	13.68	0.03	0	0	0.2	0.33	0.02	100.87	85.75
VMA1 ol 07_38	149	0.03	40.13	45.97	0.04	0.17	13.92	0.03	0	0.01	0.18	0.36	0	100.84	85.48
VMA1 ol 07_39	153	0.01	40	45.96	0.08	0.15	13.71	0.04	0.01	0.01	0.22	0.33	0.01	100.52	85.66
VMA1 ol 07_40	157	0	39.98	45.9	0.09	0.16	13.82	0.03	0	0	0.21	0.32	0.02	100.54	85.55
VMA1 ol 07_41	161	0.03	39.95	45.95	0.07	0.18	13.87	0.02	0	0.01	0.22	0.32	0	100.65	85.52
VMA1 ol 07_42	165	0.03	40.13	45.61	0.1	0.14	13.56	0.03	0.01	0.01	0.21	0.34	-0.01	100.15	85.71
VMA1 ol 07_43	169	0.01	39.82	45.96	0.06	0.14	13.77	0.03	0	0	0.2	0.31	0.03	100.34	85.61
VMA1 ol 07_44	173	0	40	45.84	0.04	0.15	13.74	0.04	0.01	0	0.2	0.32	0.03	100.36	85.61
VMA1 ol 07_45	177	-0.01	39.86	46.04	0.05	0.17	13.76	0.03	0	0.01	0.2	0.29	-0.01	100.4	85.64
VMA1 ol 07_46	181	0.03	40.08	46.01	0.05	0.14	13.73	0.05	0	0.01	0.21	0.33	0	100.63	85.66
VMA1 ol 07_47	185	0.03	40.01	45.92	0.04	0.16	13.72	0.02	0	0.01	0.21	0.35	0.03	100.5	85.64
VMA1 ol 07_48	189	0.01	40.22	46.01	0.08	0.18	13.73	0.04	-0.01	0.01	0.21	0.36	0	100.84	85.66
VMA1 ol 07_49	193	0.03	40.05	45.95	0.05	0.16	13.73	0.04	0	0	0.2	0.33	0	100.53	85.64
VMA1 ol 07_50	197	0.03	40.3	45.91	0.08	0.17	13.62	0.06	0	0.01	0.19	0.32	-0.01	100.68	85.73
VMA1 ol 07_51	201	0.02	40.03	46.18	0.09	0.16	13.71	0.03	0	0.01	0.2	0.34	0.04	100.8	85.72
VMA1 ol 07_52	205	0.01	40.15	45.89	0.09	0.17	13.63	0.03	0	0.01	0.2	0.36	0.05	100.57	85.72
VMA1 ol 07_53	209	0.02	39.93	46.01	0.09	0.16	13.67	0.04	0	0.02	0.2	0.33	0.02	100.5	85.71
VMA1 ol 07_54	213	0.01	39.92	46.07	0.1	0.14	13.76	0.04	0	0.01	0.22	0.33	0.04	100.63	85.65
VMA1 ol 07_55	217	0.02	40.14	45.86	0.06	0.15	13.66	0.05	0	0	0.2	0.28	0.01	100.42	85.68
VMA1 ol 07_56	222	0.02	40.05	45.89	0.06	0.16	13.54	0.05	0.01	0	0.2	0.32	0.03	100.31	85.80
VMA1 ol 07_57	226	0.02	40.09	45.68	0.08	0.18	13.62	0.04	0	0.01	0.21	0.31	0.01	100.25	85.67

Sample	Dist (μm)	Na_2O	SiO_2	MgO	Al_2O_3	MnO	FeO	Cr_2O_3	K_2O	TiO_2	CaO	NiO	P_2O_5	Total	Mg#
VMA1 ol 07_58	230	0.01	40.38	45.66	0.06	0.16	13.54	0.03	0	0.01	0.21	0.35	-0.02	100.39	85.74
VMA1 ol 07_59	234	0.03	39.79	46.07	0.08	0.14	13.87	0.04	0	0.01	0.2	0.34	0.01	100.57	85.55
VMA1 ol 07_60	238	0.01	40.26	45.77	0.04	0.15	13.56	0.03	-0.01	0.01	0.21	0.3	0	100.34	85.75
VMA1 ol 07_61	242	0.01	39.96	45.82	0.06	0.17	13.61	0.03	0	0.01	0.22	0.33	0.02	100.23	85.72
VMA1 ol 07_62	246	0.02	40.34	45.93	0.08	0.17	13.63	0.04	0	0.01	0.21	0.38	0	100.8	85.73
VMA1 ol 07_63	250	0.03	40.24	45.75	0.09	0.16	13.63	0.05	0	0.01	0.21	0.36	0.02	100.56	85.68
VMA1 ol 07_64	254	0.02	39.98	45.87	0.07	0.19	13.58	0.02	0	0	0.22	0.31	0.02	100.27	85.76
VMA1 ol 07_65	258	0.01	40.21	45.94	0.05	0.16	13.66	0.02	0	0.02	0.22	0.36	0.02	100.67	85.70
VMA1 ol 07_66	262	0.01	40.18	45.87	0.08	0.15	13.68	0.05	0	0.01	0.2	0.31	0.01	100.55	85.67
VMA1 ol 07_67	266	0.02	40	45.81	0.06	0.16	13.71	0.04	0.01	0.02	0.2	0.34	0.01	100.39	85.62
VMA1 ol 07_68	270	0.02	40.36	46	0.08	0.16	13.77	0.03	0	0.02	0.21	0.32	0.02	100.99	85.62
VMA1 ol 07_69	274	0.02	40.14	45.83	0.07	0.2	13.6	0.04	0	0	0.2	0.32	0.01	100.42	85.73
VMA1 ol 07_70	278	0.02	40.32	46.16	0.07	0.15	13.71	0.05	0	0.02	0.21	0.35	0.01	101.07	85.72
VMA1 ol 07_71	282	0.02	40.66	45.9	0.07	0.18	13.58	0.03	0	0.01	0.19	0.34	0.02	101	85.77
VMA1 ol 07_72	286	0.01	40.31	45.84	0.04	0.16	13.71	0.04	0	0.01	0.21	0.29	0.03	100.64	85.63
VMA1 ol 07_73	290	0.02	40.29	46.05	0.07	0.15	13.73	0.03	0	0.01	0.2	0.35	0.02	100.93	85.67
VMA1 ol 07_74	294	0.03	40.12	46.09	0.09	0.16	13.66	0.02	0	0.01	0.2	0.36	0.01	100.75	85.74
VMA1 ol 07_75	298	0.02	39.97	45.89	0.1	0.19	13.65	0.04	-0.01	0.01	0.21	0.3	0.01	100.39	85.70
VMA1 ol 07_76	302	0.03	40.3	45.9	0.05	0.17	13.72	0.04	0	0.01	0.21	0.3	0	100.74	85.64
VMA1 ol 07_77	306	0.02	40.04	45.94	0.05	0.14	13.71	0.04	0	0	0.19	0.32	0.02	100.48	85.66
VMA1 ol 07_78	310	0.02	40.19	46.11	0.09	0.16	13.58	0.03	0	0.01	0.21	0.27	0.01	100.68	85.82
VMA1 ol 07_79	314	0.01	39.86	45.98	0.07	0.14	13.59	0.03	0	0.01	0.2	0.32	-0.01	100.21	85.78
VMA1 ol 07_80	318	0.02	40.13	45.99	0.06	0.16	13.61	0.05	0	0.01	0.22	0.33	0	100.58	85.76
VMA1 ol 07_81	322	0.03	40.07	45.97	0.05	0.14	13.7	0.05	0	0.01	0.22	0.35	0.02	100.6	85.68
VMA1 ol 07_82	326	0.01	40.27	45.86	0.07	0.16	13.65	0.04	0.01	0.01	0.21	0.33	0.03	100.65	85.69
VMA1 ol 07_83	330	0.03	40.45	46.09	0.07	0.17	13.77	0.05	0	0	0.19	0.32	0.03	101.17	85.65
VMA1 ol 07_84	334	0.02	39.89	45.94	0.09	0.14	13.69	0.02	-0.01	0.01	0.22	0.33	0.01	100.35	85.68
VMA1 ol 07_85	338	0.02	39.93	45.82	0.06	0.15	13.77	0.03	0.01	0	0.22	0.32	0.05	100.39	85.57
VMA1 ol 07_86	342	0.03	40.19	45.92	0.08	0.17	13.64	0.03	0	0	0.2	0.32	-0.01	100.57	85.72
VMA1 ol 07_87	346	0	40.22	45.86	0.05	0.18	13.76	0.05	0	0.01	0.2	0.37	0.03	100.73	85.59
VMA1 ol 07_88	350	0.01	40.46	45.91	0.07	0.13	13.61	0.04	0	0.01	0.2	0.34	0.01	100.79	85.74
VMA1 ol 07_89	354	0.02	40.22	45.8	0.09	0.19	13.55	0.04	0	0.02	0.21	0.3	-0.01	100.43	85.77
VMA1 ol 07_90	358	0.02	40	45.89	0.08	0.16	13.56	0.02	0	0	0.2	0.3	0	100.25	85.78
VMA1 ol 07_91	362	0.03	40.37	46.05	0.03	0.18	13.8	0.04	0	0.01	0.22	0.37	0.01	101.11	85.61
VMA1 ol 07_92	367	0.02	40.07	45.8	0.07	0.13	13.73	0.05	0	0	0.2	0.38	0.01	100.46	85.60
VMA1 ol 07_93	371	0.03	40.16	45.93	0.06	0.16	13.73	0.02	0	0	0.2	0.3	0.02	100.62	85.64
VMA1 ol 07_94	375	0.02	40.22	45.64	0.07	0.16	13.72	0.05	0	0.01	0.2	0.33	0.02	100.45	85.57
VMA1 ol 07_95	379	0.02	40.07	45.96	0.06	0.18	13.72	0.03	0	0.01	0.21	0.33	0	100.59	85.66
VMA1 ol 07_96	383	0.01	40.07	46.02	0.08	0.14	13.74	0.01	0	0.01	0.21	0.35	0.03	100.67	85.65

Sample	Dist (μm)	Na_2O	SiO_2	MgO	Al_2O_3	MnO	FeO	Cr_2O_3	K_2O	TiO_2	CaO	NiO	P_2O_5	Total	Mg#
VMA1 ol 07_97	387	0.01	39.96	45.99	0.11	0.16	13.67	0.03	0	0.01	0.2	0.31	0.02	100.46	85.71
VMA1 ol 07_98	391	0.01	39.93	45.9	0.07	0.15	13.61	0.02	0.01	0.02	0.2	0.3	0	100.24	85.74
VMA1 ol 07_99	395	0	39.86	45.96	0.1	0.18	13.66	0.02	0.01	0.01	0.19	0.31	0.01	100.3	85.71
VMA1 ol 07_100	399	0.01	40.04	46.1	0.09	0.17	13.69	0.04	0	0.02	0.21	0.32	0.01	100.7	85.72
VMA1 ol 07_101	403	0.01	40.15	45.93	0.09	0.19	13.59	0.03	0	0.02	0.21	0.29	0.02	100.53	85.76
VMA1 ol 07_102	407	0.02	39.98	45.67	0.07	0.17	13.7	0.03	0	0.01	0.18	0.34	0.02	100.19	85.60
VMA1 ol 07_103	411	0.01	39.86	46.11	0.09	0.16	13.7	0.03	0	0.02	0.19	0.32	0.02	100.52	85.71
VMA1 ol 07_104	415	0.02	40.26	45.91	0.07	0.19	13.71	0.03	0	-0.01	0.21	0.34	0.03	100.76	85.65
VMA1 ol 07_105	419	0.03	40.19	45.93	0.08	0.17	13.82	0.05	0.01	0.01	0.21	0.33	0.02	100.84	85.56
VMA1 ol 07_106	423	0.03	40.23	45.77	0.09	0.17	13.73	0.03	0	0.01	0.21	0.32	0.02	100.6	85.60
VMA1 ol 07_107	427	0.01	39.76	45.95	0.1	0.18	13.63	0.03	0	0.01	0.21	0.32	0.02	100.23	85.73
VMA1 ol 07_108	431	0.01	40.32	45.95	0.08	0.17	13.75	0.04	0	0.01	0.21	0.3	0.02	100.87	85.63
VMA1 ol 07_109	435	0.02	39.85	45.93	0.07	0.17	13.74	0.05	-0.01	-0.01	0.21	0.33	0.01	100.35	85.63
VMA1 ol 07_110	439	0	40.11	46.06	0.08	0.15	13.72	0.03	0	0.01	0.2	0.3	0.03	100.69	85.68
VMA1 ol 07_111	443	0.02	40.14	45.85	0.09	0.17	13.76	0.04	0	0.01	0.22	0.34	0.02	100.67	85.59
VMA1 ol 07_112	447	0.02	40.1	45.97	0.09	0.17	13.61	0.03	-0.01	0.01	0.21	0.35	0.02	100.57	85.76
VMA1 ol 07_113	451	0.01	40.37	45.96	0.09	0.15	13.67	0.05	0	0.01	0.22	0.32	0	100.85	85.70
VMA1 ol 07_114	455	0.03	40.64	45.81	0.06	0.18	13.85	0.05	0	0.02	0.21	0.35	-0.01	101.19	85.50
VMA1 ol 07_115	459	0.03	40.03	45.88	0.05	0.17	13.56	0.02	0	0.02	0.21	0.29	0.01	100.28	85.78
VMA1 ol 07_116	463	0.01	40.37	46.01	0.08	0.14	13.57	0.05	0	0.01	0.21	0.3	0	100.73	85.80
VMA1 ol 07_117	467	0.02	39.96	45.7	0.08	0.13	13.71	0.04	0	0.01	0.21	0.32	-0.01	100.17	85.59
VMA1 ol 07_118	471	0.01	40.4	45.95	0.05	0.16	13.69	0.01	0	0	0.2	0.33	0	100.81	85.68
VMA1 ol 07_119	475	0.02	40.22	45.73	0.04	0.17	13.67	0.02	0	0	0.2	0.34	0.01	100.41	85.64
VMA1 ol 07_120	479	0.01	40.13	45.76	0.07	0.16	13.62	0.04	0	0	0.22	0.34	0.02	100.35	85.69
VMA1 ol 07_121	483	0.02	39.83	46.06	0.05	0.16	13.78	0.02	0	0.01	0.2	0.36	0.03	100.52	85.63
VMA1 ol 07_122	487	0.01	40.06	45.85	0.06	0.18	13.73	0.04	0	0.01	0.2	0.31	0.01	100.47	85.62
VMA1 ol 07_123	491	0.03	40.05	45.79	0.06	0.18	13.71	0.03	-0.01	0.01	0.21	0.33	0.04	100.44	85.62
VMA1 ol 07_124	495	0.01	40.23	45.83	0.07	0.15	13.79	0.03	0.01	0.01	0.2	0.33	0.02	100.69	85.56
VMA1_ol 09_01	0	1.93	46.27	4.76	15.51	0.19	9.95	-0.01	1.22	2.98	13.49	0.02	1.07	97.38	46.03
VMA1_ol 09_02	2	0.64	45.03	11.37	8.18	0.15	8.46	0.12	0.04	3.53	22.37	0.02	0.3	100.22	70.55
VMA1_ol 09_03	4	0.4	42.67	17.26	6.73	0.19	12.74	0.03	0.02	3.07	17.12	0.03	0.23	100.47	70.72
VMA1_ol 09_04	6	0.03	38.9	39.1	0.11	0.35	21.08	0.02	0.01	0.08	0.67	0.09	0	100.44	76.78
VMA1_ol 09_05	8	0.02	38.71	39.92	0.02	0.28	20.18	0.02	0.01	0.06	0.52	0.11	0.02	99.86	77.91
VMA1_ol 09_06	10	0.01	38.84	40.77	0.06	0.37	19.5	0.03	0	0.05	0.46	0.12	0	100.2	78.84
VMA1_ol 09_07	12	0	38.94	40.97	0.04	0.31	19.07	0.04	0.01	0.04	0.45	0.1	0.03	100	79.29
VMA1_ol 09_08	14	0.01	39.35	41.47	0.04	0.27	18.8	0.02	0	0.03	0.41	0.11	0.03	100.55	79.72
VMA1_ol 09_09	16	0.01	38.99	41.43	0.06	0.29	18.56	0.02	0	0.04	0.41	0.11	0.03	99.97	79.92
VMA1_ol 09_10	18	-0.01	39.09	41.89	0.03	0.27	18.37	0.01	0	0.04	0.4	0.16	0.03	100.29	80.26
VMA1_ol 09_11	20	0	38.97	41.83	0.03	0.29	17.96	0.03	-0.01	0.04	0.37	0.16	0	99.68	80.59

Sample	Dist (μm)	Na_2O	SiO_2	MgO	Al_2O_3	MnO	FeO	Cr_2O_3	K_2O	TiO_2	CaO	NiO	P_2O_5	Total	Mg#
VMA1_ol 09_12	22	0.01	39.25	42	0.05	0.27	17.9	0.02	0	0.02	0.38	0.13	0.03	100.05	80.70
VMA1_ol 09_13	24	0	39.22	42.64	0.02	0.24	17.65	0.01	0.01	0.03	0.37	0.2	0.04	100.44	81.15
VMA1_ol 09_14	26	0.01	39.49	42.5	0.02	0.27	17.38	0.02	0	0.02	0.36	0.13	0.02	100.24	81.34
VMA1_ol 09_15	28	0.01	39.14	42.6	0.02	0.3	17.22	0.04	0	0.04	0.37	0.14	0.03	99.91	81.51
VMA1_ol 09_16	30	0.01	39.77	42.85	0.05	0.25	17.18	0.04	-0.01	0.02	0.36	0.18	0.03	100.73	81.64
VMA1_ol 09_17	32	0.01	39.4	42.62	0.04	0.26	17.07	0.03	0	0.03	0.36	0.16	0.05	100.04	81.65
VMA1_ol 09_18	34	0.02	39.45	43.12	0.02	0.25	17.11	0.03	0	0.03	0.34	0.17	0.02	100.56	81.79
VMA1_ol 09_19	36	0.02	39.28	42.94	0.03	0.27	17.1	0.04	0	0.03	0.34	0.15	0.02	100.24	81.74
VMA1_ol 09_20	38	0.03	39.57	43.2	0.07	0.26	16.77	0.04	0	0.04	0.33	0.19	0.04	100.54	82.12
VMA1_ol 09_21	40	0.01	39.48	43.17	0.03	0.21	16.64	0.03	0.01	0.02	0.34	0.19	0.03	100.17	82.22
VMA1_ol 09_22	42	0.01	39.59	43.02	0.03	0.25	16.78	0.03	0	0.02	0.32	0.17	0.04	100.25	82.05
VMA1_ol 09_23	44	0	39.42	43.41	0.04	0.22	16.96	0.03	0	0.02	0.25	0.21	0.04	100.61	82.02
VMA1_ol 09_24	46	0.03	39.37	42.86	0.04	0.23	16.79	0.04	0	0.02	0.23	0.19	0.02	99.83	81.98
VMA1_ol 09_25	48	0.02	39.45	43.24	0.04	0.24	16.95	0.03	0	0.01	0.23	0.25	0.04	100.48	81.97
VMA1_ol 09_26	50	0.02	39.67	43.07	0.04	0.25	16.92	0.04	0	0	0.22	0.19	0.02	100.44	81.94
VMA1_ol 09_27	52	0.01	39.69	43.27	0.05	0.21	16.96	0.03	0	0.03	0.22	0.26	0.03	100.75	81.97
VMA1_ol 09_28	54	0.01	39.63	43.25	0.07	0.24	17.1	0.03	0	0.01	0.22	0.18	0.03	100.75	81.85
VMA1_ol 09_29	56	0.02	39.43	43.04	0.06	0.27	16.75	0.02	0	0.01	0.23	0.24	0.02	100.12	82.08
VMA1_ol 09_30	58	0.03	39.7	43.23	0.06	0.23	16.77	0.04	-0.01	0.01	0.22	0.23	0.03	100.53	82.13
VMA1_ol 09_31	60	-0.01	39.15	43.41	0.07	0.22	16.78	0.02	0	0.02	0.21	0.22	0	100.1	82.18
VMA1_ol 09_32	62	0.02	39.63	43.41	0.06	0.21	16.7	0.04	0.01	0.02	0.21	0.22	0.02	100.55	82.25
VMA1_ol 09_33	64	0.03	39.53	43.45	0.04	0.17	16.73	0.04	0	0.03	0.23	0.22	0.03	100.5	82.24
VMA1_ol 09_34	66	0.02	39.51	43.41	0.05	0.2	16.54	0.03	0	0.02	0.2	0.19	0.02	100.19	82.39
VMA1_ol 09_35	68	0.01	39.23	43.39	0.04	0.23	16.62	0.03	0	0.02	0.2	0.21	0.02	99.99	82.31
VMA1_ol 09_36	70	0	39.51	43.35	0.06	0.22	16.49	0.03	-0.01	0.01	0.22	0.23	0	100.11	82.41
VMA1_ol 09_37	72	0.01	39.42	43.57	0.04	0.23	16.67	0.03	0	0.02	0.23	0.23	0.02	100.46	82.33
VMA1_ol 09_38	74	0.03	39.42	43.42	0.05	0.22	16.54	0.04	0	0.02	0.19	0.21	0.02	100.16	82.39
VMA1_ol 09_39	76	0	39.3	43.57	0.06	0.19	16.69	0.03	0	0.02	0.21	0.21	0.01	100.28	82.31
VMA1_ol 09_40	78	0.02	39.57	43.36	0.07	0.2	16.69	0.04	0	0.02	0.2	0.22	0.04	100.43	82.24
VMA1_ol 09_41	80	0.02	39.43	43.69	0.04	0.21	16.71	0.02	0	0.01	0.22	0.22	0.02	100.58	82.33
VMA1_ol 09_42	82	0.03	39.86	43.66	0.04	0.2	16.61	0.04	0	0.01	0.21	0.27	0	100.93	82.41
VMA1_ol 09_43	84	0	39.56	43.6	0.08	0.2	16.55	0.01	0	0.01	0.2	0.28	0.02	100.52	82.44
VMA1_ol 09_44	86	0.01	39.77	43.58	0.08	0.23	16.67	0.02	0	0.01	0.21	0.27	0.03	100.88	82.33
VMA1_ol 09_45	88	0.01	39.58	43.31	0.03	0.22	16.48	0.03	0	0.02	0.21	0.28	0.01	100.18	82.41
VMA1_ol 09_46	90	0.01	39.73	43.2	0.04	0.2	16.49	0.01	0	0.02	0.2	0.26	0.01	100.17	82.36
VMA1_ol 09_47	92	0.02	39.65	43.69	0.05	0.24	16.66	0.04	0	0.02	0.21	0.18	0.02	100.78	82.38
VMA1_ol 09_48	94	0.01	39.69	43.43	0.03	0.19	16.68	0.03	0	0.01	0.2	0.23	0.02	100.53	82.27
VMA1_ol 09_49	96	0.03	39.39	43.53	0.06	0.2	16.57	0.03	0	0.02	0.21	0.24	0.02	100.29	82.40
VMA1_ol 09_50	98	0.02	39.52	43.23	0.06	0.22	16.54	0.05	0	0.02	0.2	0.25	0.03	100.14	82.33

Sample	Dist (μm)	Na_2O	SiO_2	MgO	Al_2O_3	MnO	FeO	Cr_2O_3	K_2O	TiO_2	CaO	NiO	P_2O_5	Total	Mg#
VMA1_ol 09_51	100	0.02	39.49	43.3	0.05	0.23	16.64	0.05	0	0.02	0.22	0.24	0.01	100.26	82.26
VMA1_ol 09_52	102	0.02	39.34	43.13	0.01	0.19	16.62	0.03	0	0.01	0.21	0.25	0.02	99.83	82.22
VMA1_ol 09_53	104	0.01	39.43	43.51	0.05	0.21	16.77	0.02	0	0.02	0.21	0.25	0.02	100.51	82.22
VMA1_ol 09_54	106	0.03	39.58	43.36	0.06	0.22	16.75	0.03	0	0.01	0.21	0.22	0.02	100.48	82.19
VMA1_ol 09_55	108	0.03	39.41	43.45	0.04	0.22	16.81	0.01	-0.01	0.02	0.22	0.25	0.01	100.47	82.17
VMA1_ol 09_56	110	0	39.42	43.26	0.07	0.21	16.67	0.02	0	0.01	0.2	0.24	0	100.1	82.22
VMA1_ol 09_57	112	0.02	39.69	43.42	0.06	0.2	16.73	0.02	0	0.01	0.23	0.26	0.03	100.66	82.23
VMA1_ol 09_58	114	0.02	39.32	43.24	0.05	0.22	16.6	0.04	0	0.01	0.22	0.28	0.02	100.02	82.28
VMA1_ol 09_59	116	0.01	39.51	43.25	0.05	0.21	16.8	0.01	0	0.03	0.21	0.22	0.02	100.33	82.11
VMA1_ol 09_60	118	0.02	39.4	43.12	0.04	0.25	16.93	0.03	0	0.02	0.21	0.21	0.02	100.25	81.95
VMA1_ol 09_61	120	0.04	39.07	43.24	0.04	0.24	16.67	0.03	0.01	0.03	0.23	0.22	-0.02	99.79	82.22
VMA1_ol 09_62	122	0.02	39.51	43.16	0.07	0.21	16.84	0.02	0	0.01	0.22	0.21	0.01	100.28	82.04
VMA1_ol 09_63	124	0.03	39.44	43.33	0.02	0.21	16.74	0.04	0	0.02	0.23	0.26	0	100.32	82.19
VMA1_ol 09_64	126	0.02	39.39	43.2	0.07	0.2	16.71	0.02	0	0.02	0.23	0.23	0.04	100.13	82.17
VMA1_ol 09_65	128	0.04	39.72	43.26	0.03	0.21	16.57	0.04	0	0.02	0.25	0.26	0.01	100.39	82.31
VMA1_ol 09_66	130	0.01	39.68	43.12	0.08	0.24	16.71	0.04	0.01	0.02	0.23	0.21	0.02	100.37	82.14
VMA1_ol 09_67	132	0.02	39.42	43.48	0.05	0.19	16.8	0.03	0	0.01	0.23	0.22	0.01	100.46	82.19
VMA1_ol 09_68	134	0.02	39.53	43.4	0.05	0.22	16.74	0.02	0.01	0.01	0.26	0.25	0.01	100.53	82.21
VMA1_ol 09_69	136	0.02	39.25	43.37	0.03	0.22	16.91	0.05	0	0.02	0.24	0.18	0	100.29	82.05
VMA1_ol 09_70	138	0.02	39.16	43.5	0.05	0.23	16.86	0.04	0	0.03	0.24	0.23	0.04	100.39	82.14
VMA1_ol 09_71	140	0.01	39.18	43.41	0.04	0.22	16.8	0.04	0	0.03	0.26	0.19	0.01	100.18	82.16
VMA1_ol 09_72	142	0	39.32	42.96	0.07	0.22	16.74	0.03	0	0.03	0.27	0.21	0.01	99.85	82.06
VMA1_ol 09_73	144	0.03	39.27	43.33	0.04	0.26	16.95	0.03	0	0.04	0.29	0.2	0.03	100.46	82.00
VMA1_ol 09_74	146	0.02	39.21	43.08	0.05	0.2	17.09	0.03	0	0.04	0.31	0.21	0	100.25	81.80
VMA1_ol 09_75	148	0.01	39.13	43.3	0.01	0.3	16.99	0.03	0.01	0.04	0.34	0.22	-0.01	100.37	81.96
VMA1_ol 09_76	150	0	39	42.88	0.05	0.27	17.37	0.04	0	0.03	0.38	0.16	0.01	100.19	81.48
VMA1_ol 09_77	152	0.02	38.85	42.3	0.05	0.3	18.18	0.03	0.01	0.06	0.45	0.16	0.02	100.43	80.57
VMA1_ol 09_78	154	0.1	38.73	38.88	0.43	0.34	20.54	0.02	0.08	0.16	1	0.09	0.02	100.38	77.14
VMA1_ol 09_79	156	0.3	38.51	34.05	1.9	0.34	21.49	0.03	0.29	0.51	2.36	0.1	0.19	100.07	73.85
VMA1_ol 012_01	0	2.5	41.96	6.32	13.82	0.16	10.92	0.01	1.4	4.2	13.73	-0.03	1	96	50.78
VMA1_ol 012_02	2	0.03	38.46	40.53	0.08	0.28	19.83	0.02	0.02	0.08	0.53	0.12	0.05	100.01	78.46
VMA1_ol 012_03	4	0.02	38.78	40.71	0.04	0.28	19.05	0.02	0	0.07	0.49	0.11	0.05	99.63	79.21
VMA1_ol 012_04	6	0.01	39.13	41.75	0.01	0.28	18.51	0.03	0	0.06	0.43	0.13	0.05	100.38	80.08
VMA1_ol 012_05	8	0.01	39.26	41.43	0	0.29	18.19	0.03	0	0.04	0.41	0.13	0.04	99.83	80.24
VMA1_ol 012_06	10	0	39.51	42.2	0.05	0.28	17.93	0.02	0	0.03	0.39	0.14	0.03	100.56	80.75
VMA1_ol 012_07	12	0.01	39.12	42.24	0.05	0.3	17.51	0.03	0	0.05	0.37	0.14	0.04	99.85	81.13
VMA1_ol 012_08	14	0.01	38.83	42.51	0.02	0.28	17.33	0.03	0	0.03	0.38	0.11	0.02	99.54	81.39
VMA1_ol 012_09	16	0.01	39.36	42.64	0.03	0.23	17.11	0.02	0.01	0.05	0.38	0.13	0.04	99.99	81.63
VMA1_ol 012_10	18	0.02	39.07	42.95	0.02	0.24	17.04	0.02	0	0.04	0.37	0.15	0.04	99.95	81.79

Sample	Dist (μm)	Na_2O	SiO_2	MgO	Al_2O_3	MnO	FeO	Cr_2O_3	K_2O	TiO_2	CaO	NiO	P_2O_5	Total	Mg#
VMA1_ol 012_11	20	0	39.19	43.06	0.04	0.27	16.88	0.03	0	0.03	0.35	0.16	0.06	100.08	81.97
VMA1_ol 012_12	22	0.02	39.65	43.14	0.05	0.25	17	0.05	0	0.03	0.31	0.21	0.03	100.75	81.90
VMA1_ol 012_13	24	0.02	39.27	43.06	0.05	0.27	17.08	0.03	0	0.02	0.28	0.18	0.01	100.28	81.80
VMA1_ol 012_14	26	0.02	38.84	42.84	0.04	0.19	17.01	0.04	0	0.03	0.27	0.16	0.04	99.48	81.78
VMA1_ol 012_15	28	0.01	39.29	43.07	0	0.22	17.13	0.04	0	0.03	0.25	0.21	0.01	100.25	81.76
VMA1_ol 012_16	30	0.02	39.48	42.9	0.07	0.2	17.12	0.03	0	0.01	0.24	0.2	0.03	100.29	81.71
VMA1_ol 012_17	32	0.01	39.52	43.28	0.04	0.2	17.14	0.03	0	0.02	0.24	0.26	0.04	100.77	81.82
VMA1_ol 012_18	34	0.01	39.46	43.21	0.04	0.22	16.9	0.03	0	0.01	0.24	0.27	0.01	100.4	82.01
VMA1_ol 012_19	36	0.02	39.49	43.11	0.06	0.22	16.77	0.03	0	0.01	0.24	0.23	0.01	100.18	82.09
VMA1_ol 012_20	38	0.01	39.38	43.56	0.07	0.25	16.55	0.02	-0.01	0.02	0.23	0.25	0.02	100.36	82.43
VMA1_ol 012_21	40	0.03	39.68	43.32	0.05	0.24	16.45	0.03	-0.01	0.02	0.21	0.25	0.04	100.31	82.44
VMA1_ol 012_22	42	0.02	39.44	43.53	0.07	0.2	16.34	0.03	0.01	0.02	0.23	0.18	0.01	100.09	82.60
VMA1_ol 012_23	44	0.02	39.68	43.97	0.07	0.21	16.18	0.04	0	0.02	0.23	0.24	0.03	100.7	82.89
VMA1_ol 012_24	46	0.02	39.72	43.74	0.04	0.19	15.99	0.03	0	0.03	0.2	0.22	0.02	100.19	82.98
VMA1_ol 012_25	48	0.01	39.39	43.51	0.09	0.19	15.92	0.04	0	0.01	0.24	0.22	0.03	99.65	82.97
VMA1_ol 012_26	50	0.01	39.63	44.25	0.04	0.22	16.18	0.05	0	0.03	0.24	0.23	0.03	100.9	82.98
VMA1_ol 012_27	52	0.03	39.52	44.03	0.05	0.18	15.73	0.02	0	0.02	0.21	0.27	0.03	100.09	83.30
VMA1_ol 012_28	54	0.01	39.53	44.32	0.06	0.19	15.83	0.01	0	0.02	0.2	0.26	-0.01	100.44	83.31
VMA1_ol 012_29	56	0.02	39.91	44.16	0.08	0.17	15.41	0.03	0	0.02	0.2	0.3	0	100.3	83.63
VMA1_ol 012_30	58	0.03	39.54	44.64	0.06	0.19	15.58	0.04	0	0.02	0.2	0.28	0.01	100.59	83.63
VMA1_ol 012_31	60	0.03	39.81	44.7	0.07	0.2	15.28	0.05	0	0.02	0.21	0.25	0.02	100.63	83.91
VMA1_ol 012_32	62	0.03	39.89	44.86	0.07	0.21	15.13	0.04	0.01	0.02	0.21	0.27	0.06	100.79	84.09
VMA1_ol 012_33	64	0	40.16	44.81	0.07	0.2	14.76	0.03	0	0.02	0.21	0.26	-0.01	100.51	84.40
VMA1_ol 012_34	66	0.01	40.13	44.94	0.06	0.18	14.85	0.05	0	0.02	0.21	0.25	0.02	100.73	84.36
VMA1_ol 012_35	68	0.01	39.96	44.94	0.05	0.21	14.54	0.06	0	0.01	0.21	0.27	0.03	100.27	84.64
VMA1_ol 012_36	70	0.01	39.79	45.15	0.05	0.16	14.57	0.04	0	0.03	0.21	0.27	0.04	100.33	84.67
VMA1_ol 012_37	72	0.03	39.73	45.06	0.1	0.17	14.42	0.06	0	0	0.21	0.26	0.01	100.05	84.78
VMA1_ol 012_38	74	0.01	39.92	45.13	0.06	0.2	14.25	0.04	0	0.01	0.21	0.31	0.02	100.17	84.95
VMA1_ol 012_39	76	0.01	40.07	45.54	0.06	0.21	14.35	0.03	0	0	0.2	0.33	0.02	100.81	84.98
VMA1_ol 012_40	78	0.01	39.78	45.62	0.05	0.18	14.1	0.05	0	0.01	0.22	0.25	0.02	100.28	85.22
VMA1_ol 012_41	80	0.01	40.23	45.69	0.04	0.19	14.14	0.05	0	0.01	0.19	0.33	0.01	100.88	85.21
VMA1_ol 012_42	82	0.01	39.85	45.32	0.07	0.16	13.89	0.03	0.01	0.01	0.2	0.26	0.03	99.83	85.33
VMA1_ol 012_43	84	0.03	40.17	46.1	0.03	0.21	14.09	0.04	0	0.03	0.2	0.29	0.01	101.19	85.36
VMA1_ol 012_44	86	0.02	39.77	45.55	0.04	0.19	13.87	0.05	0	0.01	0.2	0.26	0.03	100	85.41
VMA1_ol 012_45	88	0.03	40.37	45.92	0.05	0.17	14	0.04	0	0.01	0.21	0.31	0.01	101.13	85.39
VMA1_ol 012_46	90	0.03	39.98	45.82	0.07	0.16	13.8	0.06	-0.01	0.01	0.22	0.32	0.01	100.47	85.55
VMA1_ol 012_47	92	0.02	40.21	45.55	0.04	0.18	13.9	0.03	0	0.01	0.19	0.31	0	100.45	85.38
VMA1_ol 012_48	94	0.01	39.81	45.62	0.06	0.16	13.72	0.04	-0.01	0.01	0.21	0.28	0.01	99.93	85.56
VMA1_ol 012_49	96	0.02	40.04	45.79	0.06	0.15	13.57	0.06	0	0.01	0.21	0.32	0.02	100.24	85.74

Sample	Dist (μm)	Na_2O	SiO_2	MgO	Al_2O_3	MnO	FeO	Cr_2O_3	K_2O	TiO_2	CaO	NiO	P_2O_5	Total	Mg#
VMA1_ol 012_50	98	0.01	40.27	45.64	0.06	0.18	13.82	0.05	0	0.02	0.2	0.29	0.01	100.55	85.48
VMA1_ol 012_51	100	0.01	39.99	45.89	0.06	0.14	13.53	0.04	0.01	0.01	0.2	0.33	0.02	100.24	85.81
VMA1_ol 012_52	102	0.03	39.93	46.18	0.1	0.15	13.83	0.04	0	0.01	0.2	0.29	0.01	100.76	85.62
VMA1_ol 012_53	104	0.01	39.97	45.9	0.06	0.16	13.62	0.03	0	0.01	0.2	0.3	0.04	100.3	85.73
VMA1_ol 012_54	106	0	39.93	46.05	0.08	0.18	13.66	0.04	0	0.01	0.2	0.32	0.03	100.51	85.73
VMA1_ol 012_55	108	0.02	39.76	46.11	0.1	0.19	13.6	0.04	0	0.01	0.2	0.33	0.03	100.4	85.80
VMA1_ol 012_56	110	0.02	40.27	46.04	0.07	0.21	13.69	0.05	0	0	0.2	0.31	0.04	100.9	85.70
VMA1_ol 012_57	112	0.02	40.09	45.8	0.06	0.16	13.38	0.02	0	0	0.2	0.28	0	100.03	85.92
VMA1_ol 012_58	114	0.01	39.87	45.77	0.05	0.17	13.32	0.03	0	0.01	0.2	0.3	0.03	99.77	85.97
VMA1_ol 012_59	116	0.02	40.35	46.32	0.05	0.21	13.5	0.06	0	0	0.2	0.33	0.02	101.06	85.95
VMA1_ol 012_60	118	0.01	40.02	46.01	0.07	0.19	13.4	0.02	-0.01	0.01	0.19	0.31	0.01	100.24	85.96
VMA1_ol 012_61	120	0.01	40.42	45.75	0.04	0.15	13.32	0.03	0	0.02	0.2	0.34	-0.01	100.25	85.96
VMA1_ol 012_62	122	0	40.46	46.04	0.04	0.17	13.36	0.06	-0.01	0	0.2	0.29	0	100.62	86.00
VMA1_ol 012_63	124	0.02	40.44	46.1	0.06	0.16	13.43	0.04	-0.01	0	0.21	0.32	0	100.78	85.95
VMA1_ol 012_64	126	0.02	39.5	46.25	0.08	0.19	13.44	0.03	0	0	0.2	0.38	-0.01	100.07	85.98
VMA1_ol 012_65	128	0.01	40.38	45.76	0.08	0.15	13.31	0.06	0	0.01	0.2	0.31	0	100.25	85.97
VMA1_ol 012_66	130	0.02	40.04	46.19	0.06	0.15	13.42	0.06	-0.01	0	0.2	0.32	-0.01	100.44	85.99
VMA1_ol 012_67	132	0.02	40.35	46.06	0.07	0.17	13.33	0.03	0	0.01	0.21	0.34	0.02	100.63	86.03
VMA1_ol 012_68	134	0.02	40.06	46.01	0.09	0.16	13.11	0.03	0	0	0.2	0.33	0.03	100.04	86.22
VMA1_ol 012_69	136	0.02	40.24	46.26	0.06	0.17	13.33	0.03	0	0.01	0.2	0.32	0.02	100.66	86.08
VMA1_ol 012_70	138	0	40.17	46.09	0.07	0.18	13.56	0.04	0.01	0	0.2	0.35	0.04	100.71	85.83
VMA1_ol 012_71	140	0.01	40.16	46.16	0.04	0.15	13.3	0.03	0	0.01	0.19	0.32	0.04	100.4	86.09
VMA1_ol 012_72	142	0.03	40.11	46.49	0.04	0.16	13.32	0.02	0	0.01	0.2	0.32	0.01	100.69	86.15
VMA1_ol 012_73	144	0.02	40.29	45.89	0.08	0.17	13.33	0.05	0	0.01	0.2	0.34	0	100.37	85.99
VMA1_ol 012_74	146	0.02	40.02	46.32	0.07	0.17	13.43	0.03	0	0.02	0.19	0.38	0.02	100.66	86.01
VMA1_ol 012_75	148	0.03	39.91	46.04	0.07	0.14	13.28	0.04	0	0.01	0.19	0.32	0.04	100.06	86.07
VMA1_ol 012_76	150	0.02	39.69	46.04	0.05	0.16	13.32	0.02	0	0.01	0.19	0.35	0.01	99.86	86.04
VMA1_ol 012_77	152	0	40.09	45.94	0.1	0.16	13.26	0.04	0	0.01	0.2	0.34	0.02	100.15	86.06
VMA1_ol 012_78	154	0.01	39.97	46.53	0.07	0.16	13.42	0.02	0	0	0.19	0.33	0.02	100.72	86.07
VMA1_ol 012_79	156	0.02	40.36	46.29	0.06	0.2	13.32	0.05	0	0.01	0.18	0.32	0	100.81	86.10
VMA1_ol 012_80	158	0.02	40.29	45.96	0.05	0.15	13.34	0.04	0	0.02	0.19	0.34	0.02	100.42	86.00
VMA1_ol 012_81	160	0.01	40.19	46.12	0.06	0.15	13.25	0.03	-0.01	-0.01	0.2	0.33	0.01	100.35	86.12
VMA1_ol 012_82	162	0.01	40.29	46.35	0.06	0.16	13.38	0.03	0	0.01	0.2	0.36	-0.01	100.83	86.06
VMA1_ol 012_83	164	0.01	40.51	46.46	0.09	0.18	13.54	0.03	0	0.02	0.19	0.3	0	101.33	85.95
VMA1_ol 012_84	166	0	39.68	46.17	0.09	0.16	13.21	0.03	0	0.01	0.19	0.34	0.02	99.89	86.17
VMA1_ol 012_85	168	0.03	40.39	46.09	0.12	0.16	13.39	0.04	0	0.01	0.2	0.37	0.04	100.85	85.99
VMA1_ol 012_86	170	0.02	40.46	46.16	0.07	0.16	13.38	0.02	0	0.01	0.19	0.35	0.02	100.83	86.01
VMA1_ol 012_87	172	0.01	40.05	46.25	0.06	0.16	13.3	0.06	-0.01	0.01	0.2	0.35	0.03	100.49	86.11
VMA1_ol 012_88	174	0.02	39.8	45.9	0.08	0.15	13.18	0.04	0	0.01	0.19	0.29	0.02	99.68	86.13

Sample	Dist (μm)	Na_2O	SiO_2	MgO	Al_2O_3	MnO	FeO	Cr_2O_3	K_2O	TiO_2	CaO	NiO	P_2O_5	Total	Mg#
VMA1_ol 012_89	176	-0.01	40.14	46.04	0.07	0.2	13.21	0.05	0	0.01	0.21	0.3	0.01	100.25	86.14
VMA1_ol 012_90	178	0.02	40.27	46.06	0.05	0.14	13.22	0.04	0	0	0.19	0.34	0.03	100.36	86.13
VMA1_ol 012_91	180	0.03	40.1	46.15	0.08	0.16	13.19	0.06	0	0.02	0.2	0.36	0.02	100.37	86.18
VMA1_ol 012_92	182	0.02	39.77	46.29	0.09	0.16	13.23	0.03	0	0.01	0.21	0.35	0.02	100.18	86.18
VMA1_ol 012_93	184	0	40.19	46.02	0.03	0.14	13.23	0.04	0	0.02	0.2	0.34	0.01	100.23	86.11
VMA1_ol 012_94	186	0	40	45.98	0.09	0.17	13.34	0.04	0	0.01	0.19	0.31	0.03	100.14	86.00
VMA1_ol 012_95	188	0	40.31	46.17	0.08	0.17	13.34	0.02	0	0.01	0.2	0.32	0.03	100.64	86.05
VMA1_ol 012_96	190	0.02	39.95	46.42	0.08	0.17	13.32	0.06	0	0.01	0.19	0.32	0.01	100.54	86.13
VMA1_ol 012_97	192	0.02	40.07	46.19	0.06	0.18	13.24	0.04	0	0.01	0.19	0.37	0.03	100.39	86.15
VMA1_ol 012_98	194	0.03	39.93	46.3	0.09	0.17	13.26	0.03	0.01	0.01	0.18	0.35	0	100.37	86.16
VMA1_ol 012_99	196	0.02	39.93	46.28	0.07	0.16	13.36	0.05	0	0.01	0.2	0.34	0.01	100.43	86.06
VMA1_ol 012_100	198	0.02	40.25	46.38	0.08	0.16	13.36	0.02	-0.01	0.01	0.2	0.38	0.04	100.88	86.09
VMA1_ol 012_101	200	0.02	40.51	46.24	0.07	0.19	13.45	0.05	0	0.02	0.19	0.32	0.02	101.07	85.97
VMA1_ol 012_102	202	0.01	40.39	45.92	0.07	0.17	13.3	0.02	0	0	0.19	0.35	0.04	100.47	86.02
VMA1_ol 012_103	204	0.01	39.93	46.38	0.09	0.17	13.39	0.02	0	0.01	0.19	0.34	0.05	100.58	86.06
VMA1_ol 012_104	206	0.01	39.97	46.56	0.04	0.17	13.34	0.04	0	0	0.19	0.36	0.04	100.74	86.15
VMA1_ol 012_105	208	0.02	40.01	46.17	0.06	0.17	13.36	0.04	0	0.01	0.2	0.37	-0.01	100.39	86.03
VMA1_ol 012_106	210	0.03	40.36	46.31	0.07	0.16	13.47	0.04	0	0.01	0.18	0.38	0.04	101.06	85.97
VMA1_ol 012_107	212	0.03	40.09	46.09	0.07	0.13	13.35	0.04	0	0.01	0.18	0.33	0.01	100.33	86.02
VMA1_ol 012_108	214	0.01	40.03	46.08	0.06	0.19	13.29	0.04	0	0.01	0.21	0.33	0.05	100.3	86.07
VMA1_ol 012_109	216	0.03	40.54	46.16	0.1	0.14	13.42	0.05	0	0.02	0.2	0.34	0.03	101.03	85.98
VMA1_ol 012_110	218	-0.01	40.4	46.06	0.07	0.17	13.38	0.04	0	0.01	0.19	0.3	0.04	100.65	85.99
VMA1_ol 012_111	220	0.02	40.45	46.29	0.05	0.17	13.47	0.01	0	0	0.19	0.32	0.02	100.99	85.97
VMA1_ol 014_01	0	3.27	45.71	4.03	15.82	0.17	11.11	0.02	1.82	2.81	10.77	0	1.13	96.66	39.27
VMA1_ol 014_02	4	0.53	43.33	11.44	9	0.11	8.06	0.38	0.01	4.15	23.02	0.02	0.24	100.3	71.67
VMA1_ol 014_03	8	0.55	44.2	11.62	8.53	0.12	7.99	0.32	0.01	4	22.9	0.02	0.25	100.5	72.16
VMA1_ol 014_04	12	0.6	44.55	11.75	8.44	0.13	8.16	0.11	0.04	3.78	22.6	0	0.25	100.41	71.96
VMA1_ol 014_05	16	0.01	39.24	41.2	0.03	0.32	18.87	0.04	-0.01	0.06	0.49	0.1	0.03	100.38	79.56
VMA1_ol 014_06	20	0	39.45	41.7	0.05	0.28	18.26	0.02	0	0.05	0.4	0.1	0.04	100.34	80.28
VMA1_ol 014_07	24	0.02	39.54	42.15	0.06	0.26	17.88	0.04	0	0.04	0.4	0.15	0.04	100.57	80.78
VMA1_ol 014_08	28	0.01	39.25	43.01	0.03	0.26	17.22	0.05	0	0.04	0.34	0.15	0.02	100.38	81.66
VMA1_ol 014_09	32	0.02	39.43	43.34	0.04	0.27	16.8	0.03	0	0.02	0.34	0.14	0.05	100.5	82.14
VMA1_ol 014_10	36	0.03	39.15	42.68	0.06	0.22	17.13	0.05	0	0.02	0.27	0.18	0.02	99.81	81.62
VMA1_ol 014_11	40	0.01	39.49	42.68	0.03	0.24	17.34	0.04	0	0.01	0.24	0.2	0.01	100.28	81.44
VMA1_ol 014_12	44	0.02	39.34	42.64	0.04	0.22	17.27	0.02	0	0.01	0.25	0.19	0.01	100.02	81.49
VMA1_ol 014_13	48	0.04	39.63	42.86	0.07	0.26	17.13	0.04	0	0.02	0.23	0.21	0.01	100.51	81.68
VMA1_ol 014_14	52	0.02	39.4	43.05	0.1	0.22	16.96	0.04	0.01	0.02	0.24	0.21	0.02	100.28	81.90
VMA1_ol 014_15	56	0.03	39.66	43.19	0.06	0.18	16.84	0.04	0	0.02	0.23	0.19	0.02	100.45	82.05
VMA1_ol 014_16	60	0.03	39.56	43.31	0.05	0.22	16.74	0.02	0	0.02	0.22	0.24	0.02	100.43	82.18

Sample	Dist (μm)	Na_2O	SiO_2	MgO	Al_2O_3	MnO	FeO	Cr_2O_3	K_2O	TiO_2	CaO	NiO	P_2O_5	Total	Mg#
VMA1_ol 014_17	64	0.03	39.65	43.35	0.07	0.24	16.72	0.04	0	0.02	0.22	0.2	0.05	100.58	82.21
VMA1_ol 014_18	68	0.02	39.27	43.28	0.05	0.2	16.65	0.04	-0.01	0.01	0.22	0.25	0.02	100.01	82.25
VMA1_ol 014_19	72	0.01	39.45	43.33	0.07	0.21	16.94	0.04	0	0.01	0.21	0.26	0	100.53	82.01
VMA1_ol 014_20	76	0.01	39.68	43.16	0.04	0.19	16.94	0.02	-0.01	0.02	0.22	0.18	0.03	100.48	81.95
VMA1_ol 014_21	80	0.01	39.36	43.1	0.03	0.21	17.02	0.02	0	0.01	0.21	0.24	0.01	100.24	81.86
VMA1_ol 014_22	84	0.04	39.49	42.8	0.06	0.2	17.33	0.01	0	0.01	0.2	0.22	0.02	100.38	81.49
VMA1_ol 014_23	88	0.01	39.51	42.73	0.02	0.18	17.55	0.01	-0.01	0.02	0.19	0.17	0.02	100.41	81.27
VMA1_ol 014_24	92	0.03	39.03	42.49	0.08	0.24	17.63	0.02	0	0.03	0.2	0.15	-0.01	99.9	81.12
VMA1_ol 014_25	96	0.03	39.19	42.42	0.04	0.19	18.14	0	0.01	0.04	0.19	0.13	0	100.37	80.65
VMA1_ol 014_26	100	0.02	39.46	42.27	0.07	0.2	18.39	0	0	0.04	0.17	0.07	0.02	100.71	80.38
VMA1_ol 014_27	104	0.02	39.42	41.99	0.09	0.21	18.81	0.01	0	0.05	0.18	0.03	0.02	100.84	79.92
VMA1_ol 014_28	108	0.02	38.89	41.69	0.07	0.21	19	0	0	0.04	0.16	0.05	0	100.13	79.64
VMA1_ol 014_29	112	0.02	39.16	41.45	0.07	0.22	19.04	0.01	0	0.04	0.15	0.07	0.03	100.26	79.51
VMA1_ol 014_30	116	0.01	38.98	41.45	0.1	0.15	19.4	0	-0.01	0.05	0.16	0.07	0.01	100.37	79.20
VMA1_ol 014_31	120	0.03	39.14	41.4	0.08	0.17	19.4	-0.01	0	0.03	0.16	0.05	0.01	100.46	79.18
VMA1_ol 014_32	124	0.02	39.15	41.38	0.08	0.17	19.64	-0.01	0	0.05	0.16	0.05	0.01	100.7	78.97
VMA1_ol 014_33	128	0.01	38.99	41.06	0.07	0.21	19.46	0.01	0	0.04	0.16	0.07	0	100.09	79.00
VMA1_ol 014_34	132	0.02	38.81	41.04	0.05	0.19	19.5	0.01	0	0.05	0.16	0.05	0	99.88	78.95
VMA1_ol 014_35	136	0.02	39.23	41.22	0.07	0.19	19.79	0	-0.01	0.04	0.15	0.06	0.02	100.77	78.78
VMA1_ol 014_36	140	0.02	38.93	41.07	0.03	0.17	19.64	-0.01	-0.01	0.05	0.15	0.05	-0.01	100.08	78.85
VMA1_ol 014_37	144	0.01	38.98	41.22	0.08	0.15	19.7	0.01	0	0.05	0.14	0.04	0.03	100.42	78.86
VMA1_ol 014_38	148	0.03	38.78	41.12	0.05	0.17	19.72	0.01	0	0.05	0.15	0.05	0.01	100.13	78.80
VMA1_ol 014_39	152	0.01	39.19	41.48	0.03	0.16	19.74	0	0.01	0.04	0.16	0.07	0.02	100.91	78.93
VMA1_ol 014_40	156	0.02	38.81	41.2	0.05	0.21	19.62	0	0	0.04	0.16	0.04	0.01	100.16	78.92
VMA1_ol 014_41	160	0.01	39	41.12	0.03	0.15	19.78	0	0	0.03	0.16	0.06	0.02	100.37	78.75
VMA1_ol 014_42	164	0.02	38.83	41.03	0.09	0.17	19.5	0	0	0.04	0.15	0.09	0.01	99.92	78.95
VMA1_ol 014_43	168	0.02	39.13	41.31	0.07	0.19	19.66	0.01	0	0.04	0.16	0.09	0.02	100.69	78.93
VMA1_ol 014_44	172	0.03	38.68	40.99	0.09	0.21	19.67	0.01	0	0.04	0.16	0.02	0.01	99.9	78.79
VMA1_ol 014_45	176	0.02	39.23	41.23	0.07	0.16	19.73	0.01	0	0.04	0.15	0.06	-0.01	100.68	78.84
VMA1_ol 014_46	180	0.04	38.89	41.32	0.05	0.19	19.7	-0.01	0	0.04	0.16	0.07	0.02	100.46	78.90
VMA1_ol 014_47	184	0.03	39.18	40.92	0.06	0.18	19.56	0	0	0.03	0.16	0.03	-0.01	100.16	78.85
VMA1_ol 014_48	188	0.01	39.3	41.12	0.07	0.17	19.67	0	0	0.03	0.16	0.06	0.01	100.59	78.84
VMA1_ol 014_49	192	0.02	39	41.32	0.05	0.16	19.62	0.01	0	0.03	0.14	0.07	-0.01	100.41	78.97
VMA1_ol 014_50	196	0.02	38.93	41.3	0.06	0.18	19.74	0.01	0	0.04	0.15	0.08	-0.01	100.49	78.86
VMA1_ol 014_51	200	0.01	39.05	41.1	0.03	0.19	19.51	0.01	0	0.04	0.17	0.05	0	100.16	78.97
VMA1_ol 014_52	204	0.03	39.35	41.2	0.09	0.18	19.51	-0.01	0	0.03	0.15	0.08	0.01	100.62	79.01
VMA1_ol 014_53	208	0.01	39.44	41.11	0.06	0.2	19.76	-0.02	0	0.02	0.15	0.02	0	100.75	78.76
VMA1_ol 014_54	212	0.03	38.9	41.11	0.03	0.18	19.73	0.02	-0.01	0.03	0.16	0.05	-0.01	100.22	78.79
VMA1_ol 014_55	216	0.02	38.95	41.28	0.09	0.17	19.64	-0.01	0	0.03	0.17	0.04	0	100.39	78.93

Sample	Dist (μm)	Na_2O	SiO_2	MgO	Al_2O_3	MnO	FeO	Cr_2O_3	K_2O	TiO_2	CaO	NiO	P_2O_5	Total	Mg#
VMA1_ol 014_56	220	0.03	38.9	41.11	0.05	0.14	19.58	0.02	0	0.03	0.14	0.04	0	100.05	78.91
VMA1_ol 014_57	224	0.03	39.21	41.24	0.08	0.17	19.65	0	0.01	0.03	0.14	0.07	-0.01	100.61	78.91
VMA1_ol 014_58	228	0.04	39.03	41.15	0.06	0.19	19.54	0.01	-0.01	0.03	0.15	0.07	-0.01	100.24	78.96
VMA1_ol 014_59	232	0	39.05	41.29	0.08	0.17	19.58	0.02	-0.01	0.02	0.16	0.07	0.01	100.46	78.99
VMA1_ol 014_60	236	0.01	39.13	41.1	0.03	0.19	19.44	-0.02	0	0.03	0.15	0.07	0	100.13	79.03
VMA1_ol 014_61	240	0.03	39.11	41.25	0.08	0.19	19.48	0	0	0.04	0.15	0.07	0.01	100.42	79.06
VMA1_ol 014_62	244	0.02	39.27	41.36	0.05	0.17	19.46	0.01	0	0.02	0.16	0.09	0	100.61	79.12
VMA1_ol 014_63	248	0.02	39.25	41.04	0.05	0.13	19.48	0.01	0.01	0.01	0.16	0.08	-0.01	100.22	78.97
VMA1_ol 014_64	252	0.02	39.02	41.33	0.06	0.17	19.45	0	0.01	0.03	0.15	0.05	-0.02	100.26	79.11
VMA1_ol 014_65	256	0.01	39.27	41.38	0.06	0.18	19.39	0.01	0	0.03	0.16	0.06	0.01	100.56	79.18
VMA1_ol 014_66	260	0	39.03	41.26	0.06	0.18	19.46	0	-0.01	0.03	0.15	0.08	0	100.23	79.08
VMA1_ol 014_67	264	0.02	39.03	41.35	0.09	0.18	19.22	0	0.01	0.04	0.16	0.09	-0.01	100.16	79.32
VMA1_ol 014_68	268	0.02	39.17	41.54	0.04	0.2	19.26	-0.01	0	0.03	0.14	0.09	0	100.48	79.36
VMA1_ol 014_69	272	0.02	39.56	41.46	0.04	0.22	19.09	-0.02	0	0.03	0.14	0.08	0	100.62	79.47
VMA1_ol 014_70	276	0.01	39.12	41.6	0.06	0.19	19.2	0.01	0	0.03	0.15	0.09	0	100.46	79.43
VMA1_ol 014_71	280	0.04	39.23	41.49	0.07	0.2	19.28	0	0	0.03	0.15	0.08	0	100.56	79.32
VMA1_ol 014_72	284	0	38.91	41.58	0.05	0.16	19.16	0	0	0.03	0.16	0.09	-0.02	100.13	79.46
VMA1_ol 014_73	288	0.01	39.26	41.76	0.04	0.17	19.22	0.01	0	0.03	0.15	0.09	0.02	100.76	79.48
VMA1_ol 014_74	292	0	38.76	41.74	0.06	0.18	19.01	-0.02	0	0.04	0.14	0.06	-0.03	99.95	79.65
VMA1_ol 014_75	296	0.01	39.01	41.69	0.07	0.19	19.15	0.01	0	0.02	0.13	0.09	0	100.37	79.51
VMA1_ol 014_76	300	0.01	39.1	41.65	0.01	0.18	19.17	-0.01	0	0.03	0.16	0.05	-0.01	100.33	79.48
VMA1_ol 014_77	304	0.01	38.84	41.82	0.06	0.19	19.31	-0.01	0	0.03	0.15	0.08	-0.01	100.46	79.43
VMA1_ol 014_78	308	0	39.17	41.54	0.02	0.18	19.24	-0.01	0	0.03	0.14	0.09	-0.01	100.39	79.38
VMA1_ol 014_79	312	0.02	39.09	41.57	0.05	0.19	19.41	0	0	0.03	0.15	0.05	0.02	100.59	79.24
VMA1_ol 014_80	316	0.04	38.61	41.46	0.06	0.19	19.33	0.01	0	0.02	0.17	0.07	0	99.97	79.27
VMA1_ol 014_81	320	0.02	39.32	41.41	0.09	0.15	19.22	-0.01	0	0.03	0.16	0.08	0.01	100.47	79.34
VMA1_ol 014_82	324	0.02	39	41.38	0.06	0.16	19.34	0.02	0	0.03	0.14	0.08	-0.02	100.21	79.23
VMA1_ol 014_83	328	0	39.2	41.66	0.05	0.18	19.27	0	0	0.04	0.16	0.09	-0.01	100.65	79.40
VMA1_ol 014_84	332	0.02	38.77	40.93	0.07	0.21	18.98	0.01	0	0.03	0.15	0.05	-0.02	99.21	79.36
VMA1_ol 014_85	336	0.02	39.15	41.3	0.05	0.19	19.53	0.01	0	0.03	0.17	0.03	-0.01	100.47	79.03
VMA1_ol 014_86	340	0.01	38.85	41.04	0.06	0.17	19.36	0.01	0	0.03	0.14	0.08	-0.02	99.74	79.07
VMA1_ol 014_87	344	0.02	38.93	41.12	0.05	0.16	19.4	0	0	0.03	0.15	0.11	-0.02	99.95	79.07
VMA1_ol 014_88	348	0	38.61	41.17	0.08	0.18	19.42	0.01	0	0.04	0.16	0.1	0.01	99.79	79.07
VMA1_ol 014_89	352	0.03	39.09	41.15	0.05	0.18	19.41	0	0.01	0.02	0.15	0.07	-0.01	100.17	79.08
VMA1_ol 014_90	356	0.02	38.87	41.35	0.07	0.17	19.63	-0.01	0	0.04	0.15	0.09	0	100.38	78.97
VMA1_ol 014_91	360	0.02	39.26	41.26	0.08	0.16	19.52	0	0.01	0.04	0.16	0.09	0.01	100.61	79.03
VMA1_ol 014_92	364	0.02	39.19	41.3	0.04	0.15	19.64	0.01	0	0.04	0.17	0.06	-0.03	100.59	78.94
VMA1_ol 014_93	368	0.01	38.86	41.43	0.06	0.16	19.71	0.01	0	0.03	0.16	0.08	0	100.51	78.93
VMA1_ol 014_94	372	0.03	38.94	41.22	0.06	0.2	19.76	0.01	0	0.04	0.16	0.08	-0.02	100.48	78.81

Sample	Dist (μm)	Na_2O	SiO_2	MgO	Al_2O_3	MnO	FeO	Cr_2O_3	K_2O	TiO_2	CaO	NiO	P_2O_5	Total	Mg#
VMA1_ol 014_95	376	0.01	39.37	41.29	0.05	0.14	19.49	-0.01	0	0.03	0.15	0.09	0.01	100.6	79.06
VMA1_ol 014_96	380	0.01	38.89	41.22	0.08	0.19	19.64	0.01	0	0.03	0.17	0.06	-0.03	100.27	78.91
VMA1_ol 014_97	384	0	39.24	40.95	0.05	0.16	19.59	-0.01	0	0.04	0.18	0.08	-0.01	100.27	78.84
VMA1_ol 014_98	388	0	39.04	41.22	0.08	0.16	19.61	0.01	0	0.04	0.18	0.07	0.01	100.43	78.93
VMA1_ol 014_99	392	0.02	38.89	41.2	0.08	0.18	19.64	0	0	0.03	0.16	0.04	0	100.23	78.90
VMA1_ol 014_100	396	0.02	38.98	41.26	0.04	0.19	19.5	0	0.01	0.03	0.18	0.06	0.01	100.28	79.04
VMA1_ol 014_101	400	-0.01	38.92	40.92	0.06	0.17	19.45	0.01	0	0.03	0.15	0.05	0	99.77	78.95
VMA1_ol 014_102	404	0.01	38.79	41.1	0.04	0.15	19.63	0	0	0.03	0.16	0.04	0.02	99.99	78.87
VMA1_ol 014_103	408	0.02	39.19	41.06	0.02	0.18	19.59	-0.01	0.01	0.03	0.17	0.1	-0.02	100.35	78.89
VMA1_ol 014_104	412	0.03	38.96	41.03	0.08	0.17	19.49	0	0.01	0.04	0.17	0.05	-0.01	100.02	78.96
VMA1_ol 014_105	416	0.01	39.18	40.96	0.05	0.15	19.54	0.02	0.02	0.02	0.17	0.06	-0.03	100.16	78.89
VMA1_ol 014_106	420	0.02	38.84	41.22	0.06	0.2	19.29	0.02	0.05	0.03	0.18	0.05	-0.01	99.94	79.21
VMA1_ol 014_107	424	0.01	39.32	40.92	0.09	0.17	19.3	0.01	0.02	0.02	0.17	0.09	0	100.12	79.08
VMA1_ol 014_108	428	0.02	38.74	41.3	0.05	0.15	19.38	-0.01	0.02	0.03	0.17	0.05	0.01	99.92	79.16
VMA1_ol 014_109	432	0.02	39.19	41.3	0.03	0.18	19.37	-0.01	0	0.04	0.16	0.06	-0.02	100.35	79.17
VMA1_ol 014_110	436	0.02	39.09	41.35	0.07	0.17	19.34	0.01	0.01	0.02	0.16	0.08	0.02	100.36	79.22
VMA1_ol 014_111	440	0.01	39.3	41.4	0.06	0.17	19.31	0.01	0	0.03	0.16	0.07	0.01	100.54	79.26
VMA1_ol 014_112	444	0	39.02	41.24	0.07	0.16	19.5	0.01	0.01	0.02	0.17	0.07	0.01	100.29	79.03
VMA1_ol 014_113	448	0.02	39.13	41.53	0.09	0.18	19.25	0.01	0.01	0.03	0.18	0.04	0	100.48	79.36
VMA1_ol 014_114	452	0.02	39.07	41.36	0.05	0.21	19.14	0.01	0.01	0.02	0.18	0.09	0.02	100.19	79.39
VMA1_ol 014_115	456	0	39.35	41.44	0.05	0.18	19.12	0	0	0.04	0.19	0.07	0.01	100.46	79.44
VMA1_ol 014_116	460	0.01	38.96	41.76	0.04	0.19	18.77	0.01	0.01	0.03	0.18	0.07	-0.02	100.01	79.86
VMA1_ol 014_117	464	0.02	39.17	41.61	0.06	0.18	18.7	0.01	0.01	0.04	0.18	0.11	0	100.09	79.86
VMA1_ol 014_118	468	0	39.34	41.95	0.05	0.19	18.68	0.02	0.01	0.04	0.19	0.13	-0.01	100.59	80.01
VMA1_ol 014_119	472	0.02	39.39	42.03	0.06	0.2	18.24	0	0.01	0.05	0.16	0.07	-0.01	100.22	80.42
VMA1_ol 014_120	476	0.02	39.06	42.19	0.06	0.18	18.38	0.02	0.01	0.04	0.16	0.08	0.01	100.19	80.36
VMA1_ol 014_121	480	0.03	39.44	42.24	0.03	0.22	18.17	0.01	0.01	0.02	0.16	0.12	-0.01	100.45	80.56
VMA1_ol 014_122	484	0.02	39.39	42.63	0.05	0.19	17.83	0.02	0	0.03	0.19	0.12	0.02	100.49	81.00
VMA1_ol 014_123	488	0.03	39.73	42.41	0.04	0.2	17.52	0.02	0	0.04	0.17	0.12	-0.02	100.27	81.19
VMA1_ol 014_124	492	0.03	39.61	42.95	0.06	0.2	17.44	0.02	0	0.05	0.2	0.16	0	100.71	81.45
VMA1_ol 015_01	0	1.95	45.5	3.36	16.71	0.19	12.13	0.01	2.18	3.1	9.67	-0.01	1.22	95.99	33.05
VMA1_ol 015_02	4	0.34	40.09	34.29	1.97	0.41	22.87	0	0.22	0.3	1.28	0.06	0.2	102.05	72.77
VMA1_ol 015_03	8	0.01	38.44	39.76	0.03	0.33	20.7	0.01	0.01	0.07	0.51	0.07	0.01	99.96	77.40
VMA1_ol 015_04	12	0.02	39.04	40.92	0.05	0.31	19.41	0.02	0	0.05	0.51	0.09	0.02	100.43	78.98
VMA1_ol 015_05	16	0.01	38.95	41.21	0.04	0.28	18.9	0.02	0	0.04	0.46	0.14	0.02	100.07	79.54
VMA1_ol 015_06	20	0.01	38.92	41.42	0.03	0.28	18.6	0.01	0	0.05	0.42	0.15	0.03	99.92	79.88
VMA1_ol 015_07	24	0.01	38.96	41.92	0.04	0.29	18.32	0.03	0	0.04	0.42	0.13	0.01	100.18	80.31
VMA1_ol 015_08	28	0.03	39.29	42.47	0.06	0.27	17.56	0.04	0.01	0.04	0.39	0.14	0.05	100.33	81.17
VMA1_ol 015_09	32	0.02	39.06	42.76	0.05	0.28	17.25	0.04	0	0.03	0.37	0.15	0.05	100.07	81.55

Sample	Dist (μm)	Na_2O	SiO_2	MgO	Al_2O_3	MnO	FeO	Cr_2O_3	K_2O	TiO_2	CaO	NiO	P_2O_5	Total	Mg#
VMA1_ol 015_10	36	0.02	39.5	43.25	0.06	0.25	16.92	0.03	0	0.03	0.36	0.15	0.03	100.62	82.00
VMA1_ol 015_11	40	0.04	39.22	42.98	0.04	0.25	17.34	0.04	0.01	0.03	0.27	0.2	0.04	100.45	81.54
VMA1_ol 015_12	44	0.02	39.43	42.67	0.04	0.23	17.23	0.03	0.01	0.02	0.27	0.2	0.02	100.17	81.53
VMA1_ol 015_13	48	0.02	39.25	43.09	0.03	0.25	17.3	0.03	0.01	0.02	0.26	0.22	0.04	100.51	81.62
VMA1_ol 015_14	52	0.01	39.4	42.99	0.07	0.21	17.29	0.04	0	0.02	0.24	0.23	-0.01	100.48	81.59
VMA1_ol 015_15	56	0.03	39.38	42.97	0.07	0.24	17.15	0.04	0.01	0.03	0.23	0.23	0	100.37	81.71
VMA1_ol 015_16	60	0.02	39.58	43.4	0.03	0.24	17	0.03	0	0.01	0.24	0.23	0.01	100.8	81.98
VMA1_ol 015_17	64	0.02	39.38	43.19	0.04	0.22	16.86	0.06	0.01	0.02	0.24	0.24	-0.01	100.26	82.03
VMA1_ol 015_18	68	0.03	39.56	43.17	0.04	0.22	16.85	0.04	0.01	0.01	0.22	0.22	0.04	100.43	82.04
VMA1_ol 015_19	72	0.02	39.36	43.11	0.06	0.21	16.84	0.01	0	0.01	0.22	0.24	0.03	100.11	82.02
VMA1_ol 015_20	76	0.02	39.32	43.56	0.06	0.24	16.94	0.02	0.01	0.02	0.22	0.21	0.02	100.63	82.09
VMA1_ol 015_21	80	0.04	39.47	43.26	0.09	0.23	16.93	0.05	-0.01	0.02	0.21	0.24	0.01	100.53	82.00
VMA1_ol 015_22	84	0.02	39.65	43.29	0.07	0.2	16.86	0.04	0	0.03	0.23	0.18	0.02	100.58	82.07
VMA1_ol 015_23	88	0.02	39.34	43.26	0.08	0.2	16.83	0.02	0	0.03	0.24	0.18	0.03	100.23	82.08
VMA1_ol 015_24	92	0.03	39.42	43.17	0.05	0.28	16.98	0.04	0	0.02	0.22	0.22	0.06	100.5	81.92
VMA1_ol 015_25	96	0.01	38.96	43.69	0.06	0.2	16.78	0.05	0	0.04	0.23	0.21	0.04	100.28	82.27
VMA1_ol 015_26	100	0.03	39.43	43.32	0.04	0.2	16.81	0.04	-0.01	0.02	0.23	0.21	0.01	100.33	82.12
VMA1_ol 015_27	104	0.02	39.32	43.39	0.03	0.22	16.77	0.02	0.01	0.02	0.25	0.19	0.01	100.25	82.18
VMA1_ol 015_28	108	0.02	39.71	43.51	0.04	0.21	16.62	0.04	-0.01	0.02	0.24	0.2	0.02	100.62	82.35
VMA1_ol 015_29	112	0.01	39.43	43.85	0.05	0.24	16.04	0.03	0	0.02	0.22	0.23	0.02	100.13	82.97
VMA1_ol 015_30	116	0.01	39.84	44.29	0.04	0.2	15.74	0.04	0	0.01	0.2	0.24	0	100.62	83.38
VMA1_ol 015_31	120	0.03	39.56	44.36	0.06	0.2	15.65	0.04	0	0.02	0.22	0.24	0	100.36	83.48
VMA1_ol 015_32	124	0.03	40.18	44.51	0.05	0.18	15.29	0.03	0	0.02	0.22	0.23	0.01	100.75	83.84
VMA1_ol 015_33	128	0.03	39.9	44.75	0.04	0.21	15.18	0.04	0	0.01	0.22	0.19	0.04	100.59	84.01
VMA1_ol 015_34	132	0.03	40.02	44.76	0.1	0.17	15.02	0.03	0	0.02	0.23	0.29	0	100.67	84.16
VMA1_ol 015_35	136	0.02	39.86	45	0.06	0.19	14.98	0.06	0	0.02	0.21	0.27	0.02	100.69	84.26
VMA1_ol 015_36	140	0.03	39.51	45.04	0.06	0.17	14.96	0.03	0.01	0.02	0.2	0.26	0.03	100.31	84.29
VMA1_ol 015_37	144	0.02	40.02	45.01	0.05	0.16	15.06	0.04	0	0.01	0.23	0.28	0.02	100.9	84.20
VMA1_ol 015_38	148	0.03	39.94	45.02	0.04	0.18	15.11	0.05	0	0.01	0.19	0.26	0.03	100.85	84.15
VMA1_ol 015_39	152	0.02	39.71	44.53	0.06	0.19	15.26	0.04	0	0	0.2	0.26	0.04	100.32	83.88
VMA1_ol 015_40	156	0.02	39.9	44.46	0.05	0.15	15.4	0.04	0	0.01	0.2	0.24	0	100.48	83.73
VMA1_ol 015_41	160	0.04	39.7	44.63	0.02	0.19	15.66	0.05	0	0.01	0.19	0.2	-0.01	100.66	83.55
VMA1_ol 015_42	164	0.03	39.93	44.34	0.06	0.19	15.87	0.03	0	0.02	0.2	0.23	0.01	100.91	83.28
VMA1_ol 015_43	168	0.04	39.6	43.93	0.08	0.21	16.08	0.03	0	0.01	0.23	0.2	-0.01	100.4	82.96
VMA1_ol 015_44	172	0	39.51	43.51	0.03	0.21	16.54	0.02	0	0.03	0.23	0.18	0.01	100.27	82.42
VMA1_ol 015_45	176	0	39.55	43.05	0.02	0.22	16.92	0.04	0.01	0.03	0.22	0.18	0.04	100.27	81.93
VMA1_ol 015_46	180	0.03	38.88	40.53	0.05	0.28	19.46	0.03	0.01	0.04	0.43	0.16	0.03	99.94	78.78
VMA1_ol 015_47	184	0.03	38.79	40.48	0.13	0.29	19.03	0.03	0.02	0.04	0.5	0.15	0.01	99.51	79.13
VMA1_ol 015_48	188	0.02	39.51	42.85	0.05	0.27	17.33	0.03	0.01	0.04	0.31	0.22	0.01	100.64	81.51

Sample	Dist (μm)	Na_2O	SiO_2	MgO	Al_2O_3	MnO	FeO	Cr_2O_3	K_2O	TiO_2	CaO	NiO	P_2O_5	Total	Mg#
VMA1_ol 015_49	192	0.02	39.38	43.13	0.03	0.22	16.95	0.05	0	0.03	0.26	0.2	0.02	100.29	81.94
VMA1_ol 015_50	196	0.02	39.65	43.19	0.06	0.19	16.94	0.04	0	0.02	0.22	0.26	0.01	100.6	81.96
VMA1_ol 015_51	200	0.05	39.46	43.42	0.13	0.2	16.87	0.02	0.01	0.01	0.21	0.24	0.01	100.63	82.10
VMA1_ol 015_52	204	0.02	39.49	43.13	0.04	0.21	17.09	0.01	0	0.03	0.17	0.2	0	100.41	81.81
VMA1_ol 015_53	208	0.03	39.46	43.31	0.06	0.22	17.15	0.03	0.01	0.01	0.17	0.25	-0.02	100.67	81.82
VMA1_ol 015_54	212	0.03	39.24	43.11	0.02	0.22	17.37	0.02	0.01	0.02	0.15	0.22	-0.01	100.39	81.56
VMA1_ol 015_55	216	0.02	39.19	43	0.02	0.17	17.46	0.02	0	0.02	0.15	0.29	0.01	100.36	81.45
VMA1_ol 015_56	220	0.03	39.53	42.71	0.08	0.19	17.46	0.02	0	0.02	0.14	0.19	-0.01	100.36	81.34
VMA1_ol 015_57	224	0.02	39.28	42.74	0.04	0.22	17.7	0	0	0.02	0.12	0.23	0	100.38	81.15
VMA1_ol 015_58	228	0.03	39.46	42.45	0.06	0.2	17.83	0.01	0	0.02	0.13	0.24	0.04	100.47	80.93
VMA1_ol 015_59	232	0.04	39.41	42.59	0.01	0.2	17.95	0.01	0	0.02	0.12	0.27	0.01	100.63	80.88
VMA1_ol 015_60	236	0.04	39.34	42.4	0.02	0.2	18.16	0.02	0	0.01	0.12	0.27	0.04	100.61	80.63
VMA1_ol 015_61	240	0.03	39.08	42.5	0.03	0.18	18.36	0.02	0	0.01	0.11	0.2	-0.01	100.52	80.49
VMA1_ol 015_62	244	0.03	39.13	42.2	0.08	0.24	18.3	-0.01	0	0.03	0.11	0.28	0.03	100.42	80.43
VMA1_ol 015_63	248	0.04	38.85	42.19	0.03	0.23	18.36	0.02	0	0.02	0.11	0.23	0.01	100.09	80.38
VMA1_ol 015_64	252	0.04	39.45	41.88	0.05	0.24	18.53	-0.01	0.01	0.01	0.1	0.2	0.01	100.5	80.11
VMA1_ol 015_65	256	0.01	39.15	41.94	0.06	0.18	18.53	0.01	0	0.01	0.11	0.25	0.01	100.25	80.14
VMA1_ol 015_66	260	0.03	39.4	42.11	0.03	0.19	18.57	0.02	0.01	0.02	0.1	0.23	0	100.71	80.17
VMA1_ol 015_67	264	0.02	39.07	42.1	0.01	0.19	18.62	-0.01	0	0.02	0.11	0.22	0.01	100.35	80.12
VMA1_ol 015_68	268	0.02	39.21	42.03	0.03	0.19	18.84	0	0	0.01	0.11	0.21	0.03	100.68	79.91
VMA1_ol 015_69	272	0.02	38.99	41.96	0.03	0.22	18.76	0.01	0	0.02	0.12	0.23	0.02	100.38	79.95
VMA1_ol 015_70	276	0.02	39.29	41.91	0.03	0.19	18.4	0.01	0	0.01	0.13	0.23	0	100.21	80.24
VMA1_ol 015_71	280	0.03	38.78	41.94	0.04	0.2	18.62	0.01	0	0.02	0.11	0.27	-0.01	100	80.06
VMA1_ol 015_72	284	0.03	39.1	42.01	0.08	0.18	18.78	0	0	0.02	0.12	0.19	0	100.5	79.95
VMA1_ol 015_73	288	0.03	38.9	41.86	0.03	0.18	18.63	0.01	0	0.02	0.11	0.26	0.01	100.04	80.02
VMA1_ol 015_74	292	0.01	39.2	41.89	0.01	0.18	18.69	0.01	-0.01	0.01	0.1	0.24	0.01	100.35	79.98
VMA1_ol 015_75	296	0.01	38.86	41.82	0.06	0.21	18.63	0	0	0.02	0.11	0.24	0.02	99.97	80.01
VMA1_ol 015_76	300	0.03	38.89	41.78	0.03	0.18	18.67	0.01	0	0.02	0.12	0.24	-0.01	99.96	79.96
VMA1_ol 015_77	304	0.03	39.02	41.9	0.05	0.21	18.77	0	0.01	0.01	0.1	0.27	0	100.36	79.92
VMA1_ol 015_78	308	0.03	39.28	41.81	0.04	0.2	18.75	-0.01	0	0.02	0.1	0.24	0.02	100.5	79.90
VMA1_ol 015_79	312	0.06	38.92	42.17	0.04	0.21	18.64	-0.01	0.01	0.01	0.1	0.27	0.02	100.46	80.13
VMA1_ol 015_80	316	0.02	39.18	41.73	0.06	0.18	18.39	0.01	0	0.02	0.11	0.22	0	99.93	80.18
VMA1_ol 015_81	320	0.04	39.01	42.06	0.03	0.2	18.71	0	0.01	0.01	0.1	0.22	-0.01	100.38	80.03
VMA1_ol 015_82	324	0.02	39.2	41.83	0.06	0.19	18.74	-0.01	0.01	0.01	0.11	0.23	0.01	100.41	79.92
VMA1_ol 015_83	328	0.04	39.15	41.8	0.05	0.2	18.7	0.01	0	0.01	0.12	0.26	0.01	100.37	79.94
VMA1_ol 015_84	332	0.02	39.24	41.84	0.07	0.19	18.78	0.01	0	0.02	0.11	0.23	0.01	100.53	79.88
VMA1_ol 015_85	336	0.03	39.12	41.94	0.07	0.22	18.78	0	0	0.02	0.11	0.21	0.01	100.51	79.92
VMA1_ol 015_86	340	0.03	38.99	41.88	0.05	0.2	18.63	0.01	0	0.02	0.11	0.27	0.01	100.19	80.03
VMA1_ol 015_87	344	0.02	38.91	42.01	0.03	0.2	18.59	0.03	-0.01	0.02	0.1	0.22	-0.02	100.12	80.11

Sample	Dist (μm)	Na_2O	SiO_2	MgO	Al_2O_3	MnO	FeO	Cr_2O_3	K_2O	TiO_2	CaO	NiO	P_2O_5	Total	Mg#
VMA1_ol 015_88	348	0.03	39.02	41.78	0.04	0.23	18.75	0.01	0	0.02	0.1	0.27	0	100.24	79.89
VMA1_ol 015_89	352	0.01	39.08	41.73	0.06	0.21	18.73	0	0	0.02	0.11	0.25	0.01	100.2	79.89
VMA1_ol 015_90	356	0.03	39.1	41.93	0.04	0.19	18.68	0.01	0	0.03	0.1	0.25	0.01	100.37	80.00
VMA1_ol 015_91	360	0.03	38.94	41.94	0.06	0.19	18.63	0	0	0.02	0.1	0.25	0	100.14	80.05
VMA1_ol 015_92	364	0.03	39.11	42.09	0.04	0.19	18.74	0.01	0	0.02	0.11	0.21	0	100.55	80.01
VMA1_ol 015_93	368	0.02	39.29	42	0.06	0.2	18.56	0.01	0	0.02	0.09	0.29	0.04	100.58	80.13
VMA1_ol 015_94	372	0.02	39.17	42.13	0.03	0.22	18.65	0.01	0	0.02	0.12	0.21	0.02	100.61	80.11
VMA1_ol 015_95	376	0.03	38.71	41.8	0.05	0.21	18.74	0.02	0	0.02	0.13	0.23	0.04	99.97	79.90
VMA1_ol 015_96	380	0.04	39.22	41.92	0.03	0.19	18.78	0	0	0.02	0.11	0.23	0	100.53	79.92
VMA1_ol 015_97	384	0.03	39.23	41.76	0.05	0.21	18.69	0	0.01	0.02	0.11	0.24	0.01	100.35	79.93
VMA1_ol 015_98	388	0.03	39.25	41.9	0.05	0.24	18.73	0.01	0	0.02	0.12	0.25	0.01	100.6	79.95
VMA1_ol 015_99	392	0.01	38.41	42.01	0.03	0.19	18.73	0	0.01	0.01	0.12	0.25	0.01	99.79	79.99
VMA1_ol 015_100	396	0.03	39.52	41.97	0.02	0.18	18.68	-0.01	0	0.02	0.11	0.27	-0.01	100.77	80.02
VMA1_ol 015_101	400	0.02	38.88	41.86	0.03	0.18	18.59	-0.01	0.01	0.01	0.11	0.24	0.03	99.95	80.06
VMA1_ol 015_102	404	0.04	39.02	41.72	0.08	0.21	18.64	0.02	0.01	0.02	0.12	0.21	-0.03	100.08	79.96
VMA1_ol 015_103	408	0.03	39.12	41.96	0.03	0.18	18.68	0.01	0	0	0.13	0.22	0	100.34	80.02
VMA1_ol 015_104	412	0.23	39.13	41.98	0.05	0.24	18.7	-0.01	0.02	0.02	0.11	0.23	0.03	100.74	80.01
VMA1_ol 015_105	416	0.03	38.95	41.95	0.07	0.18	18.53	0.01	0	0.04	0.11	0.2	0.01	100.08	80.14
VMA1_ol 015_106	420	0.04	39.2	41.74	0.04	0.17	18.57	0	0	0.02	0.13	0.25	0.01	100.15	80.03
VMA1_ol 015_107	424	0.02	38.97	41.98	0.02	0.18	18.78	0.01	0.01	0.02	0.11	0.22	0.01	100.33	79.94
VMA1_ol 015_108	428	0.04	39.43	41.84	0.04	0.21	18.72	-0.01	0.01	0.01	0.1	0.27	0.01	100.67	79.94
VMA1_ol 015_109	432	0.02	39.1	42.02	0.08	0.21	18.75	0.02	0.01	0.02	0.11	0.23	0.02	100.59	79.98
VMA1_ol 015_110	436	0.04	39.14	41.61	0.08	0.16	18.81	0.01	0	0.02	0.12	0.24	0.01	100.24	79.77
VMA1_ol 015_111	440	0	39.52	41.88	0.04	0.24	18.5	0	0	0.01	0.12	0.23	-0.01	100.54	80.14
VMA1_ol 015_112	444	0.03	39.17	41.86	0.07	0.19	18.66	-0.01	0.01	0.02	0.11	0.24	0	100.33	80.00
VMA1_ol 015_113	448	0.01	39.24	42.06	0.1	0.2	18.8	0	0	0.02	0.1	0.22	-0.01	100.74	79.95
VMA1_ol 015_114	452	0.02	39.17	41.78	0.05	0.22	18.76	0	0	0.02	0.11	0.21	-0.01	100.34	79.88
VMA1_ol 015_115	456	0.03	38.98	42	0.02	0.22	18.8	-0.01	0	0.01	0.1	0.24	0.03	100.41	79.93
VMA1_ol 015_116	460	0.03	39.28	42.03	0.02	0.21	18.71	0	0.01	0.01	0.11	0.25	0.03	100.69	80.02
VMA1_ol 015_117	464	0.03	38.94	41.99	0.02	0.22	18.61	0.02	0.01	0.03	0.11	0.25	0	100.23	80.09
VMA1_ol 015_118	468	0.08	39.29	41.96	0.05	0.25	18.8	0.01	0.01	0.02	0.11	0.23	-0.04	100.78	79.91
VMA1_ol 015_119	472	0.01	38.9	41.98	0.03	0.2	18.72	0.01	0	0.02	0.11	0.2	0.02	100.21	79.99
VMA1_ol 015_120	476	0.04	38.98	42.2	0.02	0.21	18.63	-0.01	0	0.02	0.12	0.24	0.01	100.47	80.15
VMA1_ol 015_121	480	0.04	38.86	42	0.05	0.2	18.76	0.01	0	0.01	0.12	0.19	0	100.25	79.96
VMA1_ol 015_122	484	0.03	39.38	42	0.06	0.19	18.7	0	0	0.02	0.11	0.26	0	100.75	80.01
VMA1_ol 015_123	488	0.02	38.9	41.77	0.05	0.22	18.71	-0.01	0	0.02	0.12	0.21	0.01	100.02	79.92
VMA1_ol 015_124	492	0	39.15	41.92	0.05	0.17	18.81	0.01	0	0.02	0.11	0.26	0.01	100.49	79.89
VMA1_ol 015_125	496	0.03	39.15	41.71	0.02	0.19	18.57	0	0.01	0.02	0.12	0.23	0.01	100.05	80.02
VMA1_ol 015_126	500	0	39.27	41.7	0.04	0.21	18.78	0.01	0	0.02	0.1	0.27	0	100.4	79.83

Sample	Dist (μm)	Na_2O	SiO_2	MgO	Al_2O_3	MnO	FeO	Cr_2O_3	K_2O	TiO_2	CaO	NiO	P_2O_5	Total	Mg#
VMA1_ol 015_127	504	0.03	38.99	41.94	0.05	0.19	18.75	0.01	0.01	0.03	0.11	0.22	0	100.33	79.95
VMA1_ol 015_128	508	0.03	39.19	41.87	0.09	0.22	18.64	-0.01	0	0.03	0.11	0.27	0.01	100.45	80.02
VMA1_ol 015_129	512	0.02	38.96	42	0.04	0.17	18.63	0	0	0.01	0.1	0.25	0.02	100.21	80.07
VMA1_ol 015_130	516	0	38.72	41.82	0.04	0.23	18.64	-0.01	0	0.01	0.11	0.22	0.01	99.79	80.00
VMA1_ol 015_131	520	0.01	39.33	41.89	0.06	0.23	18.77	0.01	0.01	0.02	0.11	0.22	0	100.64	79.91
VMA1_ol 015_132	524	-0.01	38.84	41.85	0.06	0.2	18.8	0.01	0	0.02	0.1	0.22	0	100.09	79.87
VMA1_ol 015_133	528	0	39.08	41.96	0.05	0.17	18.67	0.02	0	0.01	0.1	0.24	0.01	100.32	80.02
VMA1_ol 015_134	532	0.02	38.88	41.93	0.02	0.19	18.62	-0.01	0	0.02	0.1	0.22	0.01	100	80.06
VMA1_ol 015_135	536	0.01	39.12	42.18	0.04	0.19	18.83	0.02	0	0.02	0.1	0.22	0.01	100.73	79.97
VMA1_ol 015_136	540	0	39.01	42.05	0.03	0.2	18.72	-0.03	0	0.02	0.12	0.24	0.02	100.38	80.02
VMA1_ol 015_137	544	0	39.07	41.84	0.04	0.2	18.79	-0.01	0	0.01	0.13	0.24	-0.02	100.29	79.88
VMA1_ol 015_138	548	0.02	38.91	42.05	0.08	0.21	18.74	0.01	-0.01	0.02	0.1	0.23	0.02	100.38	80.00
VMA1_ol 015_139	552	0.02	39.03	42.23	0.01	0.18	18.73	0.01	0	0.01	0.12	0.25	0.01	100.6	80.08
VMA1_ol 015_140	556	0.01	39.46	41.68	0.03	0.2	18.72	0	0	0.01	0.11	0.25	0	100.47	79.87
VMA1_ol 015_141	560	0.02	38.93	41.76	0	0.22	18.55	-0.01	0	0.02	0.11	0.26	0.02	99.86	80.05
VMA1_ol 015_142	564	0.02	39.19	41.81	0	0.19	18.75	0.02	0	0.01	0.11	0.2	-0.01	100.29	79.90
VMA1_ol 015_143	568	0.02	39.18	42.1	0.04	0.21	18.83	0.01	0	0.01	0.11	0.22	0	100.73	79.94
VMA1_ol 015_144	572	0.02	39.08	41.82	0.05	0.17	18.73	0.01	0	0.01	0.1	0.23	0	100.22	79.92
VMA1_ol 015_145	576	0	38.94	41.97	0.05	0.2	18.59	-0.01	0	0	0.11	0.24	0.01	100.1	80.10
VMA1_ol 015_146	580	0.02	38.96	41.97	0.02	0.2	18.64	0.01	0	0.02	0.1	0.24	0.04	100.23	80.05
VMA1_ol 015_147	584	0.01	38.99	41.94	0.06	0.22	18.68	0.01	-0.01	0.01	0.11	0.24	-0.03	100.24	80.01
VMC3_Ol 01a_01	0	2.97	46.56	4	15.55	0.15	11.18	0.01	1.66	3.09	11.81	0.03		97.01	38.94
VMC3_Ol 01a_02	2	0.59	43.78	10.19	9.3	0.16	8.86	0.01	0.06	3.97	22.07	0.01		98.99	67.21
VMC3_Ol 01a_03	4	0.92	42.15	26.28	7.12	0.33	18	0	0.44	1.55	5.99	0.04		102.8	72.24
VMC3_Ol 01a_04	6	0	38.83	40.84	0.05	0.3	18.86	0.02	0	0.06	0.49	0.1		99.56	79.42
VMC3_Ol 01a_05	8	0.02	39.12	40.76	0.04	0.26	18.06	0.02	0	0.06	0.46	0.08		98.87	80.09
VMC3_Ol 01a_06	10	0.02	39.46	41.56	0.06	0.29	18.08	0	0.01	0.06	0.45	0.12		100.11	80.38
VMC3_Ol 01a_07	12	0	39.41	41.59	0.02	0.27	17.59	0.01	0	0.06	0.43	0.12		99.5	80.82
VMC3_Ol 01a_08	14	0.02	39.5	42.04	0.04	0.25	17.55	0.03	0.01	0.05	0.39	0.11		99.98	81.02
VMC3_Ol 01a_09	16	0.01	39.68	41.85	0.02	0.28	17.26	0.03	0	0.03	0.37	0.1		99.62	81.21
VMC3_Ol 01a_10	18	0.02	38.89	41.11	0.03	0.27	16.98	0.03	0	0.06	0.38	0.16		97.92	81.19
VMC3_Ol 01a_11	20	0.01	39.57	42.45	0.03	0.26	16.85	0.02	0	0.03	0.36	0.14		99.71	81.79
VMC3_Ol 01a_12	22	0.04	39.6	42.9	0.04	0.25	16.64	0.05	0	0.04	0.36	0.15		100.08	82.13
VMC3_Ol 01a_13	24	0.02	39.33	42.6	0.05	0.26	16.37	0.02	0	0.03	0.36	0.2		99.22	82.27
VMC3_Ol 01a_14	26	0.02	39.55	43.33	0.03	0.24	16.44	0.06	0	0.03	0.35	0.19		100.23	82.45
VMC3_Ol 01a_15	28	0.02	39.49	43.15	0.03	0.24	16.32	0.02	0	0.03	0.32	0.2		99.81	82.50
VMC3_Ol 01a_16	30	0.02	39.64	42.87	0.03	0.21	16.47	0.04	0	0.01	0.27	0.17		99.73	82.27
VMC3_Ol 01a_17	32	0.01	39.75	42.75	0.04	0.26	16.6	0.03	0	0.02	0.26	0.23		99.96	82.11
VMC3_Ol 01a_18	34	0.04	39.54	42.9	0.01	0.22	16.75	0.04	0.01	0.02	0.26	0.19		99.98	82.03

Sample	Dist (μm)	Na_2O	SiO_2	MgO	Al_2O_3	MnO	FeO	Cr_2O_3	K_2O	TiO_2	CaO	NiO	P_2O_5	Total	Mg#
VMC3_Ol 01a_19	36	0.02	39.5	43.02	0.04	0.23	16.77	0.03	0	0.02	0.25	0.2		100.08	82.06
VMC3_Ol 01a_20	38	0.02	39.18	42.92	0.01	0.21	16.85	0.04	0	0.01	0.23	0.21		99.7	81.95
VMC3_Ol 01a_21	40	0.01	39.66	42.75	0.07	0.26	16.55	0.03	0	0.02	0.23	0.23		99.81	82.16
VMC3_Ol 01a_22	42	0.01	39.55	42.87	0.05	0.23	16.57	0.05	0.01	0.02	0.24	0.16		99.75	82.18
VMC3_Ol 01a_23	44	0.02	39.64	42.85	0.05	0.22	16.45	0.05	0	0.01	0.23	0.21		99.72	82.28
VMC3_Ol 01a_24	46	0.01	39.56	43.13	0.02	0.2	16.65	0.02	0.01	0.02	0.23	0.2		100.04	82.20
VMC3_Ol 01a_25	48	0.01	39.57	43.11	0.07	0.22	16.53	0.02	-0.01	0.02	0.23	0.22		99.98	82.30
VMC3_Ol 01a_26	50	0.02	39.49	43.24	0.05	0.22	16.54	0.03	0	0.02	0.22	0.21		100.04	82.33
VMC3_Ol 01a_27	52	0.01	40.13	43.32	0.07	0.21	16.51	0.03	0	0.01	0.22	0.22		100.72	82.39
VMC3_Ol 01a_28	54	0.01	39.49	43.32	0.02	0.17	16.18	0.03	0	0.02	0.23	0.2		99.67	82.68
VMC3_Ol 01a_29	56	0.01	39.5	43.08	0.05	0.22	16.18	0.03	0	0.02	0.22	0.22		99.52	82.60
VMC3_Ol 01a_30	58	0	39.32	43.5	0.03	0.26	16.13	0.04	0	0.01	0.23	0.18		99.7	82.78
VMC3_Ol 01a_31	60	0.01	39.88	43.37	0.06	0.21	16.29	0.02	0	0.01	0.21	0.21		100.27	82.60
VMC3_Ol 01a_32	62	0.02	39.36	43.45	0.06	0.17	16.25	0.02	0	0.01	0.22	0.21		99.77	82.66
VMC3_Ol 01a_33	64	0.02	39.68	43.22	0.03	0.22	16.01	0.03	0	0.01	0.21	0.21		99.65	82.79
VMC3_Ol 01a_34	66	0	39.57	43.59	0.08	0.18	16.25	0.04	0	0.02	0.21	0.21		100.14	82.70
VMC3_Ol 01a_35	68	0	39.81	43.63	0.06	0.24	15.9	0.02	-0.01	0.02	0.21	0.24		100.11	83.03
VMC3_Ol 01a_36	70	0.02	39.49	43.83	0.06	0.2	15.74	0.05	0.01	0.02	0.21	0.23		99.86	83.23
VMC3_Ol 01a_37	72	0.03	39.69	43.51	0.05	0.2	15.8	0.02	0	0.02	0.21	0.26		99.79	83.08
VMC3_Ol 01a_38	74	0	39.42	43.95	0.08	0.21	15.59	0.04	0	0.01	0.2	0.22		99.72	83.40
VMC3_Ol 01a_39	76	0.01	39.89	44.01	0.06	0.22	15.43	0.02	-0.01	0.02	0.21	0.28		100.15	83.56
VMC3_Ol 01a_40	78	0.02	39.7	44.03	0.06	0.2	15.15	0.03	0	0.01	0.2	0.26		99.64	83.82
VMC3_Ol 01a_41	80	0.02	39.45	43.97	0.07	0.23	15.43	0.01	0	0.01	0.22	0.22		99.63	83.55
VMC3_Ol 01a_42	82	0.01	39.6	44.11	0.07	0.18	15.25	0.07	0	0.01	0.19	0.28		99.77	83.76
VMC3_Ol 01a_43	84	0	39.81	44.01	0.07	0.18	14.72	0.03	0	0.01	0.21	0.26		99.3	84.20
VMC3_Ol 01a_44	86	0.02	39.69	44.17	0.02	0.17	15.17	0.04	0	0.01	0.2	0.25		99.74	83.85
VMC3_Ol 01a_45	88	0.01	39.74	44.35	0.06	0.18	15.05	0.04	0	0.02	0.18	0.22		99.85	84.01
VMC3_Ol 01a_46	90	0.01	39.88	44.67	0.08	0.21	14.56	0.04	0.01	0.01	0.2	0.24		99.91	84.54
VMC3_Ol 01a_47	92	0.03	40.17	44.74	0.04	0.17	14.64	0.04	0.01	0.01	0.19	0.26		100.29	84.49
VMC3_Ol 01a_48	94	-0.02	40.04	44.71	0.08	0.19	14.37	0.04	0	0.01	0.22	0.25		99.89	84.72
VMC3_Ol 01a_49	96	0.01	40.11	45.28	0.06	0.21	14.32	0.06	-0.01	0.02	0.21	0.26		100.53	84.93
VMC3_Ol 01a_50	98	0.02	39.74	45.27	0.04	0.17	14.06	0.04	0	0.01	0.2	0.25		99.81	85.16
VMC3_Ol 01a_51	100	0.02	39.96	45.07	0.04	0.19	13.88	0.05	0	0.02	0.22	0.27		99.69	85.27
VMC3_Ol 01a_52	102	0.02	40.14	45.42	0.06	0.15	13.99	0.03	0.01	0.02	0.21	0.26		100.28	85.27
VMC3_Ol 01a_53	104	0.02	40.01	45.49	0.1	0.17	14.07	0.03	0	0	0.19	0.29		100.36	85.21
VMC3_Ol 01a_54	106	0.01	40.18	45.49	0.07	0.18	13.75	0.06	0	0.01	0.21	0.29		100.25	85.50
VMC3_Ol 01a_55	108	0.02	40.05	45.47	0.03	0.17	13.63	0.03	0	0	0.2	0.31		99.91	85.60
VMC3_Ol 01a_56	110	0.01	39.92	45.51	0.04	0.17	13.49	0.01	0	0	0.2	0.29		99.66	85.74
VMC3_Ol 01a_57	112	0.02	40.04	45.52	0.06	0.14	13.31	0.06	0	0	0.19	0.3		99.64	85.91

Sample	Dist (μm)	Na_2O	SiO_2	MgO	Al_2O_3	MnO	FeO	Cr_2O_3	K_2O	TiO_2	CaO	NiO	P_2O_5	Total	Mg#
VMC3_Ol 01a_58	114	0.01	39.78	45.66	0.06	0.15	13.63	0.04	0	0.02	0.22	0.32		99.87	85.66
VMC3_Ol 01a_59	116	0.01	40.05	45.81	0.07	0.18	13.48	0.02	-0.01	0.01	0.19	0.3		100.11	85.83
VMC3_Ol 01a_60	118	0	40.18	45.67	0.05	0.17	13.04	0.06	0	0.01	0.22	0.29		99.69	86.19
VMC3_Ol 01a_61	120	0	40.39	46.22	0.05	0.16	12.94	0.05	0	0.01	0.2	0.33		100.34	86.43
VMC3_Ol 01a_62	122	0.02	40.11	45.87	0.05	0.21	13.18	0.04	0	0.02	0.2	0.29		99.99	86.12
VMC3_Ol 01a_63	124	0.01	40.42	45.67	0.09	0.16	13.35	0.04	0	0	0.2	0.33		100.28	85.91
VMC3_Ol 01a_64	126	0.01	40.29	46.13	0.07	0.16	13.1	0.04	0	0.02	0.2	0.32		100.34	86.26
VMC3_Ol 01a_65	128	0.03	40.25	46.12	0.07	0.17	13.25	0.05	0	0	0.21	0.3		100.43	86.12
VMC3_Ol 01a_66	130	0.02	40.22	46.01	0.04	0.14	13.1	0.04	0	0	0.19	0.29		100.07	86.23
VMC3_Ol 01a_67	132	0.02	40.05	46.07	0.08	0.15	12.98	0.05	0	0.01	0.19	0.34		99.94	86.35
VMC3_Ol 01a_68	134	0	40.08	46.32	0.08	0.17	13.03	0.03	0	0.01	0.2	0.35		100.26	86.37
VMC3_Ol 01a_69	136	0.03	40.29	46.06	0.09	0.12	13.05	0.04	0	0	0.22	0.34		100.23	86.29
VMC3_Ol 01a_70	138	0.02	39.91	46.6	0.09	0.16	12.74	0.05	0	0.02	0.22	0.32		100.12	86.70
VMC3_Ol 01a_71	140	0.01	40.31	46.42	0.04	0.16	12.81	0.03	0	0.01	0.21	0.32		100.32	86.59
VMC3_Ol 01a_72	142	0.01	40.19	46.1	0.09	0.18	12.55	0.07	0	0.02	0.21	0.34		99.75	86.75
VMC3_Ol 01a_73	144	0	40.39	46.06	0.08	0.16	12.7	0.03	0.01	0.01	0.2	0.28		99.91	86.60
VMC3_Ol 01a_74	146	0.02	40.28	46.34	0.08	0.12	12.57	0.04	0	0.01	0.2	0.33		99.98	86.79
VMC3_Ol 01a_75	148	0.02	40.34	46.27	0.08	0.19	12.48	0.03	0	0.02	0.19	0.33		99.94	86.86
VMC3_Ol 01a_76	150	0.01	39.97	46.52	0.08	0.15	12.68	0.04	-0.01	0	0.2	0.25		99.89	86.74
VMC3_Ol 01a_77	152	0.01	39.88	46.6	0.06	0.13	12.68	0.03	0	0.02	0.2	0.32		99.93	86.76
VMC3_Ol 01a_78	154	0.04	40.03	46.57	0.06	0.16	12.61	0.04	0	0.01	0.18	0.31		100.01	86.81
VMC3_Ol 01a_79	156	0.02	40	46.44	0.05	0.14	12.59	0.03	0	0.02	0.18	0.3		99.76	86.80
VMC3_Ol 01a_80	158	0.01	40.24	46.43	0.03	0.16	12.5	0.02	0	0.02	0.19	0.31		99.92	86.88
VMC3_Ol 01a_81	160	0.03	40.27	46.47	0.08	0.17	12.66	0.02	-0.01	0.01	0.2	0.32		100.23	86.74
VMC3_Ol 01a_82	162	0.01	39.94	46.67	0.1	0.17	12.66	0.02	0	0.01	0.2	0.35		100.14	86.79
VMC3_Ol 01a_83	164	0	40.44	46.56	0.12	0.17	12.6	0.05	0	0	0.2	0.36		100.5	86.82
VMC3_Ol 01a_84	166	0.02	40.04	46.59	0.09	0.16	12.51	0.05	0.01	0.01	0.19	0.33		99.99	86.91
VMC3_Ol 01a_85	168	-0.01	40.62	46.38	0.06	0.19	12.41	0.03	0	0.02	0.2	0.33		100.24	86.95
VMC3_Ol 01a_86	170	0.01	40.47	46.69	0.07	0.17	12.49	0.04	0	0.01	0.2	0.33		100.49	86.95
VMC3_Ol 01a_87	172	0.03	40.07	46.55	0.06	0.13	12.62	0.03	0	0.02	0.19	0.33		100.04	86.80
VMC3_OL_14_01	0	0.02	39.09	42.07	0.06	0.26	17.47	0.04	0	0.05	0.41	0.1		99.58	81.11
VMC3_OL_14_02	4	0.01	39.42	42.83	0.06	0.24	16.95	0.04	0	0.04	0.4	0.12		100.15	81.83
VMC3_OL_14_03	8	0	39.32	42.82	0.06	0.29	16.9	0.03	0	0.04	0.39	0.17		100.04	81.87
VMC3_OL_14_04	12	0.03	39.66	43.15	0.03	0.26	16.74	0.04	0	0.03	0.39	0.19		100.5	82.13
VMC3_OL_14_05	16	0.01	39.15	42.35	0.09	0.24	16.6	0.05	0	0.04	0.35	0.16		99.07	81.97
VMC3_OL_14_06	20	-0.01	39.34	43.32	0.02	0.28	16.59	0.02	0	0.02	0.35	0.15		100.1	82.32
VMC3_OL_14_07	24	0.01	39.32	43.06	0.04	0.25	16.64	0.04	0	0.03	0.31	0.16		99.91	82.18
VMC3_OL_14_08	28	0.03	39.73	43.16	0.04	0.24	16.73	0.01	0	0.03	0.28	0.16		100.41	82.14
VMC3_OL_14_09	32	0.01	39.67	43.13	0.03	0.24	16.95	0.05	0	0.03	0.27	0.2		100.6	81.94

Sample	Dist (μm)	Na_2O	SiO_2	MgO	Al_2O_3	MnO	FeO	Cr_2O_3	K_2O	TiO_2	CaO	NiO	P_2O_5	Total	Mg#
VMC3_OL_14_10	36	0.03	39.44	43.13	0.03	0.23	17.15	0.02	0	0.02	0.26	0.18		100.47	81.76
VMC3_OL_14_11	40	0.01	39.48	43.21	0.07	0.23	17.07	0.03	0	0.02	0.24	0.16		100.55	81.86
VMC3_OL_14_12	44	0.02	39.26	42.94	0.05	0.22	17.08	0.05	0	0.02	0.24	0.21		100.11	81.76
VMC3_OL_14_13	48	0	39.54	43.06	0.06	0.21	16.92	0.04	-0.01	0.01	0.23	0.2		100.25	81.94
VMC3_OL_14_14	52	0.01	39.69	43.69	0.04	0.25	16.83	0.02	0.01	0.02	0.22	0.23		101.02	82.23
VMC3_OL_14_15	56	0.01	39.52	43.45	0.05	0.23	16.61	0.04	0.01	0.02	0.24	0.19		100.4	82.34
VMC3_OL_14_16	60	0.02	39.53	43.41	0.05	0.25	16.54	0.02	0	0.01	0.22	0.22		100.3	82.39
VMC3_OL_14_17	64	0.02	39.73	43.41	0.05	0.23	16.16	0.03	0	0.02	0.22	0.22		100.13	82.72
VMC3_OL_14_18	68	0.02	39.53	43.85	0.08	0.17	16.21	0.04	0	0.02	0.22	0.21		100.36	82.82
VMC3_OL_14_19	72	0.02	39.57	43.95	0.03	0.22	16.04	0.03	0	0.02	0.21	0.26		100.38	83.01
VMC3_OL_14_20	76	0	39.42	44.07	0.08	0.17	16.09	0.02	0	0.02	0.22	0.25		100.37	83.00
VMC3_OL_14_21	80	0.02	39.55	44.26	0.03	0.18	15.7	0.04	0	0.02	0.22	0.25		100.27	83.40
VMC3_OL_14_22	84	0.01	39.88	44.17	0.09	0.15	15.45	0.04	0	0	0.22	0.21		100.23	83.60
VMC3_OL_14_23	88	0	40.21	44.5	0.08	0.16	15.36	0.03	0	0.01	0.22	0.2		100.78	83.78
VMC3_OL_14_24	92	0.02	39.7	44.64	0.08	0.2	15.25	0.04	0	0	0.21	0.23		100.39	83.92
VMC3_OL_14_25	96	0	40.21	44.63	0.05	0.19	15.3	0.04	0	0.01	0.21	0.27		100.93	83.87
VMC3_OL_14_26	100	0.01	39.69	44.77	0.06	0.21	15.04	0.04	0	0.02	0.23	0.28		100.35	84.14
VMC3_OL_14_27	104	0.01	39.87	44.44	0.07	0.18	15.05	0.05	0.01	0.01	0.2	0.25		100.14	84.03
VMC3_OL_14_28	108	0.01	40.1	44.88	0.08	0.17	15.17	0.03	0	0.02	0.22	0.2		100.86	84.06
VMC3_OL_14_29	112	0.02	40	44.44	0.08	0.21	15.32	0.04	0	0.02	0.22	0.26		100.62	83.79
VMC3_OL_14_30	116	0	39.62	44.45	0.04	0.19	15.34	0.06	0	0.01	0.22	0.26		100.2	83.78
VMC3_OL_14_31	120	0.01	39.92	44.21	0.05	0.2	15.65	0.03	0	0.01	0.23	0.23		100.57	83.43
VMC3_OL_14_32	124	0.02	39.79	44.22	0.04	0.17	15.6	0.03	0	0.01	0.22	0.22		100.36	83.48
VMC3_OL_14_33	128	0.01	39.6	44	0.05	0.21	16.06	0.03	0	0.01	0.22	0.26		100.48	83.00
VMC3_OL_14_34	132	0.03	39.46	43.99	0.03	0.21	16.14	0.04	0	0.01	0.21	0.21		100.37	82.93
VMC3_OL_14_35	136	0.02	39.85	43.7	0.04	0.2	16.41	0.06	-0.01	0.01	0.23	0.2		100.72	82.60
VMC3_OL_14_36	140	0.01	39.59	43.4	0.05	0.21	16.62	0.03	0	0.03	0.22	0.18		100.39	82.32
VMC3_OL_14_37	144	0.02	39.41	43.2	0.05	0.2	16.68	0.04	0	0.02	0.25	0.24		100.11	82.20
VMC3_OL_14_38	148	0.01	39.3	43.18	0.06	0.21	16.84	0.06	0.01	0.01	0.24	0.19		100.1	82.05
VMC3_OL_14_39	152	0.02	39.6	43.03	0.07	0.23	16.99	0.03	0.01	0.01	0.23	0.19		100.4	81.87
VMC3_OL_14_40	156	0.01	39.58	43.02	0.01	0.21	17.2	0.03	0	0.02	0.25	0.19		100.54	81.68
VMC3_OL_14_41	160	0.01	39.46	43.14	0.03	0.21	17.11	0.02	0	0.02	0.25	0.17		100.42	81.80
VMC3_OL_14_42	164	0.02	39.19	42.78	0.05	0.23	17.16	0.03	-0.01	0.04	0.26	0.16		99.93	81.63
VMC3_OL_14_43	168	0.01	39.38	42.82	0.01	0.24	17.04	0.03	0	0.02	0.26	0.17		99.98	81.75
VMC3_OL_14_44	172	0.02	39.47	43.44	0.03	0.23	16.85	0.03	0	0.03	0.3	0.24		100.67	82.13
VMC3_OL_14_45	176	0.02	39.51	43.42	0.02	0.27	16.54	0.03	0	0.03	0.36	0.13		100.31	82.39
VMC3_OL_14_46	180	0.01	39.36	43.01	0.06	0.28	16.81	0.01	0	0.04	0.37	0.16		100.14	82.02
VMC3_OL_14_47	184	0.03	39.47	42.45	0.04	0.27	17.58	0.05	0.01	0.06	0.39	0.16		100.51	81.15
VMC3_OL_14_48	188	1.24	40.45	20.26	8.78	0.26	15.88	0.01	1.13	1.72	5.86	0.07		96.38	69.46

Sample	Dist (μm)	Na_2O	SiO_2	MgO	Al_2O_3	MnO	FeO	Cr_2O_3	K_2O	TiO_2	CaO	NiO	P_2O_5	Total	Mg#
VMC3_OL_17_01	0	0.01	39.28	41.92	0.05	0.27	17.99	0.04	0	0.04	0.4	0.14	-0.01	100.12	80.60
VMC3_OL_17_02	4	0.02	39.6	42.52	0.02	0.25	17.22	0.02	0	0.02	0.37	0.14	-0.01	100.18	81.49
VMC3_OL_17_03	8	0	39.5	42.85	0.03	0.24	16.89	0.03	0	0.03	0.36	0.15	0.02	100.11	81.89
VMC3_OL_17_04	12	0	39.46	42.7	0.06	0.24	16.99	0.02	0	0.03	0.31	0.14	0.02	99.99	81.75
VMC3_OL_17_05	16	0.01	39.38	42.81	0.06	0.23	17.1	0.03	0	0.02	0.25	0.2	0.01	100.1	81.69
VMC3_OL_17_06	20	0	39.74	42.81	0.02	0.2	17.25	0.05	0	0.02	0.24	0.15	0.01	100.49	81.56
VMC3_OL_17_07	24	0.01	39.39	42.92	0.03	0.22	17.01	0.04	0	0.01	0.24	0.25	0.02	100.15	81.81
VMC3_OL_17_08	28	0.02	39.48	42.81	0.07	0.23	17	0.04	0	0.02	0.24	0.19	0.02	100.12	81.78
VMC3_OL_17_09	32	0.01	39.54	43.21	0.06	0.2	17.01	0.04	0	0.02	0.22	0.18	0.01	100.52	81.91
VMC3_OL_17_10	36	0.02	39.1	42.84	0.05	0.19	17.19	0.02	0	0.01	0.21	0.18	0.03	99.85	81.63
VMC3_OL_17_11	40	0.02	39.3	42.89	0.06	0.24	17.16	0.02	0	0.02	0.22	0.17	0	100.1	81.67
VMC3_OL_17_12	44	0.01	39.44	42.66	0.05	0.19	17.5	0.02	0	0.03	0.21	0.15	-0.01	100.24	81.29
VMC3_OL_17_13	48	0	39.17	42.85	0.08	0.17	17.4	0.02	0	0.04	0.22	0.14	0	100.09	81.45
VMC3_OL_17_14	52	0.01	39.52	42.69	0.07	0.2	17.63	0.03	0	0.04	0.21	0.14	0	100.54	81.19
VMC3_OL_17_15	56	0.02	39.03	42.31	0.06	0.18	17.99	0.04	0	0.04	0.2	0.09	0	99.96	80.74
VMC3_OL_17_16	60	0.01	39.2	42.12	0.04	0.17	18.08	0.04	0	0.03	0.2	0.09	-0.02	99.97	80.59
VMC3_OL_17_17	64	0.01	39.16	42.2	0.04	0.16	18.3	0.02	0	0.04	0.19	0.05	-0.01	100.17	80.43
VMC3_OL_17_18	68	0.03	39.36	42.28	0.06	0.16	17.93	0	0	0.04	0.22	0.07	-0.01	100.14	80.78
VMC3_OL_17_19	72	0.02	39.2	42.12	0.05	0.18	18.23	0.01	0	0.04	0.21	0.11	-0.01	100.15	80.46
VMC3_OL_17_20	76	0.03	39.46	42.18	0.07	0.17	18.43	0.03	0	0.06	0.2	0.08	0.02	100.73	80.31
VMC3_OL_17_21	80	0.01	39.08	42.29	0.08	0.18	18.23	0.01	0	0.06	0.21	0.08	0.01	100.23	80.53
VMC3_OL_17_22	84	0.01	39.6	42.25	0.06	0.17	18.3	0.02	0	0.06	0.2	0.04	0.01	100.72	80.45
VMC3_OL_17_23	88	0.01	39.51	42.25	0.07	0.19	18.04	0.02	0	0.06	0.2	0.05	-0.03	100.36	80.68
VMC3_OL_17_24	92	0.01	39.24	42.45	0.05	0.21	17.99	0	0	0.05	0.2	0.13	0	100.33	80.79
VMC3_OL_17_25	96	0	39.11	42.62	0.07	0.2	17.62	0	0	0.05	0.2	0.15	0	100.02	81.17
VMC3_OL_17_26	100	0.03	39.32	42.56	0.05	0.18	17.65	0.03	0	0.06	0.22	0.19	0	100.28	81.13
VMC3_OL_17_27	104	0.03	39.26	42.62	0.09	0.19	17.59	0.02	0	0.04	0.22	0.16	0	100.22	81.20
VMC3_OL_17_28	108	-0.01	39.36	42.72	0.07	0.21	17.47	0.01	0	0.05	0.21	0.22	0	100.31	81.34
VMC3_OL_17_29	112	0	39.01	42.82	0.06	0.22	17.5	0.04	0	0.06	0.21	0.18	-0.01	100.09	81.35
VMC3_OL_17_30	116	0.02	39.47	42.84	0.1	0.19	17.65	0.02	0	0.06	0.22	0.16	0.01	100.73	81.23
VMC3_OL_17_31	120	0.02	39.38	42.59	0.05	0.2	17.75	0.03	0	0.06	0.22	0.14	0.01	100.44	81.05
VMC3_OL_17_32	124	0.03	39.51	42.45	0.12	0.18	17.73	0.03	0	0.07	0.22	0.13	0.01	100.48	81.02
VMC3_OL_17_33	128	0.01	39.09	42.36	0.07	0.19	17.75	0.02	0	0.06	0.22	0.13	0	99.91	80.97
VMC3_OL_17_34	132	0	39.23	42.02	0.06	0.19	18.25	0.01	0	0.05	0.23	0.04	-0.02	100.07	80.41
VMC3_OL_17_35	136	0.01	39.23	42.03	0.05	0.17	18.3	0	0	0.05	0.23	0.08	-0.02	100.13	80.37
VMC3_OL_17_36	140	0.01	39.2	41.94	0.04	0.2	18.52	0.02	0	0.04	0.22	0.06	-0.01	100.24	80.15
VMC3_OL_17_37	144	0.02	38.7	42	0.09	0.17	18.45	0	0	0.04	0.21	0.03	-0.02	99.67	80.23
VMC3_OL_17_38	148	0.02	39.57	42.09	0.06	0.17	18.55	-0.01	0	0.05	0.2	0.07	0.01	100.78	80.18
VMC3_OL_17_39	152	0.04	38.95	42.15	0.11	0.18	18.33	0.02	0	0.06	0.21	0.07	0.02	100.14	80.39

Sample	Dist (μm)	Na_2O	SiO_2	MgO	Al_2O_3	MnO	FeO	Cr_2O_3	K_2O	TiO_2	CaO	NiO	P_2O_5	Total	Mg#
VMC3_OL_17_40	156	0.02	38.81	42.14	0.06	0.2	18.36	0.03	0	0.06	0.21	0.09	0	99.99	80.36
VMC3_OL_17_41	160	0.02	39.17	42.05	0.07	0.17	18.17	0.01	0	0.05	0.2	0.11	-0.02	99.99	80.49
VMC3_OL_17_42	164	0.02	39.02	42.27	0.04	0.18	18.2	0	0	0.05	0.21	0.12	-0.01	100.09	80.54
VMC3_OL_17_43	168	0	39.32	42.33	0.07	0.17	17.89	0.01	0	0.03	0.2	0.1	0	100.14	80.83
VMC3_OL_17_44	172	0	39.35	42.34	0.05	0.17	18	0	0	0.04	0.2	0.1	0	100.26	80.74
VMC3_OL_17_45	176	0.01	39.23	42.41	0.09	0.18	17.67	0.02	0	0.04	0.21	0.15	0	100.01	81.05
VMC3_OL_17_46	180	0.01	39.63	42.66	0.04	0.18	17.58	0.02	0	0.03	0.22	0.2	0.03	100.61	81.22
VMC3_OL_17_47	184	0.02	39.1	42.91	0.02	0.22	17.54	0.01	0	0.01	0.21	0.2	0.02	100.27	81.35
VMC3_OL_17_48	188	0.01	39.63	42.76	0.08	0.18	17.4	0.02	0	0.02	0.22	0.2	0	100.52	81.41
VMC3_OL_17_49	192	-0.01	39.38	43.07	0.03	0.21	17.33	0	0	0.01	0.22	0.16	0	100.41	81.58
VMC3_OL_17_50	196	0.01	39.35	43.06	0.06	0.18	17.2	0.03	0	0	0.2	0.19	0.07	100.35	81.69
VMC3_OL_17_51	200	0.01	39.52	42.89	0.07	0.21	17.02	0.02	0	0.01	0.22	0.19	0.01	100.17	81.79
VMC3_OL_17_52	204	0	39.23	43.11	0.05	0.22	16.88	0.02	0	0.01	0.21	0.21	0.01	99.97	81.99
VMC3_OL_17_53	208	0.02	39.39	43.03	0.05	0.24	16.98	0.03	0	0.01	0.22	0.21	0.02	100.2	81.88
VMC3_OL_17_54	212	0	39.55	43.23	0.04	0.18	16.96	0.02	0	0.02	0.22	0.22	0	100.43	81.96
VMC3_OL_17_55	216	0.02	39.36	43.4	0.07	0.18	16.91	0.03	0	0.01	0.23	0.21	0.02	100.45	82.06
VMC3_OL_17_56	220	0.02	39.51	43.05	0.05	0.22	16.94	0.05	0	0.02	0.23	0.23	0.02	100.34	81.92
VMC3_OL_17_57	224	0.02	39.4	43.09	0.03	0.24	17.06	0.03	0	0.02	0.23	0.18	0.03	100.33	81.83
VMC3_OL_17_58	228	0	39.54	43.12	0.07	0.24	17.14	0.03	0	0.01	0.22	0.22	0.01	100.61	81.77
VMC3_OL_17_59	232	0.01	38.97	43.12	0.07	0.25	17.08	0.04	0	0.01	0.23	0.21	0.02	100	81.82
VMC3_OL_17_60	236	0.01	39.56	42.98	0.05	0.26	17.22	0.04	0	0.01	0.23	0.18	0	100.54	81.65
VMC3_OL_17_61	240	0	39.2	42.87	0.06	0.21	17.13	0.02	0	0.02	0.26	0.18	0	99.95	81.69
VMC3_OL_17_62	244	0.02	39.38	42.82	0.03	0.24	17.16	0.05	0	0.02	0.25	0.19	0.02	100.18	81.64
VMC3_OL_17_63	248	0	39.12	42.65	0.01	0.24	17.25	0.03	0	0.01	0.27	0.17	0.01	99.77	81.51
VMC3_OL_17_64	252	0	39.45	42.98	0.06	0.24	17.36	0.04	0	0.03	0.28	0.21	0.01	100.65	81.53
VMC3_OL_17_65	256	-0.01	39.21	43.5	0.02	0.26	16.9	0.03	0	0.03	0.29	0.16	0.01	100.4	82.11
VMC3_OL_17_66	260	0.01	39.57	43.37	0.04	0.24	16.74	0.05	0	0.02	0.37	0.13	0.01	100.56	82.20
VMC3_OL_17_67	264	0.01	39.36	43.18	0.01	0.29	16.64	0.04	0	0.02	0.35	0.18	0.05	100.12	82.22
VMC3_OL_17_68	268	0.02	39.22	43.06	0.07	0.27	17.02	0.03	0	0.03	0.36	0.15	0.03	100.25	81.85
VMC3_OL_17_69	272	0.03	38.86	43.32	0.08	0.28	16.93	0.02	0	0.04	0.33	0.11	0.03	100.03	82.02
VMC3_OL_17_70	276	0.02	39.5	42.98	0.04	0.29	16.93	0.03	0	0.01	0.36	0.18	0.06	100.4	81.90
VMC3_OL_17_71	280	0	39.42	43.07	0.04	0.26	17.34	0.03	0	0.03	0.35	0.15	0.03	100.7	81.58
VMC3_OL_17_72	284	0	39.17	42.7	0.03	0.28	17.47	0.05	0	0.03	0.38	0.16	0.02	100.3	81.33
VMC3_OL_17_73	288	0.01	38.92	42.5	0.03	0.26	17.46	0.05	0	0.03	0.39	0.14	0.02	99.83	81.27
VMC3_OL_17_74	292	0	39.38	42.25	0	0.29	18.01	0.03	0	0.04	0.38	0.12	0.03	100.53	80.70
VMC3_OL_17_75	296	0	38.78	42.04	0.01	0.27	18.57	0.03	0	0.03	0.42	0.11	0.02	100.28	80.14
VMC3_OL_17_76	300	0.02	38.85	41.19	0.01	0.31	19	0.03	0	0.05	0.43	0.11	0.06	100.05	79.44
VMC3_OL_17_77	304	0	38.83	41.45	0.03	0.29	18.95	0.02	0	0.04	0.47	0.12	0.01	100.21	79.59
VMC3_OL_17_78	308	0.01	38.8	41.43	0.05	0.32	19.01	0.01	0	0.05	0.49	0.14	0.03	100.34	79.53

Sample	Dist (μm)	Na_2O	SiO_2	MgO	Al_2O_3	MnO	FeO	Cr_2O_3	K_2O	TiO_2	CaO	NiO	P_2O_5	Total	Mg#
VMC3_OL_17_79	312	0	38.63	40.25	0.03	0.35	19.87	0.02	0	0.07	0.58	0.1	0.03	99.93	78.31
VMC3_OL_17_80	316	1.2	43.97	8.07	12.41	0.14	9.22	0.04	0	3.9	19.81	0	0.6	99.35	60.94
VMC3_OL_17_81	320	0.38	48.15	14.08	4.2	0.14	7.22	0.27	0	2.05	22.65	0	0.26	99.4	77.66
AVF 30_ Pic 27_	0	0.69	45.27	4.44	17.04	0.22	10.92	0.11	0.68	2.84	9.91	0.02	0.9	93.03	42.02
AVF 30_ Pic 27_ol_	4	0.3	55.93	1.18	22.76	0.14	5.65	0.04	1.07	1.42	3.82	0.02	1.19	93.52	27.13
AVF 30_ Pic 27_03	8	0.08	49.28	6.31	19.85	0.21	8.61	0.03	0.29	1.24	2.99	0.02	1.09	90.01	56.64
AVF 30_ Pic 27_04	12	0.01	38.5	38.42	0.13	0.41	19.89	0.04	0.01	0.09	0.47	0.07	0.01	98.05	77.49
AVF 30_ Pic 27_05	16	0.01	38.82	41.5	0.04	0.25	17.37	0.06	0	0.06	0.39	0.13	0.05	98.68	80.98
AVF 30_ Pic 27_06	20	0.03	38.65	41.94	0.03	0.23	16.39	0.03	-0.01	0.04	0.37	0.13	0.03	97.85	82.02
AVF 30_ Pic 27_07	24	0.01	39.04	42.19	0.06	0.22	15.99	0.04	0	0.03	0.36	0.15	0.02	98.11	82.47
AVF 30_ Pic 27_08	28	0.01	38.69	42.48	0.03	0.25	15.91	0.03	0	0.04	0.35	0.15	0.03	97.97	82.64
AVF 30_ Pic 27_09	32	0.02	38.99	42.6	0.02	0.23	15.89	0.01	0	0.04	0.36	0.17	0.02	98.34	82.70
AVF 30_ Pic 27_10	36	0.02	38.79	42.49	0.05	0.25	15.85	0.03	0	0.02	0.33	0.14	0	97.97	82.69
AVF 30_ Pic 27_11	40	0.03	39.26	42.47	0.03	0.24	15.82	0.02	0.01	0.02	0.29	0.21	0.02	98.43	82.72
AVF 30_ Pic 27_12	44	0.03	39.02	42.39	0.05	0.26	16.1	0.03	0.01	0.01	0.27	0.16	-0.01	98.32	82.44
AVF 30_ Pic 27_13	48	0.02	39.1	42.44	0.02	0.22	15.99	0.03	0.01	0.02	0.25	0.2	0	98.31	82.55
AVF 30_ Pic 27_14	52	0.02	38.38	42.47	0.07	0.24	16.02	0.02	0	0.01	0.25	0.18	0.04	97.7	82.53
AVF 30_ Pic 27_15	56	0.02	39.07	42.47	0.06	0.25	15.95	0.02	0	0.01	0.26	0.2	0.03	98.32	82.60
AVF 30_ Pic 27_16	60	0.01	39.04	42.94	0.05	0.21	15.98	0.03	0	0.03	0.26	0.2	-0.01	98.71	82.73
AVF 30_ Pic 27_17	64	0.01	39.09	42.67	0.07	0.19	15.99	0.03	0	0.02	0.24	0.21	0.02	98.54	82.63
AVF 30_ Pic 27_18	68	0.02	38.78	42.78	0.04	0.22	15.72	0.03	0.01	0.01	0.23	0.21	0.01	98.07	82.91
AVF 30_ Pic 27_19	72	0.02	39.05	42.93	0.06	0.22	15.87	0.04	0	0.01	0.22	0.17	0.01	98.6	82.82
AVF 30_ Pic 27_20	76	0.01	38.57	42.64	0.07	0.21	15.74	0.04	0	0.02	0.25	0.25	0.02	97.82	82.84
AVF 30_ Pic 27_21	80	0.02	39.93	43.02	0.04	0.18	15.61	0.04	0	0.01	0.23	0.17	0.01	99.27	83.09
AVF 30_ Pic 27_22	84	0.01	39.12	43.13	0.06	0.22	15.46	0.04	0	0.01	0.22	0.18	0.02	98.48	83.26
AVF 30_ Pic 27_23	88	0.01	39.21	42.99	0.04	0.2	15.3	0.04	0.01	0.01	0.22	0.24	0.01	98.29	83.36
AVF 30_ Pic 27_24	92	0.02	39.08	43.24	0.09	0.17	15.17	0.03	0.01	0.02	0.23	0.21	0.01	98.27	83.56
AVF 30_ Pic 27_25	96	0.03	39.47	43.42	0.04	0.2	15.19	0.04	0.01	0.02	0.24	0.22	0.04	98.92	83.59
AVF 30_ Pic 27_26	100	0.03	39.19	43.79	0.06	0.24	15.07	0.03	0.01	0.02	0.24	0.23	0.01	98.91	83.82
AVF 30_ Pic 27_27	104	0.01	39.49	43.6	0.06	0.22	14.85	0.04	0	0.01	0.23	0.23	0	98.74	83.96
AVF 30_ Pic 27_28	108	0.01	39.12	43.87	0.06	0.18	14.67	0.04	0	0	0.21	0.24	0.03	98.42	84.20
AVF 30_ Pic 27_29	112	0.03	39.16	43.57	0.03	0.19	14.49	0.04	0	0.01	0.21	0.17	0.02	97.91	84.28
AVF 30_ Pic 27_30	116	0.02	39.27	43.96	0.02	0.19	14.32	0.04	0.01	0	0.21	0.2	0.02	98.27	84.55
AVF 30_ Pic 27_31	120	0	39.36	44.07	0.07	0.2	14.27	0.01	0	0.01	0.23	0.22	0.02	98.46	84.63
AVF 30_ Pic 27_32	124	0.03	37.54	43.04	0.07	0.18	14.12	0.05	0.01	0.02	0.23	0.22	0.01	95.52	84.46
AVF 30_ Pic 27_33	128	0.02	39.27	44.12	0.08	0.17	14.17	0.04	0	0.01	0.21	0.19	0.03	98.3	84.73
AVF 30_ Pic 27_34	132	0.02	39.34	44.49	0.06	0.19	14	0.06	0.01	0.02	0.22	0.25	0.01	98.66	85.00
AVF 30_ Pic 27_35	136	0.01	39.49	44.36	0.06	0.18	14.14	0.04	0	0	0.23	0.26	0.04	98.81	84.83
AVF 30_ Pic 27_36	140	0.02	39.27	44.58	0.05	0.18	14.17	0.05	0	0.01	0.21	0.23	0.02	98.79	84.87

Sample	Dist (μm)	Na_2O	SiO_2	MgO	Al_2O_3	MnO	FeO	Cr_2O_3	K_2O	TiO_2	CaO	NiO	P_2O_5	Total	Mg#
AVF 30_ Pic 27_37	144	0.01	39.51	44.41	0.05	0.19	14.34	0.04	0	0.01	0.23	0.21	-0.01	98.99	84.66
AVF 30_ Pic 27_38	148	0.02	39.5	44.3	0.02	0.19	14.12	0.02	0	0.02	0.22	0.22	0.02	98.65	84.83
AVF 30_ Pic 27_39	152	0.02	39.34	44.45	0.04	0.18	14.32	0.06	0	0.02	0.22	0.24	0.04	98.92	84.69
AVF 30_ Pic 27_40	156	0.02	39.59	44.26	0.07	0.17	14.38	0.04	0	0.01	0.22	0.22	0	98.98	84.58
AVF 30_ Pic 27_41	160	0.03	39.47	44.21	0.02	0.2	14.44	0.05	0	0.01	0.21	0.21	0.01	98.86	84.51
AVF 30_ Pic 27_42	164	0.02	39.38	44.19	0.06	0.2	14.74	0.04	0	0.01	0.23	0.27	0.01	99.15	84.24
AVF 30_ Pic 27_43	168	0.01	39.52	43.95	0.06	0.17	14.9	0.03	0.01	0.01	0.24	0.25	0	99.14	84.02
AVF 30_ Pic 27_44	172	0.01	39.25	44.1	0.01	0.2	14.99	0.04	0	0.01	0.22	0.2	0.03	99.07	83.99
AVF 30_ Pic 27_45	176	0.02	39.24	43.75	0.05	0.18	15.27	0.03	0	0.02	0.23	0.25	0	99.04	83.63
AVF 30_ Pic 27_46	180	0.02	39.08	43.56	0.06	0.2	15.12	0.04	0	0.01	0.22	0.2	-0.01	98.49	83.70
AVF 30_ Pic 27_47	184	0	39.26	43.54	0.06	0.21	15.47	0.04	0	0.01	0.22	0.23	0.01	99.08	83.38
AVF 30_ Pic 27_48	188	0.02	39.37	43.24	0.07	0.21	15.3	0.04	0	0.01	0.22	0.2	0.02	98.71	83.44
AVF 30_ Pic 27_49	192	0.02	39.43	43.23	0.04	0.19	15.43	0.03	0.01	0.01	0.24	0.22	0	98.85	83.32
AVF 30_ Pic 27_50	196	0.03	38.87	43.04	0.07	0.18	15.64	0.01	0.01	0.02	0.23	0.21	0.01	98.31	83.07
AVF 30_ Pic 27_51	200	0.04	39.45	42.94	0.03	0.23	15.9	0.02	0	0	0.23	0.18	0.02	99.05	82.80
AVF 30_ Pic 27_52	204	0.02	39.1	43.04	0.04	0.23	15.93	0.03	-0.01	0.02	0.22	0.22	0	98.85	82.81
AVF 30_ Pic 27_53	208	0.01	39.46	42.8	0.06	0.21	16.02	0.03	0	0	0.23	0.19	-0.02	98.98	82.65
AVF 30_ Pic 27_54	212	0.01	39.14	42.7	0.13	0.24	16.29	0.03	0	0.01	0.24	0.2	0.01	99.01	82.37
AVF 30_ Pic 27_55	216	0.01	39.42	42.75	0.05	0.25	16.2	0.05	0.01	0.02	0.26	0.19	0	99.22	82.47
AVF 30_ Pic 27_56	220	0	38.58	42.56	0.04	0.23	16.2	0.05	0	0.01	0.28	0.21	0.01	98.18	82.40
AVF 30_ Pic 27_57	224	0.03	39.02	42.63	0.04	0.22	16.09	0.04	0	0.01	0.27	0.14	0	98.5	82.53
AVF 30_ Pic 27_58	228	0.03	38.69	43	0.09	0.22	16.21	0.03	0	0.01	0.28	0.17	0.01	98.73	82.54
AVF 30_ Pic 27_59	232	0.03	39.32	42.66	0.06	0.25	16.05	0.03	0	0.02	0.3	0.1	0.03	98.85	82.57
AVF 30_ Pic 27_60	236	0.02	39.2	43.07	0.05	0.24	16.06	0.02	0.01	0.02	0.34	0.14	-0.01	99.16	82.70
AVF 30_ Pic 27_61	240	0.02	39.17	42.85	0.1	0.27	15.97	0.03	0	0.03	0.36	0.13	0.02	98.96	82.71
AVF 30_ Pic 27_62	244	0.02	39.19	42.77	0.05	0.25	16.2	0.03	0	0.02	0.37	0.2	0.02	99.12	82.48
AVF 30_ Pic 27_63	248	0.02	39.15	42.71	0.05	0.25	16.24	0.03	0	0.02	0.37	0.19	0.03	99.06	82.42
AVF 30_ Pic 27_64	252	0.01	38.84	42.66	0.02	0.24	16.53	0.02	0.01	0.03	0.36	0.14	0.03	98.88	82.14
AVF 30_ Pic 27_65	256	0.03	39.14	42.19	0.03	0.26	16.94	0.03	0.01	0.02	0.37	0.16	0.02	99.19	81.62
AVF 30_ Pic 27_66	260	0.01	38.53	40.94	0.07	0.32	18.18	0	0.01	0.03	0.4	0.11	0.03	98.65	80.06
AVF 30_ Pic 27_67	264	0.01	38.08	39.26	0.02	0.5	20.11	0.01	0.01	0.04	0.43	0.1	0.04	98.63	77.68
AVF 30_ Pic 27_68	268	0.68	52.9	4.19	21.43	0.16	6.74	-0.01	1.95	1.46	2.96	0.02	1.04	93.52	52.56
AVF 30_ 27_69	272	1.29	55.26	1.49	21.97	0.18	6.4	0.01	2.03	1.63	4.1	0.04	1.2	95.6	29.33
AVF 30_ Pic 27_70	276	0.93	54.67	1.46	22.28	0.14	6.34	0.02	2.3	1.49	3.88	0.03	1.23	94.75	29.10
AVF 30_ Pic 25_tr1	0	1.45	48.4	1.45	19.15	0.15	6.33	0.03	2.93	1.33	3.46	0	0.88	85.57	28.99
AVF 30_ Pic 25_02	4	0.59	43.92	11.23	7.93	0.13	7.93	0.01	0.06	3.39	21.92	0	0.27	97.38	71.63
AVF 30_ Pic 25_03	7	0.6	43.52	10.22	8.8	0.15	8.08	0.03	0.05	3.18	20.33	0.01	0.35	95.31	69.27
AVF 30_ Pic 25_04	11	0.52	42.34	11.49	8.77	0.1	8.09	0.11	0.01	3.91	21.49	-0.02	0.27	97.08	71.69
AVF 30_ Pic 25_05	14	0.05	38.07	35.16	0.77	0.38	20.09	0.06	0	0.35	2.92	0.07	0.05	97.97	75.73

Sample	Dist (μm)	Na_2O	SiO_2	MgO	Al_2O_3	MnO	FeO	Cr_2O_3	K_2O	TiO_2	CaO	NiO	P_2O_5	Total	Mg#
AVF 30_ Pic 25__06 18	0.02	37.85	38.52	0.06	0.34	18.49	0.03	0.01	0.06	0.56	0.06	0.02	96	78.78	
AVF 30_ Pic 25_trav 1_07	21	0.02	38.41	41.31	0.04	0.26	18.01	0.01	0	0.05	0.48	0.1	0.01	98.7	80.35
AVF 30_ Pic 25_trav 1_08	25	0.02	38.46	41.65	0.03	0.23	17.69	0.02	0.01	0.04	0.44	0.11	0	98.7	80.76
AVF 30_ Pic 25_trav 1_09	28	0.04	38.94	42.07	0.06	0.25	17.36	0.01	0.01	0.04	0.4	0.13	0	99.32	81.20
AVF 30_ Pic 25_trav 1_10	32	0.03	38.93	42.16	0.02	0.28	16.71	0.02	0.01	0.03	0.39	0.09	0.01	98.67	81.81
AVF 30_ Pic 25_trav 1_11	35	0.03	39.06	42.46	0.07	0.24	16.3	0.03	0.01	0.03	0.36	0.15	0.03	98.76	82.28
AVF 30_ Pic 25_trav 1_12	39	0.03	38.75	42.66	0.02	0.24	16.03	0.03	0.01	0.02	0.36	0.11	0.02	98.29	82.59
AVF 30_ Pic 25_trav 1_13	42	0.05	38.98	43.02	0.09	0.25	15.86	0	0.01	0.02	0.37	0.15	0.01	98.82	82.86
AVF 30_ Pic 25_trav 1_14	46	0.03	39.23	43.19	0.06	0.25	15.8	0.03	0.01	0.02	0.35	0.17	0.02	99.17	82.97
AVF 30_ Pic 25_trav 1_15	49	0.03	38.92	43.16	0.05	0.21	16.04	0.04	0.02	0.03	0.3	0.18	0.04	99	82.75
AVF 30_ Pic 25_trav 1_16	53	0.02	39.28	42.66	0.05	0.24	16.25	0.05	0.02	0.01	0.26	0.17	0.01	99.02	82.39
AVF 30_ Pic 25_trav 1_17	56	0.01	38.84	43.06	0.01	0.24	16.23	0.03	0.01	0.01	0.27	0.15	0.01	98.88	82.55
AVF 30_ Pic 25_trav 1_18	60	0.04	38.76	42.55	0.05	0.21	15.97	0.02	0.01	0.03	0.25	0.15	0	98.04	82.61
AVF 30_ Pic 25_trav 1_19	63	0.03	38.79	42.69	0.04	0.22	16.2	0.07	0.01	0.03	0.25	0.18	0.06	98.57	82.45
AVF 30_ Pic 25_trav 1_20	67	0.03	39.07	42.63	0.07	0.23	16.14	0.06	0.01	0.01	0.26	0.14	0.03	98.68	82.48
AVF 30_ Pic 25_trav 1_21	71	0.02	38.69	42.89	0.07	0.23	16.02	0.03	0.01	0.02	0.24	0.18	0.01	98.41	82.68
AVF 30_ Pic 25_trav 1_22	74	0.02	39.03	42.7	0.05	0.22	16.08	0.05	0	0.02	0.25	0.23	0.02	98.66	82.56
AVF 30_ Pic 25_trav 1_23	78	0.03	39.19	43.1	0.07	0.23	16.11	0.04	0.01	0.02	0.21	0.21	0.03	99.24	82.67
AVF 30_ Pic 25_trav 1_24	81	0.03	39.26	42.99	0.06	0.21	15.94	0.03	0.01	0.02	0.23	0.22	-0.01	98.99	82.78
AVF 30_ Pic 25_trav 1_25	85	0.04	39.52	42.99	0.04	0.19	16.09	0.03	0.01	0.02	0.24	0.19	0.02	99.37	82.65
AVF 30_ Pic 25_trav 1_26	88	0.03	37.17	43.29	0.07	0.2	16.05	0.03	0.01	0.02	0.24	0.21	0.02	97.34	82.78
AVF 30_ Pic 25_trav 1_27	92	0.03	32.69	43.39	0.06	0.18	15.8	0.04	0.01	0.01	0.25	0.25	-0.01	92.7	83.04
AVF 30_ Pic 25_trav 1_28	95	0.02	32.67	43.48	0.04	0.22	15.84	0.04	0	0.02	0.26	0.2	0.03	92.81	83.03
AVF 30_ Pic 25_trav 1_29	99	0.03	36.95	43.12	0.05	0.19	15.76	0.04	0.01	0.01	0.24	0.24	0.04	96.67	82.98
AVF 30_ Pic 25_trav 1_30	102	0.02	39.73	43.14	0.04	0.17	15.69	0.04	0.01	0.01	0.23	0.19	0.02	99.28	83.05
AVF 30_ Pic 25_trav 1_31	106	0.03	39.5	42.93	0.05	0.2	15.65	0.03	0	0	0.24	0.2	0.02	98.85	83.02
AVF 30_ Pic 25_trav 1_32	109	0.04	39.51	43.18	0.04	0.22	15.63	0.03	0.02	0.01	0.23	0.25	0.03	99.2	83.12
AVF 30_ Pic 25_trav 1_33	113	0.03	39.29	43.34	0.06	0.23	15.51	0.02	0.01	0.01	0.22	0.23	0.03	98.97	83.28
AVF 30_ Pic 25_trav 1_34	116	0.03	39.37	43.35	0.07	0.21	15.53	0.03	0.01	0.02	0.24	0.2	0.03	99.08	83.27
AVF 30_ Pic 25_trav 1_35	120	0.03	39.26	43.26	0.05	0.21	15.57	0.04	0.01	0	0.25	0.21	0.01	98.9	83.20
AVF 30_ Pic 25_trav 1_36	123	0.03	39.57	43.47	0.05	0.21	15.53	0.04	0.01	0.02	0.23	0.17	-0.01	99.32	83.30
AVF 30_ Pic 25_trav 1_37	127	0.03	39.01	43.38	0.06	0.16	15.52	0.02	0.01	0.01	0.22	0.22	0.01	98.65	83.28
AVF 30_ Pic 25_trav 1_38	130	0.01	39.78	43.43	0.11	0.21	15.57	0.04	0.01	0.02	0.22	0.22	0.01	99.63	83.26
AVF 30_ Pic 25_trav 1_39	134	0.04	32.97	43.95	0.03	0.21	15.56	0.03	0.01	0.01	0.21	0.2	0.05	93.28	83.43
AVF 30_ Pic 09_ol trav 1_01	0	0.85	51.59	1.85	19.73	0.14	7.95	0	1.67	1.62	6.17	0	1.05	93	29.32
AVF 30_ Pic 09_ol trav 1_02	2	0.3	50.04	4.29	18.82	0.24	9.97	0.01	0.84	1.54	3.45	0.02	0.92	90	43.41
AVF 30_ Pic 09_ol trav 1_03	4	0.03	38.14	27.45	3.82	0.53	25.33	0.01	0.07	0.32	0.86	0.01	0.15	97	65.89
AVF 30_ Pic 09_ol trav 1_04	6	0.01	37.56	35.72	0.03	0.47	22.85	0.01	0.01	0.06	0.5	0.09	0.03	97	73.59
AVF 30_ Pic 09_ol trav 1_05	8	0	38.33	38.1	0.04	0.38	19.94	0.01	0.01	0.04	0.47	0.07	0.01	97	77.30

Sample	Dist (μm)	Na_2O	SiO_2	MgO	Al_2O_3	MnO	FeO	Cr_2O_3	K_2O	TiO_2	CaO	NiO	P_2O_5	Total	Mg#
AVF 30_ Pic 09_ol trav 1_06	10	0.01	38.34	40.22	0.01	0.25	17.97	0.02	0	0.04	0.45	0.1	0.02	97	79.96
AVF 30_ Pic 09_ol trav 1_07	12	0	39.12	40.81	0.03	0.26	17.25	0.01	0.02	0.03	0.46	0.13	0.03	98	80.83
AVF 30_ Pic 09_ol trav 1_08	14	0.01	38.46	41.32	0.06	0.28	16.99	0.02	0.02	0.03	0.43	0.15	0.03	98	81.26
AVF 30_ Pic 09_ol trav 1_09	16	0	39.11	41.11	0.04	0.27	16.71	0	0.02	0.03	0.4	0.13	0.02	98	81.43
AVF 30_ Pic 09_ol trav 1_10	18	0	38.77	41.4	0.04	0.24	16.63	0	0.02	0.03	0.4	0.14	0.01	98	81.61
AVF 30_ Pic 09_ol trav 1_11	20	0.02	39.03	42.02	0.06	0.25	16.5	0	0.01	0.03	0.39	0.16	0.03	99	81.95
AVF 30_ Pic 09_ol trav 1_12	22	0.01	39.09	41.77	0.02	0.24	16.18	0.03	0.01	0.02	0.38	0.15	0.02	98	82.15
AVF 30_ Pic 09_ol trav 1_13	24	0.02	38.88	41.43	0.04	0.22	15.76	0.05	0.01	0.03	0.41	0.14	0.04	97	82.41
AVF 30_ Pic 09_ol trav 1_14	26	0.02	38.91	42.36	0.05	0.24	15.73	0.02	0.03	0.02	0.42	0.13	0.04	98	82.76
AVF 30_ Pic 09_ol trav 1_15	28	0.02	39.52	42.17	0.05	0.24	15.74	0.03	0.01	0.02	0.37	0.17	0.04	98	82.69
AVF 30_ Pic 09_ol trav 1_16	30	0.01	39.37	42.54	0.07	0.23	15.63	0.03	0.01	0.03	0.36	0.15	0.01	98	82.91
AVF 30_ Pic 09_ol trav 1_17	32	0.01	38.79	41.77	0.06	0.22	15.49	0.01	0	0.02	0.32	0.15	0.01	97	82.78
AVF 30_ Pic 09_ol trav 1_18	34	0	39.29	42.48	0.06	0.22	15.84	0.03	0	0.02	0.26	0.19	0.03	98	82.70
AVF 30_ Pic 09_ol trav 1_19	36	0.02	39.01	42.13	0.06	0.22	15.66	0.02	0.01	0.02	0.26	0.14	0.04	98	82.75
AVF 30_ Pic 09_ol trav 1_20	38	0.02	39.04	42.43	0.02	0.23	15.74	0.04	0	0.01	0.27	0.16	0.01	98	82.77
AVF 30_ Pic 09_ol trav 1_21	40	0.02	39.12	42.48	0.03	0.21	15.89	0.06	0	0.02	0.26	0.19	0.02	98	82.66
AVF 30_ Pic 09_ol trav 1_22	42	0.02	39.09	42.39	0.06	0.22	15.95	0.02	0	0.02	0.25	0.17	-0.01	98	82.57
AVF 30_ Pic 09_ol trav 1_23	44	0.02	38.88	42.7	0.04	0.24	15.91	0.03	0	0.01	0.27	0.19	0.02	98	82.71
AVF 30_ Pic 09_ol trav 1_24	46	0.16	38.74	40.08	0.53	0.19	14.48	0.03	0.18	0.02	0.56	0.23	0.04	95	83.15
AVF 30_ Pic 09_ol trav 1_25	48	0.21	39.05	38.49	0.58	0.16	14.81	0.03	0.14	0.02	0.6	0.23	0.07	94	82.25
AVF 30_ Pic 09_ol trav 1_26	50	0	38.92	42.06	0.05	0.2	15.86	0.03	0.01	0.02	0.26	0.2	0.04	98	82.54
AVF 30_ Pic 09_ol trav 1_27	52	0.01	39.22	42.47	0.06	0.21	15.58	0.05	0	0.02	0.24	0.19	0.01	98	82.93
AVF 30_ Pic 09_ol trav 1_28	54	0.01	38.94	42.57	0.07	0.21	15.61	0.04	0.01	0.02	0.25	0.25	0.01	98	82.94
AVF 30_ Pic 09_ol trav 1_29	56	0.03	39.08	42.35	0.05	0.23	15.46	0.04	0.01	0	0.26	0.19	0.02	98	83.00
AVF 30_ Pic 09_ol trav 1_30	58	0.03	39.37	42.35	0.1	0.2	15.69	0.05	0.02	0.03	0.24	0.17	0.02	98	82.79
AVF 30_ Pic 09_ol trav 1_31	60	0.04	38.78	41.75	0.28	0.2	15.3	0.03	0.04	0.02	0.29	0.17	0.02	97	82.95
AVF 30_ Pic 09_ol trav 1_32	62	0.04	38.76	42.69	0.06	0.18	15.54	0.03	0.01	0.02	0.26	0.18	-0.01	98	83.04
AVF 30_ Pic 09_ol trav 1_33	64	0.03	38.88	42.78	0.04	0.19	15.48	0.03	0.02	0	0.25	0.21	0.02	98	83.13
AVF 30_ Pic 09_ol trav 1_34	66	0.03	39.01	42.64	0.05	0.19	15.55	0.03	0.02	0.01	0.25	0.2	0.02	98	83.02
AVF 30_ Pic 09_ol trav 1_35	68	0.02	39.1	42.66	0.04	0.18	15.54	0.03	0.02	0.01	0.26	0.16	0.01	98	83.03
AVF 30_ Pic 09_ol trav 1_36	70	0.04	39.37	42.68	0.07	0.21	15.47	0.03	0.01	0.02	0.28	0.22	0.01	98	83.10
AVF 30_ Pic 09_ol trav 1_37	72	0.02	39.01	42.58	0.06	0.2	15.42	0.02	0.01	0.01	0.31	0.19	0.02	98	83.11
AVF 30_ Pic 09_ol trav 1_38	74	0.02	38.93	42.85	0.06	0.21	15.46	0.04	0.02	0.02	0.23	0.22	0.02	98	83.17
AVF 30_ Pic 09_ol trav 1_39	76	0.03	39.25	42.94	0.04	0.21	15.49	0.02	0.02	0.02	0.25	0.2	0.01	98	83.17
AVF 30_ Pic 09_ol trav 1_40	78	0.02	38.71	42.77	0.03	0.2	15.27	0.03	0.03	0	0.32	0.15	0.05	98	83.31
AVF 30_ Pic 09_ol trav 1_41	80	0.02	38.9	42.28	0.06	0.18	14.93	0.04	0.03	0.01	0.34	0.21	0.04	97	83.47
AVF 30_ Pic 09_ol trav 1_42	82	0.04	38.97	43	0.08	0.2	15.21	0.05	0.02	0	0.26	0.2	0.03	98	83.44
AVF 30_ Pic 09_ol trav 1_43	84	0.03	39.07	42.92	0.08	0.17	15.31	0.04	0.03	0.02	0.26	0.22	0.03	98	83.33
AVF 30_ Pic 09_ol trav 1_44	86	0.03	39.04	43.04	0.06	0.19	15.03	0.02	0.03	0.01	0.26	0.2	0.03	98	83.62

Sample	Dist (μm)	Na_2O	SiO_2	MgO	Al_2O_3	MnO	FeO	Cr_2O_3	K_2O	TiO_2	CaO	NiO	P_2O_5	Total	Mg#
AVF 30_ Pic 09_ol trav 1_45	88	0.04	39.65	43.25	0.08	0.21	15.08	0.04	0.02	0.02	0.26	0.22	0.02	99	83.64
AVF 30_ Pic 09_ol trav 1_46	90	0.02	39.29	43.13	0.06	0.23	15.02	0.03	0.02	0.01	0.24	0.19	0.03	98	83.66
AVF 30_ Pic 09_ol trav 1_47	92	0.03	39.35	43.11	0.06	0.21	14.93	0.05	0.02	0.01	0.25	0.19	0.02	98	83.73
AVF 30_ Pic 09_ol trav 1_48	94	0.04	39	43.28	0.08	0.18	14.75	0.05	0	0.01	0.25	0.24	0.03	98	83.95
AVF 30_ Pic 09_ol trav 1_49	96	0.01	39.09	43.45	0.05	0.17	14.94	0.03	0.01	0.01	0.26	0.21	0.02	98	83.83
AVF 30_ Pic 09_ol trav 1_50	98	0.03	39.32	43.44	0.06	0.17	14.85	0.02	0.02	0.02	0.24	0.19	0.02	98	83.91
AVF 30_ Pic 09_ol trav 1_51	100	0.02	39.33	43.43	0.06	0.18	14.69	0.03	0.02	0.01	0.24	0.2	0.03	98	84.05
AVF 30_ Pic 09_ol trav 1_52	102	0.02	39.44	43.7	0.07	0.19	14.86	0.03	0.02	0.01	0.23	0.18	-0.01	99	83.98
AVF 30_ Pic 09_ol trav 1_53	104	0.02	39.61	43.53	0.04	0.19	14.58	0.04	0.02	0.01	0.25	0.21	0.03	99	84.18
AVF 30_ Pic 09_ol trav 1_54	106	0.02	39	43.75	0.04	0.16	14.56	0.03	0.01	0.01	0.26	0.18	0	98	84.27
AVF 30_ Pic 09_ol trav 1_55	108	0.02	39.58	43.34	0.05	0.17	14.42	0.02	0.01	0.01	0.24	0.2	0	98	84.27
AVF 30_ Pic 09_ol trav 1_56	110	0.03	39.17	43.91	0.08	0.2	14.6	0.03	0.01	0.02	0.23	0.22	0.01	99	84.28
AVF 30_ Pic 09_ol trav 1_57	112	0.02	39.43	43.57	0.05	0.19	14.26	0.02	0.01	0	0.26	0.21	0.01	98	84.49
AVF 30_ Pic 09_ol trav 1_58	114	0.01	39.32	43.72	0.07	0.17	14.36	0.03	0.01	0.01	0.25	0.23	0.01	98	84.44
AVF 30_ Pic 09_ol trav 1_59	116	0.01	39.77	43.92	0.06	0.2	14.33	0.03	0	0.01	0.26	0.24	0.01	99	84.53
AVF 30_ Pic 09_ol trav 1_60	118	0.03	39.05	43.86	0.08	0.18	14.13	0.04	0	0.02	0.24	0.23	0.02	98	84.69
AVF 30_ Pic 09_ol trav 1_61	120	0.03	39.32	43.49	0.04	0.19	14.17	0.03	0	0.01	0.27	0.19	0.01	98	84.55
AVF 30_ Pic 09_ol trav 1_62	122	0.03	39.34	44.21	0.08	0.19	14.25	0.03	0.02	0.01	0.24	0.23	-0.01	99	84.69
AVF 30_ Pic 09_ol trav 1_63	124	0.03	39.63	43.8	0.1	0.2	13.94	0.05	0.02	0.01	0.23	0.25	-0.01	98	84.85
AVF 30_ Pic 09_ol trav 1_64	126	0.01	39.37	44.05	0.04	0.16	13.95	0.05	0.02	0.01	0.22	0.23	0	98	84.91
AVF 30_ Pic 09_ol trav 1_65	128	0.02	39.54	43.97	0.05	0.18	13.91	0.04	0.01	0.01	0.23	0.23	0	98	84.93
AVF 30_ Pic 09_ol trav 1_66	130	0.01	39.19	44.13	0.03	0.16	13.77	0.03	0	0.01	0.23	0.23	0.02	98	85.10
AVF 30_ Pic 09_ol trav 1_67	132	0.01	39.17	43.87	0.05	0.2	13.84	0.06	0	0.02	0.23	0.26	-0.01	98	84.96
AVF 30_ Pic 09_ol trav 1_68	134	0.02	39.49	44.16	0.07	0.15	13.84	0.06	0	0.02	0.23	0.21	0.01	98	85.05
AVF 30_ Pic 09_ol trav 1_69	136	0.02	39.81	44.01	0.06	0.22	13.57	0.05	0	0.01	0.23	0.24	0.01	98	85.25
AVF 30_ Pic 09_ol trav 1_70	138	0.02	39.35	44.18	0.07	0.18	13.77	0.05	0.01	0.01	0.24	0.23	0	98	85.12
AVF 30_ Pic 09_ol trav 1_71	140	0.01	39.66	44.48	0.08	0.17	13.85	0.02	0.01	0.01	0.23	0.23	0.02	99	85.13
AVF 30_ Pic 09_ol trav 1_72	142	0.02	39.38	44.13	0.05	0.18	13.77	0.04	0.01	0	0.22	0.22	0	98	85.10
AVF 30_ Pic 09_ol trav 1_73	144	0.01	39.52	44.42	0.06	0.18	13.65	0.05	0.01	0.01	0.21	0.27	0	98	85.30
AVF 30_ Pic 09_ol trav 1_74	146	0.01	39.73	44.42	0.04	0.15	13.61	0.03	0.01	0.02	0.24	0.22	0	98	85.33
AVF 30_ Pic 09_ol trav 1_75	148	0.01	39.53	44.13	0.08	0.16	13.63	0.04	0.01	0.01	0.23	0.26	0	98	85.23
AVF 30_ Pic 09_ol trav 1_76	150	0.01	39.34	44.31	0.09	0.19	13.55	0.05	0.01	0.02	0.24	0.23	0.03	98	85.36
AVF 30_ Pic 09_ol trav 1_77	152	0.02	39.77	44.01	0.09	0.18	13.26	0.05	0.01	0.01	0.24	0.24	0	98	85.54
AVF 30_ Pic 09_ol trav 1_78	154	0.02	39.43	44.68	0.1	0.16	13.56	0.04	0.01	0.01	0.25	0.26	0.02	99	85.45
AVF 30_ Pic 09_ol trav 1_79	156	0.02	39.78	44.47	0.07	0.18	13.23	0.06	0	0.01	0.23	0.28	0.03	98	85.70
AVF 30_ Pic 09_ol trav 1_80	158	0.02	39.78	44.45	0.08	0.13	13.34	0.03	0.01	-0.01	0.23	0.19	0.03	98	85.59
AVF 30_ Pic 09_ol trav 1_81	160	0.02	39.81	44.64	0.03	0.14	13.49	0.02	0.01	0.02	0.24	0.23	0.02	99	85.50
AVF 30_ Pic 09_ol trav 1_82	162	0.03	39.5	44.62	0.06	0.12	13.33	0.04	0	0.01	0.23	0.28	0.02	98	85.65
AVF 30_ Pic 09_ol trav 1_83	164	0.02	39.74	44.57	0.08	0.16	13.27	0.05	0.02	0.01	0.24	0.22	0.01	98	85.69

Sample	Dist (μm)	Na_2O	SiO_2	MgO	Al_2O_3	MnO	FeO	Cr_2O_3	K_2O	TiO_2	CaO	NiO	P_2O_5	Total	Mg#
AVF 30_ Pic 09_ol trav 1_84	166	0.02	39.82	44.73	0.05	0.16	13.34	0.03	0.01	0.01	0.24	0.26	0.03	99	85.67
AVF 30_ Pic 09_ol trav 1_85	168	0.03	39.68	44.6	0.05	0.17	13.13	0.05	0.01	0.01	0.24	0.24	0.02	98	85.83
AVF 30_ Pic 09_ol trav 1_86	170	0.03	39.48	44.58	0.08	0.16	13.18	0.04	0.01	0	0.23	0.25	0.01	98	85.77
AVF 30_ Pic 09_ol trav 1_87	172	0.03	39.71	44.51	0.07	0.17	13.14	0.03	0.01	0.02	0.24	0.26	0.01	98	85.79
AVF 30_ Pic 09_ol trav 1_88	174	0.01	39.44	44.72	0.08	0.18	13.2	0.04	0.01	0.01	0.24	0.26	0.02	98	85.79
AVF 30_ Pic 09_ol trav 1_89	176	0.03	39.74	44.53	0.04	0.19	13.09	0.05	0.02	0.01	0.25	0.28	0.03	98	85.84
AVF 30_ Pic 09_ol trav 1_90	178	0.02	39.76	44.49	0.07	0.18	12.96	0.02	0.02	0.01	0.25	0.26	0	98	85.95
AVF 30_ Pic 09_ol trav 1_91	180	0.01	39.61	44.81	0.06	0.18	13.15	0.05	0.02	0	0.24	0.3	0.04	98	85.86
AVF 30_ Pic 09_ol trav 1_92	182	0.02	39.59	45.1	0.08	0.19	13.17	0.03	0.01	0	0.25	0.25	0.03	99	85.92
AVF 30_ Pic 09_ol trav 1_93	184	0.01	39.56	44.59	0.06	0.16	13.12	0.04	0.02	0.02	0.24	0.24	-0.01	98	85.83
AVF 30_ Pic 09_ol trav 1_94	186	0.02	39.66	45.16	0.07	0.16	13.11	0.04	0.01	0.01	0.26	0.28	0	99	86.00
AVF 30_ Pic 09_ol trav 1_95	188	0.03	39.81	44.83	0.08	0.15	13.14	0.05	0.02	0.01	0.23	0.22	0.03	99	85.88
AVF 30_ Pic 09_ol trav 1_96	190	0	39.68	44.99	0.07	0.16	13.26	0.04	0.01	0.02	0.24	0.24	0.03	99	85.81
AVF 30_ Pic 09_ol trav 1_97	192	0.02	40.09	45.25	0.07	0.16	13.08	0.06	0.01	0.01	0.24	0.28	0.01	99	86.05
AVF 30_ Pic 09_ol trav 1_98	194	0.03	39.76	45.53	0.06	0.18	13.22	0.05	0.01	0.01	0.24	0.25	-0.01	99	85.99
AVF 30_ Pic 09_ol trav 1_99	196	0.02	39.95	45.15	0.05	0.15	13.17	0	0	0	0.25	0.27	0.02	99	85.94
AVF 30_ Pic 09_ol trav 1_100	198	0.02	39.91	45.22	0.06	0.15	13.14	0.05	0	0.02	0.23	0.28	0.02	99	85.98
AVF 30_ Pic 09_ol trav 1_101	200	0.03	39.93	45.37	0.08	0.17	13.04	0.04	0.01	0.01	0.21	0.25	0.01	99	86.11
AVF 30_ Pic 09_ol trav 1_102	202	0.04	39.58	45.31	0.07	0.15	12.98	0.05	0.01	0	0.22	0.27	-0.01	99	86.15
AVF 30_ Pic 09_ol trav 1_103	204	0.04	39.68	45.16	0.07	0.19	13.05	0.05	0.01	0.01	0.22	0.26	0.02	99	86.05
AVF 30_ Pic 09_ol trav 1_104	206	0.02	39.68	45.39	0.08	0.15	13.06	0.06	0.01	0.01	0.25	0.25	0.01	99	86.10
AVF 30_ Pic 09_ol trav 1_105	208	0.03	39.71	45.34	0.09	0.16	12.93	0.05	0.01	0.02	0.24	0.26	0.02	99	86.21
AVF 30_ Pic 09_ol trav 1_106	210	0.02	39.53	45.76	0.09	0.14	13.08	0.04	0.01	0.02	0.23	0.24	0	99	86.18
AVF 30_ Pic 09_ol trav 1_107	212	0.02	39.89	45.43	0.08	0.19	13.12	0.02	0.01	0.02	0.23	0.27	0.01	99	86.06
AVF 30_ Pic 09_ol point_1		-0.01	38.11	36.66	0.1	0.44	22.29	0.01	0.02	0.07	0.58	0.05	0.05	98	74.57
AVF 30_ Pic 09_ol point_2		0	39.14	41.93	0.07	0.26	17.32	0.02	0	0.03	0.41	0.13	0.04	99	81.19
AVF 30_ Pic 09_ol point_3		0.02	38.2	39.78	0.05	0.27	18.59	0.01	0.02	0.03	0.69	0.1	0	98	79.23
AVF 30_ Pic 09_ol point_4		0.46	45.4	12.18	7.09	0.09	7.16	0.34	0.01	3.13	21.91	0	0.25	98	75.20

Sample	Dist (μm)	Na_2O	SiO_2	MgO	Al_2O_3	MnO	FeO	Cr_2O_3	K_2O	TiO_2	CaO	NiO	P_2O_5	Total	Mg#
AVF 30_ Pic 09_pt_5		0.53	42.46	10.99	8.71	0.12	7.78	0.14	0.01	4.22	21.72	0.06	0.27	97	71.57
AVF 30_ Pic 08_01	0	0.47	46.41	12.28	5.69	0.14	8.04	0.02	0.02	2.59	21.99	0.01	0.26	97.93	73.14
AVF 30_ Pic 08_02	2	0.58	44.29	10.9	8.09	0.15	8.52	0	0.02	3.37	21.78	0.02	0.3	98.02	69.52
AVF 30_ Pic 08_03	4	0.62	43.22	10.52	9.06	0.13	8.4	0	0.01	4.07	21.99	0.02	0.29	98.32	69.06
AVF 30_ Pic 08_04	6	0.6	43.08	10.49	8.88	0.14	8.42	0.01	0	4.1	22	0.01	0.3	98.01	68.95
AVF 30_ Pic 08_05	8	0.56	42.99	10.66	9.01	0.1	8.23	0.01	0.01	4.02	22.05	0	0.27	97.9	69.78
AVF 30_ Pic 08_06	10	0.56	42.7	10.57	9.3	0.14	8.36	0.02	0.02	3.85	21.78	-0.02	0.24	97.53	69.27
AVF 30_ Pic 08_07	12	0.6	43.15	10.8	9	0.16	9.22	0.02	0.09	3.44	19.99	0	0.3	96.77	67.62
AVF 30_ Pic 08_08	14	0.37	40.74	18.18	4.65	0.31	16.89	0.02	0.02	1.8	12.16	0.05	0.2	95.41	65.74
AVF 30_ Pic 08_09	16	0.25	39.91	22.09	3.47	0.39	20.19	0.01	0.01	1.18	8.41	0.04	0.14	96.09	66.11
AVF 30_ Pic 08_10	18	0.01	38.57	38.61	0.09	0.37	20.6	0.02	0	0.06	0.48	0.05	0.03	98.9	76.96
AVF 30_ Pic 08_11	20	0.01	38.9	40.23	0.01	0.29	18.34	0.03	0.01	0.04	0.44	0.08	0.01	98.38	79.63
AVF 30_ Pic 08_12	22	0.02	38.79	41.2	0.07	0.29	17.54	0.01	0	0.04	0.44	0.09	0.03	98.53	80.72
AVF 30_ Pic 08_13	24	0.01	39.37	41.61	0.04	0.27	17.29	0.02	0.01	0.03	0.42	0.14	0.02	99.24	81.10
AVF 30_ Pic 08_14	26	0.01	38.8	41.7	0.06	0.27	17.21	0.01	0.01	0.04	0.4	0.16	0.03	98.7	81.20
AVF 30_ Pic 08_15	28	0.03	39.27	41.57	0.06	0.26	16.73	0.03	0	0.04	0.39	0.16	0.04	98.58	81.58
AVF 30_ Pic 08_16	30	0.01	38.77	41.69	0.04	0.24	16.75	0.02	0.01	0.03	0.38	0.14	0.05	98.12	81.61
AVF 30_ Pic 08_17	32	0.01	39.35	42.07	0.07	0.27	16.64	0.02	0	0.02	0.36	0.17	0.03	99.02	81.84
AVF 30_ Pic 08_18	34	0.02	39.2	42.11	0.04	0.26	16.78	0.03	0	0.04	0.36	0.16	0.09	99.08	81.73
AVF 30_ Pic 08_19	36	0.01	38.93	42.17	0.04	0.27	16.62	0.02	0.01	0.03	0.35	0.14	0.03	98.61	81.89
AVF 30_ Pic 08_20	38	0.02	39.13	42.55	0.04	0.25	16.56	0.04	0.01	0.03	0.35	0.16	0.05	99.17	82.08
AVF 30_ Pic 08_21	40	0	39.38	42.79	0.08	0.22	16.33	0.04	0	0.03	0.35	0.16	0.01	99.38	82.37
AVF 30_ Pic 08_22	42	0.02	39.41	42.69	0.07	0.24	15.92	0.04	0.01	0.02	0.34	0.14	0	98.89	82.70
AVF 30_ Pic 08_23	44	0	39.34	43.18	0.07	0.25	15.91	0.05	0	0.02	0.33	0.16	0.02	99.34	82.87
AVF 30_ Pic 08_24	46	0.02	39.42	42.91	0.06	0.25	15.79	0.02	0	0.03	0.31	0.19	0.03	99.03	82.89
AVF 30_ Pic 08_25	48	0.01	39.53	43.01	0.04	0.23	16.08	0.02	0	0.01	0.29	0.18	0.01	99.4	82.66
AVF 30_ Pic 08_26	50	0.01	38.94	42.71	0.03	0.18	16.13	0.04	0	0.02	0.27	0.18	0.02	98.52	82.52
AVF 30_ Pic 08_27	52	0.02	39.36	42.8	0.06	0.24	16.26	0.04	0	0.02	0.25	0.17	0.04	99.27	82.43
AVF 30_ Pic 08_28	54	0.01	39.08	42.61	0.06	0.23	16.22	0.02	0	0.02	0.25	0.18	0	98.67	82.40
AVF 30_ Pic 08_29	56	0.02	39.38	42.66	0.03	0.22	16.38	0.03	0.01	0.01	0.24	0.19	0	99.17	82.28
AVF 30_ Pic 08_30	58	0.02	39.14	42.43	0.07	0.23	16.47	0.01	0	0	0.24	0.16	0.04	98.81	82.12
AVF 30_ Pic 08_31	60	0	39.52	42.65	0.08	0.2	16.34	0.05	0	0.02	0.23	0.2	0.05	99.33	82.31
AVF 30_ Pic 08_32	62	0.01	39.37	42.92	0.05	0.22	16.22	0.02	0	0.02	0.24	0.19	0.06	99.32	82.51
AVF 30_ Pic 08_33	64	0.02	39.18	42.58	0.04	0.23	16.13	0.04	0	0.02	0.23	0.18	0.02	98.67	82.47
AVF 30_ Pic 08_34	66	0.02	39.17	42.85	0.06	0.21	16.03	0.04	0	0.01	0.23	0.17	0.04	98.82	82.65
AVF 30_ Pic 08_35	68	0.01	39.4	42.86	0.07	0.23	16.13	0.06	0	0	0.22	0.25	0.04	99.28	82.57
AVF 30_ Pic 08_36	70	0.01	39.14	42.93	0.04	0.21	16	0.05	0	0.02	0.24	0.2	0.03	98.86	82.71
AVF 30_ Pic 08_37	72	0.01	39.35	42.99	0.04	0.2	15.89	0.03	0	0.01	0.23	0.22	0.01	99	82.83
AVF 30_ Pic 08_38	74	0.02	39.32	43.16	0.07	0.17	16.04	0.03	0	0.02	0.22	0.15	0.03	99.23	82.75

Sample	Dist (μm)	Na_2O	SiO_2	MgO	Al_2O_3	MnO	FeO	Cr_2O_3	K_2O	TiO_2	CaO	NiO	P_2O_5	Total	Mg#
AVF 30_ Pic 08_39	76	0.03	39.66	43.1	0.05	0.21	15.79	0.01	0	0.02	0.23	0.2	0.03	99.31	82.95
AVF 30_ Pic 08_40	78	0.02	39.37	43.28	0.06	0.2	15.64	0.03	0	0.02	0.22	0.22	0.01	99.09	83.14
AVF 30_ Pic 08_41	80	0.03	39.66	43.58	0.06	0.19	15.66	0.04	0	0.02	0.22	0.21	0.02	99.71	83.22
AVF 30_ Pic 08_42	82	0.01	39.75	43.52	0.05	0.2	15.56	0.04	0	0.01	0.23	0.23	0	99.6	83.29
AVF 30_ Pic 08_43	84	0.02	39.29	43.47	0.07	0.21	15.5	0.04	0	0.01	0.21	0.22	0.01	99.07	83.33
AVF 30_ Pic 08_44	86	0.03	39.51	43.77	0.06	0.2	15.41	0.06	0	0.02	0.22	0.21	0.04	99.52	83.51
AVF 30_ Pic 08_45	88	0.03	39.78	43.89	0.08	0.16	15.15	0.05	0	0	0.22	0.22	0.01	99.59	83.78
AVF 30_ Pic 08_46	90	0.01	39.5	43.78	0.07	0.15	14.98	0.03	0	0.01	0.22	0.24	0.03	99.04	83.90
AVF 30_ Pic 08_47	92	0.01	39.77	43.98	0.07	0.17	15.04	0.01	0	0.01	0.22	0.25	0.03	99.57	83.90
AVF 30_ Pic 08_48	94	0.02	39.56	43.86	0.06	0.17	14.92	0.05	-0.01	0.02	0.23	0.26	0.04	99.17	83.97
AVF 30_ Pic 08_49	96	0	39.44	44.1	0.06	0.19	14.85	0.04	0	0.02	0.22	0.26	0.02	99.21	84.11
AVF 30_ Pic 08_50	98	0.01	39.49	43.91	0.06	0.18	14.75	0.02	0	0.02	0.22	0.25	0.01	98.91	84.14
AVF 30_ Pic 08_51	100	0.03	39.61	43.87	0.07	0.21	14.59	0.02	0	0.02	0.21	0.21	0.03	98.86	84.28
AVF 30_ Pic 08_52	102	0.01	39.87	43.97	0.07	0.16	14.61	0.05	0	0	0.22	0.24	0	99.19	84.29
AVF 30_ Pic 08_53	104	0.02	39.61	44.21	0.05	0.2	14.42	0.05	0	0.01	0.23	0.24	-0.01	99.02	84.53
AVF 30_ Pic 08_54	106	0	39.66	44.25	0.05	0.21	14.48	0.05	0	0.01	0.21	0.2	0	99.11	84.49
AVF 30_ Pic 08_55	108	0.03	39.5	44.38	0.06	0.18	14.42	0.03	0	0.02	0.21	0.18	0.01	99.02	84.58
AVF 30_ Pic 08_56	110	0.03	39.6	44.32	0.09	0.15	14.3	0.03	0	0.02	0.21	0.22	0.04	99.01	84.67
AVF 30_ Pic 08_57	112	0.02	39.67	44.45	0.06	0.21	14.24	0.04	0	0.01	0.2	0.26	0	99.16	84.77
AVF 30_ Pic 08_58	114	0.02	39.6	44.56	0.06	0.18	14.25	0.03	0	0.01	0.22	0.23	0.02	99.18	84.79
AVF 30_ Pic 08_59	116	0.02	40.2	44.54	0.08	0.18	14.08	0.06	0	0.03	0.22	0.23	0.04	99.68	84.94
AVF 30_ Pic 08_60	118	0.02	39.42	44.21	0.06	0.18	14.16	0.02	0	0.02	0.2	0.25	0.06	98.59	84.77
AVF 30_ Pic 08_61	120	0.01	39.51	44.21	0.09	0.17	14.07	0.03	0	0.02	0.21	0.26	0.02	98.59	84.85
AVF 30_ Pic 08_62	122	0.01	39.3	43.96	0.22	0.19	13.93	0.03	0	0.01	0.21	0.26	0.02	98.15	84.91
AVF 30_ Pic 08_63	124	0.01	39.57	44.49	0.12	0.16	13.92	0.04	0	0.02	0.22	0.23	0.03	98.81	85.07
AVF 30_ Pic 08_64	126	0.04	38.98	42.98	0.39	0.18	13.46	0.05	0	0.03	0.21	0.24	0.04	96.59	85.06
AVF 30_ Pic 08_65	128	0.01	38.64	43.3	0.36	0.17	13.47	0.07	0	0.02	0.21	0.21	0.03	96.5	85.14
AVF 30_ Pic 08_66	130	0.02	38.42	45.05	0.37	0.18	13.37	0.04	0.01	0.02	0.21	0.26	0.01	97.96	85.73
AVF 30_ Pic 08_67	132	0.01	39.99	44.75	0.05	0.17	13.59	0.04	0	0	0.21	0.27	0.06	99.13	85.44
AVF 30_ Pic 08_68	134	0.01	39.65	44.93	0.09	0.18	13.43	0.04	0	0.01	0.2	0.25	0.04	98.83	85.64
AVF 30_ Pic 08_69	136	0.02	40.02	44.63	0.07	0.19	13.48	0.04	0	0.01	0.19	0.28	0.03	98.96	85.51
AVF 30_ Pic 08_70	138	0.03	39.81	45.11	0.03	0.16	13.46	0.03	0	0.01	0.2	0.25	0	99.08	85.66
AVF 30_ Pic 08_71	140	0.02	39.75	45.01	0.07	0.18	13.34	0.05	0	0.02	0.21	0.3	0.03	99	85.74
AVF 30_ Pic 08_72	142	0.01	39.65	44.78	0.08	0.18	13.36	0.03	-0.01	0	0.2	0.26	0.01	98.57	85.66
AVF 30_ Pic 08_73	144	0.02	40.15	45.3	0.07	0.17	13.32	0.06	0	0.02	0.22	0.27	0	99.6	85.84
AVF 30_ Pic 08_74	146	0.02	39.92	45.17	0.04	0.14	13.26	0.05	0.01	0	0.2	0.31	-0.01	99.13	85.86
AVF 30_ Pic 08_75	148	0.03	40.34	45.41	0.05	0.17	13.2	0.05	0	0.02	0.21	0.29	0.01	99.77	85.98
AVF 30_ Pic 08_76	150	0.01	39.56	45.16	0.09	0.16	13.08	0.03	-0.01	0	0.21	0.28	0.02	98.6	86.02
AVF 30_ Pic 08_77	152	0.01	39.72	44.94	0.06	0.18	12.92	0.03	0	0.02	0.23	0.27	0.02	98.4	86.11

Sample	Dist (μm)	Na_2O	SiO_2	MgO	Al_2O_3	MnO	FeO	Cr_2O_3	K_2O	TiO_2	CaO	NiO	P_2O_5	Total	Mg#
AVF 30_ Pic 08_78	154	0.02	39.93	45.61	0.06	0.16	13.04	0.04	0	0.01	0.2	0.3	0.02	99.39	86.18
AVF 30_ Pic 08_79	156	0	40.04	45.4	0.09	0.15	12.83	0.05	0.01	0	0.19	0.3	0.01	99.06	86.32
AVF 30_ Pic 08_80	158	0.02	39.83	45.65	0.08	0.17	12.81	0.04	0	0.02	0.21	0.27	0.03	99.13	86.40
AVF 30_ Pic 08_81	160	0.03	39.88	45.66	0.06	0.14	12.82	0.04	0	0.01	0.21	0.31	0.03	99.19	86.39
AVF 30_ Pic 08_82	162	0.02	39.63	45.5	0.06	0.18	12.73	0.04	0	0.01	0.2	0.29	0.02	98.69	86.43
AVF 30_ Pic 08_83	164	0.02	39.6	45.34	0.08	0.17	12.73	0.04	0.01	0.01	0.19	0.3	0.02	98.51	86.39
AVF 30_ Pic 08_84	166	0.01	40.05	45.58	0.05	0.16	12.67	0.04	0.01	0.01	0.21	0.29	0.03	99.11	86.51
AVF 30_ Pic 08_85	168	0.03	39.98	45.84	0.07	0.17	12.73	0.03	-0.01	0.01	0.21	0.28	-0.01	99.32	86.52
AVF 30_ Pic 08_86	170	0.02	39.75	45.96	0.06	0.15	12.66	0.05	0	0.01	0.2	0.33	0.01	99.19	86.62
AVF 30_ Pic 08_87	172	0	40	45.77	0.09	0.16	12.63	0.05	0	0.01	0.19	0.31	0.01	99.22	86.59
AVF 30_ Pic 08_88	174	0.01	39.81	46.14	0.07	0.15	12.59	0.06	0	0	0.2	0.29	0.02	99.37	86.72
AVF 30_ Pic 08_89	176	0.03	40	45.88	0.07	0.15	12.51	0.03	0	0.01	0.21	0.3	0.02	99.21	86.73
AVF 30_ Pic 08_90	178	0.03	39.88	46.13	0.07	0.14	12.45	0.03	0	0	0.2	0.31	0.01	99.25	86.85
AVF 30_ Pic 08_91	180	0.03	40.25	45.88	0.1	0.14	12.41	0.02	0	0	0.22	0.32	0.02	99.39	86.82
AVF 30_ Pic 08_92	182	0.03	39.73	45.68	0.07	0.16	12.42	0.04	0	0.02	0.2	0.34	-0.01	98.68	86.77
AVF 30_ Pic 08_93	184	0.02	39.88	45.72	0.08	0.19	12.4	0.03	-0.01	0.01	0.19	0.31	0.01	98.83	86.79
AVF 30_ Pic 08_94	186	0.01	39.62	46.03	0.07	0.17	12.48	0.04	-0.01	0.02	0.2	0.28	0.04	98.96	86.80
AVF 30_ Pic 08_95	188	0.01	40.1	46.14	0.09	0.14	12.43	0.05	-0.01	0.02	0.21	0.33	0.04	99.54	86.87
WQE3_Ol 00_01	0	0.58	43.63	11.19	8.74	0.13	8.27	0.17	0.02	4.2	22.82	0.03	0.25	100.02	70.69
WQE3_Ol 00_02	2												0.22	98.37	70.55
WQE3_Ol 00_03	4	0.44	49.43	14.57	3.77	0.11	6.72	0.38	0.01	1.69	22.6	0.04	0.27	100.04	79.44
WQE3_Ol 00_04	6												0.18	97.63	73.29
WQE3_Ol 00_05	8	0.02	38.62	40.49	0.02	0.32	19.75	0	0	0.07	0.54	0.09	0.02	99.93	78.52
WQE3_Ol 00_06	10	0.01	38.76	40.85	0.04	0.29	19.24	0.02	0.01	0.05	0.48	0.12	0.03	99.9	79.10
WQE3_Ol 00_07	12	0.01	38.69	41.17	0.03	0.29	19.01	0.02	0	0.05	0.45	0.16	0.02	99.92	79.43
WQE3_Ol 00_08	14	0.02	38.65	41.26	0.02	0.29	18.68	0.03	0.01	0.04	0.43	0.09	0.02	99.54	79.75
WQE3_Ol 00_09	16	0.03	38.98	41.14	0.02	0.29	18.45	0.01	0	0.03	0.42	0.13	0	99.5	79.90
WQE3_Ol 00_10	18	0.02	38.73	41.73	0.06	0.27	18.52	0.03	0.01	0.06	0.42	0.11	0.05	99.99	80.07
WQE3_Ol 00_11	20	0.02	39.06	41.71	0.03	0.29	18.14	0.01	0.01	0.04	0.39	0.16	0.02	99.86	80.39
WQE3_Ol 00_12	22	0.02	39.2	41.69	0.05	0.31	18.14	0.01	0	0.04	0.4	0.12	0.02	100	80.38
WQE3_Ol 00_13	24	0.02	39.16	42.19	0.01	0.28	17.87	0.02	0	0.03	0.38	0.15	0.02	100.14	80.80
WQE3_Ol 00_14	26	0.01	38.83	42.25	0.04	0.28	17.75	0.03	0	0.04	0.38	0.15	0.04	99.79	80.93
WQE3_Ol 00_15	28	0.01	39.26	42.48	0.05	0.24	17.64	0.02	0	0.03	0.36	0.12	0.02	100.25	81.11
WQE3_Ol 00_16	30	0.01	38.91	42.9	0.03	0.25	17.4	0.03	-0.01	0.03	0.35	0.15	0.04	100.09	81.46
WQE3_Ol 00_17	32	0.01	39.45	42.69	0.02	0.25	17.01	0.03	0	0.03	0.35	0.16	0.02	100.02	81.73
WQE3_Ol 00_18	34	0.01	39.12	42.73	0.03	0.24	16.83	0.02	0	0.02	0.35	0.19	0.03	99.58	81.90
WQE3_Ol 00_19	36	0.02	39.24	42.71	0.05	0.24	16.82	0.02	0	0.03	0.34	0.19	0.04	99.7	81.90
WQE3_Ol 00_20	38	0.03	39.04	42.71	0.03	0.24	16.72	0.03	0	0.02	0.33	0.14	0.03	99.32	81.99

Sample	Dist (μm)	Na_2O	SiO_2	MgO	Al_2O_3	MnO	FeO	Cr_2O_3	K_2O	TiO_2	CaO	NiO	P_2O_5	Total	Mg#
WQE3_Ol 00_21	40	0.02	39.59	42.89	0.05	0.26	16.85	0.02	-0.01	0.03	0.32	0.16	0.03	100.21	81.94
WQE3_Ol 00_22	42	0.03	38.83	42.9	0.03	0.25	16.84	0.04	0	0.01	0.29	0.17	0.02	99.41	81.95
WQE3_Ol 00_23	44	0.02	39.33	42.62	0.03	0.26	17.44	0.04	0	0.01	0.29	0.17	-0.01	100.21	81.33
WQE3_Ol 00_24	46	0.02	39.42	42.48	0.03	0.24	17.56	0.04	-0.01	0.03	0.27	0.21	0	100.31	81.18
WQE3_Ol 00_25	48	0.01	39.53	42.78	0.02	0.26	17.38	0.05	-0.01	0.02	0.27	0.17	0	100.48	81.44
WQE3_Ol 00_26	50	0.02	38.76	42.58	0.06	0.24	17.3	0.03	-0.01	0.02	0.26	0.19	0.02	99.47	81.44
WQE3_Ol 00_27	52	0.02	39.29	42.8	0.05	0.23	17.53	0.04	0	0.01	0.24	0.2	0.04	100.44	81.32
WQE3_Ol 00_28	54	0.02	39.09	42.64	0.01	0.23	17.2	0.03	0	0.02	0.24	0.19	0.03	99.7	81.55
WQE3_Ol 00_29	56	0	39.31	42.91	0.07	0.24	17.21	0.04	0	0.02	0.24	0.23	0.02	100.29	81.63
WQE3_Ol 00_30	58	0.03	39.16	42.65	0	0.2	17.21	0.02	0.01	0.02	0.24	0.17	0.01	99.73	81.54
WQE3_Ol 00_31	60	0.03	39.13	42.72	0.03	0.19	17.21	0.03	-0.01	0.02	0.24	0.17	0.02	99.78	81.57
WQE3_Ol 00_32	62	0.03	39.16	42.58	0.03	0.19	17.36	0.05	0	0.03	0.24	0.22	0.04	99.92	81.39
WQE3_Ol 00_33	64	0.01	39.23	42.69	0.03	0.19	17.28	0.02	0	0.01	0.24	0.18	0.04	99.92	81.49
WQE3_Ol 00_34	66	0.02	39.12	42.94	0.06	0.22	17.15	0.02	0	0.02	0.24	0.18	0.01	99.99	81.70
WQE3_Ol 00_35	68	0.03	39.07	43.12	0.06	0.22	17.13	0.05	0	0.02	0.21	0.22	0.02	100.14	81.78
WQE3_Ol 00_36	70	0.02	39.31	42.9	0.03	0.22	17.2	0.02	0	0.02	0.24	0.24	0.03	100.22	81.64
WQE3_Ol 00_37	72	0.03	39.26	43.04	0.03	0.21	17.1	0.05	0	0.02	0.22	0.2	0.02	100.17	81.77
WQE3_Ol 00_38	74	0.02	39.26	42.92	0.04	0.23	16.81	0.02	0.01	0.02	0.22	0.24	0.02	99.8	81.99
WQE3_Ol 00_39	76	0.03	39.11	42.75	0.07	0.21	16.63	0.04	0	0.02	0.21	0.2	0.02	99.29	82.09
WQE3_Ol 00_40	78	0.01	38.9	43	0.05	0.18	17.02	0.05	0	0.02	0.23	0.24	0	99.69	81.83
WQE3_Ol 00_41	80	0.02	39.17	43.06	0.04	0.2	16.78	0.04	0.01	0.02	0.23	0.18	0.01	99.77	82.06
WQE3_Ol 00_42	82	0.02	39.32	42.92	0.05	0.23	16.95	0.03	0	0.02	0.23	0.25	0.01	100.02	81.86
WQE3_Ol 00_43	84	0.03	39.29	42.96	0.05	0.2	16.97	0.03	0	0.01	0.22	0.23	0.04	100.02	81.86
WQE3_Ol 00_44	86	0.01	39.26	42.94	0.03	0.23	17.05	0.02	0	0.02	0.22	0.18	0.02	99.98	81.78
WQE3_Ol 00_45	88	0.02	39.59	43.18	0.07	0.2	17.11	0.03	0	0.04	0.22	0.18	0.04	100.68	81.81
WQE3_Ol 00_46	90	0.03	39.17	43.22	0.09	0.23	17.22	0.01	0.01	0.02	0.24	0.2	0	100.44	81.73
WQE3_Ol 00_47	92	0.03	39.31	42.93	0.05	0.17	17.25	0.04	0	0.02	0.23	0.17	0.01	100.22	81.60
WQE3_Ol 00_48	94	0.02	39.13	42.9	0.06	0.18	17.24	0.02	0	0.02	0.24	0.14	0	99.96	81.60
WQE3_Ol 00_49	96	0.01	39.38	42.75	0.06	0.2	17.24	0.03	0	0.02	0.23	0.18	0	100.1	81.55
WQE3_Ol 00_50	98	0.02	39.21	42.77	0.07	0.21	17.31	0.01	0	0.03	0.24	0.17	0.04	100.09	81.50
WQE3_Ol 00_51	100	-0.01	39.06	42.49	0.08	0.22	17.42	0.03	0	0.03	0.24	0.1	0	99.66	81.30
WQE3_Ol 00_52	102	0.03	38.87	42.6	0.07	0.18	17.61	0.01	0	0.02	0.23	0.17	-0.02	99.78	81.18
WQE3_Ol 00_53	104	0.03	39.23	42.77	0.1	0.22	17.58	0.01	0	0.03	0.26	0.14	0	100.36	81.26
WQE3_Ol 00_54	106	0	39.29	42.64	0.08	0.2	17.55	0.01	0	0.04	0.25	0.13	0.01	100.17	81.24
WQE3_Ol 00_55	108	0	39.4	42.42	0.05	0.19	17.69	0.01	0	0.03	0.24	0.09	0.01	100.14	81.04
WQE3_Ol 00_56	110	0.01	38.98	42.62	0.08	0.17	17.79	0.01	0	0.04	0.25	0.09	-0.03	100.02	81.03
WQE3_Ol 00_57	112	0.02	38.95	42.49	0.08	0.2	17.92	0	-0.01	0.04	0.26	0.1	0	100.05	80.87
WQE3_Ol 00_58	114	0.02	39.09	42.06	0.09	0.24	17.87	0.02	0	0.04	0.24	0.08	0.02	99.78	80.75

Sample	Dist (μm)	Na_2O	SiO_2	MgO	Al_2O_3	MnO	FeO	Cr_2O_3	K_2O	TiO_2	CaO	NiO	P_2O_5	Total	Mg#
WQE3_Ol 00_59	116	0.01	39.17	42.2	0.07	0.19	17.9	0.03	0	0.04	0.27	0.06	-0.02	99.92	80.78
WQE3_Ol 00_60	118	0.04	39.09	41.93	0.05	0.17	17.79	0	0	0.05	0.23	0.07	-0.02	99.41	80.77
WQE3_Ol 00_61	120	0.02	38.93	42.21	0.08	0.18	17.87	0	-0.01	0.03	0.25	0.07	0	99.62	80.81
WQE3_Ol 00_62	122	0.01	39.34	42.26	0.11	0.19	18.1	0	0	0.05	0.24	0.05	0.01	100.36	80.63
WQE3_Ol 00_63	124	0.01	38.95	42.18	0.07	0.19	18.05	-0.01	0	0.05	0.25	0.08	-0.01	99.81	80.64
WQE3_Ol 00_64	126	0.02	39.23	42.3	0.1	0.2	18.03	0.01	0	0.05	0.25	0.06	-0.01	100.24	80.70
WQE3_Ol 00_65	128	0.02	39.01	42.27	0.07	0.19	17.94	0.01	0	0.05	0.24	0.05	0	99.85	80.77
WQE3_Ol 00_66	130	0.02	39.1	42.44	0.08	0.16	17.97	0	0	0.04	0.23	0.06	0	100.1	80.81
WQE3_Ol 00_67	132	0.01	38.93	42.32	0.07	0.21	17.88	0	-0.01	0.05	0.25	0.08	-0.01	99.8	80.84
WQE3_Ol 00_68	134	0	38.95	42.3	0.1	0.22	17.73	0.01	0	0.04	0.25	0.06	0.01	99.68	80.96
WQE3_Ol 00_69	136	0	39.33	42.48	0.08	0.19	17.89	0.01	0.01	0.04	0.25	0.1	-0.01	100.35	80.89
WQE3_Ol 00_70	138	0	38.91	42.6	0.08	0.16	17.78	0.02	0	0.04	0.24	0.11	0	99.95	81.03
WQE3_Ol 00_71	140	0.03	39.35	42.57	0.08	0.21	17.46	0.02	0	0.02	0.25	0.1	0	100.08	81.29
WQE3_Ol 04_01	0	0.64	41.77	10.07	9.6	0.15	9.1	0	0.05	5.01	22.12	0.01	0.33	98.84	66.36
WQE3_Ol 04_02	4	0.55	45.55	11.79	6.86	0.1	8.07	0.16	0.03	3.06	22.42	0	0.29	98.89	72.25
WQE3_Ol 04_03	8	0.43	47.35	13.73	4.93	0.12	7.4	0.26	0.02	2.32	22.43	0.02	0.27	99.29	76.78
WQE3_Ol 04_04	12	0.4	47.88	13.91	4.61	0.11	7.27	0.32	0.01	2.15	22.32	0.02	0.27	99.27	77.33
WQE3_Ol 04_05	16	0.02	38.26	40.42	0.04	0.3	19.31	0.03	0	0.05	0.47	0.1	0.04	99.07	78.86
WQE3_Ol 04_06	20	0.05	38.52	40.52	0.06	0.29	18.39	0.02	0.26	0.05	0.57	0.14	0.07	98.94	79.71
WQE3_Ol 04_07	24	0.03	38.92	41.13	0.06	0.27	18.63	0.04	0.01	0.04	0.4	0.13	0.05	99.72	79.74
WQE3_Ol 04_08	28	0.03	38.92	42.47	0.01	0.28	17.82	0.04	0.01	0.03	0.37	0.17	0.03	100.17	80.95
WQE3_Ol 04_09	32	0.01	38.83	42.72	0.01	0.26	17.26	0.03	0	0.03	0.36	0.16	0.02	99.7	81.52
WQE3_Ol 04_10	36	0	39.36	42.9	0.04	0.25	17.04	0.03	0	0.03	0.36	0.14	0.04	100.18	81.78
WQE3_Ol 04_11	40	0.01	39.3	42.62	0.05	0.25	17.32	0.03	0	0.02	0.29	0.18	0.03	100.09	81.43
WQE3_Ol 04_12	44	0.02	39.23	42.56	0.03	0.26	17.15	0.04	0.01	0.02	0.28	0.19	0.01	99.81	81.56
WQE3_Ol 04_13	48	0	38.81	43.02	0.06	0.24	17.3	0.04	0	0.02	0.27	0.2	0.03	99.98	81.59
WQE3_Ol 04_14	52	0.01	39.03	42.66	0.03	0.23	17.1	0.03	0	0.02	0.26	0.21	0	99.57	81.64
WQE3_Ol 04_15	56	0.02	39.05	42.76	0.04	0.24	17.41	0.04	0	0.02	0.24	0.21	0.03	100.05	81.41
WQE3_Ol 04_16	60	0.01	39.11	42.77	0.06	0.23	17.25	0.04	0.01	0.02	0.25	0.19	0.01	99.94	81.55
WQE3_Ol 04_17	64	0.01	39.41	43	0.04	0.22	17	0.04	0	0.02	0.25	0.23	0.02	100.23	81.85
WQE3_Ol 04_18	68	0.01	39.51	42.98	0.03	0.22	17.07	0.04	0	0.01	0.24	0.23	0.02	100.36	81.78
WQE3_Ol 04_19	72	0.04	38.95	43.23	0.07	0.24	17.05	0.03	0	0.02	0.2	0.23	0.02	100.07	81.88
WQE3_Ol 04_20	76	0.02	39.64	43.29	0.07	0.18	16.82	0.03	0.01	0.01	0.21	0.23	0.02	100.53	82.10
WQE3_Ol 04_21	80	0.02	39.19	43.71	0.04	0.19	16.17	0.04	0	0.01	0.22	0.19	0.03	99.82	82.81
WQE3_Ol 04_22	84	0.04	39.27	43.69	0.05	0.2	16.14	0.04	0	0.03	0.21	0.24	0.01	99.92	82.83
WQE3_Ol 04_23	88	0.01	39.26	44.08	0.05	0.23	16.02	0.03	0	0.02	0.21	0.22	0.02	100.14	83.06
WQE3_Ol 04_24	92	0.02	39.62	44.22	0.07	0.22	15.65	0.02	0	0.02	0.21	0.26	0.04	100.34	83.43
WQE3_Ol 04_25	96	0.02	39.56	44.66	0.07	0.18	15.28	0.02	0	0.01	0.2	0.24	0.03	100.27	83.90
WQE3_Ol 04_26	100	0.02	39.64	44.52	0.06	0.21	14.98	0.03	0	0.01	0.21	0.22	0.04	99.93	84.12

Sample	Dist (μm)	Na_2O	SiO_2	MgO	Al_2O_3	MnO	FeO	Cr_2O_3	K_2O	TiO_2	CaO	NiO	P_2O_5	Total	Mg#
WQE3_Ol 04_27	104	0.03	39.75	45	0.06	0.16	14.52	0.04	0	0.01	0.22	0.26	0.02	100.08	84.67
WQE3_Ol 04_28	108	0.02	39.74	45.3	0.07	0.17	14.31	0.04	0	0	0.2	0.23	0.03	100.11	84.95
WQE3_Ol 04_29	112	0.01	39.62	45.56	0.07	0.16	14.23	0.03	0	0.01	0.2	0.29	0	100.19	85.09
WQE3_Ol 04_30	116	0.02	39.91	45.35	0.08	0.18	13.96	0.05	0	0.01	0.19	0.24	-0.01	100	85.27
WQE3_Ol 04_31	120	0.03	39.67	45.8	0.04	0.18	13.9	0.03	0	0.01	0.19	0.27	0.01	100.13	85.45
WQE3_Ol 04_32	124	0.01	39.91	45.64	0.07	0.2	13.87	0.05	0.01	0.01	0.21	0.3	0.02	100.3	85.43
WQE3_Ol 04_33	128	0.03	39.88	45.74	0.07	0.17	13.82	0.05	0	0.01	0.2	0.31	0.03	100.3	85.51
WQE3_Ol 04_34	132	0.02	40.16	45.96	0.05	0.19	13.78	0.06	0.01	0	0.19	0.3	0.02	100.75	85.60
WQE3_Ol 04_35	136	0.02	40.05	45.71	0.05	0.15	13.71	0.04	0	0.02	0.2	0.26	0.01	100.22	85.60
WQE3_Ol 04_36	140	0.02	40.19	45.88	0.06	0.16	13.73	0.05	-0.01	0.01	0.2	0.31	-0.01	100.6	85.63
WQE3_Ol 04_37	144	0	39.73	45.98	0.07	0.17	13.67	0.05	0	0.01	0.2	0.28	0.02	100.2	85.71
WQE3_Ol 04_38	148	0.01	40	46	0.03	0.19	13.52	0.04	0	0.01	0.21	0.34	0.01	100.35	85.85
WQE3_Ol 04_39	152	0.03	40.08	46.03	0.03	0.16	13.44	0.05	0.01	0.01	0.19	0.33	0.02	100.37	85.93
WQE3_Ol 04_40	156	0.01	39.93	46.09	0.06	0.16	13.65	0.02	0	0.01	0.2	0.3	0.02	100.46	85.75
WQE3_Ol 04_41	160	0.01	39.83	46.02	0.06	0.16	13.44	0.04	0	0	0.2	0.32	0.03	100.1	85.92
WQE3_Ol 04_42	164	0.02	40.27	46.1	0.04	0.2	13.5	0.03	0	0.02	0.21	0.27	0.02	100.69	85.89
WQE3_Ol 04_43	168	0.02	39.8	46.21	0.04	0.14	13.46	0.02	0	0.01	0.19	0.34	0.01	100.24	85.95
WQE3_Ol 04_44	172	0.01	40.29	46.1	0.07	0.17	13.33	0.03	0	0.01	0.2	0.34	0.04	100.57	86.04
WQE3_Ol 04_45	176	0.03	39.65	46.36	0.06	0.18	13.34	0.05	0	0.01	0.19	0.35	0.02	100.24	86.10
WQE3_Ol 04_46	180	0.02	39.92	46.14	0.07	0.15	13.32	0.05	0	0.01	0.18	0.26	0.03	100.14	86.06
WQE3_Ol 04_47	184	0.02	39.6	46.4	0.09	0.17	13.36	0.04	0	0.02	0.2	0.3	0	100.19	86.09
WQE3_Ol 04_48	188	0.02	39.86	46.49	0.11	0.17	13.24	0.04	0	0.02	0.2	0.32	0.03	100.5	86.22
WQE3_Ol 04_49	192	0.02	39.71	46.44	0.05	0.14	13.16	0.04	0	0.01	0.2	0.34	0.01	100.13	86.28
WQE3_Ol 04_50	196	0.01	39.87	46.41	0.08	0.15	13.19	0.03	0	0.01	0.19	0.35	0	100.29	86.25
WQE3_Ol 04_51	200	0.02	39.61	46.42	0.11	0.15	13.24	0.04	0.01	0.01	0.19	0.3	0.02	100.13	86.21
WQE3_Ol 04_52	204	0.02	39.69	46.22	0.08	0.16	13.23	0.02	0	0	0.2	0.29	-0.01	99.9	86.16
WQE3_Ol 04_53	208	0.02	39.72	46.48	0.11	0.16	13.13	0.05	-0.01	0	0.19	0.36	0	100.23	86.32
WQE3_Ol 04_54	212	0.01	39.97	46.49	0.09	0.17	13.08	0.04	0	0.01	0.18	0.31	0.03	100.38	86.37
WQE3_Ol 04_55	216	0.01	39.64	46.46	0.09	0.14	12.96	0.04	0	0.01	0.2	0.36	0.01	99.91	86.47
WQE3_Ol 04_56	220	0.03	40.01	46.58	0.09	0.14	12.99	0.05	0	0	0.21	0.3	0.02	100.42	86.47
WQE3_Ol 04_57	224	0.01	39.83	46.66	0.05	0.16	12.91	0.03	0	0.01	0.19	0.33	-0.01	100.17	86.56
WQE3_Ol 04_58	228	0.01	40.02	46.38	0.06	0.11	12.81	0.05	0.01	0	0.2	0.32	0.02	99.99	86.58
WQE3_Ol 04_59	232	0.02	39.86	46.52	0.07	0.14	12.94	0.04	0	0.01	0.21	0.35	0	100.15	86.50
WQE3_Ol 04_60	236	0.02	40.35	46.58	0.05	0.18	12.95	0.04	0	0.01	0.21	0.34	0.03	100.73	86.51
WQE3_Ol 04_61	240	0.03	39.71	46.5	0.07	0.15	12.89	0.07	0	0.01	0.2	0.37	0.03	100.01	86.54
WQE3_Ol 04_62	244	0.02	40.32	46.3	0.08	0.15	12.9	0.06	0	0	0.2	0.35	0.02	100.4	86.48
WQE3_Ol 04_63	248	0.02	39.68	46.55	0.03	0.13	13	0.05	-0.01	0	0.2	0.37	0	100.03	86.46
WQE3_Ol 04_64	252	0.02	39.95	46.43	0.06	0.16	12.74	0.05	0	0.02	0.19	0.35	0.02	99.99	86.66
WQE3_Ol 04_65	256	0.03	39.95	46.6	0.06	0.17	12.98	0.04	0	0.01	0.19	0.35	0.01	100.39	86.49

Sample	Dist (μm)	Na_2O	SiO_2	MgO	Al_2O_3	MnO	FeO	Cr_2O_3	K_2O	TiO_2	CaO	NiO	P_2O_5	Total	Mg#
WQE3_Ol 04_66	260	0.02	40.18	46.33	0.08	0.16	12.86	0.03	0	0.02	0.2	0.34	0.03	100.26	86.53
WQE3_Ol 04_67	264	0.02	39.94	46.6	0.09	0.12	12.98	0.04	0.01	0	0.21	0.34	0.03	100.38	86.49
WQE3_Ol 04_68	268	0	40.09	46.32	0.06	0.15	12.93	0.03	0	0.01	0.21	0.35	0.03	100.18	86.46
WQE3_Ol 04_69	272	0.03	39.98	46.51	0.09	0.18	12.92	0.04	0	0.01	0.19	0.31	0.01	100.26	86.52
WQE3_Ol 04_70	276	0.02	40.22	46.45	0.07	0.12	12.95	0.01	0	0.01	0.2	0.36	0	100.39	86.48
WQE3_Ol 04_71	280	0.01	40.23	46.3	0.05	0.17	13.01	0.02	0	0.01	0.21	0.38	0.02	100.42	86.38
WQE3_Ol 04_72	284	0.02	39.91	46.26	0.06	0.15	13.04	0.05	-0.01	0.01	0.21	0.33	0	100.03	86.35
WQE3_Ol 04_73	288	0.02	39.72	46.42	0.08	0.18	13.01	0.02	0	0	0.2	0.3	0.03	99.99	86.41
WQE3_Ol 04_74	292	0.01	40.01	46.17	0.09	0.16	13.06	0.04	0	0.01	0.21	0.35	-0.02	100.11	86.30
WQE3_Ol 04_75	296	0	40.18	46.25	0.09	0.18	13.16	0.06	0	0	0.22	0.34	0.02	100.51	86.23
WQE3_Ol 04_76	300	0.01	39.84	46.27	0.1	0.14	13.26	0.02	0	0.02	0.2	0.37	0.01	100.25	86.15
WQE3_Ol 04_77	304	0.02	39.98	46.27	0.07	0.12	13.27	0.04	0	0.01	0.2	0.35	0.02	100.36	86.14
WQE3_Ol 04_78	308	0.02	40	46.1	0.07	0.18	13.11	0.03	0	0.01	0.22	0.32	0.01	100.08	86.24
WQE3_Ol 04_79	312	0.04	39.68	46.18	0.05	0.16	13.19	0.02	0	0.02	0.2	0.35	0.02	99.91	86.19
WQE3_Ol 04_80	316	0.03	39.74	45.99	0.09	0.16	13.32	0.02	0	0.01	0.21	0.31	0.03	99.92	86.02
WQE3_Ol 04_81	320	0.02	39.81	46.09	0.09	0.15	13.21	0.03	-0.01	0	0.21	0.38	0.02	99.99	86.15
WQE3_Ol 04_82	324	0.01	40.18	46.08	0.09	0.16	13.27	0.04	-0.01	0.01	0.23	0.34	0.03	100.43	86.09
WQE3_Ol 04_83	328	0.01	39.64	45.87	0.1	0.15	13.29	0.02	0	0.01	0.21	0.34	0.02	99.65	86.02
WQE3_Ol 04_84	332	0.03	39.96	46.26	0.08	0.15	13.26	0.03	0	0.01	0.2	0.37	0.02	100.38	86.15
WQE3_Ol 04_85	336	0.03	40.02	46.1	0.06	0.16	13.36	0.02	-0.01	0.02	0.22	0.31	0.03	100.33	86.02
WQE3_Ol 04_86	340	0.01	40.05	46.01	0.05	0.17	13.4	0.04	0	0	0.22	0.3	0.04	100.28	85.96
WQE3_Ol 04_87	344	0.02	39.8	46.06	0.07	0.16	13.44	0.01	0	0.01	0.21	0.32	0.01	100.11	85.93
WQE3_Ol 04_88	348	0.02	40.38	45.99	0.05	0.17	13.37	0.05	0	0.02	0.22	0.32	0.01	100.59	85.98
WQE3_Ol 04_89	352	0.01	39.96	46.11	0.09	0.15	13.44	0.04	-0.01	0.01	0.23	0.37	0.02	100.43	85.95
WQE3_Ol 04_90	356	0.03	40.03	46.16	0.08	0.16	13.45	0.01	0.01	0	0.22	0.35	0.03	100.53	85.95
WQE3_Ol 04_91	360	0.03	39.89	45.88	0.06	0.16	13.47	0.03	0	0	0.21	0.37	0.01	100.1	85.86
WQE3_Ol 04_92	364	0.01	40.31	45.86	0.07	0.19	13.5	0.03	0	0.01	0.22	0.3	0.02	100.51	85.83
WQE3_Ol 04_93	368	0.02	39.78	46.1	0.06	0.17	13.44	0.02	0.01	0	0.22	0.36	0	100.2	85.94
WQE3_Ol 04_94	372	0.01	39.89	45.75	0.09	0.16	13.44	0.02	0	0.02	0.21	0.33	0.02	99.93	85.85
WQE3_Ol 04_95	376	0.02	39.72	45.87	0.07	0.15	13.53	0	0	0.01	0.2	0.34	0.03	99.94	85.80
WQE3_Ol 04_96	380	0.01	40.13	45.84	0.07	0.16	13.53	0.03	0	0.01	0.22	0.32	0	100.33	85.79
WQE3_Ol 04_97	384	0.02	39.56	46.14	0.06	0.15	13.54	0.04	0	0.01	0.21	0.36	0	100.08	85.86
WQE3_Ol 04_98	388	0.02	40.01	45.8	0.1	0.16	13.31	0.03	0	0.02	0.22	0.34	0.01	100.03	85.98
WQE3_Ol 04_99	392	0.01	40.07	46.14	0.06	0.17	13.53	0.02	0	0.02	0.21	0.35	0.02	100.6	85.87
WQE3_Ol 04_100	396	0.02	39.86	46.07	0.06	0.14	13.66	0.03	0	-0.01	0.23	0.34	0.01	100.41	85.74
WQE3_Ol 04_101	400	0.01	39.98	45.93	0.08	0.15	13.56	0.04	0	0.01	0.21	0.36	0.01	100.34	85.79
WQE3_Ol 04_102	404	0.02	39.99	45.95	0.09	0.13	13.53	0.02	0.01	0.01	0.21	0.3	0.05	100.31	85.82
WQE3_Ol 22_01	14	0.12	38.9	34.03	2.22	0.33	19.69	0.02	0.04	0.53	3.07	0.12	0.26	99.33	75.49
WQE3_Ol 22_02	16	0.02	37.91	40.32	0.15	0.32	19.18	0	0.01	0.1	0.55	0.09	0.07	98.72	78.94

Sample	Dist (μm)	Na_2O	SiO_2	MgO	Al_2O_3	MnO	FeO	Cr_2O_3	K_2O	TiO_2	CaO	NiO	P_2O_5	Total	Mg#
WQE3_Ol 22_03	18	0.02	37.95	40.63	0.05	0.28	18.89	0.03	0	0.06	0.43	0.14	0.03	98.51	79.31
WQE3_Ol 22_04	20	0	37.85	41.01	0.02	0.26	18.74	0.01	0.01	0.06	0.43	0.1	0.06	98.54	79.60
WQE3_Ol 22_05	22	0.03	38.08	41.4	0.05	0.3	18.59	0.04	0.01	0.05	0.41	0.08	0.07	99.09	79.88
WQE3_Ol 22_06	24	0.01	38.08	42	0.06	0.26	18.14	0.03	0	0.04	0.36	0.12	0.05	99.17	80.50
WQE3_Ol 22_07	26	0.02	38.03	41.75	0.01	0.28	17.87	0.02	0	0.04	0.36	0.11	0.03	98.52	80.64
WQE3_Ol 22_08	28	0.03	38.22	42.23	0.04	0.24	17.51	0.03	-0.01	0.04	0.35	0.13	0.04	98.86	81.13
WQE3_Ol 22_09	30	0	38.53	42.42	0.06	0.26	17.63	0.05	0	0.03	0.35	0.16	0.03	99.52	81.09
WQE3_Ol 22_10	32	0.01	38.33	42.57	0.05	0.27	17.26	0.04	0	0.03	0.35	0.17	0.03	99.11	81.47
WQE3_Ol 22_11	34	0.01	38.52	42.93	0.04	0.22	17.1	0.03	0	0.04	0.34	0.15	0.03	99.41	81.74
WQE3_Ol 22_12	36	0.01	38.57	43	0.05	0.26	16.99	0.04	0	0.03	0.33	0.15	0.02	99.45	81.86
WQE3_Ol 22_13	38	0.03	39.02	42.94	0.04	0.22	16.92	0.03	0	0.02	0.34	0.15	0.02	99.76	81.90
WQE3_Ol 22_14	40	0.03	38.49	42.95	0.04	0.24	16.77	0.05	0	0.03	0.32	0.17	0.02	99.11	82.03
WQE3_Ol 22_15	42	0.02	38.72	42.63	0	0.25	17.22	0.05	0	0.03	0.29	0.15	0.04	99.39	81.53
WQE3_Ol 22_16	44	0.03	38.63	42.34	0.04	0.26	17.21	0.03	0.01	0.02	0.3	0.16	0.04	99.04	81.43
WQE3_Ol 22_17	46	0.02	38.76	42.15	0.05	0.23	17.47	0.04	0.01	0.04	0.31	0.15	0.05	99.26	81.13
WQE3_Ol 22_18	48	0.02	38.88	42.21	0.03	0.24	17.16	0.04	0.01	0.03	0.31	0.16	0.04	99.13	81.43
WQE3_Ol 22_19	50	0.02	38.67	42.51	0.06	0.21	17.45	0.03	0.01	0.02	0.32	0.17	0.02	99.5	81.28
WQE3_Ol 22_20	52	0.01	38.37	42.33	0.06	0.23	17.13	0.03	0.03	0.02	0.33	0.16	0.02	98.72	81.50
WQE3_Ol 22_21	54	0.04	38.71	42.55	0.06	0.23	17.26	0.04	0.01	0.03	0.28	0.2	0.05	99.46	81.46
WQE3_Ol 22_22	56	0.02	38.69	42.75	0.06	0.27	17.26	0.04	0.01	0.03	0.28	0.2	0.03	99.64	81.53
WQE3_Ol 22_23	58	0	38.91	42.34	0.05	0.18	17.28	0.05	0.02	0.02	0.28	0.22	0.05	99.38	81.37
WQE3_Ol 22_24	61	0.02	38.79	42.07	0.06	0.21	16.9	0.05	0.03	0.02	0.35	0.21	0.03	98.74	81.61
WQE3_Ol 22_25	63	0.03	38.44	42.78	0.04	0.25	17.03	0.02	0.02	0.03	0.31	0.23	0.02	99.18	81.74
WQE3_Ol 22_26	65	0.02	38.45	42.21	0.06	0.22	16.95	0.04	0.02	0.01	0.29	0.22	0.03	98.53	81.61
WQE3_Ol 22_27	67	0	39.18	42.6	0.04	0.18	17.03	0.03	0.02	0.03	0.26	0.22	0.02	99.61	81.68
WQE3_Ol 22_28	69	0.03	38.94	42.92	0.08	0.22	16.99	0.05	0	0.01	0.23	0.25	0.03	99.76	81.83
WQE3_Ol 22_29	71	0.01	38.91	43.26	0.03	0.18	17.13	0.04	0	0.02	0.23	0.21	0.04	100.05	81.82
WQE3_Ol 22_30	73	0.03	39.37	43.1	0.08	0.2	16.8	0.03	-0.01	0.02	0.23	0.21	0.03	100.08	82.06
WQE3_Ol 22_31	75	0.02	39	43.27	0.05	0.2	16.79	0.02	-0.01	0	0.23	0.19	0.06	99.82	82.12
WQE3_Ol 22_32	77	0.03	38.92	43.36	0.04	0.21	16.91	0.04	0	0.02	0.22	0.22	0.1	100.06	82.05
WQE3_Ol 22_33	79	0.02	39.23	42.75	0.06	0.19	16.75	0.04	-0.01	0.02	0.23	0.23	0.12	99.63	81.98
WQE3_Ol 22_34	81	0.03	39.27	43.22	0.08	0.22	16.99	0.04	0	0.02	0.21	0.23	0.1	100.39	81.93
WQE3_Ol 22_35	83	0.02	39.62	43.02	0.04	0.22	16.92	0.03	0	0.03	0.21	0.16	0.15	100.42	81.92
WQE3_Ol 22_36	85	0.04	39.45	43.15	0.08	0.2	17.11	0.05	0	0.03	0.2	0.19	0.12	100.62	81.80
WQE3_Ol 22_37	87	0.03	39.28	42.79	0.02	0.19	16.8	0.05	-0.01	0.02	0.21	0.2	0.15	99.73	81.95
WQE3_Ol 22_38	89	0.01	38.8	42.96	0.04	0.2	17	0.03	0.01	0.02	0.2	0.21	0.07	99.55	81.83
WQE3_Ol 22_39	91	0.02	39.16	42.82	0.04	0.18	16.96	0.06	-0.01	0.03	0.21	0.21	0.07	99.75	81.82
WQE3_Ol 22_40	93	0.02	38.97	43	0.08	0.2	17.17	0.04	0	0.02	0.23	0.22	0.05	99.99	81.70
WQE3_Ol 22_41	95	0.03	39.06	42.97	0.03	0.23	17.02	0.03	0	0.03	0.23	0.21	0.07	99.91	81.82

Sample	Dist (μm)	Na_2O	SiO_2	MgO	Al_2O_3	MnO	FeO	Cr_2O_3	K_2O	TiO_2	CaO	NiO	P_2O_5	Total	Mg#
WQE3_Ol 22_42	97	0	38.98	42.63	0.04	0.19	16.94	0.06	0	0.02	0.22	0.19	0.06	99.34	81.77
WQE3_Ol 22_43	99	0.03	39.45	42.92	0.05	0.26	17.21	0.03	-0.01	0.03	0.21	0.2	0.09	100.47	81.64
WQE3_Ol 22_44	101	0.02	39.1	43.03	0.09	0.22	17.29	0.04	-0.01	0.03	0.21	0.18	0.07	100.27	81.60
WQE3_Ol 22_45	103	0.02	39.19	42.91	0.08	0.22	17.19	0.03	0	0.03	0.23	0.22	0.06	100.2	81.65
WQE3_Ol 22_46	105	0.01	38.62	43.01	0.06	0.22	17.03	0.04	0	0.02	0.21	0.19	0.08	99.5	81.82
WQE3_Ol 22_47	107	0.02	39.15	42.92	0.05	0.22	17.23	0.04	0	0.03	0.22	0.18	0.11	100.16	81.62
WQE3_Ol 22_48	109	0.02	39.38	42.51	0.08	0.23	17.31	0.03	0	0.03	0.22	0.24	0.1	100.14	81.40
WQE3_Ol 22_49	111	0	39	42.98	0.07	0.2	17.29	0.05	0	0.03	0.22	0.21	0.11	100.15	81.59
WQE3_Ol 22_50	113	0.01	39.01	42.88	0.04	0.22	17.08	0.03	0	0.02	0.21	0.2	0.09	99.8	81.74
WQE3_Ol 22_51	115	0.04	39.39	42.88	0.04	0.22	17.18	0.03	0	0.03	0.22	0.18	0.12	100.33	81.65
WQE3_Ol 22_52	117	0.01	38.93	42.72	0.04	0.22	17.12	0.04	0	0.03	0.23	0.23	0.09	99.66	81.64
WQE3_Ol 22_53	119	0.01	39.14	42.64	0.04	0.21	16.99	0.05	0	0.03	0.22	0.21	0.06	99.6	81.73
WQE3_Ol 22_54	121	0.01	39.16	42.75	0.03	0.22	17.18	0.06	0	0.03	0.23	0.22	0.07	99.97	81.60
WQE3_Ol 22_55	123	0.03	39	43.02	0.06	0.25	17.33	0.05	0.01	0.02	0.23	0.18	0.09	100.27	81.57
WQE3_Ol 22_56	125	0.04	38.91	42.97	0.08	0.21	16.99	0.04	0	0.05	0.22	0.22	0.05	99.78	81.85
WQE3_Ol 22_57	127	0.02	39.37	43.05	0.07	0.2	17.11	0.05	0	0.04	0.23	0.22	0.08	100.43	81.77
WQE3_Ol 22_58	129	0.01	39.07	42.81	0.09	0.28	17.03	0.04	0	0.04	0.23	0.23	0.08	99.9	81.76
WQE3_Ol 22_59	131	0.02	39.61	42.97	0.06	0.2	17.12	0.06	0	0.04	0.23	0.22	0.07	100.59	81.73
WQE3_Ol 22_60	133	0.04	38.92	42.92	0.07	0.21	16.92	0.05	0	0.04	0.23	0.22	0.06	99.66	81.89
WQE3_Ol 23_01	0	3.49	50.62	1.94	19.16	0.16	7.64	0	1.41	1.74	10.3	-0.03	1.73	98.17	31.16
WQE3_Ol 23_02	4	1.5	47.44	1.36	20.37	0.11	12.75	-0.01	3.77	2.69	5.35	-0.02	1.6	96.91	15.98
WQE3_Ol 23_03	8	0.01	37.81	32.81	0.03	0.47	23.21	0.02	0.22	0.11	0.87	0.05	0.17	95.76	71.59
WQE3_Ol 23_04	12	-0.01	38.32	40.04	0.05	0.35	19.78	0.02	0	0.07	0.5	0.1	0.04	99.28	78.30
WQE3_Ol 23_05	16	0.01	38.57	40.76	0.04	0.34	19.16	0.02	0	0.06	0.43	0.12	0.07	99.58	79.13
WQE3_Ol 23_06	20	0.01	38.44	41.09	0.03	0.33	18.77	0	0.01	0.07	0.42	0.14	0.03	99.33	79.60
WQE3_Ol 23_07	24	0.02	38.97	40.98	0.04	0.28	18.67	0.02	0	0.06	0.41	0.12	0.05	99.62	79.64
WQE3_Ol 23_08	28	0.01	38.6	41.74	0.03	0.3	18.12	0.03	0.01	0.04	0.39	0.14	0.05	99.46	80.42
WQE3_Ol 23_09	32	0.02	39.12	41.81	0.03	0.29	17.96	0.04	0	0.03	0.39	0.16	0.03	99.87	80.58
WQE3_Ol 23_10	36	0.01	38.94	42.27	0.02	0.25	17.44	0.04	0	0.06	0.36	0.13	0.04	99.56	81.20
WQE3_Ol 23_11	40	0.02	39.02	42.67	0.01	0.25	17.22	0.04	0	0.03	0.35	0.19	0.08	99.86	81.54
WQE3_Ol 23_12	44	0.01	38.72	42.29	0.04	0.22	16.64	0.04	0.02	0.04	0.37	0.15	0.05	98.59	81.92
WQE3_Ol 23_13	48	0.01	39.4	42.9	0.03	0.25	17.04	0.04	0	0.03	0.35	0.18	0.02	100.24	81.78
WQE3_Ol 23_14	52	0.02	39.08	42.45	0.04	0.25	17.03	0.03	0	0.03	0.27	0.2	0.02	99.42	81.63
WQE3_Ol 23_15	56	0.02	38.9	42.54	0.03	0.26	17.29	0.02	0.01	0.03	0.28	0.21	0.03	99.62	81.43
WQE3_Ol 23_16	60	0.03	39.14	42.24	0.02	0.22	17.21	0.02	0.01	0.02	0.26	0.2	0.02	99.4	81.40
WQE3_Ol 23_17	64	0	39.16	42.39	0.02	0.23	17.19	0.04	0.01	0.01	0.24	0.18	0.01	99.48	81.47
WQE3_Ol 23_18	68	0.01	38.98	42.91	0.03	0.23	17.01	0.05	0	0.02	0.25	0.22	0	99.73	81.81
WQE3_Ol 23_19	72	0.03	39.04	43	0.03	0.21	17.19	0.03	0	0.02	0.22	0.18	0.04	100	81.68
WQE3_Ol 23_20	76	0.02	38.87	42.88	0.06	0.21	16.81	0.04	0.01	0.03	0.24	0.2	0.03	99.41	81.97

Sample	Dist (μm)	Na_2O	SiO_2	MgO	Al_2O_3	MnO	FeO	Cr_2O_3	K_2O	TiO_2	CaO	NiO	P_2O_5	Total	Mg#
WQE3_Ol 23_21	80	0.03	39.41	43.04	0.01	0.21	16.61	0.04	0.02	0.01	0.23	0.23	0.03	99.85	82.20
WQE3_Ol 23_22	84	0.01	38.83	42.94	0.04	0.2	16.62	0.01	0	0.02	0.23	0.22	0.03	99.16	82.16
WQE3_Ol 23_23	88	0.01	39.27	43.33	0.07	0.18	16.43	0.05	0	0.03	0.22	0.25	0.08	99.93	82.46
WQE3_Ol 23_24	92	0.02	39.44	43.51	0.05	0.19	16.35	0.03	0	0.02	0.21	0.23	0.03	100.08	82.59
WQE3_Ol 23_26	100	0.01	39.22	43.4	0.04	0.24	15.93	0.05	0	0	0.22	0.21	0.08	99.4	82.92
WQE3_Ol 23_27	104	0.04	39.44	43.61	0.05	0.23	15.97	0.04	0	0.02	0.22	0.23	0.03	99.88	82.96
WQE3_Ol 23_28	108	0.02	38.94	42.75	0.12	0.2	16.3	0.06	0.01	0.03	0.26	0.19	0.07	98.95	82.38
WQE3_Ol 23_29	112	0.02	39.35	44.16	0.08	0.17	15.88	0.04	0	0.01	0.21	0.28	0.01	100.21	83.21
WQE3_Ol 23_30	116	0.01	39.27	43.97	0.03	0.18	15.57	0.03	0	0.01	0.21	0.28	0.01	99.56	83.43
WQE3_Ol 23_31	120	0.04	39.17	44.15	0.06	0.22	15.25	0.02	0.01	0.01	0.22	0.24	0.09	99.48	83.77
WQE3_Ol 23_32	124	0.03	39.45	43.96	0.05	0.18	15.36	0.04	0.01	0.02	0.21	0.25	0.11	99.67	83.61
WQE3_Ol 23_33	128	0.02	39.52	44.23	0.06	0.17	15.36	0.03	0	0.02	0.22	0.24	0.11	99.98	83.69
WQE3_Ol 23_34	132	0.02	39.28	44.3	0.09	0.17	15.43	0.05	0.01	0.02	0.23	0.26	0.15	100	83.65
WQE3_Ol 23_35	136	0.03	39.63	44.05	0.06	0.21	15.36	0.03	-0.01	0.03	0.21	0.27	0.1	99.97	83.64
WQE3_Ol 23_36	140	0.02	39.14	44.17	0.07	0.16	15.58	0.01	0	0.02	0.22	0.26	0.11	99.77	83.48
WQE3_Ol 23_37	144	0.02	39.53	44.18	0.11	0.18	15.41	0.04	0	0.01	0.24	0.28	0.08	100.08	83.63
WQE3_Ol 23_38	148	0.03	39.27	43.93	0.04	0.2	15.42	0.04	0.01	0.03	0.22	0.27	0.07	99.52	83.55
WQE3_Ol 23_39	152	0.03	39.49	44.09	0.04	0.21	15.63	0.05	0	0.02	0.22	0.29	0.07	100.15	83.41
WQE3_Ol 23_40	156	0.02	39.37	44.23	0.09	0.21	15.58	0.03	0	0.01	0.21	0.27	0.08	100.1	83.50
WQE3_Ol 23_41	160	0.02	39.8	44.17	0.06	0.21	15.48	0.02	0	0.03	0.22	0.28	0.08	100.37	83.57
WQE3_Ol 23_42	164	0.03	39.31	44.06	0.07	0.18	15.62	0.05	0.01	0.02	0.21	0.26	0.05	99.88	83.41
WQE3_Ol 23_43	168	0.01	39.46	43.71	0.09	0.21	15.66	0.04	0	0.03	0.21	0.24	0.1	99.77	83.26
WQE3_Ol 23_44	172	0.01	39.27	44.14	0.05	0.22	15.68	0.03	0	0.02	0.22	0.27	0.06	99.97	83.38
WQE3_Ol 23_45	176	0.03	39.33	44.34	0.05	0.17	15.7	0.04	0	0.02	0.21	0.23	0.07	100.19	83.43
WQE3_Ol 23_46	180	0.02	39.45	43.95	0.07	0.17	15.71	0.03	0	0.02	0.21	0.28	0.03	99.94	83.30
WQE3_Ol 23_47	184	0.02	39.3	44.07	0.06	0.2	15.66	0.02	0	0.02	0.22	0.27	0.08	99.92	83.38
WQE3_Ol 23_48	188	0.02	39.37	44.18	0.03	0.24	15.57	0.04	0	0.02	0.21	0.24	0.05	99.97	83.49
WQE3_Ol 23_49	192	0.01	39.79	44.28	0.05	0.19	15.58	0.04	0	0.02	0.2	0.26	0.02	100.44	83.52
WQE3_Ol 23_50	196	0.02	39.38	44.1	0.03	0.22	15.71	0.04	0.01	0.01	0.21	0.28	0.04	100.04	83.34
WQE3_Ol 23_51	200	0.02	39.47	43.89	0.06	0.2	15.72	0.05	0	0.01	0.22	0.29	0.04	99.96	83.27
WQE3_Ol 23_52	204	0.01	39.57	44.03	0.05	0.19	15.58	0.03	0	0.02	0.21	0.26	0.03	99.96	83.44
WQE3_Ol 23_53	208	0.01	39.74	43.92	0.05	0.19	15.64	0.02	0	0.02	0.19	0.24	0.05	100.09	83.35
WQE3_Ol 23_54	212	0.01	39.15	44.11	0.07	0.24	15.71	0.03	0.01	0.02	0.2	0.27	0.07	99.88	83.35
WQE3_Ol 23_55	216	0.02	39.38	44.19	0.07	0.19	15.75	0.03	0	0.01	0.23	0.28	0.05	100.2	83.34
WQE3_Ol 23_56	220	0.02	39.15	43.94	0.08	0.19	15.54	0.02	0	0.02	0.22	0.24	0.06	99.48	83.44
WQE3_Ol 23_57	224	0.02	39.41	44.06	0.09	0.21	15.61	0.03	0	0.03	0.23	0.24	0.03	99.96	83.42
WQE3_Ol 23_58	228	0.02	39.51	44.09	0.08	0.17	15.42	0.03	0	0.01	0.22	0.25	0.05	99.84	83.60
WQE3_Ol 23_59	232	0.01	39.29	44.06	0.06	0.17	15.39	0.03	0	0.02	0.2	0.23	0.06	99.52	83.62
WQE3_Ol 23_60	236	0.02	39.18	44.39	0.05	0.2	15.62	0.03	0	0.03	0.22	0.29	0.04	100.07	83.51

Sample	Dist (μm)	Na_2O	SiO_2	MgO	Al_2O_3	MnO	FeO	Cr_2O_3	K_2O	TiO_2	CaO	NiO	P_2O_5	Total	Mg#
WQE3_Ol 23_61	240	0.01	39.21	43.88	0.07	0.22	15.49	0.02	0.01	0.02	0.23	0.26	0.04	99.45	83.47
WQE3_Ol 23_62	244	0.03	39.35	44.31	0.08	0.18	15.59	0.02	-0.01	0.02	0.21	0.28	0.07	100.13	83.52
WQE3_Ol 23_63	248	0.03	39.62	44.15	0.07	0.24	15.5	0.05	0	0.03	0.22	0.26	0.06	100.23	83.55
WQE3_Ol 23_64	252	0.03	39.33	44.17	0.08	0.17	15.4	0.03	0	0.02	0.22	0.31	0.06	99.81	83.64
WQE3_Ol 23_65	256	0.03	39.56	44.32	0.06	0.17	15.34	0.04	0	0.02	0.21	0.29	0.03	100.06	83.74
WQE3_Ol 23_66	260	0.01	39.34	44.51	0.06	0.19	15.46	0.02	0	0.03	0.21	0.29	0	100.11	83.69
WQE3_Ol 23_67	264	0	39.46	44.19	0.04	0.21	15.31	0.02	0	0.02	0.21	0.31	0.06	99.84	83.73
WQE3_Ol 23_68	268	0.02	39.36	44.32	0.03	0.2	15.42	0.06	0	0.02	0.21	0.26	0.05	99.93	83.67
WQE3_Ol 23_69	272	0	39.69	44.03	0.07	0.19	15.21	0.04	0	0.01	0.21	0.27	0.05	99.76	83.77
WQE3_Ol 23_70	276	0.02	39.39	44.34	0.02	0.2	15.36	0.04	0	0.02	0.21	0.31	-0.02	99.88	83.73
WQE3_Ol 23_71	280	0.03	39.67	44.39	0.08	0.17	15.39	0.02	0	0.03	0.22	0.29	0.01	100.29	83.72
WQE3_Ol 23_72	284	0.01	39.44	44.12	0.1	0.19	15.2	0.03	0	0.02	0.21	0.3	0.01	99.64	83.80
WQE3_Ol 23_73	288	0.02	39.8	44.38	0.04	0.18	15.32	0.03	0.01	0.01	0.22	0.27	0.04	100.31	83.78
WQE3_Ol 23_74	292	0.02	39.77	44.31	0.06	0.18	15.26	0.04	0	0.02	0.21	0.25	0.06	100.21	83.81
WQE3_Ol 23_75	296	0.02	39.68	44.45	0.06	0.22	15.23	0.05	0	0.02	0.21	0.27	0.03	100.23	83.88
WQE3_Ol 23_76	300	0.02	39.62	44.54	0.08	0.2	15.22	0.03	0	0.01	0.2	0.29	0.03	100.23	83.91
WQE3_Ol 18_01	0	6.22	46.9	0.81	19.94	0.22	14.02	0	2.29	2.97	4.09	0.01	1.62	99.07	9.34
WQE3_Ol 18_02	4	2.31	49.88	0.43	21.4	0.15	8.49	0.01	4.31	1.73	3.51	-0.03	1.73	93.92	8.28
WQE3_Ol 18_03	8	2.81	43.04	5.9	15.29	0.45	23.95	0.02	1.45	2.94	2.68	0.02	1.51	100.06	30.51
WQE3_Ol 18_04	12	0.04	37.09	35.83	0.5	0.45	24.95	0	0.08	0.24	0.72	0.06	0.07	100.03	71.91
WQE3_Ol 18_05	16	0.01	38.52	40.55	0.08	0.31	19.07	0.01	0.02	0.08	0.48	0.09	0.05	99.27	79.12
WQE3_Ol 18_06	20	0	39	41.48	-0.01	0.28	18.34	0.03	0.01	0.07	0.44	0.11	0.07	99.82	80.13
WQE3_Ol 18_07	24	0.03	39.2	42	0.02	0.28	17.86	0.02	0	0.05	0.4	0.14	0.05	100.05	80.74
WQE3_Ol 18_08	28	0.01	39.09	42.42	0.01	0.3	17.71	0.02	0	0.03	0.41	0.15	0.02	100.17	81.02
WQE3_Ol 18_09	32	0.01	39.13	42.3	0.04	0.28	17.51	0.03	0	0.04	0.38	0.18	0.04	99.93	81.15
WQE3_Ol 18_10	36	0.01	39.22	42.48	0.06	0.29	17.33	0.01	0	0.04	0.37	0.14	0.03	100.01	81.38
WQE3_Ol 18_11	40	0	38.79	42.67	0.02	0.23	17.15	0.03	0	0.04	0.37	0.14	0.02	99.46	81.60
WQE3_Ol 18_12	44	0.02	39.06	42.86	0.04	0.26	17.09	0.02	0	0.04	0.36	0.17	0.05	99.96	81.72
WQE3_Ol 18_13	48	0.02	39.4	42.88	0.05	0.26	17.23	0.02	0	0.03	0.33	0.17	0	100.39	81.60
WQE3_Ol 18_14	52	0.02	39.12	42.7	0.03	0.24	16.92	0.04	0.01	0.03	0.3	0.19	0.03	99.64	81.81
WQE3_Ol 18_15	56	0.02	39.52	42.35	0.05	0.26	17.39	0.04	0	0.03	0.28	0.2	0.02	100.17	81.28
WQE3_Ol 18_16	60	0.01	39.15	42.67	0.02	0.25	17.43	0.02	0	0.04	0.28	0.19	0	100.08	81.36
WQE3_Ol 18_17	64	0.02	39.17	42.75	0.02	0.23	17.46	0.02	0	0.02	0.27	0.19	0.05	100.2	81.36
WQE3_Ol 18_18	68	0.01	39.1	42.56	0.04	0.22	17.57	0.04	0.01	0.03	0.26	0.21	0.01	100.04	81.20
WQE3_Ol 18_19	72	0	39.27	42.84	0.06	0.23	17.38	0.05	0	0.03	0.27	0.17	0.02	100.32	81.46
WQE3_Ol 18_20	76	0.02	39.51	42.98	0.04	0.24	17.6	0.03	0	0.02	0.24	0.18	0.02	100.88	81.32
WQE3_Ol 18_21	80	0.03	39.36	42.83	0.03	0.24	17.24	0.04	0	0.02	0.24	0.2	0.04	100.26	81.58
WQE3_Ol 18_22	84	0.02	39.19	42.82	0.04	0.23	17.32	0.04	0	0.02	0.23	0.18	0.02	100.11	81.51
WQE3_Ol 18_23	88	0.01	39.37	42.99	0.06	0.24	17.37	0.03	0	0.02	0.24	0.21	0.02	100.55	81.52

Sample	Dist (μm)	Na_2O	SiO_2	MgO	Al_2O_3	MnO	FeO	Cr_2O_3	K_2O	TiO_2	CaO	NiO	P_2O_5	Total	Mg#
WQE3_Ol 18_24	92	0.01	39.28	42.97	0.07	0.2	17.21	0.06	-0.01	0.02	0.24	0.22	0.01	100.28	81.65
WQE3_Ol 18_25	96	0.03	39.34	43.06	0.03	0.22	17.34	0.02	0.01	0.03	0.23	0.2	-0.01	100.49	81.57
WQE3_Ol 18_26	100	0.01	39.2	43.11	0.02	0.2	17.17	0.01	0	0.01	0.23	0.25	0.02	100.22	81.74
WQE3_Ol 18_27	104	0.01	39.35	43.05	0.03	0.23	17.19	0.03	0	0.01	0.23	0.2	-0.02	100.31	81.70
WQE3_Ol 18_28	108	0.01	39.26	43.08	0.04	0.2	17.2	0.04	0	0.02	0.23	0.18	0.03	100.3	81.70
WQE3_Ol 18_29	112	0.01	39.26	43.16	0.04	0.2	16.87	0.04	0	0.01	0.22	0.19	0.01	100.03	82.02
WQE3_Ol 18_30	116	0.02	39.21	43.21	0.03	0.22	16.95	0.04	0	0.02	0.21	0.24	0.03	100.17	81.96
WQE3_Ol 18_31	120	0.01	39.31	43.24	0.05	0.2	16.88	0.04	0	0.01	0.23	0.19	0	100.16	82.03
WQE3_Ol 18_32	124	0.03	39.21	43.21	0.04	0.23	16.67	0.04	0	0.01	0.2	0.24	0.01	99.89	82.21
WQE3_Ol 18_33	128	0.01	39.49	43.46	0.07	0.21	16.83	0.04	0	0.01	0.22	0.2	-0.01	100.52	82.15
WQE3_Ol 18_34	132	0.02	39.43	43.4	0.05	0.2	16.75	0.03	0	0.01	0.21	0.2	-0.01	100.29	82.20
WQE3_Ol 18_35	136	0.02	39.52	43.46	0.02	0.25	16.76	0.04	0	0.01	0.21	0.25	0	100.55	82.21
WQE3_Ol 18_36	140	0	39.51	43.48	0.06	0.21	16.81	0.01	0	0.02	0.21	0.21	0.02	100.53	82.18
WQE3_Ol 18_37	144	0.03	39.76	43.69	0.03	0.21	16.65	0.02	-0.01	0.02	0.23	0.27	0.02	100.94	82.39
WQE3_Ol 18_38	148	0.02	39.42	43.38	0.08	0.25	16.72	0.04	0	0.02	0.22	0.22	0.02	100.39	82.22
WQE3_Ol 18_39	152	0.02	39.62	43.33	0.03	0.21	16.58	0.03	0.01	0.02	0.22	0.22	0.04	100.33	82.33
WQE3_Ol 18_40	156	0.03	39.17	43.61	0.04	0.2	16.61	0.01	0	0.01	0.23	0.24	0	100.15	82.39
WQE3_Ol 18_41	160	0.01	39.41	43.61	0.07	0.23	16.75	0.04	0	0.02	0.21	0.23	0.01	100.59	82.27
WQE3_Ol 18_42	164	0.01	39.5	43.49	0.05	0.24	16.63	0.03	0	0.02	0.22	0.23	0.01	100.41	82.34
WQE3_Ol 18_43	168	0.02	39.22	43.46	0.02	0.2	16.81	0.03	0	0.02	0.22	0.24	-0.01	100.23	82.17
WQE3_Ol 18_44	172	0.03	39.1	43.31	0.07	0.22	16.83	0.02	0	0.01	0.23	0.19	0	100.01	82.10
WQE3_Ol 18_45	176	0.02	39.47	43.21	0.07	0.2	16.79	0.03	0	0.02	0.22	0.22	0.02	100.27	82.10
WQE3_Ol 18_46	180	0.03	38.97	43.55	0.08	0.21	16.84	0.01	-0.01	0.03	0.21	0.23	0.01	100.16	82.17
WQE3_Ol 18_47	184	0.02	39.5	43.5	0.02	0.23	17.08	0.04	0	0.02	0.21	0.22	0.03	100.86	81.95
WQE3_Ol 18_48	188	0	39.38	43.44	0.04	0.23	17	0.01	0	0.01	0.23	0.22	0.01	100.57	82.00
WQE3_Ol 18_49	192	0.02	39.47	42.98	0.09	0.23	17.04	0.03	0	0.03	0.21	0.21	0	100.31	81.81
WQE3_Ol 18_50	196	0.01	39.36	43.28	0.03	0.23	16.93	0.05	0	0.02	0.23	0.2	0.02	100.37	82.00
WQE3_Ol 18_51	200	0.03	39.61	43.13	0.07	0.21	16.99	0.04	0	0.02	0.23	0.23	0.02	100.58	81.90
WQE3_Ol 18_52	204	0.01	39.39	43.34	0.05	0.22	17.15	0.03	0	0.03	0.22	0.17	0	100.6	81.83
WQE3_Ol 18_53	208	0.03	39.2	43.21	0.03	0.21	17	0.05	0	0.02	0.22	0.17	0.03	100.17	81.92
WQE3_Ol 18_54	212	0.01	38.98	43.16	0.06	0.21	17.2	0.05	0	0.02	0.22	0.23	0.03	100.17	81.73
WQE3_Ol 18_55	216	0.01	39.43	42.9	0.03	0.2	17.19	0.03	-0.01	0.02	0.23	0.21	0	100.24	81.65
WQE3_Ol 18_56	220	0.02	39.22	43.12	0.03	0.19	17.34	0.03	0	0.02	0.22	0.18	-0.01	100.36	81.59
WQE3_Ol 18_57	224	0.01	39.24	43.22	0.05	0.22	17.31	0.03	0	0.01	0.22	0.19	0.01	100.51	81.65
WQE3_Ol 18_58	228	0.03	39.35	43.11	0.07	0.2	17.27	0.04	-0.01	0.02	0.23	0.23	0.04	100.57	81.65
WQE3_Ol 18_59	232	0	39.11	42.9	0.05	0.24	17.27	0.02	0	0.02	0.22	0.25	0.02	100.09	81.58
WQE3_Ol 18_60	236	0.02	39.15	43.03	0.03	0.22	17.25	0.02	0	0.01	0.22	0.22	0.01	100.18	81.64
WQE3_Ol 18_61	240	0	39.44	42.91	0.05	0.24	17.36	0.04	0	0.02	0.24	0.17	0.01	100.46	81.50
WQE3_Ol 18_62	244	0	38.88	43.03	0.07	0.27	17.24	0.06	0	0.01	0.22	0.18	0.01	99.96	81.65

Sample	Dist (μm)	Na_2O	SiO_2	MgO	Al_2O_3	MnO	FeO	Cr_2O_3	K_2O	TiO_2	CaO	NiO	P_2O_5	Total	Mg#
WQE3_Ol 18_63	248	0.01	39.35	42.98	0.07	0.26	17.32	0.04	0	0.01	0.23	0.22	0.02	100.52	81.56
WQE3_Ol 18_64	252	0.02	39.33	42.89	0.03	0.24	17.33	0.03	-0.01	0.02	0.24	0.17	0.01	100.29	81.52
WQE3_Ol 18_65	256	0.02	38.99	42.68	0.02	0.22	17.28	0.06	0	0.01	0.24	0.22	0	99.76	81.49
WQE3_Ol 18_66	260	0.01	39.09	42.86	0.05	0.25	17.46	0.04	0	0	0.24	0.18	0.01	100.2	81.40
WQE3_Ol 18_67	264	0.02	39.46	42.73	0.07	0.24	17.36	0.03	-0.01	0	0.24	0.21	0.01	100.36	81.44
WQE3_Ol 18_68	268	0.01	38.95	42.84	0.05	0.19	17.51	0.03	0	0.02	0.25	0.22	0	100.06	81.35
WQE3_Ol 18_69	272	0.01	39.03	42.85	0.04	0.22	17.55	0.02	0	0.02	0.25	0.17	0	100.15	81.32
WQE3_Ol 18_70	276	0.02	38.94	42.79	0.05	0.23	17.34	0.04	0	0.02	0.24	0.18	0	99.84	81.48
WQE3_Ol 18_71	280	0.03	39.36	42.97	0.04	0.23	17.41	0.04	0	0.02	0.27	0.19	0	100.57	81.48
WQE3_Ol 18_72	284	-0.01	39.05	42.93	0	0.27	17.31	0.03	-0.01	0.01	0.25	0.21	0.03	100.08	81.55
WQE3_Ol 18_73	288	0.01	39.35	42.69	0.06	0.27	17.48	0.04	0	0.02	0.26	0.16	0	100.34	81.32
WQE3_Ol 18_74	292	0.02	38.84	42.95	0.04	0.26	17.42	0.04	0	0.02	0.26	0.19	0	100.03	81.46
WQE3_Ol 18_75	296	0.02	39.16	42.78	0.07	0.24	17.54	0.05	0	0.03	0.27	0.18	0	100.34	81.30
WQE3_Ol 18_76	300	-0.01	38.87	43.01	0.07	0.24	17.47	0.04	0	0.03	0.26	0.2	0.03	100.19	81.44
WQE3_Ol 18_77	304	0.02	39.04	42.68	0.05	0.25	17.44	0.03	0	0.03	0.28	0.16	0.05	100.02	81.35
WQE3_Ol 18_78	308	0.02	38.71	42.81	0	0.22	17.35	0.06	0	0.03	0.28	0.2	0.06	99.72	81.48
WQE3_Ol 18_79	312	0.01	39.09	42.99	0.03	0.26	17.16	0.06	0	0.03	0.28	0.18	0.03	100.12	81.70
WQE3_Ol 18_80	316	0.01	39.15	43.03	0.04	0.24	17.15	0.05	0	0.03	0.32	0.17	0.04	100.22	81.73

Table C1.3. Glass major element composition from the Waitomokia volcano (New Zealand), obtained by electron microprobe and expressed in %. Data from the Waitomokia volcano (New Zealand).

Sample	SiO2	TiO2	Al2O3	FeOt	MnO	MgO	CaO	Na2O	K2O	Cr2O3	P2O5	TOTAL
VMC3 ol01a	45.23	3.07	15.70	11.11	0.20	4.24	10.81	4.95	2.04	0.01	1.09	98.44

Table D1.1. Plagioclase major element compositions obtained by electron microprobe, expressed in %. Data from Montserrat.

Sample	Distance (microns)	Na_2O	Al_2O_3	SiO_2	K_2O	CaO	FeO	MgO	P_2O_5	TiO_2	MnO	Total
MT75_point0		5.10	28.60	54.63	0.13	11.36	0.26	0.02	0.12	0.01	0.01	100.24
MT75_point1		1.71	33.46	46.44	0.02	17.31	0.49	0.09	0.19	0.01	0.00	99.72
MT75_point2		2.83	31.54	48.99	0.05	15.64	0.59	0.10	0.17	0.02	0.01	99.94
MT75_point3		5.27	28.28	55.13	0.12	11.26	0.30	0.01	0.11	0.01	0.01	100.50
MT75_point4		5.72	27.53	55.91	0.14	10.37	0.29	0.02	0.10	0.00	0.00	100.08
MT75_point5		5.18	28.58	54.93	0.12	11.31	0.33	0.02	0.11	0.01	0.01	100.60
MT75_point6		3.03	32.00	49.79	0.06	15.04	0.33	0.01	0.16	0.00	0.01	100.43
MT75_point7		5.55	28.01	55.35	0.13	10.69	0.23	0.01	0.11	0.01	0.00	100.09
MT75_point8		5.59	27.81	55.98	0.14	10.54	0.28	0.01	0.10	0.01	0.01	100.47
MT75_point9		5.73	27.72	55.73	0.14	10.65	0.30	0.02	0.11	0.01	0.01	100.42
MT75_point10		2.13	32.01	47.12	0.04	16.48	0.60	0.09	0.18	0.02	0.00	98.67
MT75_point11		2.32	32.52	48.09	0.06	16.48	0.64	0.10	0.18	0.02	0.01	100.42
MT75_point12		5.03	28.81	54.06	0.12	11.76	0.34	0.01	0.13	0.01	0.00	100.27
MT75_point13		4.12	30.16	52.06	0.10	13.32	0.34	0.02	0.13	0.01	0.01	100.27
MT75_traverse19	0	1.28	33.70	44.52	0.03	18.10	0.48	0.03	0.18	0.01	0.01	98.34
MT75_traverse19	20.06	0.97	34.23	44.82	0.00	18.68	0.52	0.06	0.19	0.01	0.00	99.48
MT75_traverse19	40.13	1.02	34.28	45.22	0.01	18.51	0.50	0.09	0.19	0.01	0.00	99.83
MT75_traverse19	60.19	1.32	33.96	45.64	0.02	18.21	0.56	0.08	0.19	0.01	0.00	99.99
MT75_traverse19	80.26	1.27	33.70	45.92	0.02	18.10	0.54	0.07	0.18	0.01	0.01	99.82
MT75_traverse19	100.32	1.26	33.75	45.53	0.02	18.42	0.57	0.08	0.18	0.01	0.00	99.82
MT75_traverse19	120.39	1.45	33.84	45.93	0.02	17.96	0.54	0.09	0.19	0.01	0.00	100.03
MT75_traverse19	140.45	1.48	33.55	46.30	0.02	17.91	0.58	0.08	0.18	0.01	0.00	100.11
MT75_traverse19	160.51	1.48	33.89	45.86	0.01	17.99	0.58	0.04	0.19	0.01	0.01	100.06
MT75_traverse19	180.58	2.58	32.04	48.69	0.05	15.92	0.74	0.13	0.16	0.02	0.01	100.34
MT75_traverse19	200.64	2.78	31.31	48.65	0.05	15.52	0.74	0.12	0.16	0.02	0.01	99.36
MT75_traverse19	220.71	2.80	31.78	48.83	0.05	15.67	0.61	0.10	0.17	0.03	0.01	100.05
MT75_traverse19	240.77	2.33	32.67	47.28	0.04	16.75	0.63	0.08	0.16	0.03	0.02	99.99
MT75_traverse19	260.84	3.20	30.85	50.14	0.07	14.41	0.50	0.05	0.16	0.02	0.00	99.40
MT75_traverse19	280.9	3.86	30.21	51.40	0.07	13.55	0.51	0.05	0.15	0.02	0.00	99.82
MT75_traverse19	300.97	4.56	29.37	52.79	0.08	12.52	0.51	0.04	0.13	0.02	0.01	100.03
MT75_traverse19	321.03	4.09	30.05	52.09	0.10	13.50	0.86	0.05	0.15	0.05	0.01	100.95

Table D1.2. Orthopyroxene major element compositions obtained by electron microprobe, expressed in %. Data from Montserrat

Sample	Na_2O	Al_2O_3	SiO_2	K_2O	CaO	FeO	MgO	P_2O_5	TiO_2	MnO	Total
MT75_point14	0.03	0.48	51.17	0	0.58	24.84	20.98	NA	0.07	1.56	99.71
MT75_point15	0.02	0.5	51.83	0	0.57	24.7	20.9	NA	0.07	1.54	100.13
MT75_point16	0.03	1.05	53.65	0.02	1.63	16.13	26.95	NA	0.21	0.52	100.19
MT75_point17	0.02	0.94	53	0	1.72	18.17	25.54	NA	0.21	0.6	100.20

The End